Proceedings of
2019 IPL SYMPOSIUM ON LANDSLIDES

16 – 19 September 2019
UNESCO Headquarters in Paris, France

Organized by
The International Consortium on Landslides (ICL)

Sponsored by
The United Nations Educational, Scientific, Cultural Organization (UNESCO)

Picture on the cover page
Ichihara landslide in Hiroshima after the heavy rainfall in July 2018
Taken from UAV by Kyoji Sassa, Khang Dang, and Nguyen Duc Ha

2019 IPL SYMPOSIUM ON LANDSLIDES

16 – 19 September 2019
UNESCO Headquarters in Paris, France

Kyoji Sassa・Khang Dang *Editors*

Organized by
International Consortium on Landslides (ICL)

Sponsored by
The United Nations Educational, Scientific, Cultural Organization (UNESCO)

Editors
Kyoji Sassa, Khang Dang
International Consortium on Landslides
Kyoto, Japan

This proceedings is registered in the Online Public Access Catalog of the National Diet Library of Japan

ISBN 978-4-9903382-5-1

Published by: The International Consortium on Landslides

Contents

Experience of CENACID-UFPR in landslides related disasters

Lima, Renato Eugenio[1], Acordes, Fabiane Aline[2], Talamini, Adriana Ahrendt [3]

1) Federal University of Parana, Center for Scientific Support in Disasters (CENACID-UFPR), Curitiba-Brazil, Curitiba-Brazil, 80.045-115, 773 R. José de Alencar, e-mail: renatolima@ufpr.br

2) Federal University of Parana, Center for Scientific Support in Disasters (CENACID-UFPR), Curitiba-Brazil, 524 São Mateus Street, e-mail: fabiane.acordes@gmail.com

3) Federal University of Parana, Center for Scientific Support in Disasters (CENACID-UFPR), Curitiba-Brazil, 210, Av. Cel. Francisco H. dos Santos, e-mail: adrianatalamini@ufpr.br

Abstract The Center for Scientific Support in Disasters (CENACID-UFPR) is a special unit of the oldest university of Brazil, the Federal University of Paraná. The purpose of the center is to provide scientific and technical support to governments, civil protection agencies, research institutions, non-governmental organizations and community, both national and international, in the theme of risk management and disaster response. It also proposes actions to mitigate and respond to emergencies, and provides training on emergency response and accident prevention. CENACID was requested to provide scientific support in national and international emergencies associated with mass movements, such as landslides, mudflows and debris, dam breaks, gravitational mass movements associated with earthquakes and others. The center provided scientific knowledge in natural and anthropogenic environmental disasters, particularly in Brazil and South and Central America. CENACID specialists in various disciplines can be requested in emergencies, and one of the group's priorities is the investigations into emergency risk analysis associated with situations of gravitational mass movements.

Keywords CENACID, Scientific Support, Disasters, Landslide

History

The Center for Scientific Support in Disasters (CENACID-UFPR) is a special unit of the Federal University of Paraná (UFPR). It was created by a group of the members of the Interdisciplinary Nucleous for Environment and Development of the university in 2000. The members were looking for methodological approach to the sustainable development and the group produced some interdisciplinary tools to face the complexity of the development problems.

The group's reflections realized the importance of natural and man-made disasters for sustainable development. The group is leaded by Geologists, Biologists and Engineers and at this stage include Geologists, Engineers, Biologists and Physicians.

General purpose of CENACID

CENACID-UFPR's mission is to reduce the loss and suffering of people in disaster situations. For this, the center has a group of trained scientists prepared to contribute to emergency missions and to collaborate in disaster situations, providing scientific knowledge (Fig. 1).

The contribution can be of different types depending on the disaster and each specific situation.

Types of scientific support

Each specific situation requires different scientific contributions and it is not easy to discover what is important, possible and useful in disaster response.

Normally the community affected, including the government, do not know what kind of scientific support could be useful to reduce the disaster (social, economic and environmental consequences of the hazardous process).

Basic financial support is provided by Federal University of Parana and, depending on each situation, may receive additional donations from different partners. In the past, we have received financial support for disaster response missions from Civil Protection agencies, the Ministry of Foreign Affairs, UN agencies, OCHA, companies, local and state governments, etc.

Some of the typical contributions provided by the CENACID mission to a disaster area are:

- Rapid general risk evaluation;
- Support to the disaster management;
- Support to the government committees;
- Emergency risk mapping;
- Understand and explain to government leaders and representatives the geological hazardous process;
- Analysis of the hazardous process and preparation of a prognosis of the disaster evolution;
- Support to national and international agencies involved in disaster response;
- Recommendations for the disaster recovery phase;
- Explanations to the community about the natural or artificial disaster-related process, including information for the press and media services.

- Study each type of disaster-generating process to be able to apply this knowledge to future disaster situations.
- Understand and study hazardous processes in each disaster, accident or risk situation to learn from each specific situation and be able to use that experience in future situations.

Figure 1 Bridge fall over the Capivari River caused by landslides, affecting the most important Brazilian highway that connects the southeastern and southern regions (2005).

Methodology of the scientific disaster response of CENACID-UFPR

The center has developed its own methodology for scientific disaster response. This methodology is followed in every disaster or risk situation in which the CENACID group is called or offers support.

The center has regular follow-up on key situations that can result in disasters and receives information from the authorities, the press, UN agencies and other sources, about accidents and disasters.

The action of the center is based on the scientific approach and aims for rapid analysis of the hazardous process and its main characteristics. The group aims to apply an integrated, cooperative and interdisciplinary approach.

The CENACID-UFPR methodology for scientific disaster response is based in some general principles as follows:

- Recognizing and understand the hazardous process.
- Rapid assessment of the risks, including secondary risks.
- Support to the disaster management.
- Immediate preparation of a proposal for urgent action.
- Registration of the facts at the “VICON-desastres” GIS, which is a Geographic Information System developed by the members of the center.
- Pragmatic situational approach, considering cultural, economic, political conditions, etc. of the affected region.

The CENACID-UFPR mission protocol has four phases to respond disaster situations (Fig. 2):

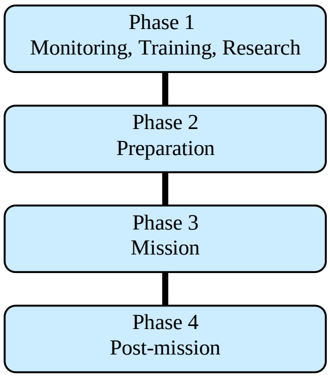

Figure 2 Scheme of CENACID-UFPR mission protocol.

Phase 1 – MONITORING, TRAINING, RESEARCHING

In the continuous monitoring phase, the CENACID team carries out the following activities:

- Permanent monitoring;
- Scientific research on hazardous processes and disasters;
- Conducting CENACID Training Courses (Fig. 3);
- Participation in meetings, seminars, scientific congresses, etc.
- Selection of disaster situations where CENACID team could be helpful, on demand or chosen;
- Deciding whether or not to launch each mission;
- Alert to CENACID members;
- Selection of the team for the disaster response mission using as criteria a) availability b) area of expertise and c) experience in previous missions of CENACID (Fig. 4).

Figure 3 Preliminary Training Course of CENACID.

Figure 4 Basic Training Course that prepares the participants to be a leader of mission.

Phase 2 – PREPARATION

The "Preparation" phase is critical to the success of the mission. It is also the fastest part of the cycle. It includes team tasks for the selected team and for the coordination of the mission.

Tasks for selected team:

- To gather information about the accident;
- To look for general information (maps, roads, language, dangerous facilities, etc.);
- Others.

Tasks for the coordination of the mission:

- Define and provide the transportation of the team to the disaster area;
- Prepare the resources needed for the mission. Local authorities contacts, travel money for each person, visas, etc.;
- Insurance for mission members in case of an international mission;
- "Mission Plan".

Phase 3 – MISSION

Carrying out a disaster relief mission is the center's most important task, and an important step towards achieving CENACID-UFPR's goal.

During this phase the team has a long list of activities to implement including: arrival and initial contacts, selection of priorities, definition of action plan, field activities, indication of urgent action proposal for local managers, information management, database organization, contacts with authorities, mandatory Mission Report, preparation of the recommendations, transfer of responsibilities to local agents, disaster exit (Fig. 5).

Figure 5 "Mission" phase to respond a landslide accident in a small city of Paraná State, Brazil (2018).

Phase 4 – POST-MISSION

"Post Mission" includes the preparation of supplementary reports, mission evaluation, return to the "monitoring" phase, complementary research and training courses. It also includes the preparation of scientific articles and conferences on the natural and anthropic processes involved in the disaster.

All CENACID scientific missions have a "lessons learned" seminar with the entire group, including non-mission members.

General experiences of CENACID

CENACID has sent science missions to almost 100 risk and disaster situations. The group was sent to offer scientific support in landslides, mass flows, floods, earthquakes, hurricanes, tornadoes, volcanic activities and tropical storms. Accidents such as the breaking of dams and collapses in karst urban areas have also been scientifically supported in different locations. In addition, environmental accidents such as oil spills in watersheds and coastal areas were also supported by the center's scientists.

Since 2000, CENACID's specially trained scientists have contributed to disaster response or prevention in over 65 hazardous processes with over 100 field missions. These missions benefited 11 countries in South and Central America, the Caribbean region, and Africa.

Most of the knowledge and products available are related to the natural processes associated in each case, such as risk analysis, evolution of landslides, dispersion of materials, secondary risks, etc.

Experiences of CENACID with landslides disasters

Approximately 50% of all disasters assisted by the center are related to gravitational mass movements (Fig. 6). This group includes accidents caused exclusively by landslides, as well as those in which landslides are not the threatening process. Examples are situations where landslides trigger disasters of other type, as in the case of disruption of dams by mass movements, and those disasters where landslides are the consequence of another process, such as landslides triggered by earthquakes.

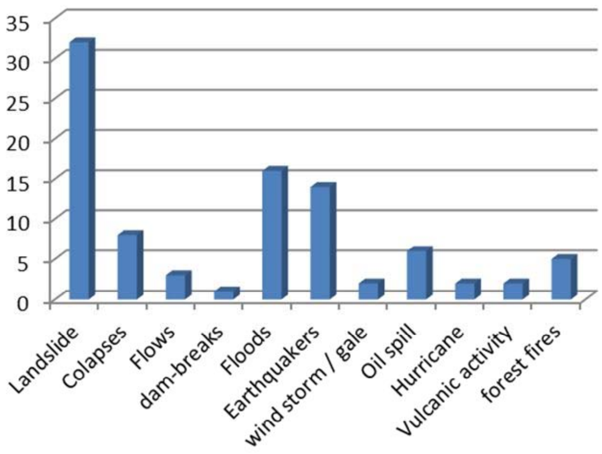

Figure 6 Comparative graphic showing the percentage of mass movements related disasters. (TOTAL 91)

Examples of landslides disaster response results

The mega-disaster of Santa Catarina State, Brazil (2008)

This disaster caused by an estimated 4000 landslides affected 42 municipalities in the state of Santa Catarina in southern Brazil and involved more than two million people.

The first landslides occurred on November 22, 2008, affecting the cities of Joinville and Itapoá in the coastal region. As the period of heavy rains continued on the night of November 22-23, 30 municipalities were heavily affected with significant losses and damage. The entire region ran out of power and water, communications services became inoperative, and roads were disrupted. This disaster resulted in one million people affected, 78707 homeless and 134 deaths. In the region 10,000 houses were totally destroyed.

Haiti earthquake (2010)

In 2010, during the Haiti earthquake, Brazil was the leader of the United Nations peacekeeping force in the country. The Government of Haiti and the force commander requested a CENACID mission to support overall decision-making in the disaster. The mission also aimed to provide an analysis of associated secondary risks, including landslide risk analysis.

The scientists identified different types of gravitational mass movements including translational landslides, sensitive-clay collapses and small flows.

The CENACID report indicated many risk areas (Fig.7) and situations, including growing concern about the risk of landslides in the next rainy season following the earthquake.

Despite the report's recommendations, it was not possible to prevent 17 people from dying from landslides caused by the next rainy season.

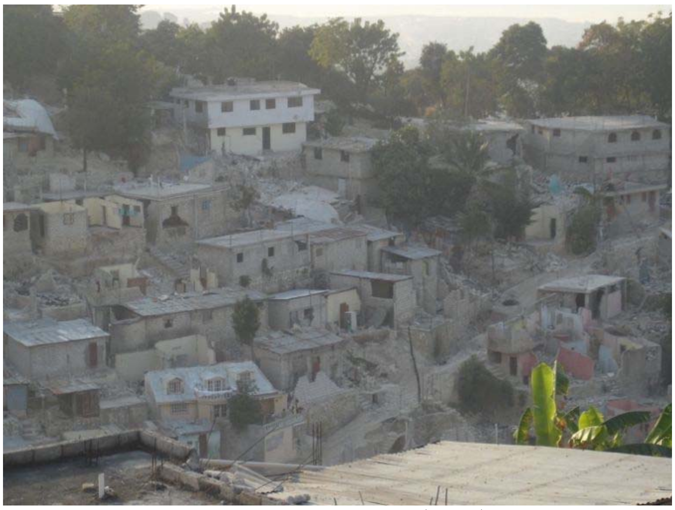

Figure 7 - Region in Port-au-Prince (Haiti) affected by the earthquake and mapped by CENACID as risk area for landslides.

The mega-disaster associated with landslides - Rio de Janeiro State, Brazil (2011)

On the night of January 11-12, 2011, the cities of Nova Friburgo, Teresópolis and Petrópolis, in the mountainous region of Rio de Janeiro State, were strongly affected by the mass flows and translational landslides of this huge disaster (Fig. 8). The number of deaths recorded was 916 and 200 people disappeared.

CENACID has estimated more than 5,000 landslides of different types that have caused complete destruction of entire neighborhoods in urban and rural areas.

These geological processes have caused serious damage to infrastructure, and thousands of homes, secondary and main roads, communication systems and sanitation services have been damaged or destroyed (Fig.9).

CENACID's mission of landslide-generated disaster specialists was sent to the disaster area immediately, responding to a request from the state and federal governments, providing emergency risk analysis and important disaster management guidance.

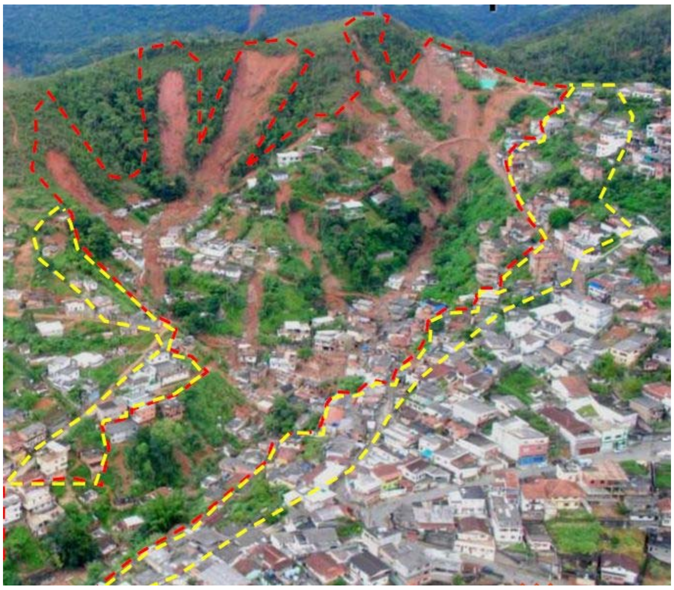

Figure 8 - Urban area affetcted by a serius of translational landslides in the disaster of Rio de Janeiro, 2011 showing deiferen levels of risk. (Photo by DRM-RJ)

As with all CENACID missions, the "Relative Rapid Landslide Analysis" (RRLA) methodology (Lima, 2013) was used to urgently assess the risk associated with landslides, resulting in over 500 risk areas quickly analyzed in conjunction with of the Geological Service of the State of Rio de Janeiro, indicating immediate evacuation in approximately 120 situations.

Figure 9 - Church in rural area of the city of Teresópolis affected by flow type mass movement in the State of Rio de Janeiro.

Restricted landslide disaster in Rio Branco do Sul, Paraná State, Brazil (2018)

A series of mass movements reached the city of Rio Branco do Sul with 32,500 inhabitants and 814 Km2. In this accident several small to medium size landslides occurred in the urban area of the municipality. The 15 observed landslides were triggered by heavy rainfall, which reached 29.49 millimeters in 20 minutes at its most intense period.

Damage to buildings and urban infrastructure was noted, such as the destruction of houses, streets and parts of the sanitation system. The largest movement reached 250m3 (Fig. 5) and destroyed houses and the street. In addition, collapses occurred in areas of karstic terrain, caused by hydrogeological changes related also to rapid and intense precipitation.

The rupture of the Brumadinho dam, Brazil (2019)

In recent years, Brazil has been hit by many situations of catastrophic rupture of dams with significant impact on the environment and hundreds of loss of life.

The last important situation was the break of the dam in the “Córrego do Feijão” iron mine, property of a Brazilian international mining company.

The dam break in a rotational slip process generated a gravitational flow of mass movement that destroyed the whole valley up to a distance of eight kilometers from the mine. This flow was responsible for the most terrible loss of life for dam-related disasters in the country's history, with 262 confirmed deaths and 41 missing people.

In this disaster situation, the CENACID team provided a quick overview of the disaster, including immediate mapping of the disaster area.

The “flow destructive capability map" (Fig. 10) as well as the “flow internal directions map" (Fig. 11) useful for search and rescue groups were urgently prepared and made available. These two are new types of useful disaster response maps proposed by the CENACID team.

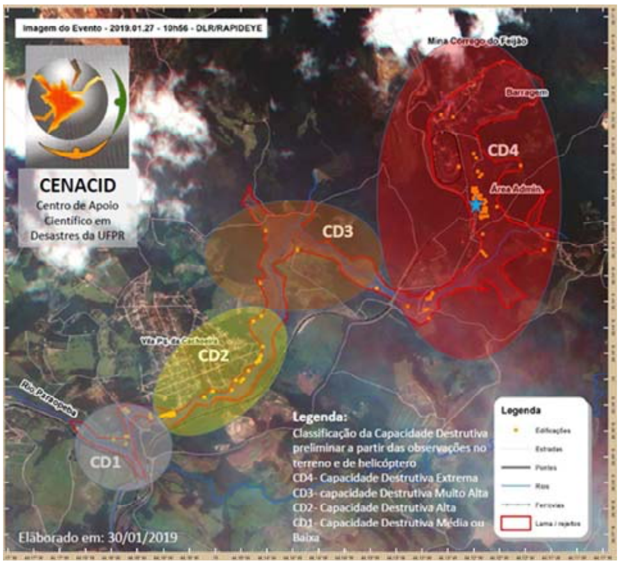

Figure 10 Map of destructive capability (CD) of the flow in the affected region - destructive capability increasing from grey to red color.

The team's typical approach is to try to provide the scientific support that could be most useful for each different situation, as in this case where specific maps were provided that assisted firefighters in the immediate response to the disaster.

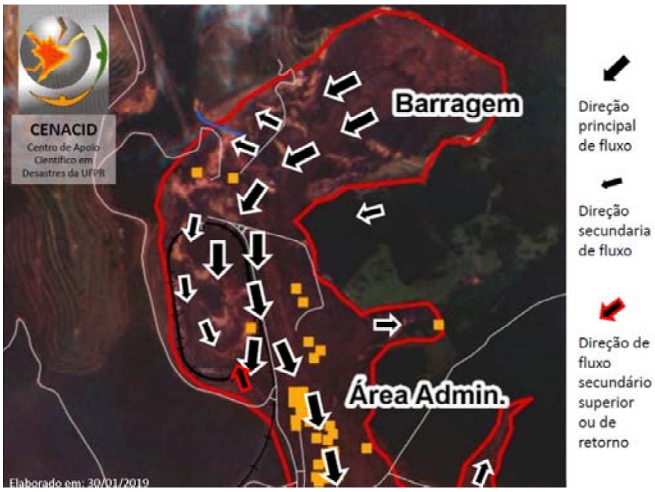

Figure 11 Map of flow internal directions providing information to search and rescue activities.

Also in the Brumadinho disaster, CENACID scientists conducted a rapid assessment of key environmental impacts and threats, including studies of sediment and associated contaminant flow along the Pirapó River basin.

Conclusions

In addition to being useful for landslide prevention, the CENACID group's experience in landslide-related disasters has demonstrated the importance of understanding landslide processes to facilitate disaster response and recovery.
It also demonstrated the importance of a trained scientific group to provide the necessary scientific support in the disaster response.

References

Lima, R. E. (2013) New Approach to Rapid Risk Evaluation in Disasters Related to Landslides. Landslide Science and Practice, Spatial Analysis and Modelling. Margotitini, C., Canuti, P. and Sassa, K. S. (eds) London. (ISBN: 97-3-642-31309-7).

CENACID-UFPR (2008). Relatório da Missão em 03/12/2008. CENACID-UFPR, Curitiba. 5p.

CENACID-UFPR (2008). Relatório da Missão em 04/12/2008. CENACID-UFPR, Curitiba. 2p.

CENACID-UFPR (2010). Informação Parcial de Atividades Haiti (19/02/10). CENACID-UFPR, Curitiba. 4p.

CENACID-UFPR (2018). Relatório 01 - Avaliação de áreas visitadas com deslizamentos e área com subsidência em região cárstica em Rio Branco do Sul – Paraná. CENACID-UFPR, Curitiba. 8p.

CENACID-UFPR (2019). Relatório 01 – Missão CENACID emergencial para apoio a resposta ao desastre relacionado ao rompimento da barragem de rejeitos da Mina Córrego do Feijão, pertencente a Cia. Vale do Rio Doce, no município de Brumadinho-MG. CENACID-UFPR, Curitiba. 32p.

A New Generation of Rigid Debris-resisting Barriers System in Hong Kong

Julian S.H. Kwan[(1)], Anthony L. Wong [(1)]

1) Geotechnical Engineering Office, Civil Engineering and Development Department, Government of the Hong Kong S.A.R., Email: anthonywong@cedd.gov.hk; Telephone: (+852) 2762 5360

Abstract Reinforced concrete rigid barriers are commonly used debris flow mitigation measures in Hong Kong. Under the threat of climate change, the chance of occurrence of more intense debris flow incidents becomes imminent. Recently, an initiative to revamp the design approach and to improve the robustness of the risk mitigation measures has been taken forward for addressing challenges of climate change. This calls for an optimisation of the design approach and an enhanced residual risk management. A series of technical development work has been conducted with an aim to establishing a displacement-based approach for assessment of stability of rigid barrier, and developing sensors for detection of debris flow impacts on the barriers by adopting novel Internet of Things (IoT) and sensing technologies. With the corroboration by large-scale physical experiments and analytical studies, the displacement-based approach is shown to be effective in optimising the design of barriers when it is compared with the conventional design approach involving limit equilibrium analysis. For debris impact detection, a reliable sensor has been developed and demonstrated capable of transmitting warning signals to designated mobile devices for the purposes of triggering timely emergency responses. The outcomes of the study would bring about advances in the design and practice of debris flow hazard mitigations.

Keywords Debris-resisting barrier; Debris flow; Displacement-based approach Climate change; Early Warning; Internet of Things

Introduction

Since 2010, Landslip Prevention and Mitigation Programme (LPMitP) has been launched in Hong Kong and is managed by the Geotechnical Engineering Office (GEO) to systematically tackle landslide risk associated with vulnerable natural hillsides with an aim to reducing the risk to an as low as reasonably practicable level. More than a hundred of rigid debris-resisting barriers have been constructed to safeguard assets and human settlements in their downstream areas (see Fig. 1).

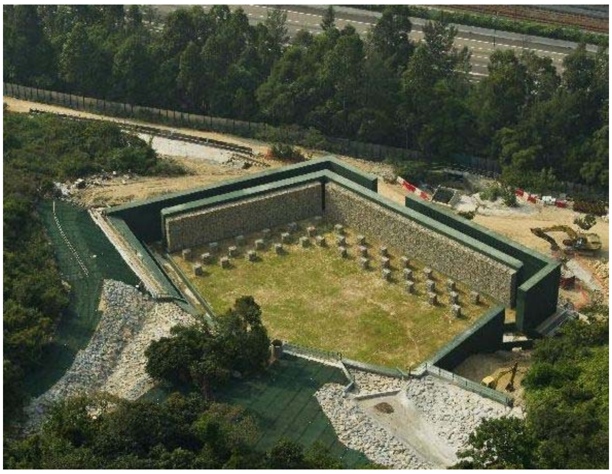

Figure 1 Rigid debris-resisting barrier constructed in Hong Kong

Under the impact of climate change, extreme rainfall events will become more frequent and intense. While landslides in Hong Kong are typically rain-induced, various studies showed that extreme rainfall could overwhelm the current slope safety system in Hong Kong (Ho et al. 2017). To cope with such unprecedented challenge, the practice of slope safety management in Hong Kong has evolved progressively. This paper introduces one of the recent technical advancements made by the GEO in respect of a new generation of rigid debris-resisting barrier system which addresses the formidable challenge of climate change. The salient features of this new system and the pertaining technical development work are presented, followed by a discussion of the overall improvement brought about.

Climate change in the context of slope safety in Hong Kong

Hong Kong has a mountainous topography and natural terrain covers 60% of its 1100 km² of the total land area. The natural terrain is typically mantled by weak saprolite or colluvium, which are susceptible to shallow landslides and small to medium-scale debris flows. According to the local landslide inventory, there would be one landslide per annum in every 2 km² of natural hillside on an average. With an insufficient supply of flat land, rapid urban development has been expanding closer to the hillsides and the landslide problem becomes particularly acute. To deal with natural terrain landslide risk, various risk mitigation measures have been constructed by the LPMitP to protect the public. Amongst these measures, rigid debris-resisting barrier made by reinforced concrete is a common option to mitigate sizeable debris flows.

In recent years, Hong Kong has been pummelled by climate change. The hourly rainfall record at the Hong Kong Observatory was broken several times in the past few decades, whereas it used to take several decades to break such record in the past. A comprehensive meteorological research has been conducted to study the probable climatic changes that will affect Hong Kong (EB 2015), and it indicates that extreme rainfall events will become more frequent and intense. While landslides in Hong Kong are typically rain-induced, various studies showed that extreme rainfall could result in an increased susceptibility and frequency of landslide initiation and an aggravation of mobility of landslide debris (Ho et al. 2017). Scale of landslides is envisaged to escalate as a result of the higher erosion power of more mobile debris. These factors could stretch the capacity of the rigid barriers and the landslide emergency system to their limit.

Features of new generation of rigid debris-resisting barrier system

In response to climate change, a holistic revamp of the practice of slope safety management has been initiated and a new generation of rigid debris-resisting barrier system has been developed. The design new barrier system will follow a novel design philosophy for assessment of the debris containment capability. This helps to produce optimised design of rigid debris-resisting barriers and devise rational design requirements of barriers to cope with the more intense debris flow events as a result of climate change. On the other hand, tailor-made instrumentations, which utilise smart technology to suit the specific conditions in Hong Kong, are to be installed in the new barrier system for the purpose of landslide detection. It can transmit warning signals to designated mobile devices for the purposes of triggering timely emergency responses in extreme landslides and improve the capability of residual landslide risk management. The new barrier system is developed based on the following two facets of technical development work, which will be elaborated in the coming sections: -

(1) Facet 1: novel design philosophy against boulder impacts scenarios for optimising the structural requirement of rigid barriers; and

(2) Facet 2: deployment of smart technology for immediate landslide detection for expediting emergency response.

Facet 1 - Novel design philosophy

General

Rigid barriers in Hong Kong are usually massive and take a quarter-size of a standard swimming pool (see Fig. 1). Mobilisation of construction materials uphill, extensive earthworks for site formation and construction of substantial foundations, e.g. tie-backs or mini-piles in remote hillside, which contribute to a high construction cost, poor constructability and various environmental concerns. Escalating the foundation requirements of rigid barrier is not a pragmatic mean to deal with the possibly larger scale and mobility of debris flows under the influence of climate change. Thus, a change in the design philosophy which could optimise the structural requirement of rigid barriers is needed (Kwan et al. 2017; Lam et al. 2018b; Law et al. 2019). The following technical development work has been carried out to (1) identify the potential areas of improvement in the current design practice, (2) establish analytical basis of a new design guidance, and (3) verify the robustness of the new design solutions.

Centrifuge test

In 2015, centrifuge modelling of debris containing boulder inclusions impacting on model rigid barriers was conducted, and impulsive force spikes of boulder impacts were observed (see Fig. 2). This is in great contrast to the more quasi-static nature of pure debris impact without boulder inclusions (Song et al. 2017). However, the prevailing design philosophy treats boulder impact as a constant pseudo-static force using conventional limit equilibrium principle (Kwan 2012).

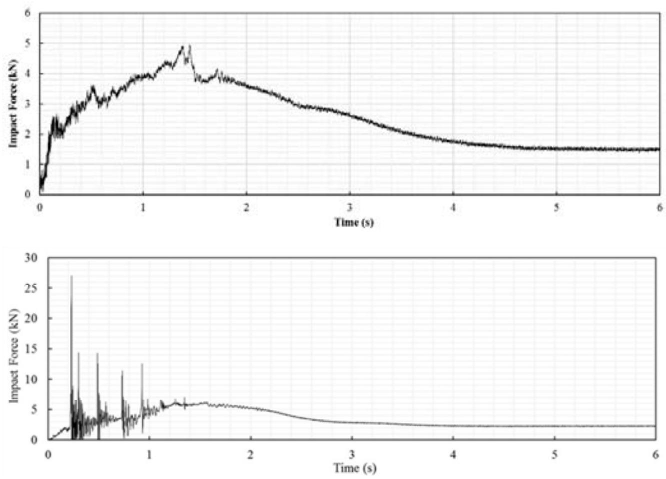

Figure 2 Time history of impact force of (a) pure debris matrix (top); and (b) debris with clastic boulders (bottom)

A review of literature was conducted and limit equilibrium analyses is a common design criteria for rigid barriers in many regions (ASI 2013; CAGHP 2018; MLR 2006; NILIM 2007; SWCB 2005; Vandine 1996). Limit equilibrium analyses work well in the conventional design of geotechnical structures, e.g. earth-retaining walls, which sustain primarily static loads. Application of conventional static design philosophy to rigid barriers to deal with momentary boulder impact is often the primary source of conservatism contributing to a bulky design of rigid barrier associated with extensive tie-backs.

Analytical study

In 2016, a novel displacement-based design philosophy, borrowed from concepts in earthquake engineering (Newmark 1965; Kramer 1996), has been proposed in view that boulder impacts are also impulsive and transient. Under this novel philosophy, if a limiting movement of rigid barrier is allowed under a boulder impact scenario, impact energy can be dissipated through work done against the movement of the barrier. This saves the need of providing extensive structural restraints for maintaining the barrier in static equilibrium.

An estimate of translational and rotational movement of the rigid barrier subject to boulder impact would be required and that, the conventional force-based philosophy of satisfying a minimum factor of safety against sliding and overturning would not be required. The geotechnical stability of the rigid barrier would be robust by limiting the estimated barrier displacement. By allowing energy dissipation through the movement of the barrier, it saves the need of providing extensive structural restraints (e.g. tie-backs or piled foundations) for maintaining the barrier in a static equilibrium condition. The formulations of displacement-based approach for the prediction of barrier's rotation and translation are given below, and the derivation and assumptions involved are detailed in Lam and Kwan (2016).

$$\Delta_{C.G.} = \frac{KE_0}{Mg} \times \frac{\kappa h}{r}\left(\frac{1+COR}{1+\kappa}\right)^2 \qquad [1]$$

$$\Delta = \frac{KE_0}{(Mg - uA)\tan\delta}\lambda\left(\frac{1+COR}{1+\lambda}\right)^2 \qquad [2]$$

where $\Delta_{C.G.}$ is rise of the barrier's centre of gravity due to rotation of barrier; Δ is translation of barrier; H is height of barrier; KE_0 is initial kinetic energy of boulder; M is mass of barrier; g is acceleration due to gravitation; r is distance between the axis of rotation and the point of impact; κ is I_θ/mhr (where I_θ is the mass moment of inertia of barrier); COR is coefficient of restitution of boulder and barrier after impact; λ is ratio of mass of barrier and boulder; u is uplift pressure of groundwater; A is contact area of groundwater and base of barrier; and δ is interface friction angle of barrier and ground.

Laboratory-scale impact tests

The formulae of displacement-based approach was rigorously derived. Notwithstanding this, two series of small-scale pendulum impact tests were carried out to verify this approach in collaboration with the University of Melbourne (see Fig. 3). Concrete barrier was constructed and was impacted by iron sphere under different impact velocities. The barrier's translational and rotational movements were measured using laser sensors. Yong et al. (2019) and Lam et al. (2018a) reported the test setup and measurement results. They found that the measured movements matched well with the predicted movements based on the analytical solutions.

Figure 3 Small-scale pendulum impact tests for verification of new design philosophy

Large-scale impact tests

The verification of displacement-based approach was progressed towards boulder impact scenarios with a higher impact energy and a series of flume tests were conducted. The flume was developed by the Hong Kong University of Science and Technology and is in total 28 m long, 2 m wide and 1 m deep (see Fig. 4). To simulate a realistic boulder-barrier interaction, an L-shaped reinforced concrete model rigid barrier weighing about 5 tonnes was constructed at the deposition zone. The model barrier was founded on a layer of compacted granitic fill materials and was set free to slide and rotate during the impact process.

Five impact tests involving different impact scenarios (i.e. different number and size of boulders) were carried out. The displacement of the barrier (both transient and permanent) was measured using the laser sensors installed behind the model barrier. High speed camera was installed to capture the impact process and to estimate the impact velocity of the boulders when approaching the model barrier (See Fig. 5).

To verify the displacement-based approach, the measured movement of the model barrier was compared with that predicted using the analytical equations. The results demonstrated that the extent of sliding and rotational movements of barrier predicted by the displacement-based approach is generally conservative (see Tab. 1).

Figure 4 Flume test facility for verification of new design philosophy

Figure 5 Snapshot of a flume test for verification of new design philosophy

Table 1 Results of flume tests

Test No.	Quantity and Size of Boulders	Observed Impact Velocity (m/s)	Measured Sliding Movement (mm)	Predicted Sliding Movement (mm)
K1	1 no. of 200 mm boulder	7.0	< 0.1	0.1
K2	10 nos. of 200 mm boulders	7.0	< 0.5	< 0.5
K3	10 nos. of 400 mm boulders	8.0	2.0 - 2.9	4.0 - 6.3

Further study using numerical analyses

To address scale-dependent problem of physical tests, three-dimensional finite-element analyses were conducted using the commercially available computer package LS-DYNA. Yong et al. (2019) validated a set of numerical inputs which are suitable for the analysis of geotechnical stability of rigid barrier. Making use of similar numerical approach, scaled-up numerical analyses were conducted. Snapshots of two analyses are shown below.

The rotational and translational movement of the model barrier have been obtained from LS-DYNA simulation and compared with that predicted using displacement-based approach (see Fig. 6). More numerical analyses are given in Yong et al. (2019) and Lam et al. (2018a).

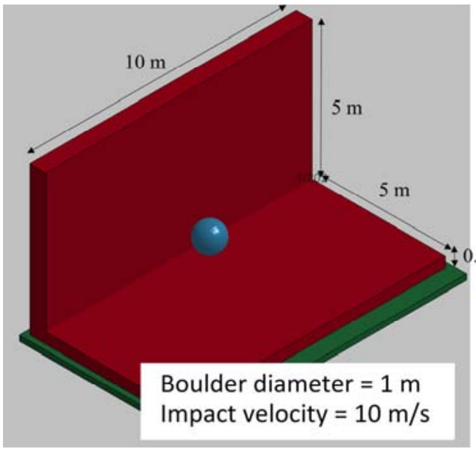

Model LS1

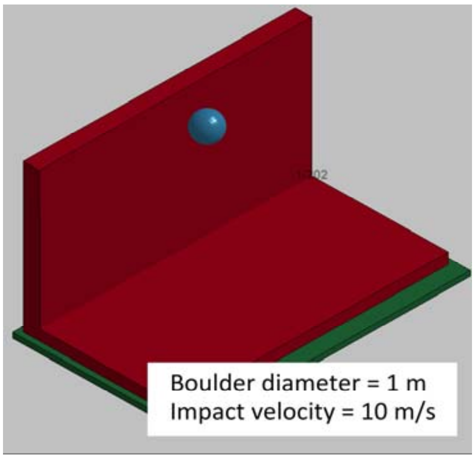

Model LS2

Model No.	Movement Obtained from LS-DYNA Simulation	Predicted Movement Based on Displacement-based Approach
LS1	Sliding of 1.3 mm	Sliding of 1.4 mm
LS2	Rotation of 0.02°	Rotation of 0.09°

Figure 6 Numerical Model LS1 (Top) and LS2 (Bottom) for verification of new design philosophy

Development of Smart Barrier System

General

Rigid barriers are capable of retaining landslide debris with a designated volume. In case of exceptionally massive or recurrent landslides triggered by extreme rainfall scenarios (see Fig. 7) which exceed the designated volume, the barriers may be overwhelmed and overflow of debris to the downstream may occur. In addition, there have been cases that barriers had intercepted landslide debris in the field without being noticed for quite some time after the landslides had occurred, due to their inaccessibility and obstructed visibility. To facilitate timely emergency responses to the above situations, a Smart Barrier System has been developed to provide alerts to the government agencies and relevant stakeholders when landslide debris impacting onto a barrier is detected. This system has been tailor-made to suit the local conditions of natural hillsides in Hong Kong.

Figure 7 Multiple landslides occurred in Lantau, Hong Kong in 2008

Design consideration

The development of this Smart Barrier System needs to overcome two key challenges: -

(1) The system is exposed to hot, humid and vegetated outdoor environment in Hong Kong without any power supply. It is therefore designed to be robust against adverse outdoor environment, nominal power consumption and sustainable by harvesting solar energy alone.

(2)The wireless communication among the IoT devices and with the cloud platform is not stable at remote and heavily vegetated sites, especially in rainy weathers. The communication module of the Smart Barrier System has to be optimised for exceptional efficiency and redundancy.

Prior to the development of Smart Barrier System, a search of landslide detection systems which are commercially available was conducted. These systems can be classified according to their position of installation. They can either be installed to monitor initiation of landslide at source area (e.g. inclinometer, acoustic signal detector), or to detect moving debris along debris trail or at the location of mitigation measures (e.g. geophones, trip wires). For those installed at the source area, soil movement is normally monitored. While landslides in Hong Kong normally involve brittle failure and the soil movement at the incipient of landslides is abrupt, detection of soil movement could not give adequate response time. On the other hand, source areas and trails of debris flows are located in remote hillside with no proper access. Maintenance of instruments is practically difficult. In view of this, landslide detection systems installed at the deposition zone of debris and the landslide risk mitigation measures are considered more effective. As regard the mechanism of landslide detection, monitoring of seismic wave (e.g. geophones) could sometimes give false alarm. The use of acoustic detector requires specific understanding of relationship between acoustic wave and soil movement, which could be cumbersome if these detectors are put in various geological or hydrogeological conditions. Besides, the use of off-the-shelf components for building an instrumentation system could be fraught with difficulty in terms of high power consumption (due to limited customisation), especially at remote and outdoor locations in Hong Kong. As no electricity supply and landline connection are available in those remote areas, the power supply by solar power panels is often not adequate to support the off-the-shelf instrumentation. Moreover, the lack of integrated hardware and software protection in the off-the-shelf instrumentation could result in costly repair and maintenance work.

With these considerations, a Smart Barrier System has been tailor-made and developed based on the following criteria:
(a) Robust and reliable in outdoor environment;
(b) Low power consumption; and
(c) Low maintenance requirement.

System architecture

The Smart Barrier System was developed with a simple system architecture targeting at timely detection of landslides instead of sophisticated measurements of the dynamics of landslide impacts. The components of the system are grouped into four categories, viz. the debris impact detection modules, the signal transmission system, the monitoring instrumentation and the power supply system (see Fig. 8). Real-time landslide detection is realised through deployment of an array of wireless impact switches mounted on the barrier. Real-time data or images recorded by the monitoring instrumentation, including tailor-made laser depth gauges (for debris flow thickness measurement) and digital cameras (for capturing photographic images), can be viewed through the mobile application to take cognisance of the field situations. These inter-connected IoT instruments are linked to a cloud-based Information Technology platform with native mobile application, which facilitates timely and informed emergency responses by the emergency responders.

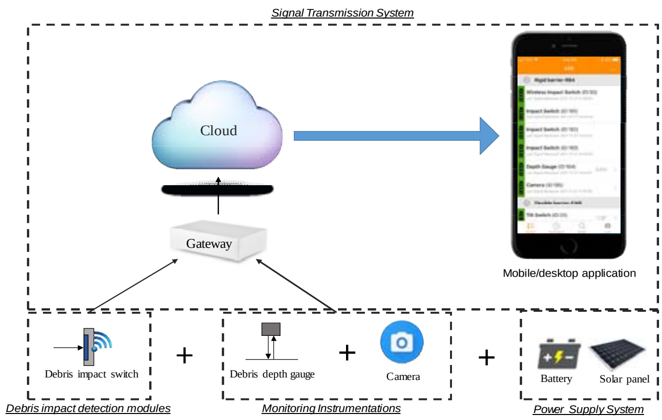

Figure 8 System architecture of Smart Barrier System

Alert trigger mechanism and operation

The debris impact switch is housed in a 300 mm by 450 mm box. The box is installed at the back of the barrier wall stem. When the front face of the box is subject to a physical hit, two wired metal plates in the impact switch, originally set uncontacted, will be pressed together, completing an electric circuit to give a signal of landslide debris impact. In addition to the impact switch, the debris depth gauge installed at the crest of the rigid barrier monitors the debris depth behind the barrier. It is programmed to make a measurement every five hours. If the depth gauge measures a depth exceeding certain threshold, it will trigger an alert signal. When there is an alert signal either sent by the debris impact switch or the debris depth sensor, the system will command the digital camera to capture a photographic image of the barrier retention zone, and the frequency of depth measurement will increase. The alert, depth data and photographic images are transmitted to desktop/mobile devices via a 4G mobile network. Officers can remote control the digital camera to capture additional images via the desktop/mobile application.

Besides, in order to facilitate monitoring of the survivability of the prototype Smart Barrier System, a special feature is incorporated in the system. The system is configured to transmit its battery power level to the mobile/desktop devices at regular interval. This kind of "heartbeat" signals together with the continual feedback from the monitoring devices (i.e. the debris depth gauges) allow us to monitor the condition of the system and the need for maintenance.

Implementation of Smart Barrier System

Flume test

The performance of Smart Barrier System was tested using the flume facility as discussed in Section 4.5. Debris impact switches were installed on the model barrier to receive strike from debris materials (see Fig. 9). Debris mix was designed to mimic the characteristics of local debris flow materials. A series of flume tests were conducted which successfully demonstrated the capability of the system.

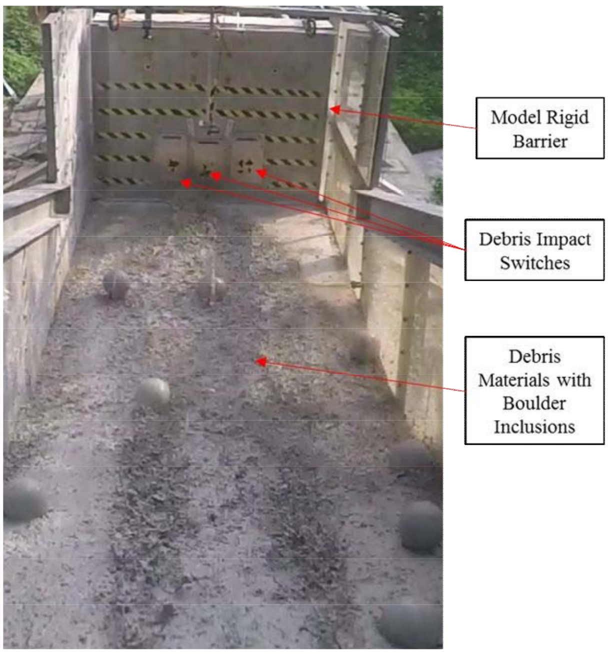

Figure 9 Debris flow flume test for examining the performance of Smart Barrier System

Trial field installation

The Smart Barrier System has been installed at a number of rigid barriers in Hong Kong for in-situ testing and proof-of-concept purposes (see Fig. 10). As the system has been exposed to outdoor environment subject to true weather conditions, the durability of the system can also be tested.

Figure 10 Trial field installation of Smart Barrier System

Case study - pilot landslide emergency plan for a local hospital

This section presents a case of practical deployment of Smart Barrier System. In order to deal with potential debris flows which could affect a local hospital, rigid barrier was constructed in its uphill. In view that massive landslide could occur and overflow the rigid barrier, Smart Barrier System has been deployed at the barrier to improve the emergency preparedness of the hospital (see Fig. 11).

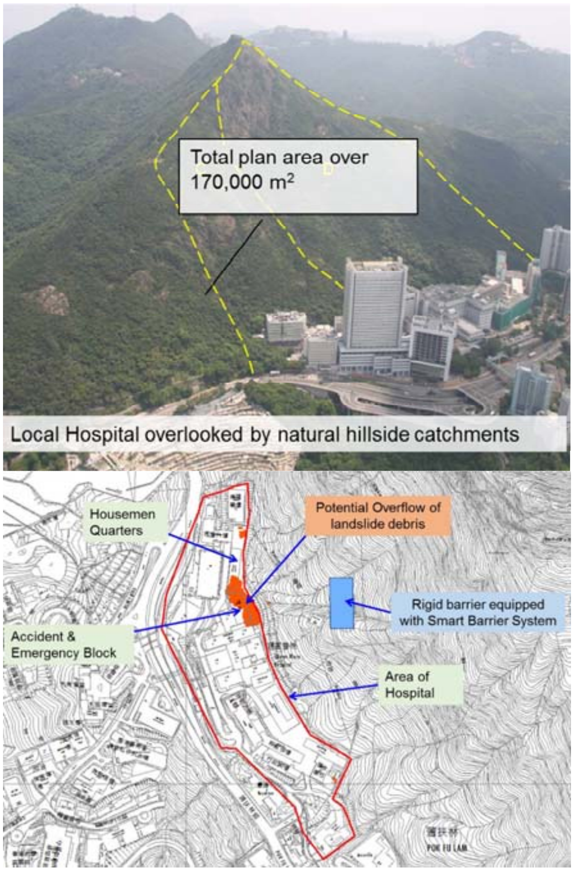

Figure 11 Practical deployment of Smart Barrier System in a local hospital

A landslide emergency handbook was formulated through series of liaisons with the stakeholders in the hospital and a concise workflow was incorporated for the frontline staffs of the hospital and the GEO. Also, the GEO has been planning an emergency drill with a view to enhancing the emergency preparedness of different stakeholders.

Overall improvement brought by the new system

Using the novel design philosophy (i.e. Facet 1), in gist, there would be a reduction of the earthwork required for site formation, less consumption of construction materials, and a dispensable need of structural restraints i.e. soil nails and pile foundation. An example of such enhancement is shown in Fig. 12. In this example, reductions of construction cost from about HK$10M ($1.3M USD) to about HK$5M ($0.6M USD), and construction time from about 20 months to about 12 months are envisaged. In addition to a significant reduction in construction cost and time, the new system brings about intangible benefits of improved constructability and minimisation of adverse impacts to the natural environment.

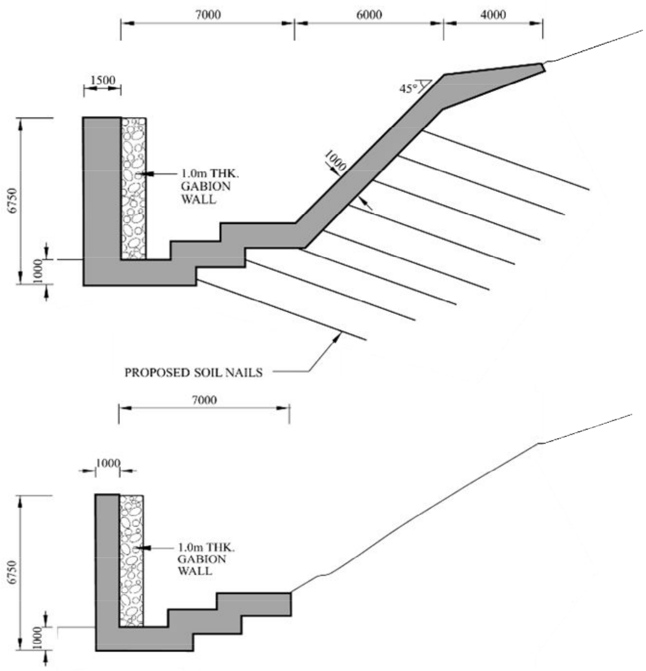

Figure 12 Comparison of design of rigid barrier based on (a) the prevailing design philosophy (top); and (b) the new design philosophy (bottom)

With the deployment of new Smart Barrier System (i.e. Facet 2), swift emergency response can be provided, which elevates the overall capability of residual landslide risk management.

Summary

The new rigid debris-resisting barrier system has been developed by integrating two technical development work. It is developed to address the geo-hazard of natural terrain landslides under the impact of climate change. With the novel design philosophy for rigid barriers, barriers of optimised design requirements can be constructed to accommodate a larger magnitude of landslide. The use of tailor-made early warning with smart technology could improve emergency preparedness. All in all, the new barrier system enhances the community's resilience against the impacts of climate change.

Acknowledgement

This paper is published with the permission of the Head of the Geotechnical Engineering Office and the Director of Civil Engineering and Development, the Government of the Hong Kong Special Administrative Region.

References

ASI (2013) ONR 24801 Protection Works for Torrent Control - Static and Dynamic Actions on Structures. Austrian Standard Institute, Austria.

CAGHP (2018) Specification of Design for Debris Flow Prevention (T/CAGHP 021-2018). China Association of Geological Hazard Prevention, 55 p. (in Chinese)

EB (2015) Hong Kong Climate Change Report 2015. Environmental Bureau, HKSAR Government, 21 p.

Ho K K S, Lacasse S, Picarelli L, (2017) Preparedness for Climate Change Impact on Slope Safety. Slope Safety Preparedness for Impact of Climate Change, ed. by K Ho, S Lacasse, Picarelli L, CRC Press, 1-42.

Kramer S L, (1996) Geotechnical Earthquake. Engineering. Prentice Hall, 653 p.

Kwan J S H, (2012) Supplementary Technical Guidance on Design of Rigid Debris-resisting Barriers (GEO Report No. 270). Geotechnical Engineering Office, Hong Kong, 88 p.

Kwan J S H , Lam H W K, Wong L A, Sze E H Y, (2017) Advances in Design of Debris-resisting Barriers in Hong Kong. THE HKIE-IEM-CIE Tripartite Seminar 2017 - Geotechnical Engineering Solutions for Natural Disaster Mitigation.

Lam C, Kwan J S H, (2016) Displacement-based Assessment of Boulder Impacts on Rigid Debris-resisting Barriers - A Pilot Study (Technical Note No. TN 9/2016). Geotechnical Engineering Office, Hong Kong, 66 p.

Lam C, Yong A C Y, Kwan J S H, Lam N T K, (2018a) Overturning stability of L-shaped rigid barriers subjected to rockfall impacts. Landslides, 15(7): 1347-1357.

Lam N T K, Yong A C Y, Perera J S, Kwan J S H, Lam H W K, Wong L A, (2018b) Flexural Response of Reinforced Concrete Barriers subject to Boulder Impact. Second JTC1 Workshop - Triggering and Propagation of Rapid Flow-like Landslides, The Second Joint Technical Committee on Natural Slopes and Landslides (JTC1) of Federation of International Geo-engineering Societies.

Law R P H, Sze E H Y, Wong L A, (2019) Revolution of Rigid Landslide Debris-resisting Barrier for Strengthening Resilience against Climate Change. (The HKIE Innovation Awards for Young Members 2019, Entry of Grand Prize for Category II - An Innovative Application of Engineering Theories).

MLR (2006) Specification of Geological Investigation for Debris Flow Stabilization. DZ/T 0220-2006, National Land Resources Department, China, 32 p (in Chinese).

Newmark N M, (1965) Effects of earthquakes on dams and embankments. Géotechnique, vol. 15, pp 139-159.

NILIM (2007) Manual of Technical Standard for Designing Sabo Facilities against Debris Flow and Driftwood. Technical Note of NILIM No. 365, Natural Institute for Land and Infrastructure Management, Ministry of Land, Infrastructure and Transport, Japan, pp 73 (in Japanese).

Song D, Ng C W W, Choi C E, Zhou G G D, Kwan J S H, Koo R C H, (2017) Influence of debris flow solid fraction on rigid barrier impact. Canadian Geotechnical Journal, 54(10):1421–1434.

SWCB (2005) Manual of Soil and Water Conservation. Soil and Water Conservation Bureau, Taiwan, 692 p (in Chinese).

VanDine D F, (1996) Debris Flow Control Structures for Forest Engineering. Ministry of Forests, British Columbia, Canada, 68 p.

Yong A C Y, Lam C, Lam N T K, Perera J S, (2019) Analytical Solution for Estimating Sliding Displacement of Rigid Barriers Subjected to Boulder Impact. Journal of Engineering Mechanics, 2019, 145(3): 04019006.

Historical review of catastrophic events caused by landslides and debris flows in Colombia from 1987 to 2017

Guillermo Ávila[1], Juan Rojas[2]

1) Universidad Nacional de Colombia, Department of Civil and Agricultural Engineering, Bogotá, email: geavila@unal.edu.co

2) Universidad Nacional de Colombia, Department of Civil and Agricultural Engineering, Bogotá, email: jusrojassu@unal.edu.co

Abstract Today is possible to have landslide inventories and much information is available; however the analysis of such information is not always exhaustive and may be lost among too many data. This research seeks to compile and analyse information from official landslide databases in Colombia, but complemented with other sources as technical reports and newspapers reports about landslides or debris flows in a 31 years window, causing at list 10 or more death persons. The results show that the most critical year was 1994 with the Páez debris flow triggered by an earthquake, that caused 128 death and 429 missing fallowed by 1987 Villa Tina Landslide with more than 500 people death and more than 2400 affected people and by 2017 Mocoa debris flow that caused 338 deaths.

Most of the events were associated to intense rain periods produced by La Niña episodes. The most critical months in terms of number of events were April and December and the most affected district was the Antioquia Department. The single event that most victims caused was the Villa Tina.

Keywords Landslide inventory, debris flow, damage, fatalities.

Introduction

Landslides and debris flows periodically affect the Andean region of Colombia, where most of the people live. The moderate or intermediate impact landslides are normally related to the rainy seasons and despite they do not bring too much attention, in conjunction, they produce important economic or environmental impacts and in certain cases they also cause some deaths and injuries to people, instead catastrophic landslides and debris flows are less frequent but individually they produce severe impacts in terms of greater number of fatalities and injuries, significant economic or environmental losses, interruption of normal social activities, etc. and for those reasons they mobilize enormous national and international resources and attract the attention of the public opinion.

The analysis of severe catastrophic events permits to identify the major deficiencies but also the positive actions in the national risk management process. In order to evaluate the impact of extraordinary events occurred during the last 31 years, a systematic review of natural hazard events databases, official reports, technical articles and newspapers reports was carried out and the information was processed to identify aspects as temporal and spatial variability of large impact events and main causes and effects.

Previous works related to landslide inventories and analysis of consequences in Colombia have been developed by Montero et al (1985) for the Colombian road network; The OSSO Corporation Colombia in association to La Red and UNISDR since 1994 developed an international database of disasters effects called DesInventar (OSSO et al, 2019); Ojeda and Donnelly (2006) analysed the impact of landslides in towns and cities of Colombia; the World Bank (Banco Mundial, 2012) complied the occurrence and effects of different type of natural hazards, including landslides from 1970 to 2011 and made an analysis of the general risk management. The Colombian Geological Service (Servicio Geológico Colombiano, SGC, 2017) with the collaboration of many universities in the country, actualized the geological and geomorphological information and developed a landslide susceptibility and hazard map at a scale of 1: 100.000 and they also developed the Mass Movement Information System (SIMMA), an open access official landslides database. Sepúlveda and Petley (2015) present analysis of landslides in Colombia from a regional perspective in Latin America and Rojas (2018) made an initial compilation and analysis of catastrophic events based on aforementioned sources.

General characteristics of the study area

Most of the main cities in Colombia are located in the Andean region, conformed by tree cordilleras that extend from southwest to northeast. The cordilleras are controlled by a complex geological fault system that has been generated by the interaction between the

Caribbean Plate, the Nazca Plate and the South America Plate. The Central Cordillera is the oldest (cretaceous) and the highest of the tree (5750 m over sea level), it is geologically the most complex, conformed by Tertiary continental sediments, Cretaceous volcanic sequences and Palaeozoic schists (Ojeda and Donnelly, 2006). The Eastern Cordillera is predominantly conformed by Cretaceous sedimentary rocks, but also there are present metamorphic and granitic rocks, covered by more recent by glaciofluvial and colluvial deposits (Montero, 2003). In the Western Cordillera appear interbedded sequences of sedimentary and igneous rocks (Ojeda and Donnelly, 2006).

The geological faults pattern is characterized by a predominant direction NNE that controls the tree mountain ranges orientation. Between the Central and the Western Cordillera is present the Cauca-Romeral fault complex and between Central and Eastern Cordillera is located the Magdalena fault complex. Within the Central Cordillera is located the Palestina fault and in the eastern side of the Eastern Cordillera is located the Frontal Eastern Cordillera fault. A secondary fault pattern is also present in the central and northern parts of the country with prevalent direction NNW. The main secondary orientation faults are Bucaramanga-Santa Marta fault and Oca fault. In Fig. 1 are indicated the main geological faults superimposed on the landslide hazard map 1:100.000 elaborated by de Colombian Geological Service (Servicio Geológico Colombiano, 2017).

An independent orographic peripheral system is the Sierra Nevada de Santa Marta, located in the Caribbean coast which reaches a height of 5775 m over sea level (the highest elevation place in Colombia). Precambrian igneous and metamorphic rocks appear in this area, cover in many places by sedimentary rocks. The region is mainly inhabited by indigenous communities with low population density and most of the stability problems are associated to intensive erosion with not catastrophic events reported.

Catastrophic events classification and sources of information

According to Colombian legislation "Natural catastrophes are those changes in the physical environment, identifiable in time and space, that produce massive and indiscriminate damage to the population and that collectively affect a community, such as earthquakes, tsunamis, volcanic eruptions, floods, landslides and debris flows." (Decree No 3990 of 2007, Ministry of Social Protection). In the frame of the cited decree, when a given event is declared by the authorities as "catastrophic", special attention is given in terms of rapid flow of economic and logistic help to attend the emergency situation.

In the context of the present article, catastrophic events are only related to landslides and debris flows occurred between 1987 and 2017 and in order to have a more simple and general way to identify those events from the available information we consider catastrophic events as those that caused 10 or more human fatalities.

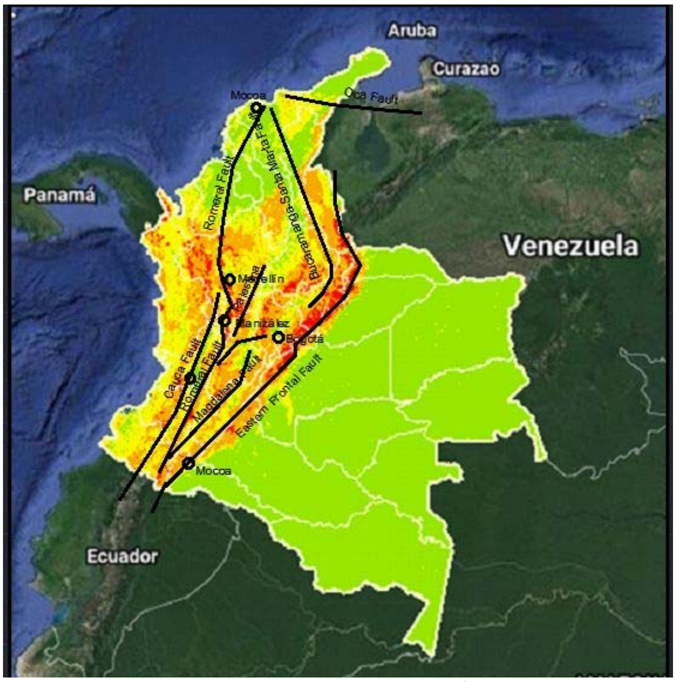

Figure 1 Main geological faults in Colombia (locazation on the ladslide hazard map (1:100.000) developed by the colombian Geológical Service)

Catastrophic landslide events were consulted from the Landslide Information System (SIMMA) that is the official landslide database, developed and administrated by the Colombian Geological Service. SIMMA has tree modules: Consult module, Load and Edition Module and Reception of Information Module. The Consulting Module permits to consult by location (municipality or department) and by type of landslide. The reported information is the location (geographic coordinates), the date of the event and the date of the report, geographic references as rivers, roads, etc., and the effects of the event in terms of number of death and missed people, number of affected people and number of affected houses. It also permits to observe the location in the landslide hazard map at scale 1:100.000 and, when available, shows information about details of the landslide as description of the event, type of event (landslide, debris flow, etc.) and sub type of event (rotational, translational, etc.), type of material, type of deposit, soil moisture condition, activity, volume of displaced material, type of cover material, possible causes, secondary effects, schematic representation, pictures or videos. This technological platform is very important for the systematic organization of the information; however during the research it was observed that not all the information is complete and unique, for what a deep depuration is required.

A second source of information was DesInventar (OSSO-Colombia, La Red, UNISDR, 2019), that since 1994 compiles, from official agencies and from newspaper reports, the small, medium and large impacts of natural events in nine Latin American Countries, including Colombia. This source is important in terms of information about the effects but the main drawback is that geographic coordinates are not always available and for that reason the localization of the events is only approximated to the nearest town. A third source of information was the Consolidated National Emergencies Report, elaborated by the National Disaster Risk Management Unit (UNGRD) that consolidates annual information since 1998, however this source is mainly oriented to register the annual economic investments in disaster prevention and it is not exhaustive in technical descriptions of the events. Although the tree mentioned information repositories should have the same information they are not integrated and in many cases there are important discrepancies that make difficult the analysis of information and for that reason it was necessary to contrast with official technical reports, technical papers, newspapers and internet reports, trying to obtain the most reliable data.

1985 Armero debris flow as reference catastrophic event

The most catastrophic natural event that has ever affected Colombia is the Nevado del Ruiz debris flow (November 13, 1985), caused by a minor eruption of El Ruiz volcano, located in the Central Cordillera, that melted about 10% of the glacial cap (Mojica et al, 1985) and subsequently produced an immense debris flow that totally cover the municipality of Armero, killing more than 22.000 people and causing injuries to more than 5.000 people. Locally this event is better known as Armero debris flow. According to Shuster et al (2002), the economic loses were about $212 million (1985 US Dollars).

Although the information about the probable eruption of el Ruiz Volcano was available before the event and there was also a volcano hazard map (that had well defined possible debris flow zones) the evacuation decisions were not taken in a timely manner, for that reason, this major event meant an inflection point in the Colombian risk management because, by one side, authorities and people realized about the very strong consequences that a natural event may produce and by the other side, the disaster revelled the importance of the scientific investigation in earth sciences, the necessity of a strong organizational risk management agency and the importance of an opportune, clear and persuasive communication of the risk situations to the exposed communities.

Types and temporal distribution of catastrophic events

The total number of events (catastrophic and non-catastrophic) from 1987 to 2017 reported in the SIMMA inventory is 6307 of which 4198 correspond to landslides (67 %), 972 correspond to flows (15%), considering in this category debris flows, earthflows, mudflows and debris avalanches, and 1137 correspond to rock falls (18%), as shown in Figure 2.

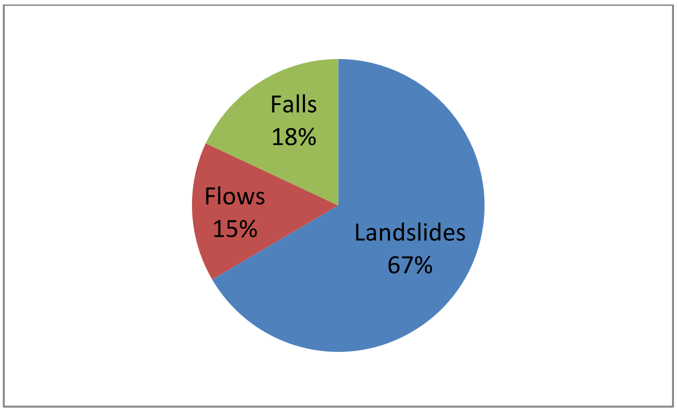

Figure 2 Percentage of catastrophic events from 1987 to 2017, according to the type o event.

The number of deaths plus missing persons in the same period was 2579, giving a mean value of 83 victims per year, which is higher than the value of 59 reported by Ojeda and Donnely (2006) for the period 1993 to 2004. Total number of grouped events each year, including catastrophic and non-catastropic, is shown in Fig. 3, together with the associated victims (deaths plus missing). From 1987 to 2001 the number of events is relatively low, varying from 7 to 65, but since 2002, the number of events tended to increase. The higher number of events occurred from 2005 to 2015 with a pick value of 868 events in 2013. This strong increase in the number of events may be partially associated to a better and more systematic registration of events from 2005 and partially to extreme rainy years during that period.

During the same time interval, there were 37 catastrophic events (according to the classification of 10 or more fatal victims), which represent only the 0,6 % of the total events, with a mean value of 1,2 catastrophic events per year. However, the number of deaths plus missing people caused for those 37 events was 2432, representing the 94% of the total. This reflects the very high impact of catastrophic events in loss of life.

The most critical events during the evaluation period occurred in 1987 (Villatina landslide, 500 deaths), in 1994 (Páez debris flow triggered by an earthquake, 128 death, and 429 missing) and 2017 (Mocoa debris flow, 338 deaths).

Most of the landslides and debris flows are associated to rain events. Colombia is located in the Intertropical Convergence Zone and this condition implies that very frequent and intense rains occur. There are typically two rainy seasons: one in April-May and the other in October-November, showing peak values in June and October. Normal conditions are strongly altered by Southern Oscilation Index (SOI), especially by La Niña episodes (SOI greater than +7) that induce exceptional rainfalls. The mean annual rainfall for the

Andes is around 1500 mm but in the exterior slopes is about 4000 mm and in the Pacific coast may reach up to 6000 mm (Rodriguez, 2006).

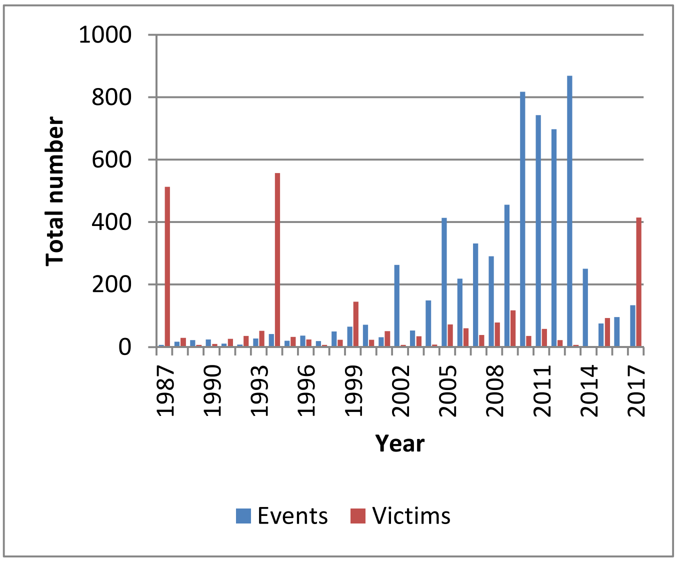

Figure 3. Total number of events and victims (deaths plus missing) from catastrophic and non-catastrophic landslides, debris flows and rock falls, from 1987 to 2017.

The distribution of number of events per year is shown in Figure 4. During the 31 years of evaluation in 18 years one event occurred, in 8 years zero events and the most critical year in number of catastrophic events was 2011, coincident with a very intense La Niña Event.

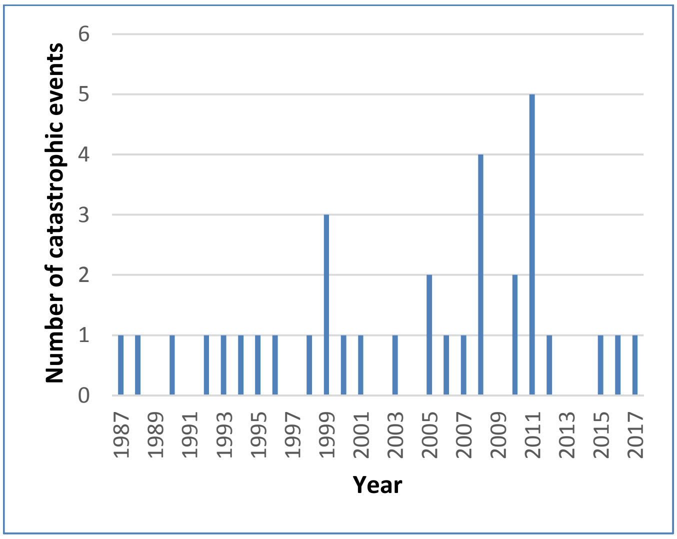

Figure 4 Number of catastrophic events each year from 1987 to 2017.

The monthly distribution of catastrophic events is shown in Figure 5. Most of the events have occurred in April- May and in October-December and therefore they are clearly associated to the predominant bimodal rain conditions.

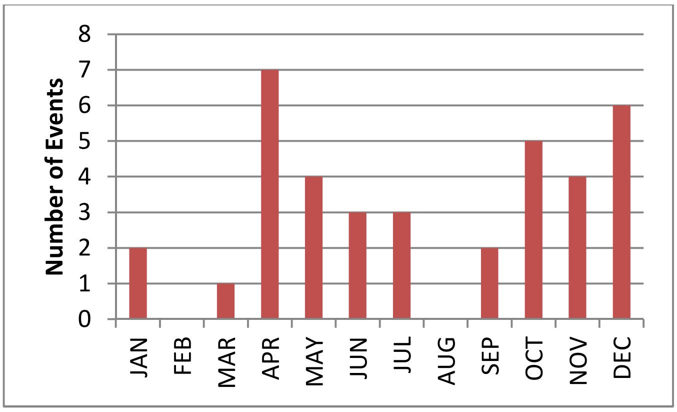

Figure 5 Monthly distribution of catastrophic events from 1987 to 2017.

Spatial distribution of catastrophic landslide events

The location of events in the Colombian map is shown in Fig. 6 where the three main events (Villa Tina, Páez and Mocoa) are highlighted.

Figure 5 Spatial distribution of catastrophic events in Colombia from 1997 to 2017.

70% of the events were presented in the Central Cordillera, 24% in the Eastern Cordillera and only 6% in the Western Cordillera, as shown in Figure 6. Politically and administratively Colombia is divided in 32 departments. The department with greater number of events was Antioquia (40%), followed by Caldas (16%), Cauca (11%) and Nariño (8%) as is illustrated in Figure 7.

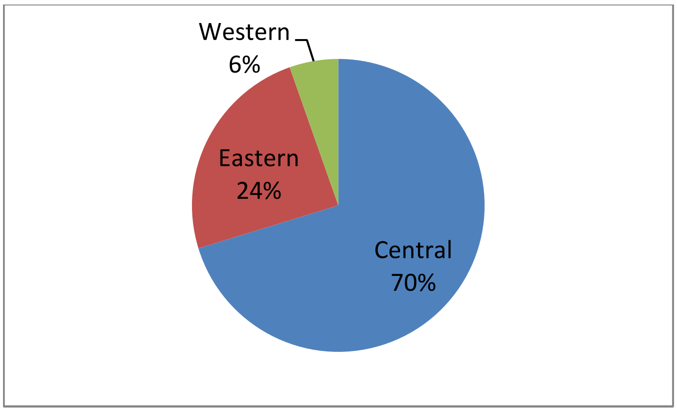

Figure 6 Percentage distribution of catastrophic events in the tree mountain ranges of Colombia.

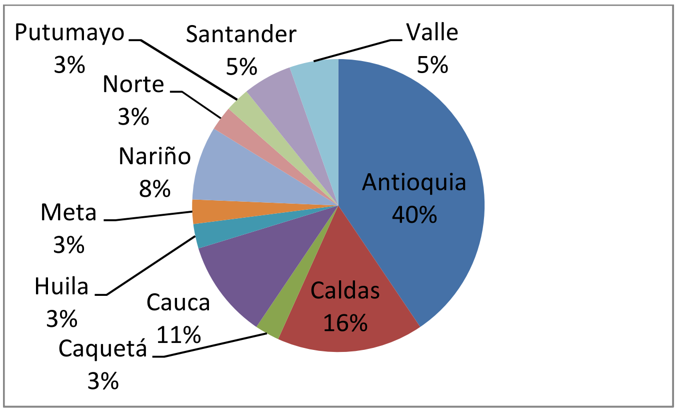

Figure 7 Distribution of catastrophic events in Colombian departments.

Characteristics of the most impacting catastrophic events

The list of catastrophic events is shown in Tab. 1 and a brief description of the most critical events (those causing more than 50 deaths) is presented below:

Villatina Landslide (September 27, 1987). This landslide occurred in the city of Medellín (Antioquia) in the neighbourhood of Villatina. It is one of the most catastrophic events produced by a single and relatively small landslide of about 40.000 m^3 of residual soil (Ojeda & Velasquez, 1996), because it caused 500 deaths, affected a further 1300 and destroyed 120 houses (Ojeda & Velasquez, 1996, Ojeda and Donnelly, 2006; SGC, 2019; UNGRD, 2019). The families were of very low income and most of the houses were informal constructions. The event occurred at 2:40 PM on a Sunday day. It was a translational landslide on residual soil followed by a very fast debris flow that did not permit people to evacuate. Even though there had been no rainfall many days before the event, the infiltration of water in the soil from a water-supply pond located in the upper part of the slope was the main cause of the landslide (Shuster et al, 2002).

Páez debris flow (June 6, 1994). As a consequence of an earthquake of magnitude 6.4 (Monday 3:47 PM), more than 3000 single and low deep translational landslides were triggered in a very steep slopes of the Cauca department (Ávila et al, 1996) and rapidly they fell into the Páez and other tributary rivers and formed a very large debris flow that swept several homes located on the bank of the rivers. The final number of deaths and missing is not clear but most of them were indigenous people of the Páez community. Cardona (1995) stated that 128 people died, 429 were missed and 207 were injured. 1664 houses were totally destroyed and 3160 affected (by the combination effects of the earthquake, landslides and debris flows).

Filadelfia Landslide (Nov 22, 2001). This event of rock fall and landslide occurred in an old abandoned gold mine in the municipality of Filadelfia (Caldas department) at 5:45 AM. At that moment about 26 persons that were looking for gold were buried by the fallen material. Immediately the other miners came to help but a second rock fall also buried them (El Tiempo, 2002). A total of 51 persons died, 32 were injured and 14 were missing (UNGRD, 2001). The old mine had been declared as unsafe previously but many low income people with little mining experience continued working informally, trying to find few grams of gold. The rain that fell the previous days detonated the instability.

Bello debris flow (Dec 5, 2010). This event occurred at 2:45 PM in the municipality of Bello (Antioquia) a city very close to Medellín in a neighbourhood known as La Gabriela. It was classified as a complex landslide–debris flow that occurred in sequence, after weeks of heavy rains (Aristizabal, 2010). The estimated mobilized volume was 50.000 m^3. The flow caused 85 deaths and 40 buried houses. As in the case of Villatina landslide, previously described, in the area lived poor people in precarious and informal houses, located very close to the mountainside and coincidentally in both events the day was Sunday and the hour of occurrence were almost the same, when many people were in family reunions.

Salgar debris flow (May 18, 2015). The event occurred at 2:48 AM due to heavy rains during the two previous days that produced a torrential flow at La Liboria creek, in Antioquia department, causing 78 deaths, 40 injured, 30 missing, 31 houses and two bridges destroyed and more than 1000 people affected (Servicio Geológico Colombiano, 2019). All the affected people lived very close to the riverbed and previous events of lower magnitude had occurred there causing moderate affectations.

Mocoa debris flow (Apr 1, 2017). The city of Mocoa is the capital of the Putumayo department. During the night of March 31th and in the early morning of April 1th, after prolonged and intense rain three rivers overflowed and many landslides were generated in the upper part of the basins, producing a very large torrential flow that cover part of the urban area as shown in Figure 8. According to the data reported by the Disaster Risk Management Unit, the flow caused 332 deaths, 398 injured and 77 missing people. The number of destroyed houses is not reported but the number of affected houses was 1.200. This event was very impacting in Colombia and important resources have been invested in recovery and in detail hazard studies in the affected area, particularly one developed by the Colombian Geological Service at scale 1:5000 (SGC, 2018).

Figure 8 Aerial photo of Mocoa in the zone affected by the torrential flow (El Tiempo, 2019. Picture from: Presidencia de la República).

Conclusions

Landslide risk management is a process of continues learning from foreign, but specially, from own experiences in different types of events. Catastrophic landslide and debris flows events are of particular interest because they generate significant direct impacts in terms of loss of life, injured, missing, loss of housing, damage in infrastructure and important social and economic losses. Catastrophic events attract the attention of national and international community and leave a special mark on the prevention and management processes.

During the period 1987-2017 the number of reported catastrophic and non-catastrophic events was 6307 and the total number of deaths was 2579. During the same period, a total of 37 catastrophic events (with 10 or more fatal victims) occurred in Colombia, which represents only the 0,6% of the total number of events, however, the number of deaths plus missing as a consequence of those catastrophic events was 2432, corresponding to the 94% of the total, proportion that reflects the impact of few but severe events. The mean value of catastrophic events per year was 1,2 and the mean value of deaths plus missing due to catastrophic events was 83 persons per year.

Most of the events occurred in the periods April-May and October-December, showing a clear association to bimodal rain conditions. 70% of the catastrophic events occurred in the Central Cordillera, 24% in the Eastern Cordillera and 6% in the Western Cordillera. The most affected department was Antioquia with the 40% of the events, followed by Caldas, Cauca and Nariño with 16%, 11% and 8% respectively. The five most critical events were: 1987 Villatina Landslide (500 deaths); 1994 Páez debris flow (128 deaths and 429 missing); 2001 Filadelfia landslide (51 deaths and 14 missing); 2010 Bello debris flow (85 deaths); 2015 Salgar debris flow (78 deaths, 30 missing) and Mocoa debris flow (337 deaths and 77 missing).

Although the risk management institutions in Colombia have achieved significant advances since 1985 Armero debris flow that caused more than 22.000 deaths, catastrophic events continue to occur periodically, affecting in most of the cases, the poorest people that, for economic reasons, are forced to locate themselves in highly vulnerable sectors. It is then important to recall the very well-known relationship between poverty and catastrophic events and the necessity of more economic investments, effective regulations and real controls in the land occupation, according to the results of hazard zonation studies, because in many cases hazard maps are available but evacuation and relocation programs have been very difficult to implement and is not easy to relocate people without offering them similar housing conditions in safer places.

Most of the described catastrophic events could have been avoided or at least their impact could have been reduced with the aid of efficient early warnings, and for that reason, special focus in the risk management process must be place on reducing risk conditions in critical areas by minimizing exposure and implementing efficient early warning systems.

The official landslide information system developed by the Colombian Geological Service (SIMMA) is a very important tool to systematically capture and keep the relevant information of landslides in Colombia, however it requires some additional work to complete and depurate information. Additionally it is recommended to have in this information system a final, unique and official data of landslide effects, because actually there is significant variability in the available information.

Table 1 Number of events per year with 10 or more fatal victims of landslides or debris flows from 1987 to 2017.

Event No	LOCATION	Type	Date (dd/mm/yyyy)	Deaths plus missing
1	VILLATINA	LANDSLIDE	29/09/1987	500
2	TARAZÁ	LANDSLIDE	01/07/1988	20
3	VILLAVICEN	LANDSLIDE	04/12/1990	10
4	TURBO	FLOW	19/01/1992	35
5	DABEIBA	FLOW	24/12/1993	45
6	PÁEZ	FLOW	06/06/1994	557
7	FREDONIA	LANDSLIDE	22/07/1995	23
8	BARBOSA	LANDSLIDE	08/07/1996	11
9	TOLEDO	LANDSLIDE	30/09/1996	11
10	ANORÍ	LANDSLIDE	21/01/1998	12
11	INZÁ	FLOW	09/04/1999	15
12	FLORENCIA	FLOW	04/10/1999	18
13	ARGELIA	LANDSLIDE	14/04/1999	41
14	CONTADERO	LANDSLIDE	21/05/2000	12
15	FILADELFIA	LANDSLIDE	22/11/2001	65
16	MANIZALES	LANDSLIDE	04/12/2003	16
17	CISNEROS	LANDSLIDE	05/06/2005	15
18	BELLO	FLOW	06/10/2005	40
19	MANIZALES	FLOW	18/03/2006	11
20	BUENAVENTURA	FLOW	12/04/2006	36
21	SUÁREZ	ROCK FALL	13/10/2007	24
22	SARDINATA	FLOW	24/06/2008	10
23	MEDELLÍN	LANDSLIDE	16/11/2008	12
24	MIRANDA	LANDSLIDE	26/11/2008	12
25	MEDELLÍN	LANDSLIDE	31/05/2008	27
26	LA CRUZ	LANDSLIDE	23/12/2010	13
27	LA GABRIELA	LANDSLIDE	05/12/2010	150
28	SAN VICENTE DE CHUCURÍ	FLOW	18/05/2011	12
29	FLORIAN	LANDSLIDE	15/04/2011	11
30	LA CRUZ	LANDSLIDE	12/12/2011	15
31	MANIZALES	LANDSLIDE	13/04/2011	20
32	MANIZALES	LANDSLIDE	05/11/2011	68
33	ISNOS	FLOW	06/10/2012	15
34	SALGAR	FLOW	18/05/2015	108
35	COPACABANA	LANDSLIDE	26/10/2016	16
36	MANIZALES	LANDSLIDE	18/04/2017	17
37	MOCOA	FLOW	01/04/2017	409
			TOTAL	2432

References

Aristizabal, E. (2010). Rainfall induced landslides in Colombia. http://rainfallandslidescolombia.blogspot.com/2011/01/la-gabriela-debris-flow.html [Last accessed: 25/07/2019].

Ávila G, Caro P, Cepeda H, Moreno M, Torres P and Agudelo A (1995). Zonificación para el uso del suelo en la cuenca del río Páez. In: Memorias 8th Jornadas Geotécnicas. Bogotá. Sociedad Colombiana de geotecnia, V.1 . p. 6.79-6.103.

Banco Mundial (2012). Análisis de la gestión de riesgo de desastres en Colombia: un aporte para la construcción de políticas públicas. http://documents.worldbank.org/curated/en/671321468026993367/pdf/701030ESW0P1290ESTI0N0DEL0RIESGOweb.pdf. [Last accessed: 25/06/2019].

Cardona O.D. (1995). El sismo del 6 de junio de 1994. Desastres y sociedad No4/ año 3. Especial: el desastre y la reconstrucción del Páez. 19-32. In: http://www.desenredando.org/public/revistas/dys/rdys04/dys4-1.0-nov-7-2001-ESPECIAL.pdf. [Last accessed: 5/08/2019].

El Tiempo (2002). Juicio por tragedia minera. https://www.eltiempo.com/archivo/documento/MAM-1370656. [Last accessed: 16/08/2019].

El Tiempo (2019). A dos años de la tragedia, así va la reconstrucción en Mocoa. https://www.eltiempo.com/colombia/otras-ciudades/asi-esta-mocoa-despues-de-dos-anos-de-tragedia-343996. [Last accessed: 05/09/2019].

Martinez J.M, Ávila G, Agudelo A, Shuster R. L., Casadevall T.J. and Skott K.M. (1995). Landslides and debris flows triggered by the 6 June 1994 Paez Earthquake, southwestern Colombia. Landslide News. no. 9, p. 13-15.

Montero J. (2007). Deslizamiento y flujo de tierra Villatina, Medellín, Antioquia, Colombia. Movimientos en masa en la región andina: una guía para la evaluación de amenazas. Servicio de Geología y Minería. Publicación geológica multinacional No 4. pp 262-268.

Montero J, Beltrán L and Cortés R. (1988). Inventario de deslizamientos en la red vial colombiana. Ing. Inv., Issue 17, p. 16-27, 1988. ISSN 2248-8723. Print ISSN 0120-5609.

Montero J and Ojeda J. (2005). Slopes instability in Colombia. Proc.of the International Conference on Landslide Risk Management. Balkema Publishers (Hungr, Fell, Couture & Eberhardt Editors). Vancouver, Canada. Supplementary Volume.

Mojica J, Colmenares F, Villarroel C, Macía C and Moreno M. (1985). Características del flujo de lodo ocurrido el 13 de noviembre de 1985 en al valle de Armero (Tolima, Colombia): historia y comentario de los flujos de 1595 y 1845. Geología Colombiana. Vol 14. 107-140.

Ojeda J and Donnelly L. (2006). Landslides in Colombia and their impact in towns and cities. The Geological Society of London. IAEG. Paper number 112. pp. 1-13.

OSSO-Colombia, La Red, UNISDR. (2019). Sistema de Inventario de Desastres, DesInventar . https://www.desinventar.org/es/. [Last accessed: 05/07/2019].

Rodriguez C. (2006). Earthquake-induced landslides in Colombia. Proc. Geohazards. Engineering Conferences International. http://dc.engcon ntl.org/geohazards/38. [Last accessed: 05/08/2019].

Rojas J. (2018). Eventos catastróficos por deslizamientos y avenidas torrenciales en Colombia. Trabajo de grado en Ingeniería Civil. Universidad Nacional de Colombia. Bogotá.

Sepúlveda S. A. and Petley, D.N. (2015). Regional trends and controlling factors of fatal landslides in Latin America and the Caribbean. Nat. Hazards Earth Syst. Cci. 15, 1821-1833, 2015.

https://www.researchgate.net/publication/307675184_Regional_trends_and_controlling_factors_of_fatal_landslides_in_Latin_America_and_the_Caribbean. [Last accessed: 10/08/2019].

Serna, C. (2011). La naturaleza social de los desastres asociados a inundaciones y deslizamientos en Medellín (1930-1990). Historia Crítica. No 43 Bogotá. Jan/Apr. 2011. http://www.scielo.org.co/scielo.php?script=sci_arttext&pid=S0121-16172011000100011. [Last accessed:25/07/2019].

Servicio Geológico Colombiano (2017). Las amenazas por movimientos en masa en Colombia. Una visión a escala 1:100.000. Imprenta nacional (eds). Bogotá. (ISBN 978-958-99528-8-7). 399p.

Servicio Geológico Colombiano (2018). Evaluación de amenaza por movimientos en masa en el área urbana, periurbana y de expansión del municipio de Mocoa-Putumayo a escala 1:5.000. . Internal Report. 229 pp.

Servicio Geológico Colombiano (2019). Sistema de Información de Movimientos en Masa, SIMMA. http://simma.sgc.gov.co/. [Last accessed: 01/08/2019].

Shuster R, Salcedo D and Valenzuela L (2002). Overview of catastrophic landslides of South America in the twentieth century. In: Catastrophic landslides: effects, occurrence, and mechanisms. Reviews in engineering Geology. Volume XV. Edited by Stephen G. Evans and Jerome V.DeGraff. The Geological Society of America. 411 p.

UNGRD (2019). Annual emergency report. Internal report from Nationl Desaster Risk Management Unit -UNGRD.

Different types of mass movements in the environment of active coal mining (four case studies from Czech Republic)

Jan Burda[1], Martin Veselý[1,2]

1) Brown Coal Research Institute, Dept. of Geotechnics and Hydrogeology, Most, Tř. Budovatelů 2830/3, Czech Republic, e-mail: burda@vuhu.cz

2) Charles University in Prague, Faulty of Science, Department of Physical Geography and Geoecology, Albertov 6, 128 43 Praha 2, Czech Republic

Abstract With the extend of 1100 km², the Most Basin is the largest coal basin within the Czech Republic. Numerous types of mass movements initiated by both natural as well as human triggers occurred during last century within an extensive anthropogenic relief of Most basin. Several types of local mass movements are presented in the form of four case studies. Three of them focused on different types of human triggered slope deformations (from large deep-seated to shallow high-risk landslide) in a geologically different areas (from steep mine slopes to old consolidated dumps). The last case study describes large rockslide/rock avalanche of Pleistocene/Holocene age. Massive debris accumulation of this fossil mass movement was discovered and well described as a result of open-pit mining in the half of 20th century.

Keywords Landslides, Mass movements, Opet-pit mine, Dump, Czech Republic

Introduction

Most Basin in the northwest part of the Czech Republic includes regions with a long tradition of brown coal mining. At the beginning of the second half of the 20th century, lignite mining was conducted in large open-pit mines. In many cases, this mining takes place in specific geological and geomorphic settings. The deepest open-pit mines reach dept over 200 m and from excavated overburden silty clays numerous internal as well as external dumps were created. These dumps form 100 m high (in extreme cases over 200 m) anthropogenic slopes always with complicated stability.

Many authors (Kalvoda et al., 1990, 1994; Rybář and Novotný, 2005; Rybář 2006; Burda 2010; Burda and Vilímek, 2010) point out that the stability of this anthropogenic slope is complicated by slope steepness, geological and geomorphic settings, as well as climatic factors.

Four different landslide case studies from the environment of the Most Basin is presented in this paper (Burda et al., 2011 and 2013, Burda et al., 2018a, Burda et al., 2018b). The paper gives a brief overview of different types mass movements occurred in this region and also describes its morphology and triggers.

Study site

The study area is situated along the boundary between the Krušné hory Mountains and the Most Basin (coal basin) at the foot of a southeasterly facing slope near the northern margin of an open-cast mine (Škvor 1975; Malkovský 1985). The Krušné hory Mts. and the Most Basin present the main geological and geomorphological units (Balatka and Kalvoda 2006). The Krušné hory Mountains comprise orthogneisses and various crystalline rocks, while the Most Basin comprises various Cenozoic sediments dominated by Miocene claystones, a coal seam, sands, and clastic rocks.

The Most Basin (Fig. 1B), has a graben structure (Váně 1985) and genetically belongs to the tectonic system of the Eger Graben (Domácí 1977). The basin sediments span the time interval from the Oligocene to Miocene (Fig. 3). These sediments belong stratigraphically to the Paleogene-age Střezov Formation and dominantly to the Neogene-age Most Formation (Domácí 1977; Grygar and Mach 2013, Mach et al., 2017). In general, the crystalline basement is covered by various heterogeneous sediments of the lower Miocene clays, sands, and sandstones as well as denudational relict material of the Upper Cretaceous and weathered volcanic rocks—phonolite, basalt, and tuff. These Paleogene sediments pass into Miocene coal sedimentation indistinctly. The boundary between the coal seam and the Miocene clay complex is sharp, and these sediments comprise a group of clays and sandy-clays with variable carbonate occurrence. The average fill of this overlying complex can be up to approximately 175 m thick with a maximum thickness of 231 m (Malkovský 1985). Upper 20–40 m of the lacustrine silty clays is represented by soft clays; deeper parts represent stiff-fissured and stiff clays.

The Quaternary sediments predominately comprise coarse-grained gravels, sandy gravels, and clays with crystalline fragments. The thickness of sediments varies from 0.1m to 40 m, with the greatest thicknesses found to be associated with the alluvial fans of former tributaries flowing down from the Krušné hory Mountains. These alluvial fans contain mainly coarse-grained gravel, sands, loams, and crystalline fragments.

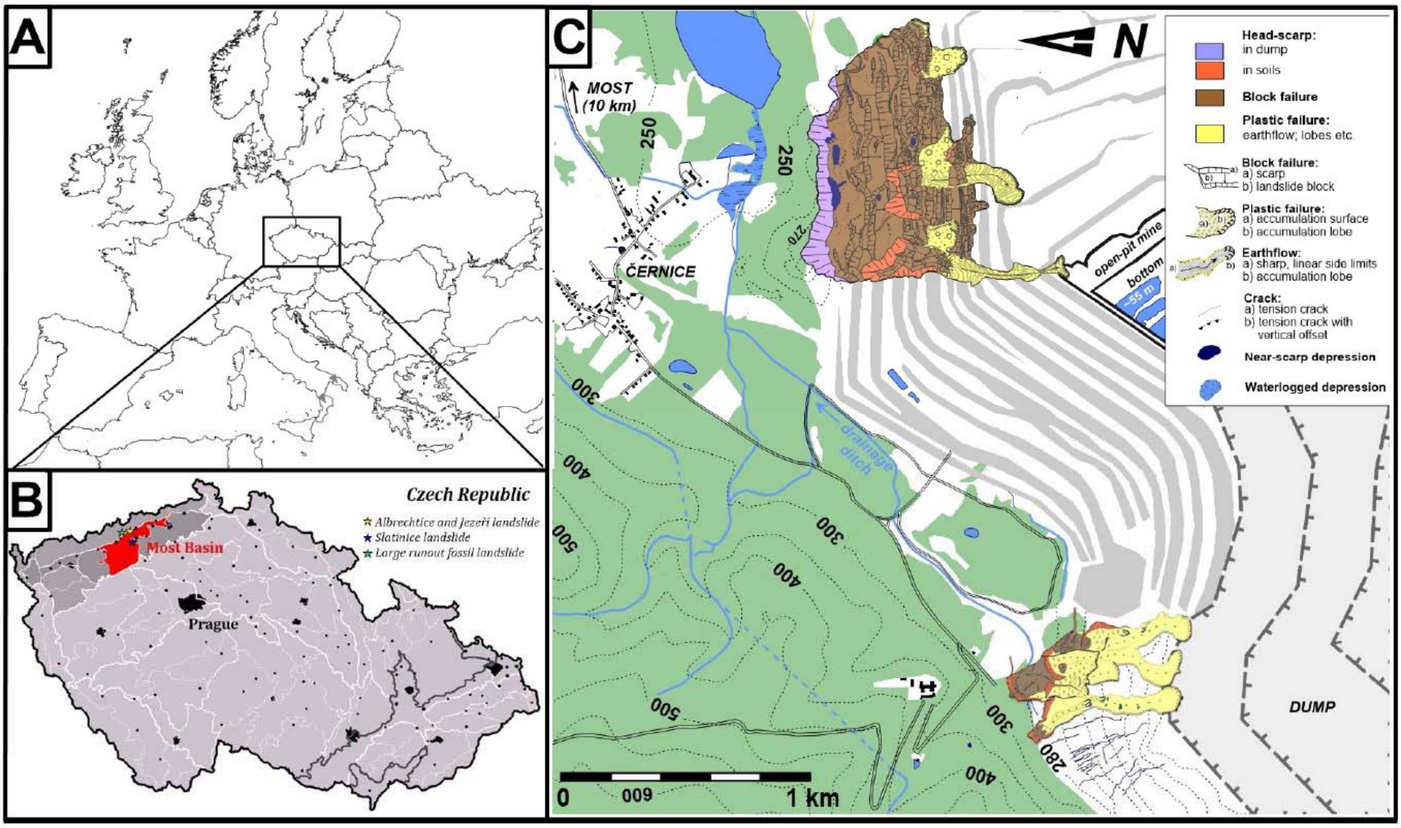

Figure 1 General position of the study site (**A, B**). A geomorphological sketch map of Albrechtice landslide case study (upper part) and Jezeří landslide case study (lower part)(**C**).

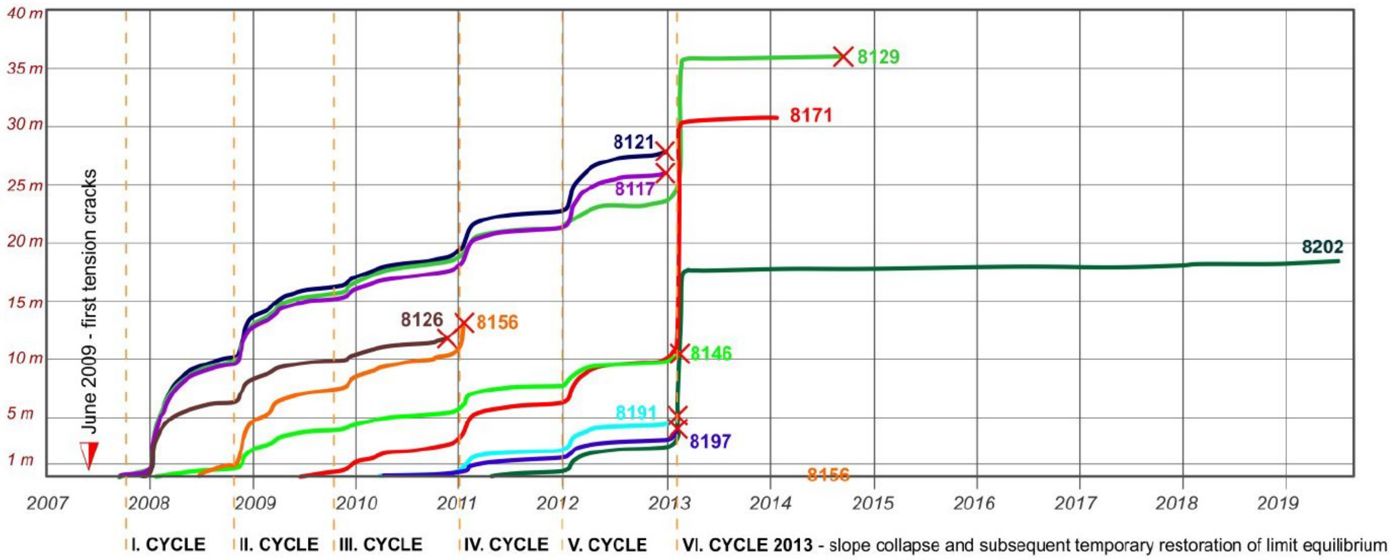

Figure 2 Monitored cumulative displacements (2007 – 2019). From the chart is evident cyclical landslide progression in the 2008 – 2013 period and temporary slope stabilization after the 2013 slope collapse.

Krušné hory Mts. consist of crystalline complexes consolidated during the Cadomian orogeny and the mantle of Lower Paleozoic rocks weakly metamorphosed during Variscan metamorphism. The study site is made up of a portion of the Kateřinohorská klenba Vault (Kalvoda et al. 1990; Vilímek 1995)—a flat anticline structure oriented in a west-east direction. The core of this vault consists of orthogenesis and metagranites, which are adjacent to a series of crystalline shales. Longitudinal and transverse faults are applied with the prevailing directions of 60°, 296°, 332°, and 700 (Král 1968; Kopecký 1989), and the foliation surface is fan like with an inclination of 50° to 70° (Marek 1983).

Case study: Albrechtice - large deep-seated landslide

The Albrechtice dump was based on untreated and dewatered original terrain. Quaternary sediments in the area under the dump are formed by very well permeable gravels of relatively large thickness. Aggregation of quaternary soils through the hopper partially reduced the flow of shallow groundwater and extensive wetlands gradually formed on the feeding side of the hopper.

The Albrechtice dump was founded by the Z50 stacker from 1954 to 1961. Part of the Albrechtice dump had to be mined again in the 1980s due to the development of new surface mining. The original area of the dump 176 ha was reduced to 43 ha and the dump volume of 31.5 million m^3 was reduced to 18.5 million m^3.

Since 2008, an evolution of a large complex landslide has been monitored and several cycles of landslide movement activity was described. The landslide is bound to an active mine slope and for miner, mining technology as well as for mining operations and coal production it has a character of serious natural hazard.

A brief overview of material and methods

The main deformation features were mapped continuously form 2011 to 2014 at a scale of 1 : 5000 using GPS.

A geodetic network of reflective prisms was placed in the study site in 2007. This could, therefore, have been used in the continuous monitoring of the nearby opencast mine (Bláha et al., 2006). This monitoring is undertaken with the Leica TCR 2003A total station and an automatic target recognition (ATR) system (Brown et al., 2007). The ATR system automatically monitors the position of all the reflective prisms at an interval of one hour. The reflective prisms are placed on 3.5m long standing pipes cemented to a depth of 2 m.

Landslide description

The landslide initially manifested itself in the emergence and opening of the tensile crack in June 2007. The first acceleration phase of the landslide, the displacement of unbearable soils by geostatic pressure of the overhung dump, was monitored from the end of September and October 2007.

The soft clays of the overlying strata, unloaded by the mining process, were the source of extensive soil deformations, leading to a initial slope failure affecting lope from the top part of the Albrechtice dump to a height of 195 m asl. (Fig. 5).

Landslide evolution

The development of mass movements in the area has been showing cyclical progressivity. Until 2015, there were 6 movement cycles, which always showed an acceleration phase during which the landslide showed decimetre movements (Fig. 2). This was followed by the main movement activity during which the landslide was moving in meters. Subsequently, there was always a temporary restoration of limit equilibrium, which resulted in stagnation or complete stabilization of the landslide movements.

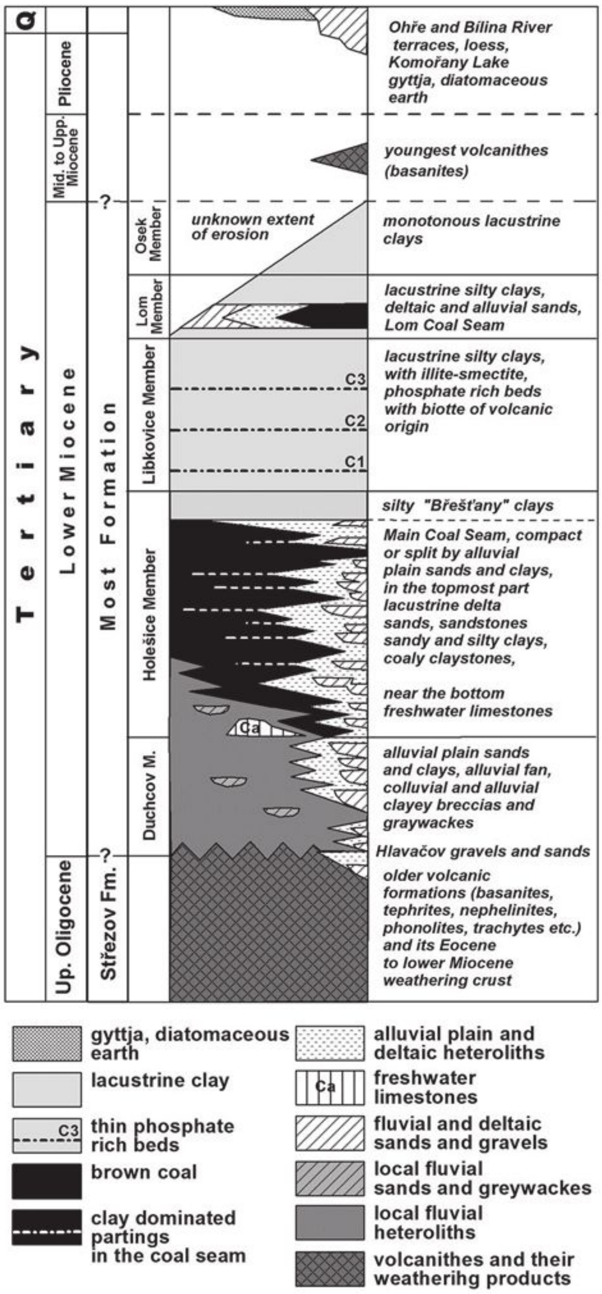

Figure 3 Stratigraphy of the Most Basin sedimentary fill (Mach et al., 2017).

During 2011, landslides occurred also below the horizon 190 m asl. During the fourth movement cycle pressure folds were documented in the slope on horizons 175-193 m asl. The extrusion was directly documented by a point lift of up to 100 mm. Except for the first movement cycle, which began in June 2007, the annual periodicity was obvious for all subsequent movement cycles; beginning of each cycle always linked to the winter period of the year (November-January), while the movement stagnation occurred always in the summer months.

Figure 4 An aerial view on the Albrechtice landslide. I the left site is remarkable up 10 m high head scarp. In the middle stabilization ground works and original landslide relief (head scarps, earthflows, tension cracks, etc.) in the lower part of the slope (foto: Burda, June 2015).

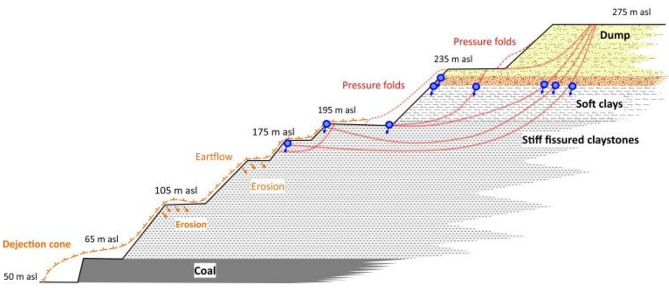

Figure 5 An idealised geotechnical cross-section across the Albrechtice landslide.

The primary cause of stability problems was the shaping of a high overburden slope with a small distance between its crest and toe as the coal seam was gradually exposed and the lowest overburden cuts. In the following years, the landslide movement was always accelerated due to climatic factors, which acted as a decisive trigger.

The evolution of the movements between 2007 and 2012 led to the development of a large complex landslide (Dikau, 2004) with difficult terrain morphology, a series of partial landslides, block landslides, earthflows and mudflows (Fig. 4). These earthflows present a serious complication for coal mining itself because their accumulation toes cover coal seam and thus its excavation is technologically more difficult, more expensive and primarily more risky.

The area affected by the landslide was calculated to be approximately 57.7 ha and the total volume of moving soils was up to 5-10 mill. m^3 (Burda et al., 2018a). Shear planes were bound to the upper soft clays (ca 227 – 190 m asl.) of the Miocene claystones additionally loaded by the consolidating masses of the Albrechtice dump, but reached even greater depths of stiff-fissured claystones under 190 m asl. (Figure 5 and 6).

Figure 6 Head scarp in stiff-fissured clays under 190 m asl. (foto: Burda, January 2013).

The long-term landslide evolution subsequently led to the collapse of the entire slope that occurred during the 6th cycle of progression in 2013. Since the landslide movement was extraordinary even for local conditions (up to 20 m), it is evident that there was a significant redistribution of the main stresses resulting in temporary restoration of the limit equilibrium. This claim was later confirmed by the overall trend of landslide movements in 2014 and 2018. After the end of the landslide movements in March 2013, there were no measurable landslide movements, this long-term trend demonstrates the overall stagnation of movement activity.

Case study: Jezeří - active earthflow

In January 2011, the area experienced a reactivation of the landslide, which can be related to failure of the Quaternary sediments. This recent failure represented one of the largest flow-like landslides of the Czech Republic (Klimeš et al., 2009) and occurred outside the active portion of the ČSA mine, with the landslide material reaching the bottom of the open-pit coal mine (Burda et al., 2013). Such reactivation was triggered by a rising water table induced by rapid snowmelt during a period of winter warming.
This landslide, its movement mechanism as well as FEM analysis, were well-desrcibed by Burda et al. (2011), Burda et al. (2013) and Vanneschi et al. (2018).

Historical and geological background

The January 2011 landslide (Fig. 7) represents the reactivation of a large complex slope deformation that has been recorded previously (Špůrek 1974; Rybář 1997). The original 1950s slope deformation occurred as a result of surface subsidence due to the collapse of galleries in older (active in 1940 - 1977) underground mine (Špůrek 1974). This deformed the entire mass of overlying rocks and, at least in part, contributed to the development of deep-seated fault planes. These subsidence induced fault planes enable water from the permanent and intermittent aquifers to infiltrate more easily into the underlying claystones and to thereby become a significant mechanical discontinuity surface.

Figure 7 An aerial overview of the landslide complex situated at the edge of the open-pit mine (foto: Burda, January 2011).

The recent headscarp and eastern extension of the reactivated landslide follow the headscarp of the earlier slope deformation from 1952. This slope deformation originally formed as a result of mining for brown coal in the Most Basin. The deep mining began at the beginning of the 20th century. It first created depressions in the overlying sedimentary layers which finally resulted in a catastrophic collapse during a landslide event that began in 1952 (Rybář 1997). This landslide led to the destruction and subsequent abandonment of the village of Eisenberg between 1952–1954. Thereafter, mining continued in the form of open-cast exploitation which further reduced the stability of the adjacent slopes.

A brief overview of material and methods

Immediately after the main movement activity in January 2011, the main deformation features were mapped at a scale of 1 : 5000 using GPS. In addition, aerial stereoscopic orthophotographs (November 2010 and March 2011) and aerial photographs (February 2011) were analysed.

The inner structure of the landslide and its vicinity was studied using the 2-D electrical resistivity tomography (ERT) which is particularly suitable for geomorphological studies as it gives insight into the subsurface (Schrott and Sass, 2006). Three profiles were measured using the Wenner–Schlumberger array in July 2010, April 2011, and October 2011. The ARES (Automatic Resistivity System) system (by GF Instruments Brno) was used for these profiles.

A geodetic network of reflective prisms was placed in the vicinity of the landslide in 2005. This could, therefore, have been used in the continuous monitoring of the nearby opencast mine (Bláha et al., 2006). This monitoring is undertaken with the Leica TCR 2003A total station and an automatic target recognition (ATR) system (Brown et al., 2007). The ATR system automatically monitors the position of all the reflective prisms at an interval of one hour. The reflective prisms are placed on 3.5m long standing pipes cemented to a depth of 2 m.

Landslide description

Landslide morphology

The landslide can be described as a complex landslide (Dikau, 2004) as it was characterised by a change in motion mechanics from sliding to flowing (Figs. 1 and 7). The body of the reactivated landslide consists of a rotated block with a length of ca. 150m and a width of ca. 120m together with a long frontal accumulation lobe that has flowed over the scarps of older earthflows.

The headscarp is located at an elevation of ca. 295 m a.s.l. It has a typical amphitheatral shape with a width of 102 m and a height of up to 13 m. In the outcrop of the headscarp it is possible to see the soil, bouldery gneiss proluvium, weathered claystones, and interbedded overlying sands.

The main scarp continues to the northeast in the form of a significant tension crack that runs for 200 m. This probably defines the unstable part of the reactivated landslide. On the western side a smooth shear plane is exposed with an inclination of up to 30°. On the eastern side a minor scarp with a height of 5–7 m defines the limit of the reactivated landslide body.

The landslide body has shifted horizontally, as determined from orthophotographic analysis. The upper part of rotated block, below the headscarp, has shifted by 12–14 m, while the middle part, including the road and artificial water channel, has shifted by 23–25m. The area of older headscarps in the lower part has shifted up to 26.4 m. At elevations of 250–265 m a.s.l., the frontal part of the landslide body was thrust over the upper overburden bench which meant that the material lost its cohesion and was subsequently deposited upon the eroded overburden benches and older earthflows (Fig.1). This accumulation lobe has a length of ca. 150 m and the characteristics of an earthflow on both the western and eastern sides where the material was fully saturated and without cohesion.

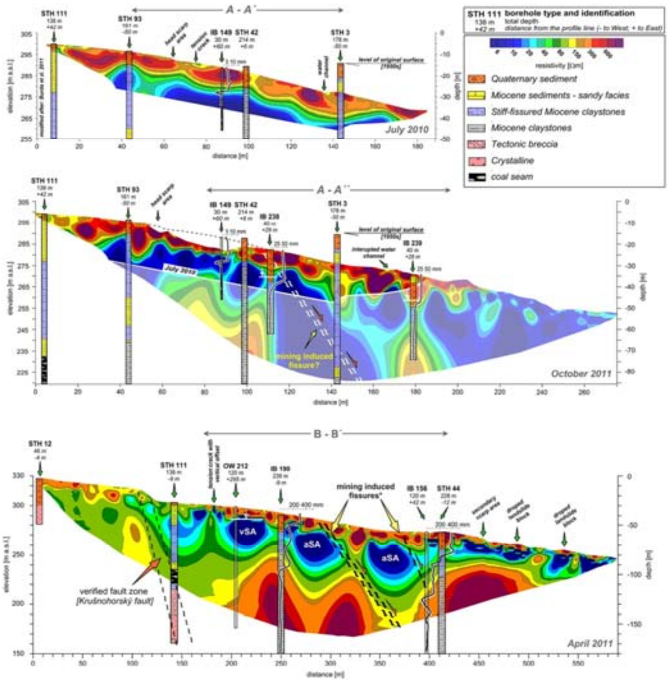

Figure 8 The ERT profiles taken across the landslide. STH: structural test hole; IB: inclinometer borehole; OW: observation well; vSA: verified shallow aquifer; aSA: assumed shallow aquifer (Burda et al., 2013).

Internal structure of the landslide

A detailed map of the mine area affected by the landsliding is shown in Fig. 1, while Fig. 8 shows the 2D Electrical Resistivity Tomography (ERT) profiles (including boreholes, inclinometers, and piezometer data).

As observed from the inclinometers shown in Fig. 8, the failure surface of the reactivated landslide (profile A-A) canbe approximately located at the interface between the Quaternary sediments and the Miocene claystone (at a depth of about 10–15 m). In addition, evidence of the old deeper landslide (dated back to 1952), described as a deepseated rotational failure (Burda et al., 2013), is present on inclinometers located along profile B-B′ , which is relatively close to the position of the reactivated shallow landslide. This suggests that the presence of two different failure mechanisms within the study area cannot be excluded.

Landslide evolution

Main movement activity

The main movement occurred in January 2011, but the movement velocity started to increase during December 2010 (Fig. 9). Between 9 and 14 January 2011, the daily rate of movement increased steadily to 20mmday–1. On 15 January at 8:01 p.m., reflective prism No. 178 was measured for the last time, with a total accumulative displacement of 777 mm. The ATR system, assuming that it had not been completely destroyed, would be able to find the reflective prism if it was within 5.5 m of its previous position (Bláha et al., 2006). It is thought, therefore, that the final movements were sudden and relatively fast (m h^{-1}), with the point destroyed shortly after reactivation of the landslide.

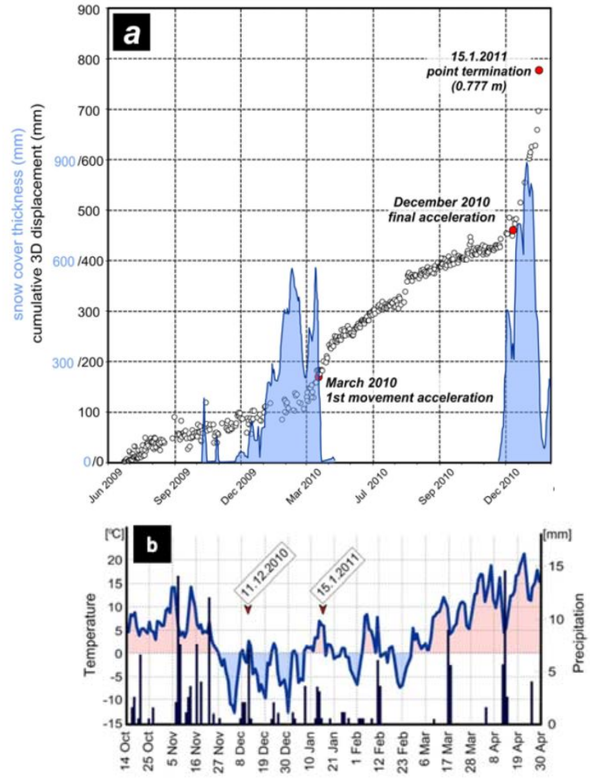

Figure 9 A cumulative three-dimensional displacement and snow melting (at NV station) versus time diagram showing the development of the landslide in the two years prior to January 2011. It is clear that there are two cycles of acceleration: the first in March 2010 and the second in December 2010 (**a**). Temperature development during October 2010 to April 2011 (**b**) (modified after: Burda et al., 2013).

Long term evolution

However, landslide evolution is well described since 1990 when monitoring based on precise levelling was found (Burda et al., 2011). Significant movements have been recorded at all four measuring sites (N1 – N4). The mean rate of movements at N1 and N2 was linear from 1993–2010 (6.4 mm yr^{-1} and 9.4 mm yr^{-1}, respectively). However, at N3 and N4 the mean rate of movements accelerated significantly after 2008 (from 19.5 mm yr^{-1} to 31.5 mm yr^{-1} and from 21 mm yr^{-1} to 55.5 mm yr^{-1}, respectively).

Landslide triggers

In 2010–2011 the peak snow cover at all stations was recorded in the second half of December, whereas in recent years it has normally occurred in the second half of January or in February (Fig. 9). The rapid cooling in late November and early December was followed by considerable warming that began on 7 January. From 7 to 16 January, the temperature did not drop below O°C. The average daily temperature reached 7°C on the 14th and 6°C on the 15th. The maximum temperature recorded during this period was 10.7°C on the 16th. It lead to rapid melting of the record snow cover with an estimated snow water equivalent of ca. 200mm (Čekal et al., 2011) and an

immediate rise in the water table . The total precipitation measured at Jezeří was 7 mm (13–15 January).
The final movement acceleration occurred at the beginning of December 2010 when a separate warming event on 11 December led to partial melting of snow and subsequent rising of water table. On 11 December the average temperature was 2.8°C and the daily maximum was 4.9° C, while there was also 7 mm of rainfall (Fig. 9). The subsequent saturation of the material led to the mobilisation of the older earthflow masses.

Case study: Slatinice - large deep-seated landslide in dump

In 1983 there was a large landslide affected an active internal dump Slatinice (placed approx. 3 km south of the town of Most). The landslide affected 80% of the total dump volume and with a 59.5 million m^3 it was by then the largest recent landslide within the Most basin. The landslide had a major impact (attenuation) on coal mining throughout the whole mining area, and we are still struggling with its consequences. In these days, strategic engineering networks are being built in this high-risk area.

Historical and geological background

The Slatinice open-pit mine was established in 1958 as part of the openings in the Bylany-Slatinice area. At the end of the sixties and early seventies, open-pit mine started coal seam excavations in the southern side of the volcanic Ressl hill. Until 1971, the uncovered foot part of Ressl Hill (3 – 20°) was an open pit and thus was exposed to precipitations and erosion.
Dumping of the Slatinice inner dump in the place of this undrained and inclined basement started in 1972. The dump was formed from a 240 m a.s.l., westward to 235 to 230 m a.s.l. across the exposed basement of the open-pit mine. Thus the exposed area of the inclined basement was divided axially in the north-west/south-east direction. The disadvantage was that the dump formed a dam on a very inclined basement and prevented both surface runoff as well as groundwater runoff. This had a deteriorating effect on the stability of the dump. The operation of the Slatinice Dump, placed on a completely non-drained inclined basement of former open-pit mine Slatinice, has been associated with a number of stability problems since 1970s (Orlt, 1998).
The rapid development of coal-mining led to an overall increase in soils deposited in the dump at the turn of the 1980s. This situation led to a excssive overburdening of the dump and culminated in a large landslide in May 1983.

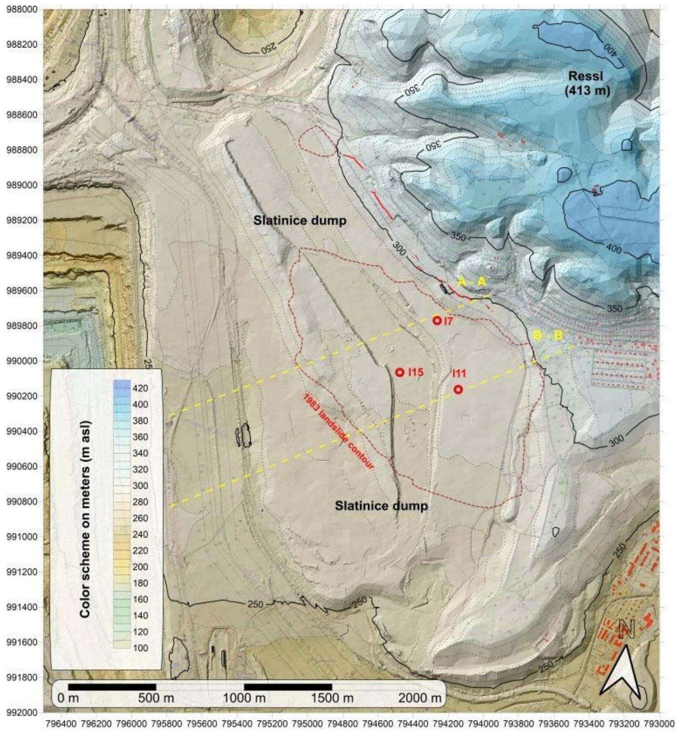

Figure 10 Actual (2018) DEM of the Slatinice dump study site with marked cross-sections and inclinometers.

A brief overview of material and methods

The situation in Slatinice dump area was mapped by aerial photogrammetry and geodetical survey.
In Slatinice dump the regular inclinometric monitoring is used since 2014. Thy system of 26 inclinometric boreholes are periodically measured on Slatinice dump body in present. Boreholes No. I7A, I11 and I15A are situated in the area formerly affected by landslide event in 1983 (Fig 10). They are the best example, that former landslide, now over-dumped, is still influencing the whole dump body stability.

Landslide description

The soil material in upper parts in scarp area could be initiated to move by minor rotational or translational movements, however the majority of soil mass was transported in linear direction, mostly parallel to the bed of the dump body. Thus, it can be described as a translational landslide of affecting vast complex area of the Slatinice dump.
The digital elevation model has been generated, based on the earlier maps of situation before and after the event of 1983. The DEMs show rapid terrain development of Slatinice dump before the landslide (Fig 11 and 12), when height of the dumps slope reached over 75 m.
Based on situation model after the landslide (Fig 13), the terrain level vertical change map was created (Fig 14), which shows the impact of landslide movement on dump body elevation.

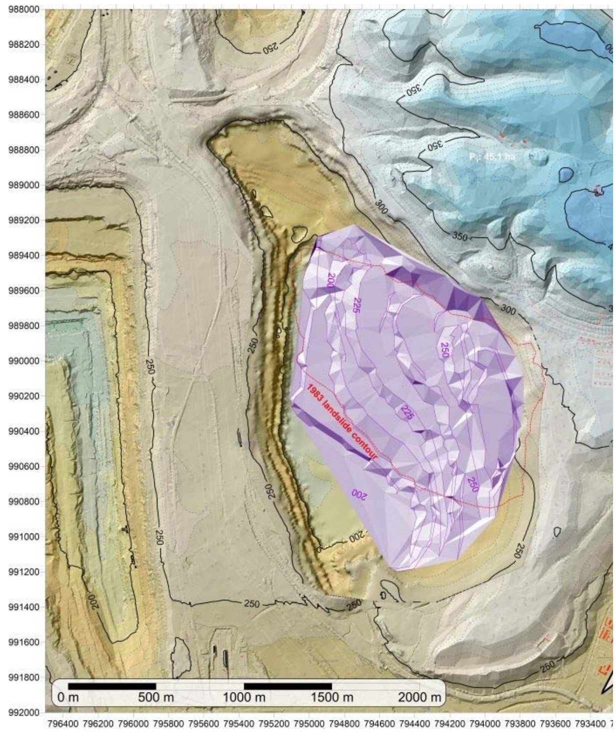

Figure 11 DEM of the Slatinice dump before the landslide – situation in 1982.

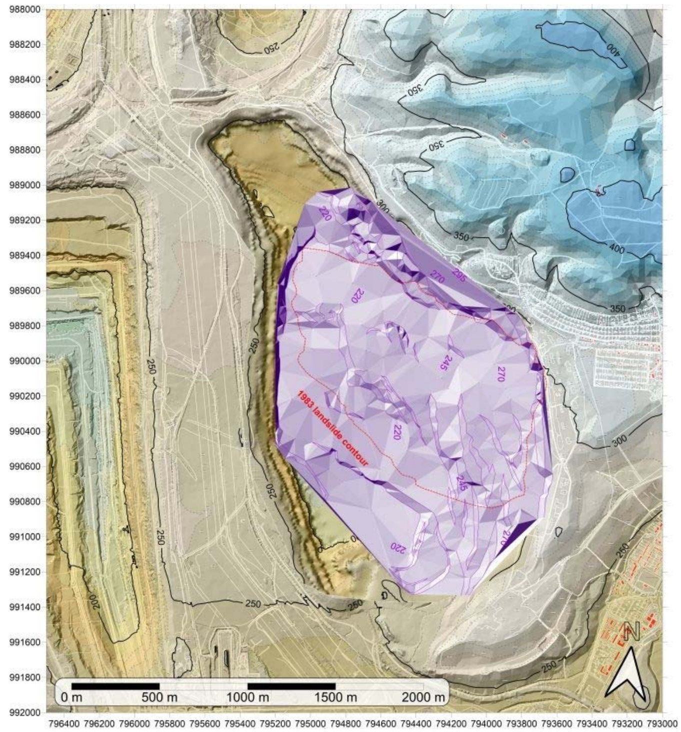

Figure 13 DEM of the Slatinice dump shortly after the landslide – situation in 09/1983.

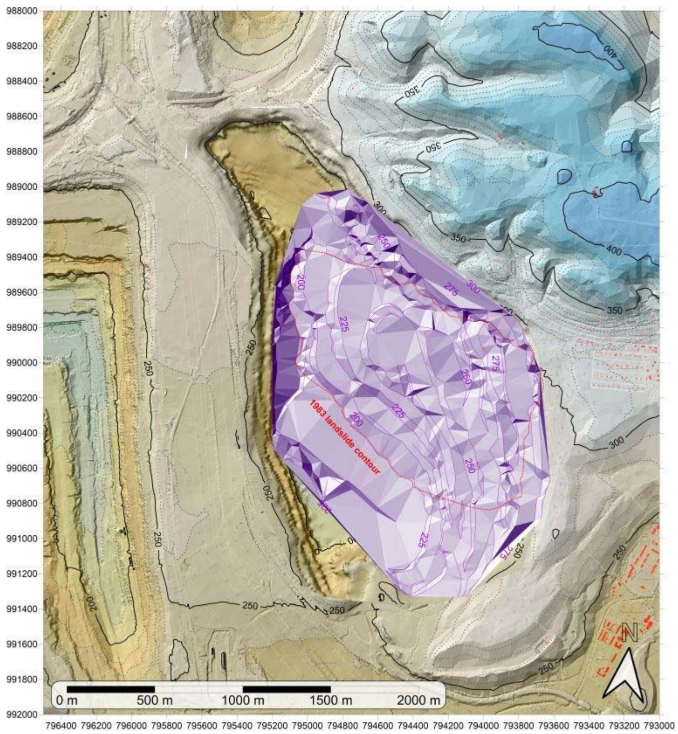

Figure 12 DEM of the Slatinice dump before the landslide – situation in 03/1983.

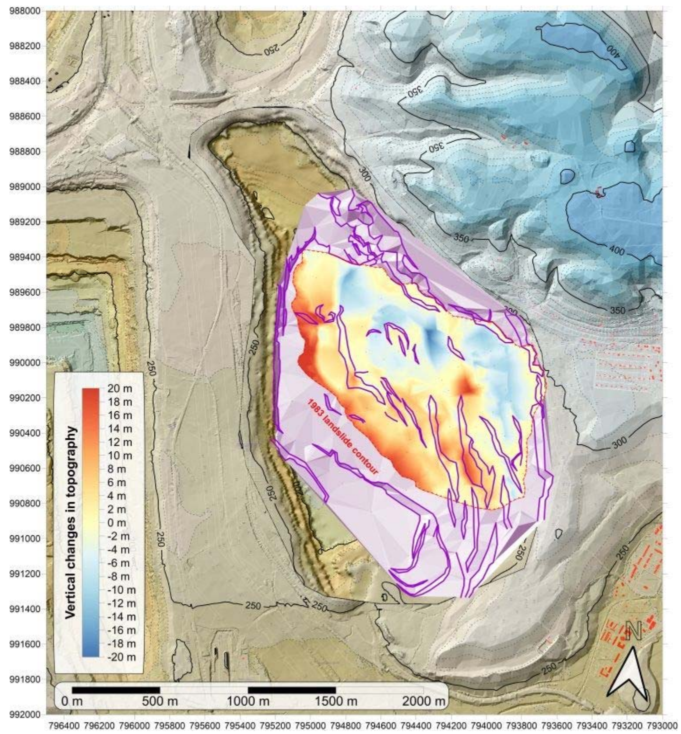

Figure 14 Vertical changes in dump topography induced by 1983 landslide activity.

Inclinometric monitoring

Inclinometer No. I7A is situated almost on the axe of cross-section A. The largest deformations were detected in last 15 months of monitoring regularly at a depth of 54,0 meters below ground level (227,8 m a.s.l.) where the most significant horizontal displacement reached 36 mm in total. The average rate of displacement growth was 2,4 mm per month. The height level of a detected potential slip surface corresponds with the base of layer representing low cohesive materials in geotechnical model (Fig. 16). The zone marked as "landslide" in the model corss-sections was verified during last years by the grid of static penetration probes. It should represent the zone of material disturbed and degraded by landslide movement in 1983. The potential slip surface at 227,8 m a.s.l. is situated approximately on contact between the landslide and its slippery zone.

The similar situation was detected by the inclinometer borehole I15A situated on the lower level of the present dump further from the cross-section A axis. The potential slip zone was observed in two zones simultaneously, with peaks at level 47,0 below ground level (220,2 m a.s.l.) and 55,0 below ground level (215,2 m a.s.l.) (Fig 15b). The total horizontal displacement at a depth of 55,0 meters, which is more significant, reached the rate of deformation growth 1,2 mm per month in average. The horizontal deformations in both mentioned levels represent the initiating slip displacements in the zone with lowered cohesion materials. Both depth levels are situated inside the layer of landslide zone in cross-ssection A (Fig 16), which reaches over 30 m in thickness in this location.

Inclinometer borehole No. I11 is situated on the line of cross-section B at 283,28 m a.s.l. The most significant slip displacement was examined at a depth 52,0 meters, height level 231,3 m a.s.l. (Fig 15) Total horizontal displacement reached value 17,3 mm in last 15 months with average rate of displacement growth 1,2 mm per month. In case of inclinometer I11 the zone of failure is narrow, sharply limited and it is obviously related to the top layer of the zone of landslide materials in geotechnical model.

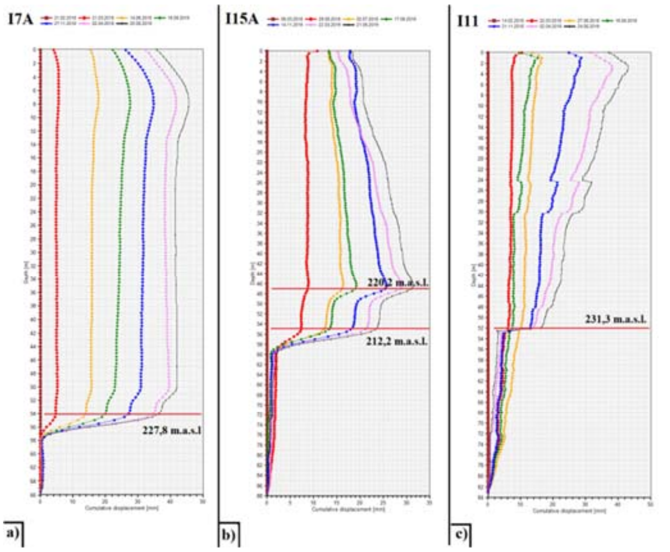

Figure 15 Total horizontal displacements measured in inclinometers I7A (a), I15A (b), and I11 (c) situated in the area of former landslide from year 1983

Case study: Large runout fossil landslide

The deposits of a large runout landslide11 cover up to 778,000 m² on the south-east facing slopes of the Krušné Hory Mts. in the north-west part of the Czech Republic (Fig. 17). Many fossil slope deformations on the toe of the geomorphological expressive structural slopes of the Krušné Hory Mts. have already been described (Zmítko 1983; Špůrek 1974; Váně 1960), but the deformation under Mt. Jezeř (706 m a.s.l.; near the Jezeří landslide described above) is quite exceptional due to its morphometric characteristics.

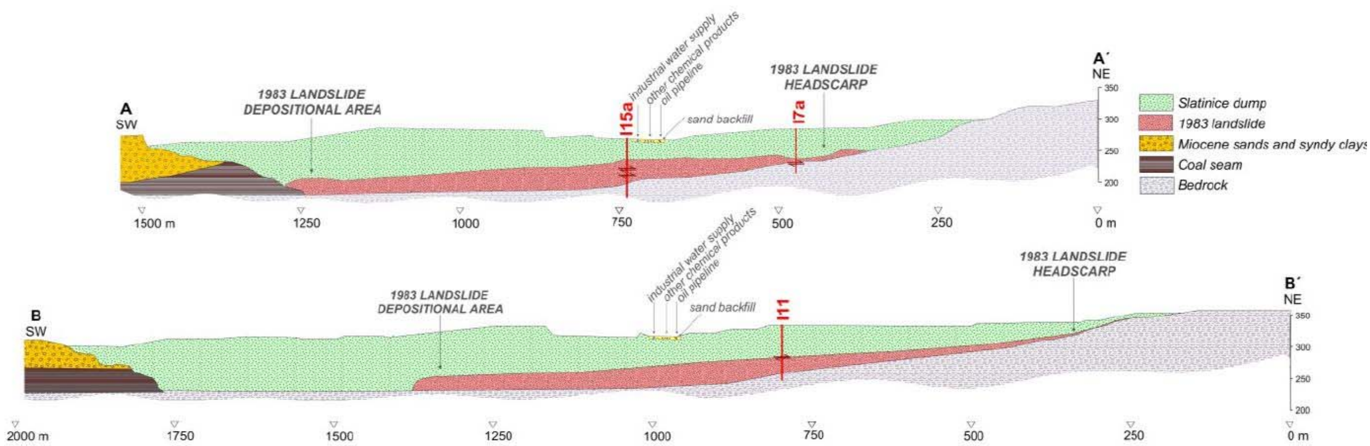

Figure 16 Cross-sections across the Slatinice dump area with position of inclinometric boreholes I7a, I11 and I15a and 1983.

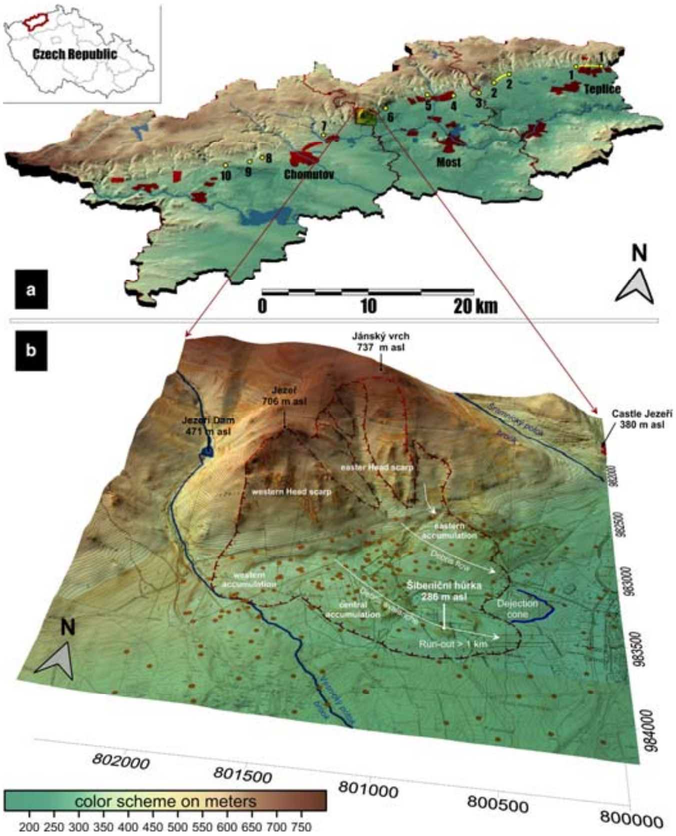

Figure 17 A detailed 3-D view of the study site seen from south-DEM based on digitizing of military topographic maps of the Czech Republic from 1952 (Burda et al., 2018)

Historical and geological background

The landslide was first described at the end of the 1950s; Váně (1960) mapped massive gneiss blocks deposited 1 km away from the mountain foothills. These blocks formed a morphologically significant hill named Šibeniční hůrka (285.9 m a.s.l.) and was previously considered as an *in situ* gneiss outcrop. During the mining was proved these are accumulation and additional studies of Špůrek (1974), Marek (1979), Rybář (1981), Zmítko (1983), and Růžičková et al. (1987) described this accumulation as a Pleistocene product of repeated rocksliding with a total volume of approximately 20mil. m^3 and an accumulation runout distance of up to 1 km from the foothills.

The described landslide is situated in the foothills below the Mt. Jezeř (706 m) and Mt. Jánský vrch (737 m). Both south-east-facing mountains are characterized by having slopes with a gradient of more than 30° (rarely more than 40^{o}).

The landslide deposits line the south-east foothills of the Krušné hory Mts. and run out into the Most Basin, which is a Neogene syn-rift basin between the České středohoří Mts. and Doupovské hory Mts. in the east and massif of the Krušné hory Mts. in the north-west (Fig. 17). The Krušné hory Mts. and the Most Basin present the main geological and geomorphological units (Balatka and Kalvoda 2006).

The uplift of the Krušné hory Mts. in the Miocene–Pleistocene along the Krušnohorský Fault expressed by the monoclonal folding of basin sediments near the edge of the mountains (Malkovský 1977). Also, as a result of uplift, the foothills are characterized by numerous slope failures from the Miocene, Pleistocene, and late Holocene (Zmítko 1983; Kalvoda 1995).

The piedmont area, including the Most Basin, has a graben structure (Váně 1985) and genetically belongs to the tectonic system of the Eger Graben (Domácí 1977). The basin sediments span the time interval from the Oligocene to Miocene. These sediments belong stratigraphically to the Paleogene-age Střezov Formation and dominantly to the Neogene-age Most Formation (Domácí 1977; Grygar and Mach 2013).

A brief overview of material and methods

Military topographic maps of the Czech Republic from 1952 were geo-referenced, digitized, and used to reconstruct the original landscape from a pre-mining age. The crucial aspect of this research consisted of an analysis of 216 boreholes drilled between 1941 and 2008. During a detailed review of the borehole profiles, attention was paid to a proper assessment of the Quaternary base and description and analysis of the character and texture of the Quaternary deposits. geological model, including the original 1950s surface, was compiled and analysed in a GIS. This analysis enabled a better estimation of the landslide area and volume.

The surface hardness measuring is a method of dating the relative age of rocks (Goudie 2006). Stone blocks and rock walls in situ were tested for compressive strength using a Schmidt hammer type N, which works with an impact energy of 2.207 Nm. The device measures the rebound value (R) on a scale of 10–100 R. The methodology according to Engel (2007) was used in this study and mean R values were used for an approximate age estimation, compared to an age-calibration curves from the Krkonoše Mts. (Czech Republic) described by Engel (2007) and Černá and Engel (2011).

Landslide description

Landslide morphology

Geomorphological sketch map presents the main features both in the accumulation zone as well as in the scarp area (Fig. 18). The accumulation part is 1180 m long, 1200 wide with relative relief of approximately 110 m. The total volume was set between 25.4 million m^3 and 27.4 million m^3. The deposits covered an area of 778,000 m^2, but the total contoured area, including the scarp area, is 939,000 m^2 with a maximum length of 1650 m.

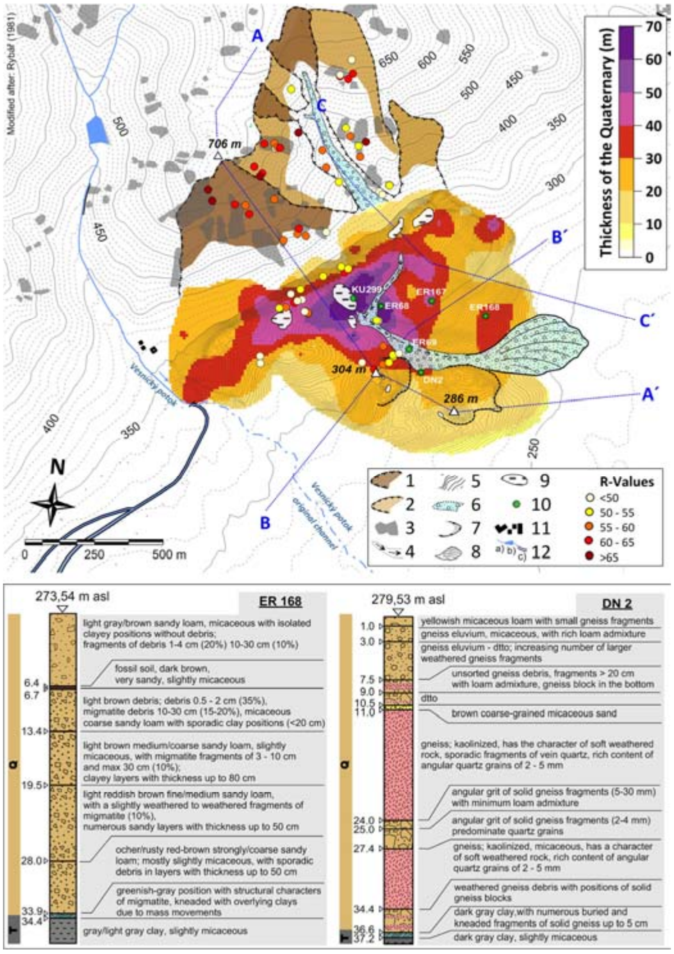

Figure 18 Top: geomorphological sketch map of the landslide with marked positions of cross-sections. Legend: 1—scarp area with expressive margins; 2—scarp area without expressive margins according to Rybář 1981; 3—rock outcrops, small ridges and rock groups; 4—gullies with occasional streams; 5—the main deposit area (contour interval 1 m); 6—fluvial sediments; 7—expressive accumulation toes with hummocky surface; 8—proluvial cone; 9—shallow colluvial depression; 10—boreholes mentioned in the text; 11—buildings and houses; 12a—stream with natural channel, b—dam, c—artificial stream channel. Bottom: geological description of ER 168 and DN 2 borehole profiles (Burda et al., 2018)

Internal structure of the landslide

The maximum thickness of the accumulated material is 72.1 m. The head scarp area can be divided into two parts. The western part under Mt. Jezeř (706 m a.s.l.) has a morphologically expressive facetted character (fault slope), with gneiss outcrops and rock walls on the surface. These rock outcrops *in situ* are concentrated at an elevation of 400 to 450 m a.s.l. up to the peak of Mt. Jezeř (Fig. 18) and this part of the slope is also the steepest—above 400 m a.s.l., the steepness rises from 20 to 25° to over 30° and in places over 40°.

Morphologically less expressive eastern head scarp area has an amphitheatrical shape which surrounds an expressive erosion gully in the middle. The gully is 550 m long, 50–120 m wide, and in the upper part splits in two particular scarp areas, which are morphologically more distinct than the rest of the eastern scarp area. This large gully is predisposed tectonically (Rybář 1981) and is filled by fluvial sediments at the bottom. The upper edge of this source area reaches up to 730m a.s.l. Some rock outcrops are located around the central gully, but in general, rock walls and rock outcrops are less common comparing to the western source area.

The whole landslide accumulation can be divided in three main parts: western and central part—both directly below the western scarp area of Mt. Jezeř and the eastern part extends up to the valley of Vesnický brook. The central and eastern accumulation parts are separated from each other by a shallow broad valley.

The surface of the western accumulation part is indistinct without expressive accumulation forms. The maximum Quaternary thickness reaches 38.5 m in the flat valley of Vesnický brook (Fig. 18). This landslide accumulation also diverted the flow of Vesnický brook and resulted in a small meander. The deposits have a character of angular boulder gneiss debris (fragments of size 100–300 mm up to 20%) with a several-meter-thick layer of loamy sand in the Quaternary basement. Sandy layers represent the material of the original alluvial fan, which was later buried due to the mass movement deposits. Recently, streamerosion cut across these deposits and formed a new flat valley with steep slopes and was filled with alluvial sediments (Fig. 18).

The central part of the landslide accumulation was almost completely excavated due to the mining in the 1970s and 1980s. The central part was clearly demarcated by 10–15° sharp and approximately 10 m high linear side walls from the west and by a broad depression from the east. The accumulation has a runout character with an irregular hummocky surface and two expressive elevations. These elevations were formed by one or more large blocks of solid coarsegrained gneiss up to thousands of m^3 (Špůrek 1974; Rybář 1981). Both elevations represented the most recent runout phases and were characterized by a 15–30° step south-east-facing slope with small dry depressions on top. The maximum length of the runout from the mountain foothills to the older indistinct accumulation toe at approximately 252 m a.s.l., reaches 1180 m. The max. thickness of the landslide deposits reaches up to 72.1 m. The area with Quaternary sediments' thickness exceeding 40 m is linked to a depression, which is evident in the pre-Quaternary basement—in the Tertiary sediments and partly in the crystalline fundament (Fig. 18).

The character of landslide deposits was described well in borehole DN 2 from 1958 (Quaternary sediments thickness of 36.6 m). In the upper 7.5 m, the material has the character of gneiss colluvium with a rich loam admixture and an increasing number of larger weathered gneiss fragments. Kaolinized and weathered soft gneiss with angular fragments or blocks of solid gneiss follow in the next 29.5 m and pass into a 0.6-m-thick layer of dark gray clay, solid gneiss fragments, and soft weathered gneiss debris, which are kneaded together. A similar character of landslide deposits was described in numerous other boreholes in this part of the landslide. The matrix facies consist of unsorted and strongly weathered gneiss debris, often colonized and with a rich loam admixture texturally interspersed with angular gneiss fragments to 30 mm (up to 30%). The block facies include large solid or slightly weathered blocks of coarse-grained gneiss or migmatite from 20 cm to boulders in size of meters. The contact of the Quaternary landslide material and the Tertiary layers comprises of dark gray clay, with numerous buried and kneaded fragments of solid gneiss up to 5 cm. A similar geological profile, including solid gneiss blocks, was found in many boreholes within the central accumulation.

The eastern landslide accumulation was excavated almost completely in the past up to the crystalline rocks of the Krušné hory Mts. This fan-shaped accumulation was up to 630 m long with a surface inclination of 10–15° in forehead part and 5–10° at the crown. The character of landslide deposits is slightly different from the landslide accumulation in the central part, which is evident from geological borehole ER 168. Large blocks of weathered gneiss are missing; accumulation has the character of slightly gray or brown sandy loam with relatively small angular fragments (up to 50 cm) of gneiss debris or migmatite (proportionally 10–20%). Like in DN2 borehole, the contact of Quaternary landslide material and lower Tertiary layers comprises a dark gray clay, with numerous buried fragments of solid gneiss kneaded due to mass movements. A similar geological profile, including a layer with kneaded clays and gneiss debris, was described in several others boreholes.

Schmidt hammer testing

Rock hardness measurements were performed on 72 sampling sites suitable for the Schmidt hammer test. For comparison, 12 sampling sites were chosen outside the landslide area. Differences of R values from all three sampling sites were statistically significant with $p < 0.05$. The result of t test showed statistically very significant difference ($p = 0.0008$) between both samples from scrap area and outside the landslide area. R values from the accumulation zone and the scarp area showed significant difference too ($p = 0.0073$). Statistically less significant difference was found within the data from accumulation area and outside the landslide area ($p = 0.0329$).

The compressive strength R values for the head scarp are in the range of 43.5 to 69.9, with a mean value of 57.8 and mean standard deviation of 4.0 (Fig. 18). In the accumulation zone, R values are in the range of 44.5 to 68.7, the mean value is 53.9, and the mean standard deviation is 4.2. These values represent rocks with different levels of strength/weathering (modified after Selby 1980), from very high strength rocks (> 65) to rocks with lower strength (< 50). The rocks of the head scarp area have significantly higher R values than the deposits in the accumulation. From the eight highest values, with an R value of over 65, only two were situated on boulders in the accumulation zone and over 70% of the sampling sites in the landslide accumulation zone are in the lower half of the dataset (Fig. 18). Rock outcrops in the western head scarp area are characterized by higher R values (43.5–69.9; avg. 59.2), compared to the eastern part of the head scarp area (47.0–65.1; avg. 54.8). In the western part, the slopes are steep (more than 30° and up to 90° on the exposed rock walls) with a higher inclination than the eastern part of the scrap area; rock outcrops are also larger and more common here. Sampling sites with different R values are distributed in both the western and eastern scarp areas. High strength rocks (R value > 60) are placed in the upper site of the western part, while the middle of the slope is characterized by R values of between 50 and 60, and two sampling sites with medium and low strength are situated lower on the slope. This elevation dependence is not conclusive in the eastern part; on the contrary, the rock strength is distributed irregularly throughout slope with a slight decreasing trend in rock strength towards the east.

The terrain of the original landslide accumulation was more modified due to open-cast mining; these excavations removed the southern rim of the landslide accumulation and also its surface layers. However, older debris material, including large gneiss blocks and boulders, were exposed due to these excavations. Five sampling sites were tested on a large blocky accumulation (crown at 262–267 m a.s.l.) under the former nameless elevation (304 m a.s.l.), and the R values span from 49.6 to 55.4. Another 24 smaller exposed gneiss blocks or boulders were tested in the rest of the accumulation zone, whereby the R values varied from 44.9 to 66.0. Different R values represent different landslide events placed rather randomly within the accumulation. The lowest R values (< 50) were detected rather closer to the mountain foot, and a cluster of the most similar R values (mean standard deviation 1.5) concentrated to one place is the exposed blocky accumulation mentioned above. The highest R values (> 60) were found on medium-size boulders, one of which is located on the current surface near the blocky accumulation and two are close to the mountain foot.

Present landslide interpretation

Based on the existing knowledge, we conclude that the slope deformation (or its western part) is a rockslide-rock avalanche, whereby the presence of water was crucial and allowed the transport of the material up to 1200 m. The water could be injected into the mobilized matrix from stiff, fissured, water-saturated Miocene sediments at the foot of the mountains or earlier due to snow or permafrost melting. If we consider the approximate age determined based on the Schmidt hammer testing, the largest movements probably occurred at the end of the Pleistocene. During this age, the large Lake Komořany formed in the Most Basin immediately below the slopes of the Mt. Jezeř and Mt. Jánský vrch (Jankovská 1987). Its maximum surface area is estimated to be 52–57 km^2, at a length of 13 km and a width of 9.5 km (Schlesinger 1871;

Zapletal 1954). Sediments of this lake were found at 230 m a.s.l. (Jankovská 1983), whereas the rock avalanche sediments were at a higher gradient (Fig. 18); we conclude that the accumulation did not reach the lake. The groundwater level in the area of the lake was near the surface and because the average annual temperature ofMost Basin was 4 °C in the Younger Dryas (Jankovská 1987), regelation processes were also intensive (to a depth of up to several tens of meters; Marek 1983). In themountains, the average annual temperature was 0° C, slopes were without tree vegetation, and only covered by tundra vegetation (Jankovská 1987). According to the expected scenario, a rockslide-rock avalanche could occur as a result of warming at the end of the stadial, as a result of rising temperatures melting the snow cover and permafrost. Rising groundwater levels and filling of the tectonic cracks by melting water could also be one of the possible triggering factors.

Three main landslide events were identified based on extensive Schmidt hammer sampling. For these events, similar R values were found on the sampling objects placed both in the head scarp area and the accumulation zone. These documented events can be understood as rapid landslide periods with various different extents. The approximate age of these events was estimated using the regression equation assembled by Engel (2007). Due to the inaccuracy of the Schmidt hammer method and the variability of measured values (Viles et al. 2011; Goudie 2006), we hypothesized that a single event can have results ranging from hundreds to several thousand years. Following this approach, it was found that the tested rock outcrops, blocks, and boulders are from a recent age up to approximately 15,200 yBP. Three main events were identified—evidence was found both in the scarp area and accumulation area. Because most of the accumulation was removed, it is possible that the blocks, older than those we found during the fieldwork, were also excavated and so it cannot be excluded that the maximum age of the oldest slope deformations may be higher.

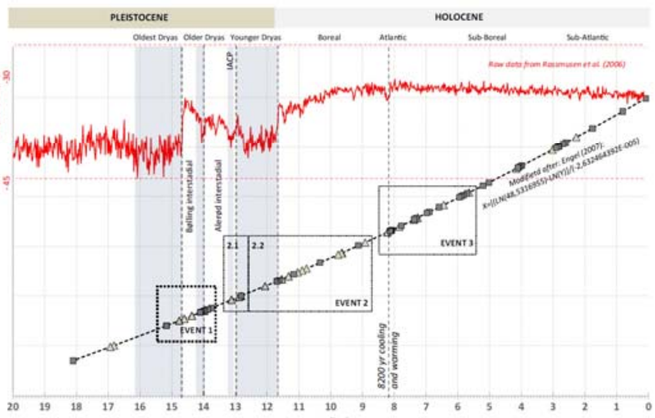

Figure 19 Rough age determination of analysed rock faces by age-calibration by Engel (2007) showing the postulated events and late glacial climatic trends as recorded in the NGRIP Greenland ice core (Rasmussen et al. 2006)

Individual events are always represented by clusters of points (11–20), which oscillate around major climate fluctuations at the end of the Pleistocene and Holocene (Rasmussen et al. 2006). Both events 1 and 2 could be associated with warming in the Bølling oscillation between the Oldest Dryas and Older Dryas stadials, and with warming in Younger Dryas (11,700 yBC) at the end of the last glacial period. Per our assumptions, event 3 is of a Holocene age, possibly associated with climate fluctuation in Atlantic (8200 yBC). Especially for events 2 and 3 (see Fig. 19), we hypothesize that they may be several mass movement events (a possible example could be event 2.1, which could be associated with the end of the Intra-Allerød Cold Period (ICAP)) acquired in a short interval (in hundreds of years), which cannot be further specified by timeline correlations based on Schmidt hammer testing. Of course, all of the events have a considerable time span; however, they are related to climatic fluctuations, because we assume that ideal climatic conditions occurred during these periods for the emergence of such extensive slope deformations.

Summary

Mining activities are accompanied by the necessity of continuous geotechnical exploration, when full knowledge of the deposit does not end until it is extracted. Therefore, it is not always possible to provide a uniform physical interpretation of the area before it is uncovered, even when a detailed geomechanical survey is available. Despite the development of mining technology allowed the open-pit mining even in the most complicated areas of the Most basin, what has not changed in principle is the riskiness of mining activities manifested in a wide range of accidents up to emergency conditions, caused by landslides of smaller and larger scale.

Each opening of the bearing and its gradual excavation over a period of several decades is a huge intervention in the equilibrium stress state of the basin filling and often also of the underlying rocks. As a result, the massif is damaged by loading cycles, weakening the original state of stress.

In addition to stratification or layering, irregular textures and predisposed areas often occur, which are a frequent cause of slope instability. Mass movements of various forms, and on a much larger scale than today, occurred at the turn of Pleistocene and Holocene. Their origin was due to denudation of low-strength sediments and extreme climatic and morphological conditions in the period of glacial and post-glaical climate. In the marginal parts of the Most basin, a number of fossil landslides are encountered or can be expected.

Compared to landslides on overburden cuts, which directly endanger the safety of mining machines, large-scale complex slope failures where sliding and run-off are applied mainly result in the loss of coal substance. This is a very unfavorable accompanying phenomenon of large mass movements caused by progressive failure of the massif. Additional efforts to extract the remaining coal substance are not always adequate to the effort. It is typical for mining practice that variants of possible alternative solution of stability problems are very limited and from this point of view it is desirable to realize the scope of overburden work in due time and scope.

A small example of the present states of art mentioned in the paper only outlines a wide range of knowledge of generations of mining experts. Even from today's perspective, geomechanical expertise cannot be qualified as fully manageable. However, considerable progress has been made with new possibilities for modeling the behavior of the massif in changing force fields, which should always be confronted with the real behavior of the massif through powerful control systems.

Acknowledgments

The paper was funded by the Research Fund for Coal and Steel grant project “847227-SUMAD-RFCS-2018.

References

Book_or_book_chapter__author_surname A A, Author_surname B B, Author C, (2009) Title of book. EditorSurname A (eds). Publisher and location. (ISBN _number_). 450p.

CD-ROM_author_surname A A, Author_surname B B, Author C, (2009) Title of CD ROM. (CD-ROM), ASCE Press, Reston, Va.

Conf_paper_author_surname A A, Author_surname B B, Author C, (2009) Title of paper. Proceedings of 30th Canadian Symposium on Remote Sensing, 22-25 June 2009. Lethbridge AB., Canada. pp. 310-321.

Journal_paper_author_surname N P, Anotherone K, Thelastone P O (2009) Title of paper. Canadian Journal of Remote Sensing. 35(2): 244-253.

Report_author_surname A A, Author_surname B B, Author C, (2009). Title of report. Publisher and location. (ISBN _number_). 50p.

Theses and dissertations _author_surname A A, Author_surname B B, Author C, (2009) Title of Theses and/or dissertations . MS thesis, DPRI Kyoto Univ., Kyoto, Japan.

Web_site_author_name_surname A A, Author_surname B B, Author C, (2009). Title of Page. URL: http://_ [Last accessed: full date].

Balatka B, Kalvoda J (2006) Geomorfologické členění reliéfu Čech. Kartografie Praha, Praha, p 79.

Bláha J, Blín J, Stanislav P (2006) Nový system sledování bočních svahů lomu ČSA, Zpravodaj Hnědé uhlí (1): 20–27.

Brown, N., Kaloustian, S., and Roeckle, M. (2007) Monitoring of open pit mines using combined GNSS satellite receivers and robotic total stations. URL: http://www.leica-geosystems..com/downloads123/zz/monitoring/geomos/tech_paper/Brown_Monitoring_with_combined_GNSS_and_robotic_total_stations.pdf [last accessed: 10 October 2011].

Burda J, Žižka L, Dohnal J (2011) A monitoring of recent mass movement activity in anthropogenic slopes of the Krušné Hory Mountains (Czech Republic). Natural Hazards and Earth System Science (9): 119-128.

Burda J, Hartvich F, Valenta J, Smítka V, Rybář J (2013) Climate-induced landslide reactivation at the edge of the Most Basin (Czech Republic) – progress towards better landslide prediction. Natural Hazards and Earth System Science (13): 361-374.

Burda J, Žižka L, Fultner J, Pletichová M (2015) Aktualizace hydrogeologických a geotechnických skutečností v oblasti Slatinice v roce 2015. Unpublished Technical Report (055/18), VUHU, Most, Czech Republic, 142p.

Burda J, Veselý M, Žižka L (2018a) Complex information of outer dump sites - locality Albrechtice. Zpravodaj hnědé uhlí (1): 3-11.

Burda J, Veselý M, Řehoř M, Vilímek V (2018) Reconstruction of a large runout landslide in the Krušné hory Mts. (Czech Republic). Landslides (15): 423-437.

Černá B, Engel Z (2011) Surface and sub-surface Schmidt hammer rebound value variation for a granite outcrop. Earth Surf Process Landf (36): 170–179.

Dikau R. (2004) Mass Movement. Goudie A. (eds) Encyclopedia of Geomorphology, pp. 644–652.

Engel Z (2007) Measurement and age assignment of intact rock strength in the Krkonoše Mountains, Czech Republic. Z Geomorphol (51): 69–80.

Goudie AS (2006) The Schmidt hammer in geomorphological research. Prog Phys Geogr (30): 703–718.

Grygar T, Mach K (2013) Regional chemostratigraphic key horizons in the macrofossilbarren siliciclastic lower Miocene lacustrine sediments (Most Basin, Eger Graben, Czech Republic). Bull Geosci 88(3): 557–571.

Jankovská V (1983) Palynologische Forschung am ehemaligen Komořany-See (Spätglazial bis Subatlantikum). Věstník Ústředního ústavu geologického 58 (2): 99–107.

Jankovská V (1987) Vývoj vegetace na Mostecku na základě pylových analýz sedimentů Komořanského jezera. In: Severočeská příroda (20):113

Kalvoda J (1995) Geomorphological analysis of levelling measurements between Mikulovice village and Jezeri Castle in the Krusne Hory Mountains. Acta Univ Carol Geogr 30, Supplem.: 139–160.

Kalvoda J, Stemberk J, Vilímek V, Zeman A (1990) Analysis of levelling measurements of the Earth’s surface movements on the geodynamic polygon Mikulovice - Jezeří in the Krušné hory Mts. Proc. 6th Int. IAEG Cong., 6–10 August 1990 Amsterdam, 3, Balkema, Rotterdam, Brookfield, pp. 1631– 1637.

Kalvoda J, Vilímek V, Zeman A (1994) Earth’s surface movements in the hazardous area of Jezeří kastle, Krušné hory Mts. GeoJournal 32(3): 247–252.

Klimeš J, Vilímek V, Omelka M (2009) Implications of geomorphological research for recent and prehistoric avalanches and related hazards at Huascaran, Peru. Nat Hazards 50(1): 193–209.

Kopecký A (1989) Neotektonika severočeské hnědouhelné pánve a Krušných hor. Sbor Geol Věd Geol 44: 155–170.

Král V (1968) Geomorfologie vrcholové části krušných hor a problém paroviny. Rozpravy Československé akademie věd 78(9): 42–49.

Mach, K., Žák, K., Teodoridis, V., Kvacek, Z. (2017) Consequences of Lower Miocene CO 2 degassing on geological and paleoenvironmental settings of the Ahníkov/Merkur Mine paleontological locality (Most Basin, Czech Republic). Neues Jahrbuch für Geologie und Paläontologie - Abhandlungen 285(3): 235-266.

Malkovský M (1977) Důležité zlomy platformního pokryvu severní části Českého masívu. Ústř Úst Geol (14): 7–12.

Malkovský M (ed) (1985) Geologie Severočeské hnědouhelné pánve a jejího okolí. Academia, Praha, 424p.

Marek J (1979) Šibeniční hůrka u Dřínova před odtěžením. Uhlí 27(11):498–501

Marek J (1983) Inženýrsko-geologický průzkumu stability zámku Jezeří v předpolí uhelného velkolomu. Geolog Průzk (25): 234–236.

Orlt O. (1998) Geotechnický model vnitřní výsypky Vršany a výsypky Slatinice. Unpublished Research Report (107/98), VÚHU, Most, Czech Republic, 70p.

Rasmussen SO, Andersen KK, Svensson AM, Steffensen JP, Vinther BM, Clausen HB, Siggaard-Andersen M-L, Johnsen SJ, Larsen LB, Dahl-Jensen D, Bigler M, Röthlisberger R, Fischer H, Goto-Azuma K, Hansson ME, Ruth U (2006) A new Greenland ice core chronology for the last glacial termination. J Geophys Res Atmos 111(6): 2156–2202.

Růžičková E, Zeman A, Hurník S (1987) Vývoj jihovýchodního okraje Krušných hor a Mostecké pánve v mladším kenozoiku. Sbor Geol Věd, ŘA (18): 9–72.

Rybář J (1981) Inženýrsko-geologické hodnocení stabilitních poměrů předpolí povrchových velkolomů při úpatí Krušných hor. Stabilitní řešení svahů a jejich zabezpečení, Sborník přednášek semináře, Most, pp 76–93.

Rybář J. Novotný J. (2005) Impact of climatic factors on stability of natural and anthropogeneous slopes. Zpravodaj Hnědé uhlí (3): 13–28.

Schlesinger L (1871) Festschrift zur Erinnerung an die Feier des 10. Gründungstages im Jahre 1871. Geschichte des Kummerner Sees bei Brüx, Praha, 26p.

Schrott, L. and Sass, O. (2008) Application of field geophysics in geomorphology: advances and limitations exemplified by case studies. Geomorphology (93): 55–73.

Schuster, R. L. and Wieczorek, G. F.: Landslide

Selby MJ (1980) A rock–mass strength classification for geomorphic purposes: with tests from Antarctica and New Zealand. Z Geomorphol (24): 31–51.

Špůrek M (1974) Sesuvné jevy u Dřínova na Mostecku. Věst Ustř Úst Geol (49): 231–234.

Vanneschi C, Eyre M, Burda J, Žižka L, Francioni M, Coggan J S (2018) Investigation of landslide failure mechanisms adjacent to lignite mining operations in North Bohemia (Czech Republic) through a limit equilibrium/finite element modelling approach. Geomorphology (320): 142 – 153.

Váně M (1960) Debris and landslides at the foot of the krušné hory Mts. Čas Min Geol 5(2): 174–177.

Váně M (1985) Geologická stavba podkrušnohorského prolomu a jeho tektogeneze. Sbor Geol Věd, Geologie (40): 147–181

Viles HA, Goudie AS, Grab S, Lalley J (2011) The use of the Schmidt hammer and Equotip for rock hardness assessment in geomorphology and heritage science: a comparative analysis. Earth Surf Process Landf 36(3): 320–333.

Vilímek V (1995) Quaternary development of Kateřinohorská Vault relief in the Krušné hory mountains. Acta Universitatis Carolinae, Geographica (30): 115–137.

Zapletal L (1954) Zbytky Komořanského jezera. Ochrana přírody 9(2): 57–58.

Zmítko J (1983) Fosilní sesuvy při podkrušnohorském výchozu pánve. Zpravodaj Hnědé uhlí (6): 12–24.

Kerala 2018 Landslides: An Overview and Preliminary Investigations

S S Chandrasekaran (1), V Senthilkumar (2)

1)Professor, School of Civil Engineering, Vellore Institute of Technology (VIT), Vellore, Tamil Nadu, India.

e mail: chandrasekaran.ss@vit.ac.in.

2)Research scholar, School of Civil Engineering, Vellore Institute of Technology (VIT), Vellore, Tamil Nadu, India

Abstract Kerala state is located in peninsular part of India. It is the third densely populated state. 47% of its land area is surrounded by Western Ghats. Western Ghats is one of the oldest mountain range which is frequently affected by landslides, especially during monsoon seasons. About 8% of area in Western Ghats of Kerala state is classified as vulnerable zones for landslides. The past landslide events indicate that, the heavy rainfall, thick soil cover and steep slopes are the major causal factors for landslides. An unprecedented very heavy rainfall during south west monsoon in the year 2018 resulted in floods and landslides across the Kerala state. According to Geological Survey of India (GSI) more than 67 major landslides and hundreds of minor landslides were reported. More than 400 people lost their lives due to floods and landslides. The extreme events resulted in severe infrastructural and environmental damages, collapse of many buildings and uprooting several trees and poles which caused complete shutdown of transport and communication for several days. The present study provides an overview of different types of landslides occurred in various locations across the Kerala state. The preliminary investigation was carried out on landslides that caused severe damages and fatalities. The investigation comprises of preliminary survey, collection of soil samples at landslide locations and laboratory investigations on index properties of soil. Based on the field observations and laboratory investigations on landslide materials, the landslides were classified according to updated Varnes classification of landslide type based on Hungr et al. 2014. The study provides the landslide dimensions and geotechnical characterization of subsoil materials involved in landslides. The overview of landslides and data of preliminary field and laboratory investigations reported in the present study provides necessary inputs for detailed investigations to assess the failure mechanism of reported landslides.

Keywords: Rainfall, Landslides, Preliminary, Investigations, Failure Mechanism

Introduction

Landslides are major hydro geological hazards in India. Himalayas and Western Ghats are among the frequently affected locations due to landslides in India. About 8% of area in Western Ghats of Kerala state is classified as vulnerable zones for landslides.The location of Kerala state is shown in fig. 1. According to district level landslide hazard zonation map of Tamil Nadu and Kerala,the Nilgiris district in Tamil Nadu and several locations in Idukki, Wayanad, Kozhikode and Malappuram districts of Kerala are very high to severe landslide hazard zones (BMPTC). The topography of Kerala is divided into three distinct regions namely highlands, midlands and lowlands with four major geological formations such as crystalline and sedimentary rocks of Archean and Tertiary age, Laterite capping on crystalline and sedimentary rocks and recent sediments (Oommen et. al. 2018).The normal rainfall for Kerala state during south west monsoon (June – August) is 1649 mm. During the 2018 monsoon season, the rainfall increased to 2344 mm, 42.17 % excess than the normal rainfall (Oommen et. al. 2018). A cumulative rainfall of 771 mm from 1st August to 20th August (140% more than the expected normal), led to numerous landslides across the state (PDNA, 2018). The major types of landslides are debris slide, earth slide, debris flow and mudflow type. The landslides caused extensive damage to houses, roads, railways, bridges, power supplies, communications networks and other infrastructure that affected the lives and livelihoods of many people in the state. According to state government, the estimated loss was about USD 3 billion (PDNA 2018).

The present study provides an overview of various types of landslides that occurred across the Kerala state in the year 2018. The preliminary investigation was carried out on landslides that caused severe damages and fatalities which includes Nenmara landslide in Palakkad district, Upputhodu landslide in Idukki district and Peringavu and Kaithakunda landslides in Malappuram district. Based on the results of the preliminary investigation the reported landslides were characterized.

Kerala 2018 Landslides – An overview

Between June 1 and August 18, 2018, Kerala experienced the worst ever floods in its history since 1924 (PDNA, 2018). During this period, the state received cumulative rainfall that was 42% in excess of the normal average rainfall.

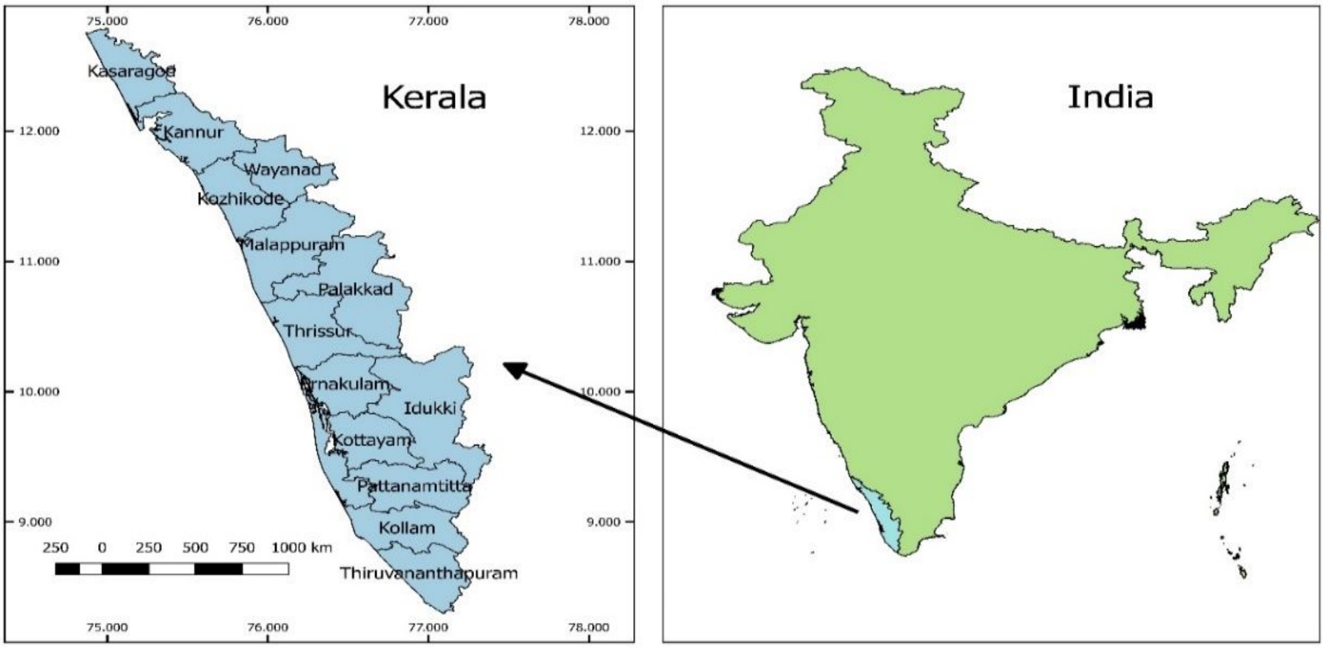

Fig. 1. Location map of Kerala

The heaviest spell of rain occurred between 1st to 20th August, in which the state received 771 mm of rain (PDNA, 2018). The torrential rains triggered several landslides and forced the release of excess water from 37 dams across the state which aggravates the impact of flood and landslide. 341 landslides were reported from 10 districts. Idukki was the worst affected district due to landslide that ravaged by 143 landslides (PDNA, 2018). Geological survey of India (GSI) carried out a preliminary assessment of 58 important landslides occurred in Kozhikode, Idukki, Wayanad, Kannur, Malappuram and Palakkad districts (Praveen et. al. 2018; Sulal and Archnana 2018; Sachin and Vishnu 2018). According to latest reports of the state government, 1,259 out of 1,664 villages spread across its 14 districts were affected. Kozhikode, Idukki, Wayanad, Kannur, Malappuram and Palakkad were worst affected in terms of damages and fatalities. The devastating floods and landslides affected 5.4 million people, displaced 1.4 million people, and led to death of 433peopleacross the Kerala state (PDNA, 2018).

Preliminary investigation and landslide Characterization

Authors carried out a post disaster site visit and identified few landslides that caused more damages and fatalities for detailed investigation. The landslides identified are Nenmara landslide in Palakkad district, Upputhodu landslide in Idukki district, Peringavu and Kaithakunda landslides in Malappuram district.The preliminary investigation was carried out to characterize the landslide. The investigation consists of preliminary survey, sample collection and laboratory testing. The landslides and its damages are shown in fig. 2. Based on the preliminary investigation, the landslides were classified based on revised Varnes landslide classification proposed by Hungret.al. (2014).The Nenmara landslide was classified as debris flow type landslide, Peringavu and Kaithakonda landslides were classified as earth slide and Upputhodu landslide was classified as mud flow type landslide.

The Nenmara debris flow type landslide occurred on the early morning of 16th August 2018. The view of landslide is shown in fig.2a. The landslide located at latitude and longitude of 10.58 and 76.61. Eight people were killed due to the landslide including a new born baby. The bodies were recovered from the debris. The landslide damaged three houses located at the toe of the landslide. The overall runout distance was observed as 200 m and average width of the landslide was observed as 60.00 m. Landslide occurred due to heavy rainfall. Daily rainfall recorded at nearby rain gauge station on the day of landslide occurrence was 220 mm.Upputhodu mud flow type landslide occurred in the evening of 17thAugust 2018 at the location of 9.89 latitude and 76.97 longitude. The view of landslide is shown in fig. 3b. Four people were killed due to landslide. Two houses were completely washed away and one house was partially damaged. Few acers of agriculture land were completely washed away. The overall runout distance of landslide was observed as about 500 m and average width of the landslide is about 50.00 m. Landslide occurred due to heavy rainfall in the Upputhodu area. The daily rainfall observed from the nearby raingauge station on the day of landslide occurrence was about 190 mm.The heavy rainfall in Nenmara and Upputhodu regions leads to infiltration of rainwater into the soil that developed the pore water pressure and seepage pressure along the failure surface was the causing factors for debris and mud flow type landslides in respective locations. The detailed investigation considering landslide simulation and rainfall infiltration modelling will be useful to understand the failure mechanism and failure process.

Authors currently investigating the Kaithakonda and Peringavu earth slide type landslides. The view of Kaithakonda and Peringavu landslides are shown in figs. 3c and 3d. The Kaithakonda landslide occurred in the midnight of 15th August 2018. The slide killed 3 people and damaged a house located at the toe. The subsoil consists of highly weathered silty sand followed by sandy silt. The rotational failure occurred due to heavy rainfall and reduction in shear strength of sandy silt layer. The daily rainfall on the day of landslide occurrence observed from the nearby rain gauge station was 221 mm. Peringavu earth slide type landslide occurred on the 15th August 2018. The view of landslide and damaged buildings are shown in fig. 3d. The landslide killed eight people and completely damaged a two-story residential building. The heavy rainfall of 221 mm on the day of landslide occurrence allows the rainwater to infiltrate into the highly weathered sandy silt layer and reduced the shear strength of the soil caused a rotational type slope failure. A numerical modelling consists of stability analysis considering the effect of rainfall infiltration in addition to the field and laboratory tests being conducted to understand the failure mechanism. Various remedial measures are to be modeled numerically in order to identify the suitable site-specific remedial measure for Kaithakonda and Peringavu rotational earth slide type landslides.

(a)

(b)

(c)

(d)

Fig. 2 Kerala 2018 Landslides, (a) Nenmara Landslide, (b) Upputhodu landslide, (c) Kaithakonda Landslide (d) Peringavu Landslide

Conclusions

The study presents an overview of various types of landslides occurred at Kerala in the year 2018. The study revealed that, accumulative rainfall of 771 mm from 1st August to 20th August (140% more than the expected normal in just 20 days) was the major causal factor for landslides across the Kerala State.The major types of landslides are debris slide, earth slide, debris flow and mudflow type. From the study it was observed that, among 14 districts in the Kerala state, Kozhikode, Idukki, Wayanad, Kannur, Malappuram and Palakkad districts were most affected in terms damages and fatalities. After the post disaster site visit, authors identified four landslides including Nenmara debris flow type landslide, Upputhodu mudflow type landslide, Kaithakonda and Peringavurotational earth slide type landslides for detailed investigation. The preliminary investigations including preliminary survey and landslide characterization provides the necessary data such as landslide type (according to Hungr et. al.2014), landslide dimensions, earth materials involved and probable casual factors will be useful for planning of detailed investigations. From the study it is suggested that, a comprehensive study consist of field investigation, laboratory testing and numerical modelling (landslide simulation and rainfall infiltration modelling and modelling of remedial measure) will be useful in order to identify the landslide triggering factors, understanding the failure mechanism and selection of suitable site-specific remedial measures

References Hungr, O., Leroueil, S. and Picarelli, L. (2014), 'The Varnes Classification of Landslide Type, An Update', Landslides 11(2), 167-194.

Oommen, T., Coffman, R., Sajinkumar, K.S. and Vishnu C. L. (2018), 'Geotechnical Impacts of August 2018 Floods of Kerala', Ntional Science Foundation, GEER Association Report, Report No. 058.

PDNA. (2018), 'Kerala Post Disaster Needs Assessment – Floods and landslides', Government of Kerala Report.

Sulal, N.L. and Archana, K. G. (2018), 'Note on Post Disaster Studies for Landslides Occurred in June 2018 at Idukki District, Kerala', Geological survey of India, Report No. M4SI/NC/SR/SU-KRL/2018/21108.

Praveen, K.R., Kumar, T.N. and Vishnu, C. S. (2018), 'Note on Post Disaster Studies for Landslides Occurred in June 2018 at Kozhikodu and Wayanad District, Kerala', Geological survey of India, Report No. M4SI/NC/SR/SU-KRL/2018/21108.

Sachin, R. and Vishnu, C. S. (2018), 'Note on Post Disaster Studies Malappuram and Palakkad Districts, KeralaDuring June 2018', Geological survey of India, Report No. M4SI/NC/SR/SU-KRL/2018/21108.

The influence of geological history in modern landslide activity on the site "Vorobyovy Gory"

Olga Barykina, Oleg Zerkal, Irina Gvozdeva, Michail Chernov

Lomonosov Moscow State University,Geological Department, Moscow, GSP-1, Leninskie Gory, 119991, Russian Federation,e-mail: barykina@geol.msu.ru

Abstract: Landslide processes in Moscow have been studied more than a hundred years. One of the landslide hazard areas is the Vorobyovy Gory – nature reserve within Moscow located on the right cut bank of the Moskva River. The study area is located in the central part of the Vorobyovy Gory covering the area from the Moscow viewpoint to the Moscow metro bridge. The slope has a typical landslide landscape. The geological strata are represented by deposits of the Carboniferous, Jurassic, Cretaceous and Quaternary systems. Deep large and long-time active landslides were formed at the right side of the valley of the Moskva River in pre-Holocene time. Currently, several zones of the "Vorobyovy Gory" landslide are active. The total volume of the landslides reaches eight million cubic meters.The article is devoted to the description of landslide development based on new data (2015 – 2019).

Based on the newly obtained data, the following conclusions can be drawn. Firstly, the territory involved in landslide processes on the Vorobyovy Gory is characterized by much larger values, both in area and in depth, than it was previously assumed. In the head part, where the displacement zone is located at depths of 80-100 m, the deformations, confined to the lower part of the Jurassic deposits, have a block character. Secondly, we can speak of a combined mechanism for the development of a large-scale landslide massif "Vorobyovy Gory", which includes plastic flow with the formation of a ridge compression, collapse with tipping, block displacement and other types of deformations. Also it is possible to distinguish both primary and secondary displacements.

The development of deep landslide deformations was confined to the level of the paleo-valley, which was lower than the current Moskva River level.

Keywords: Landslide processes, degree of reconsolidation, landslide development, combined mechanism, plastic flow, ridge compression, collapse with tipping, block displacement, primary and secondary displacements.

Introduction

Landslide processes have been studied for more than a hundred and fifty years at the territory of Moscow (Pavlov, 1890, Nikitin, 1897, Danshin, 1937, Korchebokov, 1938, Churinov, 1957, Kuntzel, 1965, Paretskaya, 1975, Barykina et al, 2017, 2019). At present, more than 200 landslide sites are known on the territory of the city, including 16 sites where large-scale slope deformations develop. One of the largest landslide areas covers the high slope of the starboard side of the Moskva River in the Vorobyovy Gory area (Vorobyovy Gory is the name of own hills in the South-West of Moscow).

Slope deformations on the Vorobyovy Gory have been documented since the beginning of the 19th century. In the middle of the XIX centurythe presence of landslides in the Vorobyovy Gory region was reflected at the Map of the Moscow Province (Schubert, 1860). Because of landslide hazard, in the middle of the twentieth century, the high-rise building, which later became the main building of the Moscow Lomonosov State University, was moved from the edge of the slope.

According to the results of previous works it was considered that landslide deformations are confined to the upper, watered part of Oxford clays, which are regional waterproofing (Danshin, 1937, Churinov, 1957, Kuntzel, 1965, Paretskaya, 1975). The base of displacement was considered to be the modern Moskva River bed.

Engineering geological setting

The characteristic of research area

The city of Moscow is located on a naturally complex territory, which is characterized by a long history of development and a variety of landscapes. The valley complex of the river occupies the most part of the city (river floodplain and its three terraces); the south-western part (where the research area is located) lies within the Teplostan upland; the eastern part is the marginal part of the Mescher lowland - a flat, weakly dissected swampy plain with low, absolute marks. Thus, the valley of Moskva riveris the main geomorphological object of the territory, occupying a significant part and crossing the city diagonally from the north-east to south-west (Fig. 1).

The relief of Moscow inherited preglacial features and was formed because of Quaternary period glaciations, as well as erosion. In the right-sided bends, the Moskva River cuts into the valley side, forming steep landslide slopes, one of which ("Vorobyovy Gory") is the study territory. The study territory is located in the central part of Vorobyovy Gory.

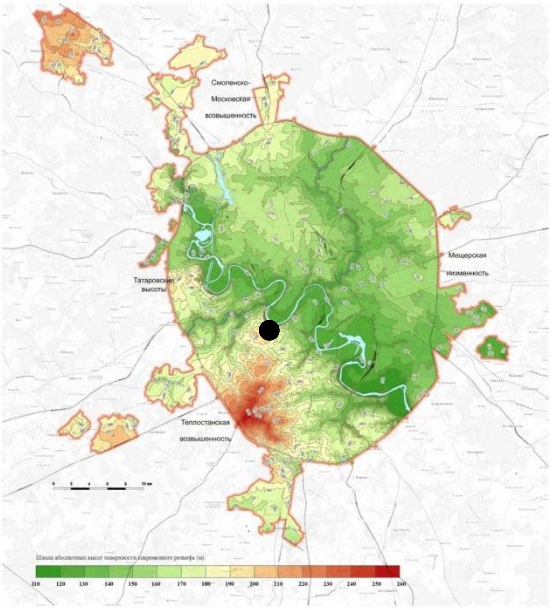

Figure 1 Hypsometric map of Moscow area. Circle - research area

Vorobyovy Gory are located on the right side of the valley of the Moskva River and represent a steep, sometimes forested slope (up to 70 m high) with a peculiar ridge-landslide relief, stretching along the river. The main scarp is well expressed in relief - its height varies from 12 to 30 m, and steepness from 25° to 40°. Erosion forms, such as ruts, gullies, ravines, etc., are developed within the slope also. The lower part of the slope adjoining the Moskva River embankment is significantly technologically altered by anti-landslide measures.

Geological setting

Rocks of the Middle Pennsylvanian of Carboniferous, Bathonian-Tithonian Jurassic, Berriassian-Aptian stages of the Lower Cretaceous, and Quaternary formations represented by morainic and aquatic-glacial accumulations take part in the near-surface structure of the watershed part of the Vorobyovy Gory (Shkolin, 2015, Barykina et al, 2017, 2019).

At the base of studied section, on the eroded surface of organogenic detrital limestones of the Myachkovskian age (the Moscovian stage of the Middle Pennsylvanian) (Fig. 2), whose roof was exposed at depths of 110-113 m, lies thin bed seam (up to 2 m) of the deposits of the Callovian stage of the Middle Jurassic, presented by dark brown carbon-bearing clays and gray-brown clays with oolites and large pebbles of limestone.

The roof of Carboniferous deposits forms a complexly organized pre-Jurassic paleorelief. It should be emphasized that the area of the Vorobyovy Gory from the

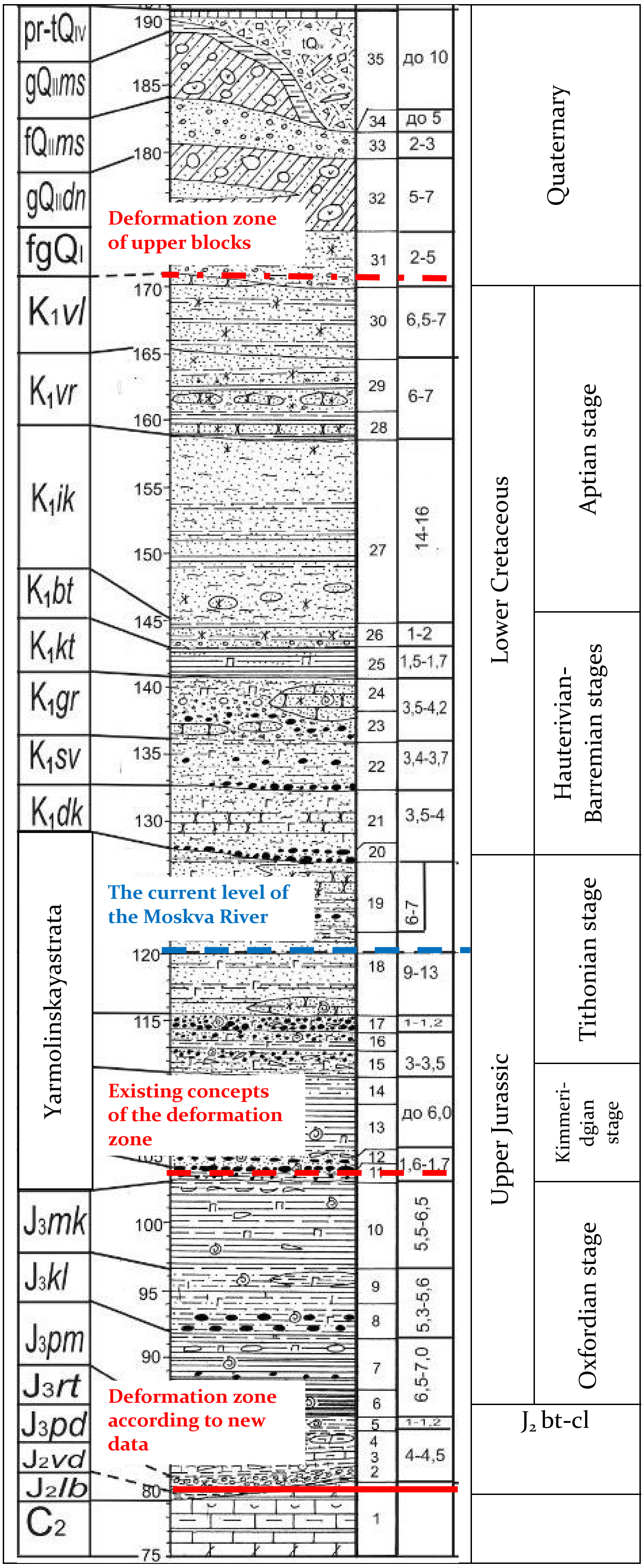

Figure 2 Summary geological column (by A.A. Shkolin, modified).The blue dotted line shows the current level of the Moscow River. The red dotted line shows the previously existing notions about the landslide deformation zone (the basis is the bottom of modern alluvium). The red solid line shows the deformation zone according to the new data.

observation deck to the metro bridge is located within the "Main pre-Jurassic paleovalley". The relative depth of its downcutting, based on the difference in marks of the base of the Jurassic formations (in comparison with the adjacent territories), reaches 40-45 m.

Five suites represent the section of the Oxfordian stage, the deposits of which overlap the callovian formations, successively from the bottom to the top (Fig. 2): podosinkovskaya suite (J_3pd) composed of gray clays with fauna of belemnites and ammonites, up to 1-2 m thick; ratkovskaya suite (J_3rt), represented by gray clays and oolitic sands with phosphorites and ammonites, up to 1 m thick; podmoskovnayasuite (J_3pm), composed of a pack of dark gray and black, dense, micaceous, fissile shaleclays up to 6.5 m thick; kolomenskaya suite (J_3kl) composed of brownish-gray and light gray clay, heavily silty, up to 6.0 m and makarievskaya suite with a capacity of up to 6.5 m. Depth of the roof of oxford clays within a high, not involved in landslide deformations, of a watershed surface is more than 90-95 m.

The yermolinskaya strata including four low-thickness suites, which lies higher in the section, overlays the Jurassic deposits and, in terms of age, covers the upper part of the Oxford Stage and the bottoms of Kimmeridgian Stage. The yermolinskaya strata is composed of black, dense, layered clays. Above the geological section, overlapping the Upper Jurassic clays, there is a pack of sands accumulating from the Tithonian to the Aptian age. The deposits of the Tithonian stage are represented by greenish-gray and green quartz-glauconite sands (Fig. 2) with numerous phosphorites, which are characterized by the presence of numerous remains of the fauna of belemnites and ammonites. Dark-gray clayey aleurites occur at the base of the Tithonian section. The Berriasian stage of the Lower Cretaceous is presented by gray-green, green fine-grained sands deposits. Overlapping their pack of hauterivian deposits is composed of green fine-grained glauconite sands. Above the section, a thin interlayering of fine and medium-grained sands (Fig. 2), light and to various degrees of ferruginous, reddish brown with interlayers of lilac-gray and beige clayey aleurites and lilac and dark gray clays represents deposits of the Barremian stage. Deposits of the Aptian stage, which crowns the thickness of the Lower Cretaceous deposits, are presented by brownish-red fine-grained sands, with a thickness of about 15.0 m, a sandy silt-clay packet of fine- and medium-grained micaceous sands. The total thickness of the sandy layer reaches (in areas with undisturbed bedding) 69-71 m. The roof of the Lower Cretaceous sands lies within a high, not involved in landslide deformations, of a watershed surface at depths of 19-20 m.

The thickness of Quaternary sediments is composed of two horizons of moraine loam (Fig. 2) with crushed stone and gravel, separated by fluvioglacial medium- and fine-grained sands formed in the interglacial epoch (Mindel-Riss). The lower horizon of loams has a thickness of up to 7 m, and the thickness of the upper horizon (the Moscow stage of glaciation) is up to 5-6 m.

The Moskva River has a depth of about 5-7 m at the site adjacent to Vorobyovy Gory. The thickness of alluvial deposits in the channel part of the valley ranges from 7 m to 10 m.

Most researchers (V.V. Kyuntzel, M.N. Paretskaya, etc.), who studied the landslides of the Vorobyovy Gory, consider the clay deposits of the Oxfordian Stage as the main deforming horizon of landslide massifs (Kuntzel, 1965, Paretskaya, 1975). In this regard, within the slope, overlapping Oxfordian formations, sandy-clayey Upper Jurassic deposits of the Tithonian Stage, Lower Cretaceous mainly sandy sediments and Quaternary glacial, fluvioglacial formations are in landslide occurrence.

ResultsconductedresearchandDiscussion

A detailed study of the cores of wells located on the surface of the watershed "plateau" near the slope edge revealed several planes of landslide sliding: in the intervals of absolute marks of 81.3 m and 82.5 m. The intervals are confined to the clays underlying the Oxford sediments. It should be noted that earlier it was believed that the territory of the high surface of the separating "plateau" is located in the part of the massif undisturbed by landslide deformations and uncover the root occurrence of rocks.

The obtained data uniquely indicate the presence in natural (not involved in the technogenic activity) occurrence, within the depth of 80-100 m, of explicit zones of landslide deformations (in the form of slip planes). This allows us to state that the deep zone of displacements extends beyond the previously accepted boundary of landslide processes, which was revealed visually by the wide development of cracks, ruptures, etc. on the slope of the Vorobyovy Gory. Based on the above information, the conclusion about the necessity to transfer the boundaries of landslide processes in the study area deep into the watershed "plateau" was done. In this case, all previously described landslide bodies should be considered as secondary, developing within a very large landslide massif, the rupture zone which is located within the modern watershed plateau. Perhaps the surface occurrence of these deep deformations are now retouched by anthropogenic re-planning of the territory during its development.

The mechanism of formation of a landslide massif

The development of landslide in the area of the Vorobyovy Gory is probably related to the location of this region within the deep pre-Jurassic paleovalley of the Moskva River, where the upper part of the Carboniferous deposits (limestones, marls) was eroded and was the accumulation of a thick series of clays during the Jurassic time. Such areas are characterized by a significant, both horizontal and vertical, variability of the geological section, active water exchange between aquifers, which in turn leads to an intensification of the development of geological processes. The data obtained during drilling confirmed the uneven boundary of the roof of Carboniferous deposits. Drilling operations have revealed a difference in the marks of the roof of the Carboniferous deposits, reaching 4-5 m. The surface of Carboniferous formations buried beneath the overlying sediments is eroded and has a complex character, and is probably one of the factors of the development of landslide processes in the Vorobyovy Gory region (Barykina et al, 2017, 2019).

Based on newly obtained data, it is possible to clarify the mechanism of landslide processes of the study territory, which is based on the features of the motion of individual elements of the landslide. In our case, we can talk about the simultaneous action of several mechanisms of deformation of soils in different parts of the slope.

The formation of the head part of the landslide massif occurred because of the displacement of large blocks composed of Mesozoic-Cenozoic deposits. This is confirmed by the presence of a series of slip planes encountered during drilling in the thickness of Jurassic clays. The thickness of such landslide blocks in the study territory, based on the drilling data, reaches 80-100 m. It should be noted that the identified slip zones are in a section at absolute elevations substantially below the current level of the river, indicating that the basis for landslide displacements was a lower erosion level, indicating the duration (in geological time) of the development of landslide deformations in the study area. Thus, the head of the modern large-scale landslide massif "Vorobyovy Gory" is a fragment of the relict landslide (according to the terminology proposed by (International, 1993)).

Three levels of landslide blocks, the surfaces of which rise above the edge of the river on 15-16 m, 29-33 m and 47-49 m respectively, form the main part of the modern large-scale landslide massif «Vorobyovy Gory». The nature of landslide displacement is reflected in the peculiarities of the variability of the structure of the geological section within each of the blocks.

Within the lower block, a normal stratigraphic sequence is established only for the lower part of the open geological section (depth 40 m and below). In this depth interval, near the riverbed part of the valley, there are clays of the Oxfordian stage (ratkovskaya, podmoskovnaya and kolomenskaya suites). Nevertheless, a certain reduction (up to 0.5-1.0 m) of thickness (as compared to the structure of undisturbed areas) was established for these deposits and an increase in the altitude of the boundaries by approximately 2 m as well. The clay of the yermolinskaya strata the tops of the Oxfordian stage - the bottom of Kimmeridgian stage) have a thickness of 12.3 m, which is more than twice higher than their thickness in undisturbed occurrence within the limits of the high watershed areas. Above the clays of the yermolinskaya strata, a zone of landslide folded rock was revealed, represented by separate fragments (pieces) of black clays of the yermolinskaya strata, up to several centimeters in diameter, located in a matrix formed by greyish-green sands of berriasian. The thickness of the folded zone is up to 1 m. The zone of landslide folded is overlaying by the displaced deposits having a reverse (!) in sequence of occurrence. At the base of the stratum, a horizon of fine-grained silty sands of the Berriasian age with a thickness of up to 2.5 m was found, above which lie Tithonian glauconite fine-grained sands (up to 1 m thick). They are covered with dark gray clayey siltstones with a thickness of less than 1 m, lying in an undisturbed state at the base of Tithonian formations. The total thickness of the pack, characterized by the reverse occurrence, is up to 5 m. Above, a zone of interlayering (0.6-0.9 m) of sand and silts of the Tithonian age and of the yermolin clay was discovered. The upper part of the section of the lower block is formed by alluvial formations (thickness up to 7 m), at the base of which there are floodplain clays.

The geological structure of landslide blocks of the middle part of the slope is not the same then the structure of the blocks in the lower part of the landslide massif. The section of the second landslide block is characterized by a certain elevation (relatively to the position within the unbroken sections of watershed plateau) of the boundaries of all the suites by 2-3 m. In the lower part of the landslide block, the thickness of the clays of the Oxfordian stage does not change. Above the section, for the clays of the yermolinskaya strata (the tops of the Oxfordian stage-the bottoms of Kimmeridgian stage), the aleurite-sand formations of the Tithonian-Berriasian stages, a reduction of each of the suites on 1-2 m is typical. A deluvial cover of redeposited Lower Cretaceous sands forms the upper part of the section of the second landslide block.

The geological structure of landslide blocks of the upper tier differs from the structure of the blocks in the middle and lower parts of the landslide massif "Vorobyovy Gory". In contrast to the structure of the middle tier of landslide blocks, where relative elevation of stratigraphic boundaries is observed, the opposite picture is observed for the upper part of the landslide massif. All stratigraphic boundaries within the upper block are reduced by approximately 1.5-2 m. However, for landslide blocks of the upper tier, as well as the structure of the middle tier of landslide blocks, the thickness of all the suites is reduced by 1-2 m, increasing in the upper part of the Lower Cretaceous formations up to 4 m.

Thereby, based on the peculiarities of the variability of the geological structure of landslide blocks, the mechanism of displacement of the modern large-scale landslide massif "Vorobyovy Gory" can be characterized as following. At the initial stage, because of moistening the upper part of the oxford clay, their transition to a plastic state occurred, which led to extrusion of clays in the direction of lowering the relief. At the same time, with the landslide movements in the lower part of the slope and the adjacent part of the river bed, aridge compression was formed, as evidenced by an increase in the thickness of the clay of the yermolinskaya strata (the upper Oxfordian stage - the bottom Kimmeridgian stage) by more than twice. In some stages of landslide displacement, because of a change in the orientation of the overlying sediments, a landslide block collapsed, accompanied by tipping (by toppling mechanism), disintegration and the subsequent formation of a landslide body in the form of a sand-clay avalanche. As the result of deformations in the lower part of the slope, a regressive development of landslide displacements with the separation of blocks has occurred in its upper part. The landslide blocks that were broken during the displacement tested tipping to the side of the slope, as evidenced by the somewhat elevated (relatively undisturbed massif) position of the stratigraphic boundaries in the middle of the slope and their reduced position in the upper part of the slope.

Separately, it should be noted that the development of the modern large-scale landslide massif "Vorobyovy Gory" occurred within the relict landslide massif (Barykina et al, 2017, 2019).

The third type of deformations developed on the slope can be attributed to relatively shallow landslides, which only capture the upper part of the geological section. With the development of these displacements, the deformation zone does not leave the Lower Cretaceous sandy-argillaceous deposits. The zone of shear deformations is located at depths of up to 20 m. This is confirmed by the drilling data, which showed, in particular, the doubling (in relation to unbiased parts) of the Apt sand deposits.

Study of the reconsolidation of clay soils

For the Mesozoic - Cenozoic clays of study area, degrees of reconsolidation from 2 to 12.6 were obtained, and a sharp increase of this indicator in a small range of depths is noted.

This effect can be largely due to the influence of the cover glaciation of this territory, in the epoch of which some of the rock strata could be in a frozen state and therefore have a much lower compressibility; therefore, the role of long-term consolidation could be significantly reduced.

As a result, the ratio between the degree of reconsolidation, on the one hand, and the maximum geostatic pressure tested by the soils in the past, and, on the other hand, with indicators of their physical and physical-mechanical properties, reflects not only the scale of denudation and maximum geostatic pressure, but also the impact (both stress and temperature) of the ice cover.

Morphological features of the microstructure of the Jurassic clays

The difference in composition, conditions of accumulation and post-sedimentation transformation of clayey material leads to a large variety of microstructures of clayey rocks, which in turn determines significant variations in the properties of these rocks. In order to identify these features, the microstructure of the three samples considered above was studied: podmoskovnaya, kolomenskay suite sand yermolinskaya strata. The X-ray phase analysis of the samples showed that the podmoskovnaya and yermolinskaya strata are characterized by a high content of smectite (42% and 58%, respectively), while the kolomenskaya suite contains 7% smectite and 37% zeolite. Samples taken from the podmoskovnaya suite and yermolinskay astrata contain 10 and 7% quartz, respectively, and 8 and 13% calcite. Whereas the kolomenskaya suite sample contains 22% quartz and 14% calcite. It should be noted that the pyrite content in the sample of the podmoskovnaya suite is high, up to 7%, and almost two times lower in the samples of the yermolinskaya strata and kolomenskaya suite (4% each).

The main features of yermolinskaya strata clays microstructure are oriented microstructure, composed of elongated carbonate clay aggregates with rare microbial skeletons (Fig. 3).

The main features of kolonenskaya suite clays microstructure are weakly oriented microstructure, composed of more isometric clay-dusty aggregates with rare sand grains of quartz and plagioclases(Fig. 3).

The main features of podmoskovnaya suite clays microstructure are undirected microstructure, composed of isometric aggregates of clay minerals with the inclusion of numerous residues of microfauna skeletons(Fig. 3).

Conclusions

Thus, based on the newly obtained data, the following conclusions can be drawn. Firstly, the territory involved in landslide processes on the Vorobyovy Gory is characterized by much larger values, both in area and in depth, than it was previously assumed, which is confirmed by the drilling data.

The revealed, deepest zones of landslide deformations are not modern as their displacement basis is located essentially below the modern level of erosion cut. Probably, deep zones of landslide deformations are the relict ones formed in the epoch of formation of the pre-glacial valley of the Moskva River.

The current observed landslide displacements are confined to either gypsometrically located oxford clays or quaternary sediments. They are secondary landslides within the boundaries of an ancient landslide massif.

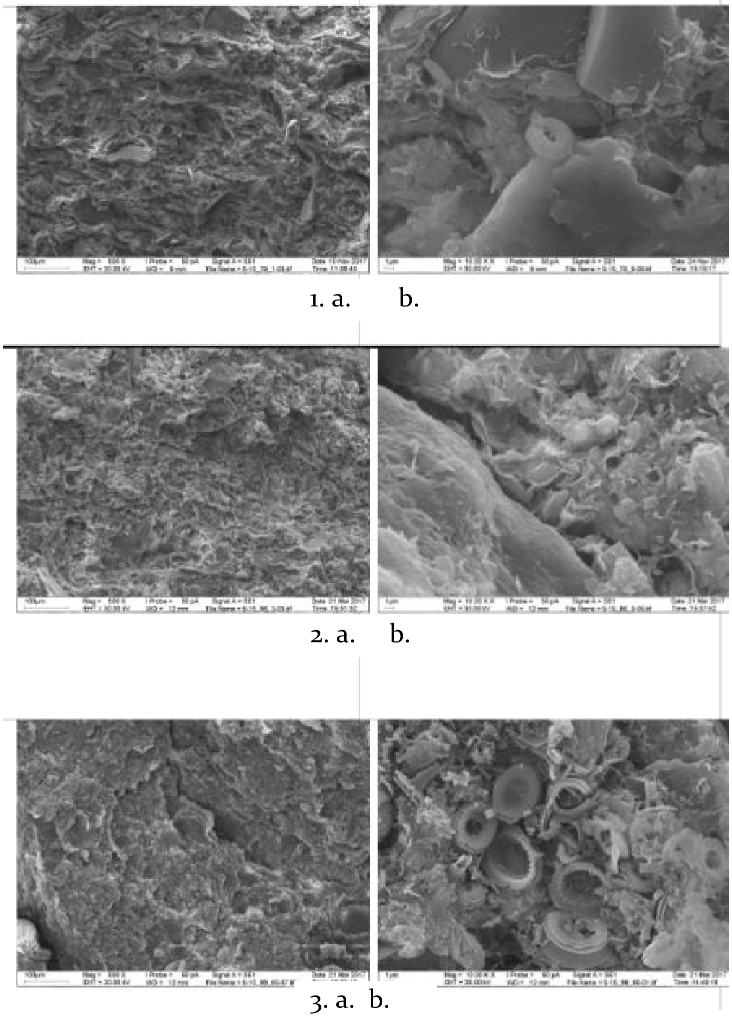

Figure 3 SEM images of Jurassic clay microstructure

1. Yermolinskaya strata: a. Increase x500. b. Increase x10000
2. Kolomenskaya suite: a. Increase x500. b. Increase x10000
3. Podmoskovnaya suite: a. Increase x500. b. Increase x10000

In the head part, where the displacement zone is located at depths of 80-100 m, the deformations, confined to the lower part of the Jurassic deposits, have a block character. Secondly, one can speak of a combined mechanism for the development of a large-scale landslide massif "Vorobyovy Gory" (according to the terminology proposed by (International, 1993)), which includes plastic flow with the formation of a ridge compression, collapse with tipping, block displacement and other types of deformations. As a part of a landslide massif, it is possible to distinguish both primary and secondary displacements.

References

Barykina O.S., Zerkal O.V., Samarin E.N., Gvozdeva I.P. (2017) On the development of landslide processes on Vorobyovy Gory (Moscow). *Engineering-geological problems of the present and methods for their solution*: Proc.conf. Geomarketing. Moscow. pp. 111-117 (in Russian)

Barykina O.S., Zerkal O.V., Samarin E.N., Gvozdeva I.P. (2019) The History of Slope Evolution - Primary Cause of its Modern Instability (by Example of the "Vorobyovy Gory" Landslide, Moscow). Natural Hazards and Risk Research in Russia: Innovation and Discovery in Russian Science and Engineering. - Springer Publ. pp. 345-361 (ISBN 978-3-319-91832-7)

Churinov M.V. (1957) Description of landslides of the right bank of the Moskva River on the site of the Lenin Mountains and the possibility of building development of this territory. Questions of hydrogeology and engineering geology: Proc. VSEGINGEO. - Gosgeoltekhizdat. Moscow. 15. pp. 62-78 (in Russian)

Danshin B.M. (1937) The geological structure of the Leninskie Hills in connection with some issues of the stratigraphy of deposits of the Cretaceous system and landslide phenomena along the banks of the Moskva River. *News of the Moscow Geological Trust.* 4. pp.3-23 (in Russian)

Danshin B.M. (1947) Geological aspects and mineral deposits of Moscow and its outskirts. *Bull. of Moscow Soc. of Naturalists*. 307 (in Russian)

Geological Atlas of Moscow, 2009

Golodkovskaya G.A., Lebedeva N.I. (1984) Engineering-geological zoning of the territory of Moscow. *Inzhenernayageologiya* [Engineering geology]. (3). pp. 87-102 (in Russian)

Gulakyan K.A., Kuntzel V.V. (1970) Classification of landslides by the mechanism of their development. Proc. VSEGINGEO. 29. pp. 58-64 (in Russian)

International Geotechnical Society's UNESCO Working Party on World Landslide Inventory (WP/WLI) (1993) *A multi-lingual landslide glossary*. Bitech Publ. Vancouver. 59

Korcheobokov NA, Romanov AV, Yakovlev S.Y. (1938) Landslides of the LeninskieGory. *Geology in the reconstruction of Moscow*. Academy of Sciences of the USSR. Moscow-Leningrad. pp. 377-390 (in Russian)

Kuntzel V.V. (1965) On the age of deep landslides in Moscow and the Moscow region, associated with Jurassic clay deposits. *Bull. Bull. of Moscow Soc. of Naturalists*. Subdiv. geol., XL (8), pp. 93-100 (in Russian)

Moscow. Geology and the city (1997). Eds. Medvedev O.P., Osipov V.I. Moscow textbooks and Kartolitographia. Moscow. 399 p. (in Russian)

Nikitin S.N. (1897) Les environs de Moscou. *Guide des excursions du VII CongresGeologique International*. St-Petersbourg. pp. 1-16

Olferiev A.G. (2012) Jurassic stratigraphic subdivisions of Moscow basin. *Bull. of Moscow Soc. of Naturalists*. Subdiv. geol., 87(4). pp. 32-55 (in Russian)

Paretskaya M.N. (1975) Dependence of the morphology of landslides extrusion of the Moscow suburbs on the strength of Jurassic clays. *Proc. VSEGINGEO*. 81. pp. 94-97 (in Russian)

Pavlov A.P. (1890) New data on the geology of the VorobyovyHills. *Bulletin of Natural Science*. (7). pp. 301-304 (in Russian)

Pavlov A.P. (1910) A note on the formation of landslides in clayey and clayey-sandy rocks. *Bull. of Moscow Soc. of Naturalists*. 4. pp. 29-30 (in Russian)

Pavlov A.V. (1911) *Memorandum to the Moscow City Council on the structure of the area along the pressure tank line - Yacht Club - Moscow River and the reasons for the slope of the uphill slope between the pressure tank and the eastern edge of the village Vorobyov.* City printing house. Moscow (in Russian)

Shkolin A.A., MalenkinaS.Y. (2015) Comparison of the types of sections of the Upper Jurassic (Volga level) -a lower chalk of the southeast of the Moscow region. *Jurassic system of Russia: problems of stratigraphy and paleogeography: Proc. VI Russian Workshop*. ALEF. Makhachkala. pp. 304-308 (in Russian)

Unified regional stratigraphic scheme of the Jurassic sediments of the East European Platform. Explanatory letter. (2012). V.V.Mitta, A.S.Alexeev, S.M.Shik, eds. GINRAS - FGUPVNIGNI. Moscow (in Russian)

Zerkal O., Barykina O., Samarin E., Gvozdeva I. (2017) The influence of paleo-landslide activity on the modern slope stability. *Proc. of 2017 IPL Symposium*, UNESCO-ICL, Paris. pp. 89-92

Landslide Risk Assessment, Mapping and Management

Valentina Svalova

Sergeev Institute of Environmental Geoscience RAS, Ulansky per., 13, Moscow 101000 Russia, v-svalova@mail.ru

Abstract The problem of geological and landslide risk management is seen as series of events leading to risk reduction, including Risk analysis, Risk assessment, Risk mapping, Vulnerability evaluation, Concept of acceptable risk, Monitoring organization, Engineering-technical methods, Insurance and others. Methodology for landslide risk assessment and mapping at urban areas is elaborated. The construction of landslide risk map in the territory of Moscow is suggested.On the basis of preliminary expert estimates, the areas of high landslide risk are in the vicinity of Moscow River and Yauza River, as well as in the areas of contrasting relief along riverbeds of paleorivers in the city center. These areas may be considered as "hot spots" on the risk map.

Keywords landslide, risk, risk assessment, risk management

Introduction

The problem of landslide risk management is seen as series of events leading to landslides risk reduction. Natural risk is a relatively new and not fully explored concept. There are many definitions of natural risk. And often a scientific study or a scientific approach to the problem begins with a presentation of the author's position and the choice of the definition of natural risk for the problem. This individualistic approach is difficult to avoid. Spores are carried out so far. For example, if there is a risk without material damage to people or not.

If one of the main systematic approaches to hazards research is their classification so now also the concept of Risk Management can be considered as new step of science development and new basement for systematic hazards investigations.

Development of the Risk concept demands the promotion of the methods for Risk Assessment and calculation. It makes the theory of Risk the scientific discipline with good mathematical background. It is necessary to elaborate common approaches to the risk calculation for different types of natural hazards. The methods of seismic risk assessment as the most promoted ones must be spread to landslides, karst, suffusion, flooding, pollution and other types of natural hazards and risks and also to complex and multi-risk.

Arising from everyday life, gambling, finance, business and building the Risk concept became the subject for scientific research and basement for systematic investigations of natural and man-made hazards and disasters.

In common sense Risk is the potential possibility to gain or lose something (life, health, property, money, environment etc.) Risk situation can arise at meeting with uncertainty resulting from action or inaction. Risk is a consequence of unpredictable outcome.

In Risk-Analysis science Risk is considered as a measure of the probability of damage to life, health, property, money or the environment. Risk is defined as the probability of the natural hazard event multiplied by the damage from possible consequences.

Risk analysis is the use of available information for hazard identification and vulnerability evaluation.

Vulnerability is the degree of loss of a given element or set of elements exposed to the occurrence of a natural or man-made hazard. It is expressed on a scale of 0 (no loss) to 1 (total loss).

Risk assessment is considered as the process of making decision on whether existing risk is acceptable or non-acceptable and implies the risk analysis and risk evaluation processes.

Sometimes Risk Assessment is considered as Risk calculation on the base of selected parameters and establishment of ranking risk criteria.

Acceptable risk is defined by the level of human and property loss that can be tolerated by an individual or community. The probability of acceptable risk is very small. The concept of acceptable risk arises from the understanding that absolute safety is an unachievable purpose

Risk management is considered as the complete process of Risk assessment and Risk reduction.

Risk reduction implies some methods and measures, as legislative, organizing, economic, engineering, information and others.

Sometimes in narrow sense Risk Management is considered as measures for Risk Reduction.

And in this sense the problem of Landslide Risk Management is seen as a series of events leading to landslides risk reduction and avoiding. It includes landslides monitoring, landslide forecast, engineering works, slopes strengthen, insurance and others.

Summarizing systematic approach to natural hazards research on the base of the Risk concept it is possible to present the next steps and scheme to establish criteria for ranking risk posed by different types of natural or man-made hazards and disasters, to quantify the impact that hazardous event or process have on population, structures and to enhance strategies for risk reduction and avoiding.

Risk Management

1. Hazard Identification;
2. Vulnerability evaluation;
3. Risk analysis;
4. Concept of acceptable risk;
5. Risk assessment;
6. Risk mapping;
7. Measures for risk reduction:
1) legislative;
2) organizational and administrative;
3) economic, including insurance;
4) engineering and technical;
5) modeling;
6) monitoring.
7) information.

According to the most common definition the Risk is the probability of the natural hazard event multiplied by the possible damage:

$R = PxD$,

where R - risk, P - probability, D - damage.
For multi-risk assessment it is possible to use sum of risks of different hazards:

$R = \sum Ri$

For Risk Maps construction it is necessary to use the Natural Hazards maps and maps of possible damage. These maps can be of local, regional, federal (sub global) and global levels.
Landslide is a major geological hazard, which poses serious threat to human population and various other infrastructures like highways, rail routes and civil structures like dams, buildings and others.
Landslides occur very often during other major natural disasters such as earthquakes, floods and volcanoes.
The word 'landslide' represents only a type of movement that is slide. However it is generally used as a term to cover all the types of land movements including falls, creep, spreads, flows and other complex movements.
A correct term to represent all these movements may be 'mass movement' or 'mass wastage'. However the term 'landslide' has been accepted and is being used commonly around the world as a synonym of 'mass wastage'.
Some main aspects of landslides risk management are considered.

Landslides risk assessment and mapping

Geological risk mapping is an important step towards solving the problem of natural risk management [1, 8, 19-25]. Due to the complexity and diversity of the problem the combination of probabilistic and deterministic approaches and expert estimates arises.
The probability of landslide process depends on the stability of the landslide slope, trigger mechanisms (precipitation, earthquakes), technological factors. The first step is studying the physical and mechanical sliding process at different conditions. Nevertheless, the landslide process mechanics is still not fully understood. Landslide prediction is not always possible. Even statistical frequency of landslides activation for a particular area varies very widely.
As an example to be considered the approach to the construction of the landslide risk map in the territory of Moscow.
Landslide processes in Moscow are well investigated [2-7, 9-18]. Landslides cover about 3% of the city, where there are 15 deep and a lot of small landslides , and the landslide hazard is mapped. Last years in Moscow there is a significant activation of landslide processes. To assess the landslide hazard the height of the slope, the landslide body volume, mass velocity, rock properties, topography of the surrounding area, the range of possible promotion landslide masses, hydrogeological conditions and trigger mechanisms have to be taken into account. Selection of taxons (special areas) varying degrees of landslide hazard in the city is completely solvable task. And gradation is possible as in the three degrees of danger (high, medium, low) as in five ones (very high, high, medium, low, not dangerous), depending on the detail of the task.
The most expensive land and buildings in Moscow are located in the city center, where are also the oldest historic buildings, the most vulnerable to natural hazards, and the most expensive new ground and underground construction, subway lines, complex traffic, and technical communications of high density. There is an increased density of population. We can assume that the closer to the center of Moscow, the greater the potential damage from possible landslide process.
Hazardous industrial production brought to Moscow's periphery. But the protected zone of Moscow on the Vorobiovy Hills and in Kolomenskoye also have high cultural value, and the potential damage there is highly evaluated. So a first approximation map of landslide risk in Moscow may be an overlay of landslide hazard maps and population density, building density, land prices, density of roads and infrastructure maps. Areas with the highest degree of landslide hazard and the highest damage are the areas of the highest landslide risk in the territory of Moscow.
The methodology for risk evaluation and mapping is suggested.
For the automated analysis of the factual material and the risk maps construction it is needed to find the intersection of the landslide hazard map and integrated

map of possible damage t.e. for each i - th fragment Ri of risk map to find the product of probability Pi of landslide event to the amount of different j - th possible damages from landslides, that could be damage to land, to buildings, to transport, to communications, to people and others:

$$R_i = P_i \sum_j D_{ij}$$

Maps of landslide hazard is necessary calibrated from 0 to 1, to reflect the probability of landslide events ($0 \le P \le 1$). Thus, gradation, for example, is possible on a scale of (0; 0,25; 0,5; 0,75; 1), where 0 corresponds to no danger of landslides, 0.25 - low, 0.5 - average 0.75 - high and 1 - a very high probability of the landslide process. This assessment is an expert in nature. In principle it is possible to construct the landslide hazard maps as the intersection of maps of factual material, such as map of relief contrast, rock strength, slope stability, speed of motion of the surface, the density of rainfall, seismicity, etc. Of course, this will require additional research and evaluation.

For a comprehensive assessment of the damage in each region it is suggested to calibrate the possible damage of each option on a three-point system (0, 1, 2), where 0 means no damage, 1 - middle, 2 - high damage. The parameters here are, for example, 1) cost of land, 2) cost of housing, 3) density of buildings, 4) population density, 5) density of roads and communications. The higher the value (the value of land, housing, etc.), the greater the damage in case of a hazardous event.

Then, the possible damage to 5 parameters for each element varies from 0 to 10.

The risk also in each element ranges from 0 to 10. This is the risk in relative terms (high-low), on 10-point scale.

$$D_i = \sum_j D_{ij},\ j = 1\text{-}5,\ D_{ij} = (0, 1, 2),\ 0 \le D_i \le 10,$$
$$0 \le R_i \le 10.$$

After defeating the map of the area into squares and calculating the risk for each square, you can get a map of the area at risk on 10-point scale.

On the basis of preliminary expert estimates, it will be the areas in the vicinity of Moscow River and Yauza River, as well as in the areas of contrasting relief along riverbeds of paleorivers in the city center.

The places of high landslide risk are Andronievskaya embankment (Figs. 1, 2), Nikolo-Yamskaya embankment (Fig. 3), Kotelnicheskaya embankment (Fig. 4), Samotechnaya Street (Fig. 5) in the center of Moscow.

Fig. 1. Andronievskaya embankment with Svjato-Andronikov monastery.

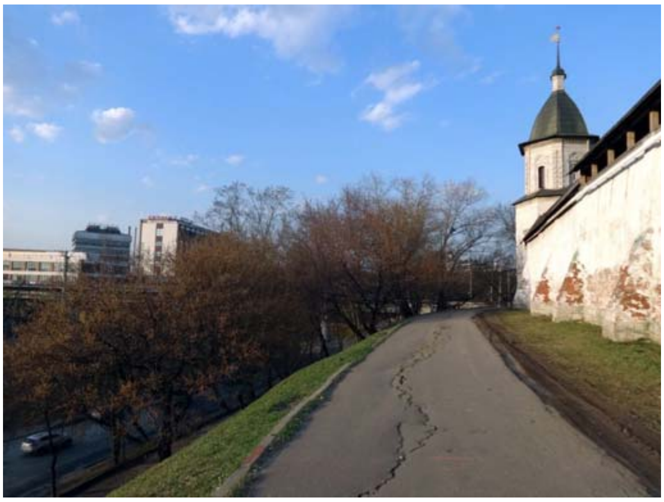

Fig. 2. Cracks near Svjato-Andronikov monastery

Fig. 3. Nikolo-Yamskaya embankment

Fig. 4. Kotelnicheskaya embankment

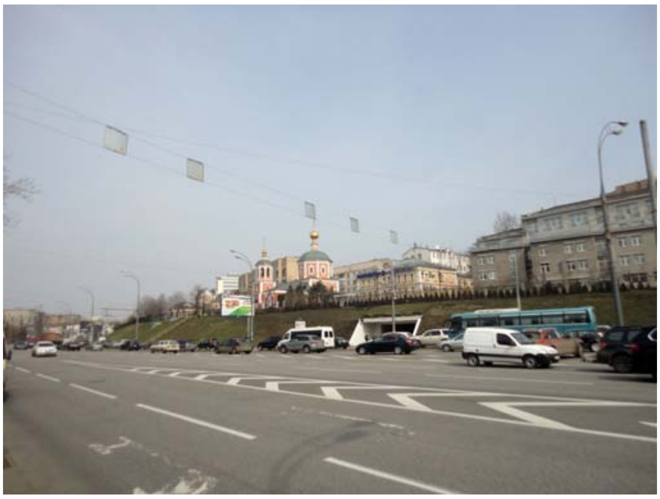

Fig. 5. Samotechnaya Street.

The places of highest landslide risk are Vorobiovy Mountains (Hills) (Figs. 6,7) and Kremlin Hill. (Figs. 8, 9). They are shown as white circles in the map of geological danger in Moscow. (Fig. 10).

Fig. 6. Vorobiovy Mountains with Moscow State University, ski-jumps and metro-bridge.

Fig. 7. Vorobiovy Mountains with building of Presidium RAS (Russian Academy of Sciences), Andreevsky monastery and new living houses.

Fig. 8. Kremlin embankment.

Fig. 9. Center of Moscow with Kremlin hill and Moscow river.

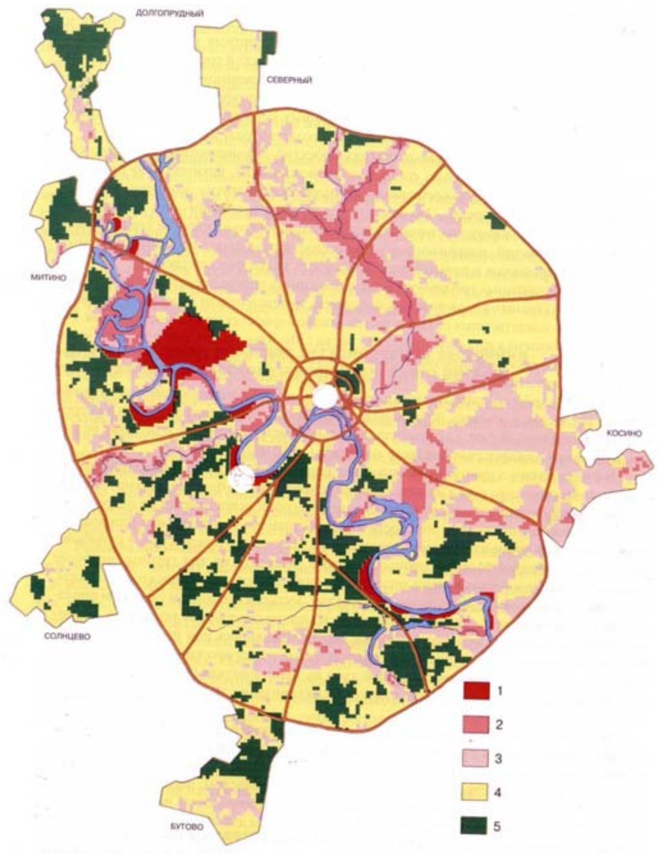

Fig. 10. Map of geological danger in Moscow. Landslides, karst, underflooding. (Osipov V.I., Kutepon V.M., Mironov O.K.) [3]. Landslides are near rivers in semi-dark (red and pink).

1 - very high danger, 2 – high, 3 - middle, 4 – low, 5 – no. White circles – risk "hot spots". Kremlin hill (center) and Vorobiovy Mountaims (south-west).

These areas may be considered as "hot spots" on the risk map. And even thought in some of these areas, the population density is not so high, the other components (cost of land, the historical importance of the object, the density of underground utilities and others) give a great contribution to the high risk assessment.

These areas must be at measures for risk management and reduction at the first line. It means monitoring organization, slope strengthen, ban of extra buildings and activity.

As additional fact it is interesting to use night cosmic photo of Moscow that reflect the density of communications and possible damage. (Fig. 11).

Fig. 11. Cosmic photo of Moscow at night.

References

1. Corominas J, van Westen C, Frattini P, Cascini L, Mallet J-P et al (2014) Recommendations for the quantitative analysis of landslide risk. Bulletin of Engineering Geology and Environment 73(2): 209-263
2. Kutepov VM, Sheko AI, Anisimova NG, Burova VN, Victorov AS et al. (2002) Natural hazards in Russia. Exogenous geological hazards. Moscow, KRUK
3. Kutepov VM, Postoev GP, Svalova VB (2004) Landslide hazards estimation on sites of modern and historical constructions in Moscow. Proceedings of 32 IGC, Italy, Florence, 2004
4. Osipov V, Medvedev (eds) (1997) Moscow. Geology and town. Moscow textbooks and kartolitografiya, Moscow
5. Osipov VI, Shojgu SK, Vladimirov VA, Vorobjev YuL, Avdod'in VP et al (2002) Natural hazards in Russia. Natural hazards and society. Moscow, KRUK
6. Postoev GP, Erysh IF, Salomatin VN et al. (1989) Artificial activation of landslides. Russia. Moscow, Nedra.
7. Postoev GP, Svalova VB. (2005) Landslides risk reduction and monitoring for urban territories in Russia. Proceedings of the First General Assembly of ICL (International Consortium on Landslides), Landslides: risk analysis and sustainable disaster management, Washington, USA, Springer, 297-303.
8. Ragozin A (ed) (2003) Natural hazards of Russia. Evaluation and management of natural risk. Moscow, KRUK
9. Svalova VB (2001) Mechanical-mathematical modeling and monitoring for landslide processes. Journal of Environmental Science nd Engineering 5(10): 1282-1287
10. Svalova VB (2011) Monitoring and modeling of landslide processes. Monitoring. Science and technology 2(7): 19-27
11. Svalova VB (2011) Landslide process simulation and monitoring. Proceedings of ENGEOPRO, Moscow
12. Svalova VB (2012) Mechanical-mathematical modeling and monitoring for landslides. Proceedings of IPL (International Program on Landslides) Symposium, UNESCO, Paris
13. Svalova VB (2014). Modeling and Monitoring for Landslide Processes. In: Linwood K (ed) Natural Disasters - Typhoons and Landslides - Risk Prediction, Crisis Management and Environmental Impacts. Nova Science Publishers, New York, p.177-198.
14. Svalova VB (2014) Mechanical-mathematical modeling and monitoring for landslide processes. IPL 163 Project. Proceedings of the World Landslide Forum 3. V. 4. Beijing, China. 24-27.
15. Svalova VB (2014) Modeling and monitoring for landslide processes: case study of Moscow and Taiwan. Proceedings of the World Landslide Forum 3. V. 4. Beijing, China. 628-632.
16. Svalova VB (2015) Mechanical modeling and geophysical monitoring for landslide processes. Proceedings of IAEG XII Congress "Engineering geology for society and territory" , v.2, Torino-2014, Italy, Springer. 345-348
17. Svalova VB (2016) Monitoring and modeling of landslide hazard in Moscow. Engineering protection 1 (12): 34-38
18. Svalova VB, Postoev GP (2008) Landslide Process Activization on Sites of Cultural Heritage in Moscow, Russia. Proceedings of the First World Landslide Forum 2008, Tokyo, Japan
19. Svalova VB (2016) Monitoring and reducing the risk of landslides in Taiwan. Monitoring. Science and technology 3:13-25.
20. Svalova VB (2016) Analysis of landslide risk in Taiwan. "Commonwealth", Russia-China scientific journal 4: 136-141
21. Svalova VB (2016) Analysis and management of risk of landslides. Scientia. Physics and Mathematics 2: 28-31
22. Svalova VB (2016). Reducing the risk of landslides. Uniform All-Russia Scientific Bulletin 2(3): 79-83.

23. Svalova VB (2016) Landslides modeling, monitoring, risk management and reduction. EESJ(East European Scientific Journal , Poland) 7(11): 43-52
24. Svalova VB (2016) Risk analysis, evaluation and management for landslide processes. Sciences of Europe (Praha, Czech Republic) 4 (6): 15-25
25. Svalova V (2017) Landslide Risk: Assessment, Management and Reduction. Nova Science Publishers, New York

Impact of low shearing resistance of ash deposit on post-fire rainfall induced debris flow

Binod Tiwari[1], Beena Ajmera[2], Rupert Bernett[1]

1) California State University, Fullerton, Office of Research and Sponsored Project, Fullerton, 1121 N. State College Blvd, ASC-230, USA e-mail: btiwari@fullerton.edu

2) North Dakota State University, Department of Civil and Environmental Engineering

Abstract Wild-fires are considered as one among very common natural disasters that are causing a significant loss of lives and properties globally. Due to global warming and climate change, loss due to the wild-fire induced natural disasters are increasing annually. While wild-fires directly trigger property loss and death by burning vegetation and trees, buildings, and other infrastructures, another secondary but very common disaster triggered by the wild-fire is post-fire debris flows. The number of post-fire rainfall induced debris flows have significantly been increased in recent years. One among such disastrous events is Montecito Debris Flow event of 2018 in Santa Barbara County of California. Soil test results on the soil and ash deposit collected from the Montecito debris flow area suggests that the residual friction angle of the ash deposit is one-third of that of the parent soil. This along with the increase in seepage velocity due to the loss of vegetation cover has been attributed to be the major triggering factors for the Montecito debris flow event. This paper includes the details of the field situation and shear test results that lead to the authors' conclusion pertinent to the debris flow trigger.

Keywords post-fire debris flow, residual friction angle, ash deposit

Introduction

Uncontrollable, unplanned blazes in areas of ignitable vegetation are known as wildfires. Wildfires also called brush fires, desert fires, vegetation fires, wildland fires, hill fires, grass fires, peat fires, etc. These fires often start unobserved, fueled by vegetation and spread by wind, they can quickly engulf hundreds of acres of land within a few hours igniting trees, homes, agricultural resources and almost anything else that they come in contact with. Verisk's 2017 Wildfire Risk Analysis found that 4.5 million homes in the United States were at high or extreme risk of wildfire. Among these, more than 2 million are in California (more than double the second riskiest state of Texas). Over the past decade, damages in excess of $5.1 billion from wildfires have been reported. Until July 3, 2019, over 20,000 wildfires burning over 1.12 million acres have been reported in the United States (National Interagency Fire Center, 2019). About 8.8 million acres were burnt in 2018 from over nearly 58,100 wildfires (National Interagency Fire Center, 2019). In 2017, nearly 71,500 wildfires were responsible for burning about 10 million acres, exceeding the 10-year average for the country (National Interagency Fire Center, 2019).

The Thomas Fire started on December 4, 2017. It burned approximately 300,000 acres of vegetation in the Santa Barbara and Ventura Counties, California, destroyed over 1000 buildings, 2 fatalities and caused damages exceeding $2.2B. Declared contained on January 12, 2018, the Thomas Fire was the largest wildfire in California's history. While the fire was ongoing, the affected area saw a series of heavy rainfall events, which triggered debris flow events in the city of Montecito in Santa Barbara County, CA at 11:30 am GMT on January 9th, 2018. These debris flow events resulted in 21 fatalities (plus another 2 missing individuals, who were presumed dead) and injuries to over 160 people. The debris flow events are also estimated to have caused at least $177 million in property damage, approximately $7 million in emergency responses (RND, Inc. 2018), and $43 million for the clean-up (Noozhawk, 2018). Over 60 residential buildings were completely damaged with an additional 450 residential buildings having partial damage. Partial damage was observed in 20 commercial buildings while 8 commercial buildings were completely damaged. In addition to the damages to the buildings, 10 to 12 feet of debris accumulated on major highways, including US 101, and local streets. The debris flow events also resulted in the loss of utilities including water, power and gas. Mudslides and debris mass blocked or washed away bridges and culverts. Figure 1 shows the debris carried in the flows.

Figure 1 Debris found in the Montecito debris mass.

Field Investigation

The field conditions after the Montecito debris flows were investigated through on-site visits and high resolution images released for public use by Google as a response to the federally declared emergency. Aerial views of the debris flow area before and after the wildfire and debris flow events are shown in Figure 2. The figure illustrates the complete loss of vegetative cover following the wildfire. Additionally, the wildfire was responsible for leaving thick deposits of ash on the ground surface and changing the properties of the top soil due to the high heat. As a result of the ash deposits, a reduction of the permeability of the soil corresponding to a substantial increase in the run-off can be expected. The exposure to the high heat from the wildfire caused a brittle and cracked surface prone to localized seepage. The high resolution imagery also indicated that the debris flow events resulted in a widening of the creek from 2 to 3 m to 20 to 40 m in width. Furthermore, evidence of loose debris mass with the potential to flow along the channel bed could also be found from the images. Two drainage basins in the area were completely filled by the debris (consisting of tree branches, roots, boulders, etc.) The debris, then, overflowed into the community, onto local roads and highways and about 100 m into the Pacific Ocean. Despite the large amount of debris involved in January 9th event, a significant amount of loose debris was still present along the creek channel with the potential to flow in the event of an intense rainfall in the future.

Laboratory Soil Testing

During the field investigations, several soil samples were collected from the bank of the creek. Any large boulders or coarse gravels were excluded from the laboratory investigations presented in this study. Results from sieves analyses (ASTM D 6913/6913M, 2017) and Atterberg limit tests (ASTM D4318, 2017) indicated that the materials classified as SP-SM (poorly graded sand with silt and gravel) and SW-SM (well graded sand with silt and gravel) per the USCS classification system.

The residual shear strength of the soils was also determined for two conditions – (a) for the soil matrix and (b) ash deposit on the soil matrix with ash to represent the condition of the soil following the Thomas wildfire. The residual shear strength measurements were conducted at normal stresses of 100, 200, 400 and 800 kPa using a GDS ring shear apparatus. The results, as shown in Figure 3, indicate that the residual shear strength of the ash in soil matrix reduced to less than one third of the original strength of the soil. This indicates that once a slope fails from the hill and the debris mass runs over the ash deposit, the debris mass can easily increase its velocity and momentum to move down the slope and travel large distances very quickly due to the extreme low residual shear strength of the ash deposit on soil matrix.

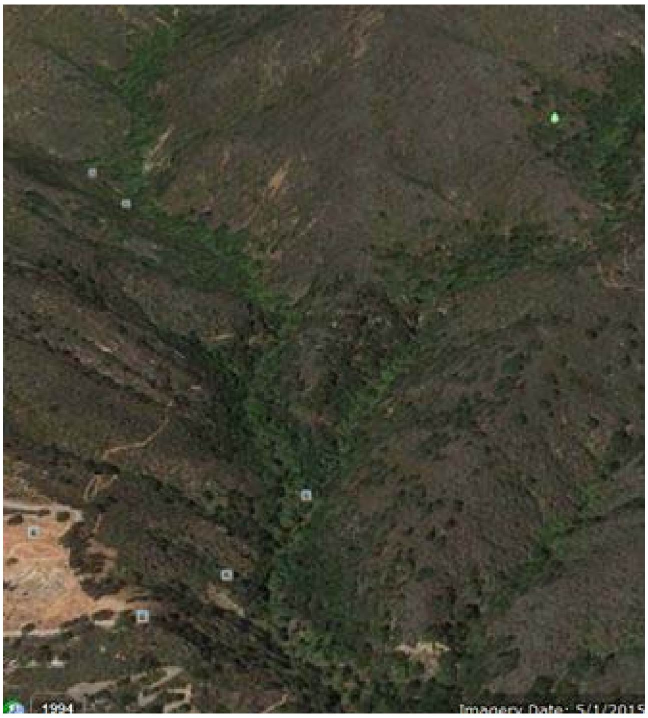

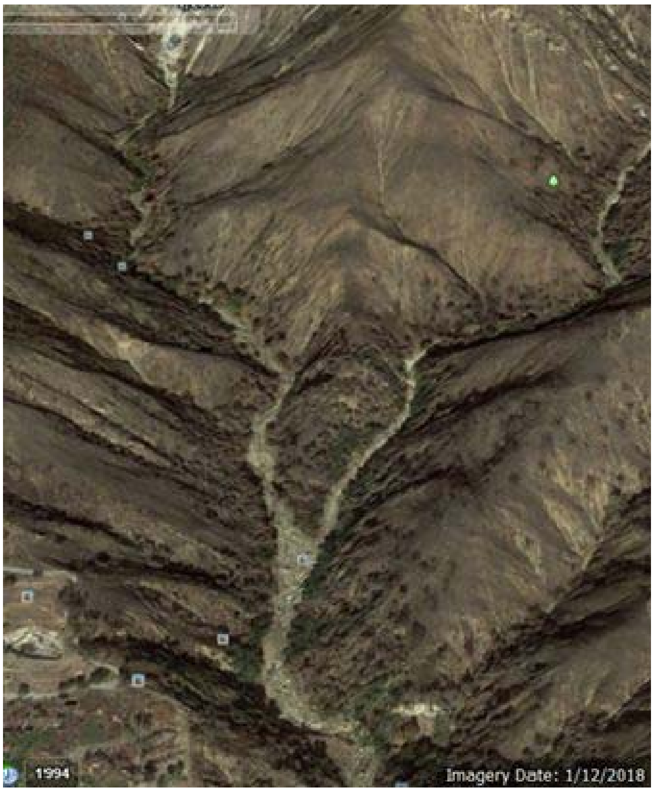

Figure 2 Google Earth imagery of the creek and watershed before (left) the Thomas Wildfire and after (right) the wildfire and Montecito debris flow events.

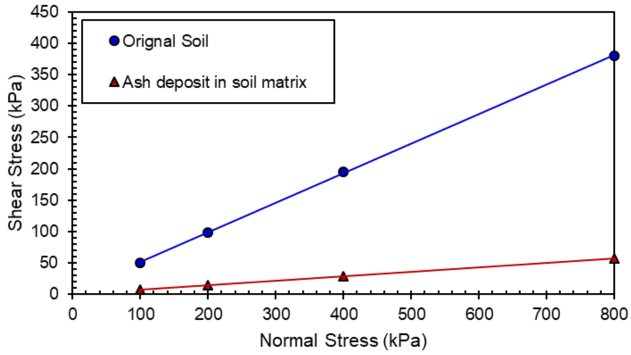

Figure 3 Residual shear strength failure envelopes for original soil and ash deposit in soil matrix.

Discussion

The Thomas wildfire, which affected the region at the same time, also contributed to the occurrence of the debris flow. As a result of the wildfire, there was a significant loss of the vegetation cover in the watershed. The extreme heat from the wildfire left the ground brittle with cracks that would allow localized seepage to occur. Furthermore, the vegetation cover was replaced by deposits of ash from the wildfire. The ash not only contributed to a reduction in the permeability of the top soil resulting in an increase in the run-off, but also provided a slippery surface for the moving debris mass quickly for a large run out distance, specifically due to a very low residual shear strength of the ash deposit on the soil matrix, which was less than one third of the residual shear strength of the original soil in the area. Finally, large quantities of debris were available along the creek channel to cause extensive damage to the area. All of these factors combined with the high rainfall intensity-duration in the January 8th to January 10th storm led to the triggering of the debris flows in the city of Montecito, CA.

Conclusion

The Thomas Wildfire that affected Southern California in December 2017 to January 2018 resulted in several fatalities and significant damage in the affected region. Furthermore, the wildfire left the city of Montecito in Santa Barbara County prone to a devastating debris flow following a high intensity rainfall in January 2018. Several causative factors contributed to the occurrence of this disaster. Specifically, the wildfire resulted in the replacement of the vegetative cover of the region with ash that resulted in a reduction in the permeability of the top soil and an increase in the run-off from rainwater. Residual shear strength measurements conducted in this study also showed that the strength of the ash deposit on the soil matrix was less than one third of the residual shear strength of original soil in the area. Therefore, the debris flow would be capable of moving at very high velocities. While the total monthly rainfall in the region was significantly lower than the rainfall in the previous years, the storm that triggered the debris flows was very intense having a rainfall intensity-duration significantly higher than the lower bound suggested by historical data for debris flows triggered in burn areas. The results from this study indicate that the debris flows occurring in Montecito after the Thomas Wildfire are a complex phenomenon.

Acknowledgement

Mr. Chris Doolittle from the Santa Barbara County is graciously thanked for providing access to the disaster area to the first author and for providing pertinent information regarding the debris flow event. The authors would like to acknowledge the support of the CSUF RCA grant that provided the financial support for this study.

References (in the alphabetical order)

ASTM D4318 (2017). "Standard Test Methods for Liquid Limit, Plastic Limit, and Plasticity Index of Soils," ASTM International.

ASTM D6913/6913M (2017). "Standard Test Methods for Particle-Size Determination (Gradation) of Soils using Sieve Analysis," ASTM International.

National Interagency Fire Center (2019). "National Interagency Fire Center Fire Information," https://www.nifc.gov/fireInfo/nfn.htm.

Noozhawk (2018). "County Estimates $46 Million Cost for Thomas Fire, Montecito Debris Flow Response, Repairs," https://www.noozhawk.com/article/county_estimates_46m_cost_thomas_fire_montecito_debris_flow_response.

RDN, Inc. (2018). "The Economic Impacts of the Montecito Mudslides: A Preliminary Assessment," RDN¸ Inc.

Update on the Landslide Research Program at the University of Alberta

Michael Hendry[(1)], Renato Macciotta [(1)]

1) University of Alberta, Edmonton, Canada

Abstract

The University of Alberta, as an ICL WCoE, continues a dynamic research program focused on landslide monitoring technologies and slow-moving landslide in heavily overconsolidated clays and (soft) shales in western Canada. This presentation will provide an overview of our new research area of the Assiniboine River Valley and an update on the research conducted at in the Thompson River Valley (the Ripley Landslide).

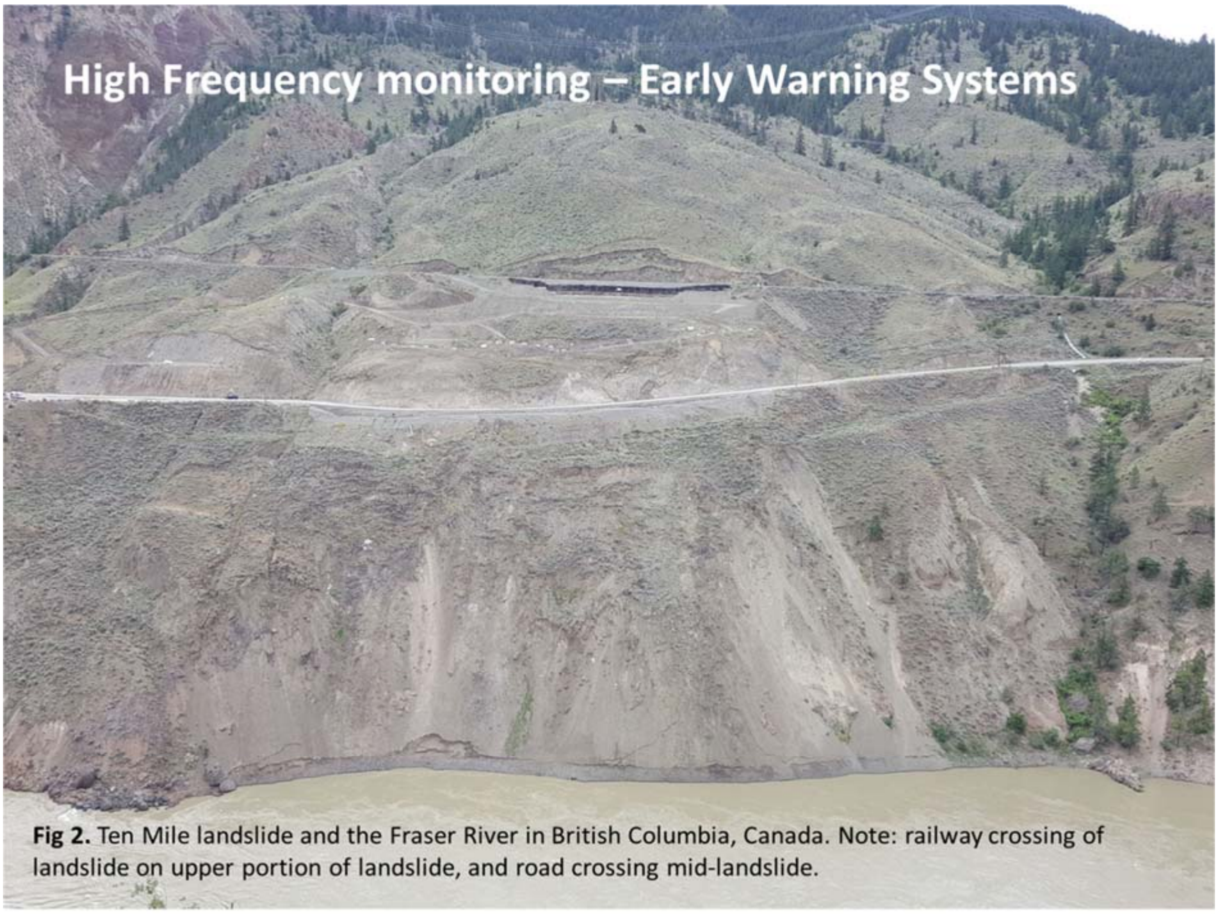

Fig 2. Ten Mile landslide and the Fraser River in British Columbia, Canada. Note: railway crossing of landslide on upper portion of landslide, and road crossing mid-landslide.

High Frequency monitoring – Early Warning Systems

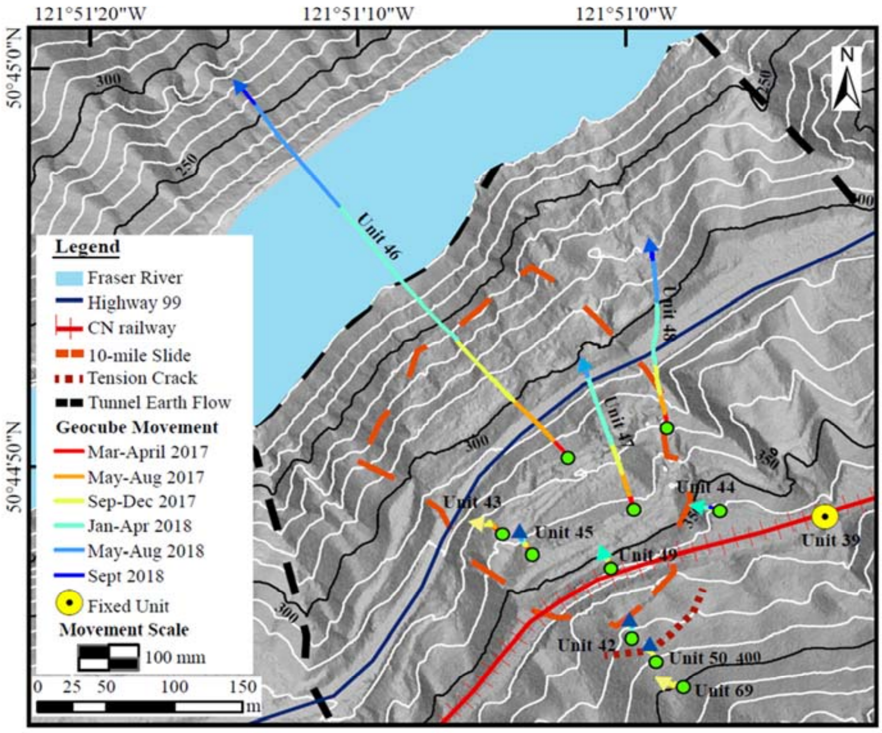

Fig 3. Cumulative displacement differing blocks of the Ten Mile landslide from displacement measurements taken at 5 minute intervals.

High Frequency monitoring – Early Warning Systems

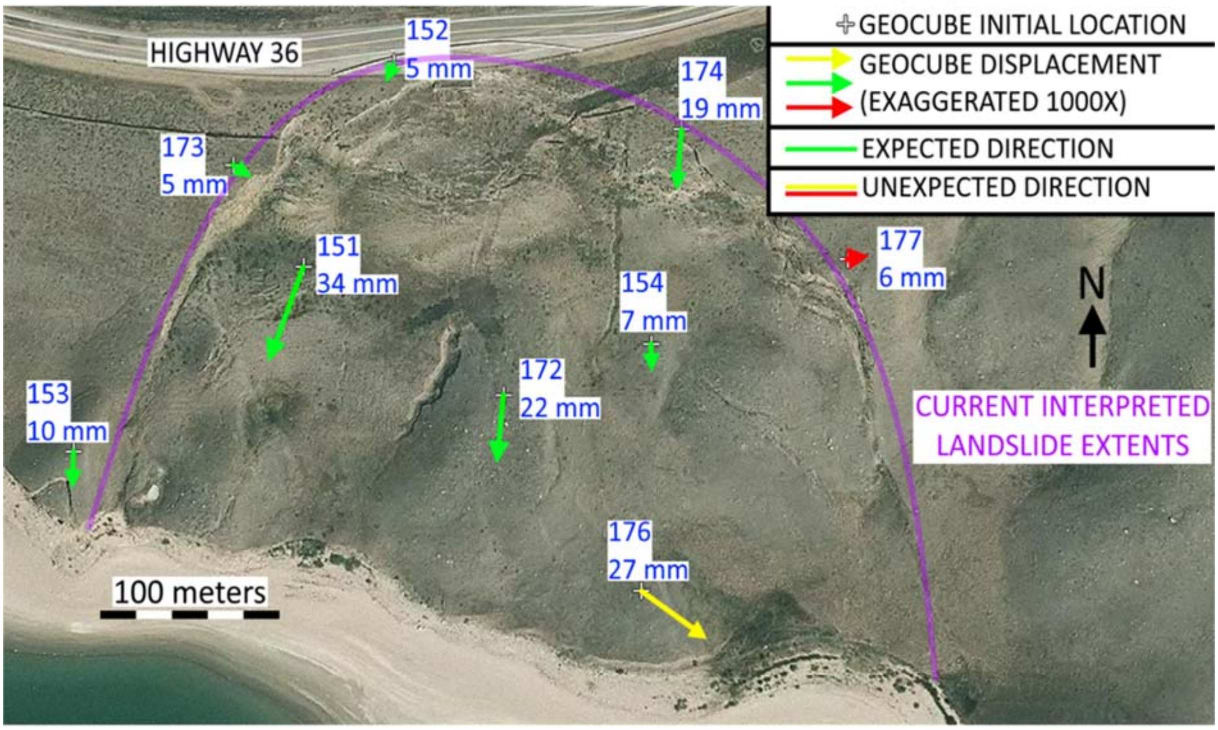

Fig 4. Cumulative displacement August 2018- August 2019 measured by GeoCubes installed at the Chin Coulee landslide in southern Alberta, Canada.

High Frequency monitoring – Early Warning Systems

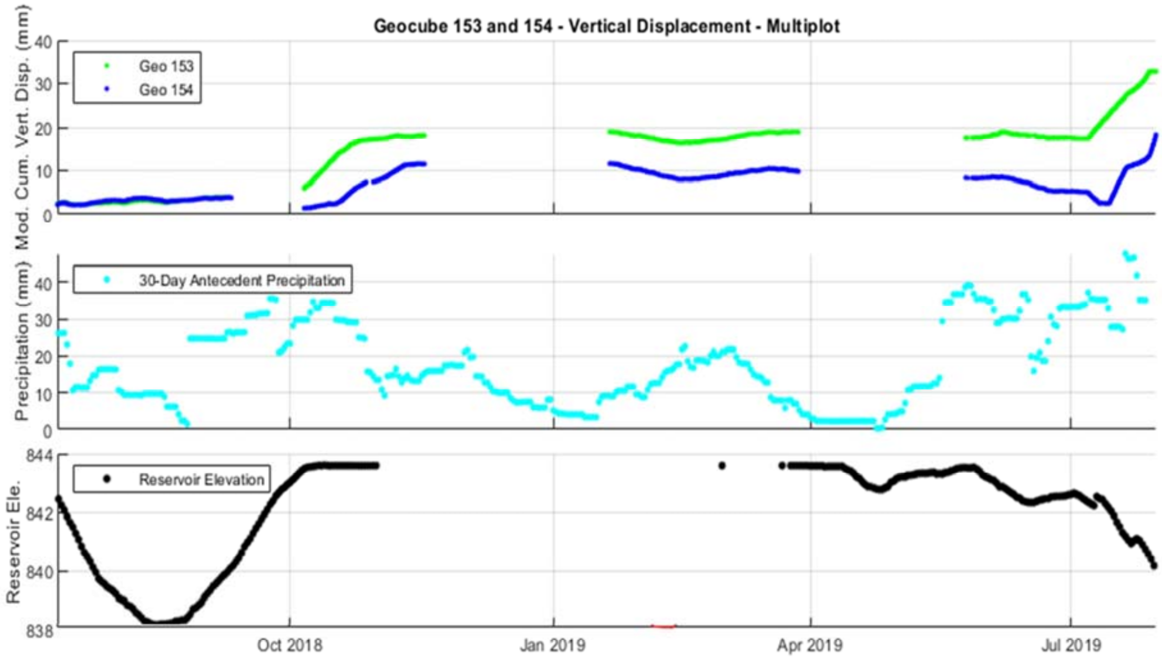

Fig 5. Geocube 176 horizontal displacement plotted versus 30-day antecedent precipitation and reservoir elevation for the Chin Coulee landslide in southern Alberta, Canada.

Remote Sensing - GB InSAR

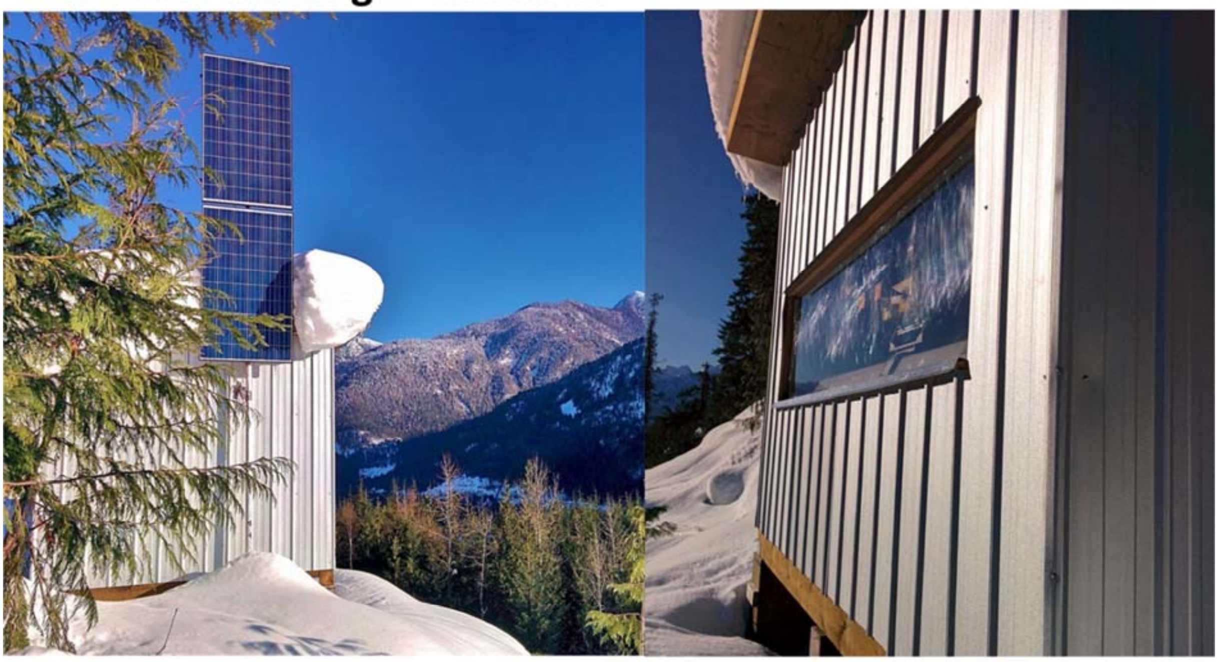

Fig 6. GB-InSAR installation up stream of the BCHydro's Revelstoke dam, British Columbia, Canada. Installation is monitoring the unstable slope at Checkerboard Creek. Note: location is remote without power supply, steep north-south valley, and some of the highest amounts of snow accumulation in Canada.

Remote Sensing - GB InSAR

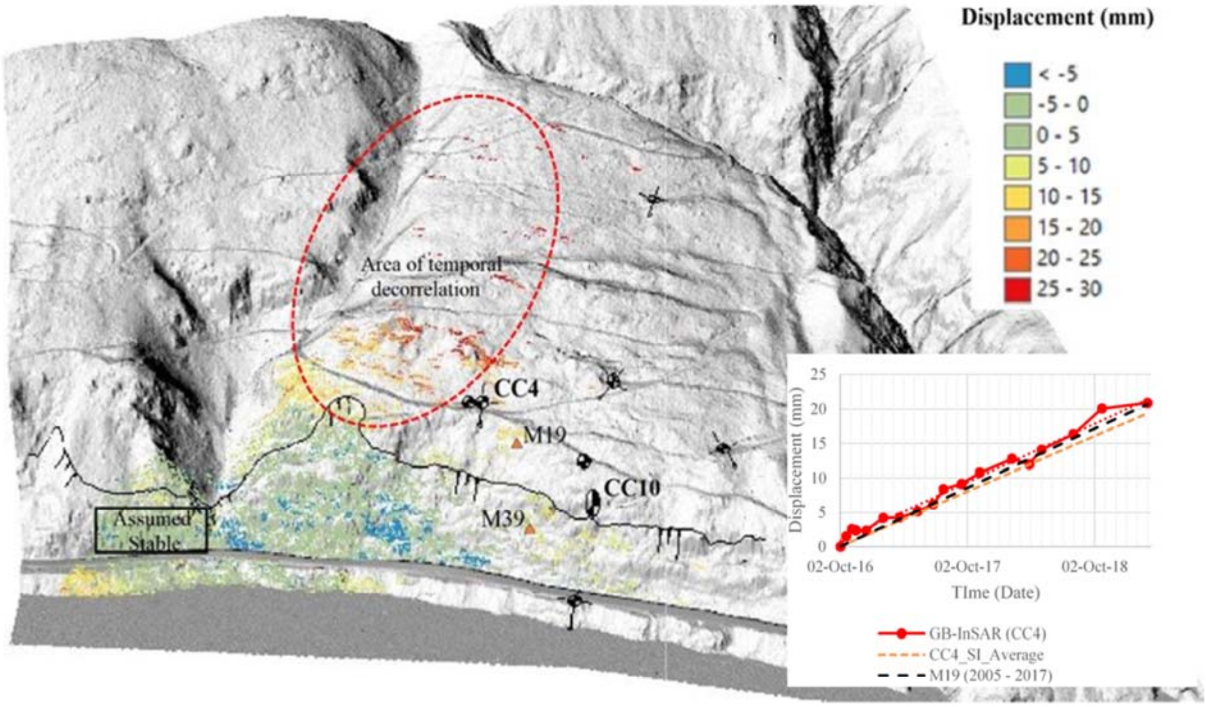

Fig 7. GB-InSAR cumulative LoS displacement map between November 15, 2016 and March 4, 2019. Locations of extensometer CC10 and slope inclinometer CC4 are noted. (*inset*) Cumulative displacement in LoS direction by discontinuous GB-InSAR compared to SI.

Fig 8. 3D model of unstable slope near Drumheller, Alberta, Canada. Monitoring of erosion processes preceding failure of slope.

Remote Sensing - Drone Photogrammetry

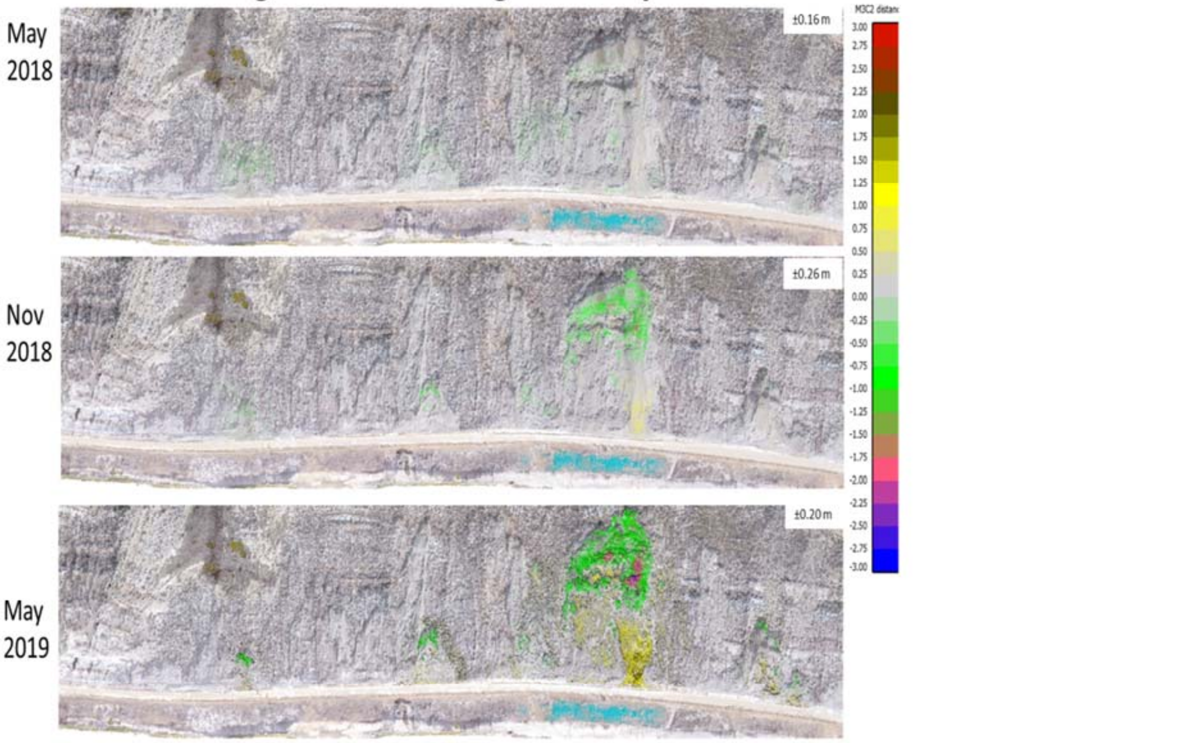

Fig 9. Drone photogrammetry used for quantifying the erosion processes that precede slope failures that impact roadway. And, development of monitoring program.

Remote Sensing - Historical Photogrammetry

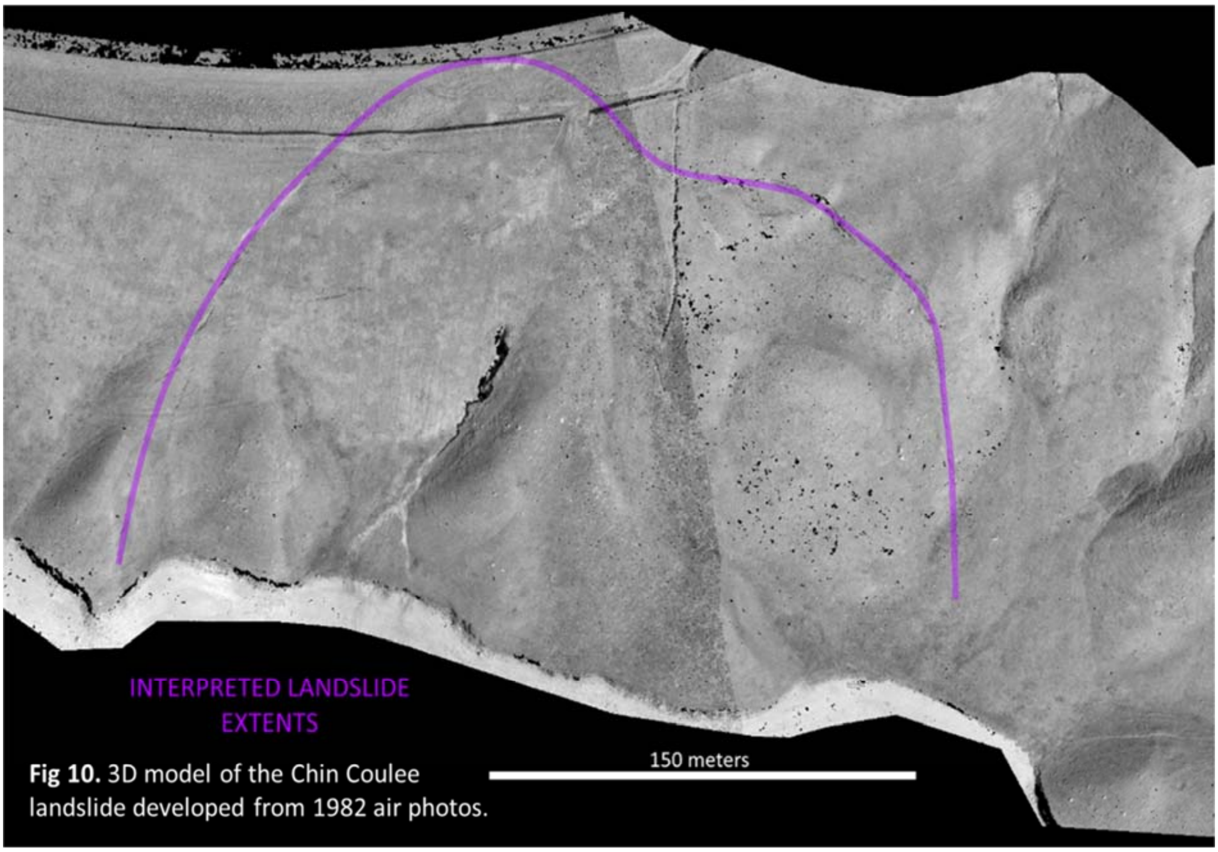

Fig 10. 3D model of the Chin Coulee landslide developed from 1982 air photos.

Remote Sensing - Historical Photogrammetry

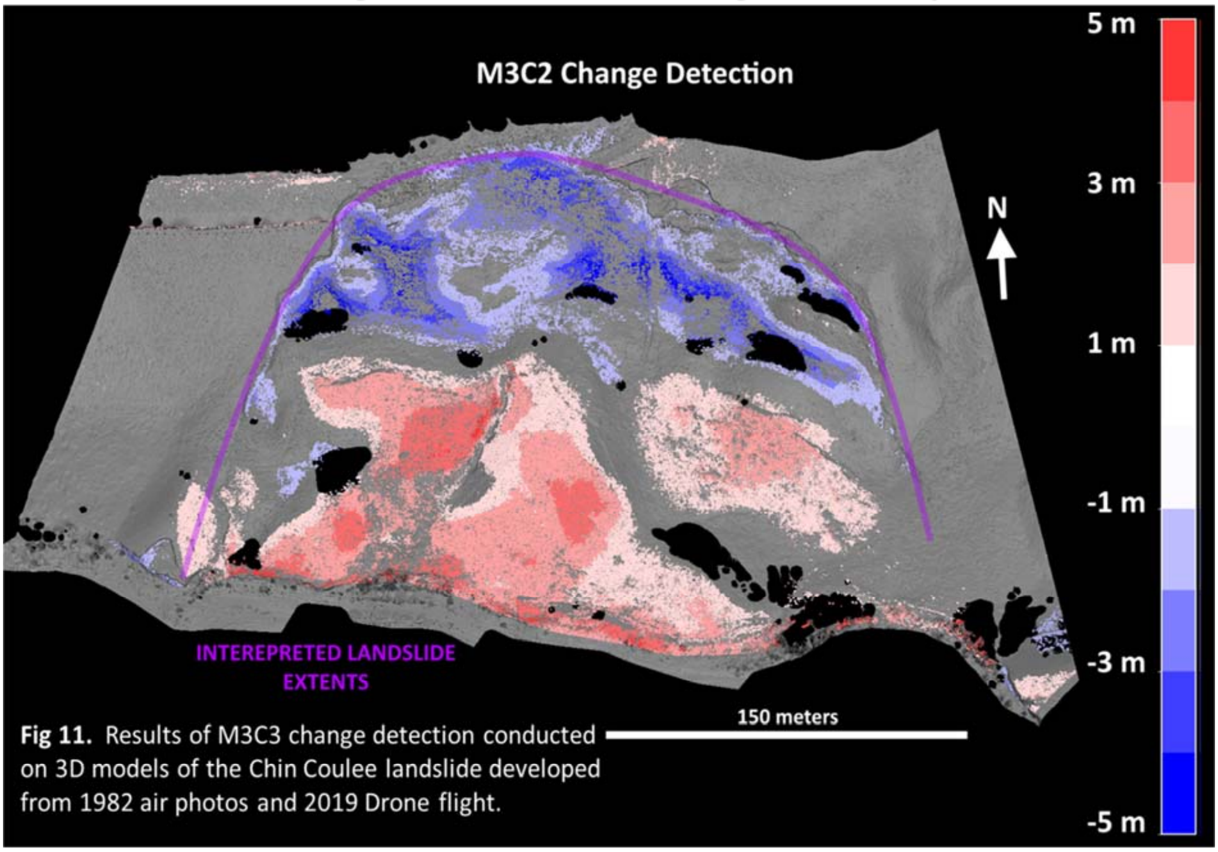

Fig 11. Results of M3C3 change detection conducted on 3D models of the Chin Coulee landslide developed from 1982 air photos and 2019 Drone flight.

Assiniboine River Valley Landslides

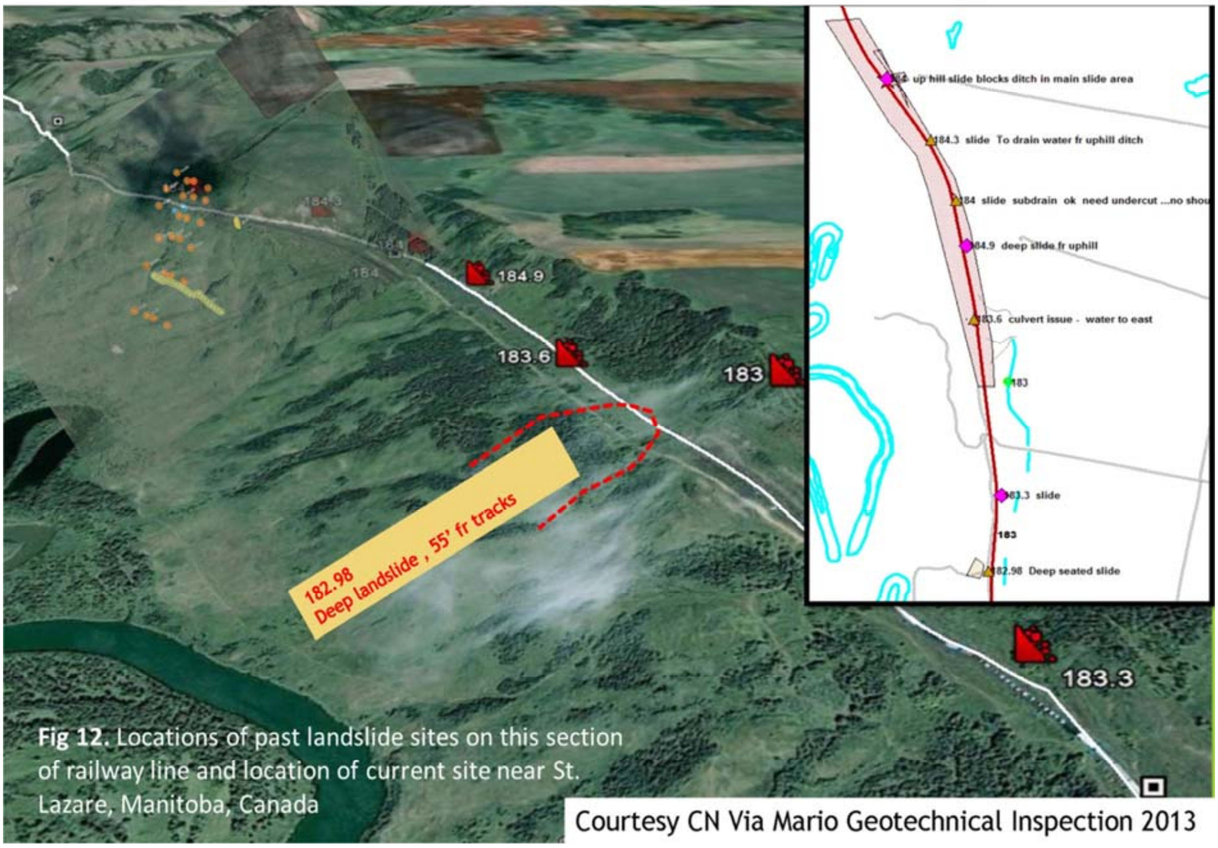

Fig 12. Locations of past landslide sites on this section of railway line and location of current site near St. Lazare, Manitoba, Canada

Courtesy CN Via Mario Geotechnical Inspection 2013

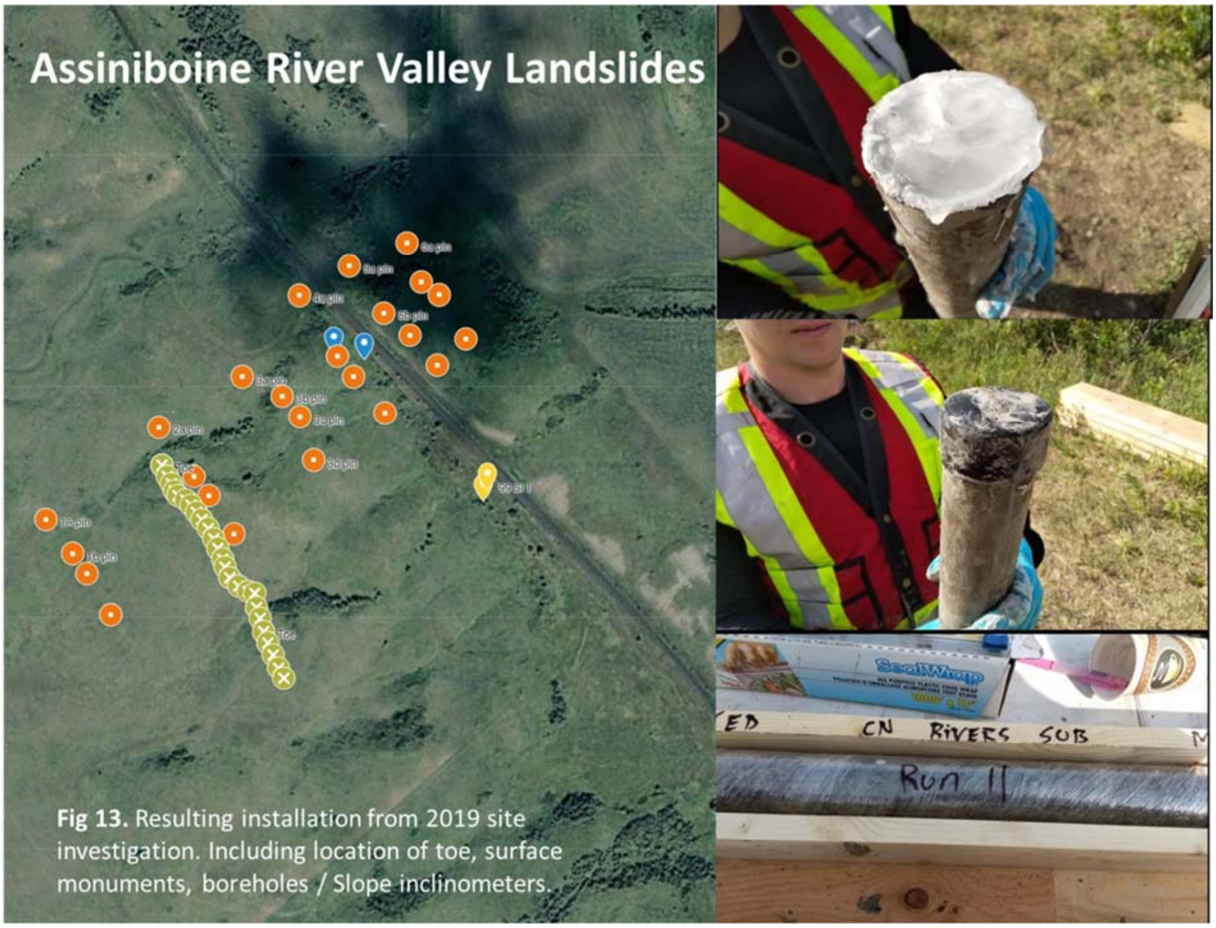

Fig 13. Resulting installation from 2019 site investigation. Including location of toe, surface monuments, boreholes / Slope inclinometers.

Landslide susceptibility mapping using GIS-based machine learning methods in Zigui basin, TGR, China

Prof./Dr. Changdong Li

China University of Geosciences, Wuhan, No. 388 Lumo Road, P.R. China
e-mail: lichangdong@cug.edu.cn

Abstract

The assessment and mapping of landslide susceptibility is crucial for the management and risk mitigation of such catastrophic geohazard in landslide-prone areas. In this presentation, a novel hybrid model based on machine learning algorithm has been developed and applied for landslide susceptibility prediction in Zigui basin, TGR, China. A database of landslide distribution in Zigui basin was first established using GIS based on remote sensing images, unmanned aerial vehicles (UAV) and field investigations. Next, self-organizing map (SOM) algorithm was used to produce a preliminary susceptibility map with four classified susceptibility zones, and two step cluster algorithm was applied to reduces the randomness of selecting the non-landslides in previous studies. Furthermore, random forest (RF) algorithm was adopted to obtain a trained SOM-RF model through labeled data set, with which the landslide susceptibility mapping in the study area was finally performed. The results show that most areas with high or very high susceptibility are located within the hydro-fluctuation belt of TGR. It's also found that the proposed SOM-RF model combined with TSC performs better prediction capacity than that of traditional RF model. Additionally, high robustness and low deviation of the proposed model are also verified.

Outline

1. Background
2. Case study
3. Discussion
4. Conclusions

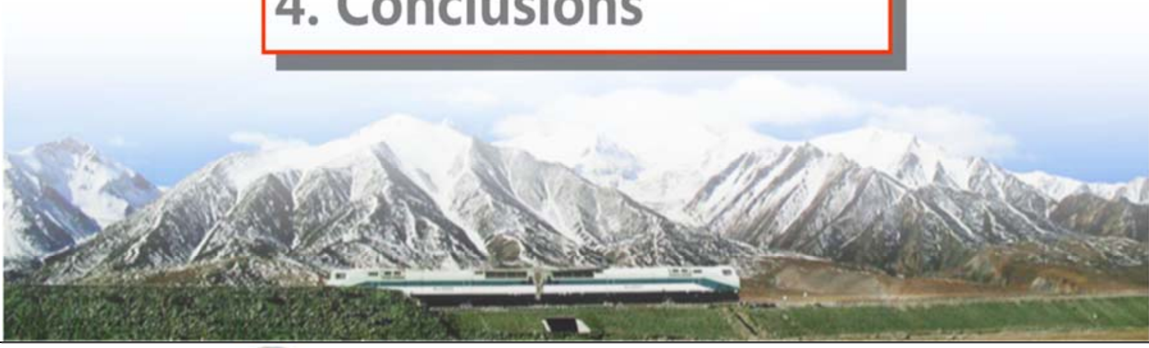

Statistics of Geo-hazards in China

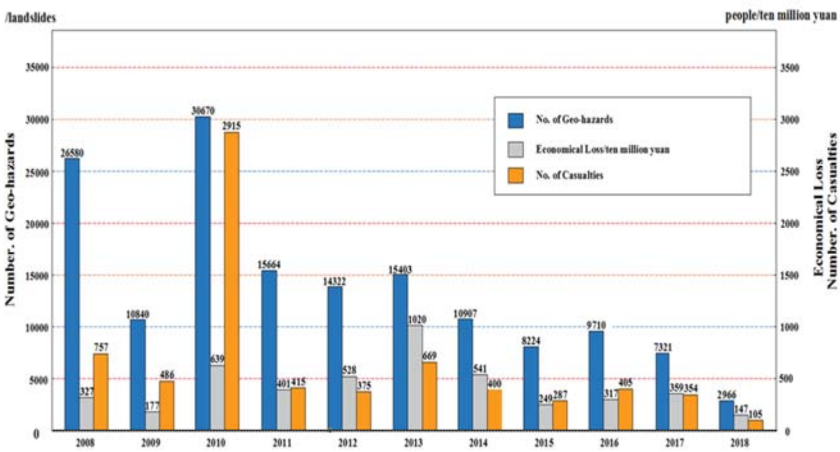

Geo-disasters in the past decade (Data from China Geological Survey)

Geo-hazards in Three Gorges Reservoir Area

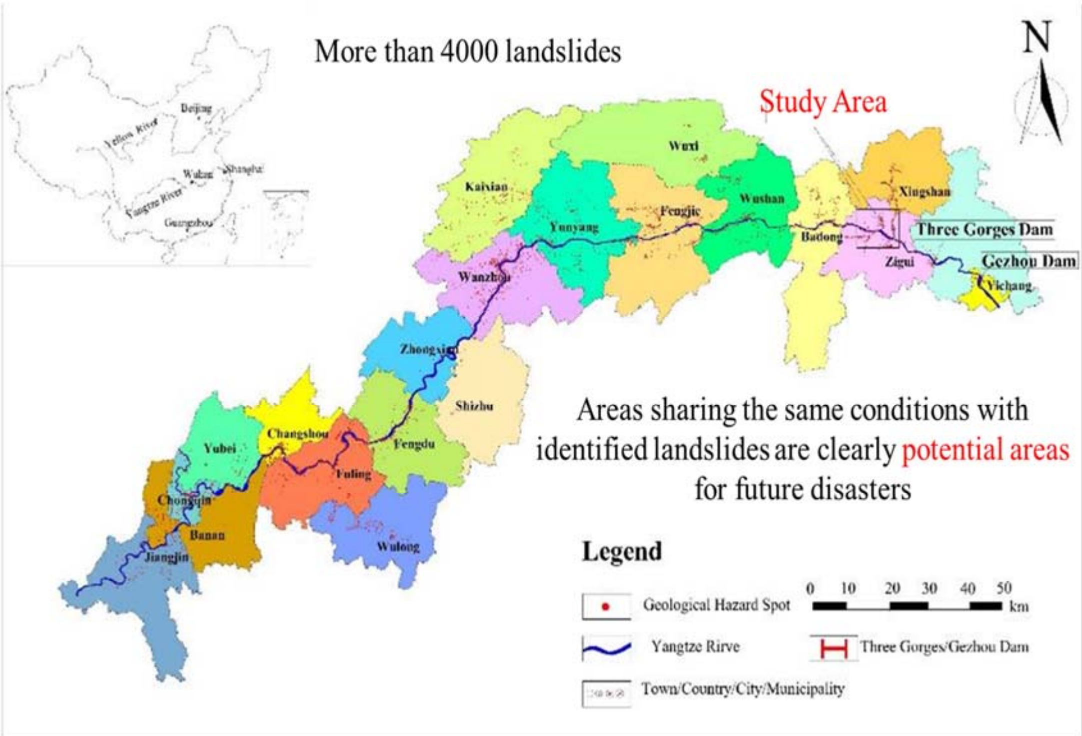

Existing methods in landslide susceptibility prediction

"3S" Technology: GPS, GIS, RS

Machine Learning: SVM, BP, DT

Underlying problems

1. Determination of influence factors
2. Selection of real non-landslide grid cells

Data collection

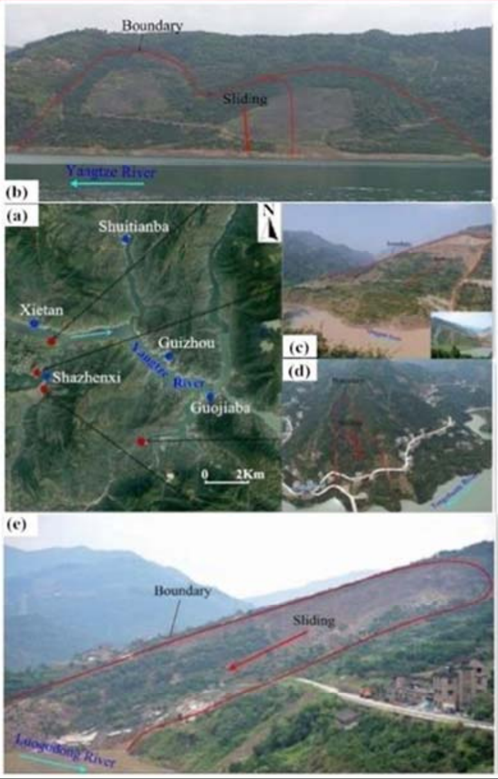

Multiple methods to obtain landslide information: field investigations and remote sensing (both from satellite and UAV), etc.

3D model by UAV images

Database establishment

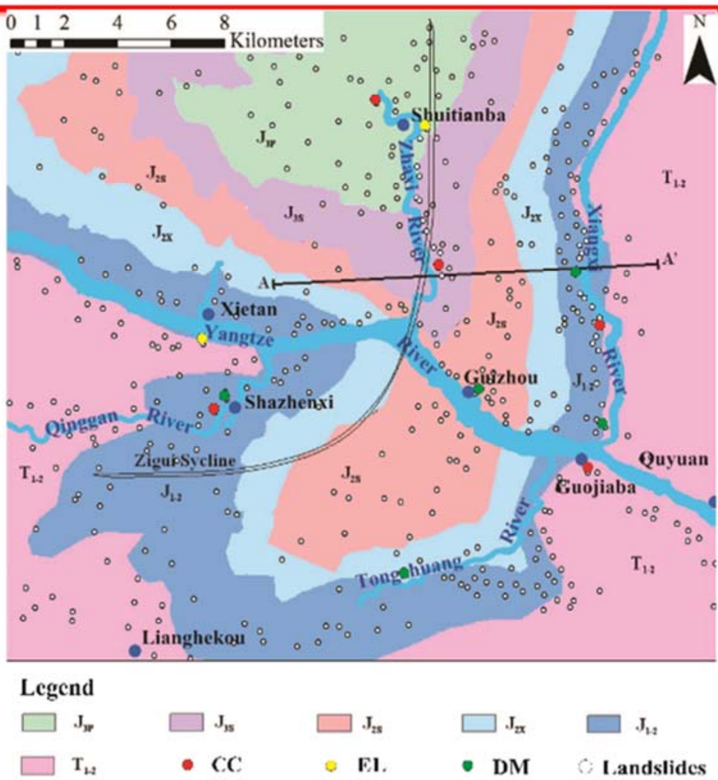

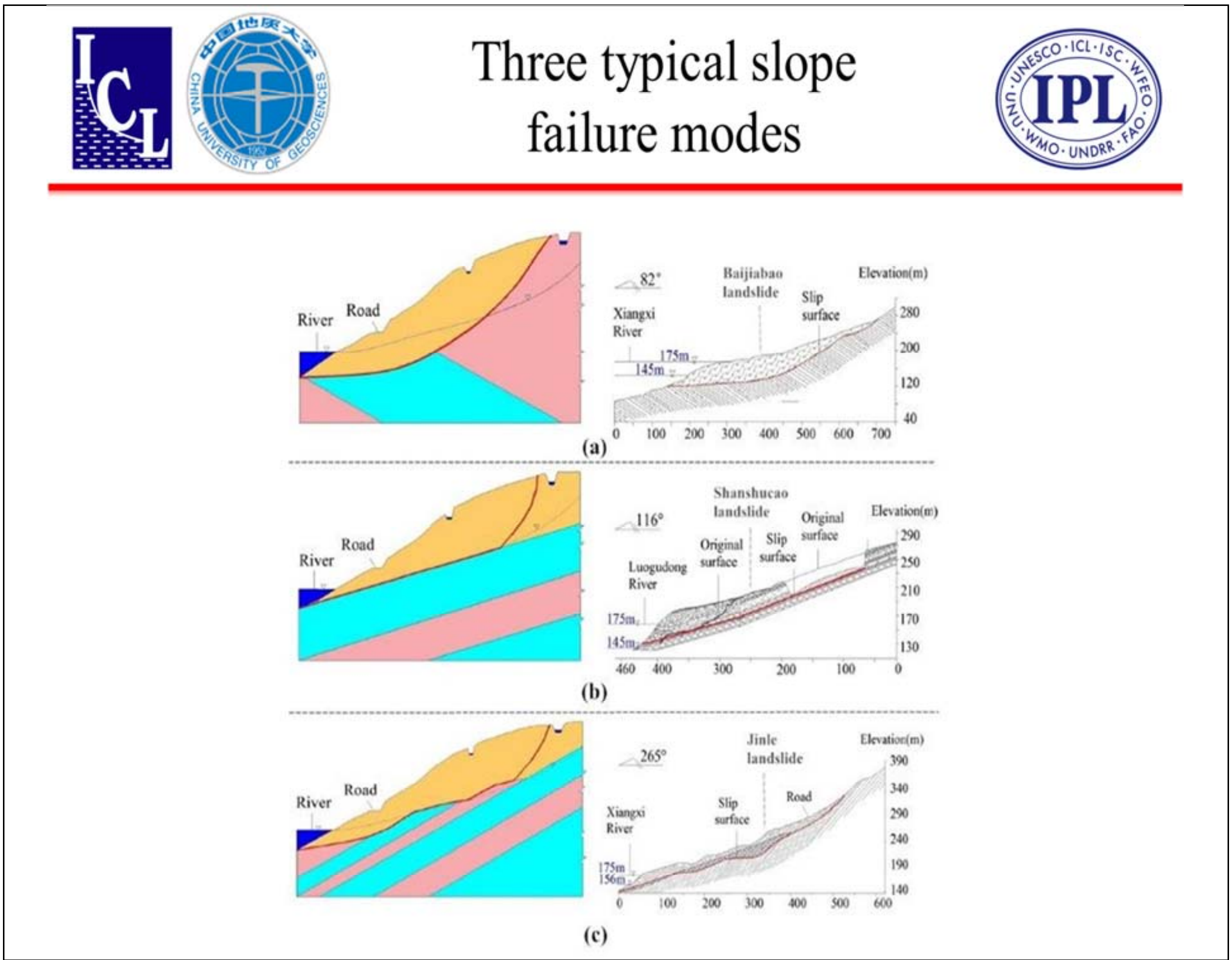
Three typical slope failure modes
River
Road
82°
Baijiabao landslide
Slip surface
Elevation(m)
Xiangxi River
175m
145m
(a)
116°
Shanshucao landslide
Original surface
Slip surface
Original surface
Elevation(m)
Luogudong River
175m
145m
(b)
265°
Jinle landslide
Road
Slip surface
Elevation(m)
Xiangxi River
175m
156m
(c)

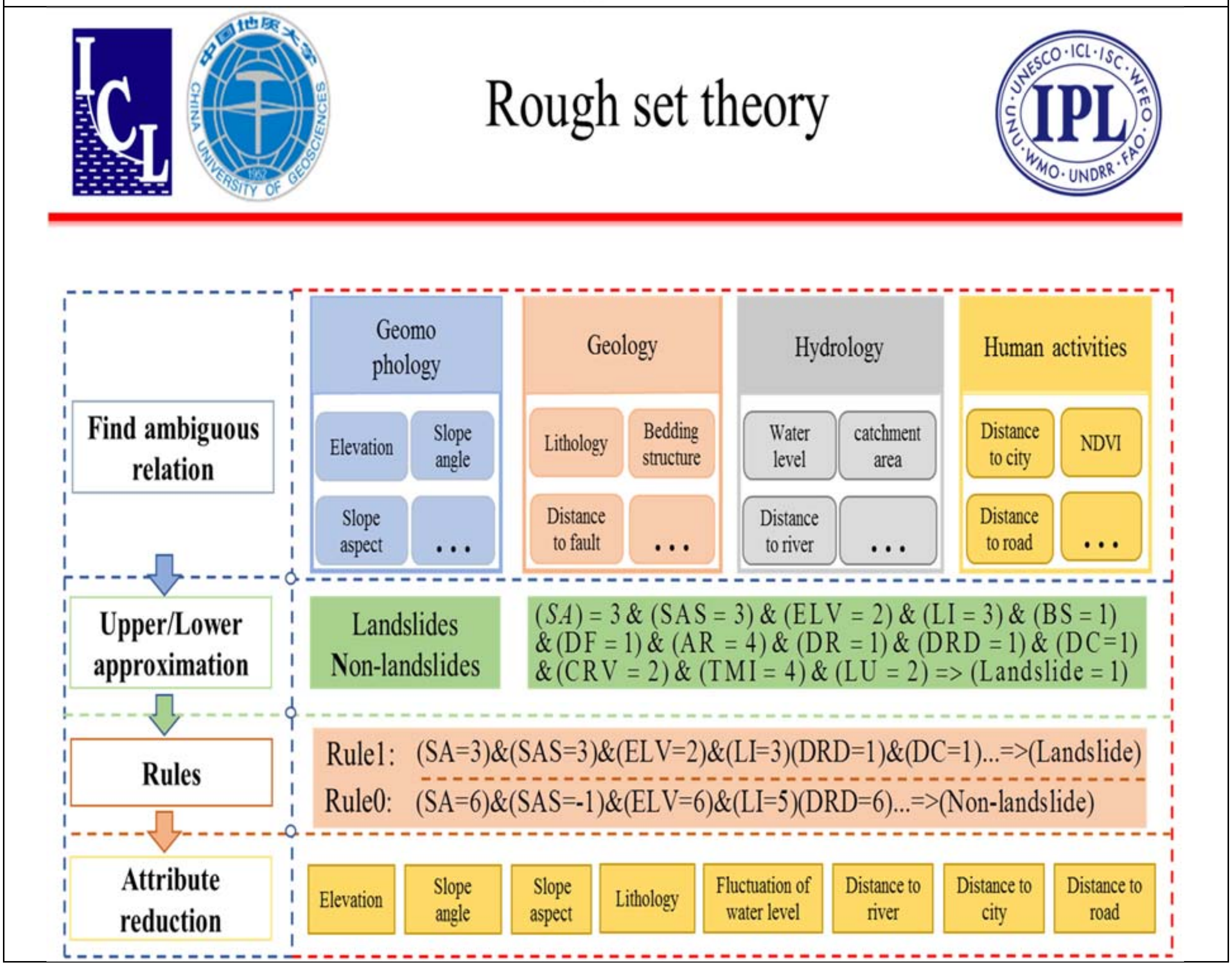
Rough set theory
Find ambiguous relation
Geomo phology
Elevation
Slope angle
Slope aspect
...
Geology
Lithology
Bedding structure
Distance to fault
...
Hydrology
Water level
catchment area
Distance to river
...
Human activities
Distance to city
NDVI
Distance to road
...
Upper/Lower approximation
Landslides
Non-landslides
(SA) = 3 & (SAS = 3) & (ELV = 2) & (LI = 3) & (BS = 1)
& (DF = 1) & (AR = 4) & (DR = 1) & (DRD = 1) & (DC=1)
& (CRV = 2) & (TMI = 4) & (LU = 2) => (Landslide = 1)
Rules
Rule1: (SA=3)&(SAS=3)&(ELV=2)&(LI=3)(DRD=1)&(DC=1)...=>(Landslide)
Rule0: (SA=6)&(SAS=-1)&(ELV=6)&(LI=5)(DRD=6)...=>(Non-landslide)
Attribute reduction
Elevation
Slope angle
Slope aspect
Lithology
Fluctuation of water level
Distance to river
Distance to city
Distance to road

Environment influencing factors databases

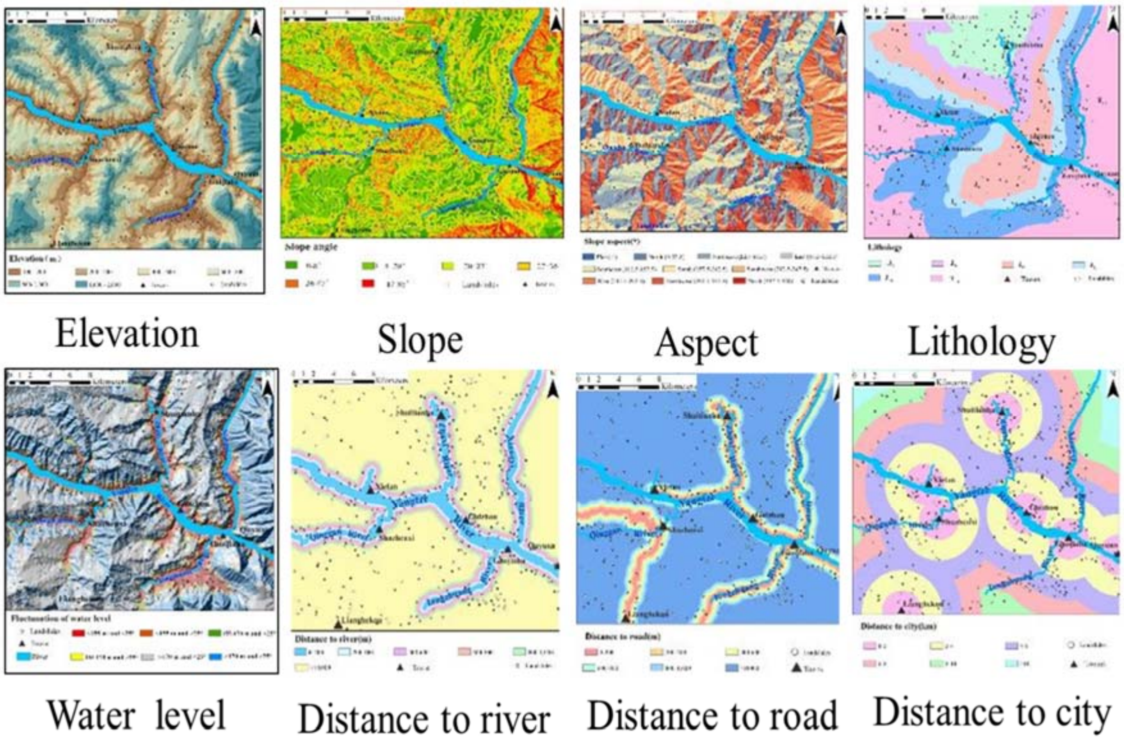

Frequency ratio

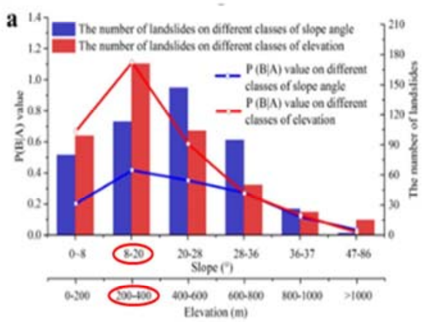

$$FR=\frac{Np_i x(S_i)/\sum_{i=1}^{n} Np_i x(S_i)}{Np_i x(N_i)/\sum_{i=1}^{n} Np_i x(N_i)}$$

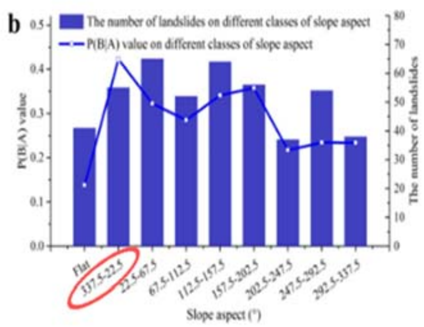

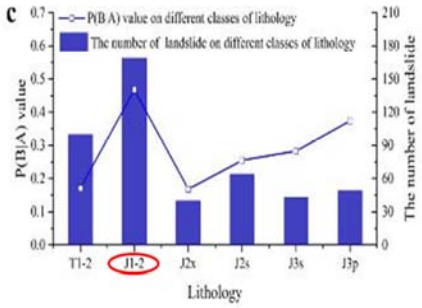

Frequency ratio

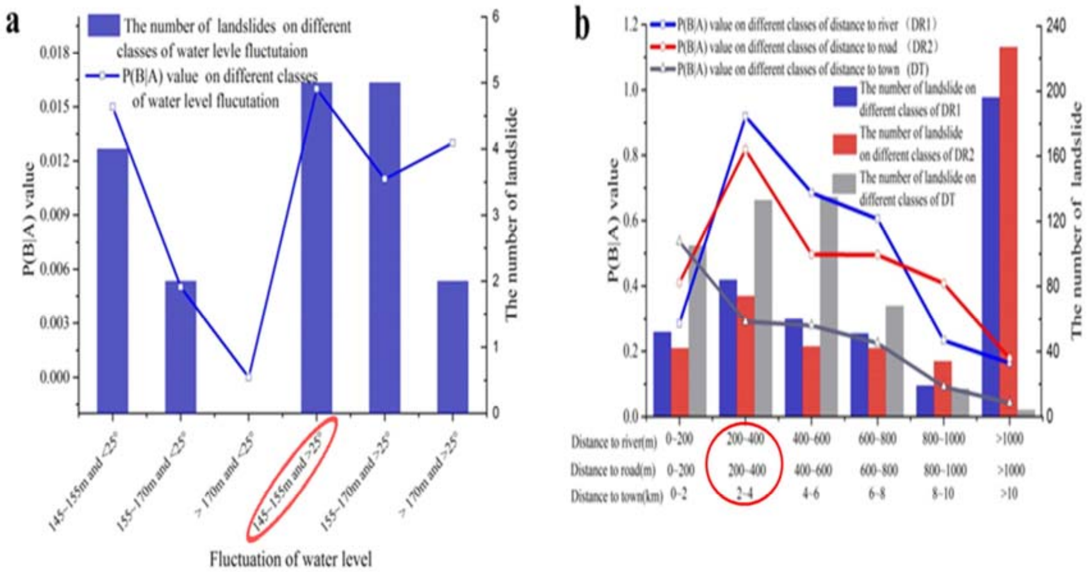

SOM & TSC

Self-Organizing Feature Map   Two Step Cluster algorithm

Unsupervised Learning

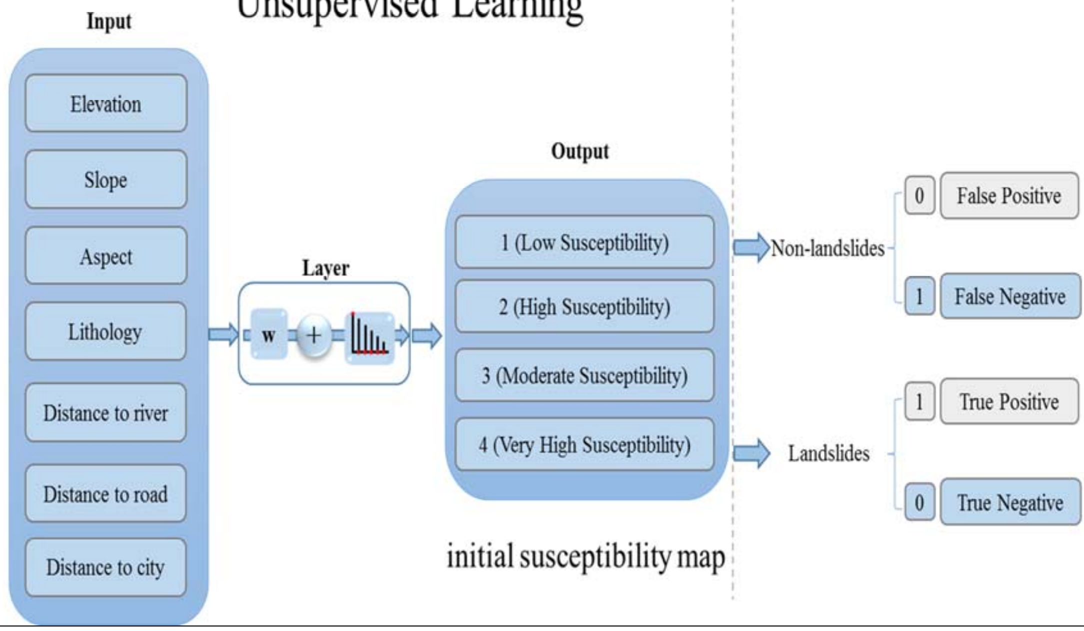

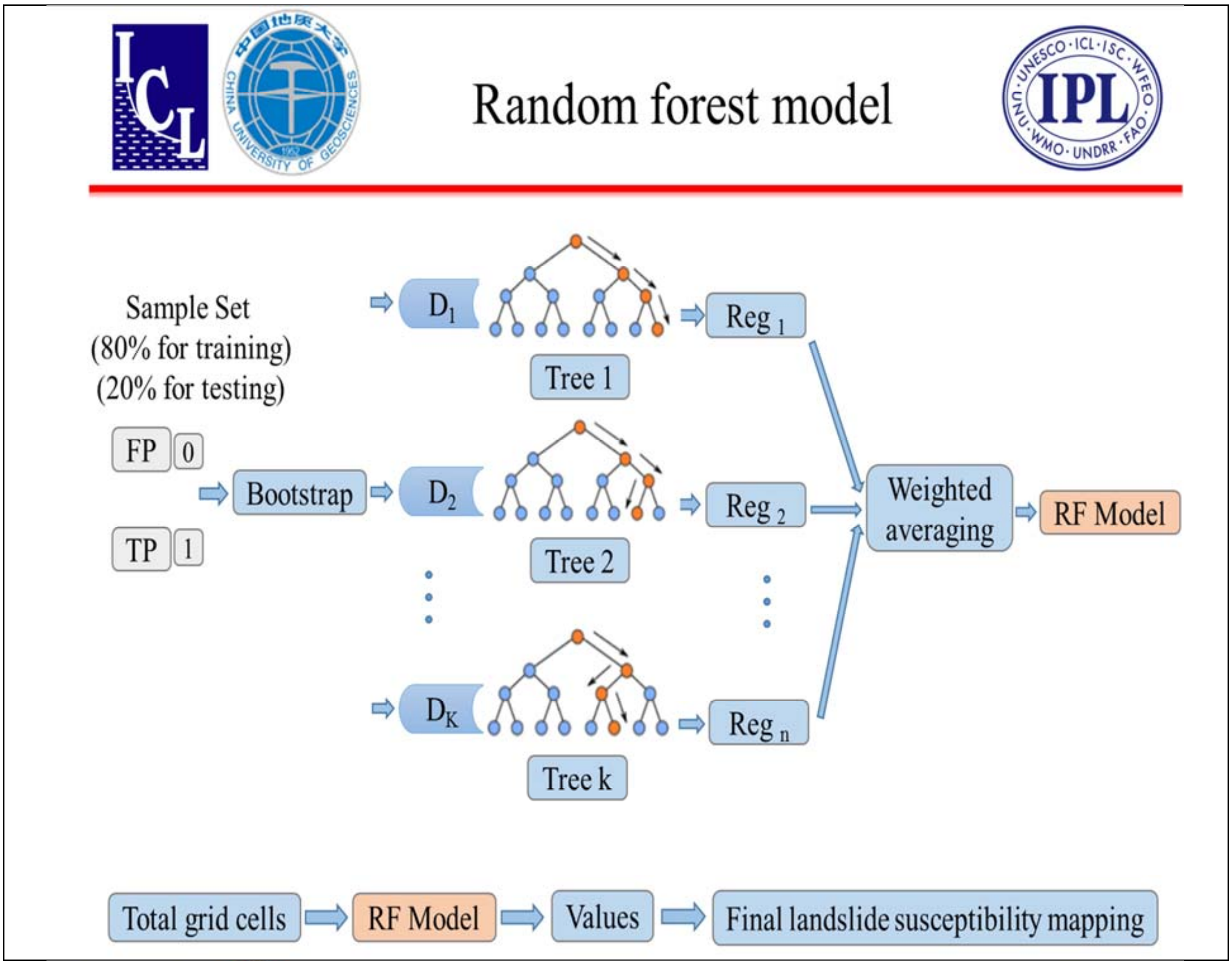
Random forest model
Sample Set
(80% for training)
(20% for testing)
FP 0
TP 1
Bootstrap
D_1
D_2
D_K
Tree 1
Tree 2
Tree k
Reg 1
Reg 2
Reg n
Weighted averaging
RF Model
Total grid cells
RF Model
Values
Final landslide susceptibility mapping

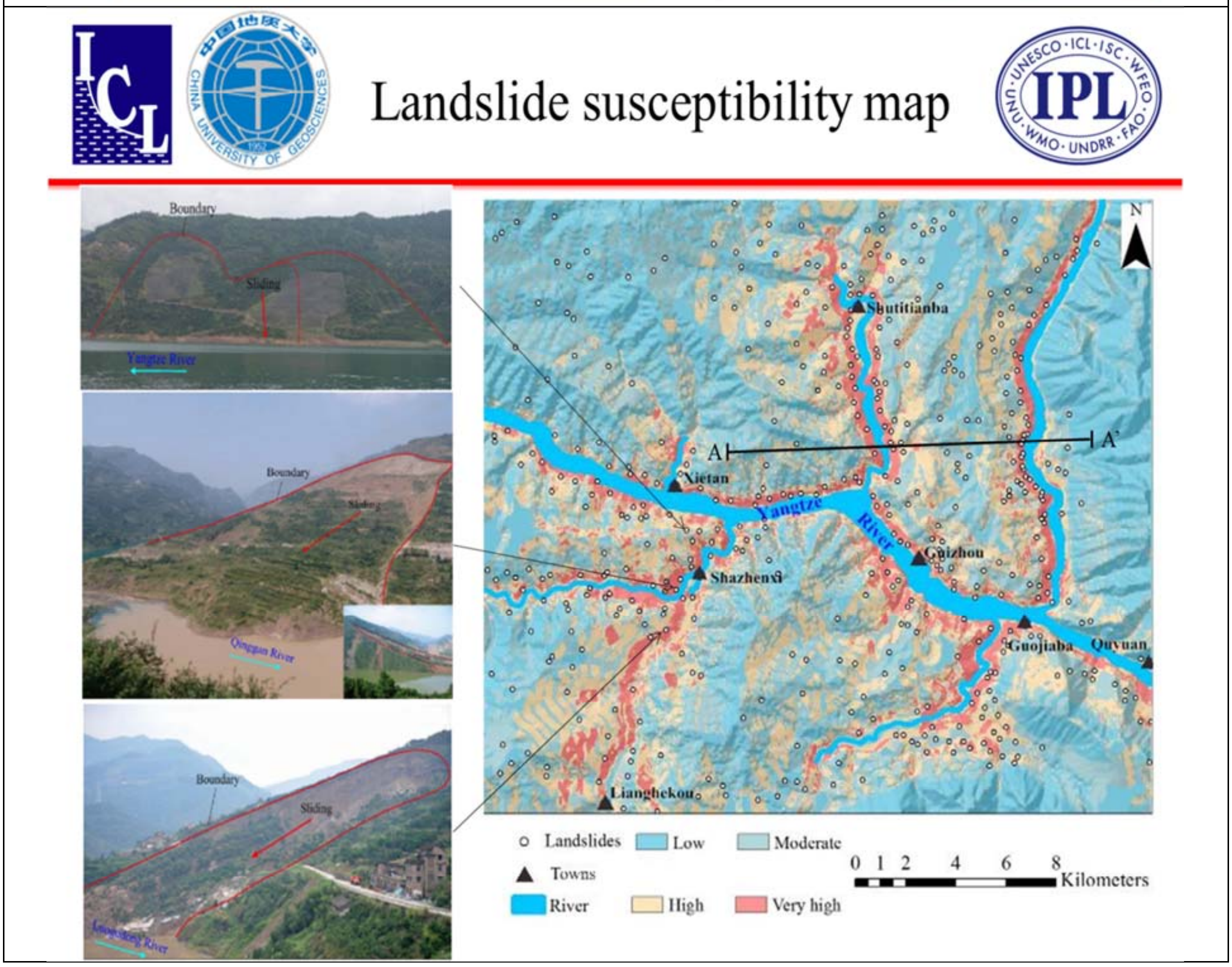
Landslide susceptibility map
Boundary
Sliding
Yangtze River
Qinggan River
A
A'
Shutitianba
Xietan
Yangtze River
Guizhou
Shazhenxi
Guojiaba
Quyuan
Lianghekou
N
Landslides
Low
Moderate
Towns
River
High
Very high
0 1 2 4 6 8
Kilometers

Results analyses

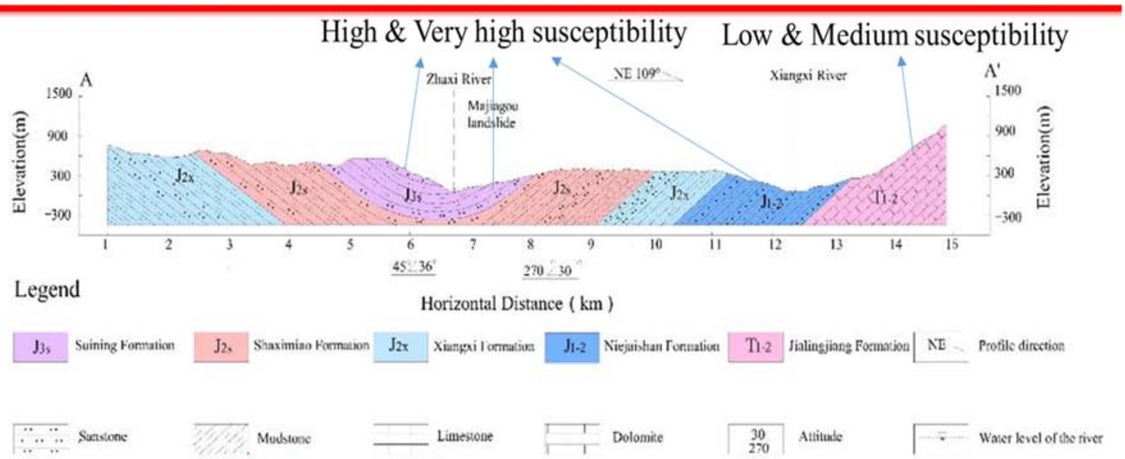

◆ Most areas with high or very high susceptibility are located within the hydro-fluctuation belt of the TGR, and most regions with moderate and low susceptibility values are distributed in the high mountains and plains.

◆ Little difference between the high susceptibility values of the west and east banks of the Zhaxi River.

◆ Considerable difference between the susceptibility of the banks of the Xiangxi River.

Verification of proposed model

RFD--Relative Failure Density

$$RFD_i = \frac{Np_i x(S_i)/Np_i x(N_i)}{\sum_{i=1}^{n}(Np_i x(S_i)/Np_i x(N_i))} \times 100$$

Npix(Si) - Number of landslides in i^{th} susceptibility area
Npix(Ni) - Number of grids in i^{th} susceptibility area

The closer the value of RFD is to 1 in very high and high susceptibility area, the better the accuracy of model is.

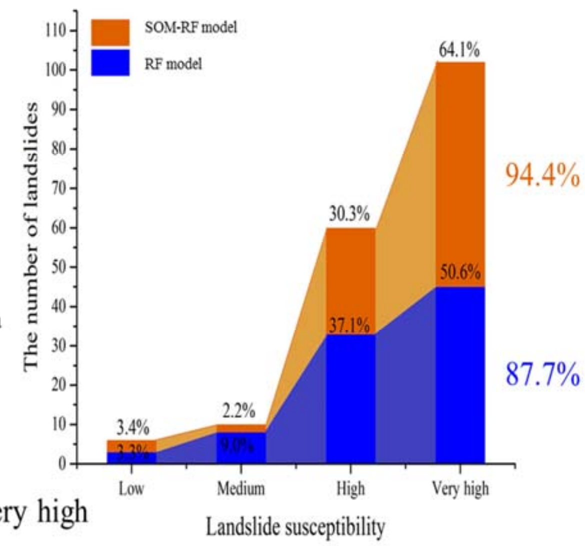

RFD Comparison of SOM-RF and RF model

Verification of proposed model

ROC--Receiver Operating Characteristic

AUC--Area Under the ROC Curve

$AUC_{(SOM-RF)} = 0.89$

$AUC_{(RF)} = 0.86$

The SOM-RF model has better accuracy than RF model.

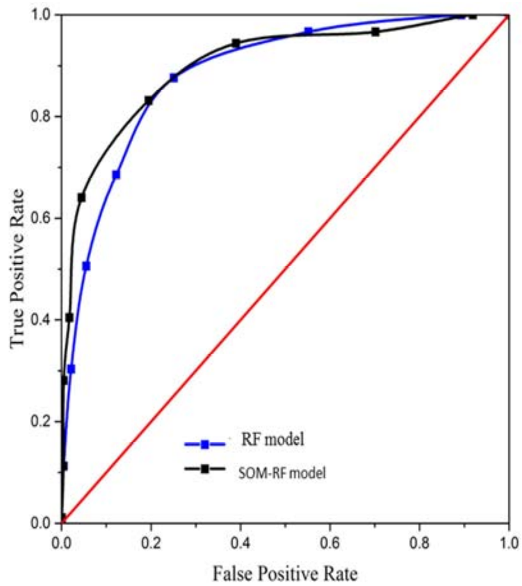

ROC Comparison of SOM-RF and RF model

Uncertainty of proposed model

Uncertainty of the model → 7 random databases → mean value / distribution

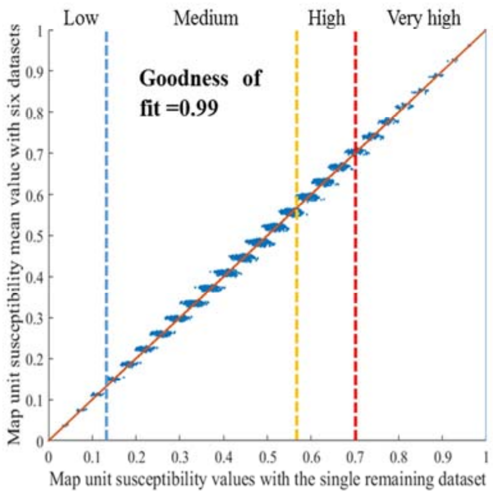

Comparing mean value by random six database with the best result by one database

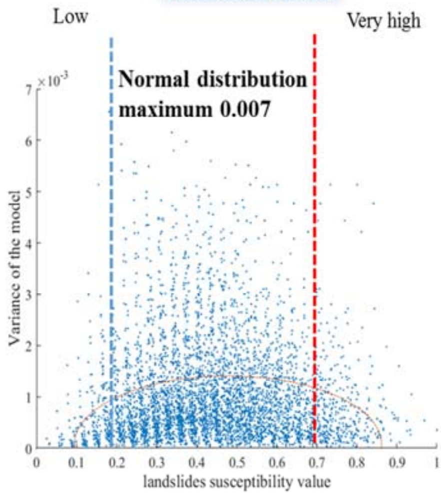

Distribution of landslide susceptibility values

Low deviation

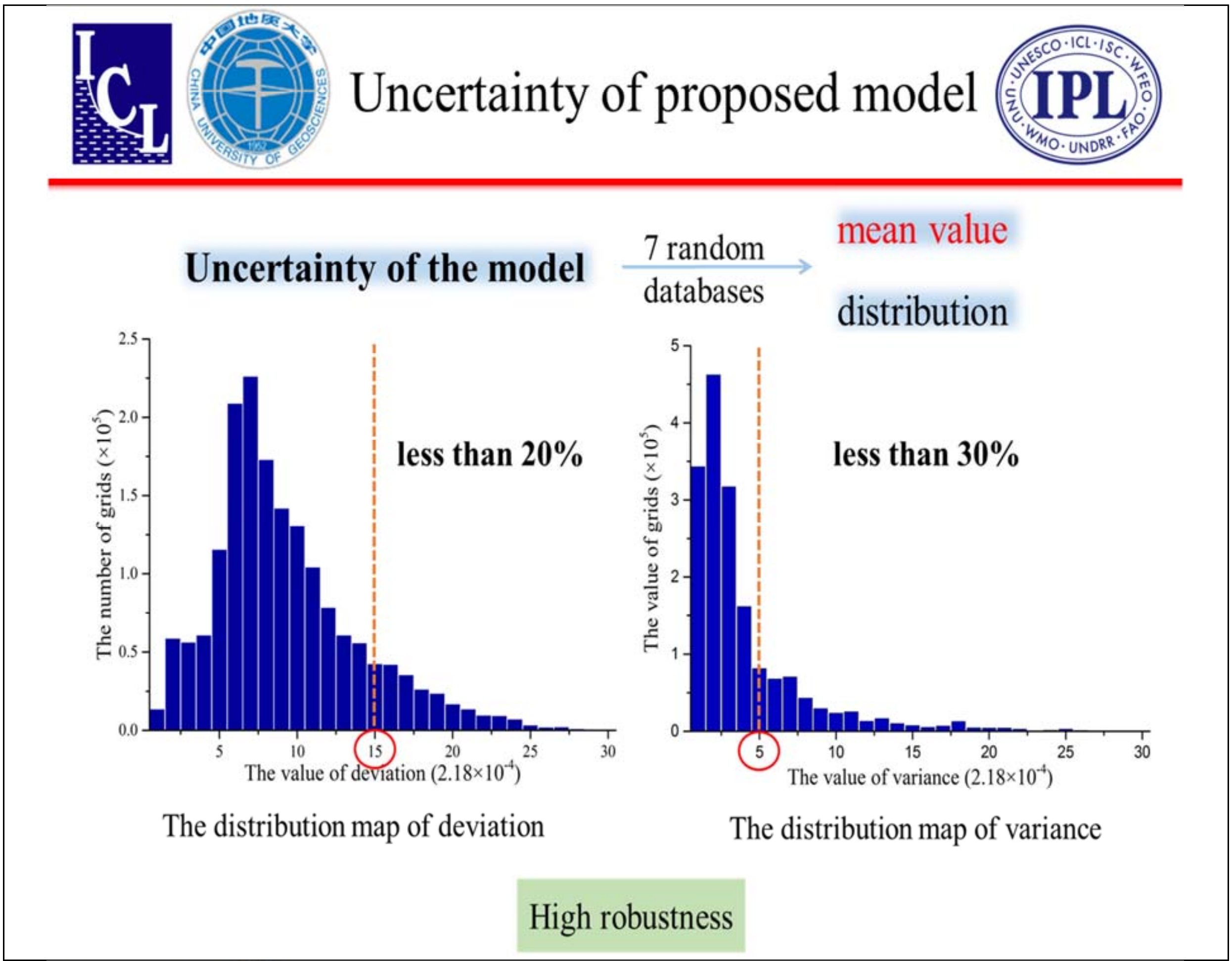
Uncertainty of proposed model
Uncertainty of the model
7 random databases
mean value
distribution
less than 20%
less than 30%
The number of grids (×10^5)
The value of deviation (2.18×10^-4)
The value of grids (×10^5)
The value of variance (2.18×10^-4)
The distribution map of deviation
The distribution map of variance
High robustness

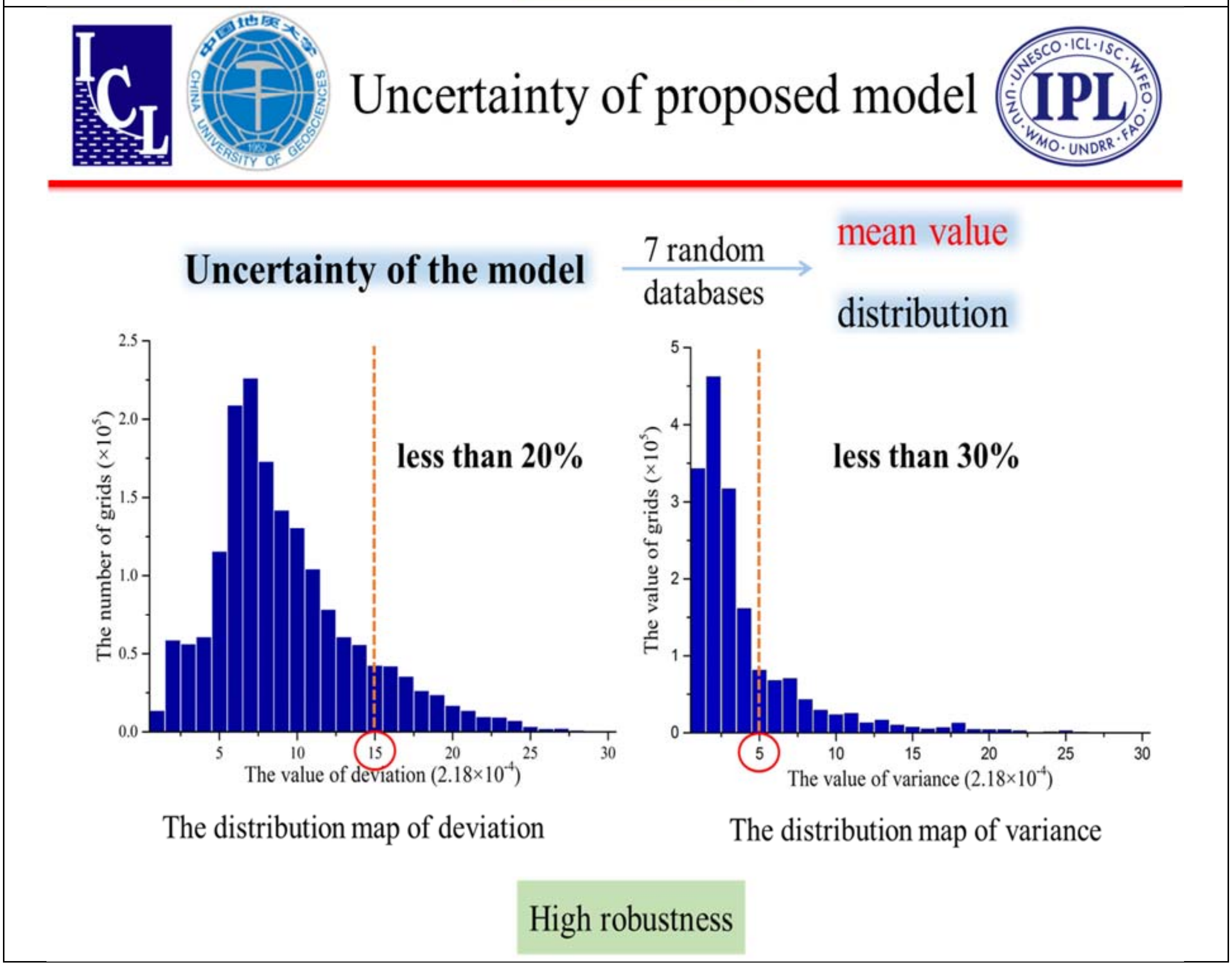
Uncertainty of proposed model
Uncertainty of the model
7 random databases
mean value
distribution
less than 20%
less than 30%
The number of grids (×10^5)
The value of deviation (2.18×10^-4)
The value of grids (×10^5)
The value of variance (2.18×10^-4)
The distribution map of deviation
The distribution map of variance
High robustness

Identifying triggering factors for individual landslide--A case study

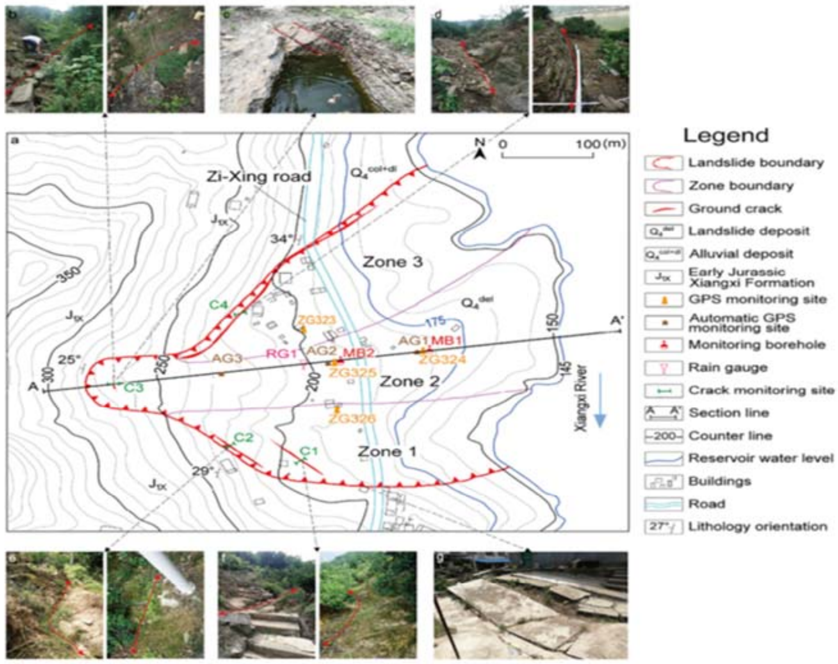

Geological map of the Baijiabao landslide and field investigation photos

Identifying triggering factors for individual landslide--A case study

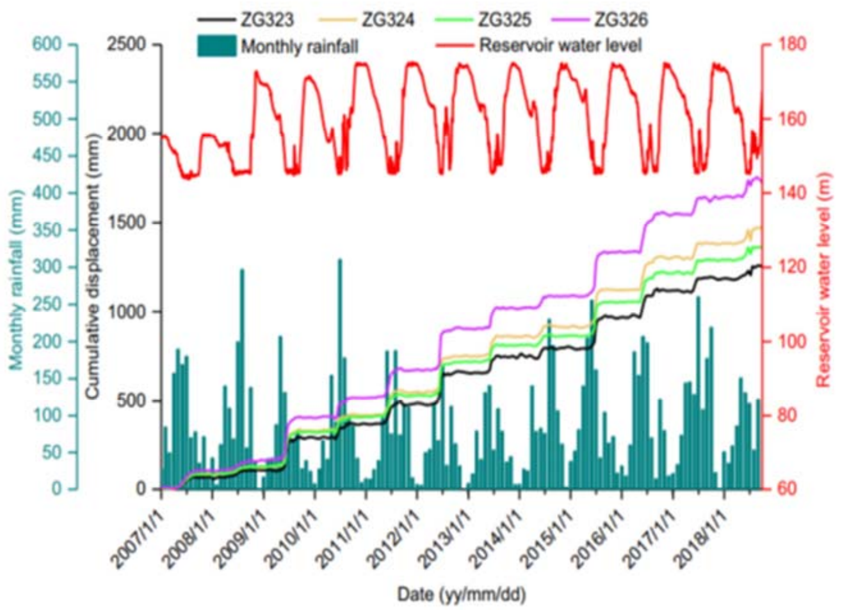

Time-series of cumulative displacement of GPS sites, monthly rainfall, and reservoir water level

Identifying triggering factors for individual landslide--A case study

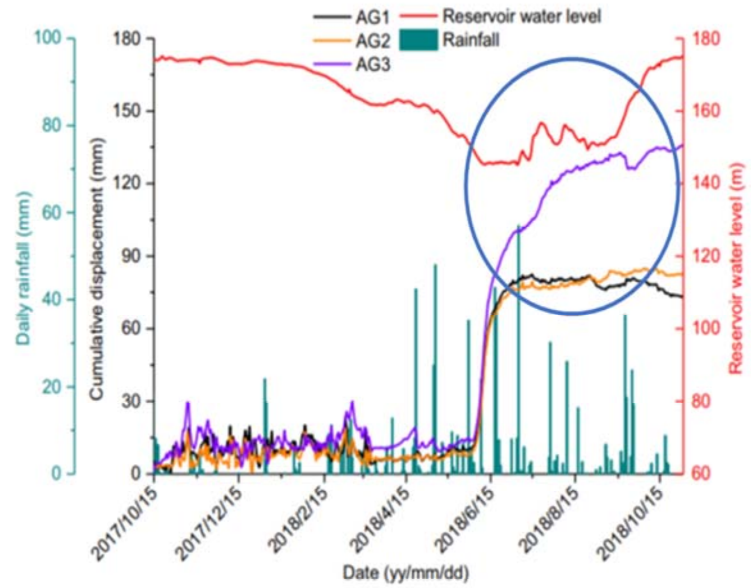

Time-series of cumulative displacement of AGPS sites, daily rainfall, and reservoir water level

Identifying triggering factors for individual landslide--A case study

Neighborhood rough set theory

Candidate attributes of daily monitoring data

Candidate condition attributes	Description
a_1'	The cumulative rainfall during the current day
a_2'	The cumulative rainfall over the previous day
a_3'	The cumulative rainfall over the previous seven days
a_4'	The cumulative rainfall over the previous fifteen day
a_5'	The cumulative rainfall over the previous thirty days
a_6'	The average reservoir water level during the current day
a_7'	The average reservoir water level over the previous day
a_8'	The average reservoir water level over the previous seven days
a_9'	The average reservoir water level over the previous fifteen days
a_{10}'	The average reservoir water level over the previous thirty days
a_{11}'	The change in the reservoir water level over the previous day
a_{12}'	The change in the reservoir water level over the previous seven days
a_{13}'	The change in the reservoir water level over the previous fifteen days
a_{14}'	The change in the reservoir water level over the previous thirty days

Significance of candidate condition attributes to daily monitoring data during rainy season.

Automatic monitoring data		a_1'	a_2'	a_3'	a_4'	a_5'	a_6'	a_7'	a_8'	a_9'	a_{10}'	a_{11}'	a_{12}'	a_{13}'	a_{14}'
AGPS	AG1	0.013	0.026			**0.026**							0.013		
	AG2	**0.013**		**0.013**		**0.013**						**0.013**			
	AG3	0.026		**0.039**								0.026	0.033		
Crack width	C1	0.031		0.035	0.012	0.016						**0.063**	0.035		
	C2	0.024		0.043	0.024							**0.063**	0.059		
	C4	0.028		0.028	0.028	0.012	0.024					**0.071**	0.039		
Deep displacement	IM1			0.013								**0.039**	0.033		
	IM2											**0.013**			

Note: Blanks mean that the significance of candidate condition attributes are <0.01. Values in bold mean the most important candidate condition attribute to the monitoring sites.

Identifying triggering factors for individual landslide--A case study

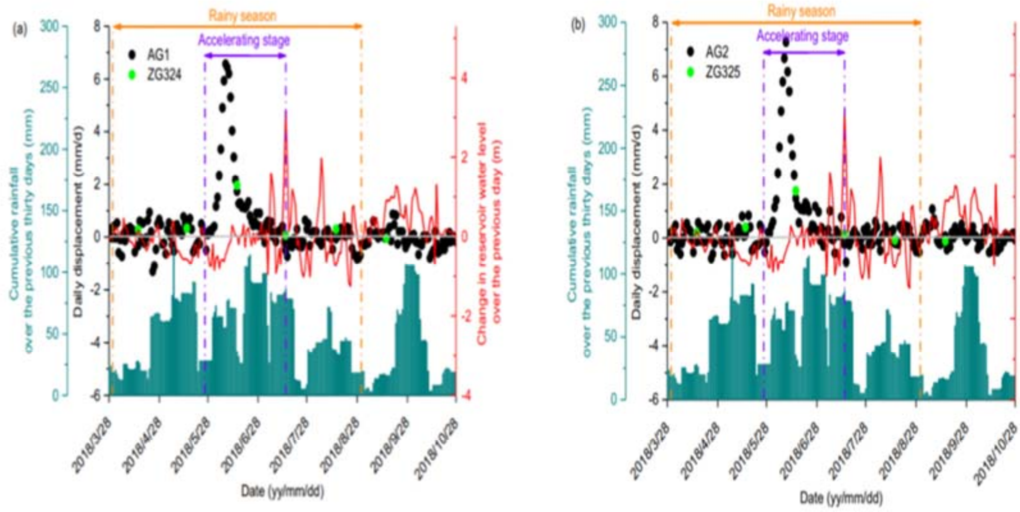

Time-dependent variation in daily rates of displacement calculated from the monthly data at the GPS sites, and directly measured at the AGPS sites

Identifying triggering factors for individual landslide--A case study

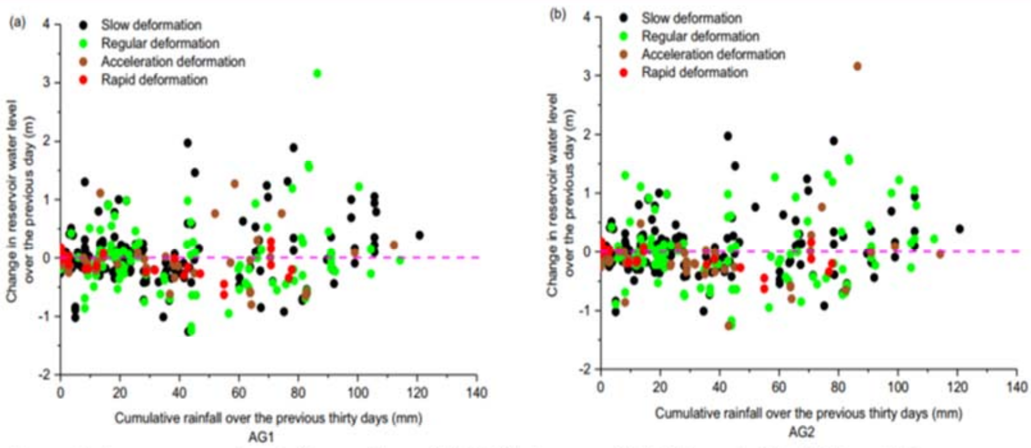

Correlation among the deformation of AGPS sites at (a) AG1 and (b) AG2 and the change in reservoir water level over the previous day and the cumulative rainfall over the previous thirty days. Most points for accelerating (brown) and rapid deformation (red) lie below the dashed purple line, showing the dependence on falling reservoir water level.

- Wenmin Yao, Changdong Li*, Qingjun Zuo, Hongbin Zhan, Robert E. Criss. Spatiotemporal deformation characteristics and triggering factors of Baijiabao landslide in Three Gorges Reservoir region, China. Geomorphology, 2019, 343:34-47.

Conclusions

◆Landslides database in the Zigui basin were identified with **remote sensing images**, field investigations and **unmanned aerial vehicle**;

◆Landslides distribution:Slope: between **8° and 28°** ;Elevation: **< 400m**; Aspect: **22.5° - 67.5°** ; Lithology: $J_{1\text{-}2}$;Distance to road and river: **< 400m**; Distance to city: **< 4km**;

◆A novel hybrid model was proposed based on the Two Step Cluster algorithm and the **Self-Organizing Map – Random Forest**;

◆TSC and SOM-RF model performs **better** prediction capacity than that of traditional RF model;

◆ **Goodness of fit 0.99** and **maximum deviation** less than **0.007** express high robustness and low deviation of the proposed model calculated by other databases.

◆The most important triggering factor depends on the particular site, **data type** and the **time interval** used to define it for the individual landslides.

Identification of ancient landslides in degraded areas of permafrost by surface trees

Wei Shan, Ying Guo

Institute of Cold Regions Science and Engineering, Northeast Forestry University
e-mail: shanwei456@163.com

Abstract

The continuous warming of the global climate has led to the continuous thawing of permafrost in permafrost regions at high latitudes, and the landslides and secondary disasters caused by permafrost degradation have gradually increased. The arbor plants are sensitive to the growth environment, such as soil moisture and temperature and so on. The distribution of tree species is determined by aerial photography and on-site investigation. The tree is drilled to determine the age of the tree. At the same time, combined with regional geomorphology analysis and high-density electrical detection on site, the landslides caused by permafrost degradation is judged, such as its age, mechanism, and sliding process and so on. It provides methods and basis for the identification of regional landslide distribution and the prevention of secondary disasters.

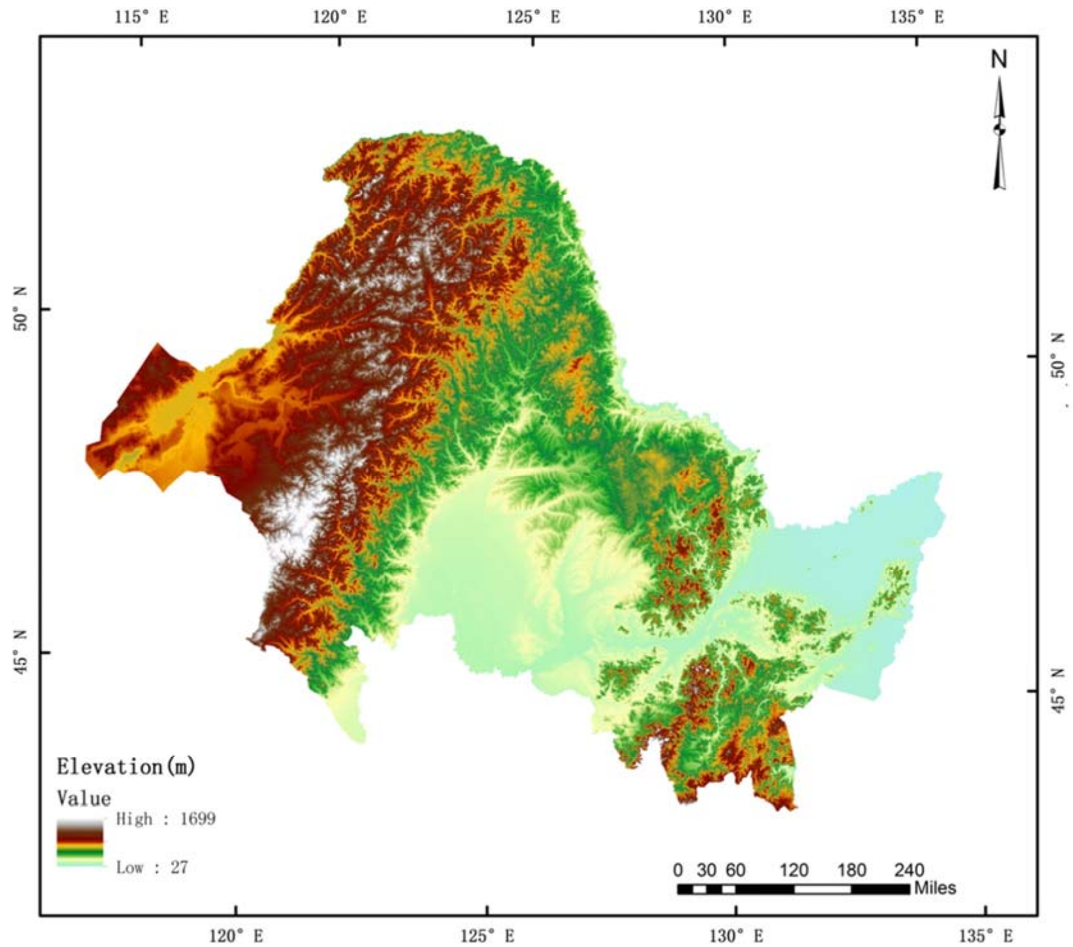
115° E
120° E
125° E
130° E
135° E
N
50° N
45° N
Elevation(m)
Value
High : 1699
Low : 27
0 30 60 120 180 240
Miles

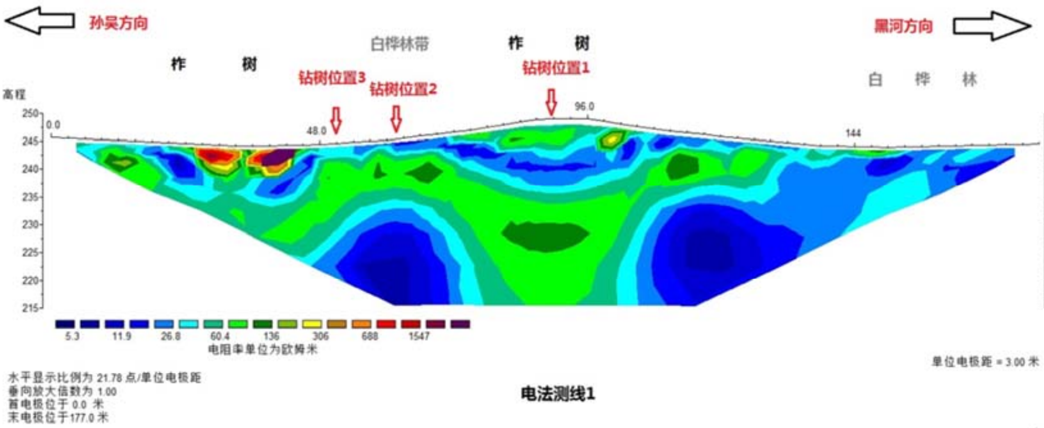
孙吴方向
黑河方向
白桦林带
柞 树
柞 树
钻树位置3
钻树位置2
钻树位置1
白 桦 林
高程
250
245
240
235
230
225
220
215
0.0
48.0
96.0
144
5.3
11.9
26.8
60.4
136
306
688
1547
电阻率单位为欧姆米
单位电极距 = 3.00 米
水平显示比例为 21.78 点/单位电极距
垂向放大倍数为 1.00
首电极位于 0.0 米
末电极位于 177.0 米
电法测线1

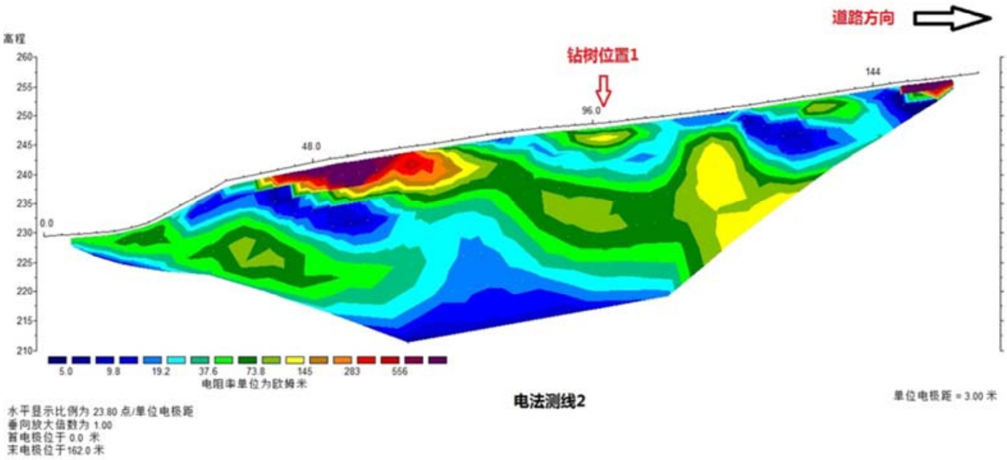
道路方向
钻树位置1
高程
260
255
250
245
240
235
230
225
220
215
210
0.0
48.0
96.0
144
5.0
9.8
19.2
37.6
73.8
145
283
556
电阻率单位为欧姆米
单位电极距 = 3.00 米
水平显示比例为 23.80 点/单位电极距
垂向放大倍数为 1.00
首电极位于 0.0 米
末电极位于 162.0 米
电法测线2

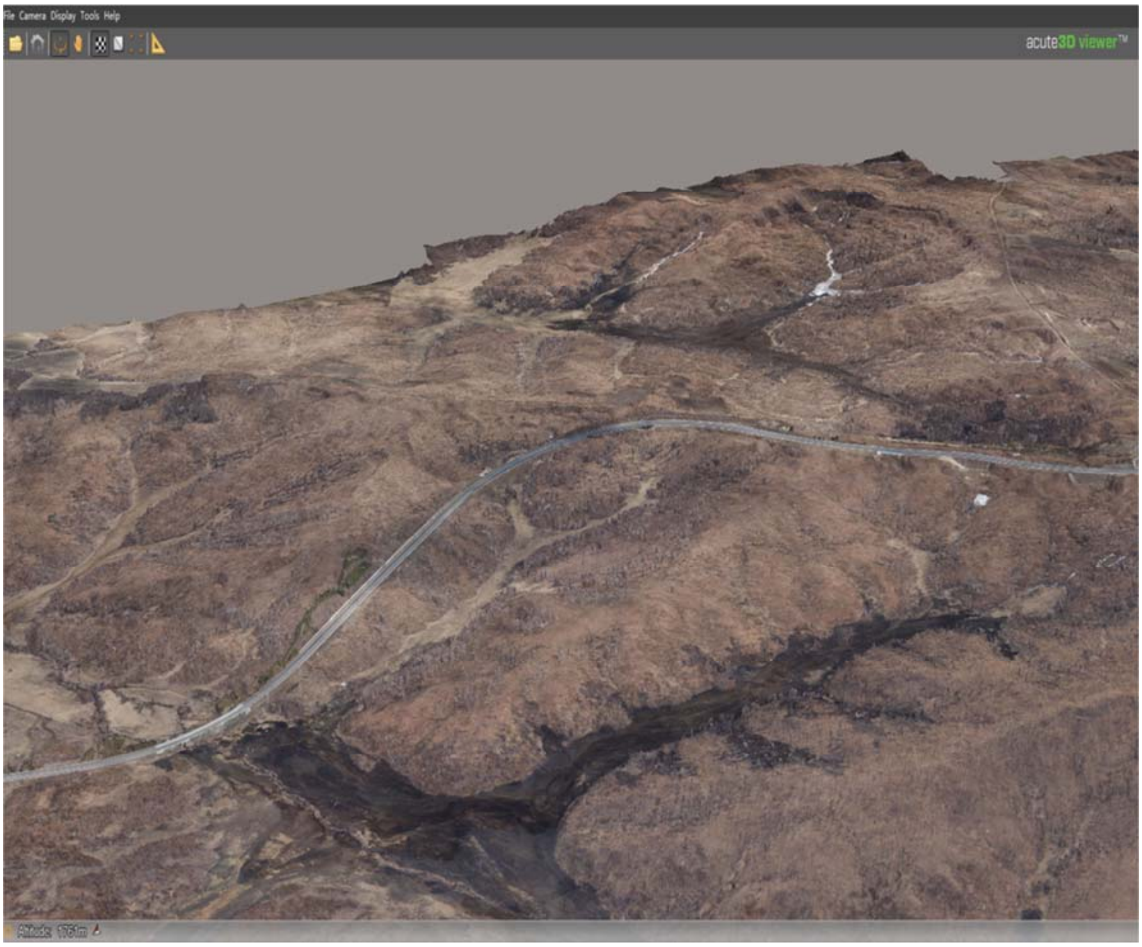
acute3D viewer™

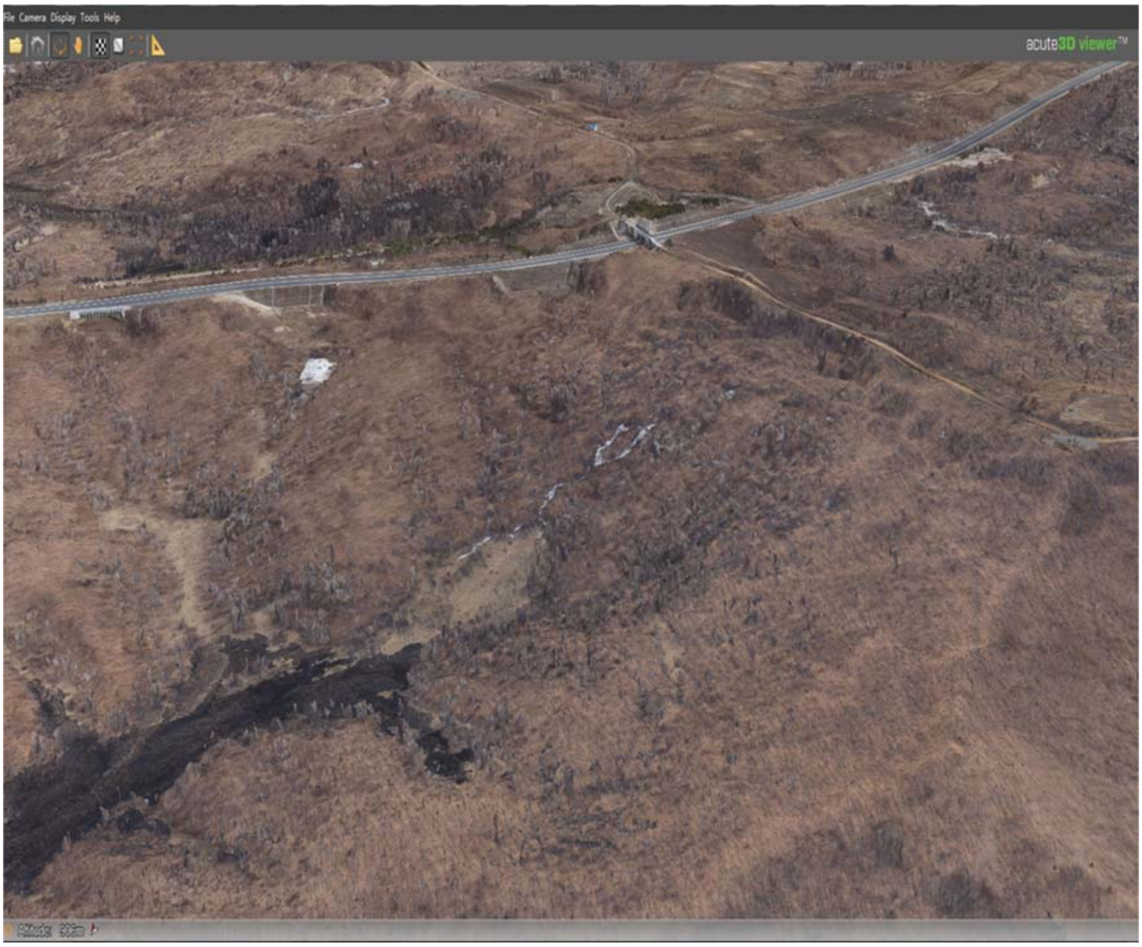
acute3D viewer™

研究区多年冻土分布特征

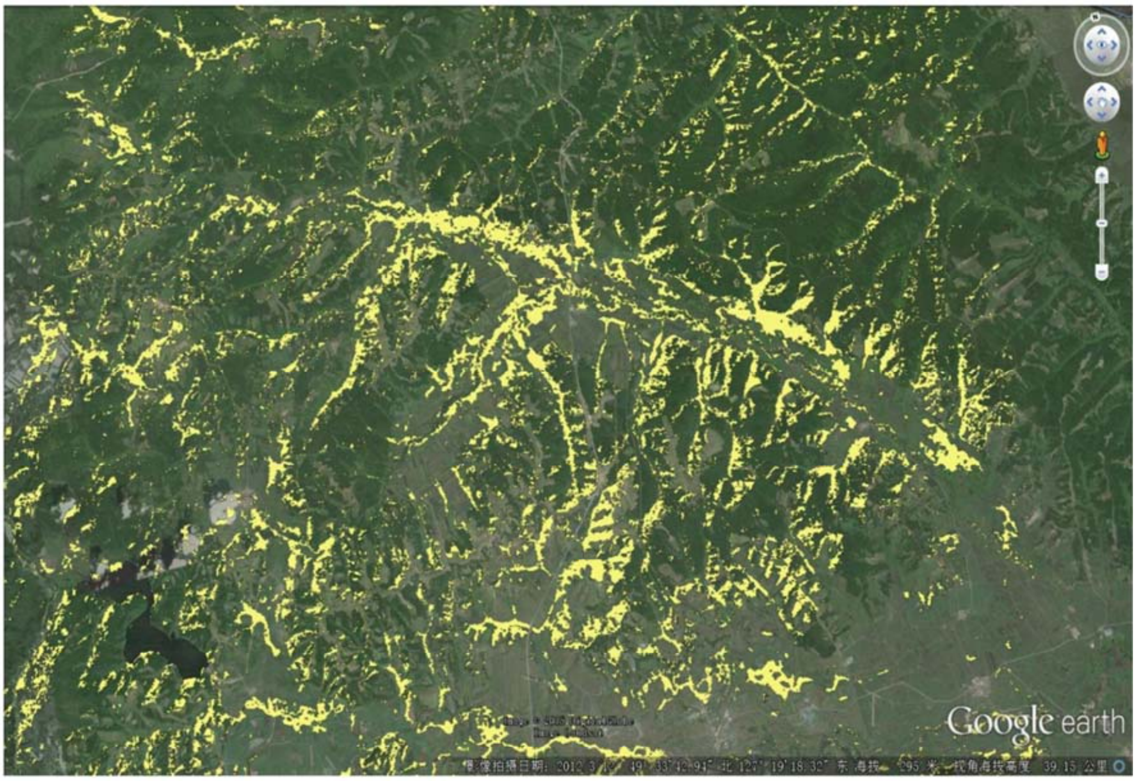

PF distribution using Landsat 7 ETM+ Imagine data,2012

冻土分布与地表形变的关系

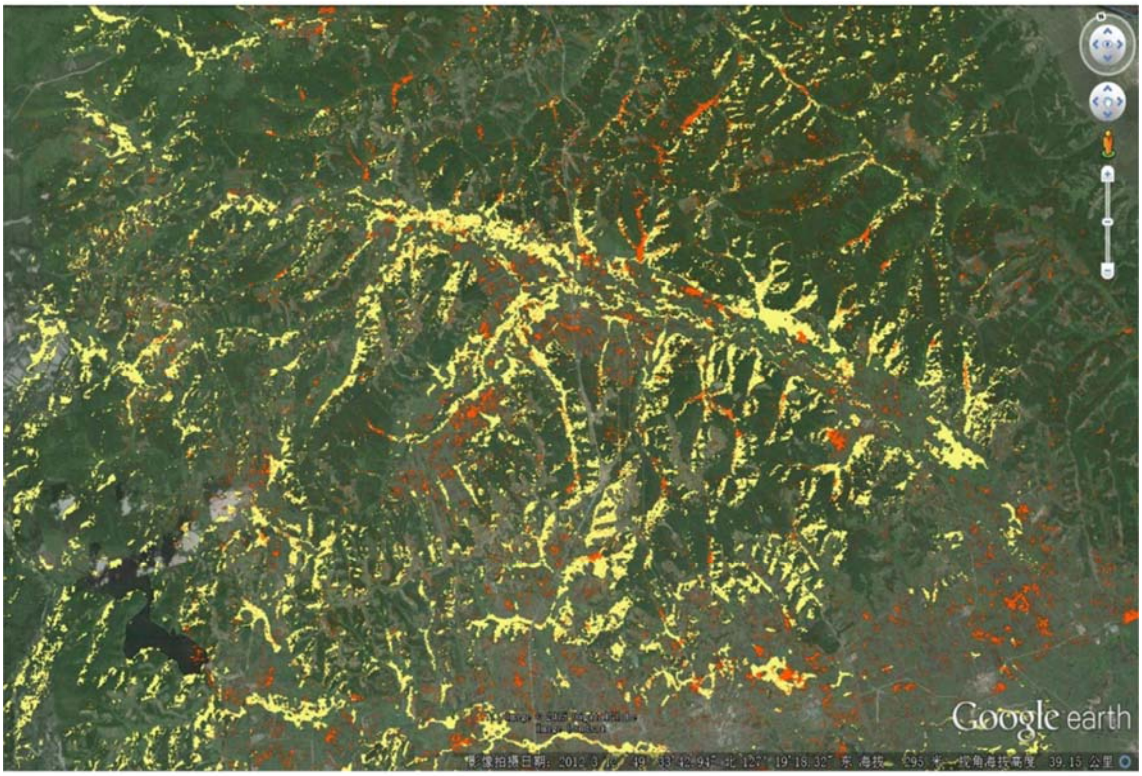

PF distribution and the surface deformation

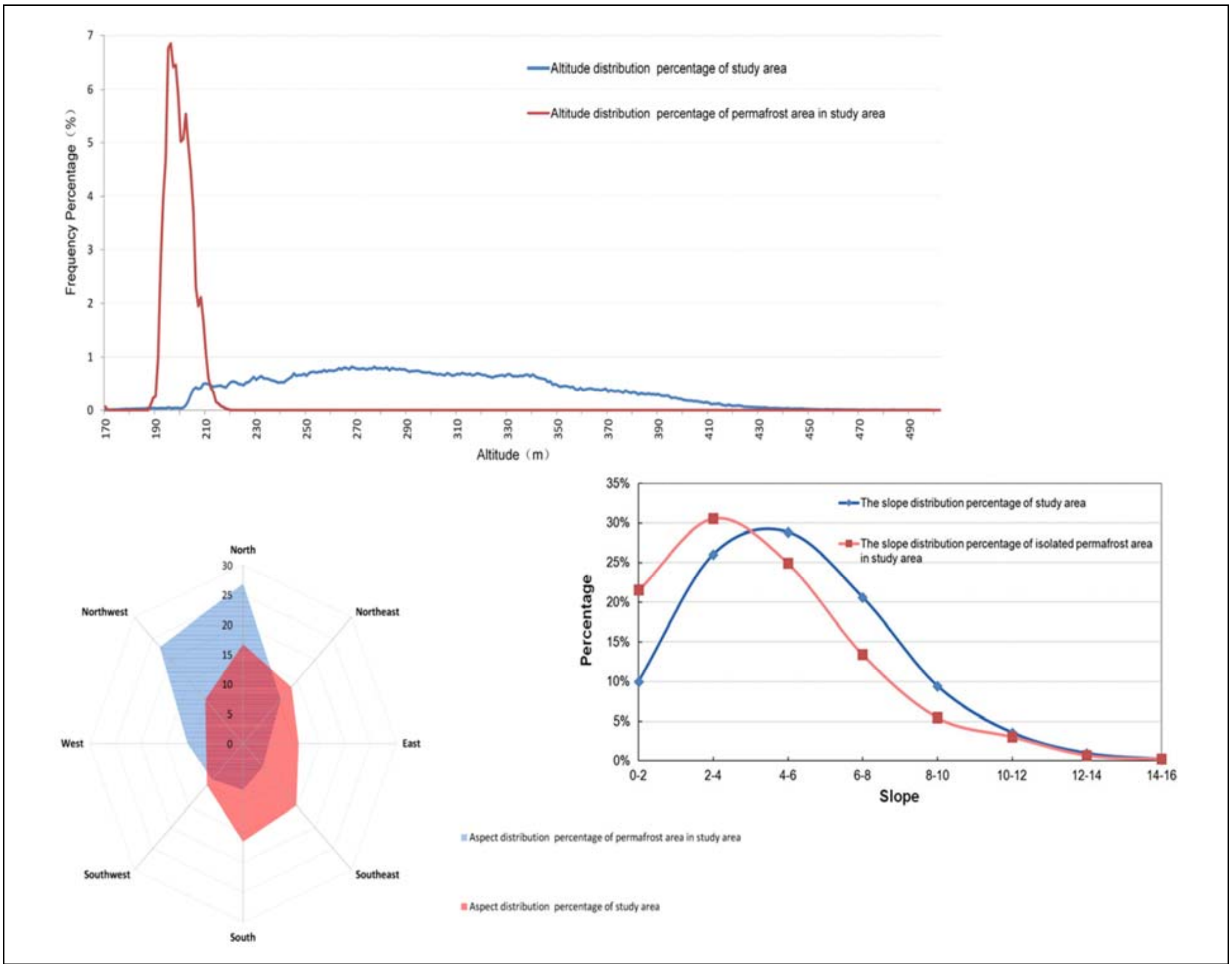
Altitude distribution percentage of study area
Altitude distribution percentage of permafrost area in study area
Frequency Percentage（%）
Altitude（m）
The slope distribution percentage of study area
The slope distribution percentage of isolated permafrost area in study area
Percentage
Slope
North
Northeast
East
Southeast
South
Southwest
West
Northwest
Aspect distribution percentage of permafrost area in study area
Aspect distribution percentage of study area

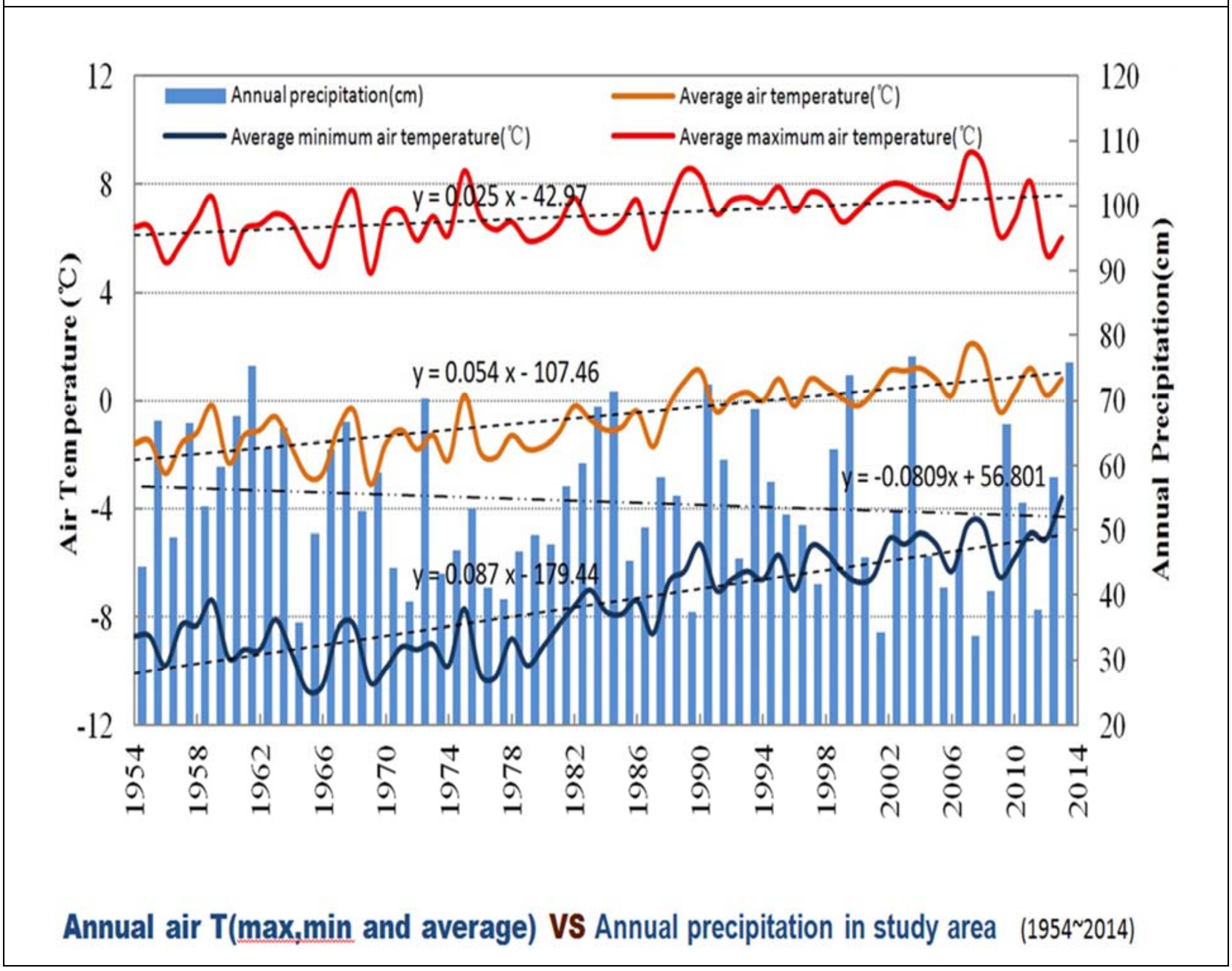
Annual precipitation(cm)
Average air temperature(℃)
Average minimum air temperature(℃)
Average maximum air temperature(℃)
y = 0.025 x - 42.97
y = 0.054 x - 107.46
y = -0.0809x + 56.801
y = 0.087 x - 179.44
Air Temperature (℃)
Annual Precipitation(cm)
Annual air T(max,min and average) VS Annual precipitation in study area (1954~2014)

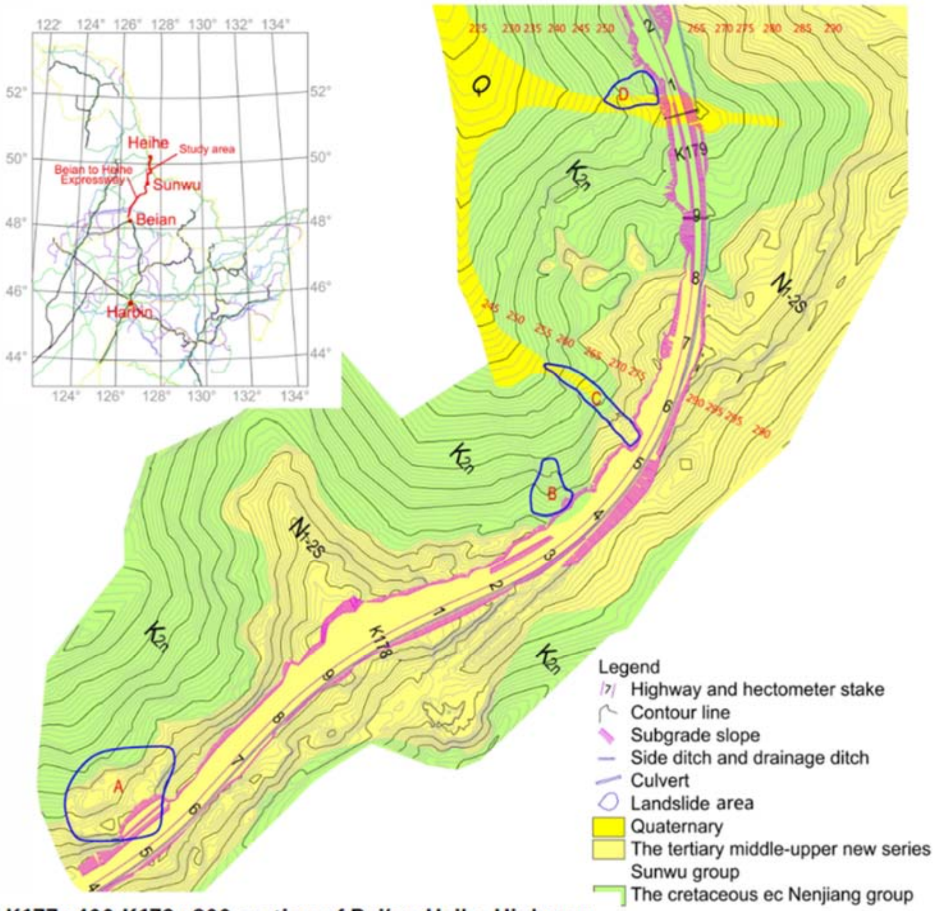

Geological map of K177+400-K179+200 section of Bei'an-Heihe Highway.

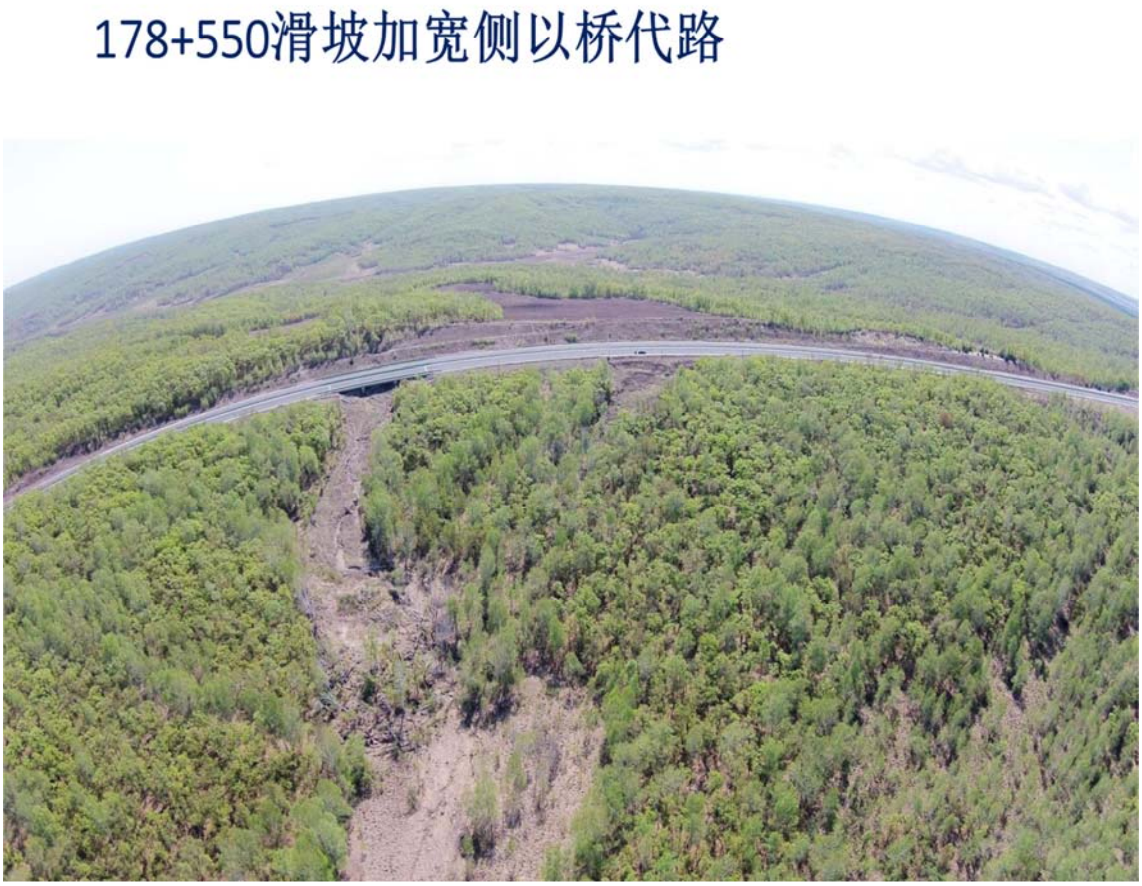

K177+550滑坡虽经抗滑桩支挡，旧滑坡前缘出现新滑坡

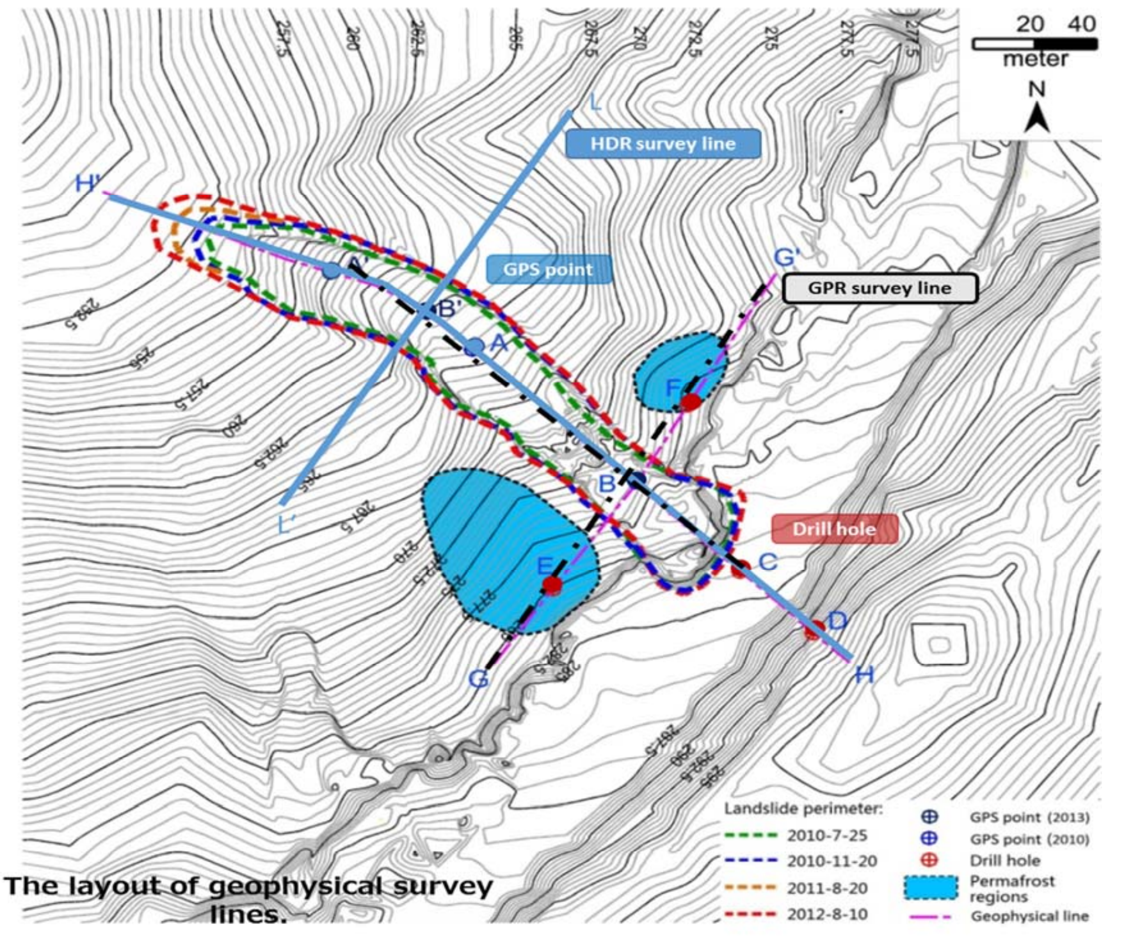

20 40
meter
N
HDR survey line
GPS point
GPR survey line
Drill hole
H'
H
L
L'
G'
G
A'
A
B'
B
C
D
E
F
Landslide perimeter:
2010-7-25
2010-11-20
2011-8-20
2012-8-10
GPS point (2013)
GPS point (2010)
Drill hole
Permafrost regions
Geophysical line
The layout of geophysical survey lines.

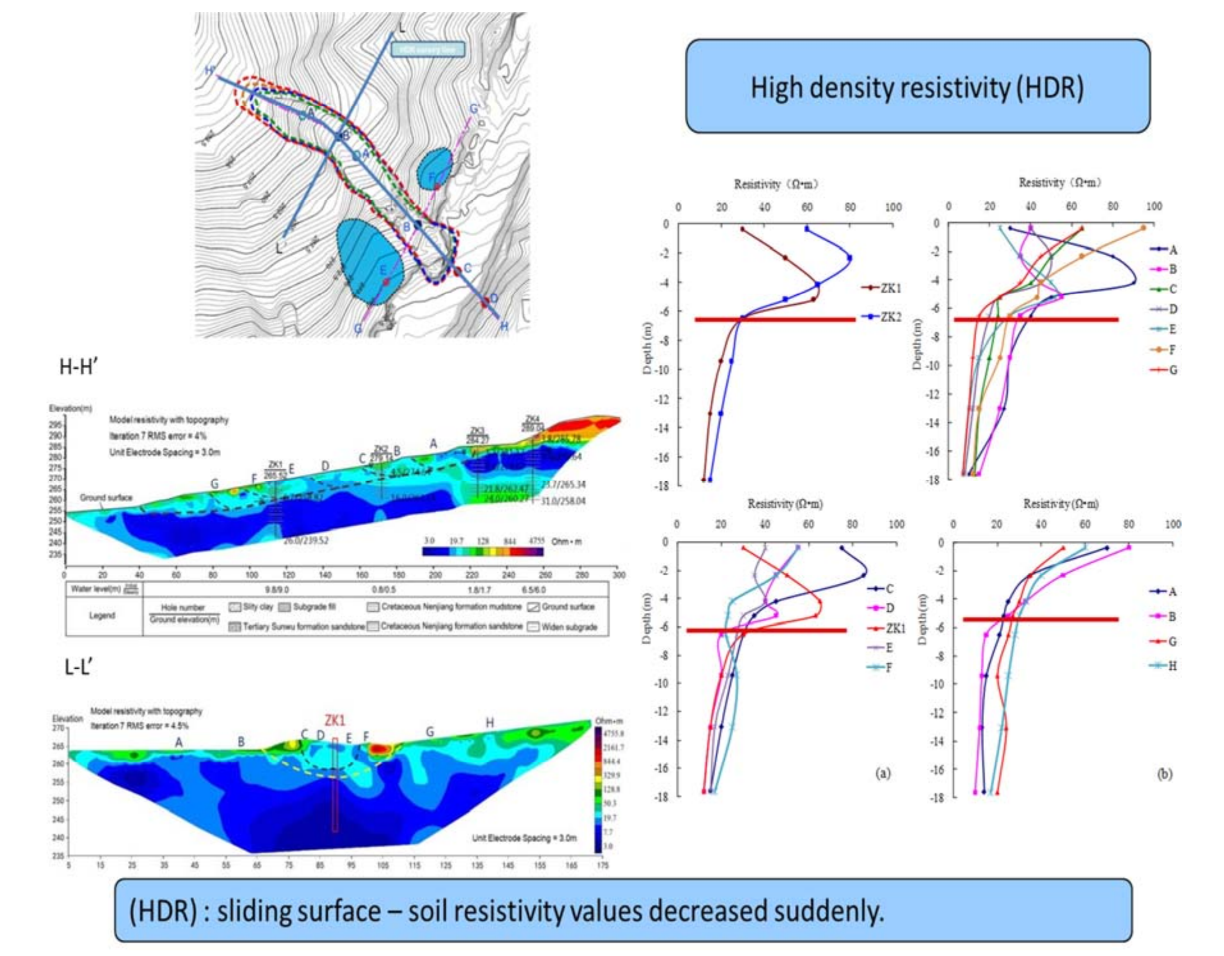

High density resistivity (HDR)
H-H'
Model resistivity with topography
Iteration 7 RMS error = 4%
Unit Electrode Spacing = 3.0m
Ground surface
L-L'
Model resistivity with topography
Iteration 7 RMS error = 4.5%
ZK1
Unit Electrode Spacing = 3.0m
Resistivity (Ω•m)
Depth (m)
ZK1
ZK2
(a)
(b)
(HDR) : sliding surface – soil resistivity values decreased suddenly.

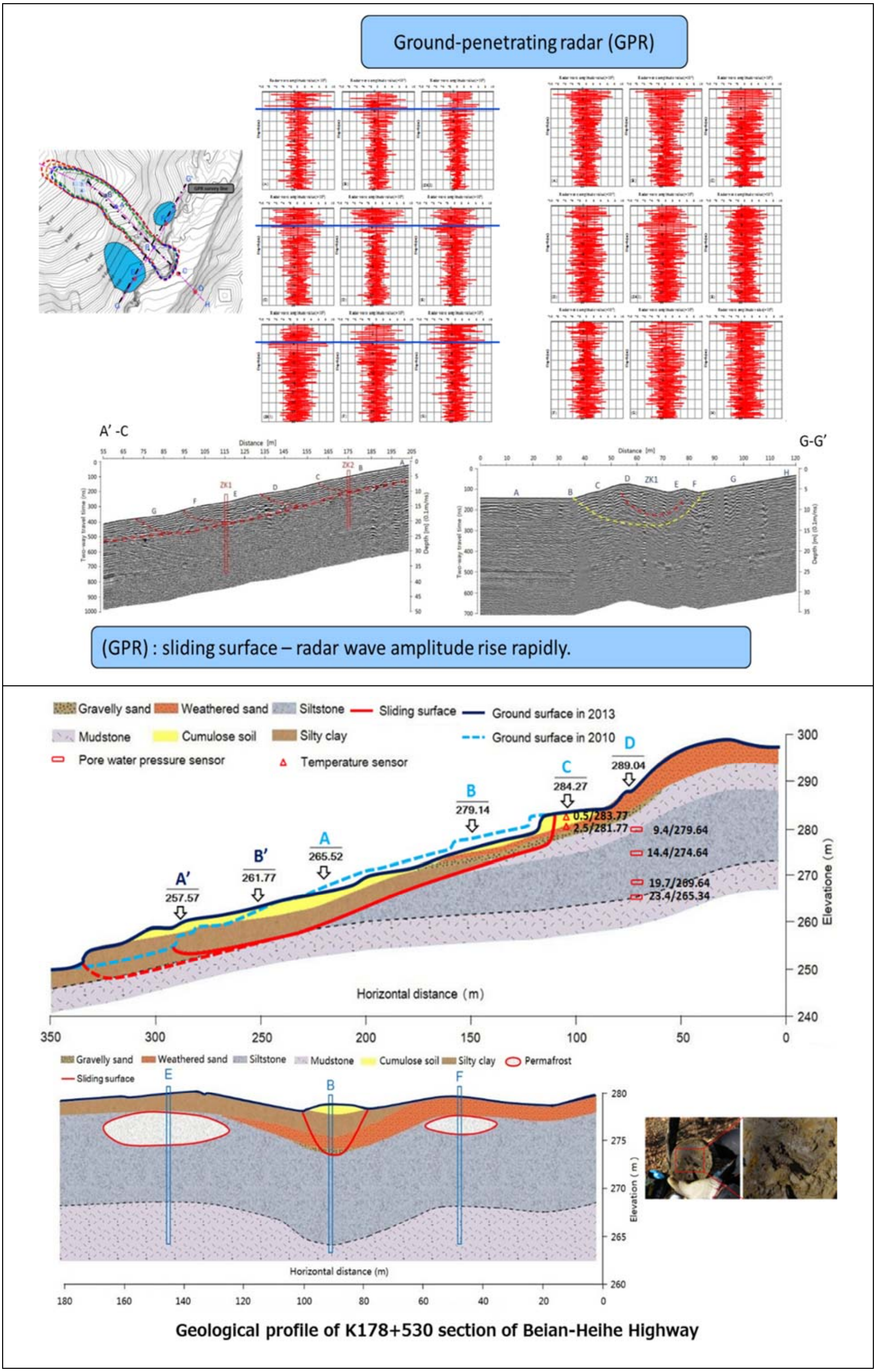
Ground-penetrating radar (GPR)
A' -C
G-G'
(GPR) : sliding surface – radar wave amplitude rise rapidly.
Gravelly sand
Weathered sand
Siltstone
Sliding surface
Ground surface in 2013
Mudstone
Cumulose soil
Silty clay
Ground surface in 2010
Pore water pressure sensor
Temperature sensor
A'
257.57
B'
261.77
A
265.52
B
279.14
C
284.27
D
289.04
0.5/283.77
2.5/281.77
9.4/279.64
14.4/274.64
19.7/269.64
23.4/265.34
Horizontal distance (m)
Elevatione (m)
Permafrost
E
B
F
Elevation (m)
Geological profile of K178+530 section of Beian-Heihe Highway

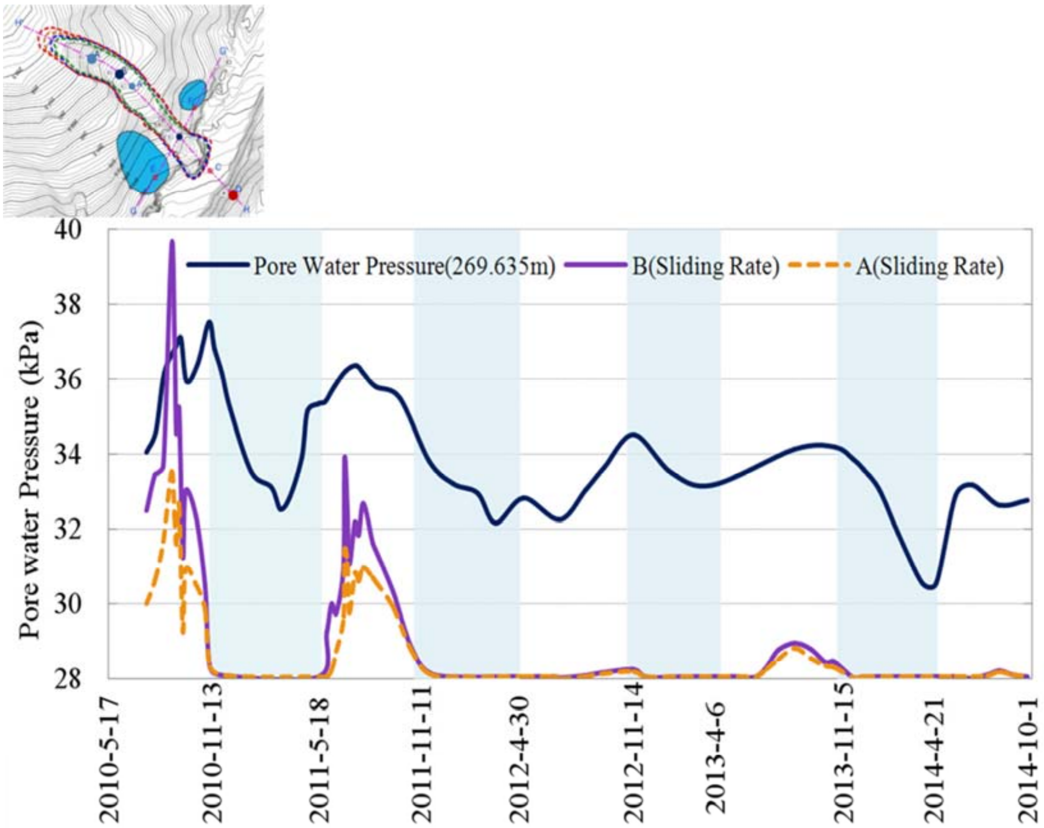

Horizontal displacement rates at point A and point B on the landslide mass and pore water pressure at point D (19.4m depth) in K178 + 530 section of Bei'an-Heihe Highway.

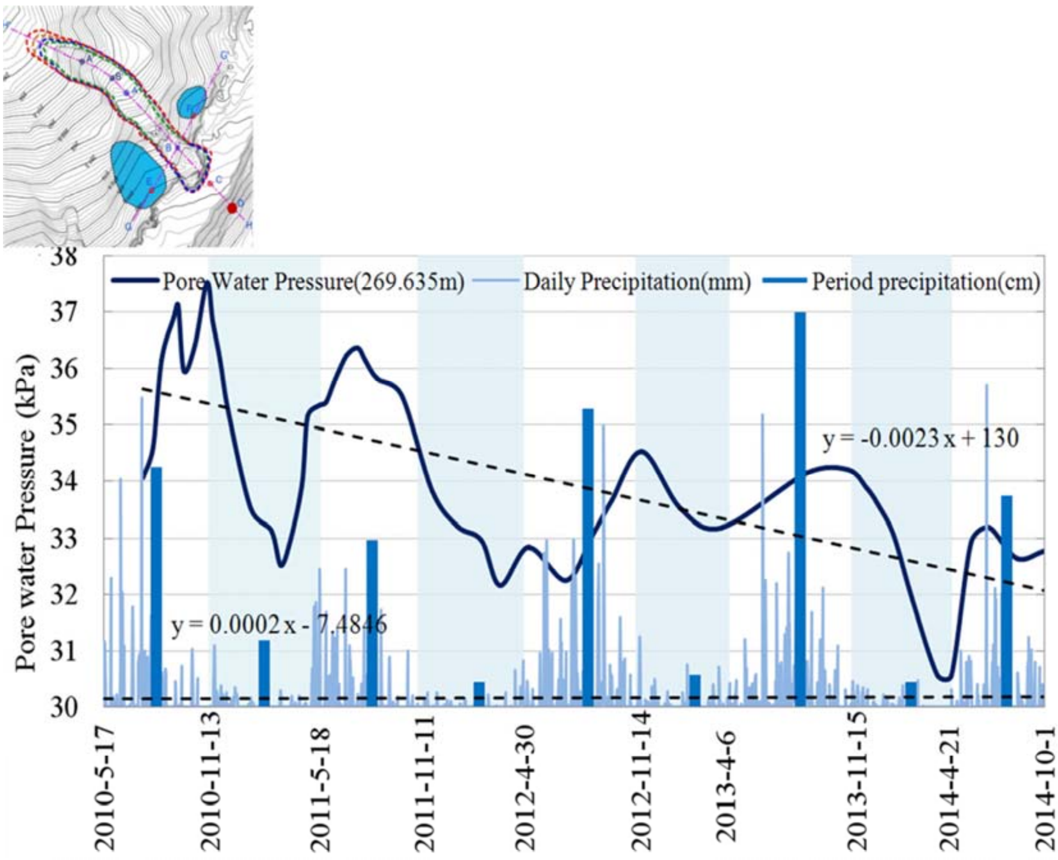

Daily precipitation and pore water pressure in the depth of 19.4 cm of D point in K178 + 530 section of Bei'an-Heihe Highway.

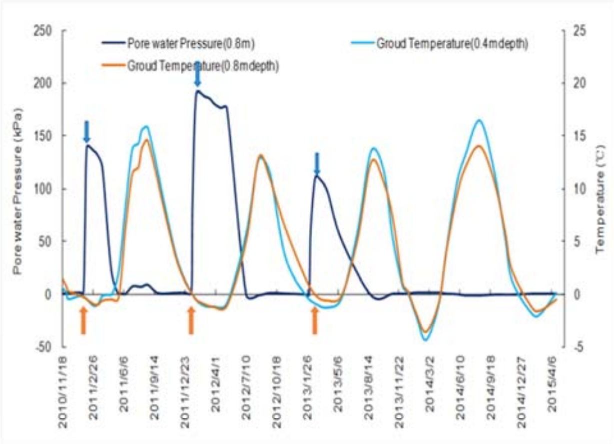

Results
& Discussion

Signal of icing :

- Icing is related to soil PWP around here. The signal of it is a sudden increasing of soil PWP accompanied by soil temperature dropped to 0 °C.(frozen front)

Icing cycles:

- Occurrence, bigger, smaller, disappearance...

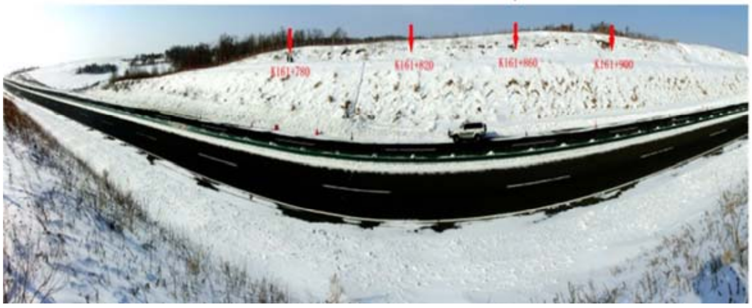

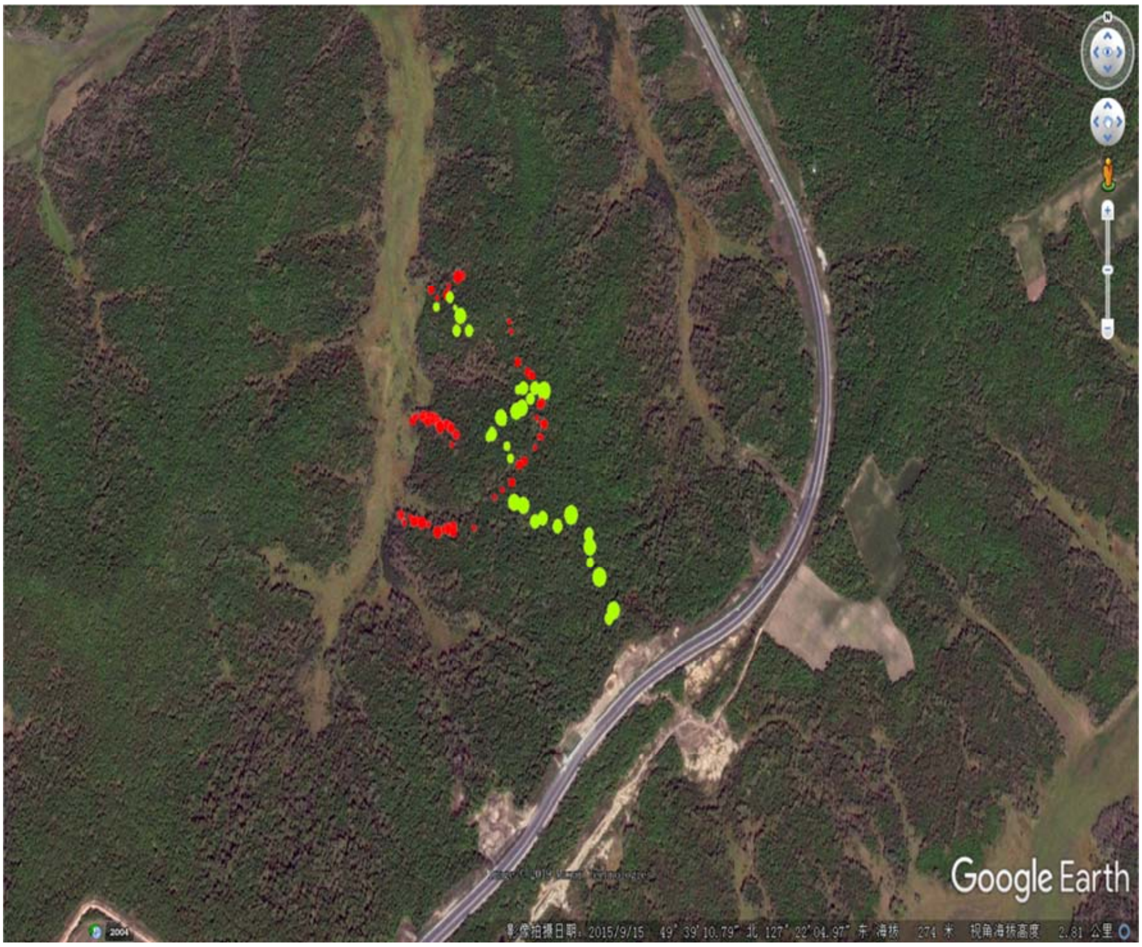
Google Earth
影像拍摄日期：2015/9/15 49°39'10.79" 北 127°22'04.97" 东 海拔 274 米 视角海拔高度 2.81 公里

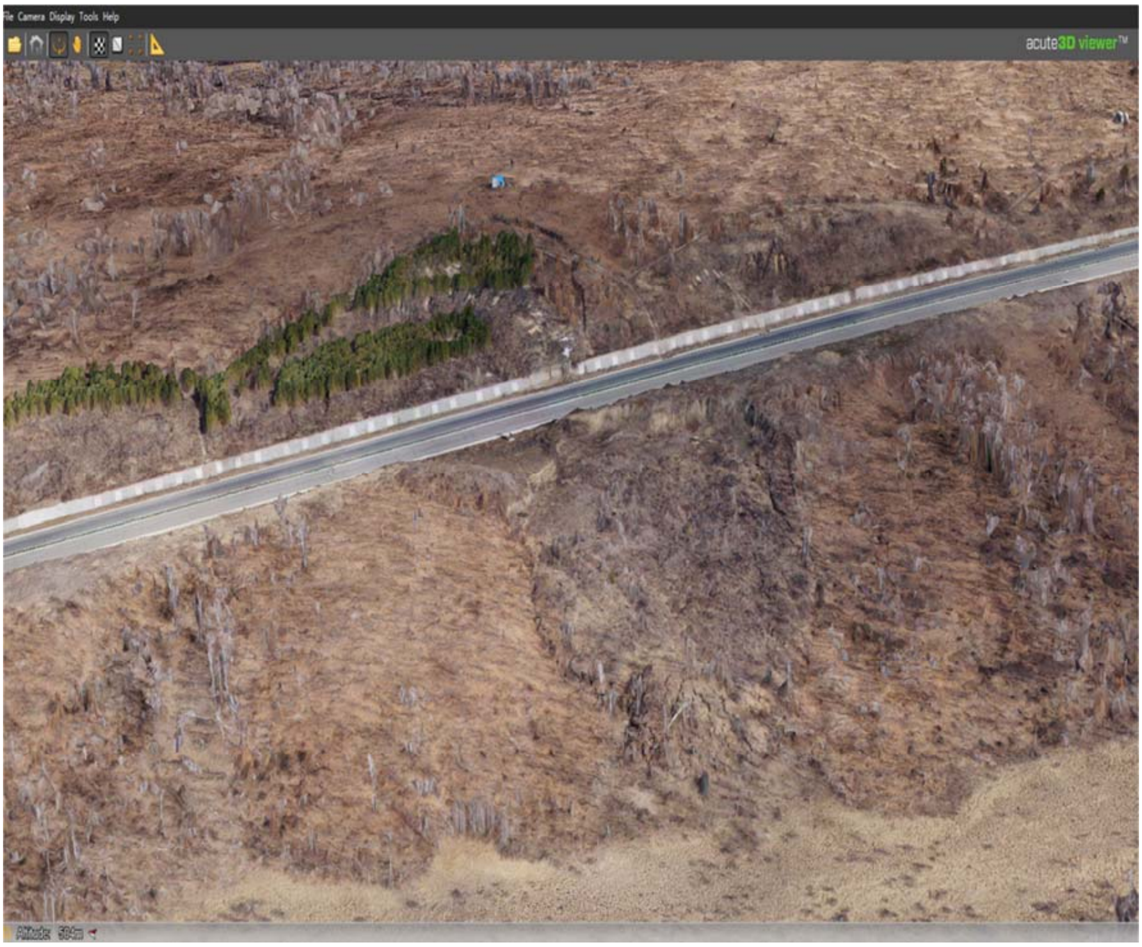
File Camera Display Tools Help
acute3D viewer™

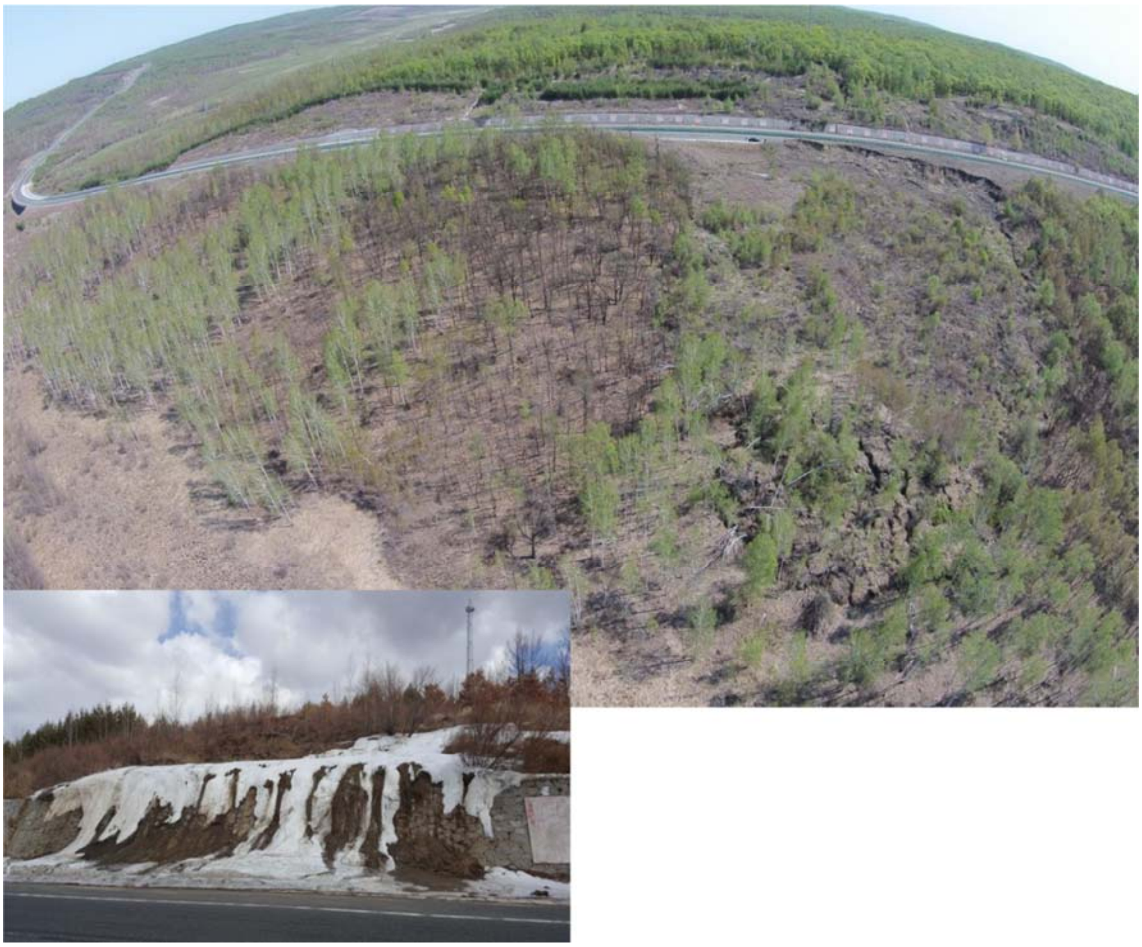


Google Earth
Google Earth

Landslide mapping from multi-sensor remote sensing imageries

Ping Lu[a], Yuanyuan Qin[a], Zhongbin Li[b], Alessandro C. Mondini[c], Nicola Casagli[d]

[a] College of Surveying and Geo-Informatics, Tongji University, Shanghai, China
[b] Center for Global Change and Earth Observations, Michigan State University, East Lansing, MI, USA
[c] CNR IRPI, Via Madonna Alta 126, Perugia, Italy
[d] Department of Earth Sciences, University of Firenze, Via La Pira 4, Firenze, Italy

Abstract

Remote sensing is an importance source for regional landslide mapping. In particular, advanced image processing approaches may increase the mapping efficiency and even make automatic landslide mapping feasible. This presentation renders some of our experiences in recent years on rapid mapping of landslides from diverse image processing approaches and remote sensing platforms. Notably, our attempts were made to rapidly generate landslide inventory from multi-sensor datasets. Landslides triggered by both rainfall, earthquake and typhoon around the world are respectively presented. We think with the increasing applications of remote sensing, this topic deserves further particular attention in the near future.

Outline

I. Research Background

II. Study Area and Data

III. Datasets and Methodology

IV. Results and Analysis

V. Conclusions

Contents lists available at SciVerse ScienceDirect

Earth-Science Reviews

journal homepage: www.elsevier.com/locate/earscirev

Landslide inventory maps: New tools for an old problem

Fausto Guzzetti [a,*], Alessandro Cesare Mondini [a,b], Mauro Cardinali [a], Federica Fiorucci [a,b], Michele Santangelo [a,b], Kang-Tsung Chang [c]

[a] CNR IRPI, via Madonna Alta 126, I-06128 Perugia, Italy
[b] Università degli Studi di Perugia, Piazza dell'Università, I-06123 Perugia, Italy
[c] Kainan University, 1, Kainan Rd., Luzhu, Taoyuan 33857, Taiwan

ARTICLE INFO

Article history:
Received 29 July 2011
Accepted 8 February 2012
Available online 23 February 2012

Keywords:
Geomorphology
Landslide
Inventory map
Remote sensing
Satellite Image
LiDAR

ABSTRACT

Landslides are present in all continents, and play an important role in the evolution of landscapes. They also represent a serious hazard in many areas of the world. Despite their importance, we estimate that landslide maps cover less than 1% of the slopes in the landmasses, and systematic information on the type, abundance, and distribution of landslides is lacking. Preparing landslide maps is important to document the extent of landslide phenomena in a region, to investigate the distribution, types, pattern, recurrence and statistics of slope failures, to determine landslide susceptibility, hazard, vulnerability and risk, and to study the evolution of landscapes dominated by mass-wasting processes. Conventional methods for the production of landslide maps rely chiefly on the visual interpretation of stereoscopic aerial photography, aided by field surveys. These methods are time consuming and resource intensive. New and emerging techniques based on satellite, airborne, and terrestrial remote sensing technologies, promise to facilitate the production of landslide maps, reducing the time and resources required for their compilation and systematic update. In this work, we first outline the principles for landslide mapping, and we review the conventional methods for the preparation of landslide maps, including geomorphological, event, seasonal, and multi-temporal inventories. Next, we examine recent and new technologies for landslide mapping, considering (i) the exploitation of very-high resolution digital elevation models to analyze surface morphology, (ii) the visual interpretation and semi-automatic analysis of different types of satellite images, including panchromatic, multispectral, and synthetic aperture radar images, and (iii) tools that facilitate landslide field mapping. Next, we discuss the advantages and the limitations of the new remote sensing data and technology for the production of geomorphological, event, seasonal, and multi-temporal inventory maps. We conclude by arguing that the new tools will help to improve the quality of landslide maps, with positive effects on all derivative products and analyses, including erosion studies and landscape modeling, susceptibility and hazard assessments, and risk evaluations.

Previous Work on Landslide Inventory Mapping

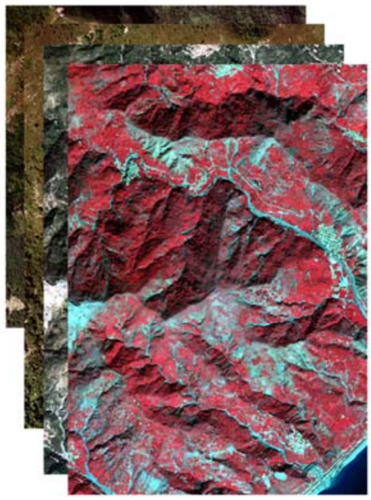

- **Data**
  - Aerial photos, remote sensing images, etc.
- **Method**
  - Visual interpretation-based, pixel-based, object-based, etc.

Limitations in the existing methods:

a) the limited degree of **automation**;
b) the limited level of **generality** and **applicability**;
c) and the increasing **complexity of remote sensing images** (spectral, spatial, and temporal resolution).

Remote Sensing of Environment 187 (2016) 76–90

Contents lists available at ScienceDirect

Remote Sensing of Environment

journal homepage: www.elsevier.com/locate/rse

Landslide mapping from aerial photographs using change detection-based Markov random field

Zhongbin Li[a,b,*], Wenzhong Shi[a], Ping Lu[c], Lin Yan[b], Qunming Wang[d], Zelang Miao[a]

[a] Department of Land Surveying and Geo-Informatics, The Hong Kong Polytechnic University, Hong Kong
[b] Geospatial Sciences Center of Excellence, South Dakota State University, Brookings, SD, USA
[c] College of Surveying and Geo-Informatics, Tongji University, Shanghai, China
[d] Lancaster Environment Center, Lancaster University, Lancaster, UK

ARTICLE INFO

Article history:
Received 27 May 2016
Received in revised form 16 September 2016
Accepted 2 October 2016
Available online 12 October 2016

Keywords:
Aerial photographs
Change detection
Landslide mapping (LM)
Markov random field (MRF)
Region-based level set evolution (RLSE)

ABSTRACT

Landslide mapping (LM) is essential for hazard prevention, mitigation, and vulnerability assessment. Despite the great efforts over the past few years, there is room for improvement in its accuracy and efficiency. Existing LM is primarily achieved using field surveys or visual interpretation of remote sensing images. However, such methods are highly labor-intensive and time-consuming, particularly over large areas. Thus, in this paper a change detection-based Markov random field (CDMRF) method is proposed for near-automatic LM from aerial orthophotos. The proposed CDMRF is applied to a landslide-prone site with an area of approximately 40 km^2 on Lantau Island, Hong Kong. Compared with the existing region-based level set evolution (RLSE), it has three main advantages: 1) it employs a more robust threshold method to generate the training samples; 2) it can identify landslides more accurately as it takes advantages of both the spectral and spatial contextual information of landslides; and 3) it needs little parameter tuning. Quantitative evaluation shows that it outperforms RLSE in the whole study area by almost 5.5% in *Correctness* and by 4% in *Quality*. To our knowledge, it is the first time CDMRF is used to LM from bitemporal aerial photographs. It is highly generic and has great potential for operational LM applications in large areas and also can be adapted for other sources of imagery data.

Limitations of previous MRF works

- ONLY based on change vector analysis (CVA)

$$\rho(I) = \left[\sum_{b=1}^{n} (I_{t_1} - I_{t_2})_b^2 \right]^{1/2}$$

- Extensive parameter tuning (manual intervention)

- ONLY tested on aerial photos, namely RGB channels

- ONLY tested on one study area/event

Objectives of Our Research

To develop an **improved** change detection-based Markov Random Field (CDMRF) method for landslide inventory mapping that have the following advantages:

a) it can map landslides over large areas **efficiently**;

b) it is **highly automatic** with minimal human interaction;

c) Generic: can be applicable over **different study areas and data**.

Study Area 1: Messina, rainfall-triggered

Event:

- Occurred on 1 October 2009
- 225 mm in 8 h, a peak of 115 mm in 3 h
- Shallow debris slides and flows
- 31 deaths, 6 people missing

IEEE GEOSCIENCE AND REMOTE SENSING LETTERS, VOL. 8, NO. 4, JULY 2011 701

Object-Oriented Change Detection for Landslide Rapid Mapping

Ping Lu, André Stumpf, Norman Kerle, and Nicola Casagli

***Abstract*—A complete multitemporal landslide inventory, ideally updated after each major event, is essential for quantitative landslide hazard assessment. However, traditional mapping methods, which rely on manual interpretation of aerial photographs and intensive field surveys, are time consuming and not efficient for generating such event-based inventories. In this letter, a semi-automatic approach based on object-oriented change detection for landslide rapid mapping and using very high resolution optical images is introduced. The usefulness of this methodology is demonstrated on the Messina landslide event in southern Italy that occurred on October 1, 2009. The algorithm was first developed in a training area of Altolia and subsequently tested without modifications in an independent area of Itala. Correctly detected were 198 newly triggered landslides, with user accuracies of 81.8% for the number of landslides and 75.9% for the extent of landslides. The principal novelties of this letter are as follows: 1) a fully automatic problem-specified multiscale optimization for image segmentation and 2) a multitemporal analysis at object level with several systemized spectral and textural measurements.**

***Index Terms*—Change detection, landslide, object-oriented**

Landsat Thematic Mapper (TM), has limited utility for landslide studies [4]. More recently, high-resolution images and Light Detection and Ranging (LiDAR) elevation derivatives have started to offer an alternative way for effective landslide mapping. Most research works, however, have been focusing on pixel-based analysis. For example, Borghuis *et al.* [5] employed unsupervised image classification in automated landslide mapping using Satellite Pour l'Observation de la Terre 5 (SPOT-5) imagery. McKean and Roering [6] also successfully delineated landslide features using measures of surface roughness from LiDAR digital terrain model (DTM). With increasing spatial resolution, however, pixel-based methods have fundamental limitations in addressing particular landslide characteristics due to finite spatial extent. Only those object characteristics allow landslides to be further assigned to different type classes and other features of similar appearance to be discarded. Such methods focusing on features instead of pixels are the basis of object-oriented analysis (OOA).

Study Area 2: Taiwan, typhoon-triggered

- Occurred on 7 August 2009, triggered by Typhoon Morakot
- 673 deaths

Study Area 3: Jiuzhaigou, earthquake-triggered

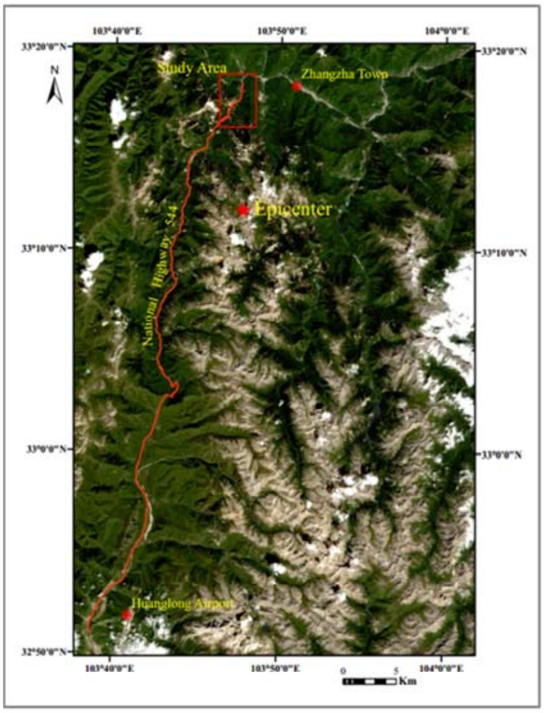

The epicenter is located at 33.20° N and 103.82° E.

Event:

An M_S **7.0 earthquake** occurred in **Jiuzhaigou County**, northeast of Sichuan Province, China on **August 8, 2017**, which induced a large number of shallow landslides.

Study area:

- About 16.5 km².
- About 9 km from the epicenter.
- Landslides distributed along National Highway 544 from Huanglong Airport to Zhangzha Town.

Multi-sensor Data

Messina

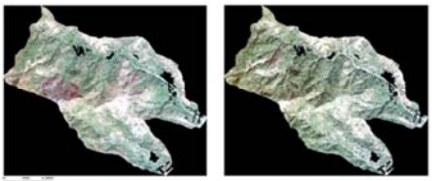

Quickbird (VHR, 2.4 m)

Taiwan

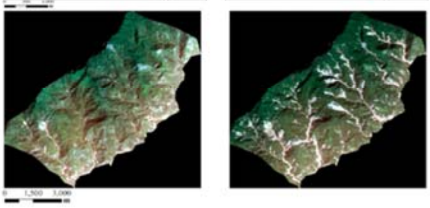

FORMOSAT-2 (HR, 8 m)

Jiuzhaigou

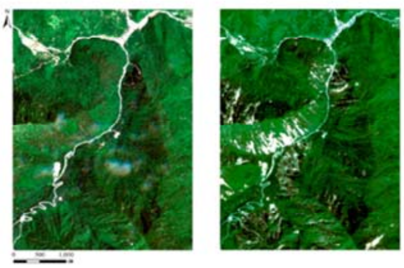

Sentinel-2 (MR, 10 m)

Landsat-8 (30 m) + Sentinel-2 (10 m)
(different sensors)

Methodology

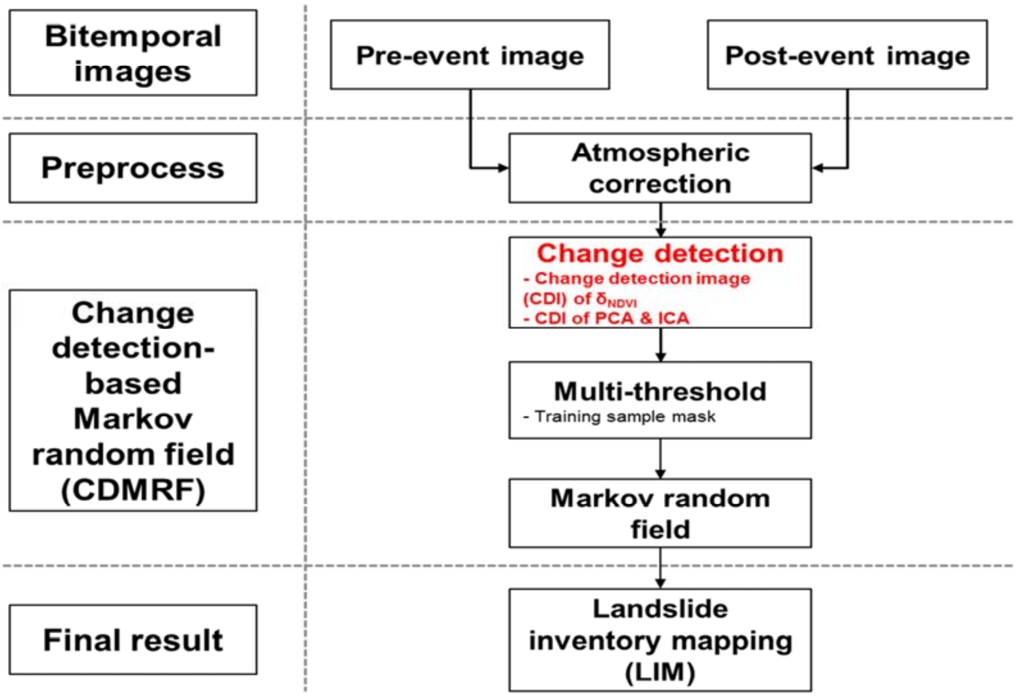

Flowchart of change detection-based Markov Random Field method for landslide inventory mapping

Markov Random Field

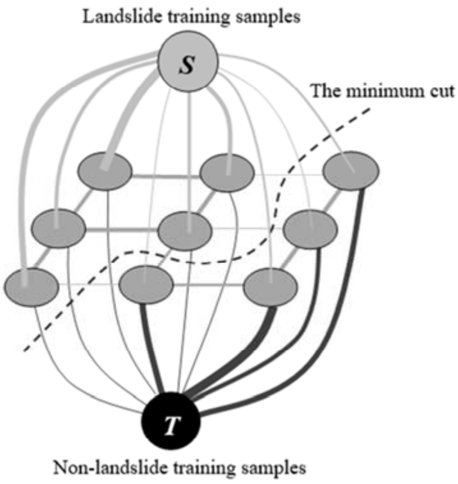

A simple diagram of MRF for a 3×3 image

Input data

- The post –event image
- Training sample mask

The Energy Function

$$E(L) = E_u(L) + \lambda \cdot E_p(L)$$

$$\hat{L} = \arg\min_{L} E(L)$$

$E_u(L)$: the unary potential.

$E_p(L)$: the pairwise potential.

$L = (l_1, l_2, \ldots, l_n)$: a label set and l_i represents the label of the ith pixel.

λ : a coefficient reflecting the relative importance between the unary and pairwise potential.

Output

- Landslide inventory mapping

Mapping Results

Messina

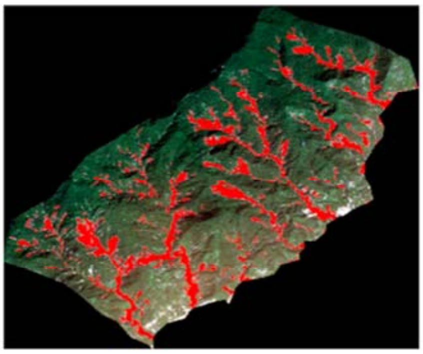

Taiwan

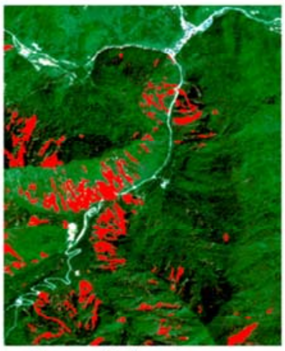

Jiuzhaigou (single sensor)

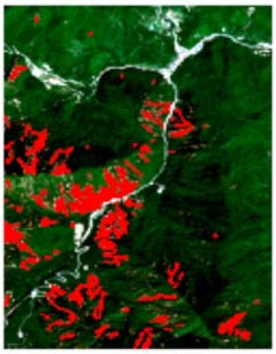

Jiuzhaigou (different sensor)

Accuracy Assessment

Quantitative evaluation results of landslides mapping through CDMRF.

Test site	CDI	Accuracy assessment results					
		Completeness (%)	Correctness (%)	Kappa coefficient	$F_{0.5}$	F_1	F_2
Messina	CVA	19.60	48.65	0.27	0.37	0.28	0.22
	δNDVI	42.83	62.34	0.50	0.57	0.51	0.46
	PCA-4	76.10	82.44	0.80	0.81	0.79	0.77
	ICA-4	88.59	82.48	0.85	0.84	0.85	0.87
Taiwan	CVA	53.50	54.89	0.52	0.55	0.54	0.54
	δNDVI	61.57	69.64	0.64	0.68	0.65	0.63
	PCA-4	81.71	87.45	0.84	0.86	0.84	0.83
	ICA-2	88.83	92.71	0.90	0.92	0.91	0.90
Jiuzhaigou (single sensor)	CVA	59.29	48.24	0.50	0.50	0.53	0.57
	δNDVI	79.01	92.78	0.85	0.90	0.85	0.81
	PCA-4	96.55	85.07	0.90	0.87	0.90	0.94
	ICA-3	86.60	77.35	0.81	0.79	0.82	0.85
Jiuzhaigou (two sensors)	CVA	35.74	46.07	0.36	0.44	0.40	0.37
	δNDVI	82.84	83.77	0.82	0.84	0.83	0.83
	PCA-4	67.90	92.50	0.77	0.86	0.78	0.72
	ICA-3	65.55	85.35	0.72	0.80	0.74	0.69

Conclusions

- NDVI, PCA, and ICA are integrated into MRF for landslide mapping

- Improved CDMRF for landslide mapping from multi-sensor data

- NDVI-, PCA-, and ICA-based MRF outperform CVA-based MRF significantly

- Applicable to map rainfall-, typhoon-, and earthquake-triggered landslides

ELSEVIER

Contents lists available at ScienceDirect

Remote Sensing of Environment

journal homepage: www.elsevier.com/locate/rse

Landslide mapping from multi-sensor data through improved change detection-based Markov random field

Ping Lu[a], Yuanyuan Qin[a], Zhongbin Li[b,*], Alessandro C. Mondini[c], Nicola Casagli[d]

[a] College of Surveying and Geo-Informatics, Tongji University, Siping Road, 1239, Shanghai, China
[b] Center for Global Change and Earth Observations, Michigan State University, East Lansing, MI, USA
[c] CNR IRPI, Via Madonna Alta 126, Perugia, Italy
[d] Department of Earth Sciences, University of Firenze, Via La Pira 4, Firenze, Italy

Rockfall structural protection of the cultural heritage in the City of Omiš, Croatia

Željko Arbanas[1], Marin Sečanj[2], Martina Vivoda Prodan[1], Sanja Dugonjić Jovančević[1], Josip Peranić[1], Sanja Bernat Gazibara[2], Martin Krkač[2], Dalibor Udovič[3], Snježana Mihalić Arbanas[2]

1) University of Rijeka, Rijeka, Faculty of Civil Engineering, Radmile Matejčić 3, Rijeka, Croatia
e-mail: zeljko.arbanas@gradri.uniri.hr
2) University of Zagreb, Faculty of Mining, Geology and Petroleum Engineering, Pierottijeva 6, Zagreb, Croatia
3) Monterra Ltd., Vukovarska 76, Rijeka, Croatia

Abstract

The City of Omiš, is situated in the middle part of the Croatian Adriatic coast, at the mouth of the Cetina River in the toe of high limestone cliffs of the Omiška Dinara Mountain. The mouth of the Cetina River was first permanently inhabited in ancient times, more than 2000 years ago, while the development of now-days City of Omiš started in 12 and 13 century. Several constructions and building, such as fortresses and churches in Omiš belong to the cultural and historical Croatian heritage. The old center of the City of Omiš, was threatened by numerous rockfall occurrences in the past that caused significant damages at residential structures and infrastructure. During the last decades several designs for rockfall protection structures were conducted, followed by installation of protection structures was conducted from 2016 to 2018. During the final design performing the detailed field investigation was carried out using field and remote sensing methods to determine rockfall sources as well as threatened zones of the city. The 2D and 3D numerical modelling and rockfall simulations were performed to determine adequate rockfall protection structures and their locations at the slope. Installed stabilization and protection structures (protection wire fences, wire meshes reinforced by steel ropes and rockbolts, and rockfall barriers) as the first stage of mitigation measures, significantly reduced the rockfall hazard in the City of Omiš. In this paper we will describe the methods of field and remote sensing investigation of the slopes, modelling and simulation of rockfall propagation, as well as selection of protection measures and their positions at the slope above the City of Omiš.

Croatian Landslide Group
IPL World Centre of
Excellence

- Rockfall, by definition a type of landslides that include detachment of the rock or several rock blocks, from mostly sub-vertical rock slope followed by rapid down-slope motion as free-falling, bouncing, rolling and sliding phases, represent a major hazard in areas characterized by steep slopes built in different rock masses.

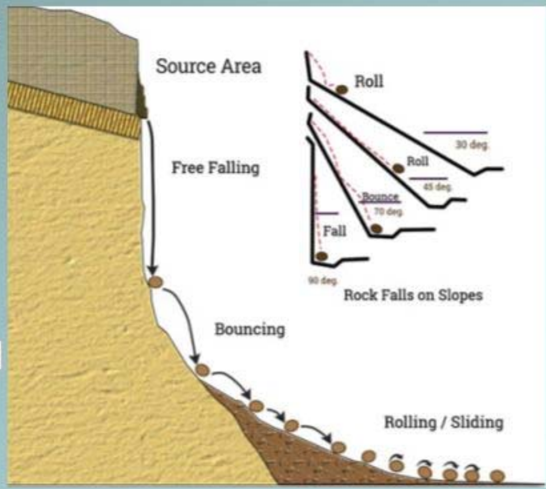

ICL Symposium, UNESCO Paris, 16-19 September 2019

Croatian Landslide Group
IPL World Centre of
Excellence

- The old town of Omiš, is situated in the middle part of the Adriatic coast, at the mouth of the Cetina River in the toe of high limestone cliffs and it is very exposed to high rockfall hazards.

ICL Symposium, UNESCO Paris, 16-19 September 2019

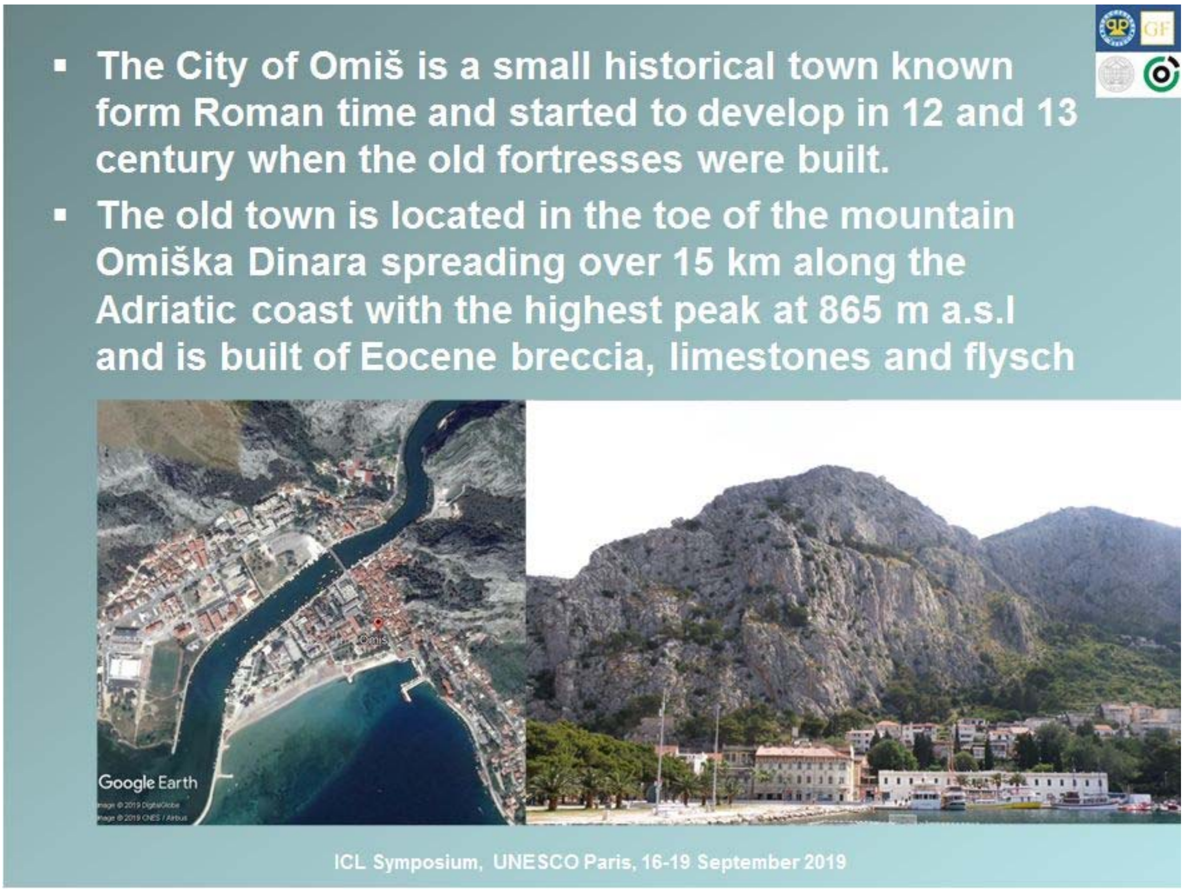

▪ The City of Omiš is a small historical town known form Roman time and started to develop in 12 and 13 century when the old fortresses were built.
▪ The old town is located in the toe of the mountain Omiška Dinara spreading over 15 km along the Adriatic coast with the highest peak at 865 m a.s.l and is built of Eocene breccia, limestones and flysch
Google Earth
ICL Symposium, UNESCO Paris, 16-19 September 2019

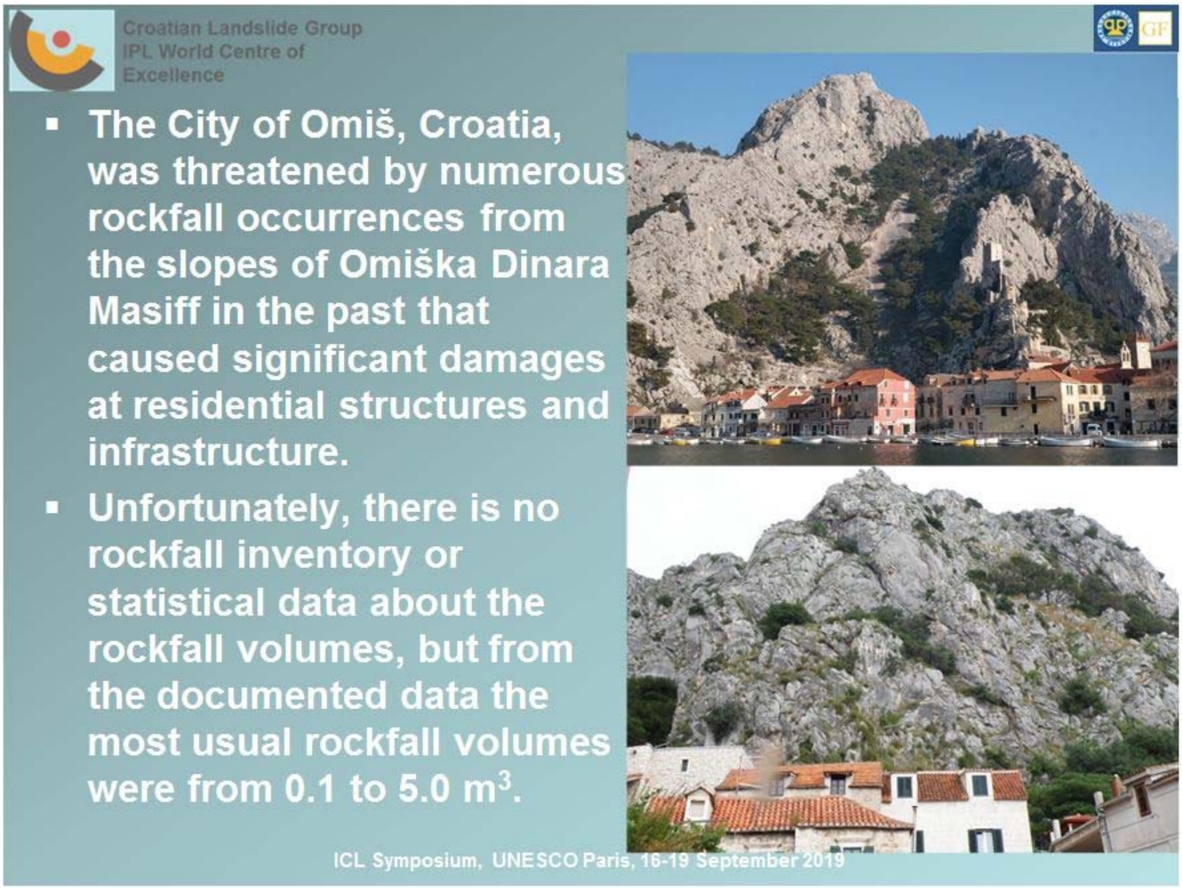

Croatian Landslide Group
IPL World Centre of Excellence
▪ The City of Omiš, Croatia, was threatened by numerous rockfall occurrences from the slopes of Omiška Dinara Masiff in the past that caused significant damages at residential structures and infrastructure.
▪ Unfortunately, there is no rockfall inventory or statistical data about the rockfall volumes, but from the documented data the most usual rockfall volumes were from 0.1 to 5.0 m^3.
ICL Symposium, UNESCO Paris, 16-19 September 2019

Croatian Landslide Group
IPL World Centre of Excellence

- Several blocks fallen from the cliffs hit directly in the houses and came through the construction in the past without any injured and human victim.
- These occurrences pointed on necessary rockfall hazard and risk analyses and rockfall protection measures.

(*www.24sata.hr*)

ICL Symposium, UNESCO Paris, 16-19 September 2019

Croatian Landslide Group
IPL World Centre of Excellence

- The administration of the City of Omiš started with rockfall protection measures design in 2008.
- In period from 2008 to 2012 preliminary and main designs for rockfall protection measures were completed for 22 identified potentially dangerous location that included several potentially unstable blocks (source zones) as well as the zones that could be reached by rockfall mass.
- The main design was set up on very poor preliminary data:
  - Old topographic maps (in scale 1:5000) were used for designing that not enabled more accurate determination of rockfall source zones and potentially unstable rock block volumes.
  - No engineering geological survey was done and no engineering geological map was created to identify rock mass structure and rock mass characteristics.
  - Potential unstable rock blocks on the slope are visually determined from the toe of the slope and approximately located in the maps.

ICL Symposium, UNESCO Paris, 16-19 September 2019

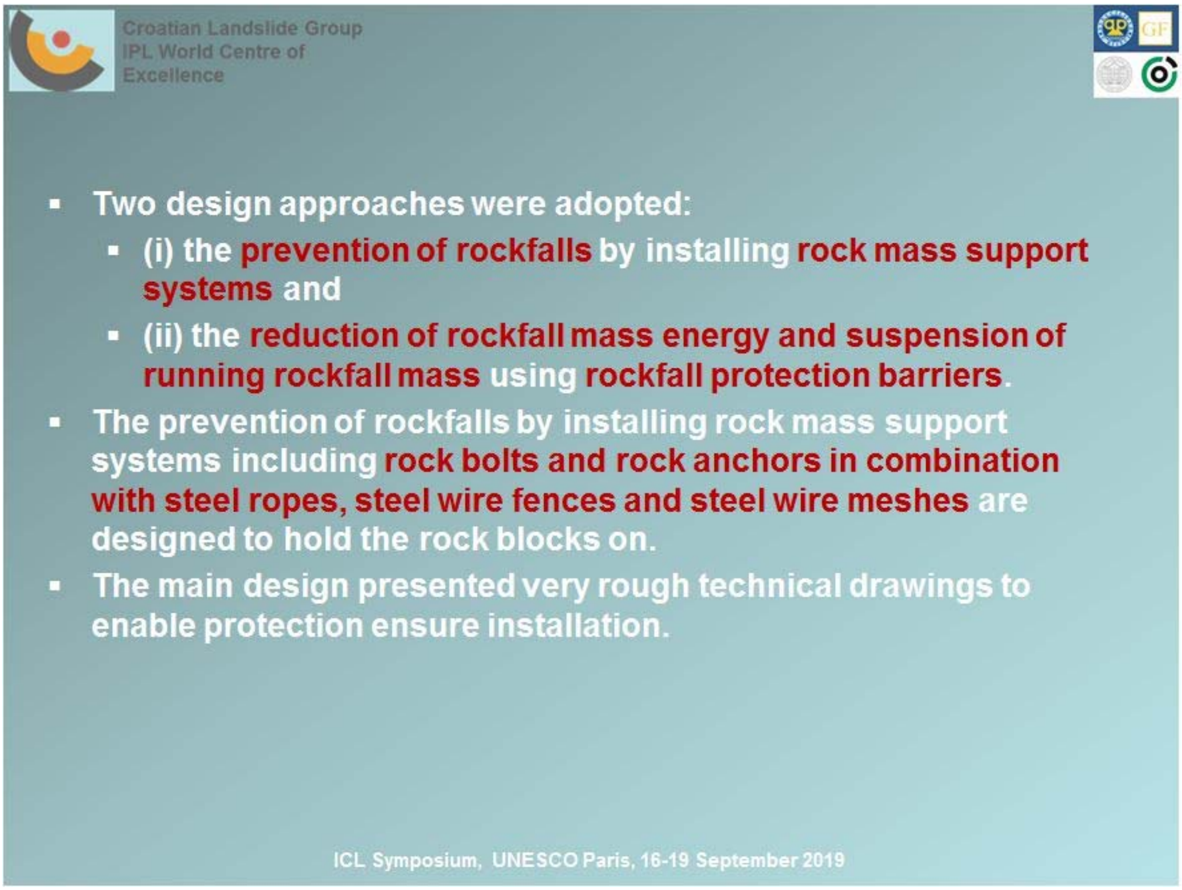
Croatian Landslide Group
IPL World Centre of
Excellence
GF
Two design approaches were adopted:
(i) the prevention of rockfalls by installing rock mass support systems and
(ii) the reduction of rockfall mass energy and suspension of running rockfall mass using rockfall protection barriers.
The prevention of rockfalls by installing rock mass support systems including rock bolts and rock anchors in combination with steel ropes, steel wire fences and steel wire meshes are designed to hold the rock blocks on.
The main design presented very rough technical drawings to enable protection ensure installation.
ICL Symposium, UNESCO Paris, 16-19 September 2019

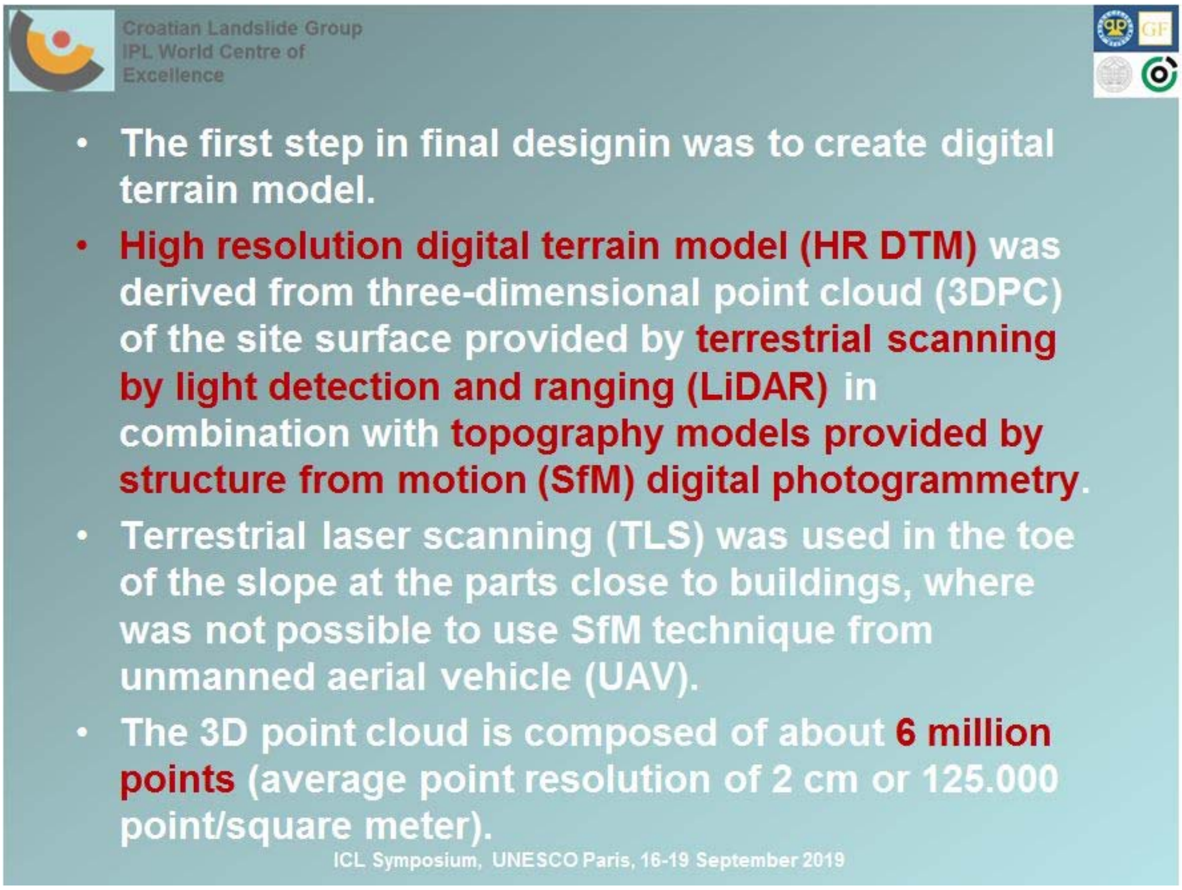
Croatian Landslide Group
IPL World Centre of
Excellence
GF
The first step in final designin was to create digital terrain model.
High resolution digital terrain model (HR DTM) was derived from three-dimensional point cloud (3DPC) of the site surface provided by terrestrial scanning by light detection and ranging (LiDAR) in combination with topography models provided by structure from motion (SfM) digital photogrammetry.
Terrestrial laser scanning (TLS) was used in the toe of the slope at the parts close to buildings, where was not possible to use SfM technique from unmanned aerial vehicle (UAV).
The 3D point cloud is composed of about 6 million points (average point resolution of 2 cm or 125.000 point/square meter).
ICL Symposium, UNESCO Paris, 16-19 September 2019

Croatian Landslide Group
IPL World Centre of
Excellence

- **High resolution digital terrain model (HR DTM) enabled:**
  - **Identification and location unstable blocks** from the main project and positioning their locations in the model
  - **Remote sensing engineering geological mapping**
  - Determination of **joint sets** and their characteristics (app. 2700 joint sets in the area): **discontinuities orientation**, **spacing** and **persistence**
  - Determination of **block volumes**

as a data for rockfall simulations and rockfall protection analyses.

ICL Symposium, UNESCO Paris, 16-19 September 2019

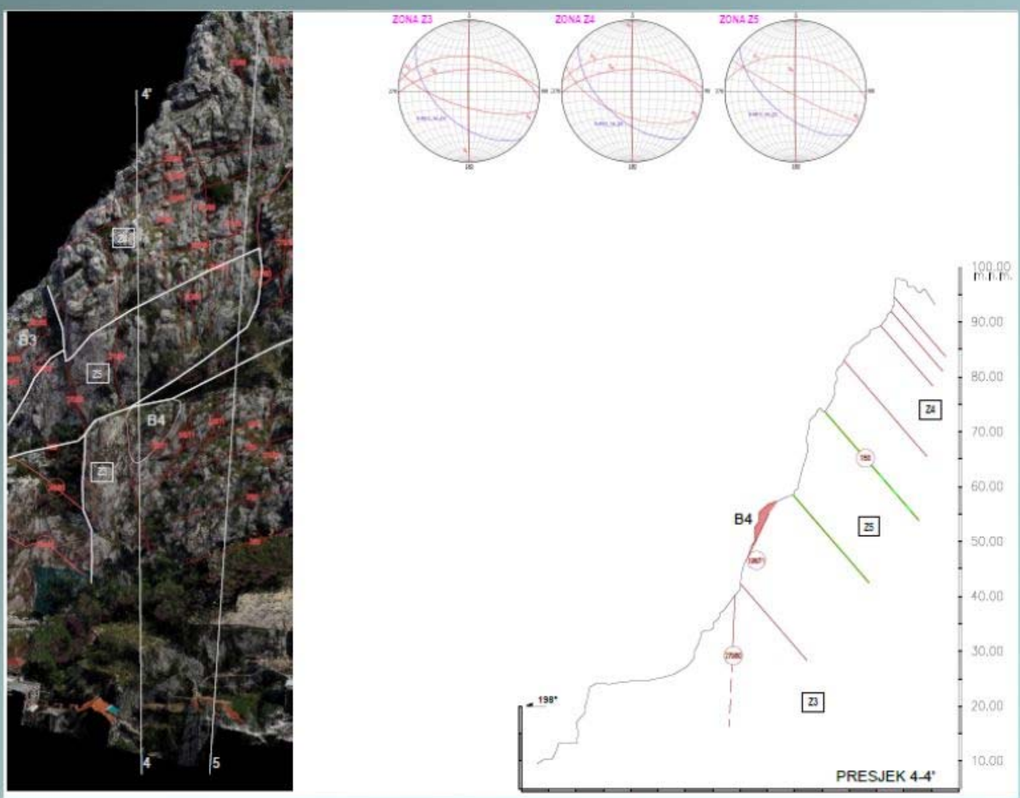

ICL Symposium, UNESCO Paris, 16-19 September 2019

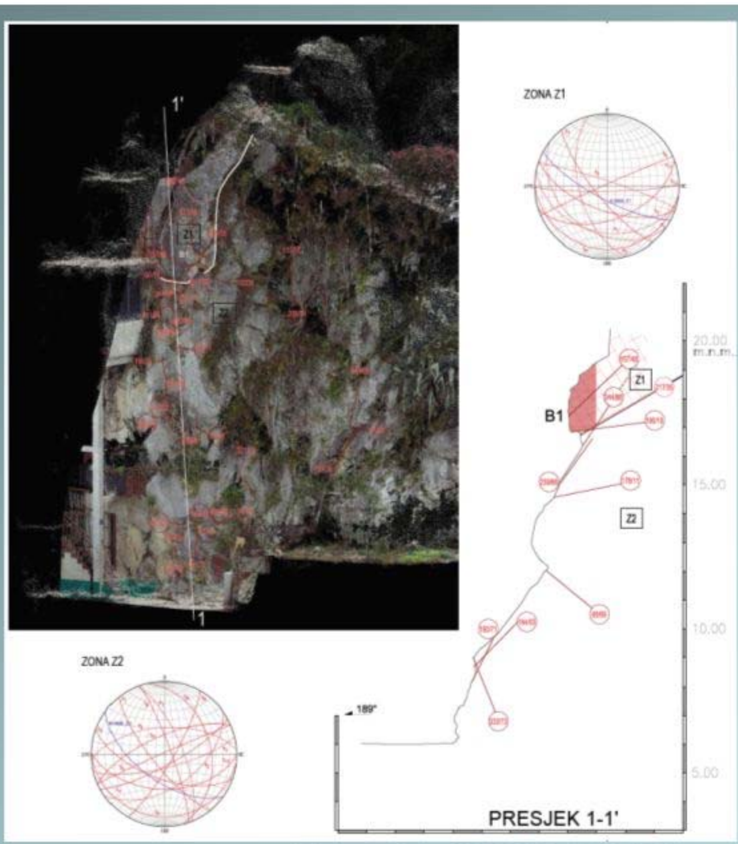

ICL Symposium, UNESCO Paris, 16-19 September 2019

Croatian Landslide Group
IPL World Centre of Excellence

- Based on rock mass and discontinuities characterization data, **spatial kinematic analysis** were conducted to identify kinematic conditions of possible **planar**, **wedge** and **toppling rock mass failure** in different parts of the slope.
- RocPro3D and RockFall software was employed to conduct the rockfall simulation.
- Position of **each barrier pole was precisely determined and defined in high resolution DTM and 3DPC** that enabled clear determination in construction stage.
- Stability analyses for potentially unstable rock blocks **defined necessary support system for each analyzed rock block** and precisely determined and **defined elements of support system in high resolution DTM and 3DPC**.

ICL Symposium, UNESCO Paris, 16-19 September 2019

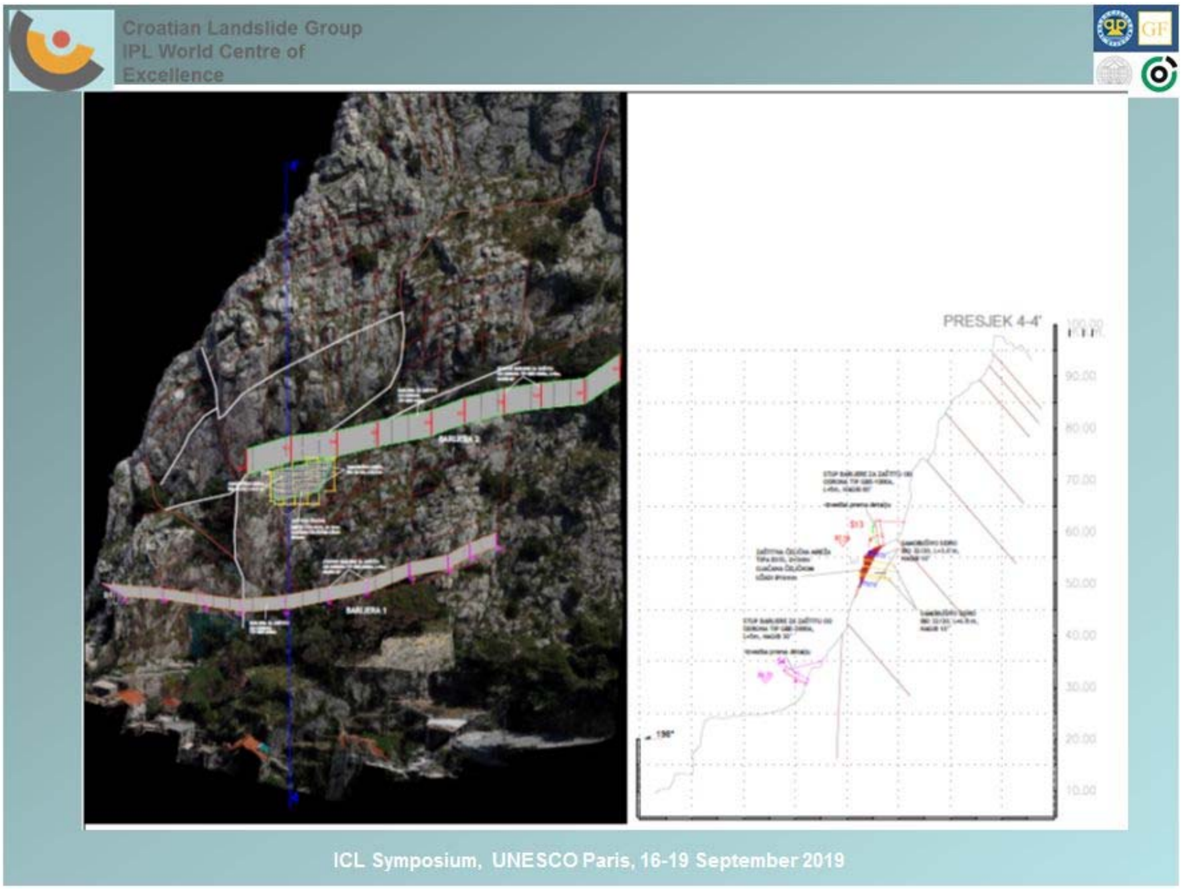
Croatian Landslide Group
IPL World Centre of
Excellence
PRESJEK 4-4'
100.00
90.00
80.00
70.00
60.00
50.00
40.00
30.00
20.00
10.00
ICL Symposium, UNESCO Paris, 16-19 September 2019

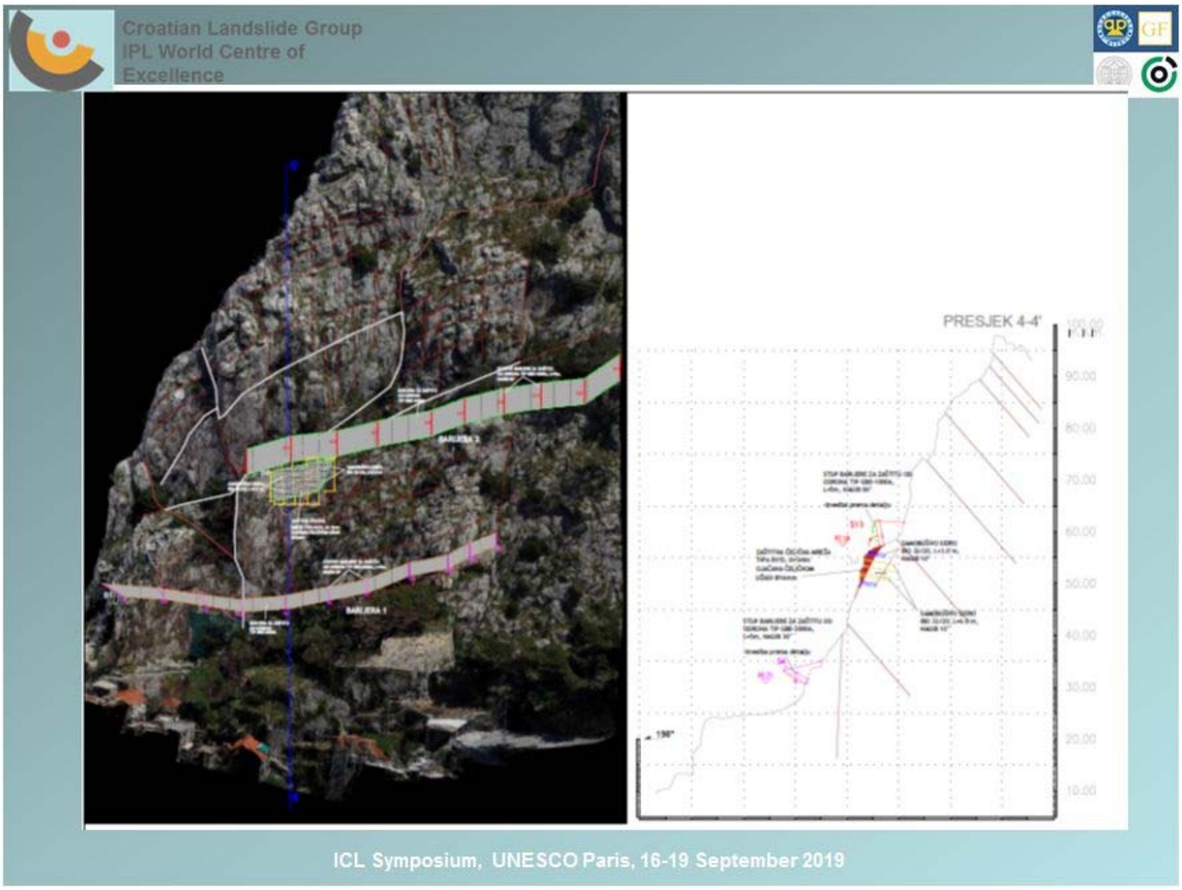
Croatian Landslide Group
IPL World Centre of
Excellence
PRESJEK 4-4'
100.00
90.00
80.00
70.00
60.00
50.00
40.00
30.00
20.00
10.00
ICL Symposium, UNESCO Paris, 16-19 September 2019

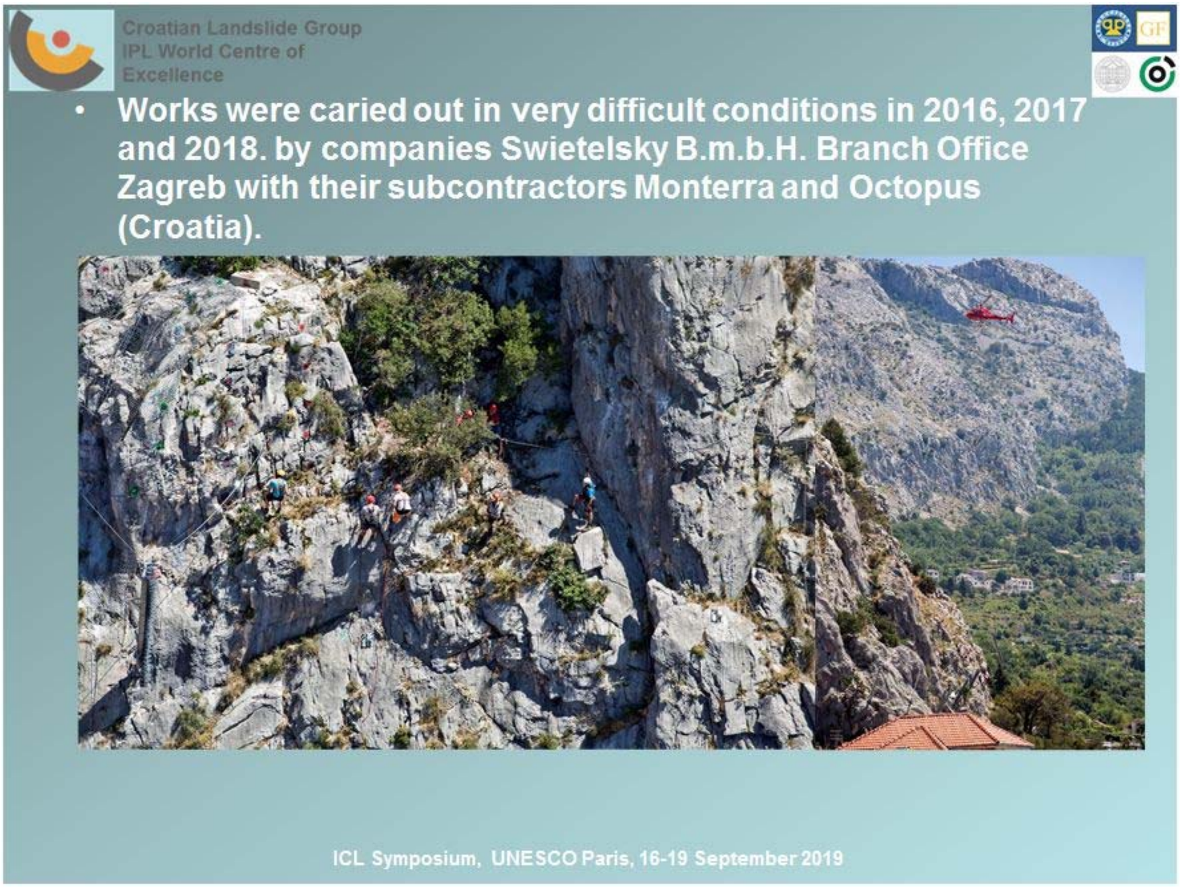
Croatian Landslide Group
IPL World Centre of
Excellence
• Works were caried out in very difficult conditions in 2016, 2017 and 2018. by companies Swietelsky B.m.b.H. Branch Office Zagreb with their subcontractors Monterra and Octopus (Croatia).
ICL Symposium, UNESCO Paris, 16-19 September 2019

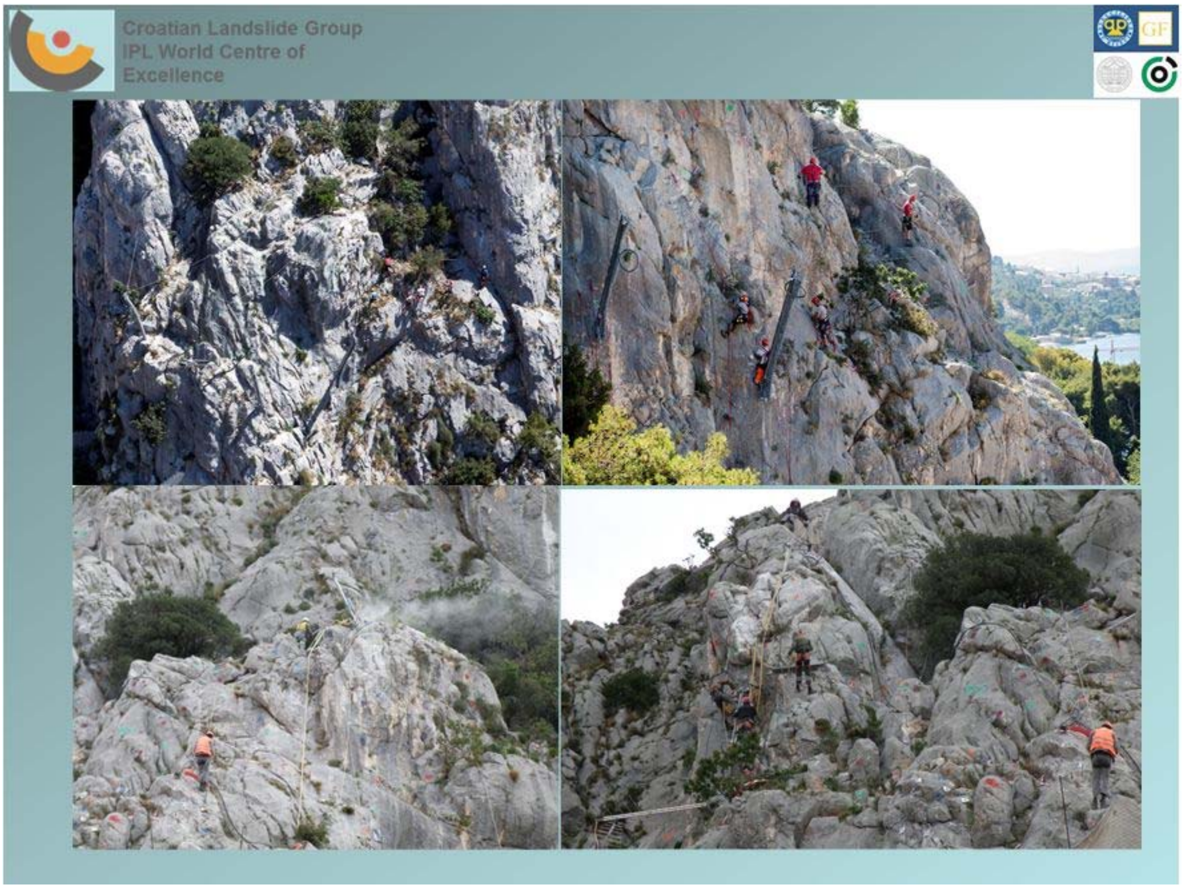
Croatian Landslide Group
IPL World Centre of
Excellence

Croatian Landslide Group
IPL World Centre of
Excellence

- **RESULTS**
- It can be concluded:
- The **rockfall hazard** at the slopes above the City of Omiš **is reduced,**
- The **rockfall risk** for the City of Omiš **is significantly diminished**, but the main risk **not adequately minimized**.

ICL Symposium, UNESCO Paris, 16-19 September 2019

Croatian Landslide Group
IPL World Centre of
Excellence

- **CONCLUSIONS**
- Construction of support systems and installation of rockfall protection barriers above the City of Omiš are completed in November 2018 according to the final design.
- Conducted analyses pointed out that the carried out protection measures will not ensure the residents and buildings in the City of Omiš from all possible rockfall events.
- To ensure full protection, it would be necessary to conduct a rockfall hazard and risk analysis that would identify rockfall potential from the slopes above the City of Omiš.
- The next stage of rockfall protection should use advanced methods in rockfall source identification and rock mass characterization to enable adequate rockfall simulations and numerical analyses in rock protect measure designing.

ICL Symposium, UNESCO Paris, 16-19 September 2019

Croatian Landslide Group
IPL World Centre of
Excellence

Thank you for your attention!

This research is conducted in the frame of the Projects:

- Rockfall hazard identification and rockfall protection in the coastal zone of Croatia, IPL Project 219
- Research of Rockfall Processes and Rockfall Hazard Assessment, University of Rijeka, uniri-tehnic-18-276

ICL Symposium, UNESCO Paris, 16-19 September 2019

Diversity of landslide types identified in Vinodol Valley (Croatia) using airborne LiDAR imagery

Petra Đomlija(1), Željko Arbanas(1), Vedran Jagodnik(1), Snježana Mihalić Arbanas(2)

1) University of Rijeka, Faculty of Civil Engineering, Rijeka, Radmile Matejčić 3, 51000
e-mail: petra.domlija@gradri.uniri.hr
2) University of Zagreb, Faculty of Mining, Geology and Petroleum Engineering, Zagreb

Abstract

Sliding and erosion processes are active in the Vinodol Valley (area of 64.57 km2) since historical time. Although these processes contribute to landscape evolution, and as well they continuously cause economic losses, systematic scientific investigations of their types, characteristics and spatial arrangement in relation to geomorphological conditions of the Vinodol Valley so far was lacking. For the study area, the bare-earth Digital Terrain Model (DTM) was created with a 1 m resolution from the elevation data acquired by airborne laser scanning using the LiDAR (Light Detection and Ranging) technology, in March 2012. Nine types of topographic datasets were derived from the high-resolution LiDAR DTM for the visual interpretation of topography of the Vinodol Valley. LiDAR derivatives were visually interpreted singularly and in combinations, in a large scale. Identification and mapping of landslide phenomena was performed according to specific criteria that were established exclusively for each landslide type. Landslides are classified according to the updated Varnes classification of landslide types. In total, ten types of landslides were identified, and a detail geomorphological historical landslide inventory was created. For 633 landslide phenomena, an accurate landslide contour could be precisely delineated, due to the visible topography of landslide features recognized on LiDAR derivatives. The most abundant landslide phenomena in the Vinodol Valley are debris slides. The spatial arrangement of landslides is distinctively irregular, whereas most of the identified debris slides are situated in numerous gullies of different types.

Vinodol Valley

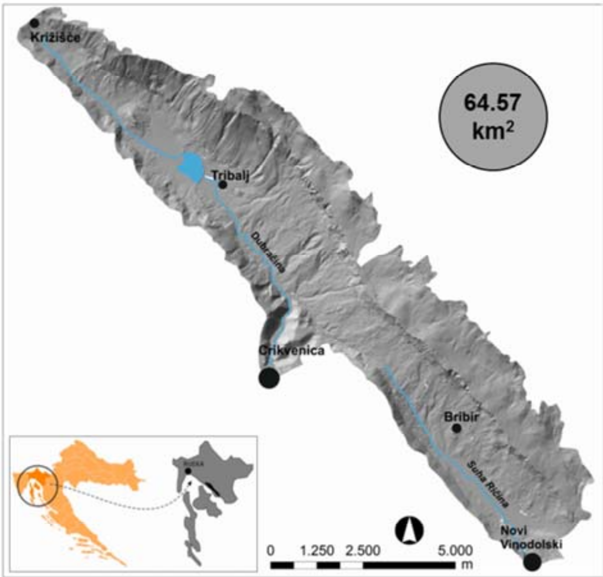

- north-western coastal part of Croatia
- rural area, with more than 50 small settlements
- dense road network
- valley flanks composed of carbonate rock mass
- inner parts and the bottom of the valley composed of flysch rock mass
- flysch bedrock mostly covered by various types of superficial deposits

Landslides and erosion - interrelated hazardous phenomena

infrastructure damages and economic losses

landscape evolution

Research motivation

- lack of detail and systematic investigations
- conventional research methods previously available
- study area covered by dense vegetation

Inovative technology

- airborne laser scanning in March 2012
- last returns density: 4.03 points/m^2
- *bare- earth* Digital Terrain Model 1 x 1 m

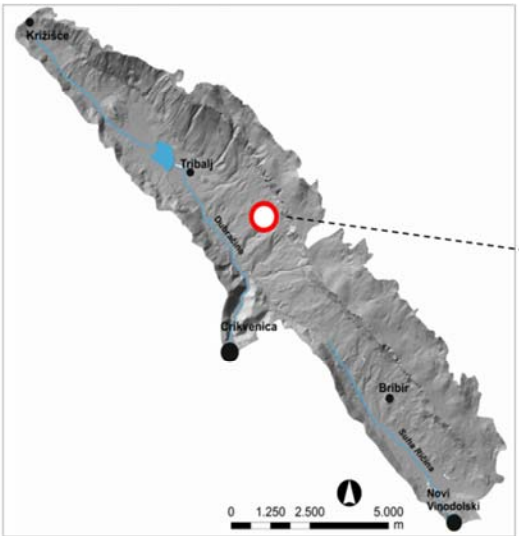

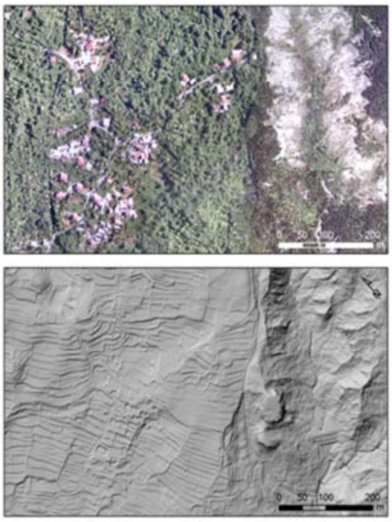

LiDAR topographic datasets

- derived from the 1 x 1 m DTM
- *ArcGIS 10.0* software tools

Hillshade map

Slope map

Contour line map

Topographic roughness map

Aspect map

Profile curvature map

Planform curvature map

Flow accumulation map

Stream power index map

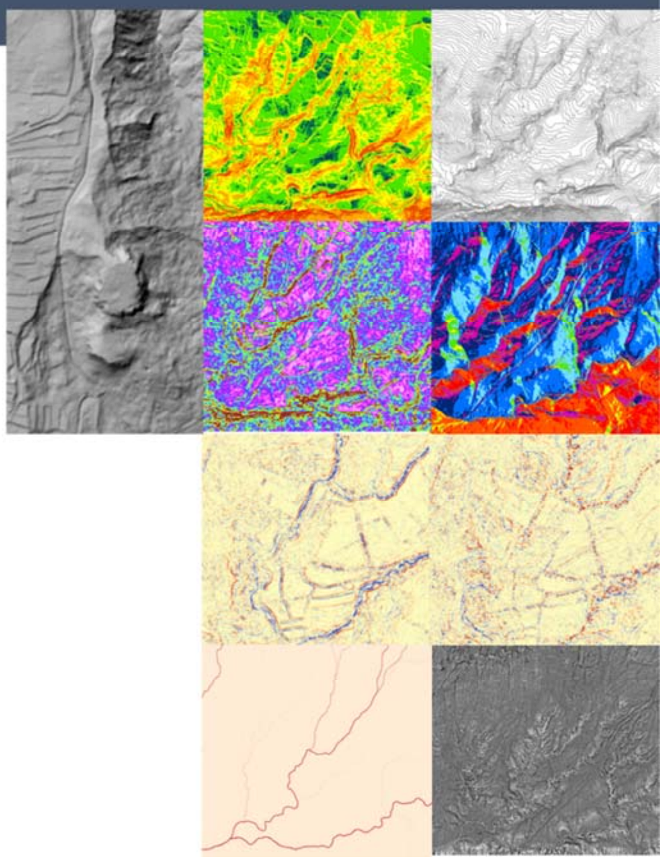

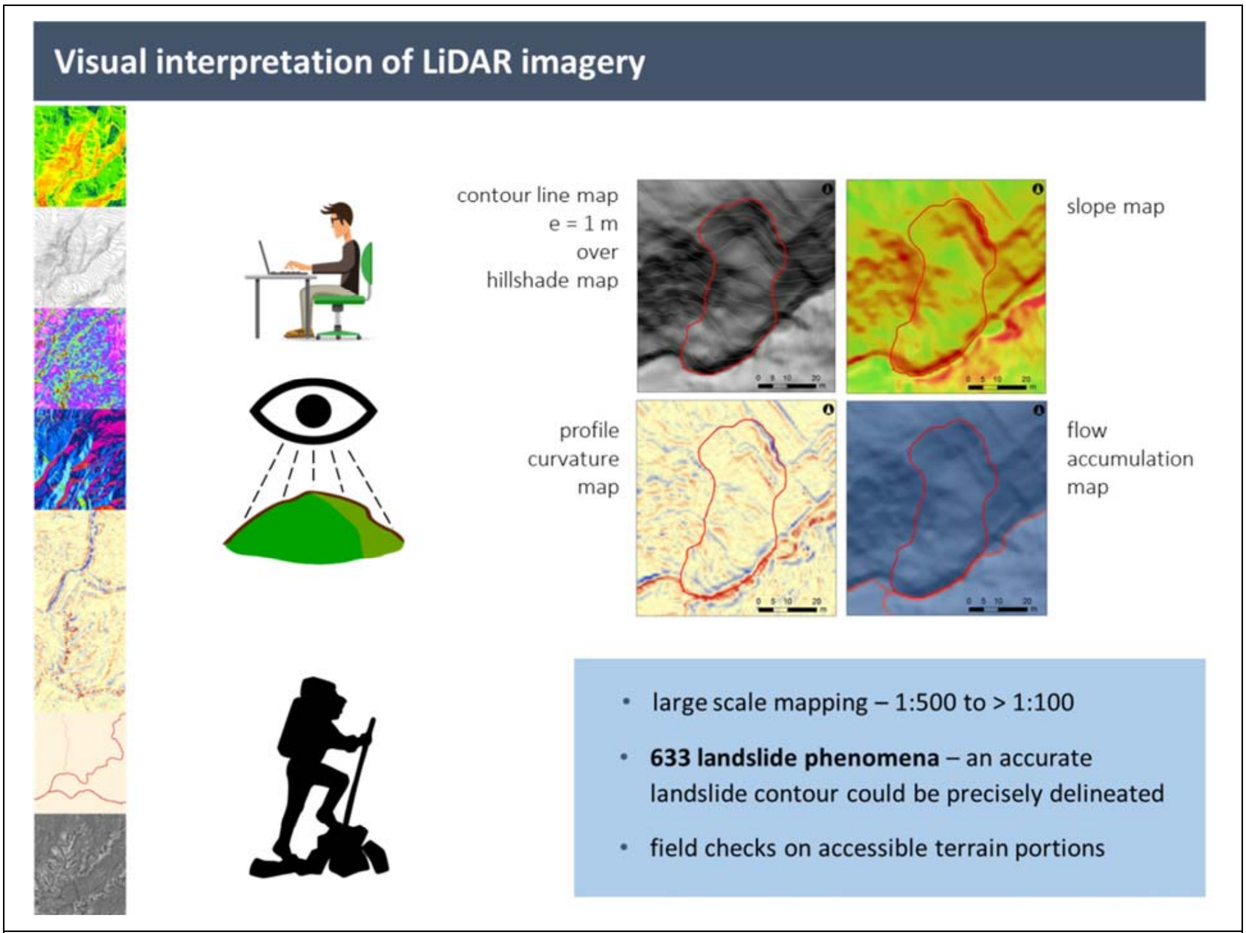
Visual interpretation of LiDAR imagery
contour line map
e = 1 m
over
hillshade map
slope map
profile
curvature
map
flow
accumulation
map
• large scale mapping – 1:500 to > 1:100
• 633 landslide phenomena – an accurate landslide contour could be precisely delineated
• field checks on accessible terrain portions

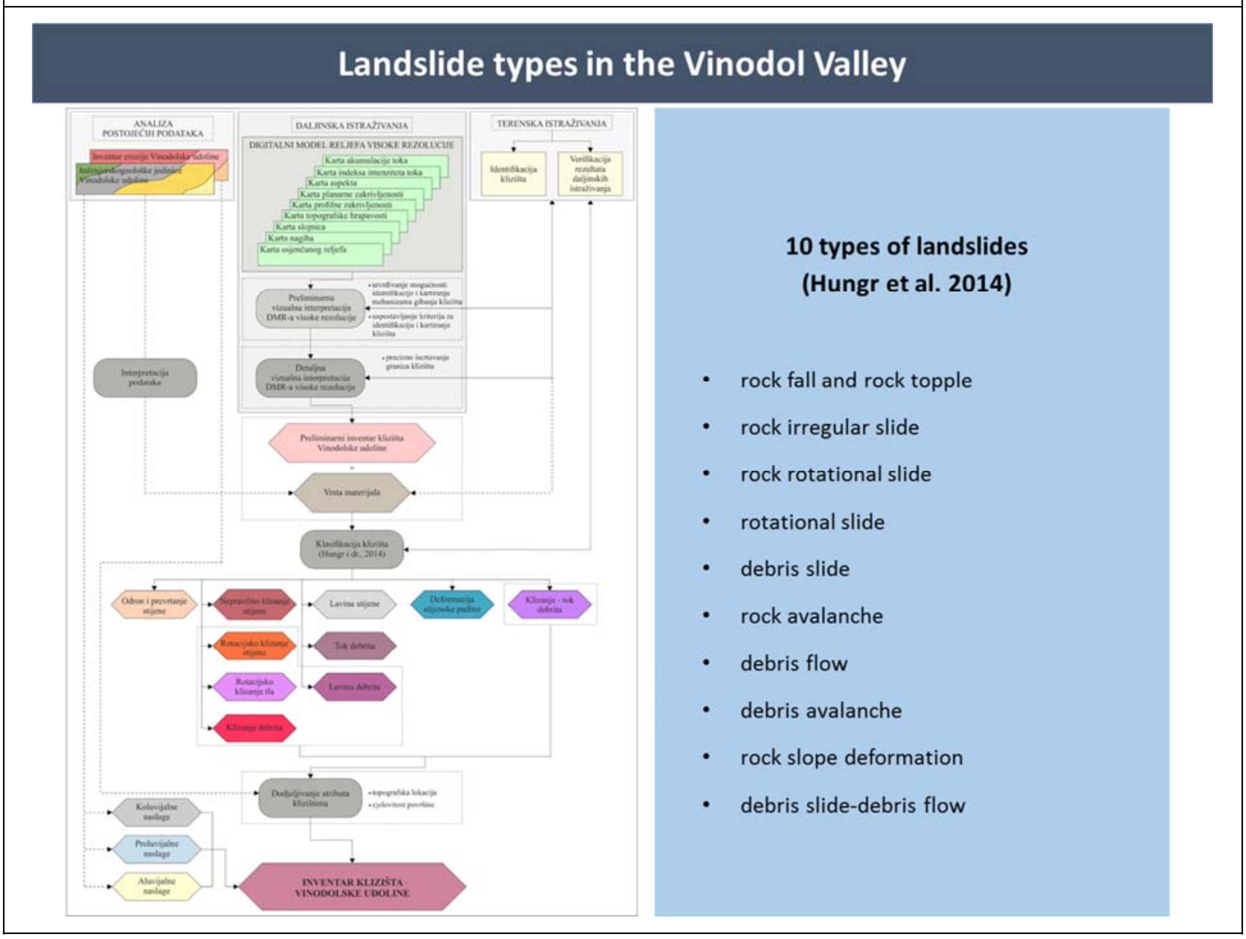
Landslide types in the Vinodol Valley
10 types of landslides
(Hungr et al. 2014)
• rock fall and rock topple
• rock irregular slide
• rock rotational slide
• rotational slide
• debris slide
• rock avalanche
• debris flow
• debris avalanche
• rock slope deformation
• debris slide-debris flow

Debris slides

- **484 phenomena in the Vinodol Valley**
- different types of debris material

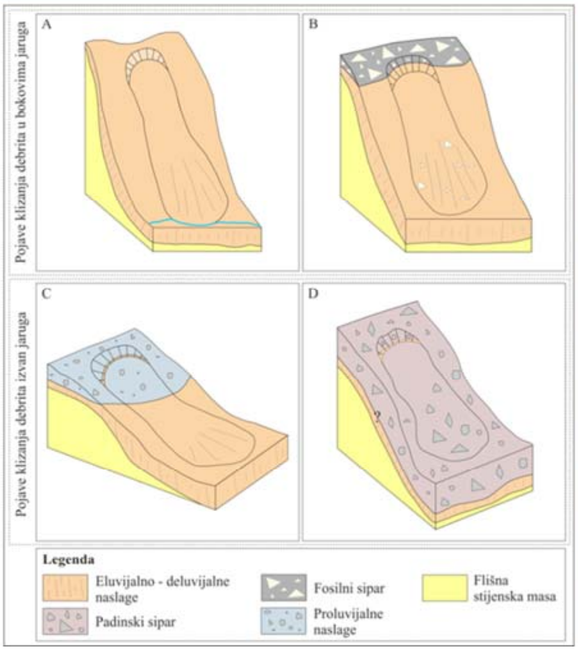

Debris slides

- 376 landslides located within gullies
- 108 landslides located on slopes outside gullies
- very small to moderate-small, shallow to moderate-shallow landslides

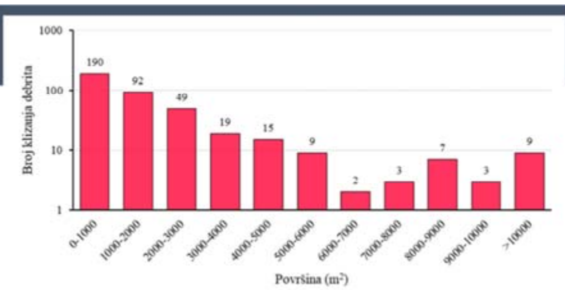

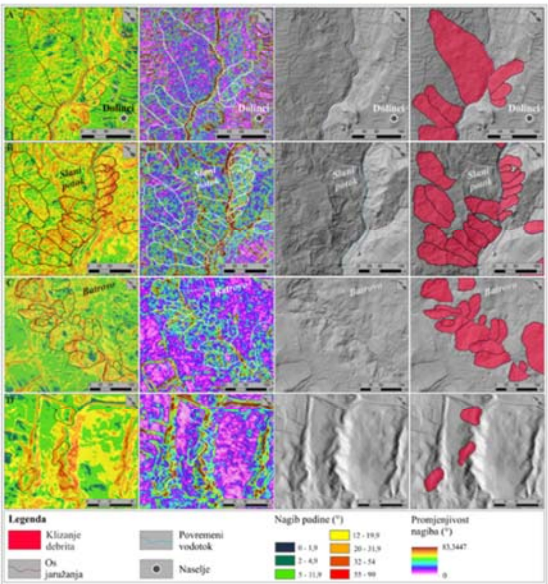

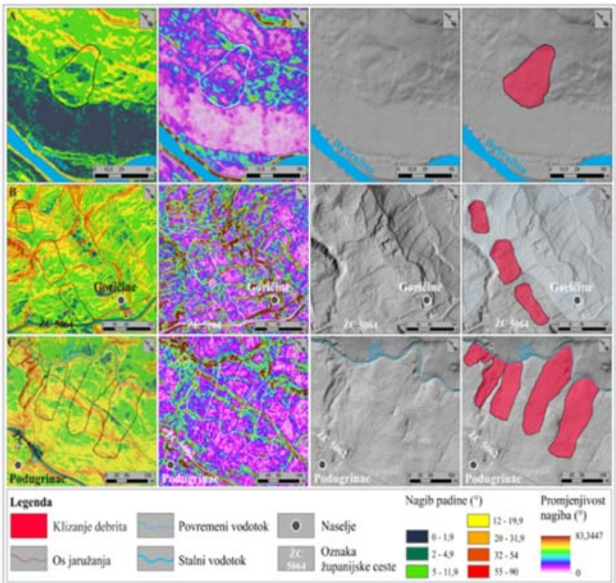

Debris slide-debris flows

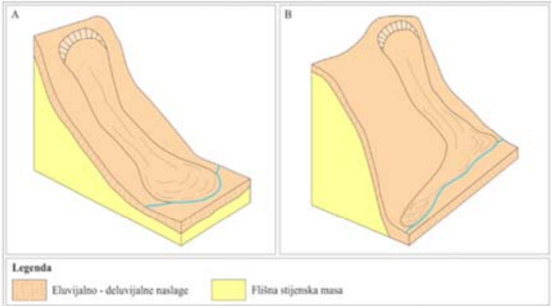

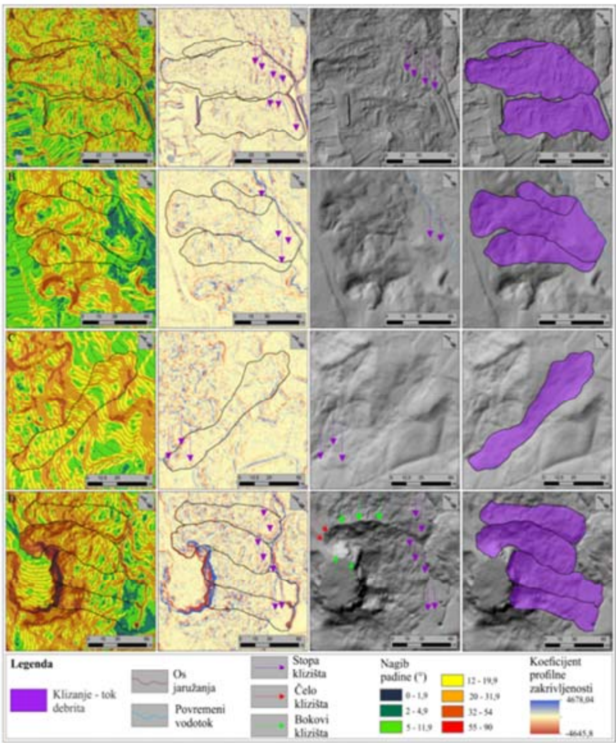

- **136 phenomena in the Vinodol Valley**
- 131 landslides located within gullies
- 5 landslides located on slopes outside gullies

- ***A-type*** – the displaced material flows to the gully thalweg
- ***B-type*** – the flow of the displaced material continues along the gully thalweg and infills the bottom of the gully challen

Debris slide-debris flows

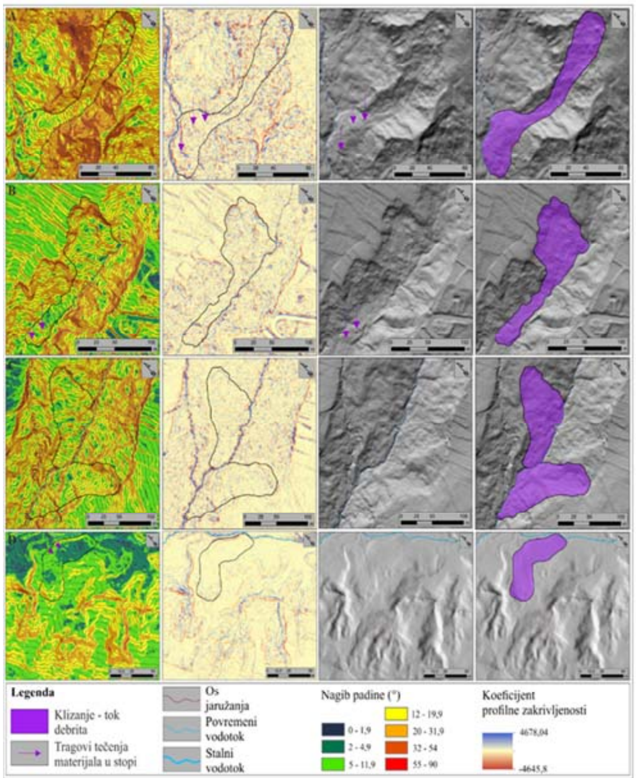

- very small to moderate-small landslides
- shallow to moderate-shallow landslides
- landslide volumes in a range between < 10^3 and 10^5 m^3

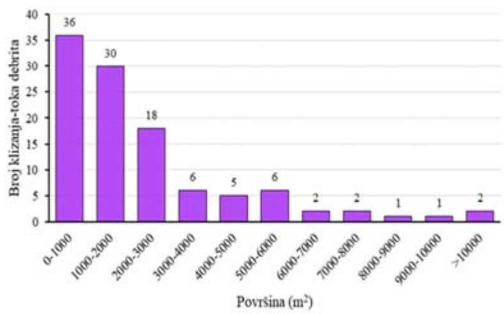

Rock falls and rock topples

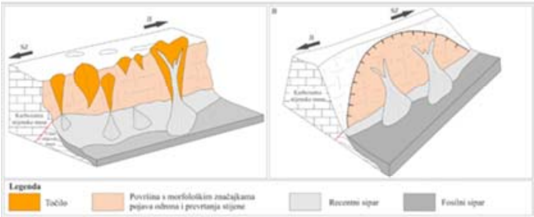

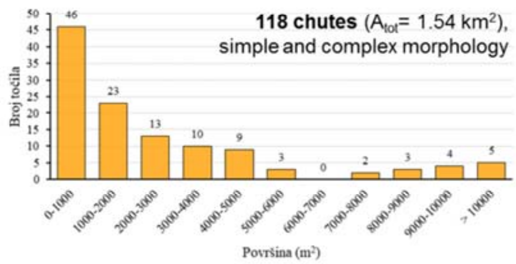

- indirectly mapped from LiDAR imagery:
  - chutes
  - free cliff face
  - recent and older talus deposits

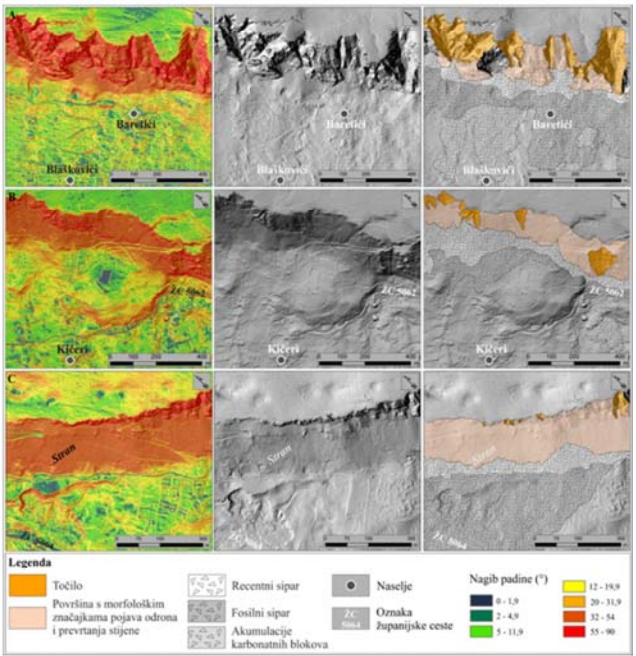

Debris flows

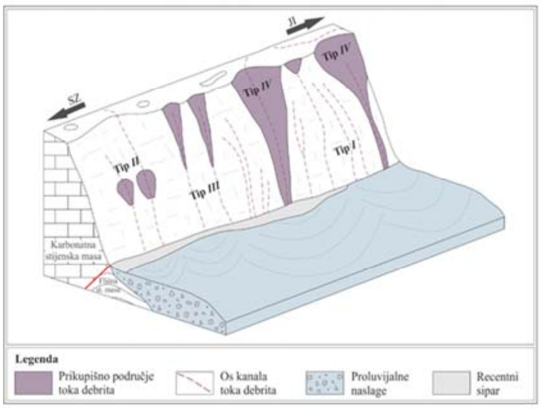

- 125 phenomena in the Vinodol Valley
- 4 morphological types of debris flow channels
- A_{uk} = 2.44 km^2

North-western part of the Vinodol Valley

- 100 phenomena
- 30 debris flow channels of *IV-type* (A_{tot} = 1.76 km^2)

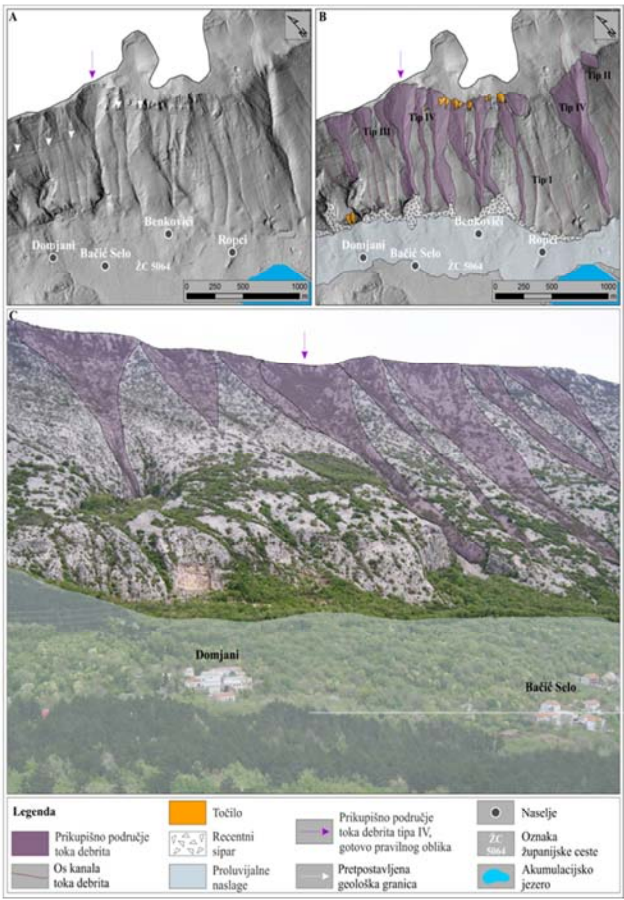

Rock rotational slides

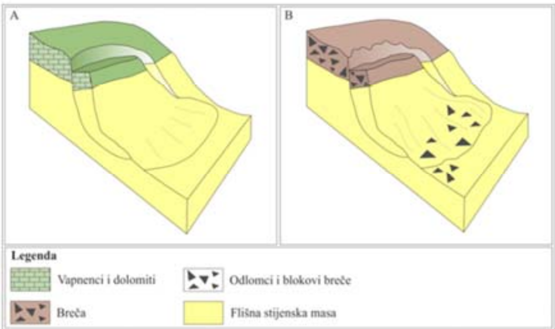

- 6 phenomena in the Vinodol Valley
- A_{min} = 3,176.84 m^2; A_{max} = 63,708.48 m^2

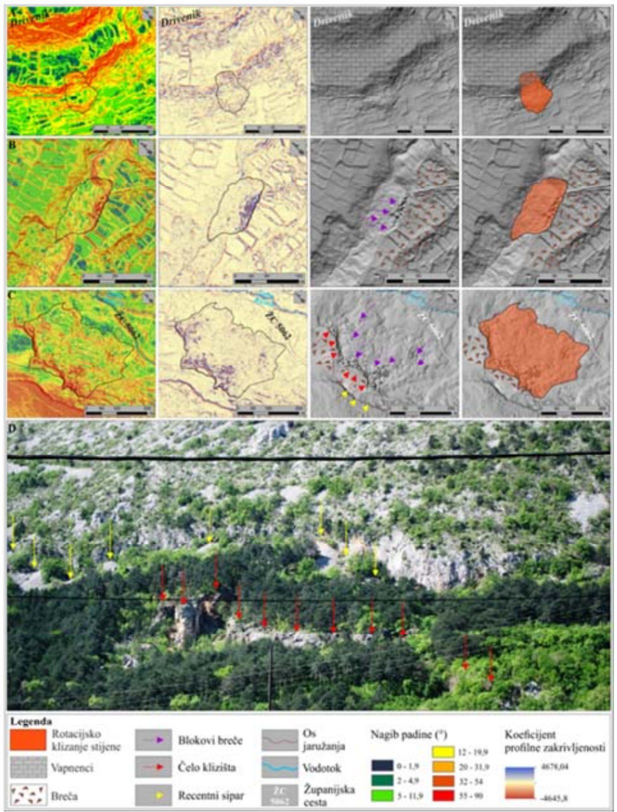

Landslide inventory of the Vinodol Valley

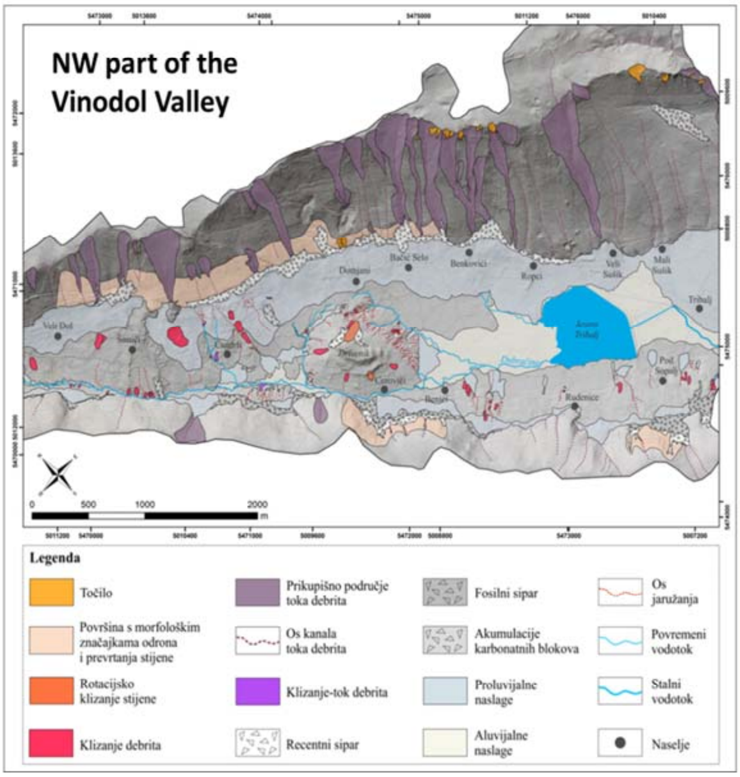

geomorphological historical landslide inventory

- ~ 6 months for preparation
- totally 840 polygons
- 633 polygons of individual landslide phenomena
- 627 landslides in soil materials
- A_{tot} = 1.41 km^2
- A_{min} = 64.80 m^2 (debris slide)
- A_{max} = 49 461.62 m^2 (debris avalanche)
- Q_3 = 2 457.37 m^2
- **7.53 km^2 (11.67 %) of the Vinodol Valley covered by landslides**

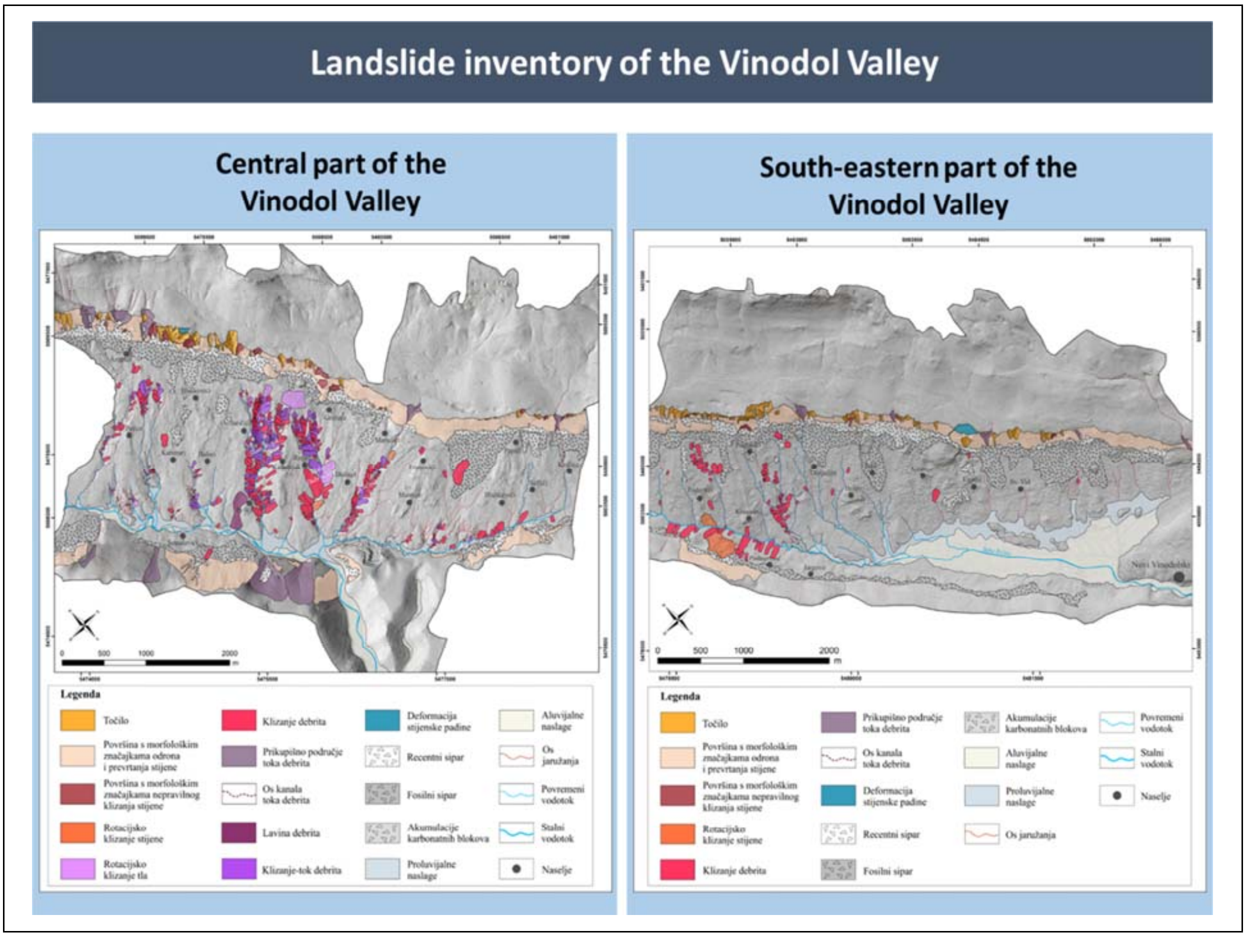
Landslide inventory of the Vinodol Valley
Central part of the Vinodol Valley
0 500 1000 2000 m
Legenda
Točilo
Površina s morfološkim značajkama odrona i prevrtanja stijene
Površina s morfološkim značajkama nepravilnog klizanja stijene
Rotacijsko klizanje stijene
Rotacijsko klizanje tla
Klizanje debrita
Prikupilno područje toka debrita
Os kanala toka debrita
Lavina debrita
Klizanje-tok debrita
Deformacija stijenske padine
Recentni sipar
Fosilni sipar
Akumulacije karbonatnih blokova
Proluvijalne naslage
Aluvijalne naslage
Os jaružanja
Povremeni vodotok
Stalni vodotok
Naselje
South-eastern part of the Vinodol Valley
0 500 1000 2000 m
Legenda
Točilo
Površina s morfološkim značajkama odrona i prevrtanja stijene
Površina s morfološkim značajkama nepravilnog klizanja stijene
Rotacijsko klizanje stijene
Klizanje debrita
Prikupilno područje toka debrita
Os kanala toka debrita
Deformacija stijenske padine
Recentni sipar
Fosilni sipar
Akumulacije karbonatnih blokova
Aluvijalne naslage
Proluvijalne naslage
Os jaružanja
Povremeni vodotok
Stalni vodotok
Naselje

Landslide risk management at the community level – lessons learned in the Andean peasant community, Cordillera Negra, Peru

Jan Klimeš(1), Ana Marlene Rosario (2), Roque Vargas(3), Pavel Raška(4), Luis Vicuña(5), Christine Jurt(5)

1) Institute of Rock Structure and Mechanics The Czech Academy of Sciences, Prague, Czechia, e-mail: klimes@irsm.cas.cz
2) Instituto Nacional de Investigación en Glaciares y Ecosystemas de Montaña, Department of Mountain Ecosystems , Huaráz, Peru
3) Instituto Nacional de Investigación en Glaciares y Ecosystemas de Montaña, Department of Glacier Research, Huaráz, Peru
4) Jan Evangelista Purkyne University, Department of Geography, Usti nad Labem, Czechia
5) University of Zurich, Department of Geography, Zürich, Switzerland

Abstract

This presentation describes the history of scientific research and landslide disaster risk reduction efforts in a small peasant community in the Rampac Grande of the Peruvian Andes. The community was hit by a catastrophic landslide in 2009, which challenged local knowledge about landslide occurrences. The DRR project performed during 2016 - 2017 illustrates the shift from refusing outside intervention to acceptance of the proposed landslide risk reduction measures and active community participation in their application and maintenance. Emphasis was placed on the role played by community representative participation during formulation of the expected outcomes of the DRR, which leads to hazard reduction through the preparation of hazard maps and landslide movement monitoring. The short-term success was documented by the construction of water tanks in the year following termination of the project. Despite of that, definition of long-term exit strategy, involving the minimum input from the outside actors, still needs to be done in order to permanently reduce the community vulnerability to the landslide risk.

Introduction

- Village of Rampac Grande, Peruvian Andes, was struck by a catastrophic landslide in 2009:
  - claiming five fatalities
  - challenging local knowledge about landslides
- Collaboration between a team of scientists (Czechia, Peru) and the local community shifted the community attitude from refusing outside intervention to acceptance of the proposed measures and active community participation on the landslide DRR.

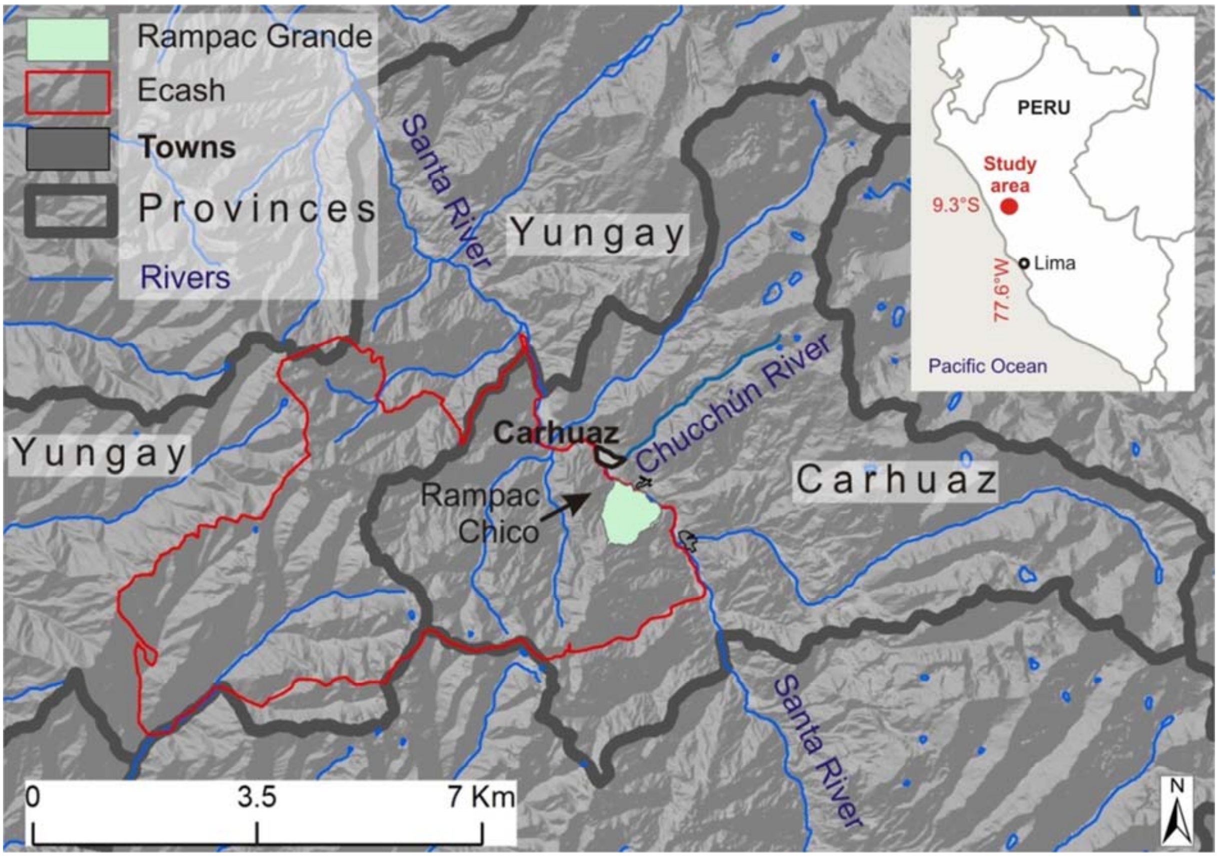

Previous research

- Unpublished reports:
  - Zamora MC (1966) Deslizamento de tierras en Rampac Chico (Carhuaz). Unpublished report Electroperu S.A., Glaciologia y Seguridad Lagunas, Huaraz, Peru
  - Zapata M (1972) Deslizamentos de tierrasen Rampac Chico, provincia de Carhuaz. Electroperu S.A., Glaciologia y Seguridad Lagunas, Huaraz, Peru
- Aricles:
  - Klimeš J, Vilímek V (2011): A catastrophic landslide near Rampac Grande in the Cordillera Negra, northern Peru. Landslides, 8:309-320.
  - Vilímek V, Klimeš J, Torres MZ (2016): Reassessment of the development and hazard of the Rampac Grande landslide, Cordillera Negra, Peru. Geoenvironemental Disasters. DOI 10.1186/s40677-016-0039-8

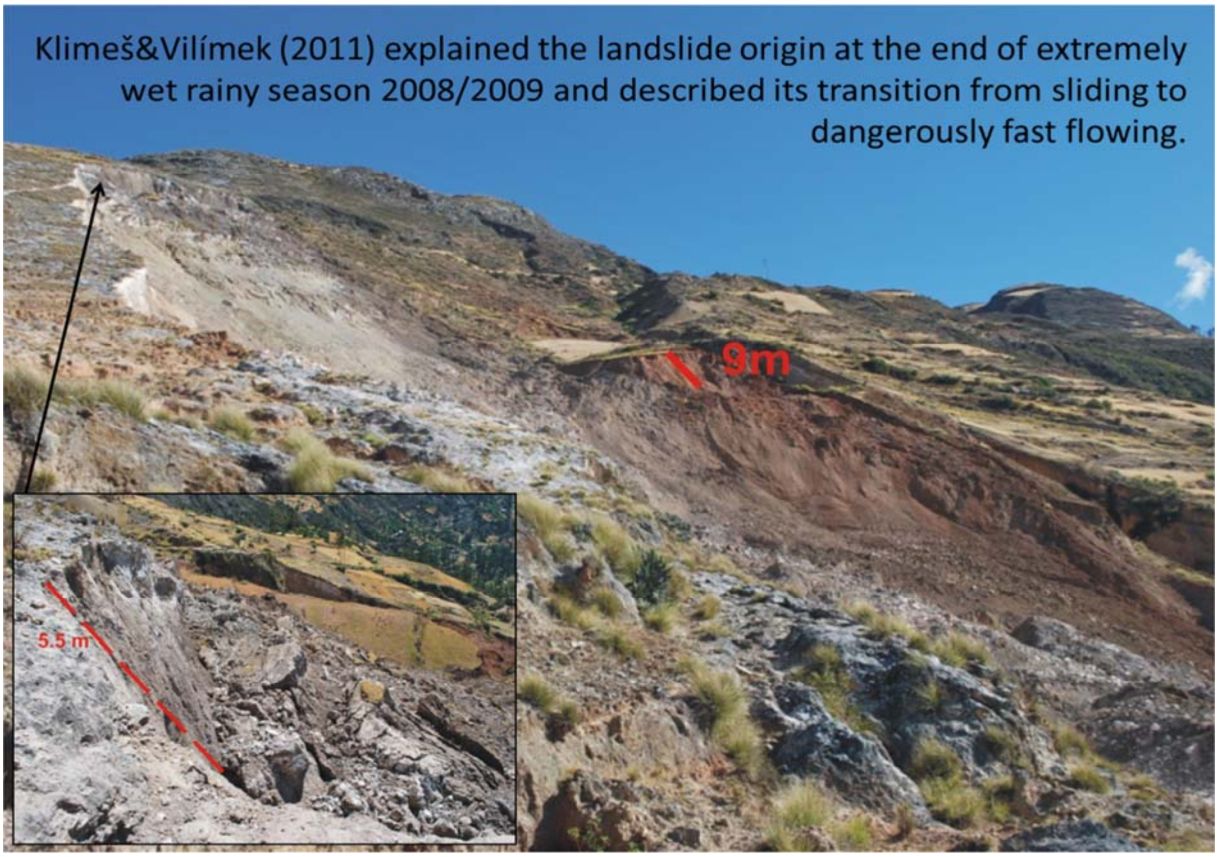
Klimeš&Vilímek (2011) explained the landslide origin at the end of extremely wet rainy season 2008/2009 and described its transition from sliding to dangerously fast flowing.
9m
5.5 m

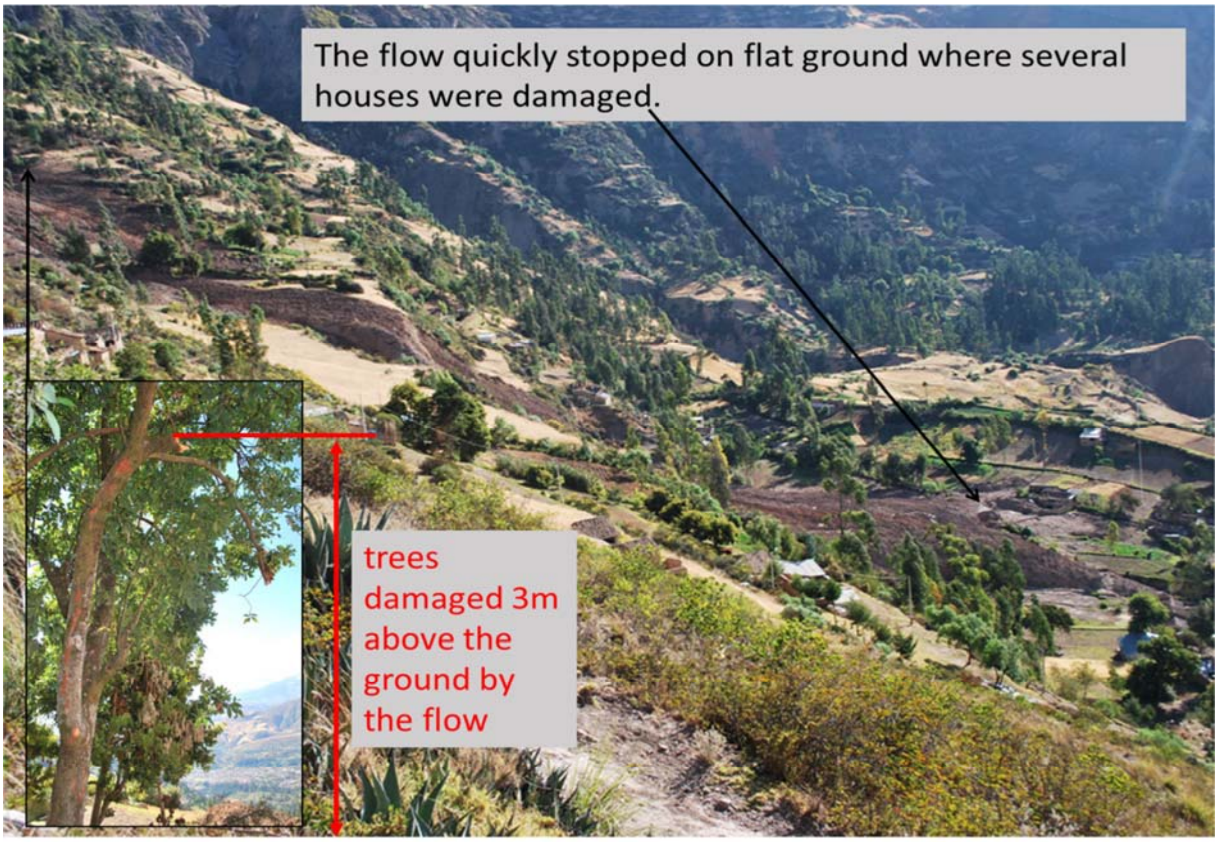
The flow quickly stopped on flat ground where several houses were damaged.
trees damaged 3m above the ground by the flow

High hazard of reactivation was identified at three parts of the landslide.

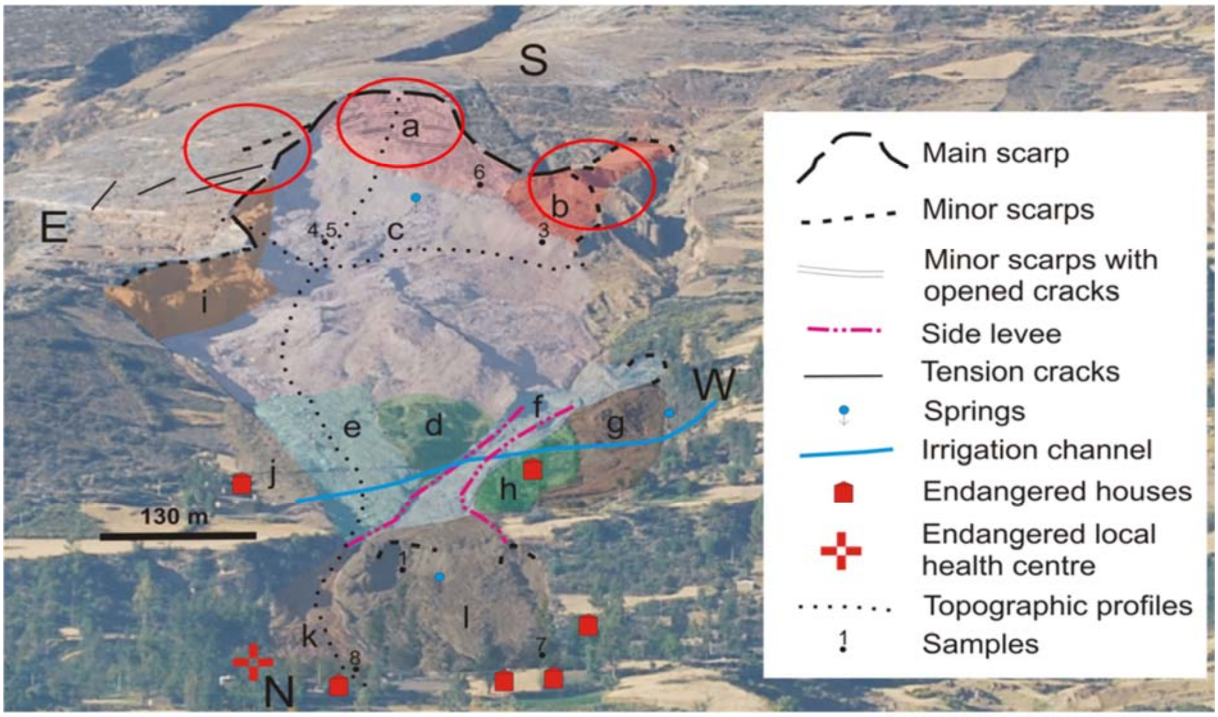

(Klimeš & Vilímek, 2011)

Social impacts of the 2009 landslide

- The Rampac Grande community was left without reliable explanation of the landslide origin.
- The community made its own explanation – illegal prospection of precious metals.
- The community did not trust to the external actors – national or foreign researchers and closed the community territory to outsiders.

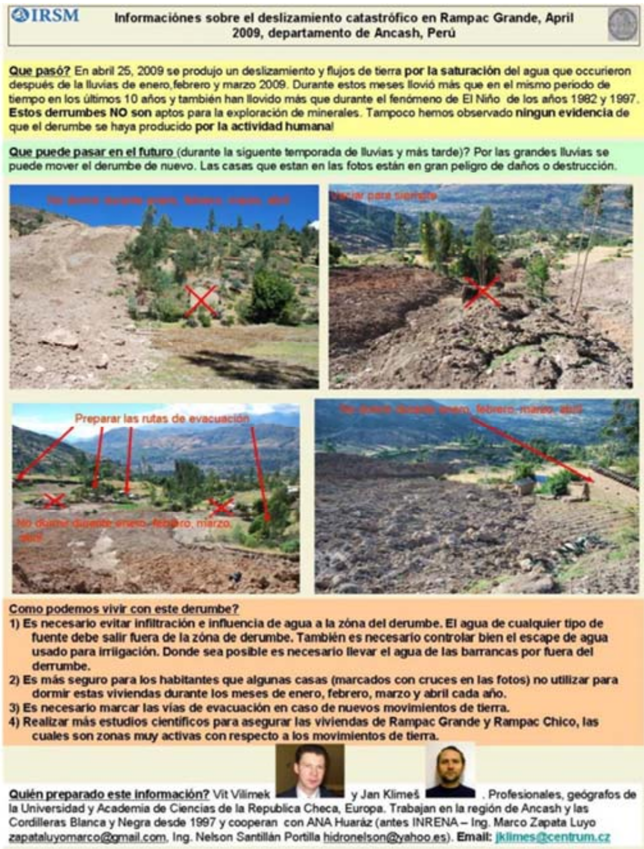
IRSM Informaciónes sobre el deslizamiento catastrófico en Rampac Grande, April 2009, departamento de Ancash, Perú

Que pasó? En abril 25, 2009 se produjo un deslizamiento y flujos de tierra **por la saturación** del agua que occurieron después de la lluvias de enero,febrero y marzo 2009. Durante estos meses llovió más que en el mismo período de tiempo en los últimos 10 años y también han llovido más que durante el fenómeno de El Niño de los años 1982 y 1997. **Estos derrumbes NO son** aptos para la exploración de minerales. Tampoco hemos observado **ningun evidencia** de que el derumbe se haya producido **por la actividad humana!**

Que puede pasar en el futuro (durante la siguente temporada de lluvias y más tarde)? Por las grandes lluvias se puede mover el derumbe de nuevo. Las casas que estan en las fotos están en gran peligro de daños o destrucción.

Como podemos vivir con este derumbe?
1) Es necesario evitar infiltración e influencia de agua a la zóna del derumbe. El agua de cualquier tipo de fuente debe salir fuera de la zóna de derumbe. También es necesario controlar bien el escape de agua usado para irriigación. Donde sea posible es necesario llevar el agua de las barrancas por fuera del derrumbe.
2) Es más seguro para los habitantes que algunas casas (marcados con cruces en las fotos) no utilizar para dormir estas viviendas durante los meses de enero, febrero, marzo y abril cada año.
3) Es necesario marcar las vías de evacuación en caso de nuevos movimientos de tierra.
4) Realizar más estudios científicos para asegurar las viviendas de Rampac Grande y Rampac Chico, las cuales son zonas muy activas con respecto a los movimientos de tierra.

Quién preparado este información? Vit Vilimek y Jan Klimeš. Profesionales, geógrafos de la Universidad y Academia de Ciencias de la Republica Checa, Europa. Trabajan en la región de Ancash y las Cordilleras Blanca y Negra desde 1997 y cooperan con ANA Huaráz (antes INRENA – Ing. Marco Zapata Luyo zapataluyomarco@gmail.com, Ing. Nelson Santillán Portilla hidronelson@yahoo.es). **Email:** jklimes@centrum.cz

Vilímek et al. (2016) confirmed adjustment of the landslide material, continuous hazard of landslide retrogressive movement and found that the community does not considers the landslide as ongoing threat – „with time the mountain will heal itself and it will be safe again“.

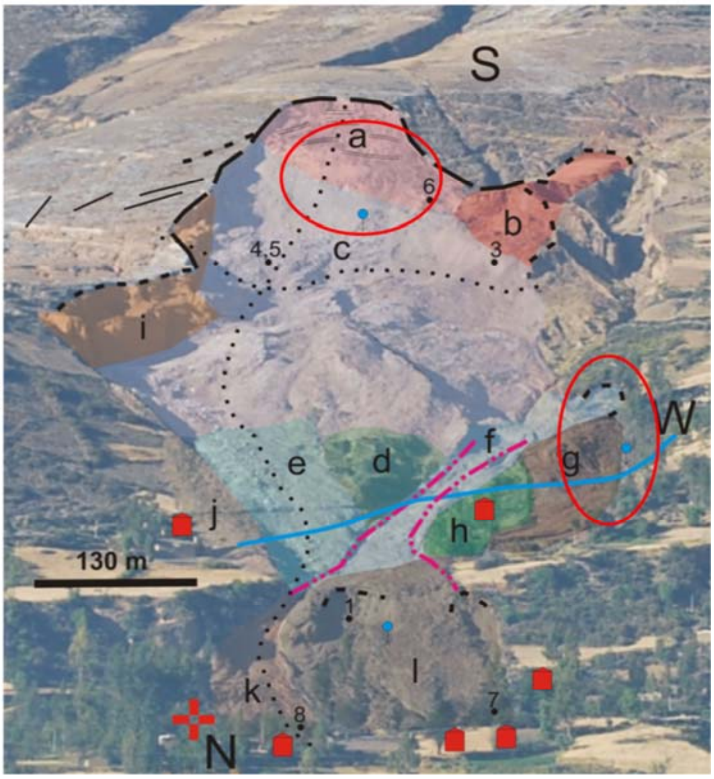

Comparison of two photographs of landslide accumulation probably explains the perceived process of „mountain healing“ (Vilímek et al., 2016).

2009

2014

Disaster risk reduction project 2016 - 2017

- Joint project of the Czech Embassy in Peru (17,600 USD) and INAIGEM, Peru (Instituto Nacional de Investigación en Glaciares y Ecosystemas de Montaña, 18,500 USD)
- Collaboration of the community and its acceptance of the project were major requirement for the project success
- **Project results described in**: Klimeš J, Guerrero AMR, Vargas R, Raška P, Vicuña L, Jurt C (2019) Community participation in landslide risk reduction, a case history from Central Andes, Peru. Landslides. https://doi.org/10.1007/s10346-019-01203-w

CZECH REPUBLIC
DEVELOPMENT COOPERATION

INAIGEM

History of landslide research and DRR activities in the Rampac Grande community, from Klimeš et al. (2019). * activities performed by the foreign research team without INAIGEM participation, comm. – community, CZ – Czech Republic, land. – landslide, RG – Regional Government, R.G. – Rampac Grande, PM - Provincial Municipality, INDECI - National Institute of Civil Defense. At the bottom of the figure, main community as well as external research group attitudes towards the landslide DRR are described.

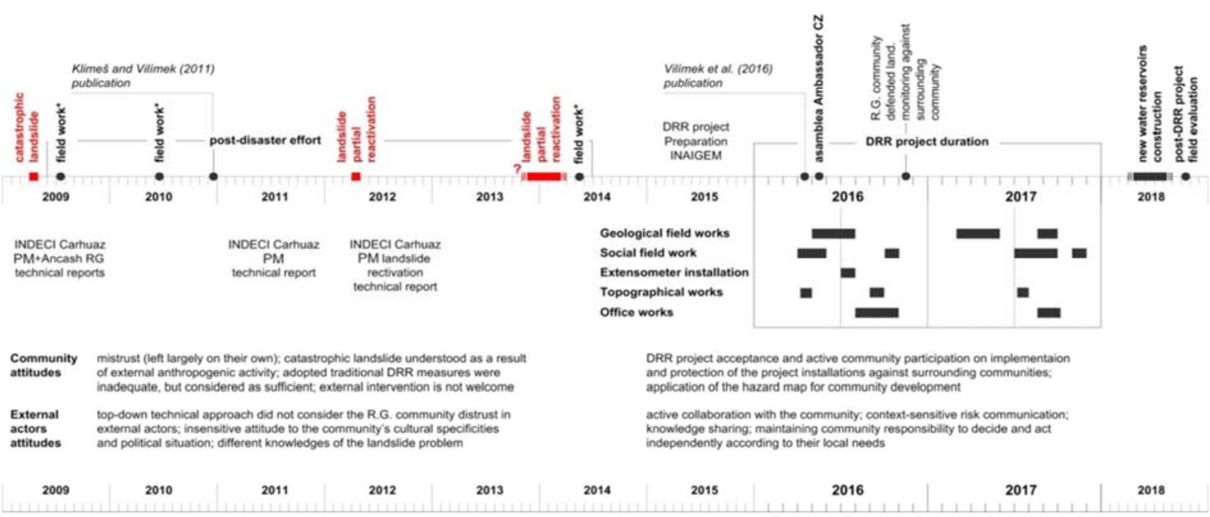

Disaster risk reduction project 2016 – 2017 – community sensitization

- Used approaches:
- Semi-structured interviews (253 community members)
- Focus group meetings (the Rampac Grande executive council and community commissions, Carhuaz PM mayor and commission)
- Meetings of the entire community („asamblea“, 4 meetings)

Disaster risk reduction project 2016 – 2017 – stakeholder prioritization

- High institutional vulnerability of local governments
- Local (e.g. provincial) governments are important sources of economic aid for the communities
- Strong authority of communities over their territory

Disaster risk reduction project 2016 – 2017 – community sensitization

- Semi-structured interviews (253 community members) used to obtain information about:
  - main regular community events (festivals, meetings) and agricultural practices
  - past landslide events and traditional landslide mitigation practices
  - explanation of the landslide hazard map

Main regular community events (festivals, meetings) and agricultural practices

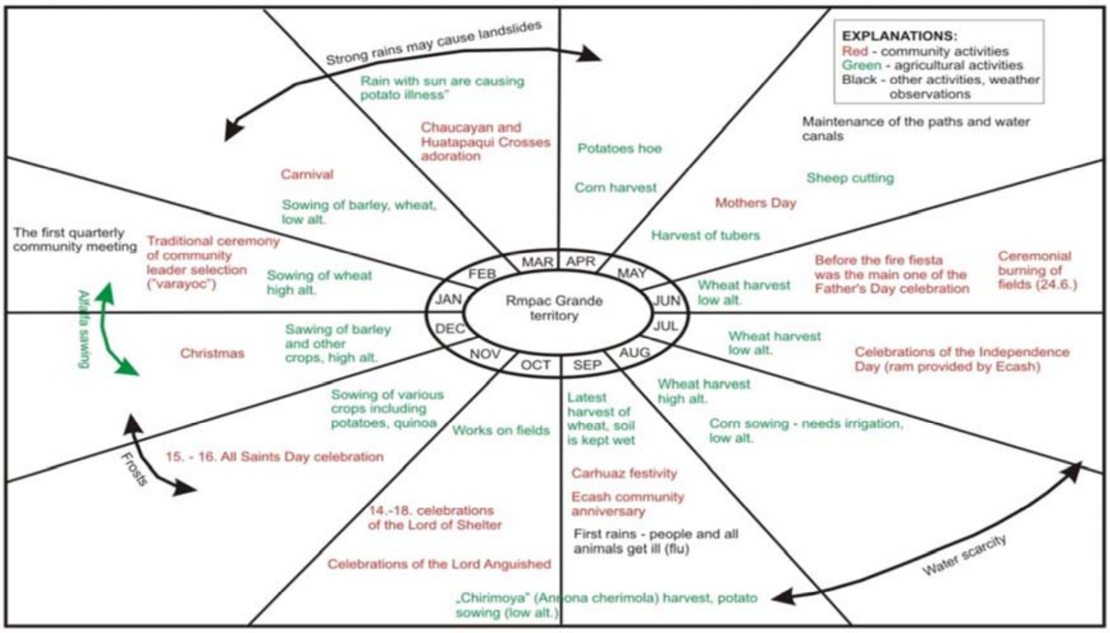

(Klimeš et al., 2019 – Online Resource 2)

Disaster risk reduction project 2016 – 2017 – community sensitization

- Focus group meetings (the Rampac Grande executive council and community commissions, Carhuaz PM mayor and commission):
  - community expectations of the project results
  - project adaptation to the community needs and understanding
  - project results explanation

Focus group meeting at the Rampac Grande basic school, presentation of the project advances, 2016

Field explanation of the landslide monitoring technique to the Rampac Grande community representatives, (Klimeš et al., 2019)

Disaster risk reduction project 2016 – 2017 – community sensitization

- Meetings of the entire community („asamblea“, 4 meetings):

i) Understand the community expectations of the DRR project

ii) Introduce and explain the scope of the project and basic benefits for the community

iii) Obtain the community agreement and commitment to collaborate on the project

iv) Present the project results


Asamblea - obtaining the community agreement and commitment to collaborate on the project


Asamblea – project results explanation translated to Quechua language
(Klimeš et al., 2019)

Disaster risk reduction project 2016 – 2017 – landslide mitigation measures

- Landslide hazard map
- Warning signs
- Landslide movement monitoring of the sites prone to the dangerous retrogressive failures

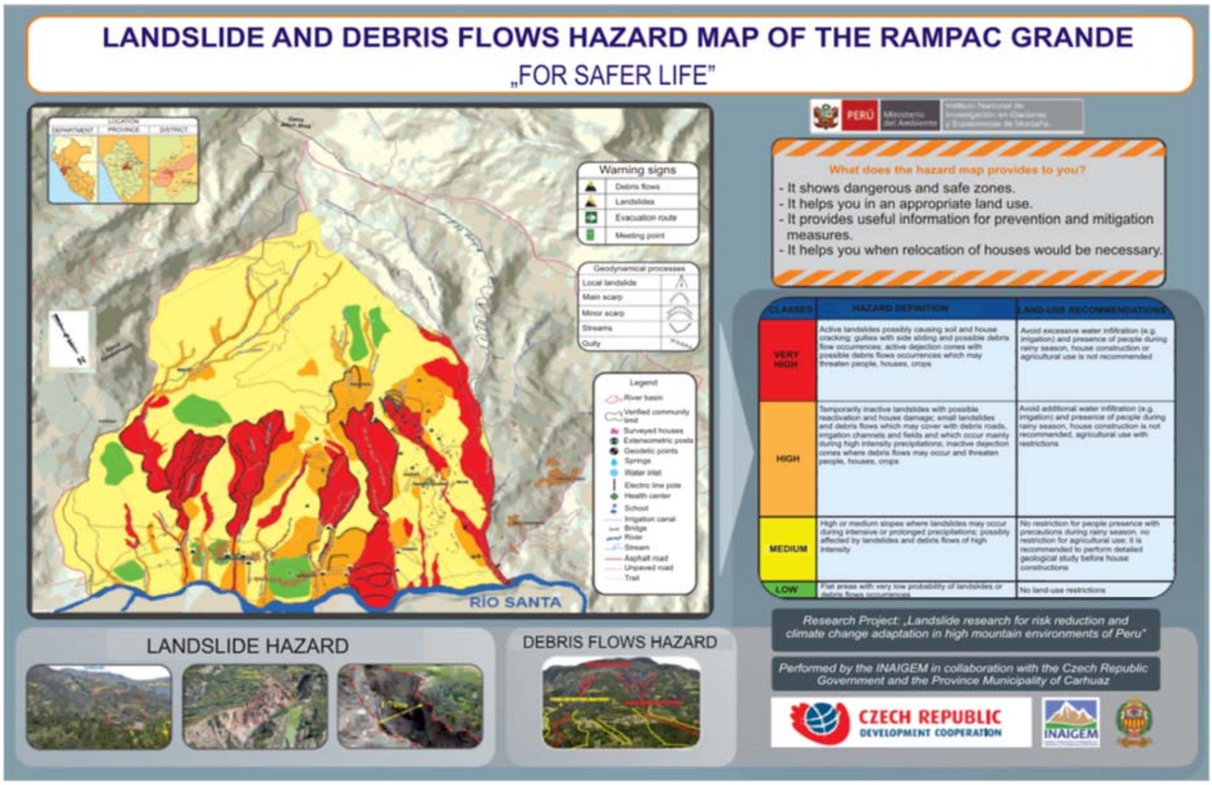

(Klimeš et al., 2019, Online Resource 3)

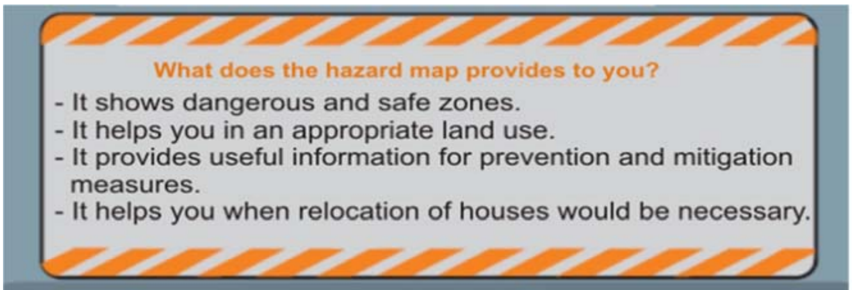

CLASSES	HAZARD DEFINITION	LAND-USE RECOMMENDATIONS
VERY HIGH	Active landslides possibly causing soil and house cracking; gullies with side sliding and possible debris flow occurrences; active dejection cones with possible debris flows occurrences which may threaten people, houses, crops	Avoid excessive water infiltration (e.g. irrigation) and presence of people during rainy season, house construction or agricultural use is not recommended
HIGH	Temporarily inactive landslides with possible reactivation and house damage; small landslides and debris flows which may cover with debris roads, irrigation channels and fields and which occur mainly during high intensity precipitations; inactive dejection cones where debris flows may occur and threaten people, houses, crops	Avoid additional water infiltration (e.g. irrigation) and presence of people during rainy season, house construction is not recommended, agricultural use with restrictions
MEDIUM	High or medium slopes where landslides may occur during intensive or prolonged precipitations; possibly affected by landslides and debris flows of high intensity	No restriction for people presence with precautions during rainy season, no restriction for agricultural use; it is recommended to perform detailed geological study before house constructions
LOW	Flat areas with very low probability of landslides or debris flows occurrences	No land-use restrictions

(Klimeš et al., 2019, Online Resource 3)

Placement of the landslide/debris flows warning signs – exact installation site was always selected by the community members

(Klimeš et al., 2019)

Landslide movement monitoring of the sites prone to the dangerous retrogressive failures

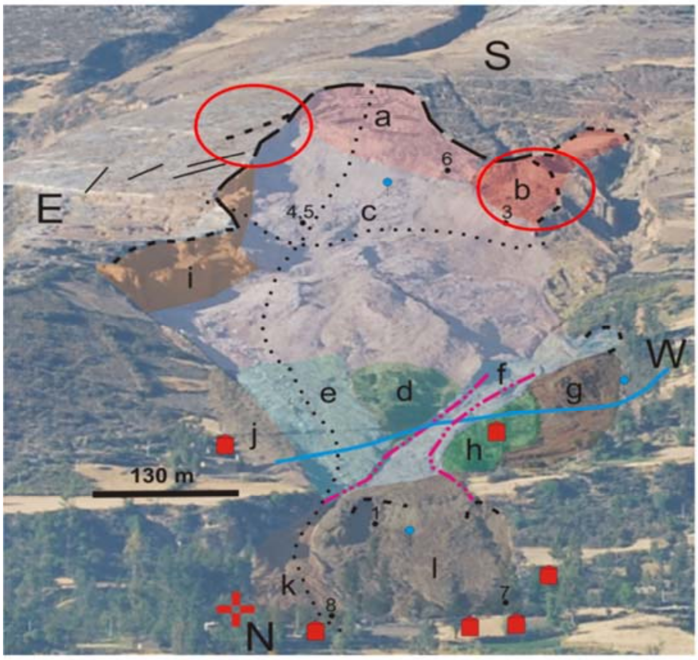

Short-term success indicators

Construction of two water reservoirs (2018, cost of 26,000 USD) – site selection and financial support of the Peruvian state were obtained using the landslide hazard map of the 2016/2017 project.

(Klimeš et al., 2019, Online Resource 4)

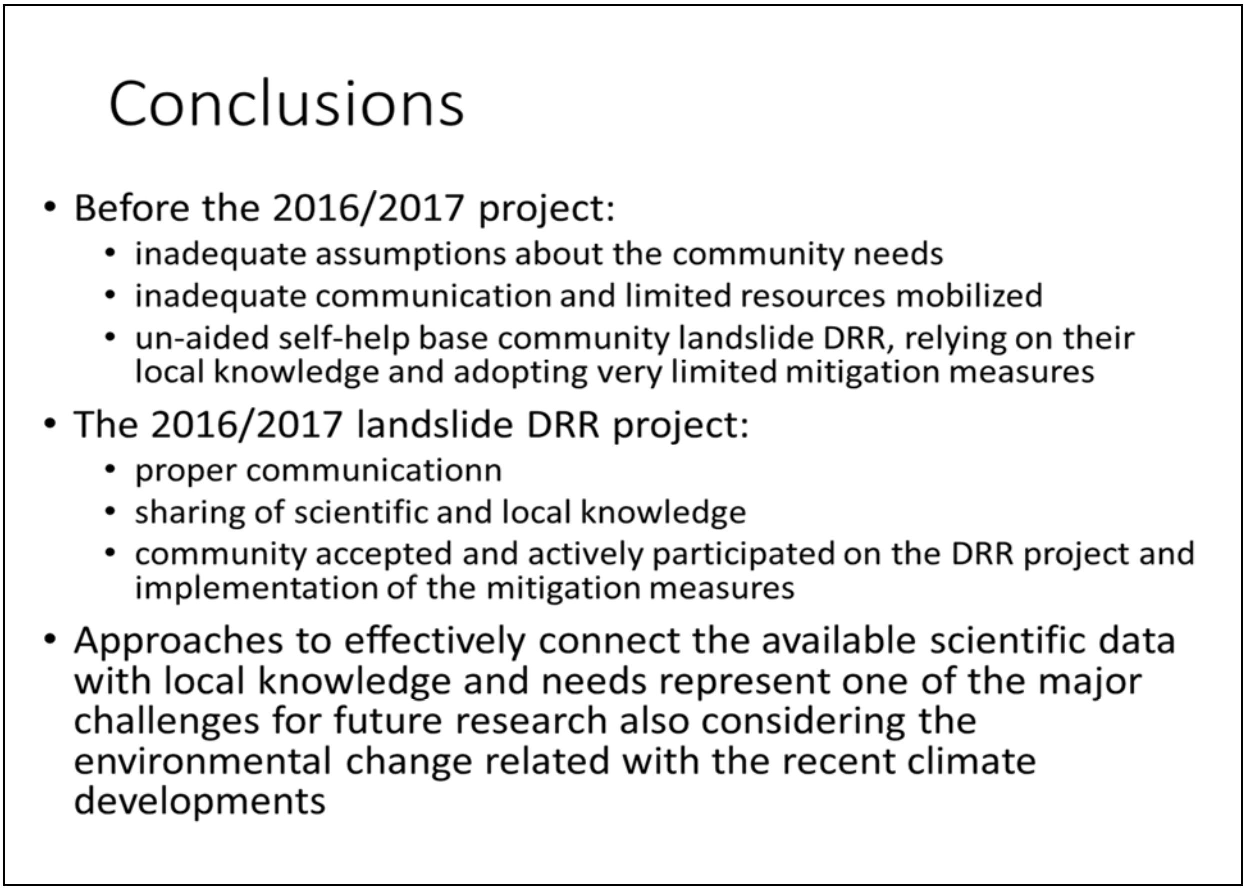
Conclusions
• Before the 2016/2017 project:
• inadequate assumptions about the community needs
• inadequate communication and limited resources mobilized
• un-aided self-help base community landslide DRR, relying on their local knowledge and adopting very limited mitigation measures
• The 2016/2017 landslide DRR project:
• proper communicationn
• sharing of scientific and local knowledge
• community accepted and actively participated on the DRR project and implementation of the mitigation measures
• Approaches to effectively connect the available scientific data with local knowledge and needs represent one of the major challenges for future research also considering the environmental change related with the recent climate developments

Geological Hazard (Landslide, Debrisflow, Rockfall) Zoning map for Tbilisi city (Georgia)

Dr. George Gaprindashvili, Dr. Emil Tsereteli, Merab Gaprindashvili

1) Department of Geology, National Environmental Agency, Ministry of Environment Protection and Agriculture of Georgia, Tbilisi, D. Agmashenebeli ave. 150, 0112
E-mail: gaprindashvili.george@gmail.com

Abstract:

Tbilisi is a capital of Georgia, occupies 504.2 sq. km, population – 1.1 mln. At present, under the conditions of increased demand on constructions, the territory of Tbilisi city is being developed under the most complex geological conditions, which is frequently accompanied by widespread occurrence and activation of hazardous geological processes, such as landslides, debris/mudflow, rockfalls, riverbank erosion. Catastrophic geological events are triggered by earthquakes, extreme hydro-meteorological events, probably on the background of global climate change, large-scale human impacts on the environment. Last period several geological disaster occurred in Tbilisi.

Since 2016 Department of Geology of National Environmental Agency under the Ministry of Environment Protection and Agriculture of Georgia started governmental program named: “Processing of Geological Hazard (Landslide, Debris/mudflow, rockfall, rock avalanche et. al) zoning map and monitoring of Tbilisi city”. Such type and scale map never was done for the capital. Project activities are processing historical material; Field Geological Survey; Inventory mapping of all type of geological hazards; Preparation of geological hazard database; preparation hazards triggering factor maps; Preparation geological hazard zoning map and report using modern methodologies. Bellow it is presented above mentioned activities conducted by Department of Geology.

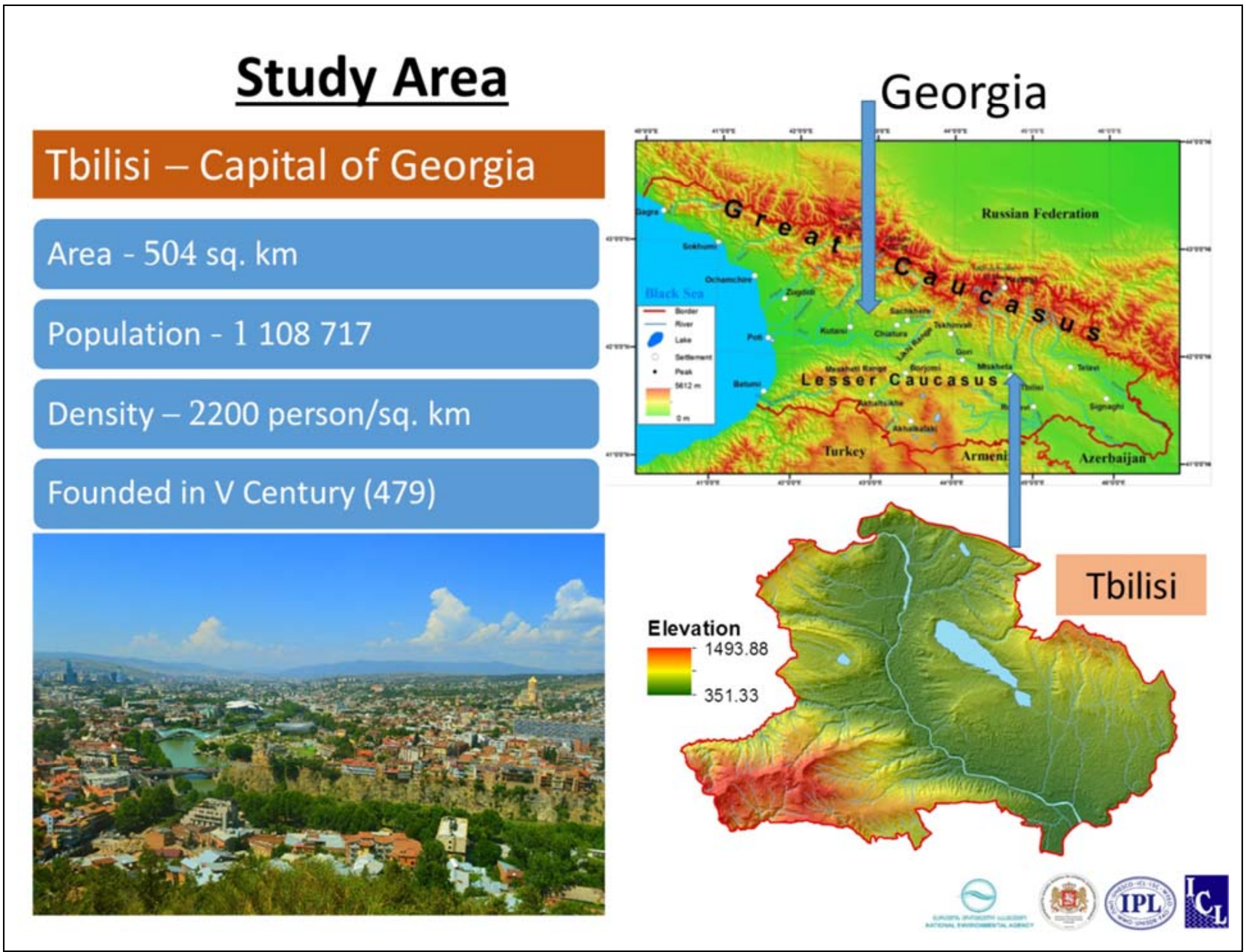
Study Area
Tbilisi – Capital of Georgia
Area - 504 sq. km
Population - 1 108 717
Density – 2200 person/sq. km
Founded in V Century (479)
Georgia
Great Caucasus
Russian Federation
Lesser Caucasus
Turkey
Azerbaijan
Tbilisi
Elevation
1493.88
351.33
IPL

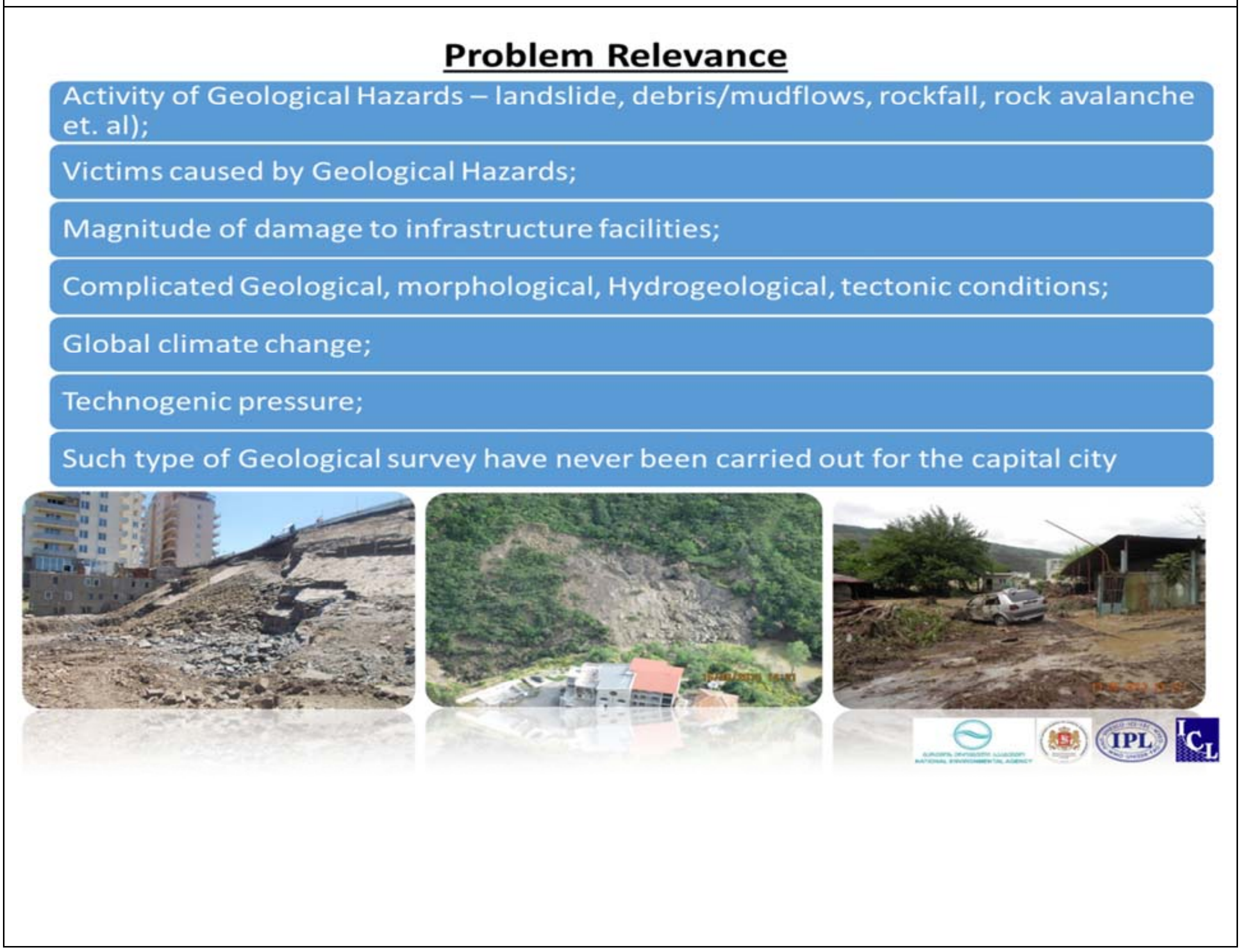
Problem Relevance
Activity of Geological Hazards – landslide, debris/mudflows, rockfall, rock avalanche et. al);
Victims caused by Geological Hazards;
Magnitude of damage to infrastructure facilities;
Complicated Geological, morphological, Hydrogeological, tectonic conditions;
Global climate change;
Technogenic pressure;
Such type of Geological survey have never been carried out for the capital city
IPL

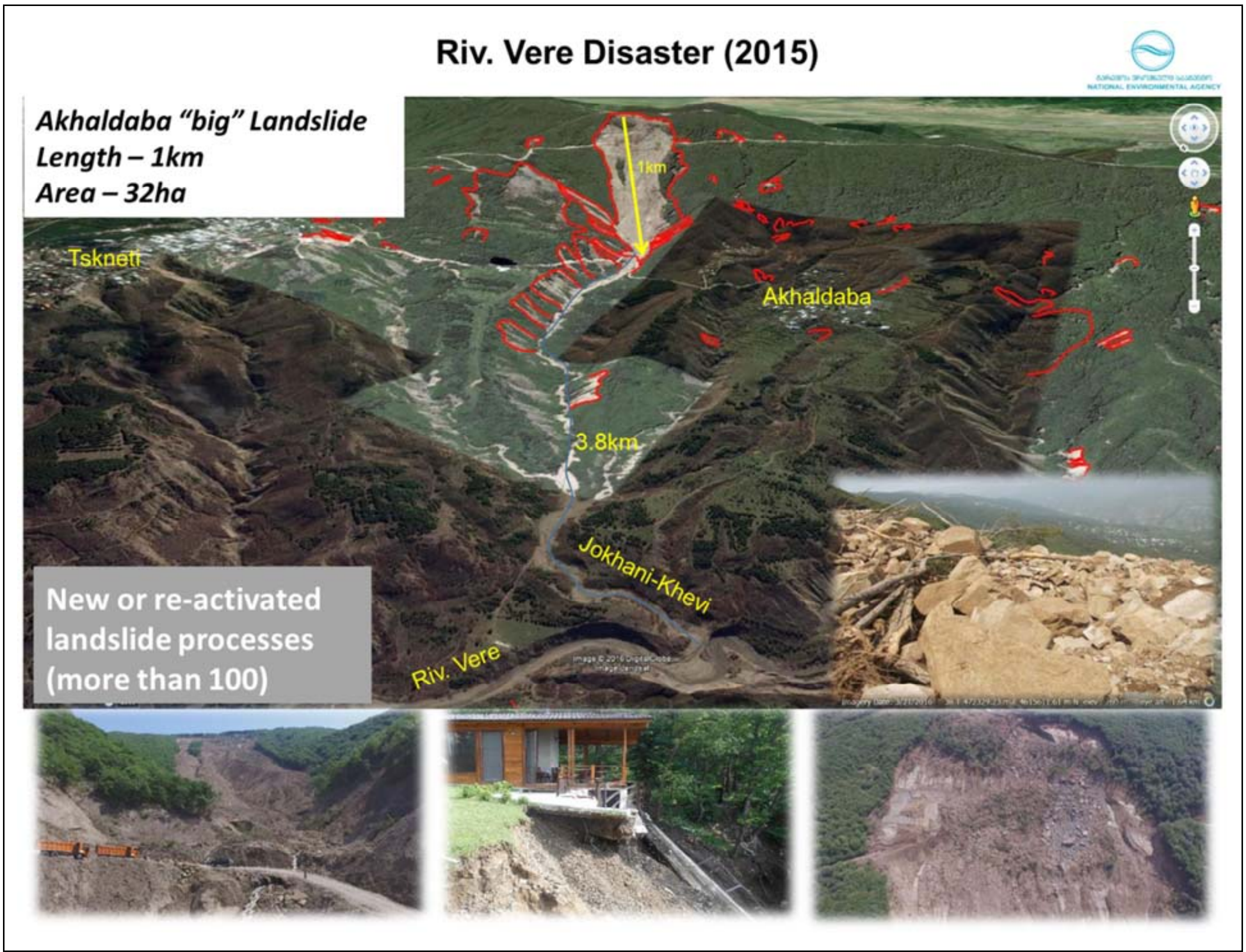
Riv. Vere Disaster (2015)
Akhaldaba "big" Landslide
Length – 1km
Area – 32ha
1km
Tskneti
Akhaldaba
3.8km
Jokhani-Khevi
Riv. Vere
New or re-activated landslide processes (more than 100)


Results
Tskneti-Akhaldaba road section
Tskneti-Samadlo road section
Akhaldaba "big" Landslide
Tskneti street (Tbilisi)
Tbilisi Zoo
Tbilisi
Number of Suffered Families – 239;
Number of Suffered Individual – 1041
Victims - 23

Ministry of Environment Protection and Agriculture of Georgia,
National Environmental Agency, Department of Geology

State Program: Geological Monitoring and Creation of State Geological Maps

Sub-Programs:

- Geological Monitoring (Spring-Autumn) and Assessment of Geological Hazards during extreme activation of Processes;
- Processing of Geological Hazard (Landslide, Debris/mudflow, rockfall, rock avalanche et. al) zoning map and monitoring of Tbilisi city
- Monitoring of Groundwater
- Processing of State Geological Maps (Geological Survey)

Project Activity

- Processing of historical (archive) data;
- Development of methodology for geological hazard assessment;
- Field geological survey;
- Identification of all type of geological processes in field conditions (landslides, debris/mudflows, rockfall, river bank erosion et. al);
- Creation of Geological Hazards Database (GIS);
- Creation of Geological Hazards Catalog/cadastres;
- Creation of Geological Hazard zoning map and geological report;
- Preparation of various thematic maps (geology, slope, aspect, etc.);

Processing of historical (archive) materials

Field geological survey

Identified all type Geological Hazards:

- **540 Landslides** (Total Area – 440.6ha, Assessed based on: hazard type and hazard risk;
- **Erosion Processes:** 1) riverbank erosion: 24.936km length; 2) Deep erosion: 4296.01m
- 70 **Debris/mudflow gorges;**
- 17 **rockfall/rock avalanche area**:

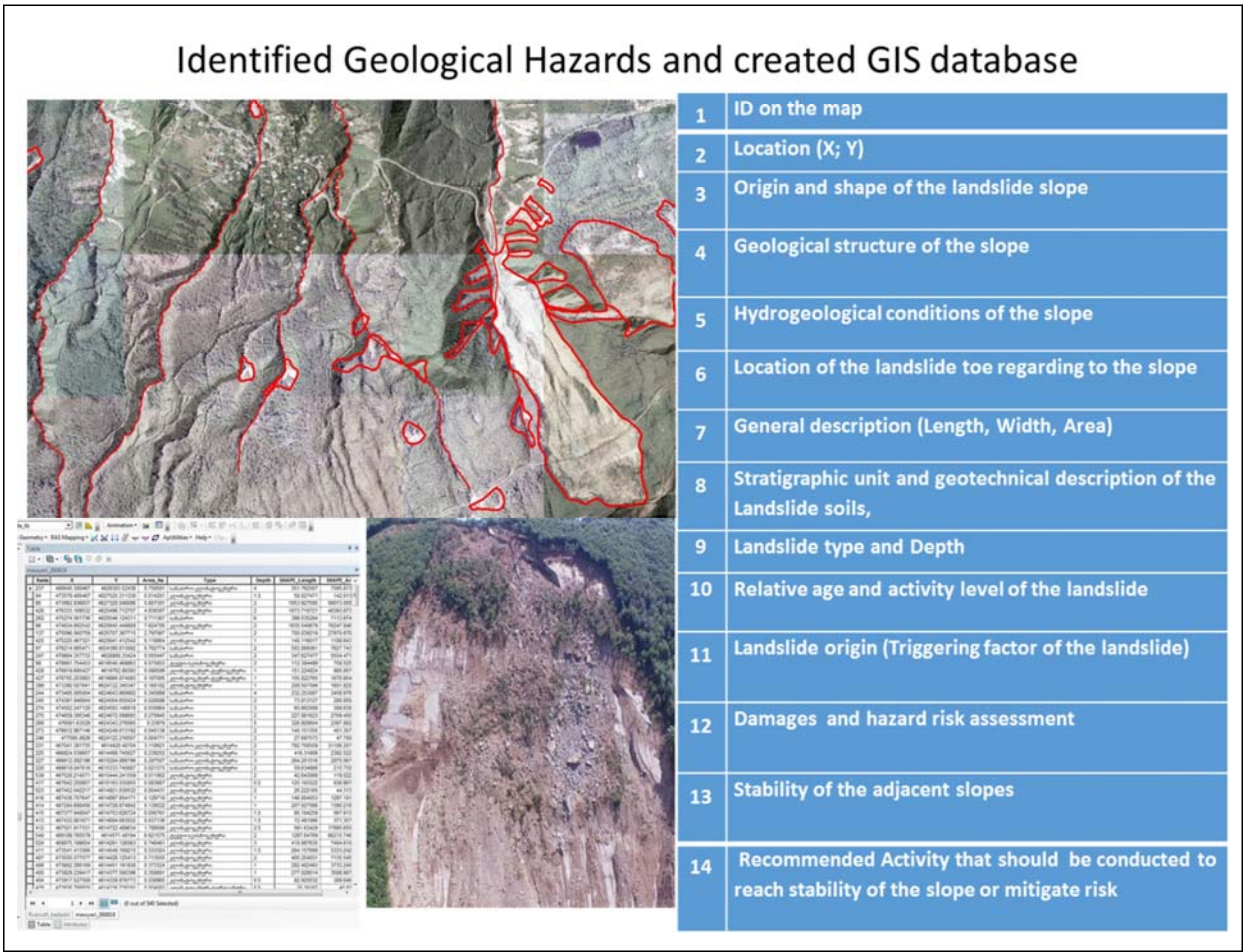
Identified Geological Hazards and created GIS database
1 ID on the map
2 Location (X; Y)
3 Origin and shape of the landslide slope
4 Geological structure of the slope
5 Hydrogeological conditions of the slope
6 Location of the landslide toe regarding to the slope
7 General description (Length, Width, Area)
8 Stratigraphic unit and geotechnical description of the Landslide soils,
9 Landslide type and Depth
10 Relative age and activity level of the landslide
11 Landslide origin (Triggering factor of the landslide)
12 Damages and hazard risk assessment
13 Stability of the adjacent slopes
14 Recommended Activity that should be conducted to reach stability of the slope or mitigate risk

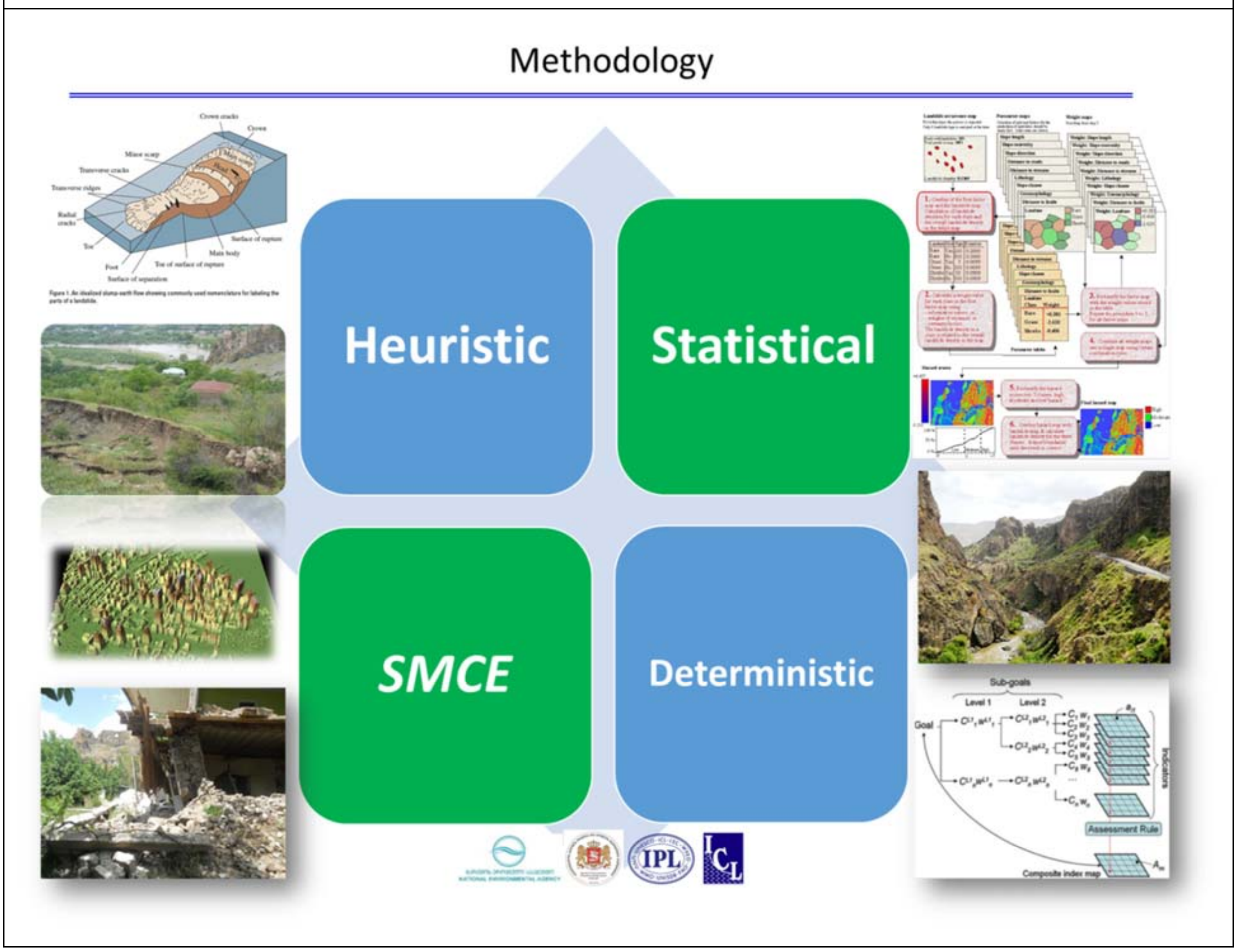
Methodology
Heuristic
Statistical
SMCE
Deterministic

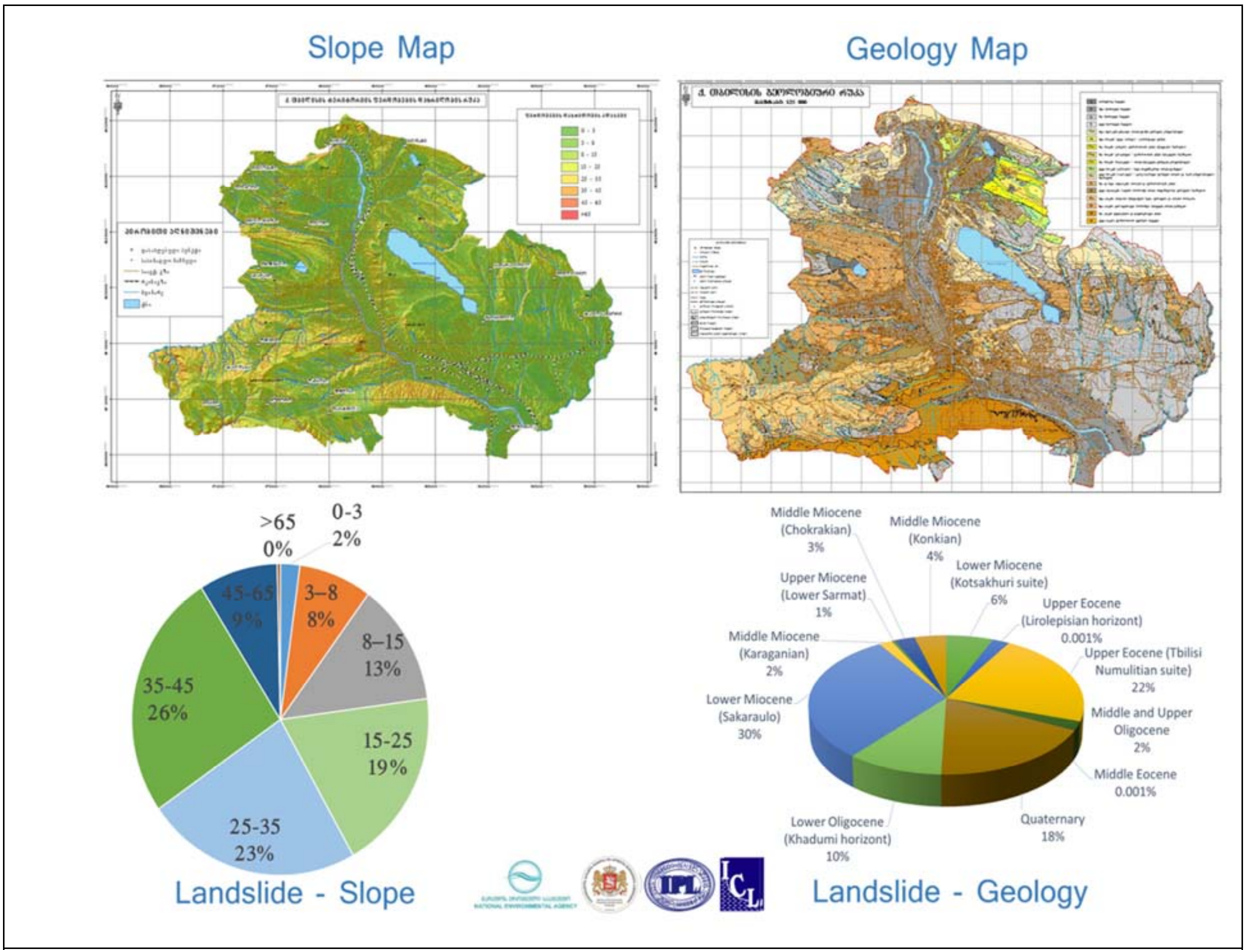
Slope Map
Geology Map
>65
0%
0-3
2%
3–8
8%
8–15
13%
15-25
19%
25-35
23%
35-45
26%
45-65
9%
Landslide - Slope
Middle Miocene
(Chokrakian)
3%
Middle Miocene
(Konkian)
4%
Lower Miocene
(Kotsakhuri suite)
6%
Upper Miocene
(Lower Sarmat)
1%
Upper Eocene
(Lirolepisian horizont)
0.001%
Middle Miocene
(Karaganian)
2%
Upper Eocene (Tbilisi
Numulitian suite)
22%
Lower Miocene
(Sakaraulo)
30%
Middle and Upper
Oligocene
2%
Middle Eocene
0.001%
Lower Oligocene
(Khadumi horizont)
10%
Quaternary
18%
Landslide - Geology
IPL
ICL

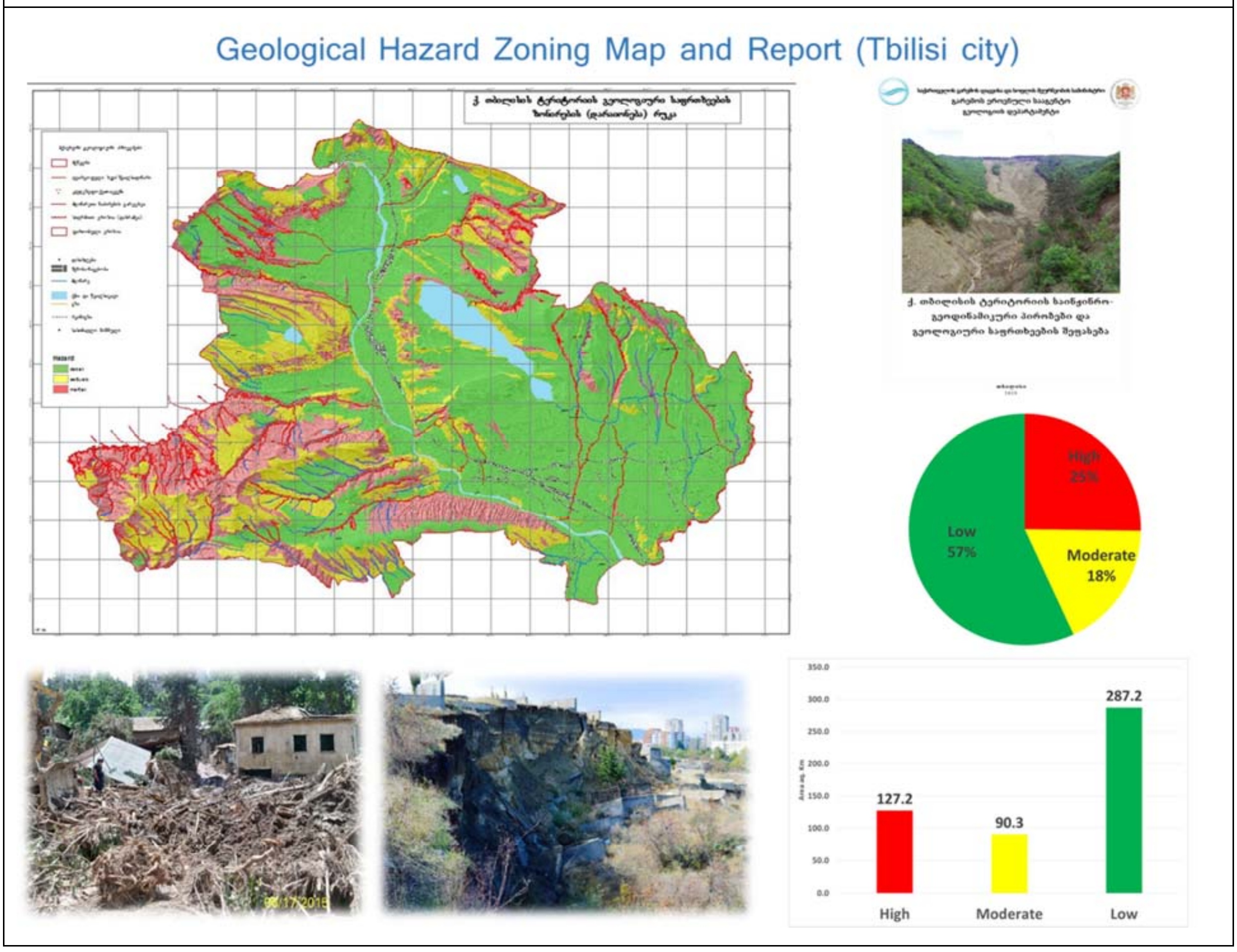
Geological Hazard Zoning Map and Report (Tbilisi city)
High
25%
Moderate
18%
Low
57%
350.0
300.0
250.0
200.0
150.0
100.0
50.0
0.0
127.2
90.3
287.2
High
Moderate
Low

Conclusions, Recommendations, Future Steps

- Prepared Geological Hazards Database;
- Prepared geological hazard zoning map and report for Tbilisi city
- Engineering measures have been developed to mitigate and eliminate hazardous geological processes;
- Map and report was sent to Tbilisi City Hall for future spatial planning of the capital (General Scheme of Tbilisi);
- The resulting geological hazard zoning map is not static, as a number of indicators have a temporal variability, and detailed scale map should therefore be updated regularly (once 2-3 years).

Landslide Early Warning System for Enhancing Disaster Resilience of the Community

Dr. Maneesha Vinodini Ramesh

Professor & Director
Amrita Center for Wireless Networks & Applications
Amrita Vishwa Vidyapeetham
maneesha@amrita.edu

Abstract

India has experienced extreme weather conditions during the last two years, 2018 and 2019, leading to large scale multi hazard events. These events have led to cascaded landslide events leading to loss of human life and large scale infrastructure damage. Climate change is contributing to increase in extreme weather conditions leading to an increase in frequency of landslides, and its unpredictability. This demands design, development and deployment of early warning systems for enhancing disaster resilience of the community. This work proposes systems, solutions and programs for multiscale landslide early warning to provide adaptive, and integrated community resilience for enhancing preparedness, response, and mitigation. A participatory approach based integrative solution has been devised and prototyped during 2019 monsoon season in Kerala, India. Enhanced community awareness, engagement, and context aware risk communication using Internet of Things (IoT)and social media based approaches have been utilized. A case study of Munnar, Kerala, India will be detailed in this work which will provide insights from the experience and perspective of enhancing disaster resilience in a rural population.

Contents

Extreme Weather & Impacts

- 2018 South West Monsoon
- MultiHazard
  - Extreme Rain - 42% departure from normal
  - Flood: 14% of total land area of Kerala
  - Landslide: 200+
  - Dam Opening: 36
  - Change in River course
- All districts of Kerala on RED alert
- Death Toll: 450+
- Displaced: 1000000+

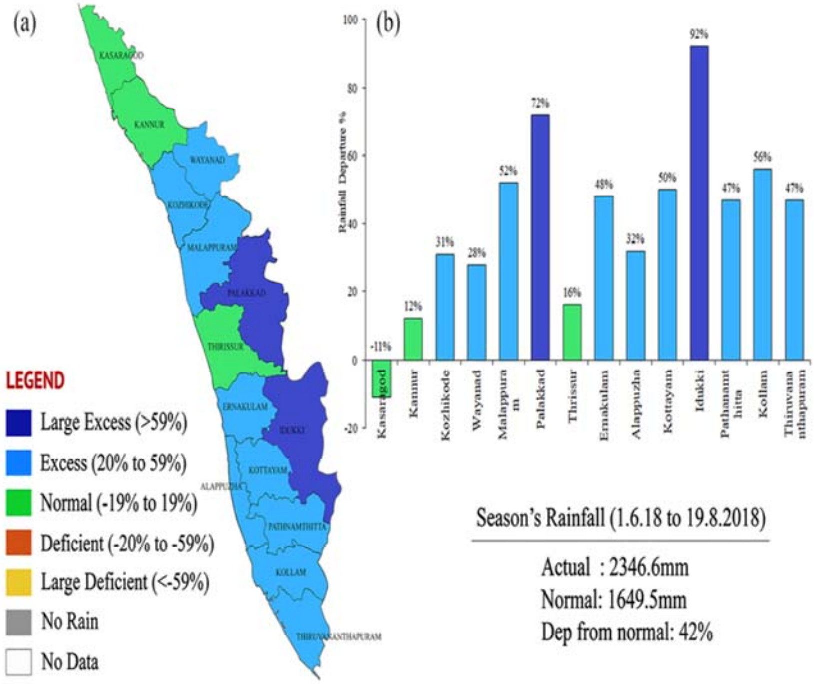

Extreme Weather & Impacts

Extreme Weather & its Impact

- Extreme precipitation events in Kerala during the years 2018 & 2019
- 2018;
  - More than 483 people died
  - 140 people missing
  - 1 million people were evacuated to relief camps
  - Property damage: US $5.8 Billion
  - 67 major landslides
- 2019
  - 121 casualties
  - Thousands of people evacuated to relief camps
  - 1789 houses damaged between August-8 to August-19
  - More than 80 landslides in a span of 2 days

Disaster Resilience

- Create Resilient Community
  - Extreme variability in weather patterns
  - Uncertainty in disaster
  - Increase in frequency of disaster
- Phase
  - Preparedness
  - Response
  - Recovery
  - Mitigation
- Scale
  - Individual
  - Community
  - Local
  - Regional

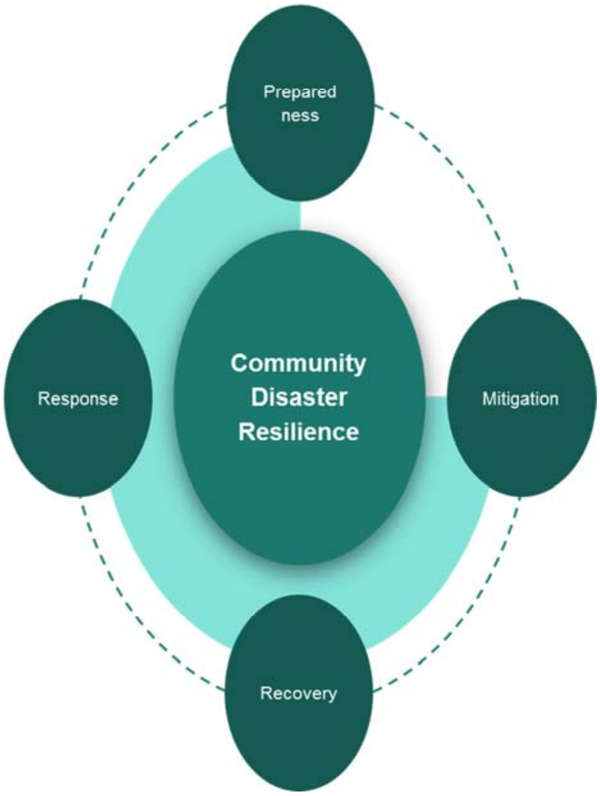

Landslide Dynamics: Challenges in Developing Systems & Solutions

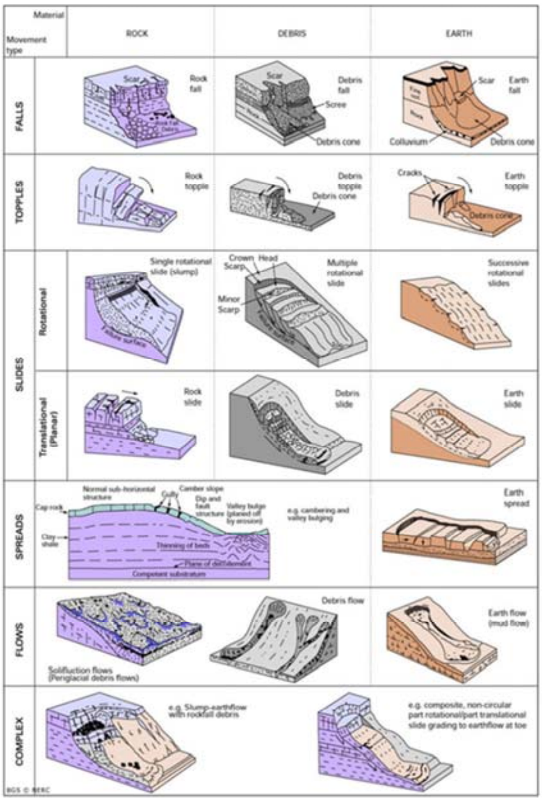

- Type of landslides are different
- Type of soil material is different
- Velocity of landslide is different
- Trigger for landslides are different
- A single EWS cannot address all the heterogeneities involved in different landslide process
- Therefore EWS needs to tailored specific to landslide types, scales and velocities with increasing level of severity

Systems & Solutions: Disaster Resilience

- Multiple Phases
  - Preparedness
  - Response
  - Recovery
  - Mitigation
- Tradeoff
  - Intervention Frequency
  - Time criticality
  - Reliability
  - Interdisciplinarity - Engineering, Management, Social
- Multi Scales
  - Individual
  - Community
  - Local
  - Regional
  - Global
- Tradeoff
  - Cost
  - Reliability
  - Scalability

Systems & Solutions: Requirements

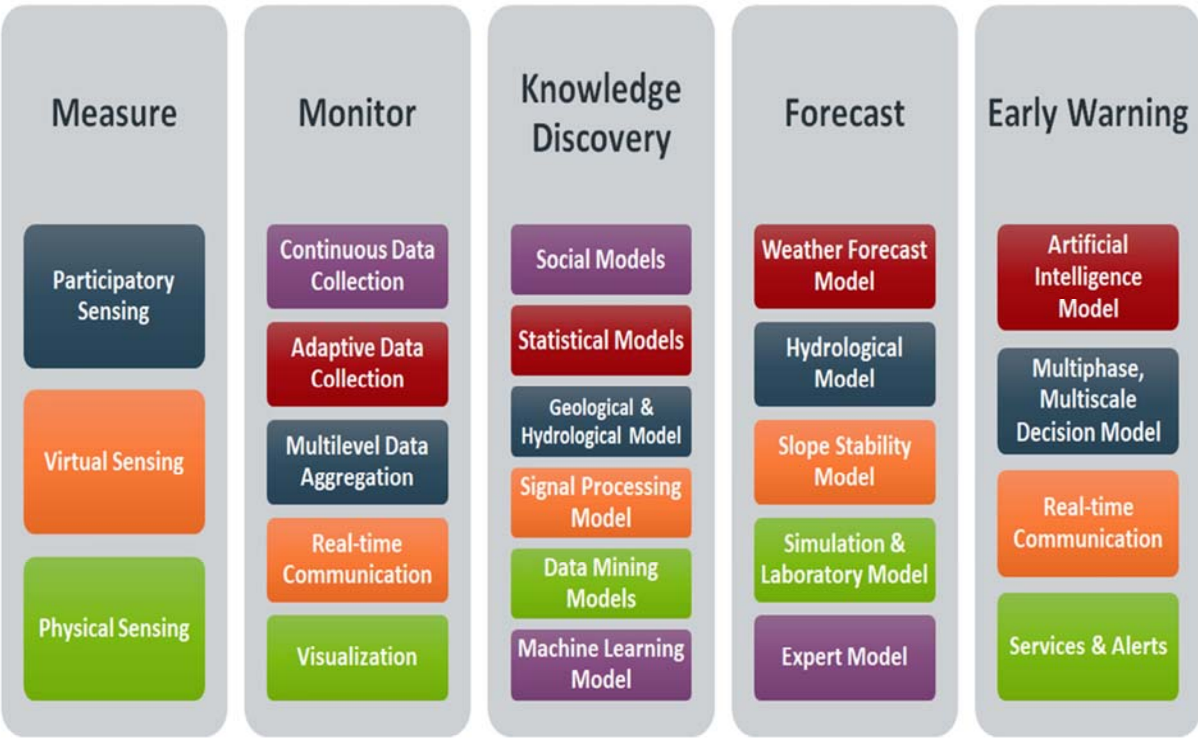

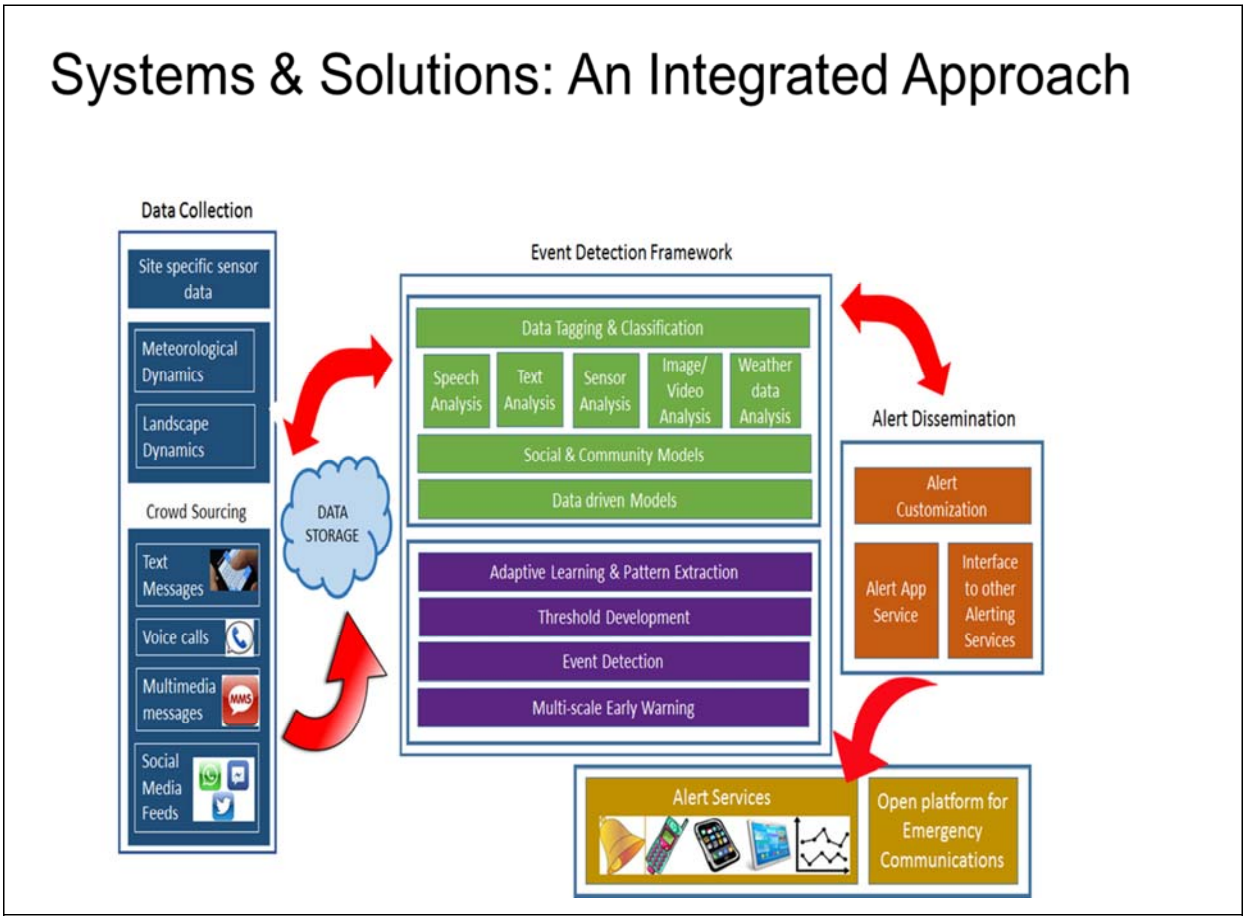
Systems & Solutions: An Integrated Approach
Data Collection
Site specific sensor data
Meteorological Dynamics
Landscape Dynamics
Crowd Sourcing
Text Messages
Voice calls
Multimedia messages
MMS
Social Media Feeds
DATA STORAGE
Event Detection Framework
Data Tagging & Classification
Speech Analysis
Text Analysis
Sensor Analysis
Image/ Video Analysis
Weather data Analysis
Social & Community Models
Data driven Models
Adaptive Learning & Pattern Extraction
Threshold Development
Event Detection
Multi-scale Early Warning
Alert Dissemination
Alert Customization
Alert App Service
Interface to other Alerting Services
Alert Services
Open platform for Emergency Communications

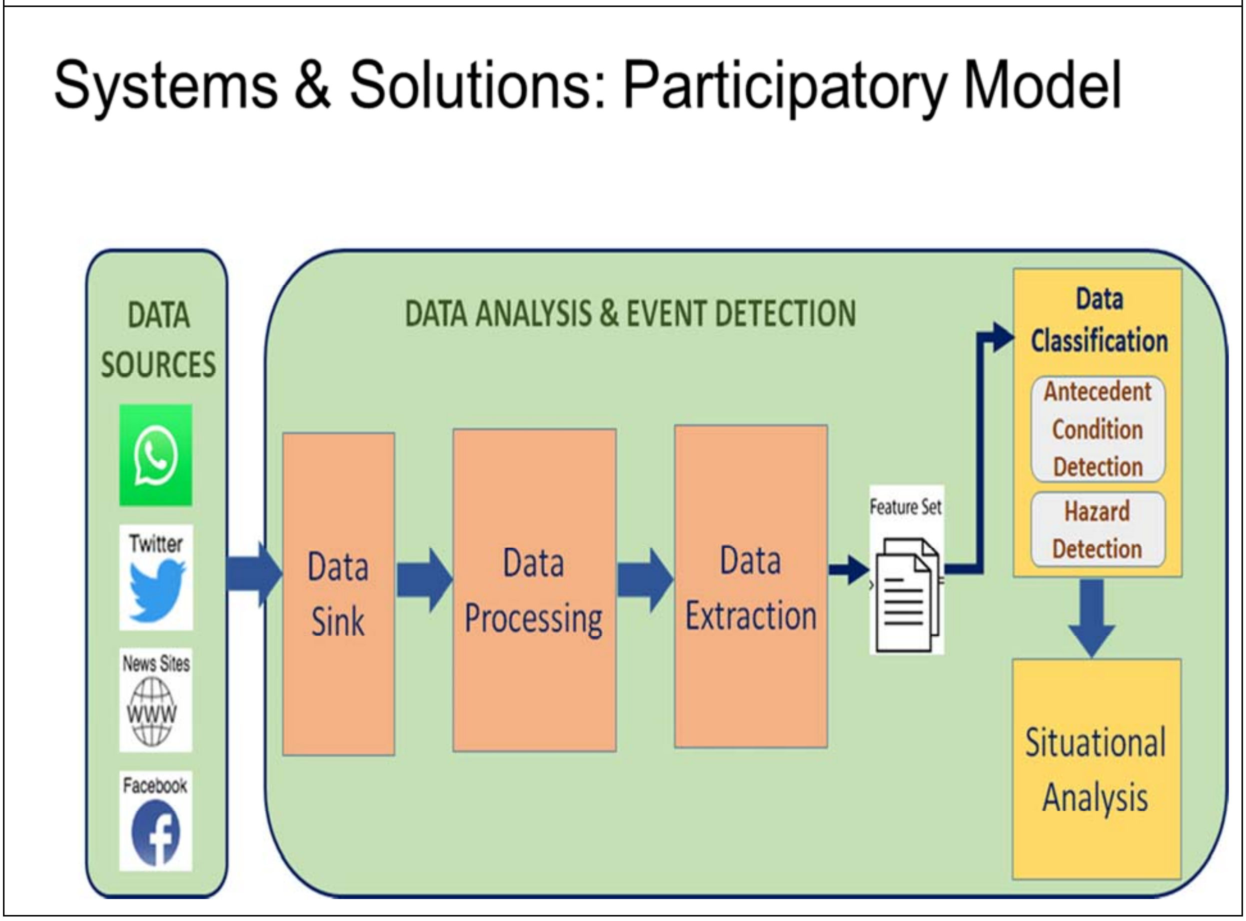
Systems & Solutions: Participatory Model
DATA SOURCES
Twitter
News Sites
WWW
Facebook
DATA ANALYSIS & EVENT DETECTION
Data Sink
Data Processing
Data Extraction
Feature Set
Data Classification
Antecedent Condition Detection
Hazard Detection
Situational Analysis

Systems & Solutions: IoT System

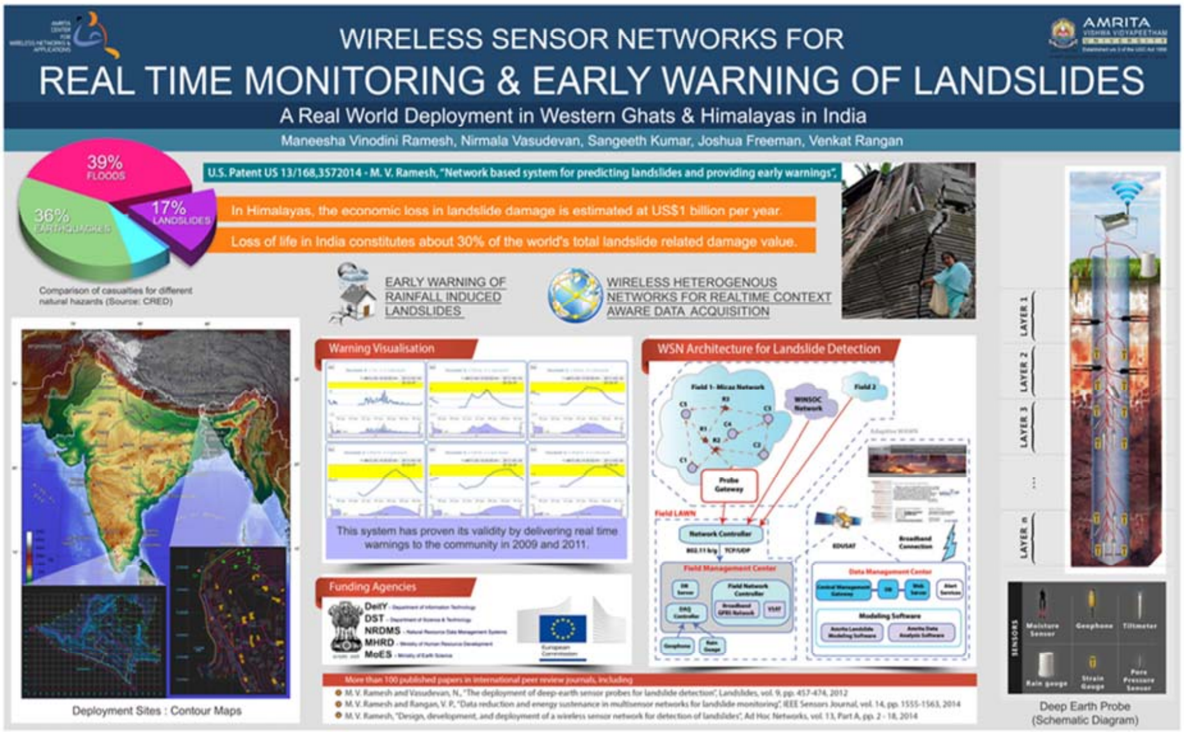

Systems & Solution: Early Warning

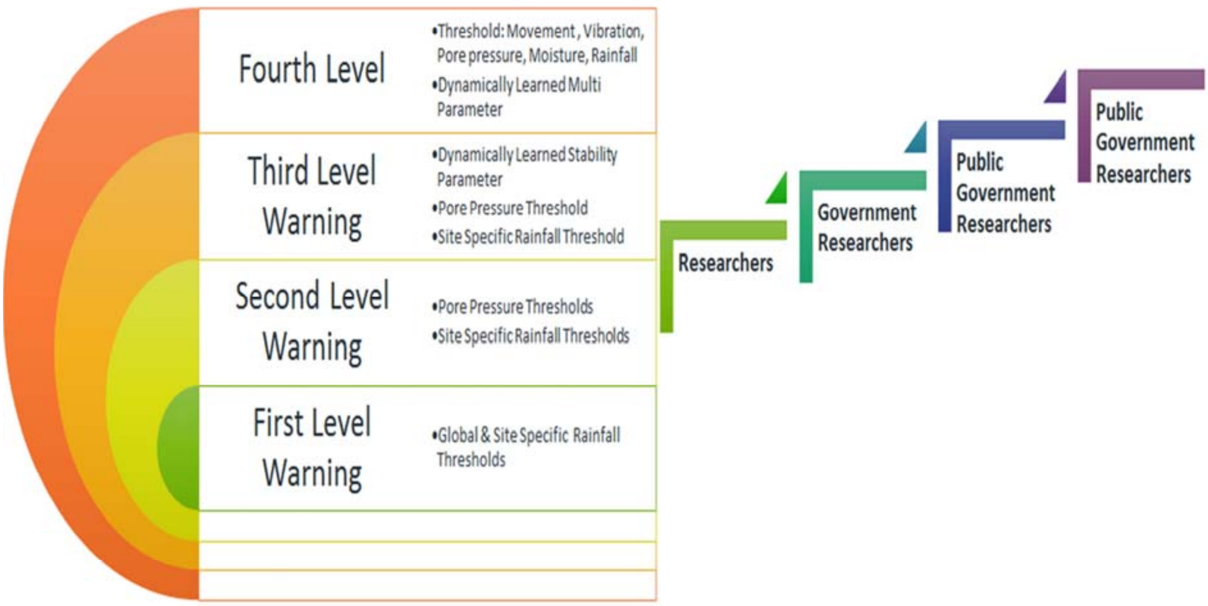

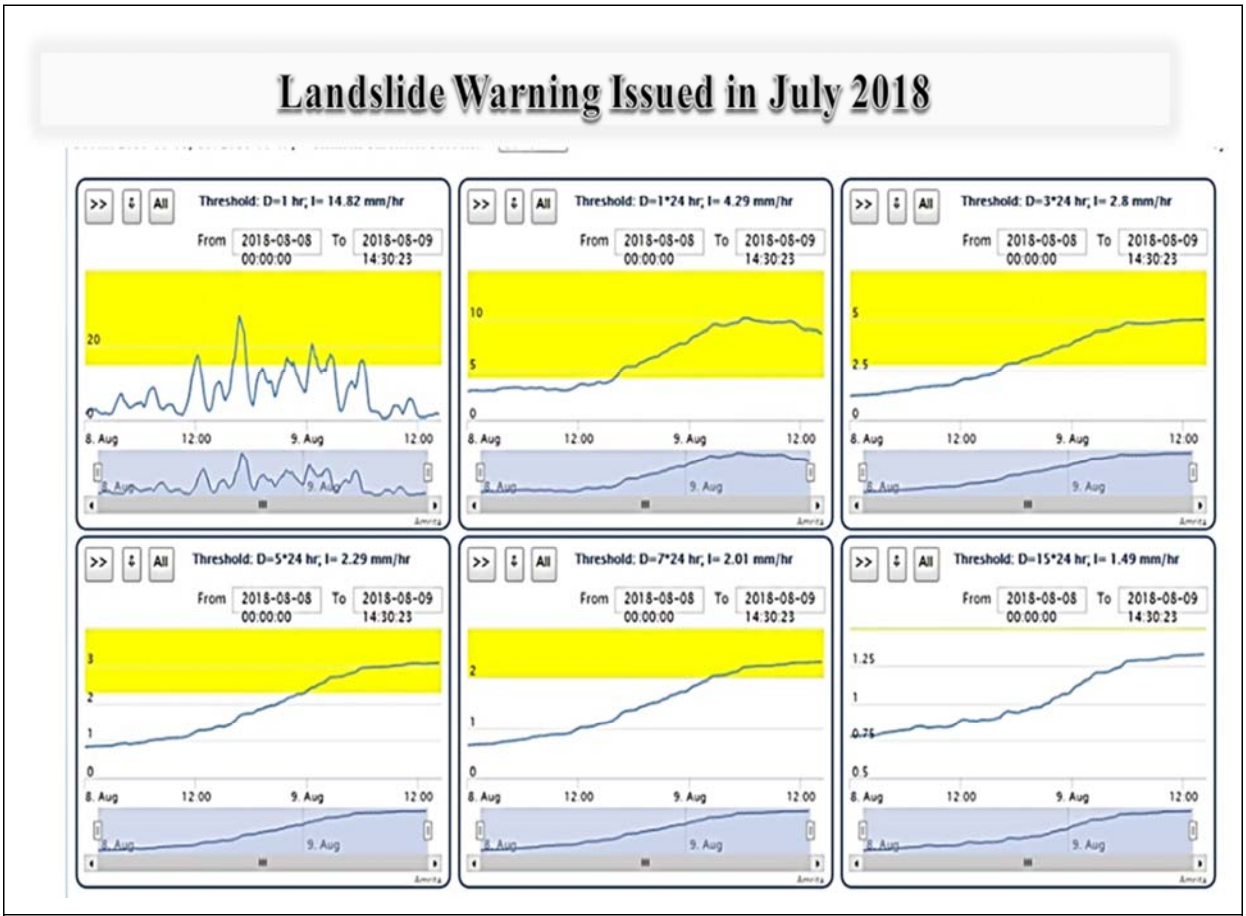
Landslide Warning Issued in July 2018
Threshold: D=1 hr; I= 14.82 mm/hr
Threshold: D=1*24 hr; I= 4.29 mm/hr
Threshold: D=3*24 hr; I= 2.8 mm/hr
Threshold: D=5*24 hr; I= 2.29 mm/hr
Threshold: D=7*24 hr; I= 2.01 mm/hr
Threshold: D=15*24 hr; I= 1.49 mm/hr
From 2018-08-08 00:00:00 To 2018-08-09 14:30:23
8. Aug
12:00
9. Aug

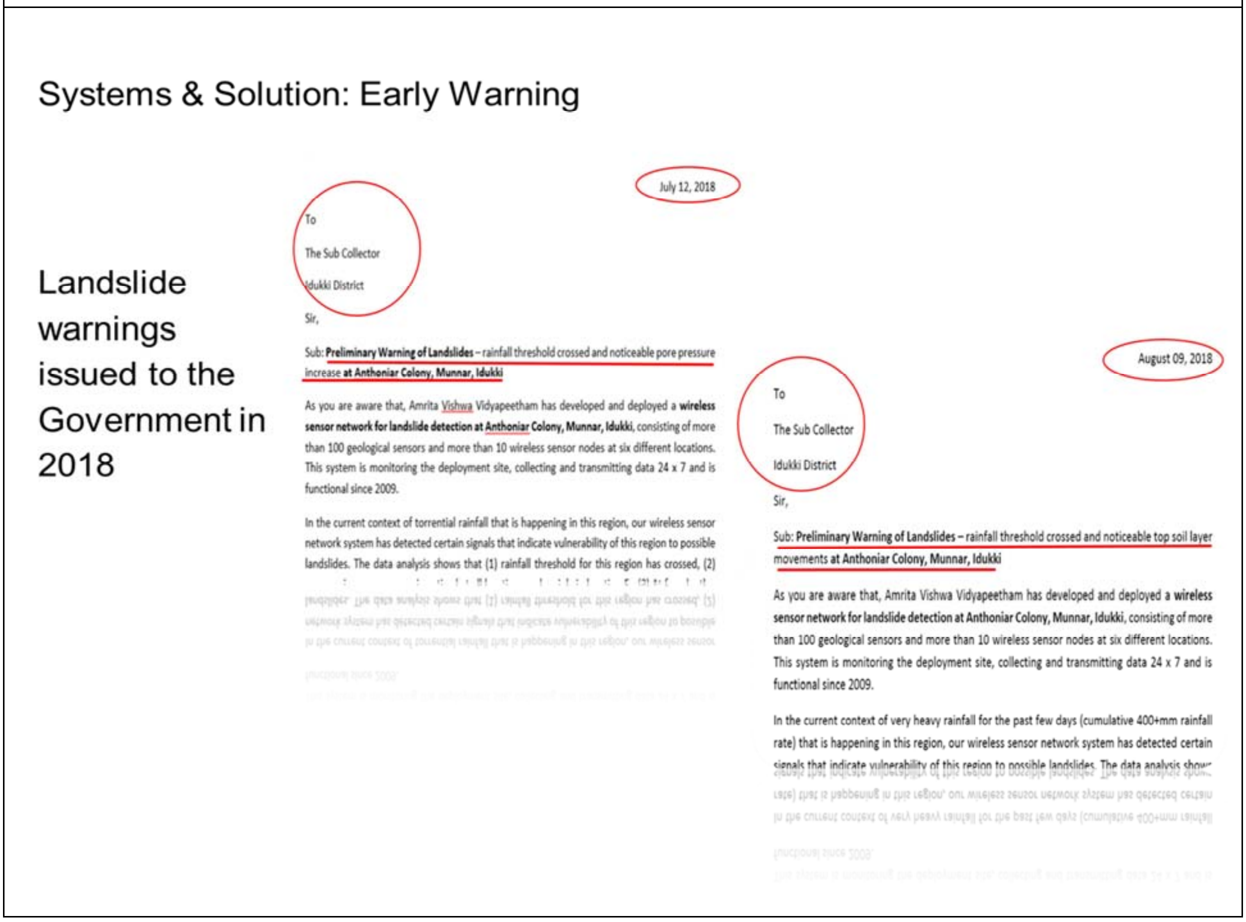
Systems & Solution: Early Warning
Landslide warnings issued to the Government in 2018
July 12, 2018
To
The Sub Collector
Idukki District
Sir,
Sub: Preliminary Warning of Landslides – rainfall threshold crossed and noticeable pore pressure increase at Anthoniar Colony, Munnar, Idukki
As you are aware that, Amrita Vishwa Vidyapeetham has developed and deployed a wireless sensor network for landslide detection at Anthoniar Colony, Munnar, Idukki, consisting of more than 100 geological sensors and more than 10 wireless sensor nodes at six different locations. This system is monitoring the deployment site, collecting and transmitting data 24 x 7 and is functional since 2009.
In the current context of torrential rainfall that is happening in this region, our wireless sensor network system has detected certain signals that indicate vulnerability of this region to possible landslides. The data analysis shows that (1) rainfall threshold for this region has crossed, (2)
August 09, 2018
To
The Sub Collector
Idukki District
Sir,
Sub: Preliminary Warning of Landslides – rainfall threshold crossed and noticeable top soil layer movements at Anthoniar Colony, Munnar, Idukki
As you are aware that, Amrita Vishwa Vidyapeetham has developed and deployed a wireless sensor network for landslide detection at Anthoniar Colony, Munnar, Idukki, consisting of more than 100 geological sensors and more than 10 wireless sensor nodes at six different locations. This system is monitoring the deployment site, collecting and transmitting data 24 x 7 and is functional since 2009.
In the current context of very heavy rainfall for the past few days (cumulative 400+mm rainfall rate) that is happening in this region, our wireless sensor network system has detected certain signals that indicate vulnerability of this region to possible landslides. The data analysis shows

Systems & Solutions: Disaster Resilience

- 24 Hour helpline established during 2018, 2019 floods and landslides in Amrita
- Amrita Kripa App: A mobile app developed by Amrita for disaster rescue

Systems & Solutions: Disaster Resilience

Amrita Kripa App: A mobile app developed by Amrita

livemint

Mumbai — one of the three children of T.K. Somashekhara Pillai (68) and Leelamma (64) — panicked when she heard about the Kerala floods. Being far away from her aged parents, she was frantically trying to contact several people to save them. She had called several helplines for immediate help. She downloaded the app from the Amrita university's website and entered her parents' details, asking for help.

Researchers at the Amrita Center for Wireless Networks & Applications (AmritaWNA) customized the Android app, called AmritaKripa, to specifically cater to the recent Kerala floods. Apart from over 3,000 entries in two days, more than 500 real time entries were from people willing to provide relief-and-rescue services. The app was used in tandem with the "Amrita Help Line" set up by students and faculty volunteers at the university's Amritapuri campus in Kollam district.

The Indian EXPRESS

Tuesday, May 21, 2019

Kerala flood: App to connect survivors with relief providers

The app allows users to request for or offer rescue, medical help, supplies such as food, clothing, medicines, shelter and services such as water, electricity, telephone. One can also report people missing, people found orphaned, either conscious or unconscious, or dead.

Adaptive and Integrated Community Disaster Resilience

Field Deployment

Community Engagement

Key Findings- I

- Single warning will not suffice the EWS, Single level warnings can lead to false alarms
- Reliability of warnings are necessary to build effective disaster resilience
- Effective Resilience Building for Preparedness require defining optimality between time criticality and reliability of the early warning
- Multiscale warning requires efficient decisions based on cost effectiveness and reliability of warning
- Scalable models for the systems and solutions are required to be used by the citizens from different socio, economic and political background
- Multi level, multi phase intervention strategies need to be designed based on the communities social, economical, and political background

Key Findings - II

- Sustainable social models need to be developed for time critical behavioral changes
- Change agents need to be identified from the community, who will act as the ambassadors for the change management and development of sustainable pathways for the prospective change
- Risk communication need to be real-time
- Community need to be trained in understanding different levels and scales of risk communication
- Administrators & policy makers need to be engaged and empowered for dynamic change management
- Education & awareness need to start from the understanding of their five capitals (Human, Natural, Finance, Social, Physical)

Conclusion

- Community Disaster Resilience is of Paramount Importance
- MultiPhase, Multiscale Integrated Approach is needed to capture the dynamics of Landslide
- Developed Systems and Solutions for Adaptive and Integrated Community Disaster Resilience
- Field Evaluated & Time Tested
- Demonstrated Success Stories

Palu Earthquake-induced Liquefaction: Toward Reconstruction and Recovery

Teuku Faisal Fathani(1), Wahyu Wilopo(1)

1) Center for Disaster Mitigation and Technological Innovation (GAMA-InaTEK), Universitas Gadjah Mada, Yogyakarta 55281
e-mail: tfathani@ugm.ac.id, wilopo_w@ugm.ac.id

Abstract

On 28 September 2018, an earthquake followed by tsunami and liquefaction in Central Sulawesi caused severe damage and resulted in a death toll of more than 2000 people. The epicenter was northeast of Palu City, at a relatively shallow depth of 10 kilometers. The earthquake was followed by a series of tsunami waves as high as 6 m. The earthquake caused liquefaction and earth flows, which affected a large 380 hectare area in Sigi District and Palu City. Sulawesi Island has several geologic structures, one of which is the Palu Koro Fault with 240 km long north to south, crossing Palu City to Bone Bay. The Palu Koro Fault is an active sinistral fault which moves north 25-30 mm/year. As a result, earthquakes often occur in the area. The 28 September 2018 earthquake was also caused by the Palu Koro Fault. Other notable phenomena caused by the 28 Sept 2018 earthquake were tsunami, liquefaction and earth flows. The liquefaction that occurred in several areas was then followed by earth flows. The liquefaction was caused by earthquake induced shaking in a soil layer dominated by saturated fluvial and alluvial sediments. The liquefaction hazard map published by the Geological Agency (2012) had already identified that Palu City had a high to very high liquefaction potential.

2018 Palu Earthquake

- The epicenter of M7.5 Earthquake was northeast of Palu City at a relatively shallow depth of 10 km.
- The earthquake was followed by a series of 6 m (max) tsunami waves.
- The earthquake caused liquefaction and earth flows, which affected 400 hectare.
- The earthquake, tsunami, and liquefaction caused severe damage and resulted in a death toll of >2000.
- Sept-Oct 2018, 21 earthquakes >M5 with ±10km depth.
- Total Loss $ 1.5 billion

Geologic Structure of Sulawesi Island

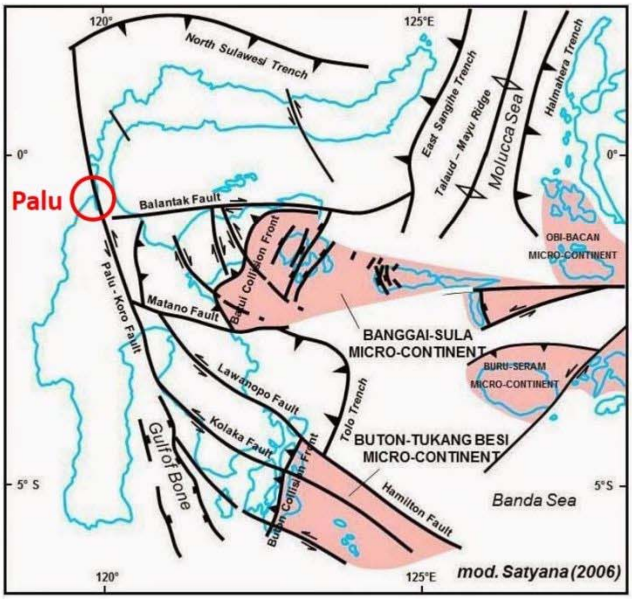

Palu Koro fault:

- An active sinistral fault which moves north 25-30 mm/year.
- 240 km long north to south, crossing Palu to Bone Bay.

1927 Earthquake

- A M6.3 earthquake which was followed by a 15 m high tsunami wave.
- Causing 2,500 casualties.

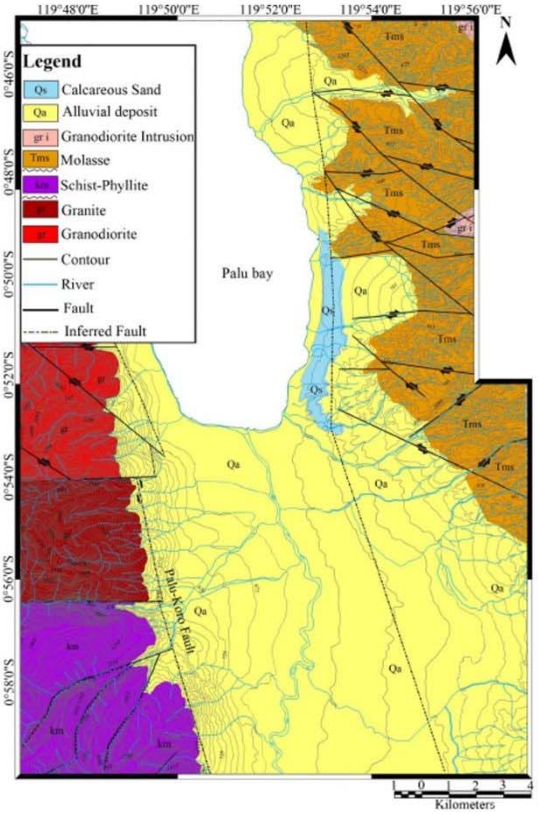

Geological Map of Palu City and surrounding area (UGM, 2013)

Geological map of Palu depression area (Pramumijoyo et al., 2013)

Microtremor Measurement in Palu City

UGM and Kyoto University (2012)

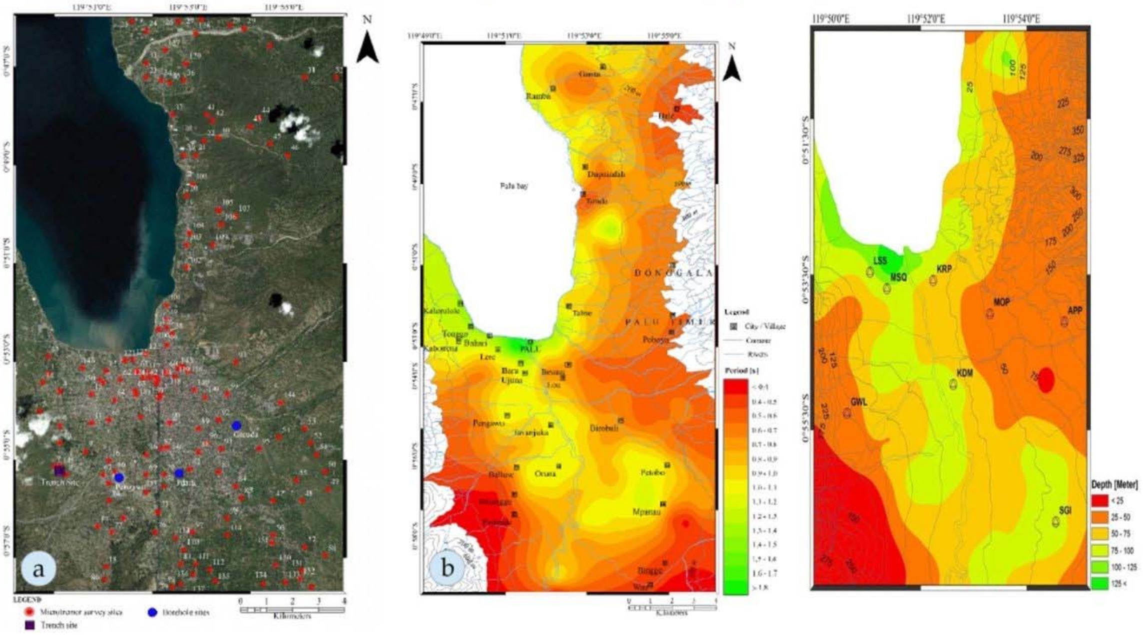

(a) Microtremor observation, boreholes sites and the situation of the trench making at Palu; (b) Spatial distributions of longer predominant period; (c) Sediment thickness

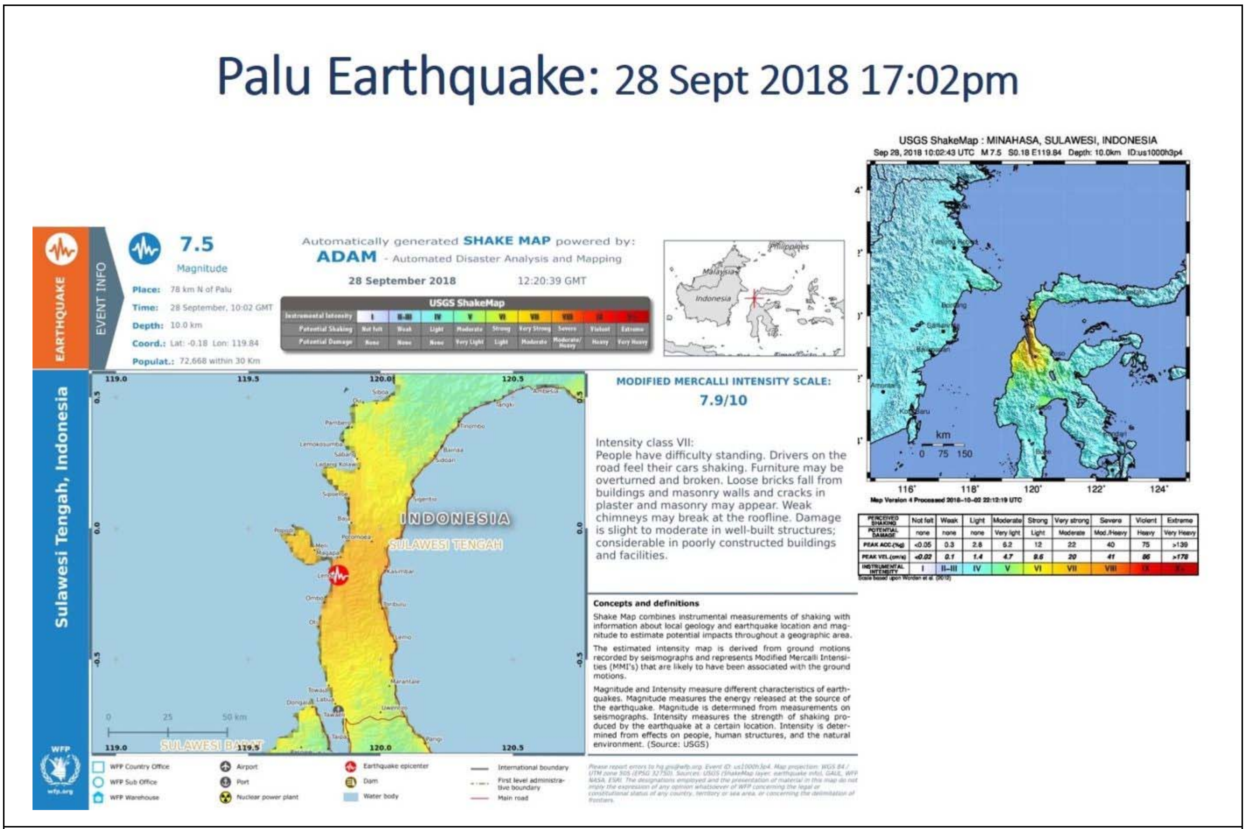
Palu Earthquake: 28 Sept 2018 17:02pm
USGS ShakeMap : MINAHASA, SULAWESI, INDONESIA
EARTHQUAKE
EVENT INFO
7.5
Magnitude
Place: 78 km N of Palu
Time: 28 September, 10:02 GMT
Depth: 10.0 km
Coord.: Lat: -0.18 Lon: 119.84
Automatically generated SHAKE MAP powered by:
ADAM - Automated Disaster Analysis and Mapping
28 September 2018
12:20:39 GMT
USGS ShakeMap
Sulawesi Tengah, Indonesia
INDONESIA
SULAWESI TENGAH
SULAWESI BARAT
MODIFIED MERCALLI INTENSITY SCALE:
7.9/10
Intensity class VII:
People have difficulty standing. Drivers on the road feel their cars shaking. Furniture may be overturned and broken. Loose bricks fall from buildings and masonry walls and cracks in plaster and masonry may appear. Weak chimneys may break at the roofline. Damage is slight to moderate in well-built structures; considerable in poorly constructed buildings and facilities.
Concepts and definitions
Shake Map combines instrumental measurements of shaking with information about local geology and earthquake location and magnitude to estimate potential impacts throughout a geographic area.
The estimated intensity map is derived from ground motions recorded by seismographs and represents Modified Mercalli Intensities (MMI's) that are likely to have been associated with the ground motions.
Magnitude and Intensity measure different characteristics of earthquakes. Magnitude measures the energy released at the source of the earthquake. Magnitude is determined from measurements on seismographs. Intensity measures the strength of shaking produced by the earthquake at a certain location. Intensity is determined from effects on people, human structures, and the natural environment. (Source: USGS)
WFP

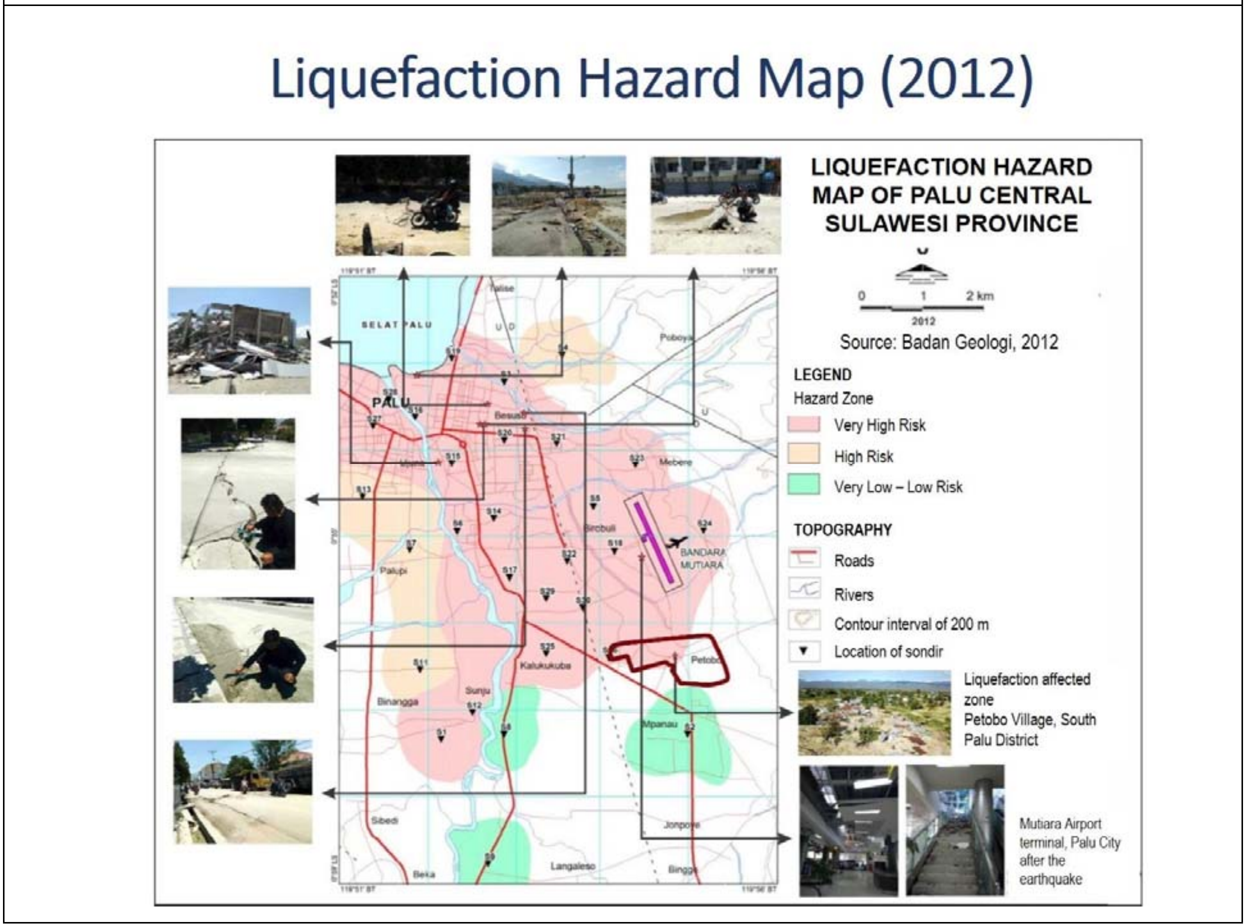
Liquefaction Hazard Map (2012)
LIQUEFACTION HAZARD MAP OF PALU CENTRAL SULAWESI PROVINCE
0 1 2 km
Source: Badan Geologi, 2012
LEGEND
Hazard Zone
Very High Risk
High Risk
Very Low – Low Risk
TOPOGRAPHY
Roads
Rivers
Contour interval of 200 m
Location of sondir
SELAT PALU
PALU
BANDARA MUTIARA
Petobo
Liquefaction affected zone
Petobo Village, South Palu District
Mutiara Airport terminal, Palu City after the earthquake

Main Liquefaction area

Balaroa

Petobo

Jono-Oge

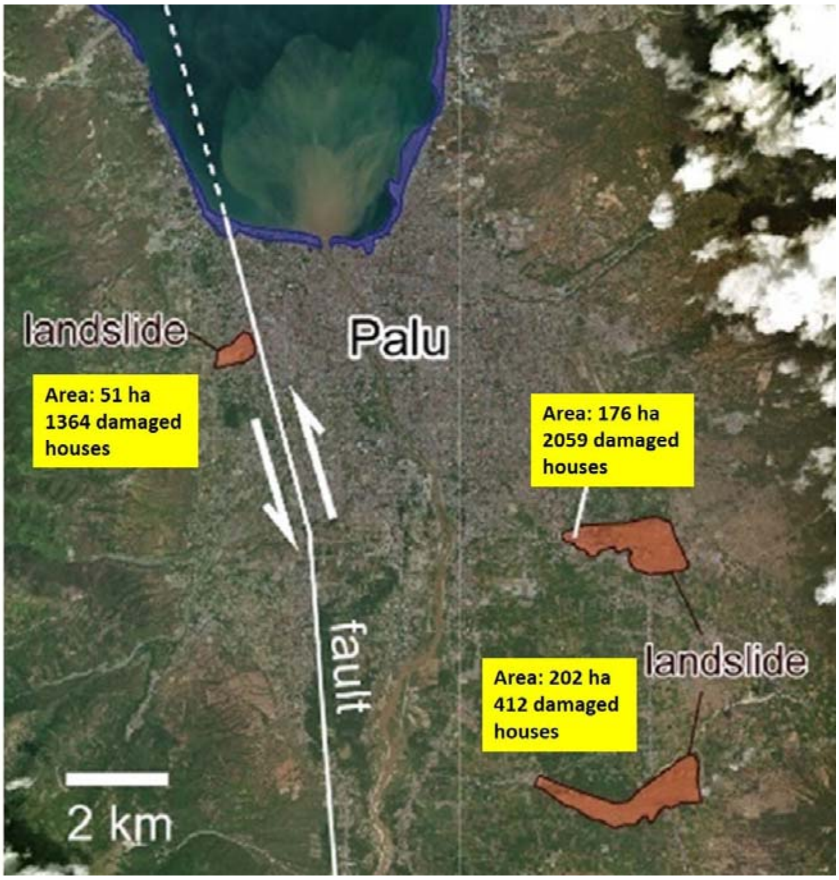

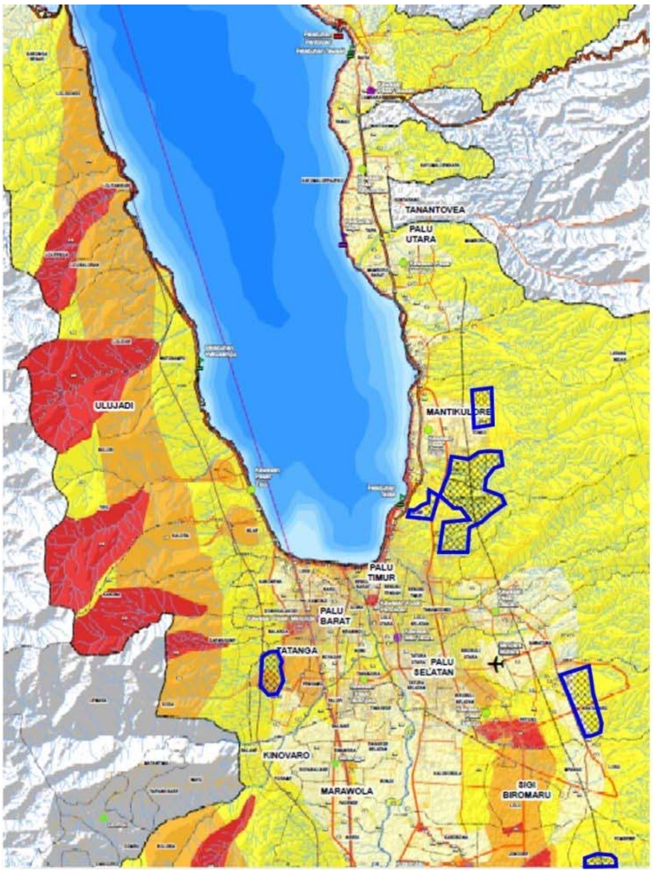

Hazard Map Zonation of Palu City and Surrounding Area

ZONA & TIPOLOGI	DEFINISI/ KRITERIA	ARAHAN SPASIAL PASCA BENCANA (KETENTUAN PEMANFAATAN RUANG)
ZRB 4 (ZONA TERLARANG) Prohibited zone	4 L : Zona likuifaksi masif pasca gempa (Seperti Kws Petobo, Balaroa, Jono Oge, Lolu, dan Sibalaya) 4 T : Zona sempadan pantai rawan tsunami minimal 100 – 200 meter dari titik pasang tertinggi (sempadan 100 m untuk Teluk Palu, kecuali di Kel. Lere, Besusu Barat, dan Talise, ditetapkan 200 m) 4 S : Zona Sempadan Patahan Aktif Palu-Koro 0-10 meter (Zona Bahaya Deformasi Sesar Aktif) 4 G : Zona Rawan Gerakan Tanah Tinggi Pasca Gempabumi Zona Rawan Gempabumi Tinggi	1. Dilarang pembangunan kembali dan pembangunan baru. Unit hunian pada zona ini direkomendasikan untuk direlokasi. 2. Diprioritaskan pemanfaatan ruang untuk fungsi kawasan lindung, RTH, dan monumen.
ZRB 3 (ZONA TERBATAS) Limited-use zone	3 S : Zona Sempadan Patahan Aktif Palu Koro pada 10-50 meter 3 L : Zona Rawan Likuifaksi Sangat Tinggi 3 T : Zona Rawan Tsunami Tinggi (KRB III) di luar sempadan pantai 3 G : Zona Rawan Gerakan Tanah Tinggi Zona Rawan Gempabumi Tinggi	1. Dilarang pembangunan baru fungsi hunian serta fasilitas penting dan berisiko tinggi (sesuai SNI 1726, antara lain rumah sakit, sekolah, gedung pertemuan, stadion, pusat energi, pusat telekomunikasi) 2. Pembangunan kembali fungsi hunian diperkuat sesuai standar yang berlaku (SNI 1726) 3. Pada kawasan yang belum terbangun dan berada pada zona rawan likuifaksi sangat tinggi maupun rawan gerakan tanah tinggi, diprioritaskan untuk fungsi kawasan lindung atau budidaya non-terbangun (pertanian, perkebunan, kehutanan)
ZRB 2 (ZONA BERSYARAT) Regulated zone	2 L : Zona Rawan Likuifaksi Tinggi 2 T : Zona Rawan Tsunami Menengah (KRB II) 2 G : Zona Rawan Gerakan Tanah Menengah 2 B : Zona Rawan Banjir Tinggi Zona Rawan Gempabumi Tinggi	1. Pembangunan baru harus mengikuti standar yang berlaku (SNI 1726). 2. Pada zona rawan tsunami dan rawan banjir, bangunan hunian disesuaikan dengan tingkat kerawanan bencananya. 3. Intensitas pemanfaatan ruang rendah.
ZRB 1 (ZONA PENGEMBANGAN) Promoted zone	1 L : Zona Rawan Likuifaksi Sedang 1 T : Zona Rawan Tsunami Rendah (KRB I) 1 G : Zona Rawan Gerakan Tanah Sangat Rendah dan Rendah 1 B : Zona Rawan Banjir Menengah dan Rendah Zona Rawan Gempabumi Tinggi	1. Pembangunan baru harus mengikuti standar yang berlaku (SNI 1726). 2. Intensitas pemanfaatan ruang rendah-sedang.

Discussion

- Shift in paradigm : focusing on Disaster Risk Reduction (DRR)
- Promoting an integrated planning in DRR
- Reconstruction and recovery should not only focus on engineering solution but include consideration of the environment sustainability and social aspect
- Consideration of multi-hazards in DRR and Recovery Planning

Debris Flow Hazard in Cyclops Mountains, Papua, Indonesia

Wahyu Wilopo(1) & Teuku Faisal Fathani(1)

1) Center for Disaster Mitigation and Technological Innovation (GAMA-InaTEK), Universitas Gadjah Mada, Yogyakarta 55281
e-mail: wilopo_w@ugm.ac.id; tfathani@ugm.ac.id

Abstract

A landslide-induced debris flow occurred in Cycloop Mountains of Papua Island on 16 March 2019. The debris flow was caused by heavy rain, which led to landslides in several locations, forming a natural dam in the river. The large water discharge prompted by excessive rainfall and the landslide materials caused the dam to collapse. The steep slope of Cycloop Mountains resulted in rapid flow of river water, bringing various sizes of flashflood materials and threatening the settlements in the surrounding areas. In response to this hazard, the Center for Disaster Mitigation and Technological Innovation Universitas Gadjah Mada conducted an intensive study to reduce the sediment-related disaster risk. The result will give a general overview on the geological condition, the potential and mechanism of sediment-related disasters, and recommendations on mitigation efforts to reduce the risk.

Background

- On Saturday March 16, 2019 there was a debris flow disaster in Sentani City, Papua, Indonesia
- This disaster resulted in 68 people died, 75 people were slightly injured and 30 people seriously injured. A total of 4,153 residents were evacuated in seven shelter locations.
- It is necessary to do an investigation to understand the debris flow mechanism and propose some mitigations strategy.

LOCATION

The study area is located in Cyclops Mountain, Jayapura District, Papua

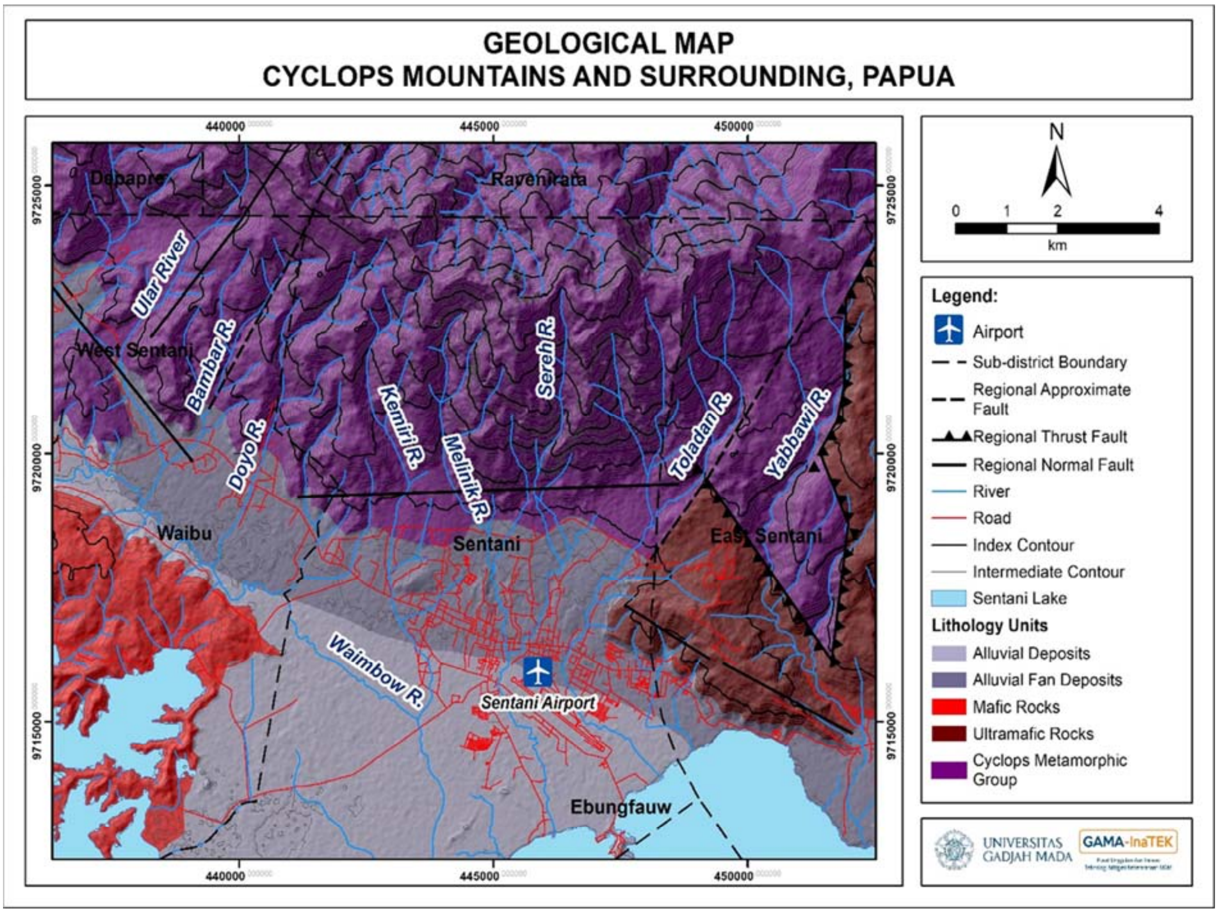
GEOLOGICAL MAP
CYCLOPS MOUNTAINS AND SURROUNDING, PAPUA
Depapre
Ravenirara
Ular River
Bambar R.
West Sentani
Doyo R.
Kemiri R.
Melinik R.
Sereh R.
Toladan R.
Yabbawi R.
Waibu
Sentani
East Sentani
Waimbow R.
Sentani Airport
Ebungfauw
440000
445000
450000
9725000
9720000
9715000
N
0 1 2 4
km
Legend:
Airport
Sub-district Boundary
Regional Approximate Fault
Regional Thrust Fault
Regional Normal Fault
River
Road
Index Contour
Intermediate Contour
Sentani Lake
Lithology Units
Alluvial Deposits
Alluvial Fan Deposits
Mafic Rocks
Ultramafic Rocks
Cyclops Metamorphic Group
UNIVERSITAS GADJAH MADA
GAMA-InaTEK

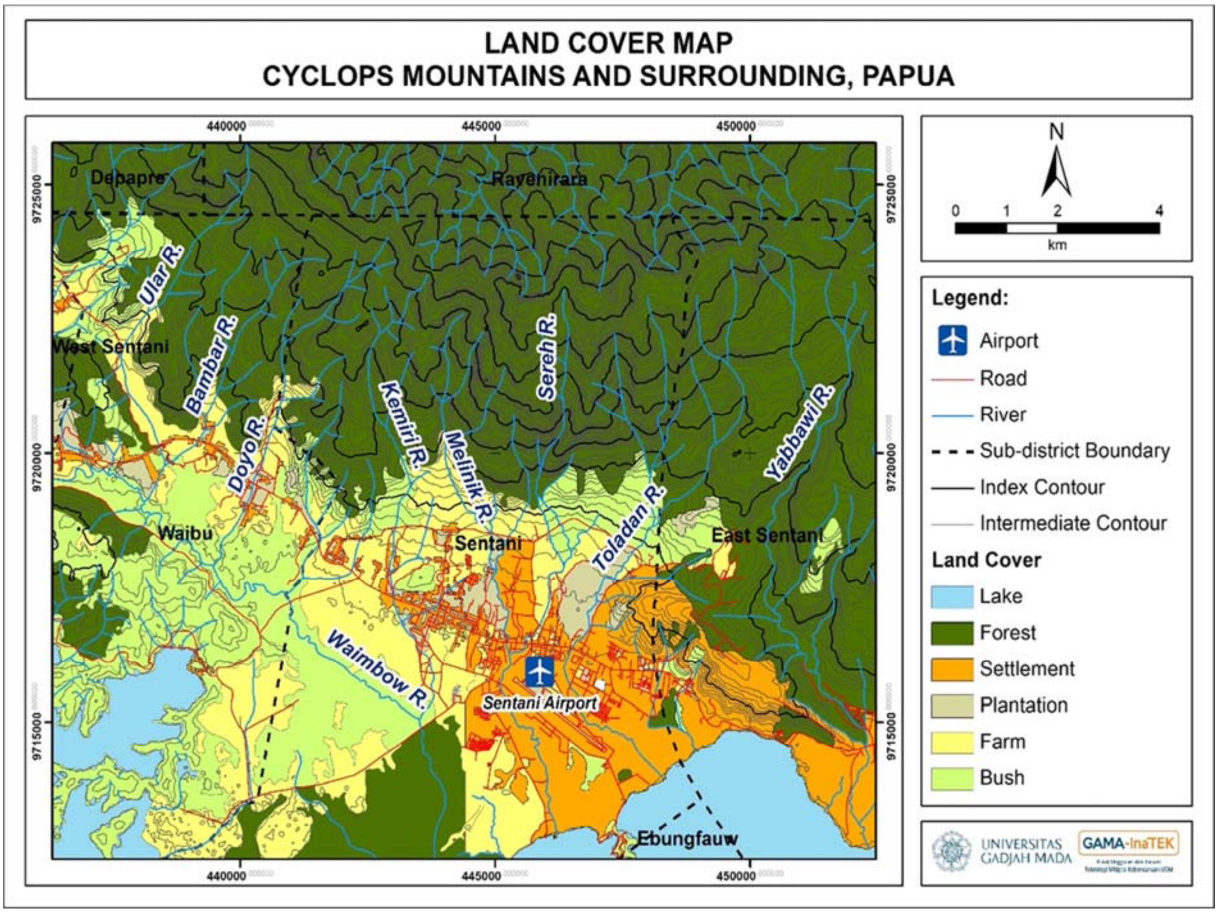
LAND COVER MAP
CYCLOPS MOUNTAINS AND SURROUNDING, PAPUA
Depapre
Ravenirara
Ular R.
West Sentani
Bambar R.
Doyo R.
Kemiri R.
Melinik R.
Sereh R.
Toladan R.
Yabbawi R.
Waibu
Sentani
East Sentani
Waimbow R.
Sentani Airport
Ebungfauw
440000
445000
450000
9725000
9720000
9715000
N
0 1 2 4
km
Legend:
Airport
Road
River
Sub-district Boundary
Index Contour
Intermediate Contour
Land Cover
Lake
Forest
Settlement
Plantation
Farm
Bush
UNIVERSITAS GADJAH MADA
GAMA-InaTEK

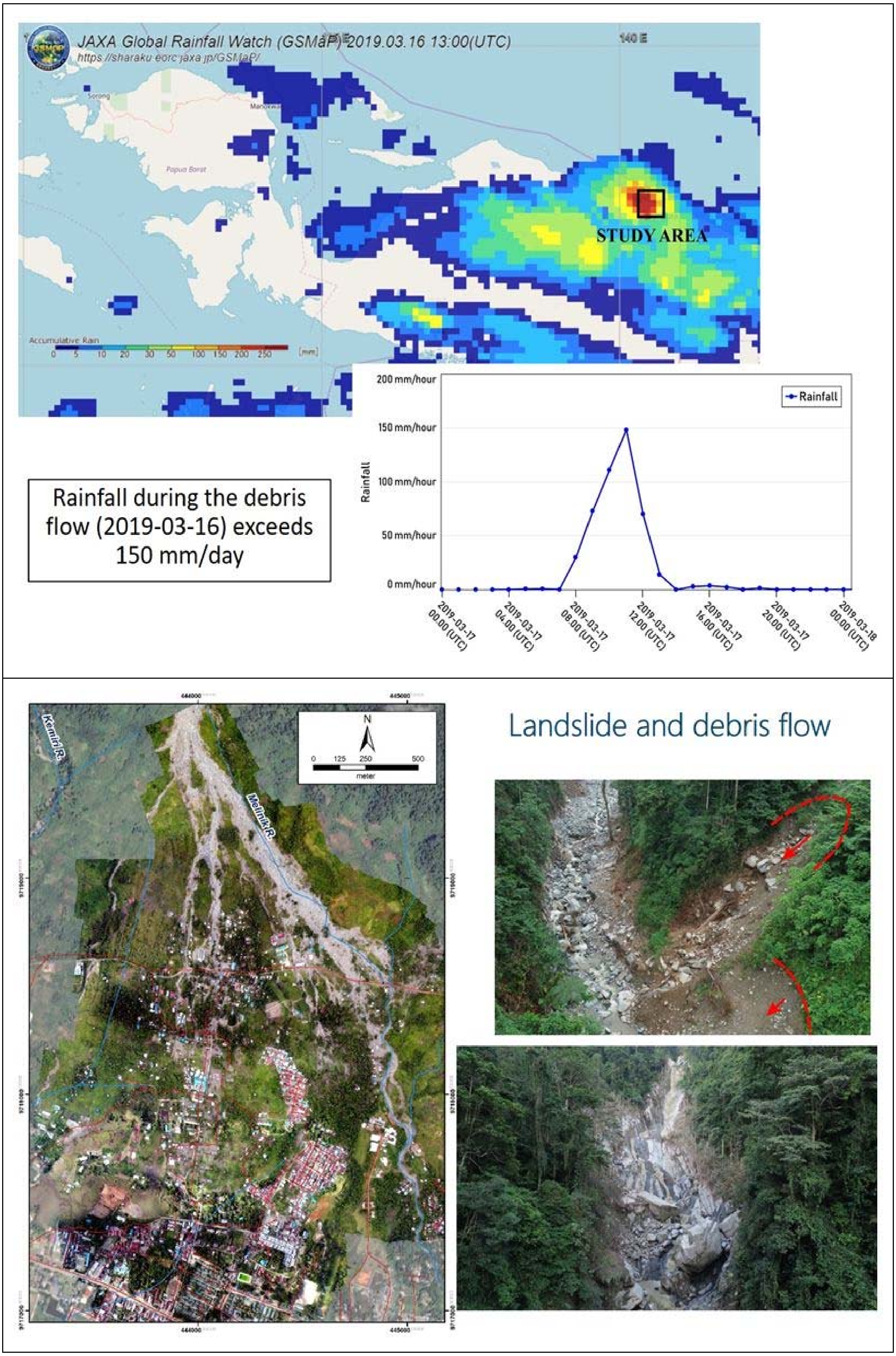
JAXA Global Rainfall Watch (GSMaP) 2019.03.16 13:00(UTC)
https://sharaku.eorc.jaxa.jp/GSMaP/
140 E
STUDY AREA
Accumulative Rain
0 5 10 20 30 50 100 150 200 250 [mm]
Rainfall during the debris flow (2019-03-16) exceeds 150 mm/day
Rainfall
200 mm/hour
150 mm/hour
100 mm/hour
50 mm/hour
0 mm/hour
2019-03-17 00:00 (UTC)
2019-03-17 04:00 (UTC)
2019-03-17 08:00 (UTC)
2019-03-17 12:00 (UTC)
2019-03-17 16:00 (UTC)
2019-03-17 20:00 (UTC)
2019-03-18 00:00 (UTC)
Kemiri R.
Melinik R.
N
0 125 250 500
meter
Landslide and debris flow

RECOMMENDATIONS

- Preventive actions not to settle in the debris flow risk zone.
- Monitoring the indication of debris flow (rainfall and landslide movement in the catchment area).
- Increasing community preparedness by implementing an early warning system.
- Maintain the flow of the river.
- Chanel modification and floodwalls.
- Reviewing land use by considering the geological aspects.

Rain-Induced Landslide Hazard Zone in West Java Province

Munawar[1], Aditya[2], Karnawati[1,2]

1) School of Meteorology Climatology and Geophysics
2) BMKG Indonesia

Abstract

Landslide dominate natural disasters in West Java. landslide induction rainfall index in alarm units per month. The index determines the correction factor to determine the spread of potential landslides. Each constituent element of landslide potential in West Java is related to one another. The pattern of distribution of landslide-inducing rainfall greatly influences how the spread of potential landslides. Most of the patterns on the spread of landslide potential are formed almost the same as the distribution of the induced rainfall. Distribution of landslide potential induced by rainfall shows the frequency of potential landslides to occur in one month. This potential for landslides is caused by the frequency of climatological rainfall that exceeds the threshold index.

Keywords: potential, prone, landslides, overlays, indices

REPUBLIKA.co.id

Home > News > Nasional

Awal Tahun, Longsor Dominasi Bencana di Sukabumi

Kamis 16 February 2017 08:50 WIB

REPUBLIKA.CO.ID, SUKABUMI -- Bencana longsor mendominasi bencana alam yang terjadi di Kota Sukabumi pada Januari hingga pertengahan Februari 2017. Kejadian bencana tersebut salah satunya dipicu oleh tingginya intensitas hujan di wilayah Sukabumi.

"Jumlah bencana yang terdata dari Januari hingga pertengahan Februari sebanak 17 kejadian," kata Kepala Seksi Pencegahan dan Kesiapsiagaan, Badan Penanggulangan Bencana Daerah (BPBD) Kota Sukabumi Zulkarnain Barhami kepada *Republika.co.id*, Kamis (16/2).

Rinciannya, sebanyak 12 kasus pada Januari dan lima kasus hingga pertengahan Februari. Zulkarnain mengatakan, kasus longsor mendominasi dibandingkan dengan yang lain yakni enam kejadian. Sementara bencana lainnya yakni angin topan atau puting beliung sebanyak empat kasus, tiga kasus kebakaran, dua kasus gempa bumi, dan dua kejadian bencana lain-lain.

Zulkarnain mengungkapkan, dalam dua hari terakhir ini terjadi dua bencana longsor di dua lokasi berbeda. Peristiwa itu terjadi di Kelurahan Karamat Kecamatan Gunungpuyuh dan Kelurahan Sukakarya Kecamatan Warudoyong.Kepala Seksi Kedaruratan dan Logistik, BPBD Kota Sukabumi Ahdar Somali menambahkan, bencana longsor di Karamat, Gunungpuyuh terjadi akibat adanya material longsor menutupi saluran air yang ada di bawahnya. Dikhawatirkan, tertutupnya saluran air dengan material longsor

REPUBLIKA.co.id

Home > News > Nasional

Kerugian Akibat Bencana di Sukabumi Capai Rp 38,1 Miliar

Rabu 06 December 2017 10:34 WIB

Rep: Riga Nurul Iman/ Red: Andi Nur Aminah

REPUBLIKA.CO.ID, SUKABUMI -- Dampak bencana di Kota Sukabumi menyebabkan kerugian yang cukup besar. Pasalnya, sejak 2013 lalu hingga September 2017 lalu tercatat jumlah kerugian akibat bencana diperkirakan mencapai Rp 38,1 miliar.

"Dari data yang dihimpun menyebutkan kerugian akibat bencana dari 2013 hingga 2016 ditaksir mencapai sebesar Rp 36 miliar," ujar Kepala Pelaksana Badan Penanggulangan Bencana Daerah (BPBD) Kota Sukabumi Asep Suhendrawan, Rabu (6/12).

Jumlah tersebut belum ditambah kerugian akibat bencana pada 2017. Asep mengatakan, dalam rentang Januari-September 2017 tercatat jumlah kerugian akibat bencana ditaksir Rp 2,1 miliar. Data kerugian ini lanjut dia dimulai sejak 2013 karena lembaga tersebut baru beroperasi dan melaksanakan tugas serta fungsinya.

Menurut Asep, mengacu pada data tersbeut menunjukkan sangat besar dampak bencana terhadap kerugian yang dialami masyarakat. Jumlah kerugian bencana ini ungkap dia membuktikan upaya optimalisasi pencegahan mitigasi dan kesiapsiagaan bencana sangat diperlukan untuk

KOMPAS.com

Home / News / Nasional

Ini Penyebab Longsor di Banjarnegara Menurut BNPB

JAKARTA, KOMPAS.com — Kepala Pusat Data dan Informasi Badan Nasional Penanggulangan Bencana (BNPB) Sutopo Purwo Nugroho menyebutkan beberapa penyebab terjadinya longsor di Dusun Jemblung, Desa Sampang, Kecamatan Karangkobar, Kabupaten Banjarnegara, Jawa Tengah.

"Dusun Jemblung di dalam peta merupakan daerah yang rawan longsor dengan intensitas sedang-tinggi," ujar Sutopo, dalam konferensi pers di Kantor BNPB, Jalan Juanda, Jakarta Pusat, Senin (15/12/2014).

Sutopo mengatakan, pada dua hari menjelang terjadinya longsor, yaitu pada tanggal 10-11 Desember, wilayah di sekitar Dusun Jemblung, Banjarnegara, diguyur hujan yang cukup deras. Akibatnya, tanah di lokasi tersebut menjadi penuh dengan air. Kemudian, menurut Sutopo, materi penyusun bukit Telaga Lele, di Dusun Jemblung, merupakan endapan vulkanik tua sehingga solum atau lapisan tanah cukup tebal dan terjadi pelapukan.

Selain itu, kemiringan lereng di bukit tersebut kurang dari 60 persen. Saat kejadian, mahkota longsor berada pada kemiringan lereng 60-80

Home Berita Daerah Internasional Fokus Kolom Blak blakan Pro

Status Jabar Siaga Bencana Banjir dan Long

Bandung - Status Jabar siaga darurat bencana banjir dan tanah longsor mulai 1 November 2017 sampai 31 Mei 2018. Masyarakat diimbau untuk selalu waspada.

Penetapan status siaga tersebut tertuang dalam surat Nomor 362/kep.1024-BPBD/2017 yang ditandatangani langsung oleh Gubernur Jabar Ahmad Heryawan pada 30 Oktober lalu.

"Provinsi Jawa Barat dalam keadaan siaga darurat bencana alam banjir dan longsor, mulai dari tanggal 1 November sampai 31 Mei 2018," kata Gubernur Jabar Ahmad Heryawan dalam rilisnya, Rabu (16/11/2017).

Pria yang akrab disapa Aher mengungkapkan penetapan status siaga bencana ini bukan tanpa alasan. Dari hasil koordinasi dan laporan dengan instansi terkait bahwa November ini sudah memasuki musim penghujan yang tentu berpotensi terjadinya banjir dan longsor.

Untuk itu, dia meminta supaya Badan Penanggulangan Bencana Daerah (BPBD) di tingkat kabupaten dan kota untuk melaksanakan upaya-upaya kesiap siagaan keadaan darurat. "Sehingga mampu meminimalisir potensi dampak bencana melalui penanganan yang bersifat cepat, tepat dan terpadu," kata Aher.

LIPUTAN6

HOME NEWS PILKADA BISNIS SHOWBIZ BOLA FOTO VIDEO GLOBAL TEKNO

Home > News > Peristiwa

Longsor di Pangandaran, F-PDIP Usul Pemetaan Daerah Rawan Bencana

Liputan6.com, Jakarta - Anggota DPR RI Fraksi PDIP Diah Pitaloka mengharapkan kementerian Sosial dan Badan Nasional Penanggulangan Bencana (BNPB) segera memberi bantuan kepada korban longsor di Pangandaran, Jawa Barat.

Diah menilai, daerah selatan Jawa Barat adalah daerah yang mempunyai tingkat kerawanan bencana yang tinggi. Sehingga perlu di bangun posko logistik bencana Jawa Barat Selatan untuk merespon cepat, terutama di musim hujan seperti saat sekarang ini.

"Bantuan harus segera didistribusikan, jangan sampai masyarakat yang menjadi korban longsor semakin menderita karena pemerintah terlambat mengambil tindakan," ujar Diah Minggu (8/10/2017).

Anggota Komisi VIII ini mengatakan, pemerintah semestinya membuat peta kawasan rawan bencana. Sehingga masyarakat yang masuk area tersebut dapat dilakukan relokasi atau diberikan pendidikan mitigasi bencana lebih intensif.

"Kita enggak selalu memberikan bantuan saat terjadi bencana, tapi kita membuat masyarakat agar terhindar dari bencana," jelas dia.

Selain itu, Diah mengungkapkan, pencegahan adalah upaya terbaik yang harus dilakukan pemerintah dan masyarakat. Karena nantinya bantuan yang diberikan oleh pemerintah tidak bisa mengembalikan anggota yang hilang akibat bencana.

Background

- Natural disasters become a serious obstacle in economic development.
- West Java Province is one of the areas with high potential for landslides.
- Information on potential landslide risks can reduce the impact of disasters.
- BMKG hold complete rainfall data where rainfall is the trigger for most landslides.

Purposes

1. Knowing the **physical** distribution of landslide potential areas in West Java Province.
2. Knowing the potential spread of landslides **due to high rainfall** in West Java Province.
3. Knowing the **distribution of landslide-prone** zones in West Java Province.

Effect of rainfall on landslides

- Aleotti (2004) conducted a study of rainfall parameters in relation to the initiation of landslides including cumulative rainfall, previous rainfall, rainfall intensity, and duration of rainfall.

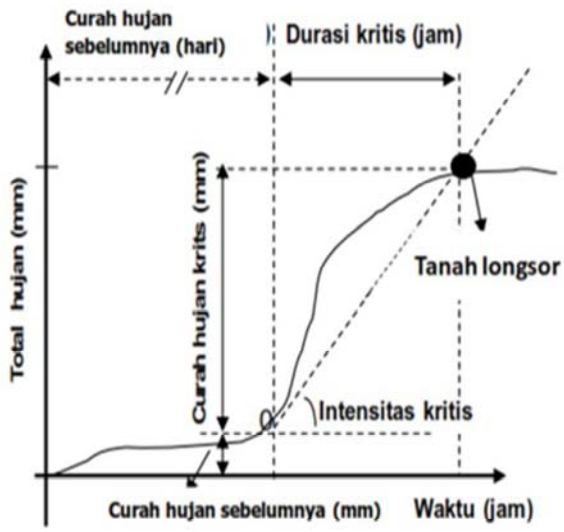

Landslide induction rain threshold

- Muntohar (2009) conducted a landslide-induced rainfall threshold study based on Chain (1980) and Jibson (1986) research by increasing the number of rain posts in the area under study.
- The results show that the rainfall threshold of Muntohar (2009) research is greater than the threshold of Chain (1980) and Jibson (1986).

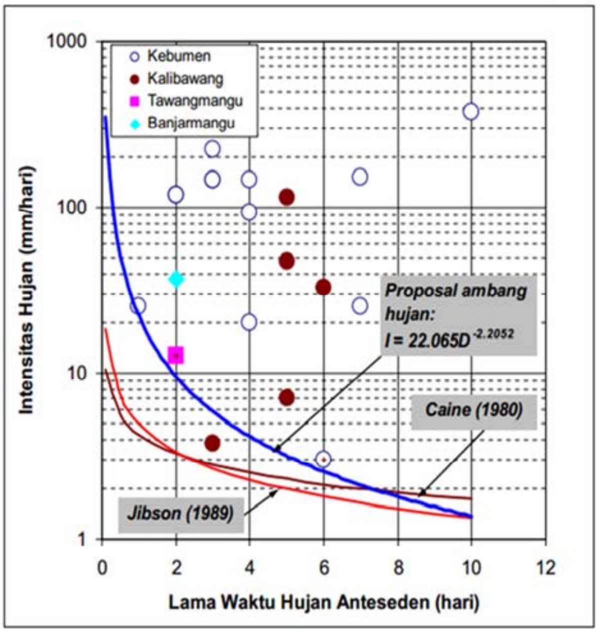

Landslide induction rain threshold

- Rohmaniah and Muntohar (2017) also examined the rain threshold for early warning of ground movements in Indonesia. One of the areas studied is West Java.
- This research resulted in the threshold of Antecedent Rain (accumulated rain that fell a few days before the landslide).
- The equation for the rain threshold curve in West Java is **$Ia = 140.05 * D^{-3.127}$**

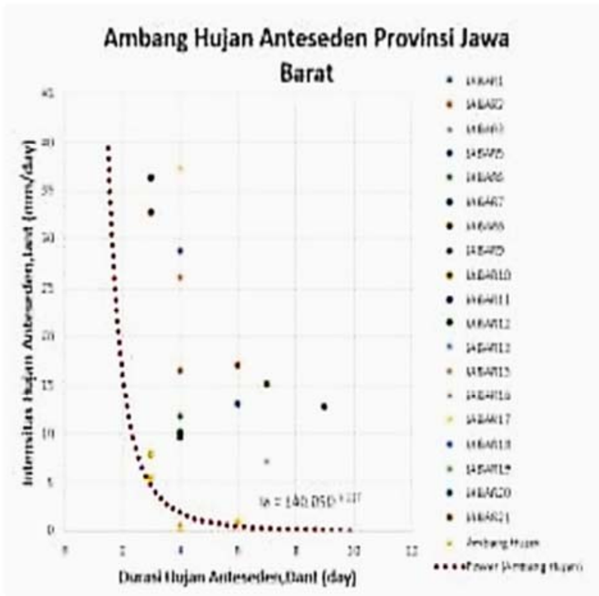

Spatial interpolation model

Interpolation is the process of estimating values in areas that are not sampled or measured, so a map or distribution of values is made in all areas (Gamma Design Software, 2005).This research resulted in the threshold of Antecedent Rain (accumulated rain that fell a few days before the landslide).

- Pramono (2008) compared the spatial interpolation method of Inverse Distance Weighting (IDW) and Ordinary Krigging.
  - The results of Pramono's (2008) research show that the IDW Method provides more accurate interpolation results than the Kriging method.

- Junita and Nanik (2012) compared the IDW, Natural Neighbor and Spline methods in the SRTM DEM interpolation.
  - The results show that the IDW method with large power has the smallest RMSE value.

Weighted overlay method

Weighted overlays are a simple bi-variate statistical method where the weights are determined based on the relationship between the factors causing landslides and the frequency of landslides (Sarkar et al., 1995).

- Panikkar and Subramaniyan (1997) conducted a landslide hazard mapping using a GIS-based weighted overlay method in the area around Dehradun and Massori of Uttar Pradesh.

Research area

- The area studied was West Java Province which located at 5.86 - 7.83 South Latitude and 106.3 - 108.8 East Longitude.

Research material

- **Soil type data**
  HWSD : http://www.fao.org/soils-portal/soil-survey/soil-maps-and-databases/harmonized-world-soil-database-v12/en/
- **Digital Elevation Model (DEM)**
  SRTM : https://earthexplorer.usgs.gov/
- **Land cover data**
  KLHK : geoportal.menlhk.go.id/arcgis/rest/services/KLHK/Penutupan_Lahan_Tahun_2016/MapServer
- **Rainfall data**
  BMKG : Bogor Climatological Station, Jawa Barat, 2000 – 2017 period.
- **Landslide data**
  BNPB : dibi.bnpb.go.id
  2000 – 2017 period.
- **Basic map of West Java region**
  BIG : portal.ina-sdi.or.id

Research Method

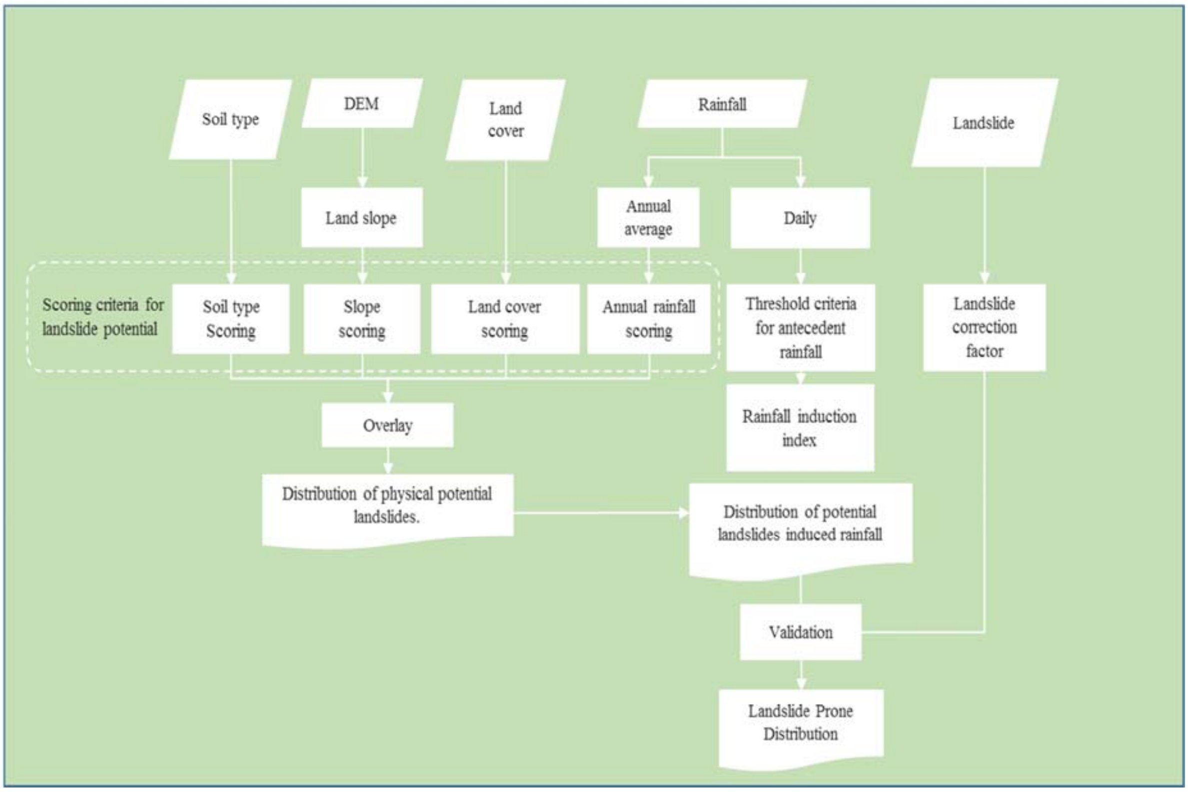

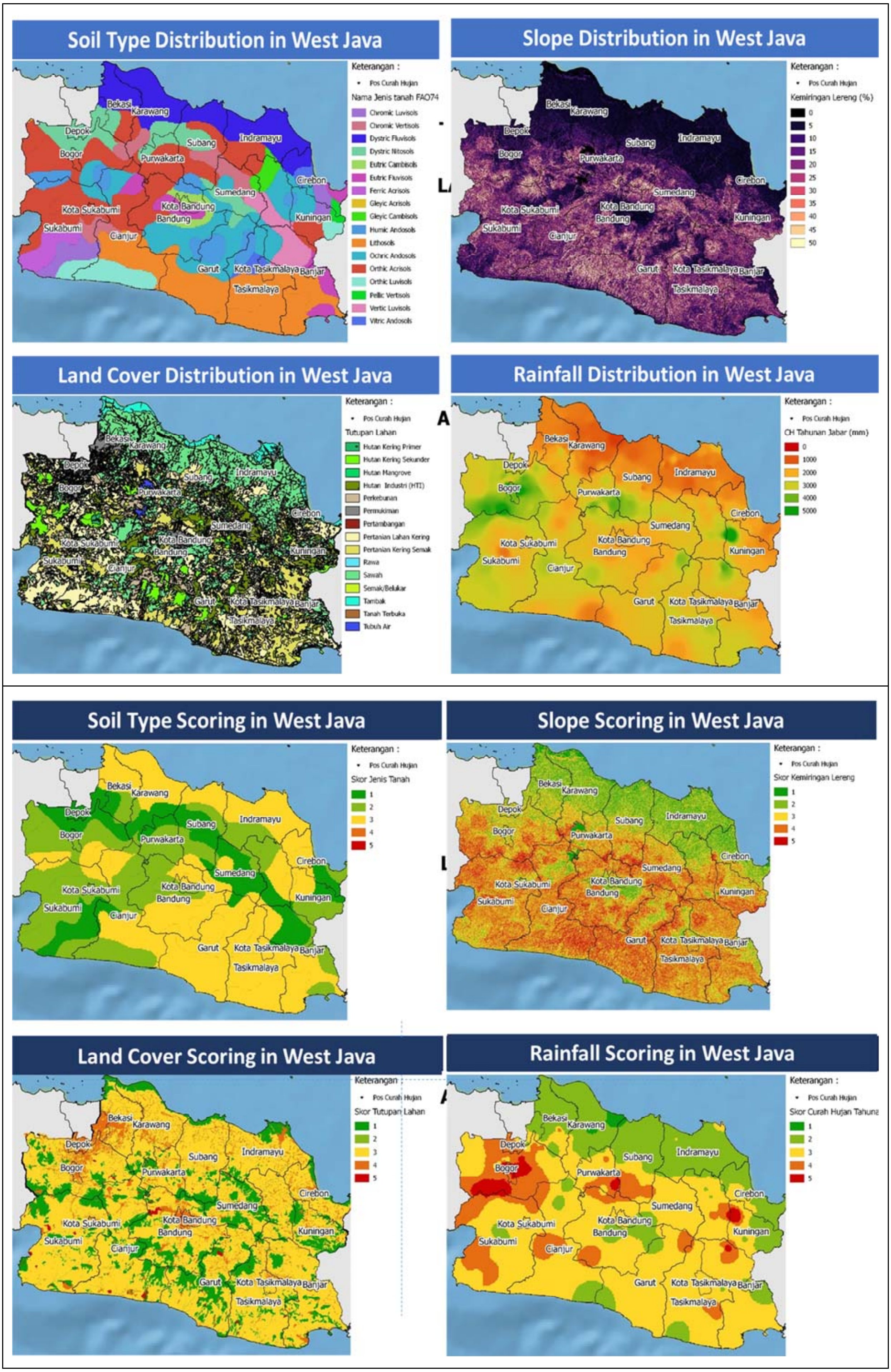
Soil Type Distribution in West Java
Keterangan :
Pos Curah Hujan
Nama Jenis tanah FAO74
Chromic Luvisols
Chromic Vertisols
Dystric Fluvisols
Dystric Nitosols
Eutric Cambisols
Eutric Fluvisols
Ferric Acrisols
Gleyic Acrisols
Gleyic Cambisols
Humic Andosols
Lithosols
Ochric Andosols
Orthic Acrisols
Orthic Luvisols
Pellic Vertisols
Vertic Luvisols
Vitric Andosols
Slope Distribution in West Java
Keterangan :
Pos Curah Hujan
Kemiringan Lereng (%)
0
5
10
15
20
25
30
35
40
45
50
Land Cover Distribution in West Java
Keterangan :
Pos Curah Hujan
Tutupan Lahan
Hutan Kering Primer
Hutan Kering Sekunder
Hutan Mangrove
Hutan Industri (HTI)
Perkebunan
Permukiman
Pertambangan
Pertanian Lahan Kering
Pertanian Kering Semak
Rawa
Sawah
Semak/Belukar
Tambak
Tanah Terbuka
Tubuh Air
Rainfall Distribution in West Java
Keterangan :
Pos Curah Hujan
CH Tahunan Jabar (mm)
0
1000
2000
3000
4000
5000
Soil Type Scoring in West Java
Keterangan :
Pos Curah Hujan
Skor Jenis Tanah
1
2
3
4
5
Slope Scoring in West Java
Keterangan :
Pos Curah Hujan
Skor Kemiringan Lereng
1
2
3
4
5
Land Cover Scoring in West Java
Keterangan :
Pos Curah Hujan
Skor Tutupan Lahan
1
2
3
4
5
Rainfall Scoring in West Java
Keterangan :
Pos Curah Hujan
Skor Curah Hujan Tahuna
1
2
3
4
5
Bekasi
Karawang
Depok
Bogor
Subang
Indramayu
Purwakarta
Cirebon
Sumedang
Kota Sukabumi
Kota Bandung
Bandung
Kuningan
Sukabumi
Cianjur
Garut
Kota Tasikmalaya
Banjar
Tasikmalaya

SOIL TYPE SCORE

× 0.25

LAND SLOPE SCORE

× 0.1875

+

LAND COVER SCORE

× 0.1875

ANNUAL RAINFALL SCORE

× 0.375

TOTAL SCORE	CLASS	COLOR SYMBOL
≤ 2,5	Safe	
> 2,5 – ≤ 3,6	Vulnerable	
> 3,6	Very vurnerable	

Direktorat Vulkanologi dan Mitigasi Bencana / DVMBG (2004)

LANDSLIDE POTENTIAL in WEST JAVA

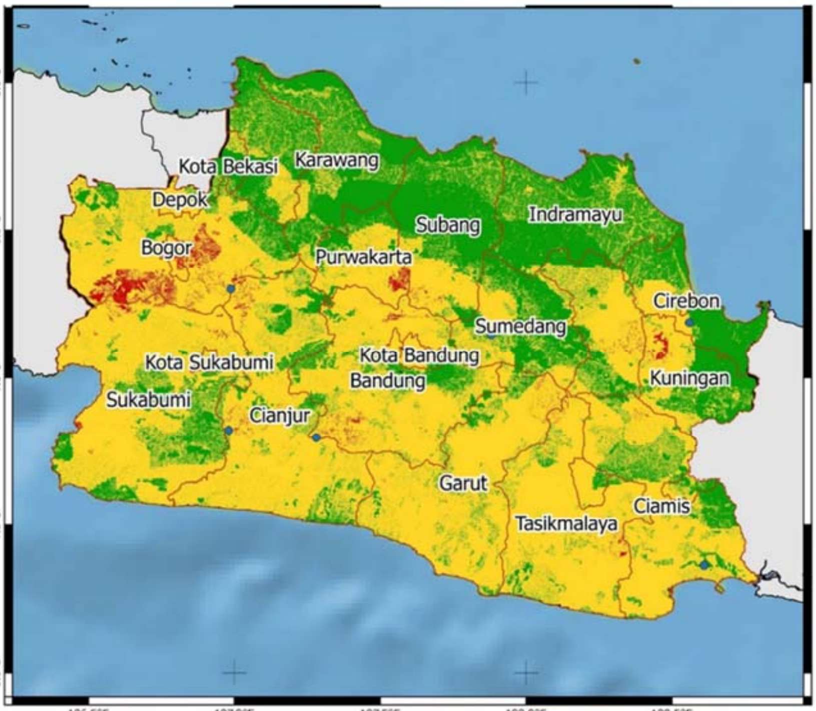

TOTAL SCORE	CLASS	COLOR SYMBOL
≤ 2,5	Safe	
> 2,5 – ≤ 3,6	Vulnerable	
> 3,6	Very vurnerable	

TESTING FOR CAUSATIVE FACTORS

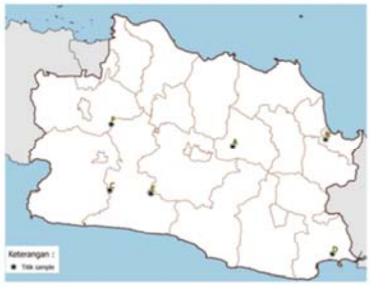

SAMPLE POINT OF LANDSLIDE OCCURRENCE

Sample	Place name	Occurance date
A	Dsn. Ciherang, Sumedang	20-09-2016
B	Gumulung Lebak, Cirebon	22-04-2017
C	Desa Waringinsari, Cianjur	01-10-2017
D	Ds. Kalijati, Pangandaran	04-06-2017
E	Ds. Cipelah, Bandung	30-10-2017
F	Tugu Selatan, Bogor	05-02-2018

Results of physical factor tests on landslides in West Java

Sample	Lat	Lon	Landslide Physical Potential	Annual Rainfall Score	Soil Type Score	Land Slope Score	Land Cover Score
A	-6.86	107.88	2.6875	3	1	4	3
B	-6.81	108.56	3.1875	3	3	4	3
C	-7.18	106.98	3.5625	4	3	4	3
D	-7.64	108.61	2.9375	3	2	4	3
E	-7.2	107.28	3.1875	3	3	4	3
F	-6.7	106.99	3.75	4	3	5	3
			TOTAL	20	15	25	18

RAINFALL INDUCTION OF LANDSLIDES

Rohmaniah dan Muntohar (2017)

	Day -2	Day -1	D-Day
Rainfall tresshold (mm/day)	≥92	≥16	≥5

Monthly alarm index = Average alarm for the month

RAINFALL INDUCTION OF LANDSLIDES

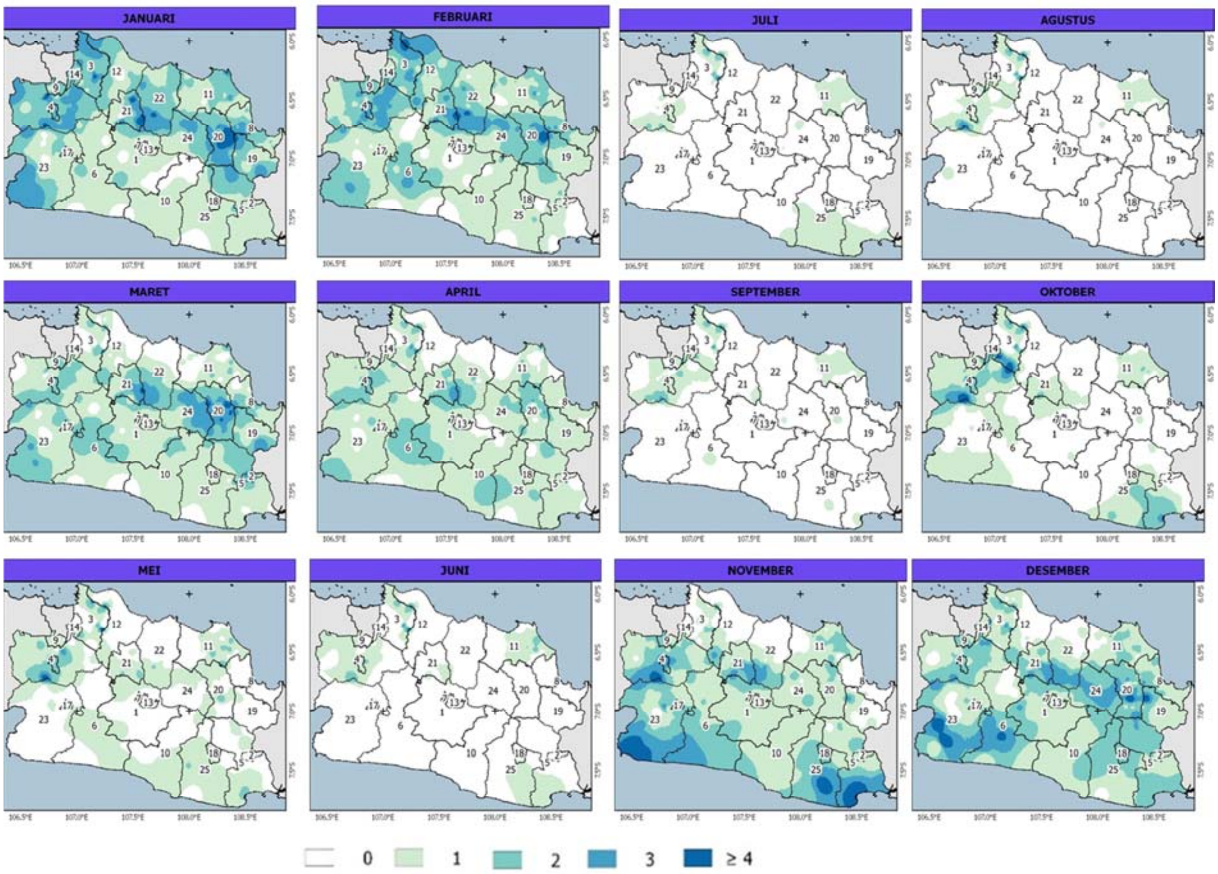

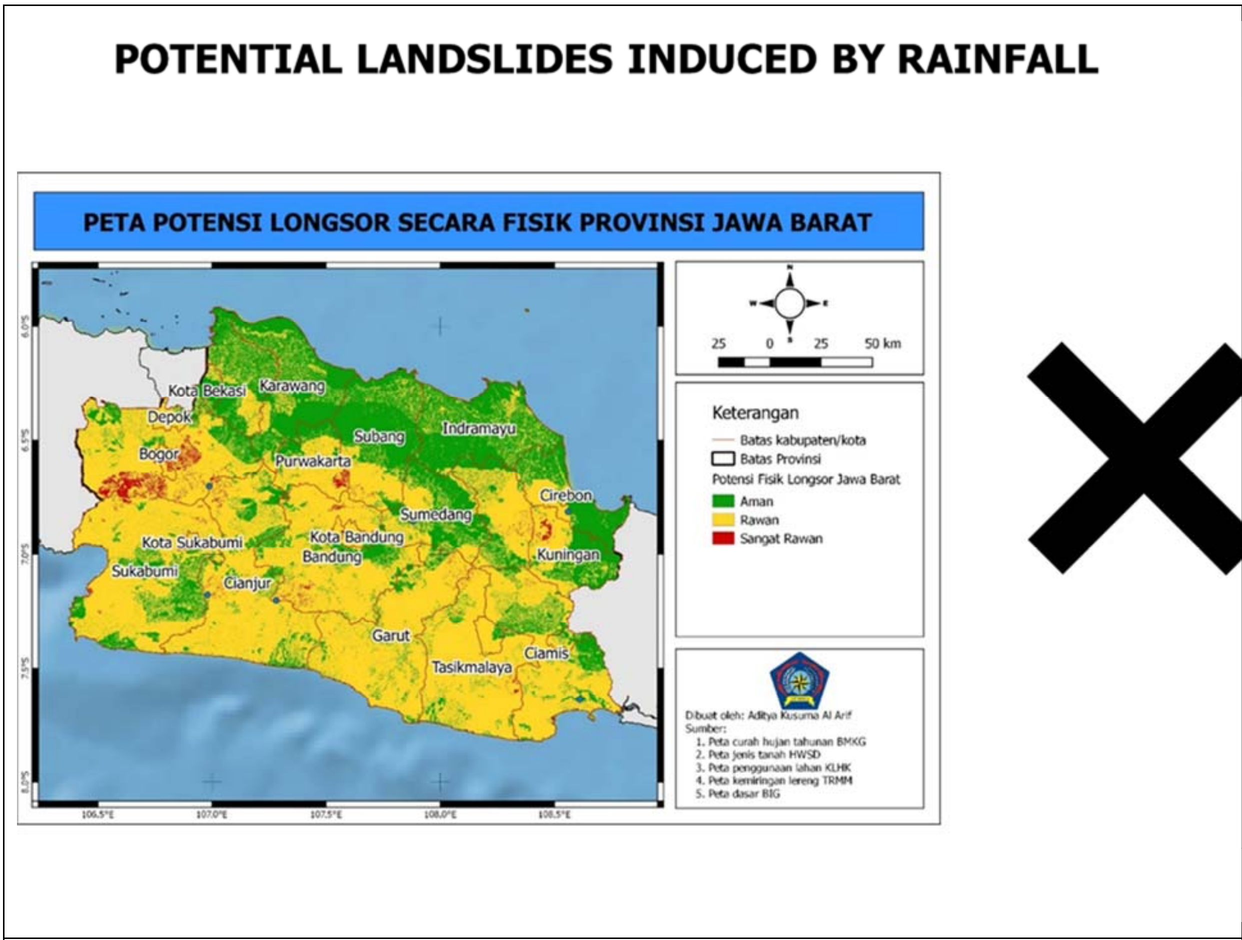
POTENTIAL LANDSLIDES INDUCED BY RAINFALL
PETA POTENSI LONGSOR SECARA FISIK PROVINSI JAWA BARAT
Kota Bekasi
Karawang
Depok
Bogor
Subang
Indramayu
Purwakarta
Cirebon
Sumedang
Kota Bandung
Bandung
Kota Sukabumi
Sukabumi
Cianjur
Kuningan
Garut
Ciamis
Tasikmalaya
25 0 25 50 km
Keterangan
Batas kabupaten/kota
Batas Provinsi
Potensi Fisik Longsor Jawa Barat
Aman
Rawan
Sangat Rawan
Dibuat oleh: Aditya Kusuma Al Arif
Sumber:
1. Peta curah hujan tahunan BMKG
2. Peta jenis tanah HWSD
3. Peta penggunaan lahan KLHK
4. Peta kemiringan lereng TRMM
5. Peta dasar BIG
106.5°E
107.0°E
107.5°E
108.0°E
108.5°E
6.0°S
6.5°S
7.0°S
7.5°S
8.0°S

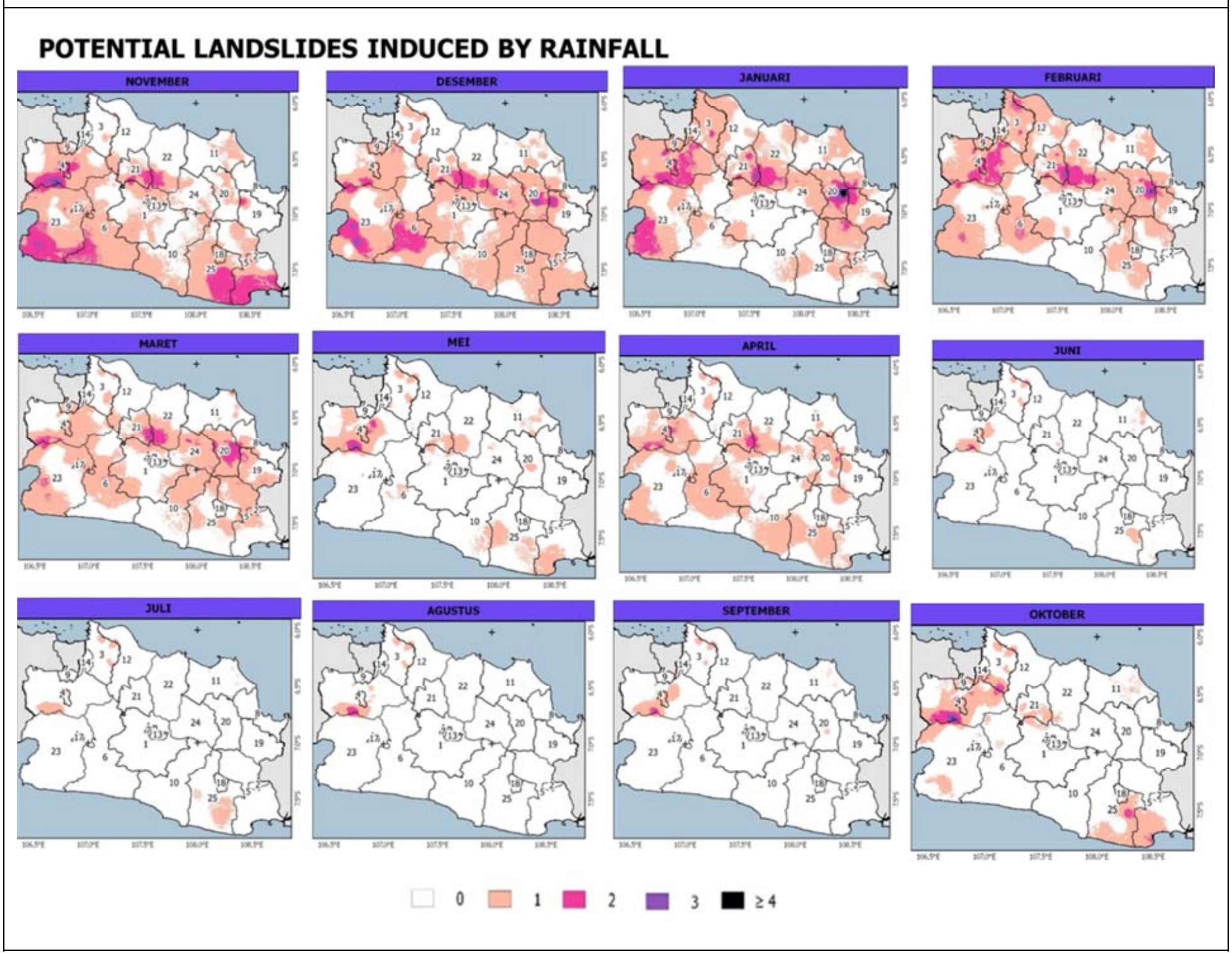
POTENTIAL LANDSLIDES INDUCED BY RAINFALL
NOVEMBER
DESEMBER
JANUARI
FEBRUARI
MARET
MEI
APRIL
JUNI
JULI
AGUSTUS
SEPTEMBER
OKTOBER
0
1
2
3
≥ 4

COMPARISON OF POTENTIAL AND REAL LANDSLIDE EVENTS

DISTRIBUTION OF LANDSLIDE PRONE IN WEST JAVA

$$\text{Correction Factor} = \frac{\text{Real event}}{\text{Potential Index}}$$

$$\text{LANDSLIDE PRONE INDEX} = \text{Correction Factor} \times \text{Potential Index}$$

DISTRIBUTION OF LANDSLIDE PRONE IN WEST JAVA

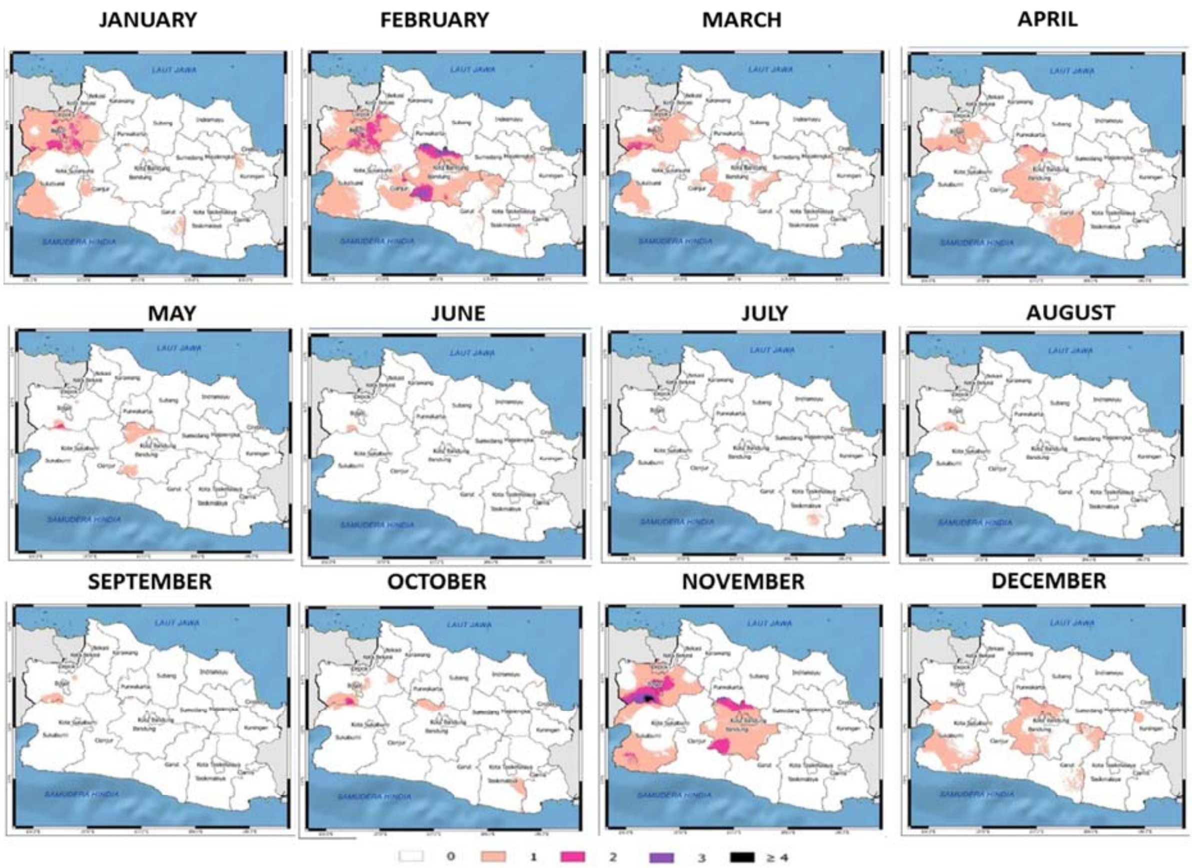

CONCLUSION:

1. Physical distribution of landslide potential areas in West Java Province is dominated by areas with “vulnerable” categories, which are generally located on the slopes of mountains or mountains that have high rainfall.

2. The distribution of areas with potential landslides induced by rainfall in West Java Province following the pattern of monsoonal seasonal.

3. The distribution of landslide-prone zones in West Java Province adjusted to the actual occurrence of landslides, in which some landslide potential models are caused by overestimate rainfall and the West Java region most prone to landslides is the southern part of Bogor Regency and the northern and southern parts of Bandung.

A preliminary large-scale assessment of landslide susceptibility in the territory of the Metropolitan City of Rome (Italy)

Carlo Esposito(1), Gian Marco Marmoni(1), Gabriele Scarascia Mugnozza(1), Alessio Argentieri(2), Giovanni Rotella(2)

1) Sapienza University of Rome, Department of Earth Sciences and CERI Research Centre.
e-mail: carlo.esposito@uniroma1.it
2) Città Metropolitana di Roma Capitale, Department of Land Planning

Abstract

Based on a research agreement with the Metropolitan City of Rome, we performed a preliminary large-scale assessment of landslide susceptibility and related exposure to risk of some relevant assets (i.e., main roads and public buildings) for the whole territory. Due to the extent of the study area (more than 5,000 km2) we partitioned the territory in sub-zones, homogeneous in terms of lithological and geomorphological features. We performed distinct analyses with the logistic regression technique, after having grouped the landslides in 4 macro-classes: slow moving landslides, rapid flows, shallow landslides and rockfall/topples. Due to the possible incompleteness of the official inventories on which the analyses relied, to train the susceptibility functions we performed a hot-spot analysis of landslide points: we selected stable points only in the cold spots. Furthermore we established a criterion to qualitatively assign a reliability level of the results in different areas. For the assessment of exposure to risk two main steps were crucial: the selection of a probability threshold to identify areas prone to first-time failures and the empirical simulation of run-out for rapid flows and rockfall/topples. The so obtained detachment and spreading areas were overlaid with exposed elements for the preliminary assessment of exposure to risk.

FUNCTIONS OF THE METROPOLITAN CITIES

From the *Provincia di Roma* (1870-2014)

to the *Città Metropolitana di Roma Capitale* (since 2015)

MAIN FUNCTIONS:

- adoption and annual updating of a **Triennial Strategic Plan** of the metropolitan area;
- **general territorial planning**;
- **mobility** and **road network**;
- promotion and coordination of the **computerization and digitization systems**;
- protection and enhancement of the **environment**;
- **data** collection and processing, **technical-administrative assistance to local authorities**;
- **school building**

Città metropolitana di Roma Capitale — SAPIENZA UNIVERSITÀ DI ROMA

Landslide susceptibility in urban and extraurban areas

- Threatening posed by the interaction between landslides and urban areas and infrastructural networks are one of the most important topics in land management;
- Landslide risk assessment represents an institutional duty of Città Metropolitana Roma Capitale (CMRC) for Civil Protection activities;
- Since 2005 and systematically since 2016, studies on landslide susceptibility have been carried out (in collaboration with DST-Sapienza), covering about 1/5 of the Rome metropolitan area (ab. 1.000 km^2)

Città metropolitana di Roma Capitale — SAPIENZA UNIVERSITÀ DI ROMA

The level of accuracy based on the duty and competence of Metropolitan City

Scale description	Indicative range of scales	Zoning methods			Zoning levels			Types of zoning		Purpose
		Basic	Intermediate	Sophisticated	Preliminary	Intermediate	Advanced	Susceptibility	Hazard	
Small	<1:100,000	*			*			*		Regional zoning - Information
Medium	1:100,000 to 1:25,000	*	(*)		*	(*)		*	(*)	Regional zoning - Information - Advisory
Large	1:25,000 to 1:5000	*	*	*	*	*	*	*	*	Local zoning - Information - Advisory - Statutory
Detailed	>1:5000	[*]	(*)	*	[*]	(*)	*	(*)	*	Site specific zoning - Information - Advisory - Statutory - Design

Cascini, 2008

Città metropolitana di Roma Capitale — SAPIENZA UNIVERSITÀ DI ROMA

The FRANARISK Project: 2007-2016

ENEA ROMA TRE UNIVERSITÀ DEGLI STUDI

(index-based Heuristic method)

$$S_f = (I_{geol} \times I_{pend}) \times \frac{\sum_n (i_n \times P_n)}{\sum_n P_n}$$

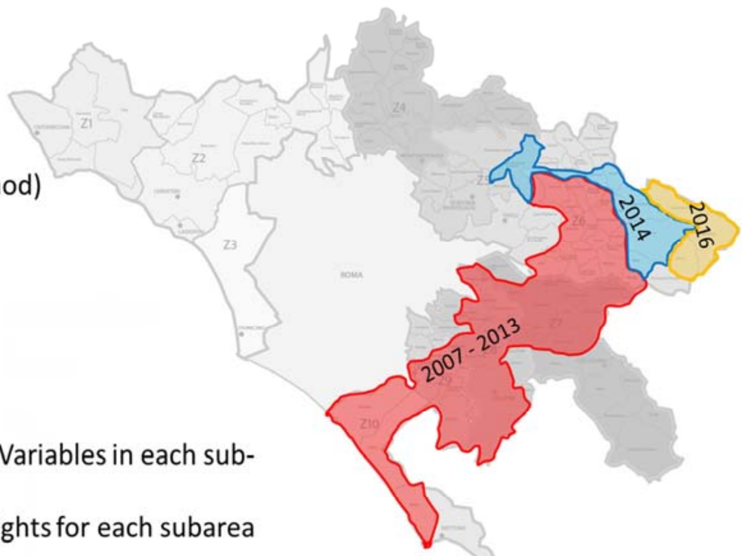

Critical Issues:

- Different Classification of Variables in each sub-area;
- Different Indexes and Weights for each subarea (municipalities);
- Spatial discontinuities and inhomogeneities of results

Città metropolitana di Roma Capitale — SAPIENZA UNIVERSITÀ DI ROMA

The FRANARISK Project: 2018-2019

- ***2018*** – Rome Metropolitan Area (CMCR)

Tasks / objectives:

- Final reclassification and **homogenization** of input predisposing variables;
- **Frequency Ratio** analyses on the **whole Rome metropolitan area (ab. 5300 km^2)**
- **Logistic Regression** on the identified physiographic domains;
- Preliminary assessment of the interaction of detachment and/or accumulation areas with selected exposed elements (roads and public building managed by CMRC)

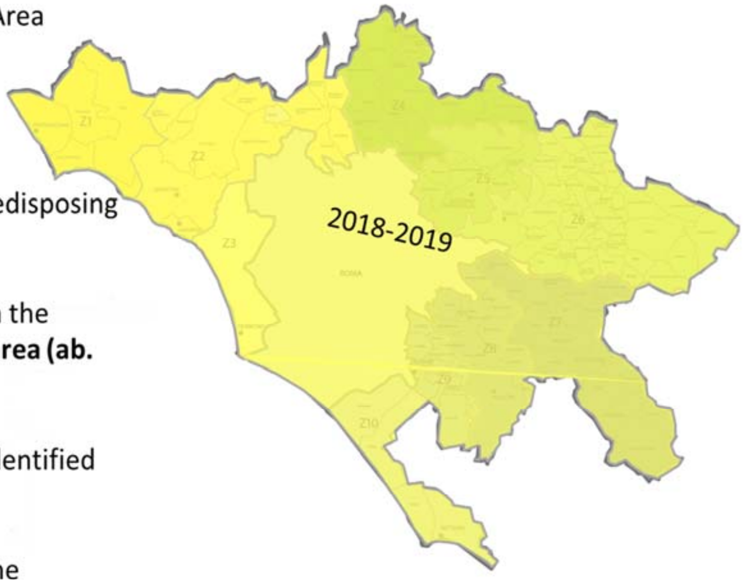

Città metropolitana di Roma Capitale

SAPIENZA UNIVERSITÀ DI ROMA

The FRANARISK Project: 2018-2019

- ***2018*** – Rome Metropolitan Area (CMCR)

Preparatory factors:

- Lithotecnical Units
- Morphometric factors (Slope, Aspect, Curvature);
- Land Cover;
- Elevation;
- Distance from streams;
- Distance from faults;
- Distance from roads;
- Wildfires;

Landslides types:

- Rockfalls/topples;
- Roto-translational slides and earth flows;
- Shallow landslides and slow creep;
- Debris flows

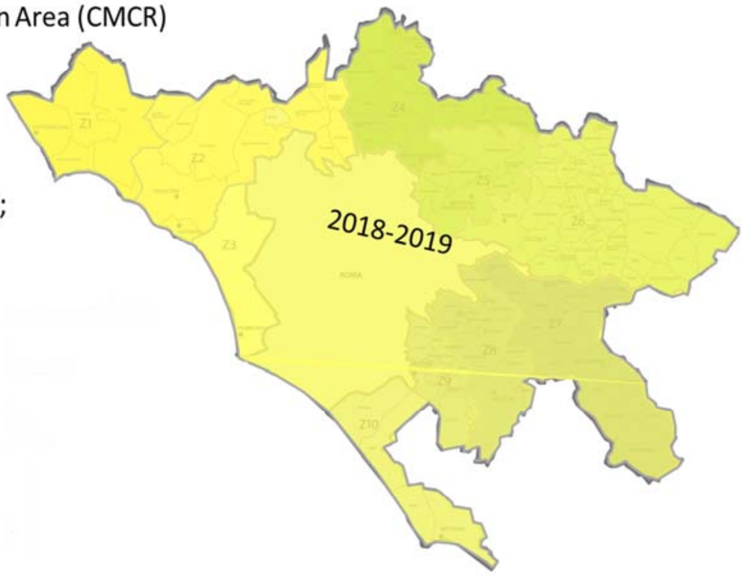

Città metropolitana di Roma Capitale

SAPIENZA UNIVERSITÀ DI ROMA

The FRANARISK Project: Landslides Dataset

Datasets:

- IFFI
- PAI
- CERI Database (*Alessi et al., 2014; Del Monte, 2016*)
- CMRC Archives

TOTAL of 2903 landslides

Landslides types frequency:

- Rockfalls/topples (n. 371);
- Roto-translational slides and earth flows (n. 254);
- Shallow landslides and slow creep (n. 287);
- Debris flows (n. 254)
- n.a. (***n. 1377***)

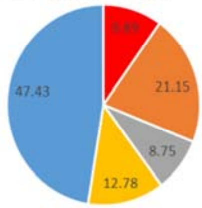

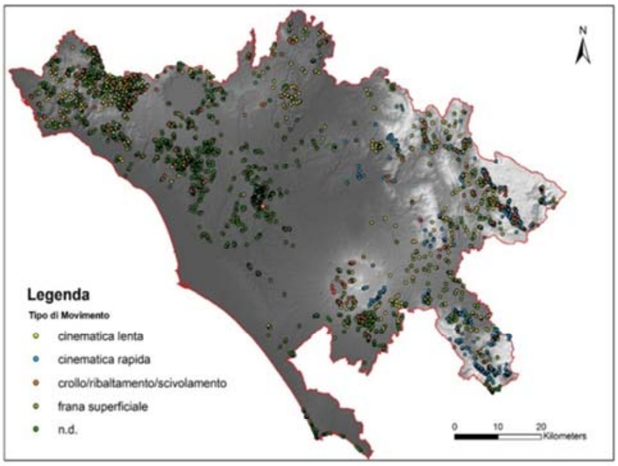

Main Issues:

- IFFI catalogue completeness/update;
- PAI applicability (lack of landslide typology).

Città metropolitana di Roma Capitale — SAPIENZA UNIVERSITÀ DI ROMA

Availability of preparatory factors

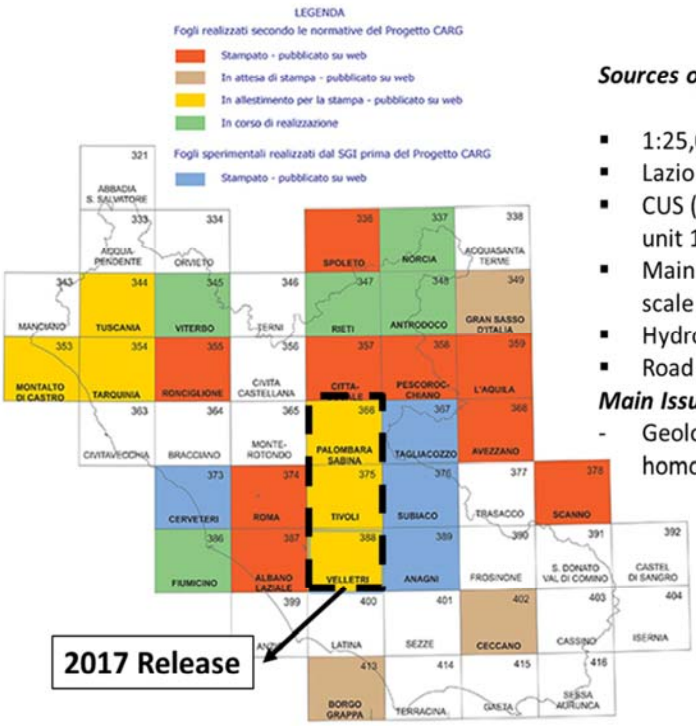

Sources of predisposing variables:

- 1:25,000 Geological Map (*Regione Lazio*)
- Lazio DTM (5m resolution);
- CUS (*Regione Lazio* land cover – mapping unit 100 x 100 m)
- Main tectonic elements (ISPRA –nominal scale 1:100,000)
- Hydrographic network (ISPRA)
- Road network (CMRC)

Main Issue:

- Geological map completeness and scale homogeneity;

REGIONE LAZIO OPEN DATA

Città metropolitana di Roma Capitale — SAPIENZA UNIVERSITÀ DI ROMA

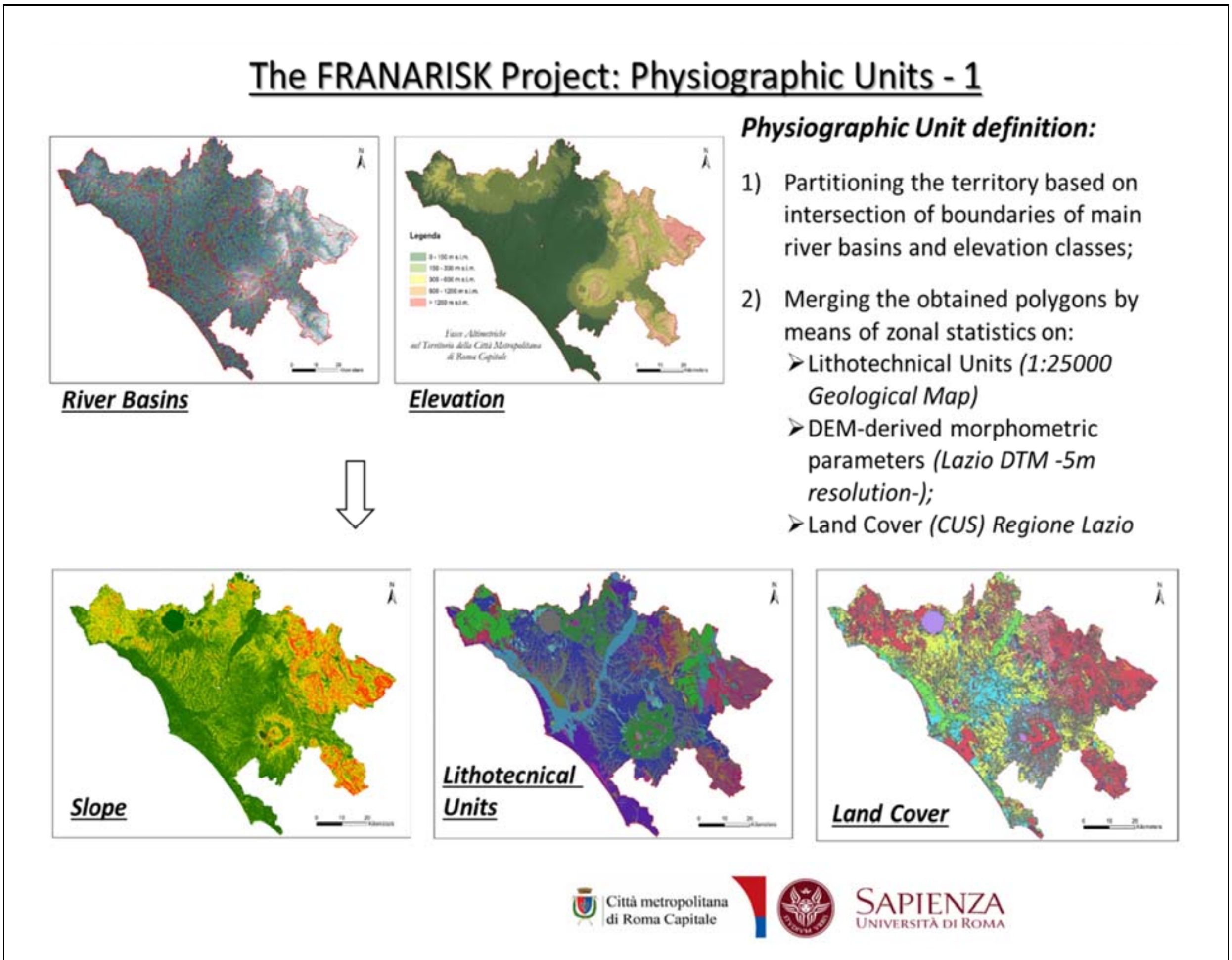

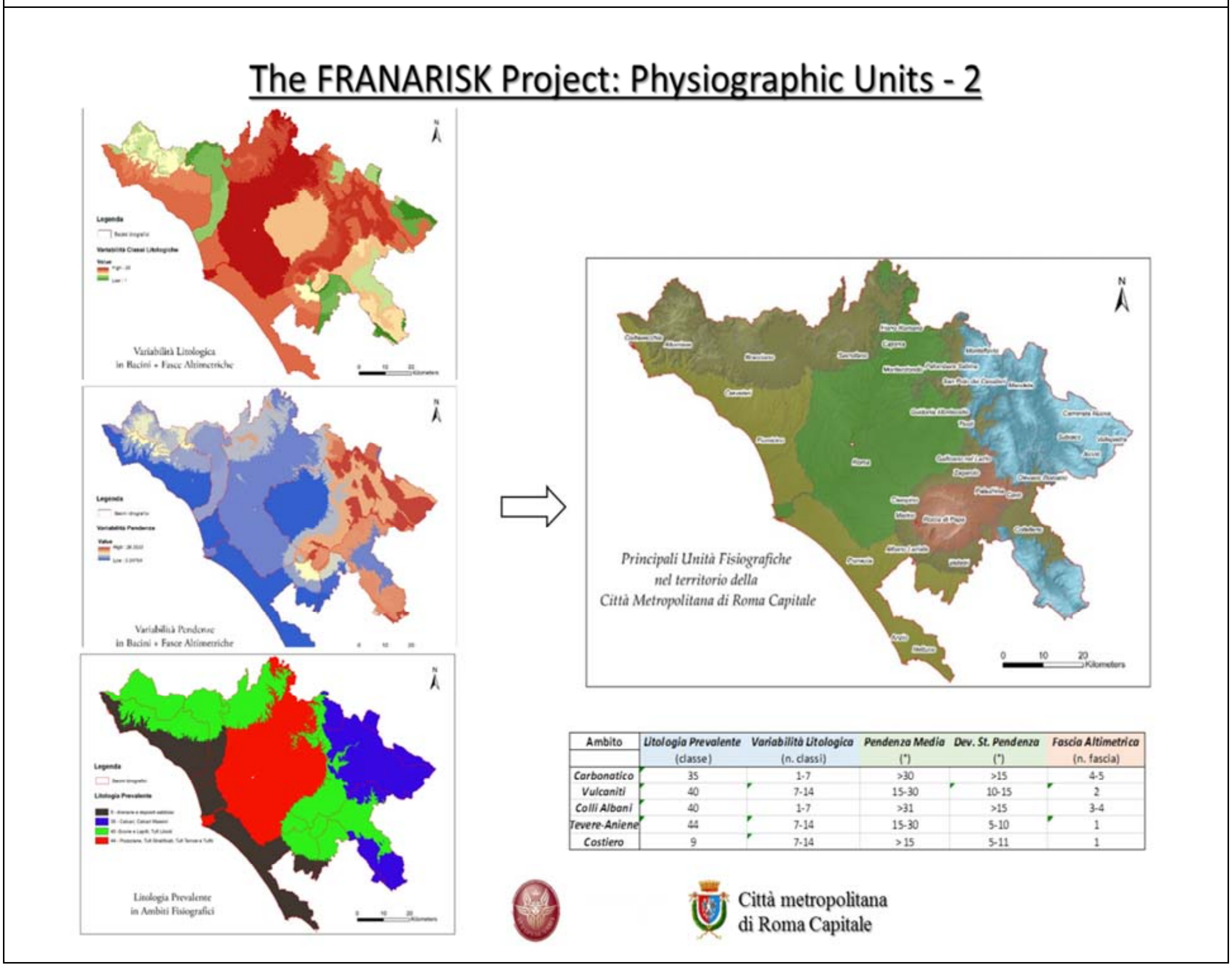

Ambito	Litologia Prevalente (classe)	Variabilità Litologica (n. classi)	Pendenza Media (°)	Dev. St. Pendenza (°)	Fascia Altimetrica (n. fascia)
Carbonatico	35	1-7	>30	>15	4-5
Vulcaniti	40	7-14	15-30	10-15	2
Colli Albani	40	1-7	>31	>15	3-4
Tevere-Aniene	44	7-14	15-30	5-10	1
Costiero	9	7-14	> 15	5-11	1

The FRANARISK Project: a preliminary look at the Landslide Susceptibility

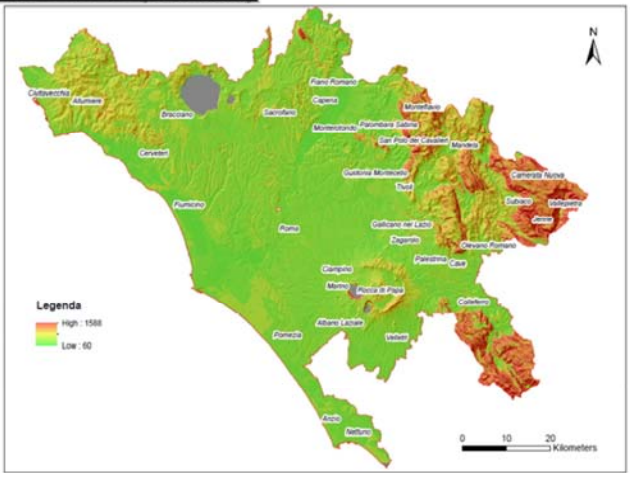

$$FR_i = \frac{\frac{n.landslides_i}{n.landslides\ tot_i}}{\frac{area_i}{area\ tot_i}}$$

$$\Downarrow$$

$$LSI = \sum_{i=1}^{n} FR_i$$

1) Rock fall/topples

2) Shallow landslides and slow creep

3) Roto-translational slides and earth flows

4) Debris flow

Susceptibility

Low

Medium-Low

Medium-High

High

Città metropolitana di Roma Capitale

SAPIENZA UNIVERSITÀ DI ROMA

The FRANARISK Project: a preliminary look at the Landslide Susceptibility

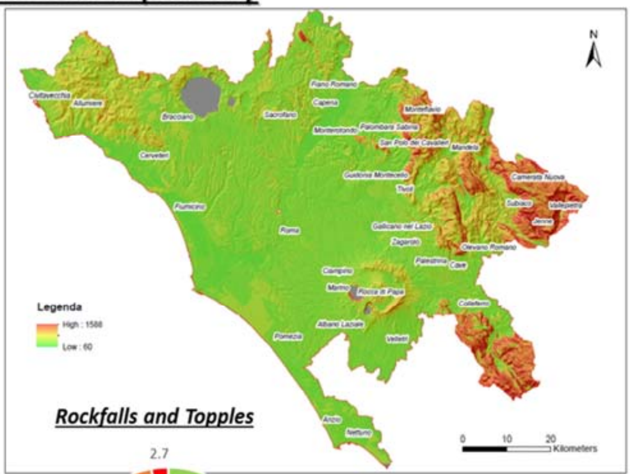

$$FR_i = \frac{\frac{n.landslides_i}{n.landslides\ tot_i}}{\frac{area_i}{area\ tot_i}}$$

$$\Downarrow$$

$$LSI = \sum_{i=1}^{n} FR_i$$

1) Rock fall/topples

2) Shallow landslides and slow creep

3) Roto-translational slides and earth flows

4) Debris flow

Rockfalls and Topples

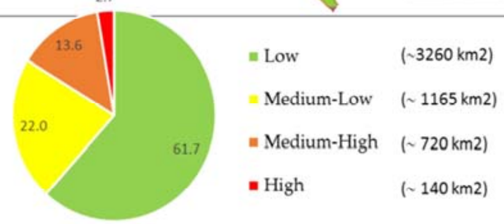

Città metropolitana di Roma Capitale

SAPIENZA UNIVERSITÀ DI ROMA

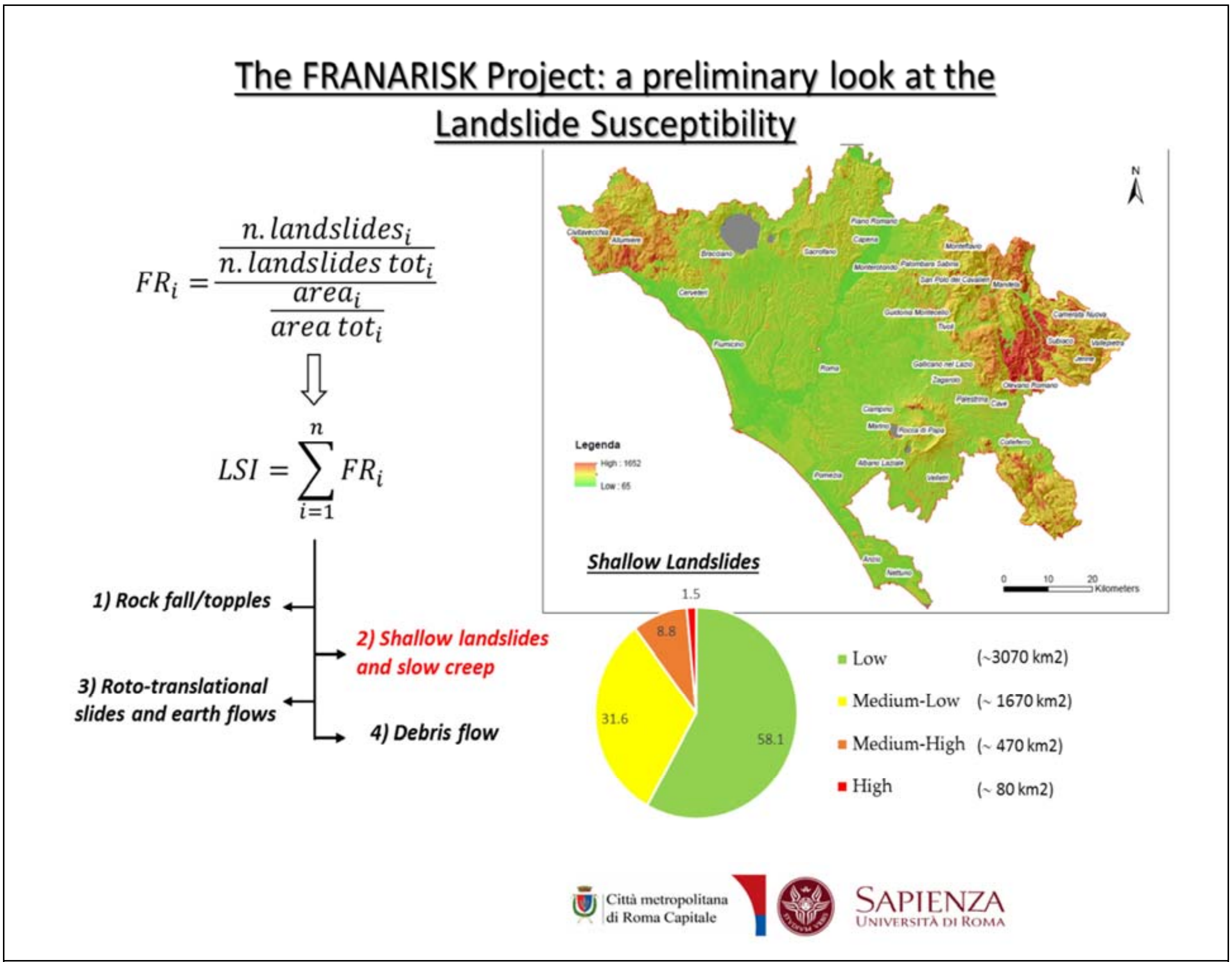
The FRANARISK Project: a preliminary look at the Landslide Susceptibility
$FR_i = \frac{\frac{n.landslides_i}{n.landslides\ tot_i}}{\frac{area_i}{area\ tot_i}}$
$LSI = \sum_{i=1}^{n} FR_i$
1) Rock fall/topples
2) Shallow landslides and slow creep
3) Roto-translational slides and earth flows
4) Debris flow
Legenda
Shallow Landslides
0 10 20 Kilometers
1.5
8.8
31.6
58.1
Low (~3070 km2)
Medium-Low (~ 1670 km2)
Medium-High (~ 470 km2)
High (~ 80 km2)
Città metropolitana di Roma Capitale
SAPIENZA Università di Roma

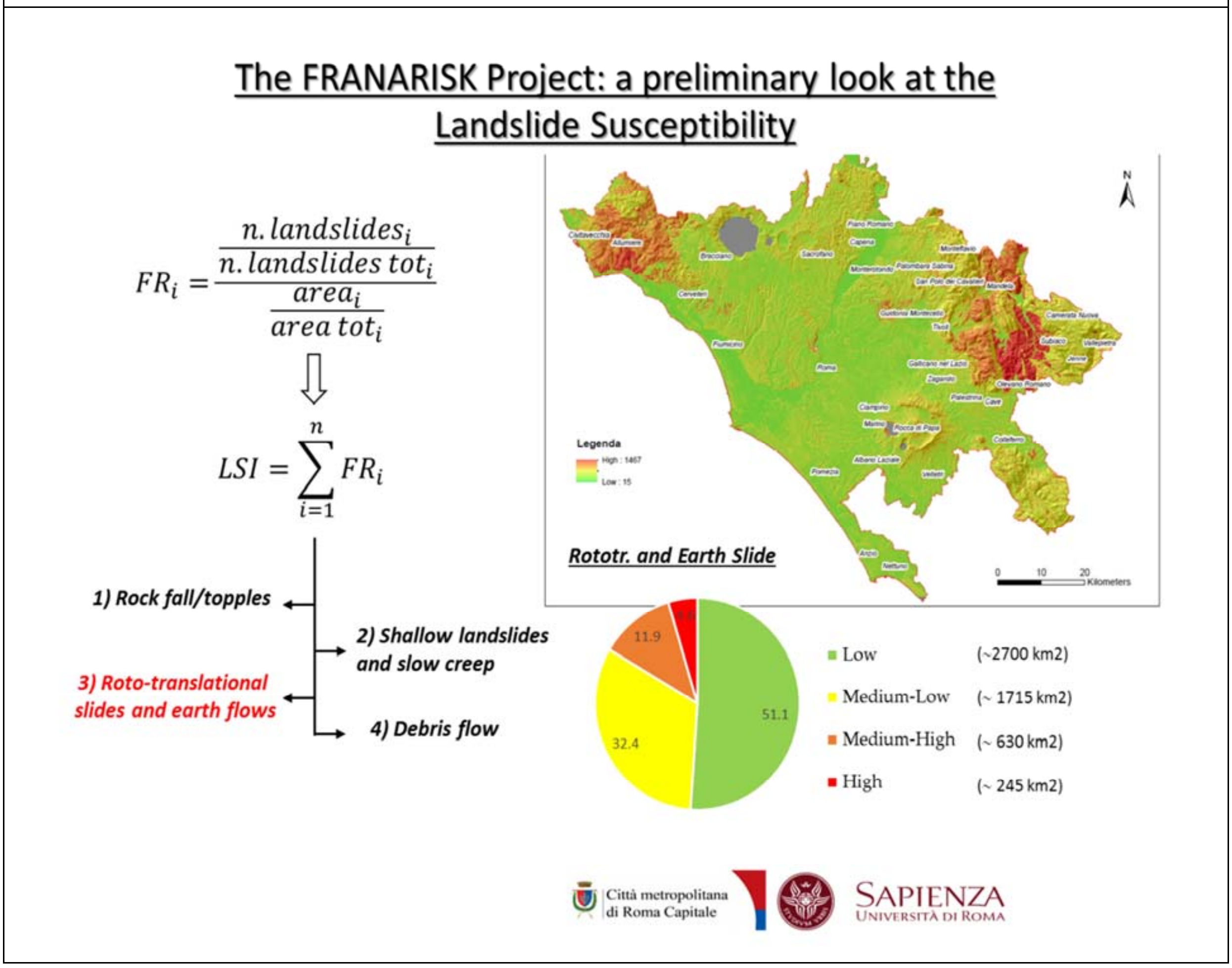
The FRANARISK Project: a preliminary look at the Landslide Susceptibility
$FR_i = \frac{\frac{n.landslides_i}{n.landslides\ tot_i}}{\frac{area_i}{area\ tot_i}}$
$LSI = \sum_{i=1}^{n} FR_i$
1) Rock fall/topples
2) Shallow landslides and slow creep
3) Roto-translational slides and earth flows
4) Debris flow
Legenda
Rototr. and Earth Slide
0 10 20 Kilometers
11.9
32.4
51.1
Low (~2700 km2)
Medium-Low (~ 1715 km2)
Medium-High (~ 630 km2)
High (~ 245 km2)
Città metropolitana di Roma Capitale
SAPIENZA Università di Roma

The FRANARISK Project: a preliminary look at the Landslide Susceptibility

$$FR_i = \frac{\frac{n.landslides_i}{n.landslides\ tot_i}}{\frac{area_i}{area\ tot_i}}$$

$$\Downarrow$$

$$LSI = \sum_{i=1}^{n} FR_i$$

1) Rock fall/topples

2) Shallow landslides and slow creep

3) Roto-translational slides and earth flows

4) Debris flow

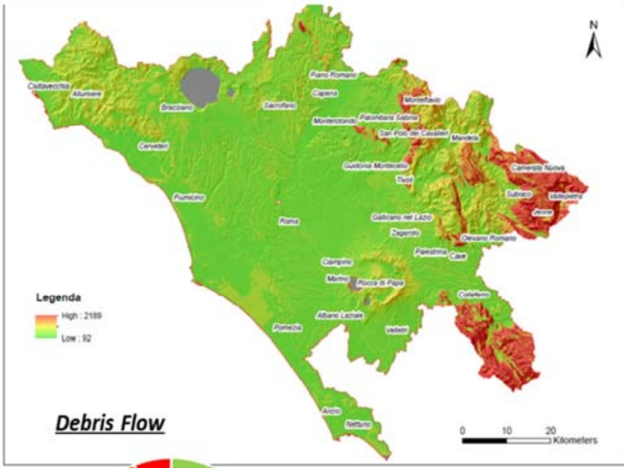

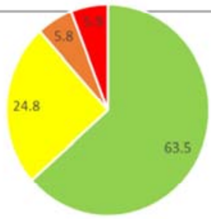

Città metropolitana di Roma Capitale

SAPIENZA UNIVERSITÀ DI ROMA

The FRANARISK Project: Landslide Susceptibility by means of Logistic Regression – Sampling strategies

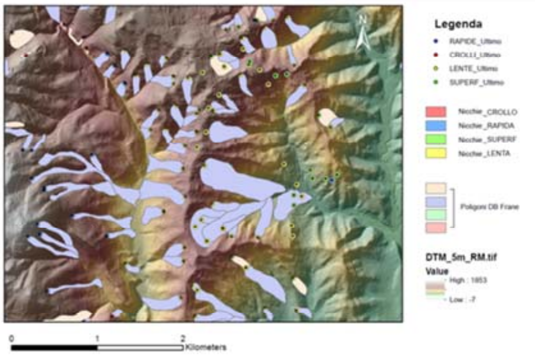

1) Definition of detachment areas

2) Sampling balance:
Stable: 60 – 70 %
Unstable 40 – 30%

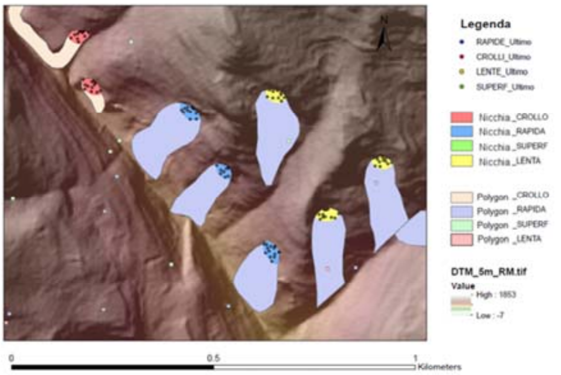

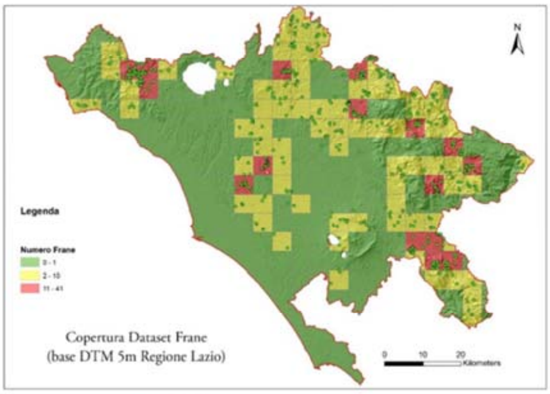

The FRANARISK Project: Landslide Susceptibility by means of Logistic Regression – Validation strategies

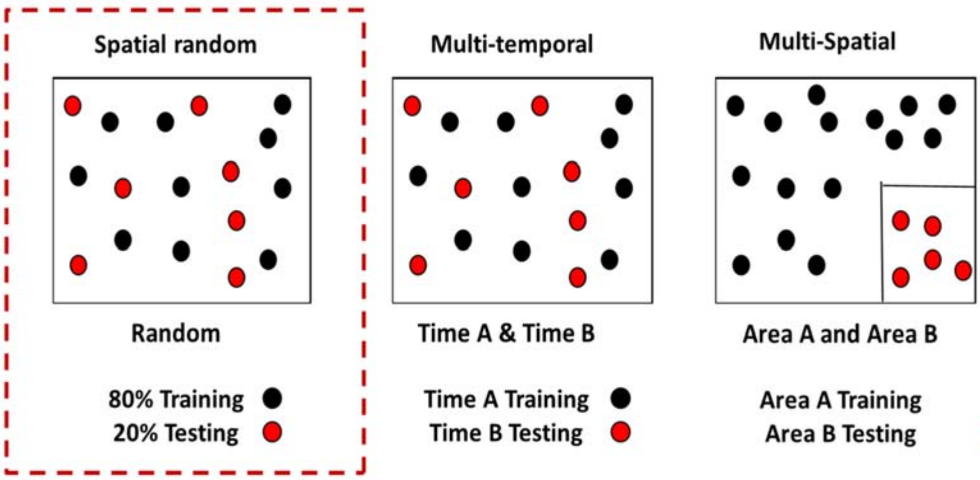

Città metropolitana di Roma Capitale

SAPIENZA UNIVERSITÀ DI ROMA

The FRANARISK Project: Landslide Susceptibility by means of Logistic Regression – Results

Tabella di classificazione[a]

			Previsto FRANA ,00	1,00	Percentuale di correttezza
Osservato					
Fase 1	FRANA	,00	3615	462	88,7
		1,00	692	2109	75,3
	Percentuale globale				83,2

a. Il valore di divisione è ,500

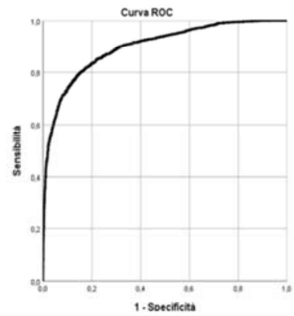

Variabili nell'equazione

		B	S.E.	Wald	gl	Sign.	Exp(B)
Fase 1[a]	lito_FR_cr	,004	,000	229,876	1	,000	1,004
	cus_FR_cro	-,001	,001	2,206	1	,137	,999
	SL_DTM_5m_	,139	,005	797,875	1	,000	1,149
	CURtot_5m_	,280	,175	2,544	1	,111	1,323
	CURplan_5m	-,305	,175	3,020	1	,082	,737
	CURprof_5m	,270	,175	2,370	1	,124	1,310
	DIST_road_	-,002	,000	399,283	1	,000	,998
	DIST_river	-,002	,000	43,929	1	,000	,998
	TPI300_RM	,030	,001	437,709	1	,000	1,030
	StreamPowl	-,140	,016	76,106	1	,000	,869
	TWI_5m_rm	,312	,038	66,811	1	,000	1,366
	Costante	-5,920	,300	388,274	1	,000	,003

a. Variabili inserite nella fase 1: lito_FR_cr, cus_FR_cro, SL_DTM_5m_ , CURtot_5m_ , CURplan_5m , CURprof_5m , DIST_road_ , DIST_river , TPI300_RM, StreamPowl , TWI_5m_rm .

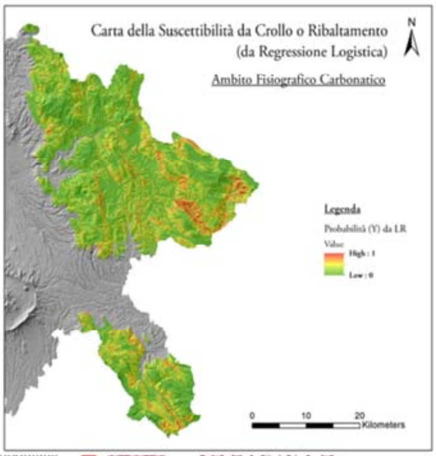

Città metropolitana di Roma Capitale

SAPIENZA UNIVERSITÀ DI ROMA

The FRANARISK Project: Landslide Susceptibility by means of Logistic Regression Results

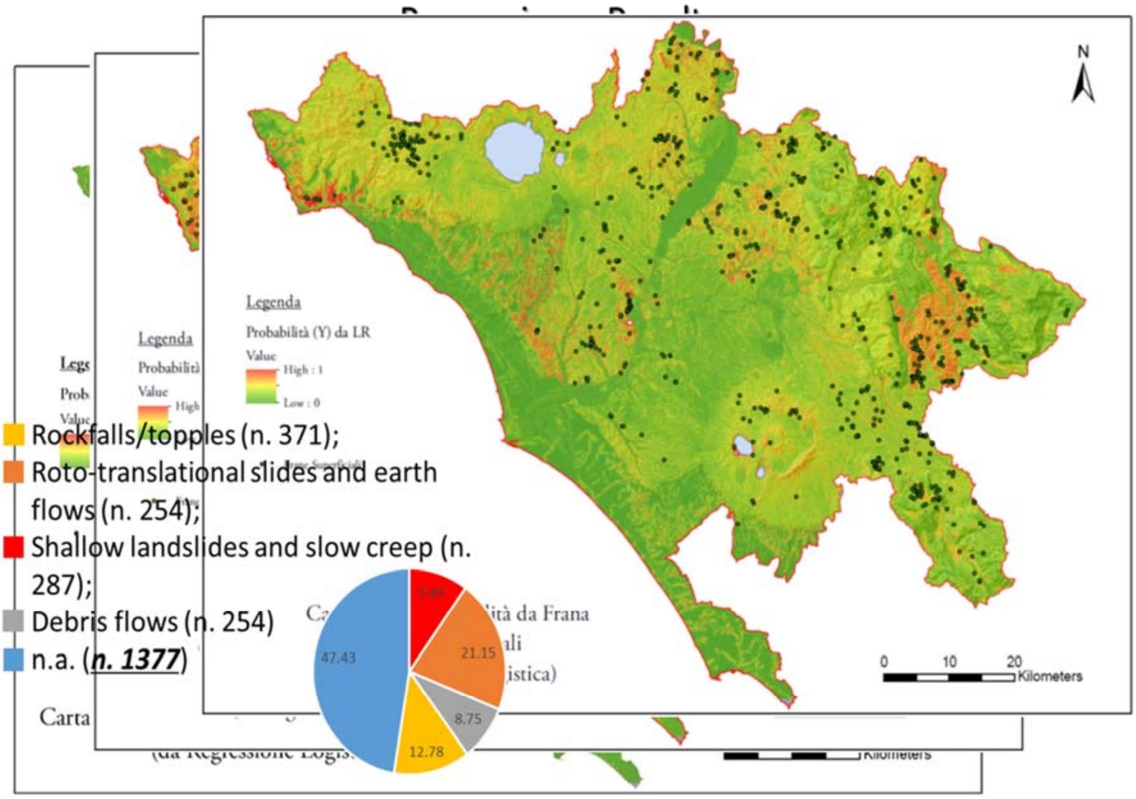

Città metropolitana di Roma Capitale — SAPIENZA Università di Roma

Evaluation of exposure to risk

Slow-moving landslides: overlay of unstable areas (already existing and first-time failures resulting from susceptibility) + buffer and exposed elements.

Fast-moving landslides: overlay of existing invasion areas (from official databases) and simulated run-out areas fed by first-time failures resutling from susceptibility **(P>95%)**

Flow-R
(Flow path assessment of gravitational hazards at a Regional scale)

UNIL | Université de Lausanne

Horton et al., 2013

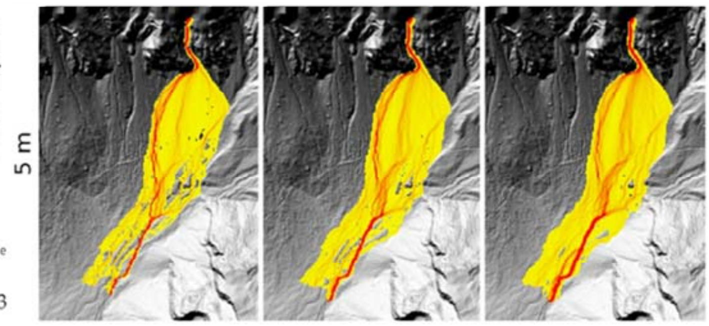

Città metropolitana di Roma Capitale — SAPIENZA Università di Roma

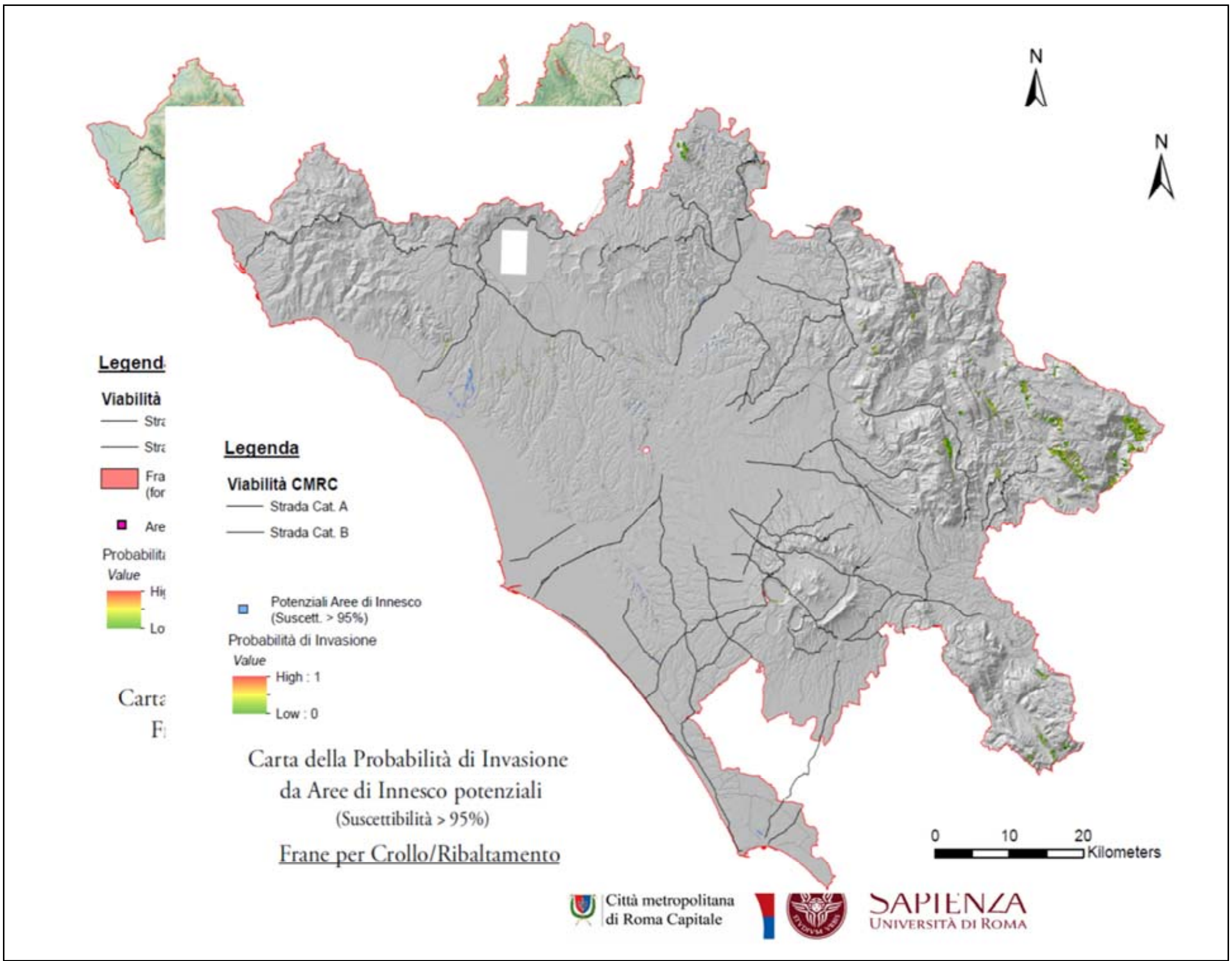

Conclusions

- The Franarisk project provided first insights in the "fragility" of the territory, highlighting significant levels of landslide susceptibility
- At the same time, it has been possible to point out the main critical issues of the available "environmental" datasets: further effort should be done to integrate such information, especially the landslide database
- Anyway, the project represents the first systematic attempt to build a uniform DB of environmental information
- The results have to be considered as a first product that must be updated and integrated to become a more efficient and reliable screening tool
- Beyond these limitations, due to the level of seismicity affecting large part of the study area, the project results can be used for preliminary screening of areas susceptible to co-seismic slope instabilities, as already established in a joint technical committee (Rome municipality, Metropolitan City of Rome, Region)

Città metropolitana di Roma Capitale

SAPIENZA Università di Roma

Advanced Technologies for LandSlides (ATLaS)

Nicola Casagli, Filippo Catani, Riccardo Fanti, Giovanni Gigli, Sandro Moretti, Veronica Tofani, Paolo Canuti

UNESCO Chair on Prevention and Sustainable Management of Geo-hydrological Hazards
Department of Earth Sciences - University of Florence, Italy

Abstract

Since 2008 the Department of Earth Sciences of the University of Florence (DST-UNIFI) has been entitled as a World Centre of Excellence (WCoE) on Landslide Risk Reduction by the Global Promotion Committee of International Programme on Landslides of UN-ISDR with a project entitled "Advanced technologies for landslides" (ATLAS).

The objective of the ATLAS project is to develop new methodologies and advanced technologies for landslide risk reduction. DST-UNIFI carries out research and development (R&D) for the prevention and management of landslides, in order to support policies and actions of risk reduction. In particular, the project focuses on the three main activities such as: 1) innovative technologies (Ground-based SAR interferometry, UAV, Laser Scanner) for landslide monitoring and early warning; 2) EO (Earth Observation) data and technology to detect, map, monitor and forecast ground deformations and 3) regional landslide forecasting models.

Concerning the first activity the DST-UNIFI performs monitoring activities of unstable slopes in order to estimate the deformational evolution of the landslide events (in space and time) and to implement the most suitable operational early warning systems (EWS) according to different critical situations. The activities of point 2 focus on the development of the satellite surveillance system exploiting the satellite data for the identification, mapping, monitoring and analysis of risk scenarios associated with landslides from local to regional scale. The last activity focus on the optimization of the regional early warning system for landslide risk by means of meteorological nowcasting and real-time forecasting of slope movements that are characterized by rapid and very fast kinematic

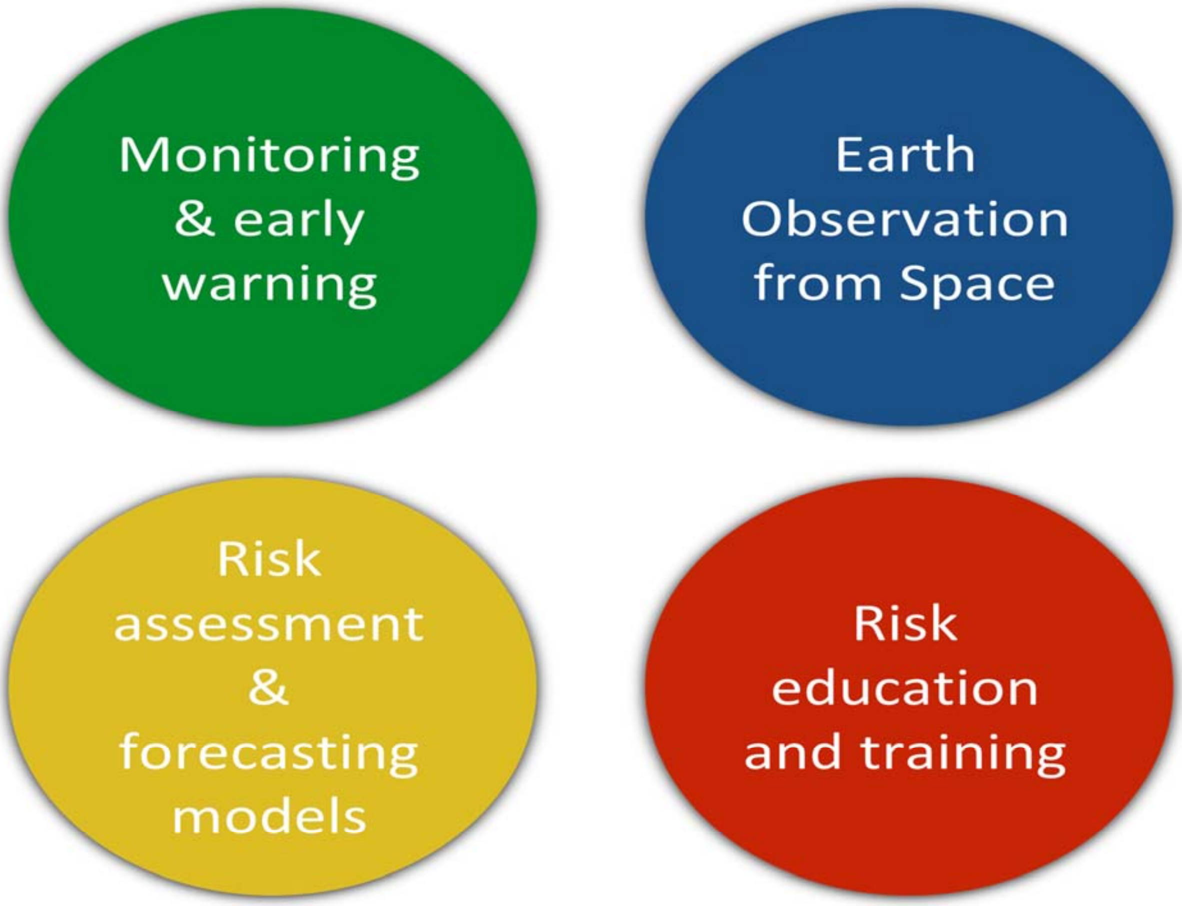
Monitoring & early warning
Earth Observation from Space
Risk assessment & forecasting models
Risk education and training


Monitoring & early warning


First application of GB-InSAR for landslide monitoring(2000)
LiSAmobile™ 5th generation
(Linear Synthetic Aperture Radar)


Multi sensor drone (SATURN)
Multi and Hyper Spectral
Laser scanner
Ground penetrating radar
PATENTED

Monitoring sites

40+ monitoring sites

6 active now

Earth Observation from Space


Radar Satellites
esa
sentinel-1
agenzia spaziale italiana
COSMO SkyMed
KEEPING AN EYE
ON THE WORLD

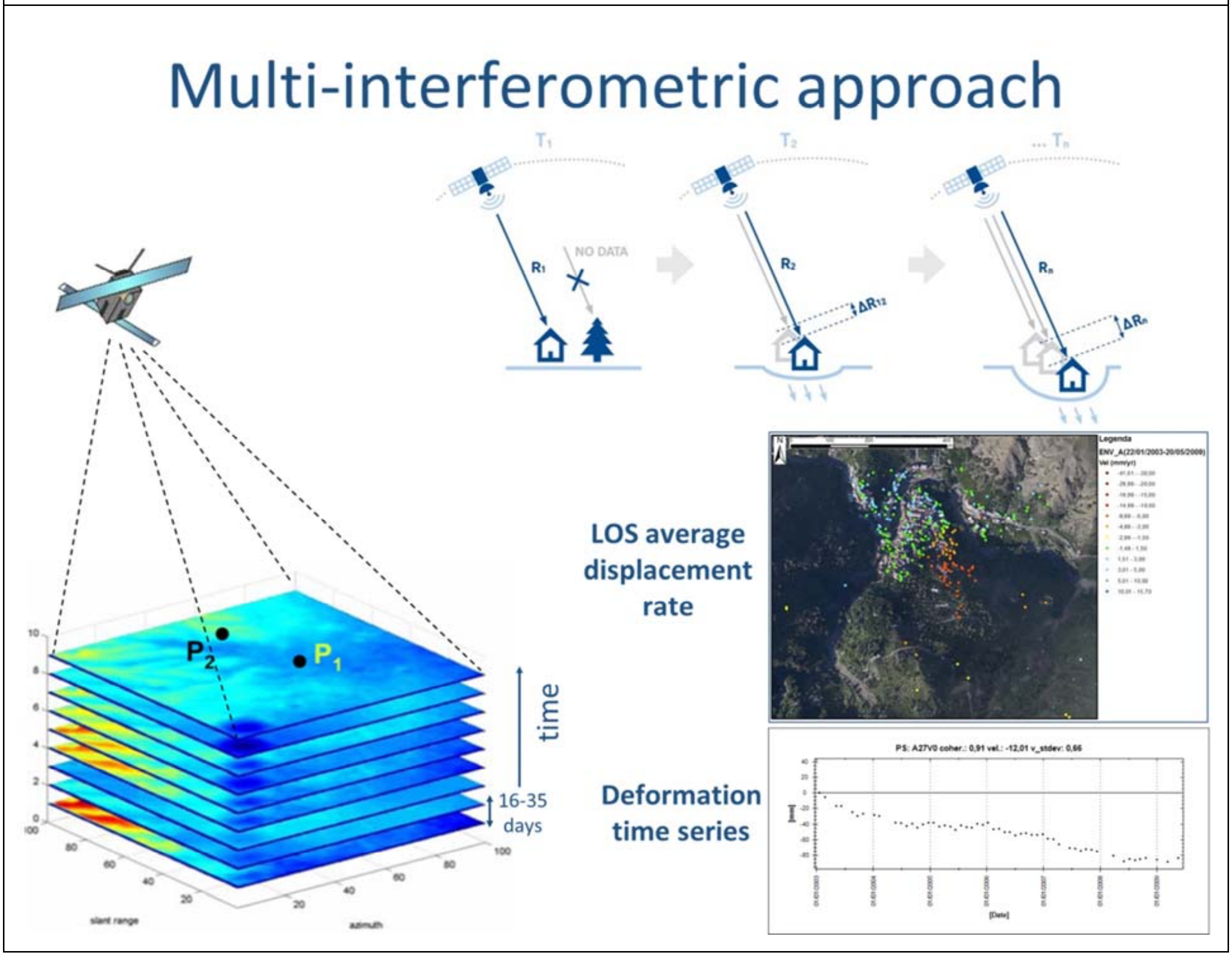
Multi-interferometric approach
T1
T2
... Tn
R1
NO DATA
R2
ΔR12
Rn
ΔRn
LOS average displacement rate
Deformation time series
P2
P1
time
16-35 days
slant range
azimuth
Legenda
PS: A27V0 coher.: 0,91 vel.: -12,01 v_stdev: 0,66
[mm]
[Date]

PS
National
Coverage

22 million of
permanent
scatterers

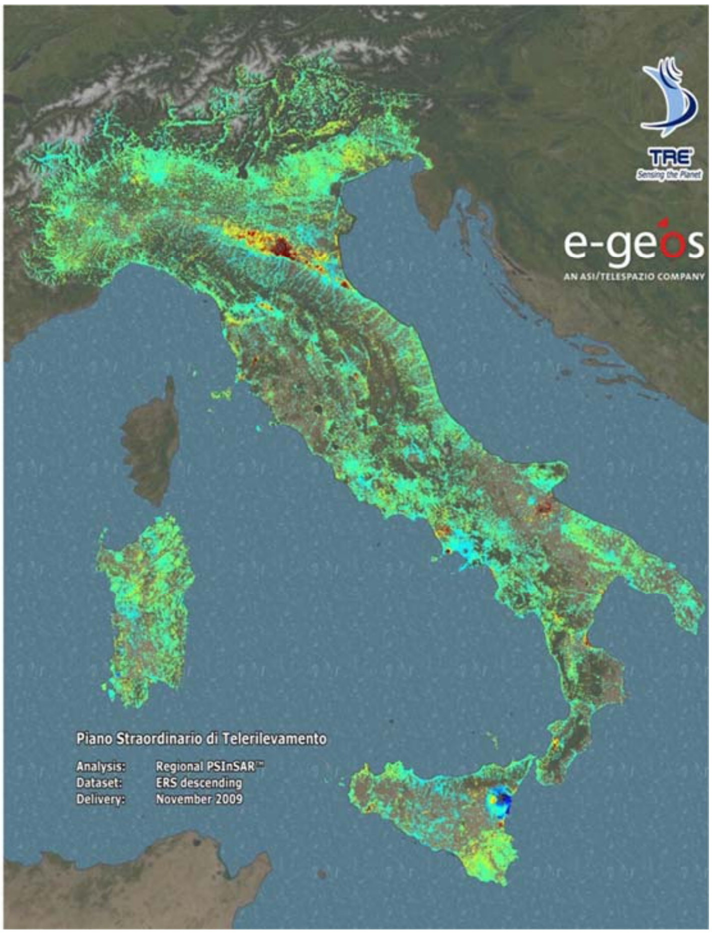

Risk assessment &
forecasting models

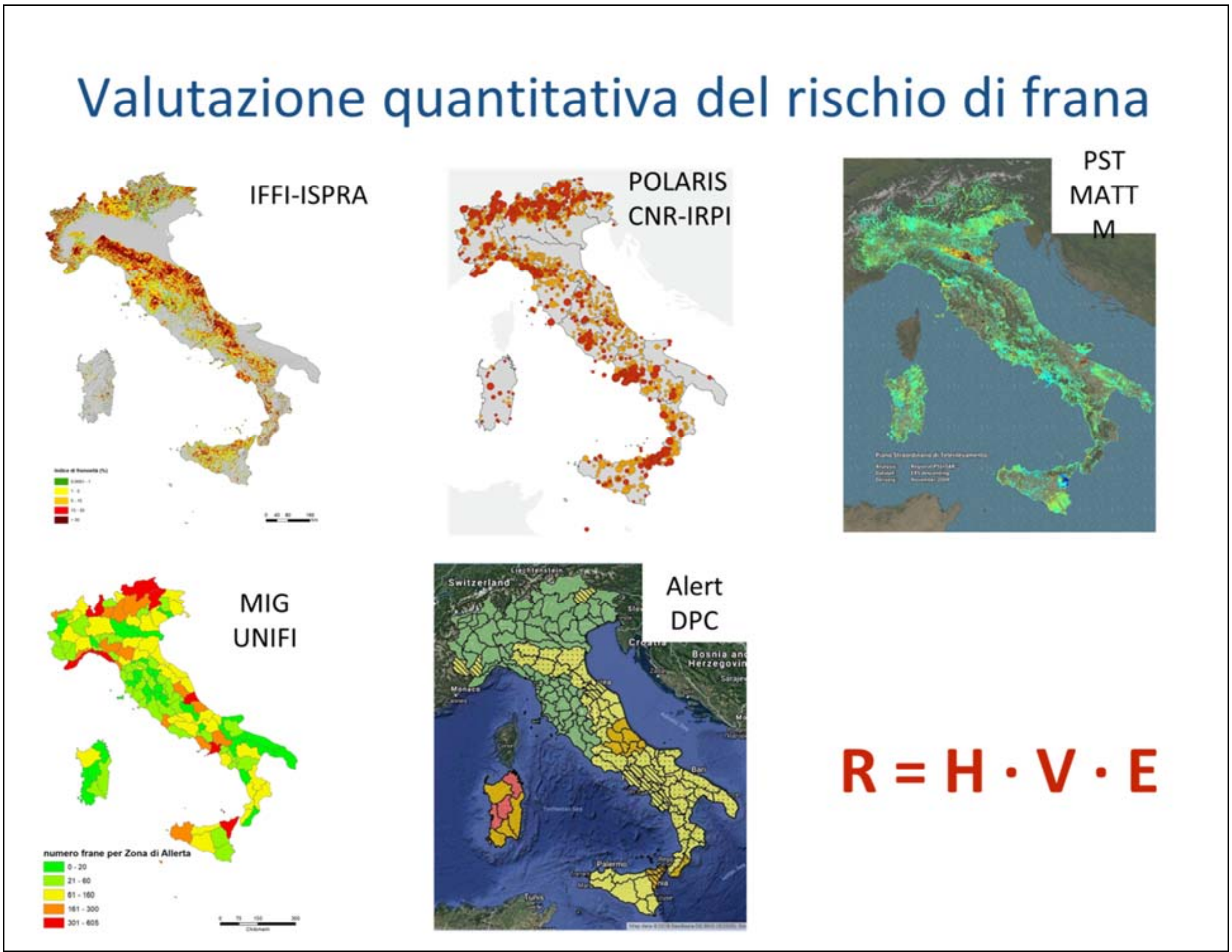
Valutazione quantitativa del rischio di frana
IFFI-ISPRA
POLARIS
CNR-IRPI
PST
MATT
M
MIG
UNIFI
numero frane per Zona di Allerta
0 - 20
21 - 60
61 - 160
161 - 300
301 - 605
Alert
DPC
R = H · V · E

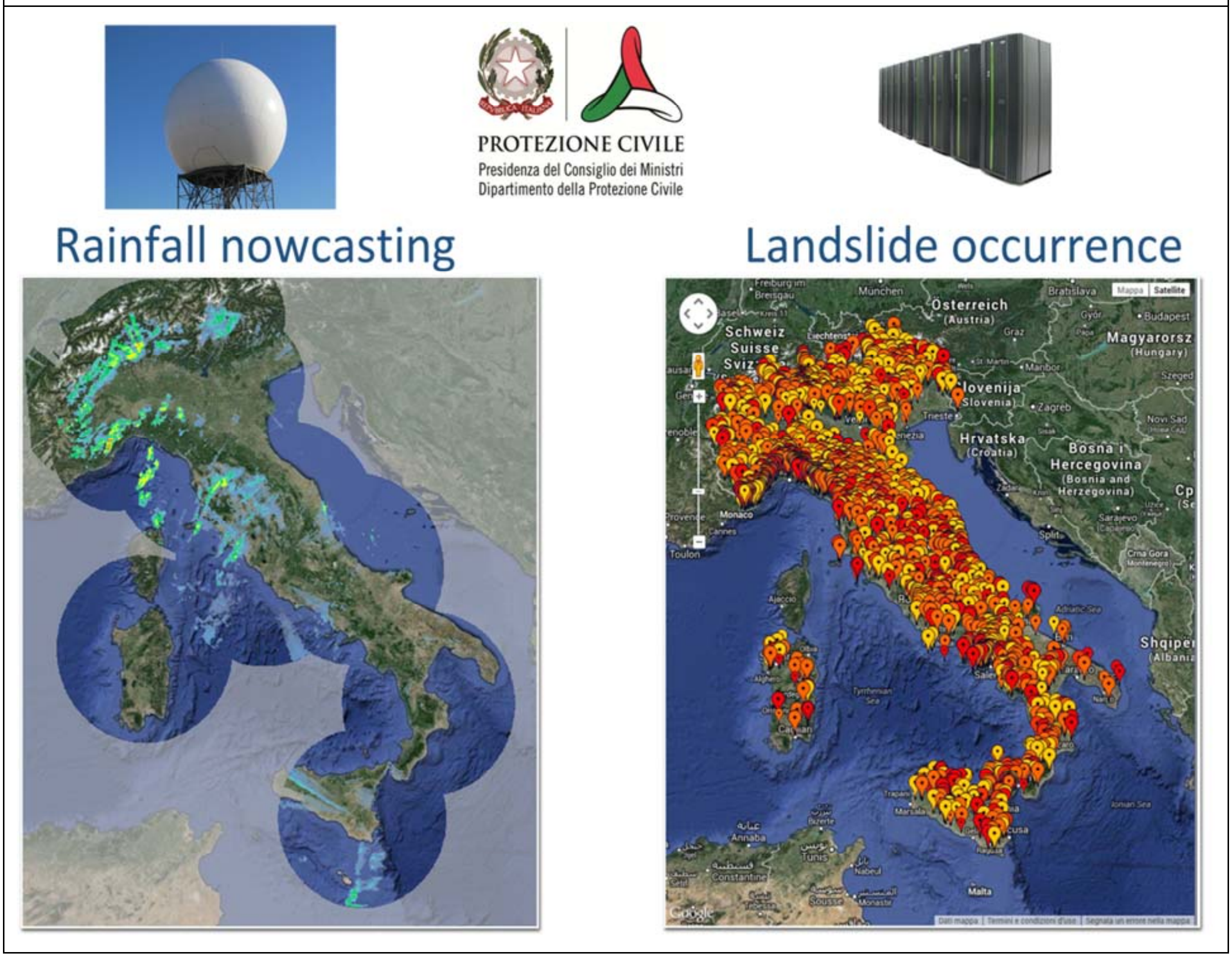
PROTEZIONE CIVILE
Presidenza del Consiglio dei Ministri
Dipartimento della Protezione Civile
Rainfall nowcasting
Landslide occurrence
Österreich
(Austria)
Schweiz
Suisse
Magyarország
(Hungary)
Slovenija
(Slovenia)
Hrvatska
(Croatia)
Bosna i
Hercegovina
Shqipëri
(Albania)

Web news data mining

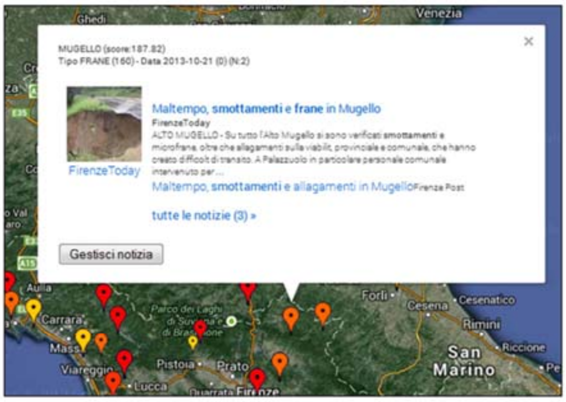

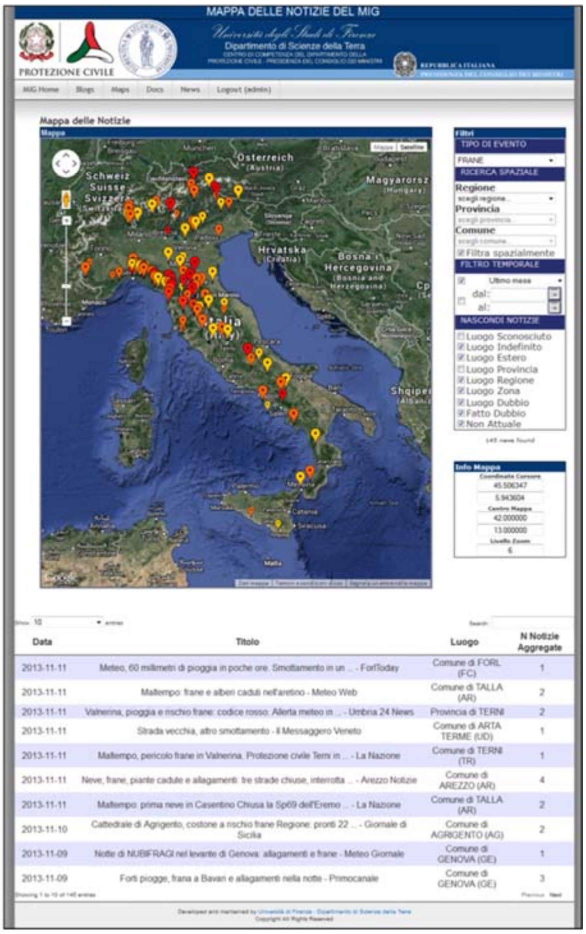

Risk education and training


International relationship
A Programme of the ICL for ISDR
INTERNATIONAL PROGRAMME ON LANDSLIDES
ISDR-ICL SENDAI PARTNERSHIPS 2015-2025 FOR GLOBAL PROMOTION OF UNDERSTANDING AND REDUCING LANDSLIDE DISASTER RISK
IPL World Centre of Excellence
INTERNATIONAL CONSORTIUM ON LANDSLIDES
ITALIAN NETWORK
INTERNATIONAL CONSORTIUM ON LANDSLIDES
Natural Sciences Sector
United Nations Educational, Scientific and Cultural Organization
University Twinning and Networking Programme
Sustainable Development Goals
THE GENEVA MILESTONE
UNESCO World Heritage
GEMs Geoengineering Master
UNESCOChair PhD Program
UNESCO Chair on the Prevention and Sustainable Management of Geo-Hydrological Hazards, University of Florence, Italy
UNIVERSITÀ DEGLI STUDI FIRENZE
PROTEZIONE CIVILE
ICGdR
INTERNATIONAL CONSORTIUM ON GEO-DISASTER REDUCTION
Geoenvironmental Disasters
JIC-Nh
Joint International Center on Natural Hazards
GADRI
Global Alliance of Disaster Research Institutes
European Commission
EUROPEAN CIVIL PROTECTION AND HUMANITARIAN AID OPERATIONS
JOINT RESEARCH CENTRE
DISASTER RISK MANAGEMENT KNOWLEDGE CENTRE


UNESCO International missions


ICL Italian Network
INTERNATIONAL
CONSORTIUM
ON LANDSLIDES
ITALIAN NETWORK
UNIMIB
UNIPV
UNIPD
UNITO
UNIPR
UNIMORE
UNIBO
UNIFI
IDS
IRPI
UNICH
ISPRA
UNIROMA
UNISANNIO
UNIBA
UNISA
UNICAL
7 full members
6 associates
1 supporter
3 coming soon

Combination of Rainfall Thresholds and Susceptibility Maps for Dynamic Landslide Hazard Assessment at Regional Scale

Veronica Tofani[1], Samuele Segoni[1], Ascanio Rosi[1], Filippo Catani[1], Nicola Casagli[1]

1) UNESCO Chair on Prevention and Sustanaible Management of Geohydrological hazards, University of Florence

Abstract

A methodology to couple rainfall thresholds and susceptibility maps for dynamic landslide hazard assessment at regional scale is presented. Both inputs are combined in a purposely-built hazard matrix to get a spatially and temporally variable definition of landslide hazard. The hazard matrix combines three susceptibility classes (S1, low susceptibility; S2 medium susceptibility; S3 high susceptibility) and three rainfall rate classes (R1, R2, R3), defining five hazard classes, from H0 (null hazard) to H4 (high hazard). The employ of the proposed procedure in a regional warning system brings two main advantages: (i) it is possible to better hypothesize when and where landslide are expected and with which hazard degree, thus fostering a more effective hazard and risk management (e.g., setting priorities of intervention); (ii) the spatial resolution of the regional scale warning system is markedly refined because from time to time the areas where landslides are expected represent only a fraction of the alert zone.

Objectives

Define a methodology to couple rainfall thresholds and susceptibility maps for dynamic landslide hazard assessment at regional scale

Advantages:

- it is possible to better hypothesize when and where landslide are expected and with which hazard degree, thus fostering a more effective hazard and risk management (e.g. setting priorities of intervention);
- the spatial resolution of the regional scale warning system is markedly refined because from time to time the areas where landslides are expected represent only a fraction of the alert zone.

Methodology

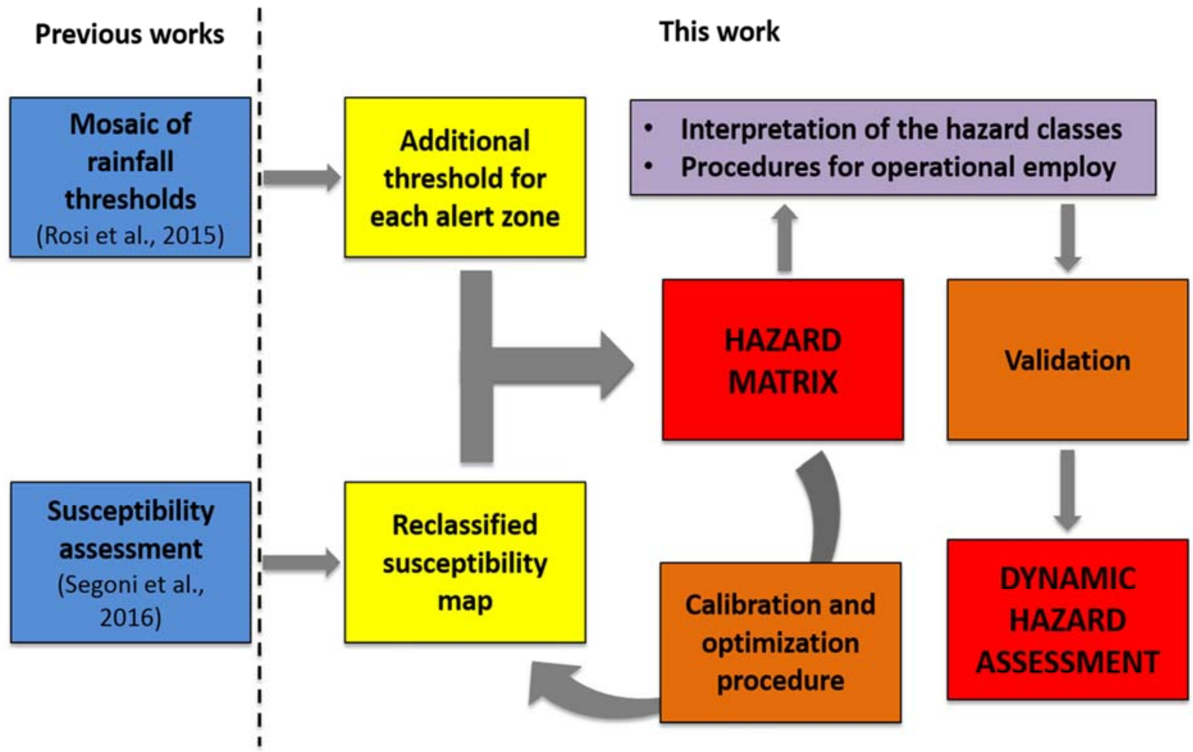

Susceptibility assessment

Random forest classification is a machine-learning algorithm for non-parametric multivariate classification

- it does not require assumptions about the distribution of the predisposing variables
- It allows the simultaneous use of numeric and categorical variables
- It takes into account the correlation and non-linearity between the variables

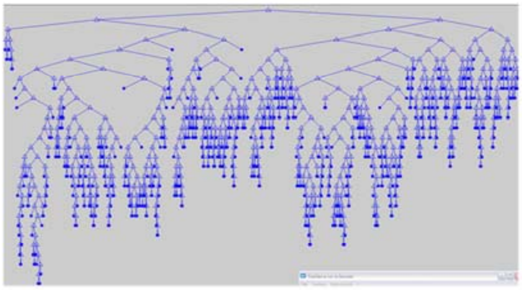

Rainfall thresholds

Statistical analysis of Intensity-Duration Data

Massive CUMulate Brisk Analyzer

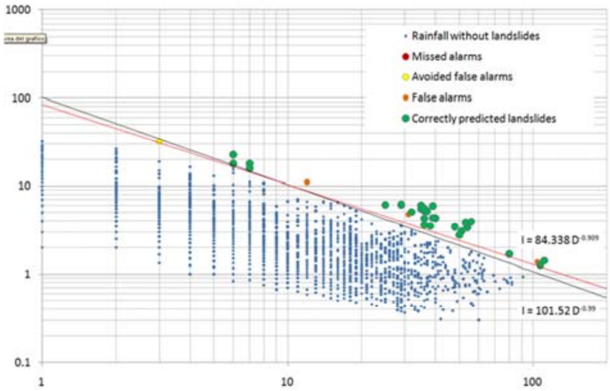

- **Intensity-duration**
- **Automated analysis**
- **Standardized approach**
- **Definition of local thresholds**
- **Balancing between false and missed alarms**

Study area

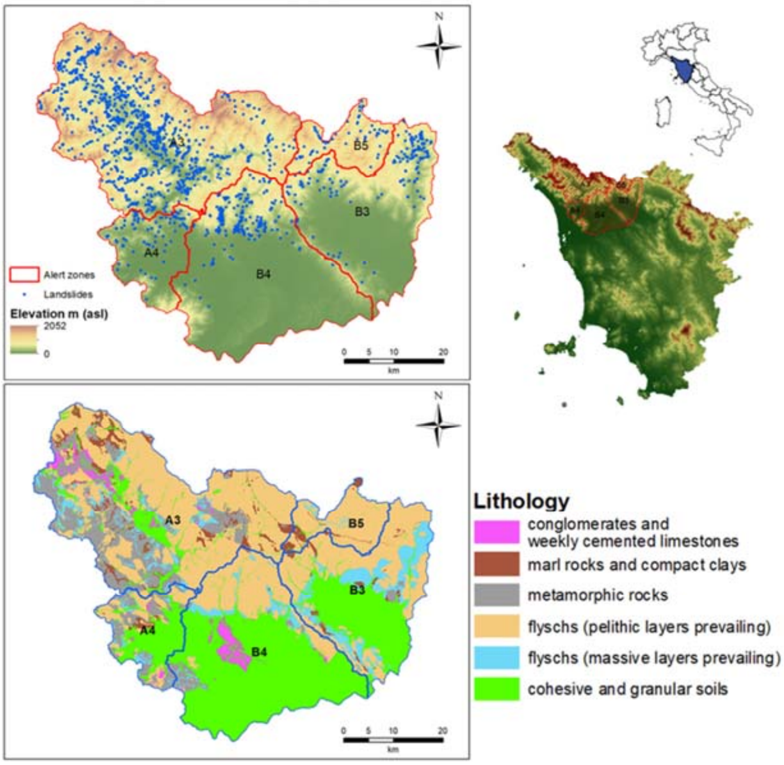

Hazard assessment

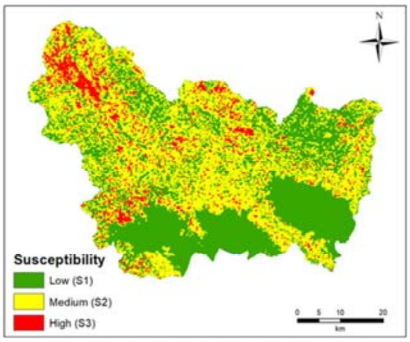

Spatial forecasting
(fine spatial resolution)
Static map (no temporal information)

Hazard matrix

	S1	S2	S3
R1	H0	H1	H2
R2	H1	H2	H3
R3	H2	H3	H4

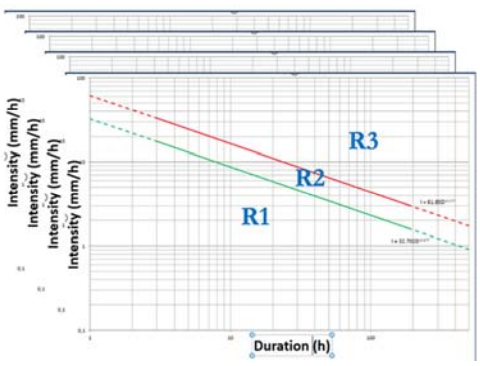

Temporal forecasting
Coarse spatial resolution (alert zone)

Hazard calibration

Susceptibilty map reclassified in 3 classes (S1, S2, S3)

Class break values calibrated:

- **using 1761 landslides from a 17 years dataset (2010 to 2016)**
- **independently in each alert zone**
- **to reach a quantitative and objective target**
- **to provide a precise meaning to the resulting hazard classes (H0, H1, H2, H3, H4).**

Alert zone	S1–S2 (%)	S2–S3 (%)
A3	4	18
A4	7	15
B3	7	22
B4	4	22
B5	7	26

Class break values for susceptibility classes for each alert zone

Interpretation of the hazard classes

H0, null hazard. No landslides are expected.

H1, low hazard. Theoretically, no landslides should be expected. However, this class encompasses a residual possibility (10%) of landslide occurrence because of errors in one of the input models, uncertainties in the data, or triggers other than rainfall.

H2, medium hazard. Landslides can be expected, since one of the inputs is high and the other is low, or they both are medium.

H3, high hazard. Either rainfall rate is at the maximum level (thus landslides can be expected also in areas with medium susceptibility) or the susceptibility is at the highest level (thus landslides can be triggered also when the rainfall rate is at a medium level of criticality).

H4, very high hazard. Highest possible level of spatial and temporal hazard.

Validation of the hazard map

Validation: we simulated an operational employ of the dynamic hazard matrix, checking the hazard class associated to each landslide occurred in the study area during the validation period.

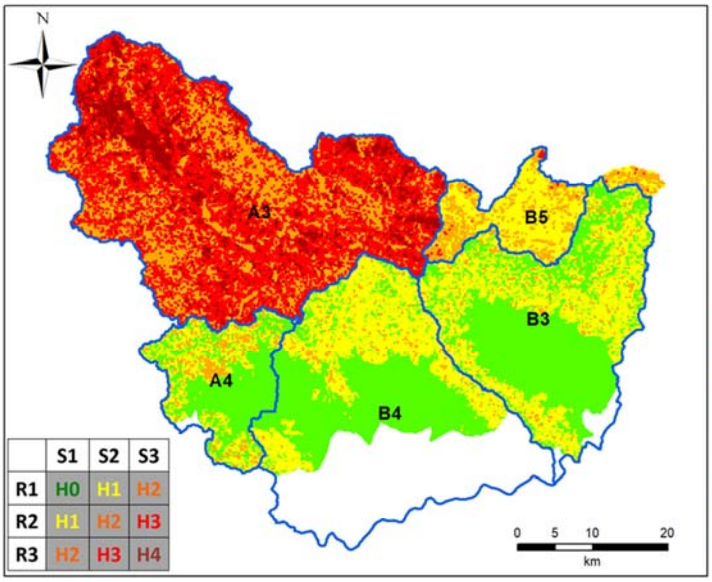

Validation period: from 01-01-2017 to 30-4-2108

39 landslides occurred.

They were forecasted as follows:
H0: 0 landslides
H1: 1 landslide
H2: 15 landslides
H3: 14 landslides
H4: 9 landslides

Conclusions

- **The proposed methodology can be applied in every area where rainfall thresholds and susceptibility maps have been previously defined.**
- **It can be used to enhance the forecasting effectiveness and the spatial resolution of regional scale early warning systems based on rainfall thresholds**
- **The calibration of the hazard matrix allows for an optimization of the forecasting effectiveness of the system, the definition of uncertainties, a better comprehension of the significance of the output hazard levels.**
- **It is possible to better hypothesize where landslides are expected and with which hazard degree, thus fostering a more effective hazard and risk management (e.g., setting priorities of intervention);**

Bibliography

Rosi, A., Lagomarsino, D., Rossi, G., Segoni, S., Battistini, A., & Casagli, N. (2015). Updating EWS rainfall thresholds for the triggering of landslides. Natural Hazards, 78(1), 297-308.

Segoni, S., Tofani, V., Lagomarsino, D., & Moretti, S. (2016). Landslide susceptibility of the Prato–Pistoia–Lucca provinces, Tuscany, Italy. Journal of Maps, 12(sup1), 401-406.

Segoni, S., Tofani, V., Rosi, A., Catani, F., & Casagli, N. (2018). Combination of rainfall thresholds and susceptibility maps for dynamic landslide hazard assessment at regional scale. Frontiers in Earth Science, 6, 85.

Laboratory physical modeling of rainfall, slope deformation and landslides triggering.

Giovanna Capparelli [(1)], Pasquale Versace[(1)], Gennaro Spolverino[(1)], Roberto Greco[(2)], Emilia Damiano [(2)], Lucio Olivares[(2)]

1) CAMILab (Laboratory of Environmental Cartography and Hydraulic and Geological Modeling), DIMES Department, University of Calabria, Ponte Pietro Bucci, cubo 42/b Rende (CS) Italy

2) University of Campania Luigi Vanvitelli, DICEA, Aversa – Napoli (Italy)

Abstract

Rainfall is the most common cause of landslides. Every year, meteorological events trigger superficial and deep landslides on the slopes, which produce many damage and victims.

The knowledge of the hydraulic processes in unsaturated soils is significant, not just for a better overall understanding of the mechanisms that control landslide triggering, but also for risk mitigation policy.

Although the literature is full of simulation models, the complexity of phenomena would impose a more detailed analysis by a well-equipped flume, with the aim of seeing rainfall infiltration processes into the granular soils, the distribution of the water content and pore pressure both in saturated and unsaturated layers and the effects in terms of slope stability.

For that purpose a physical scale model at the University of Calabria was designed and built, very useful for carrying out complex tests to analyze the response of loose soils or debris in terms of stability. Two channels compose it; the first one is adopted for analysing the triggering mechanisms, the second one for the propagation phases. Both channels are equipped with suitable sensors for monitoring the main physical variables, i.e.: spray nozzle systems, to apply a rainfall intensity; minitensiometers and TDR for measuring respectively suction values and water content; miniaturized pressure transducers for pore water pressures; laser displacement sensors.

All this is discussed here, in addition to the first results obtained from transient infiltration tests performed on pyroclastic soils sampled around Sarno area (Southern Italy - near the volcano Vesuvio) which was affected by mud flows events on 5 May 1998.

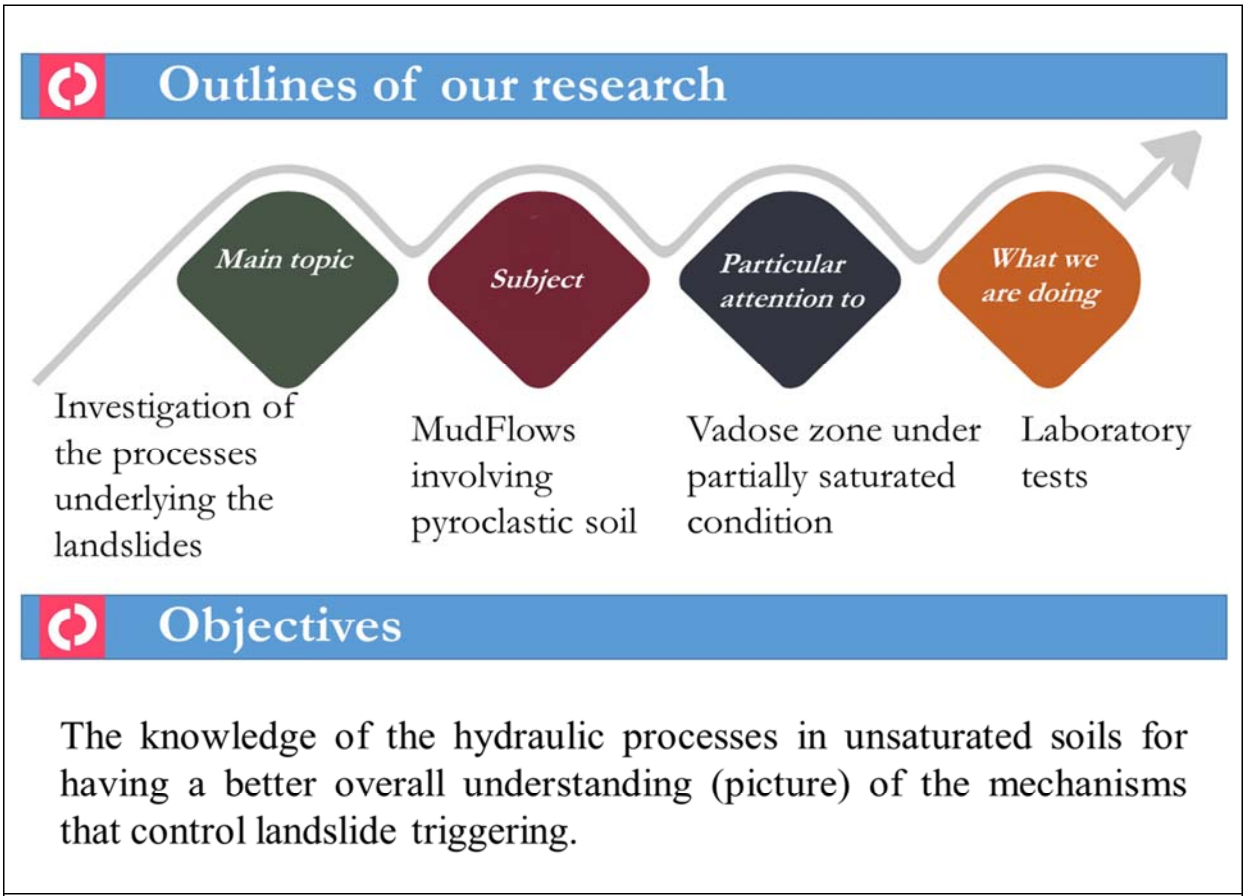
Outlines of our research
Main topic
Subject
Particular attention to
What we are doing
Investigation of the processes underlying the landslides
MudFlows involving pyroclastic soil
Vadose zone under partially saturated condition
Laboratory tests
Objectives
The knowledge of the hydraulic processes in unsaturated soils for having a better overall understanding (picture) of the mechanisms that control landslide triggering.

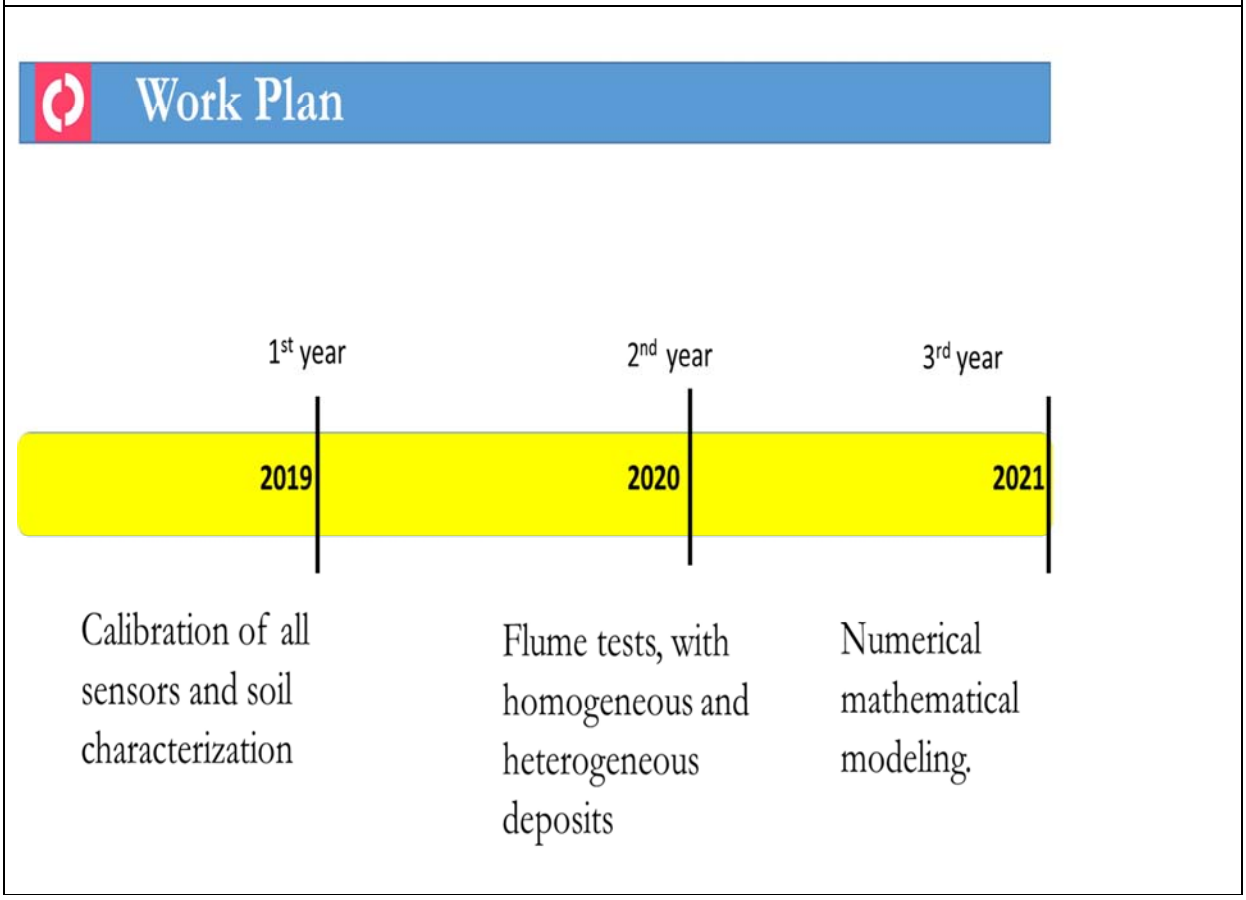
Work Plan
1st year
2nd year
3rd year
2019
2020
2021
Calibration of all sensors and soil characterization
Flume tests, with homogeneous and heterogeneous deposits
Numerical mathematical modeling.

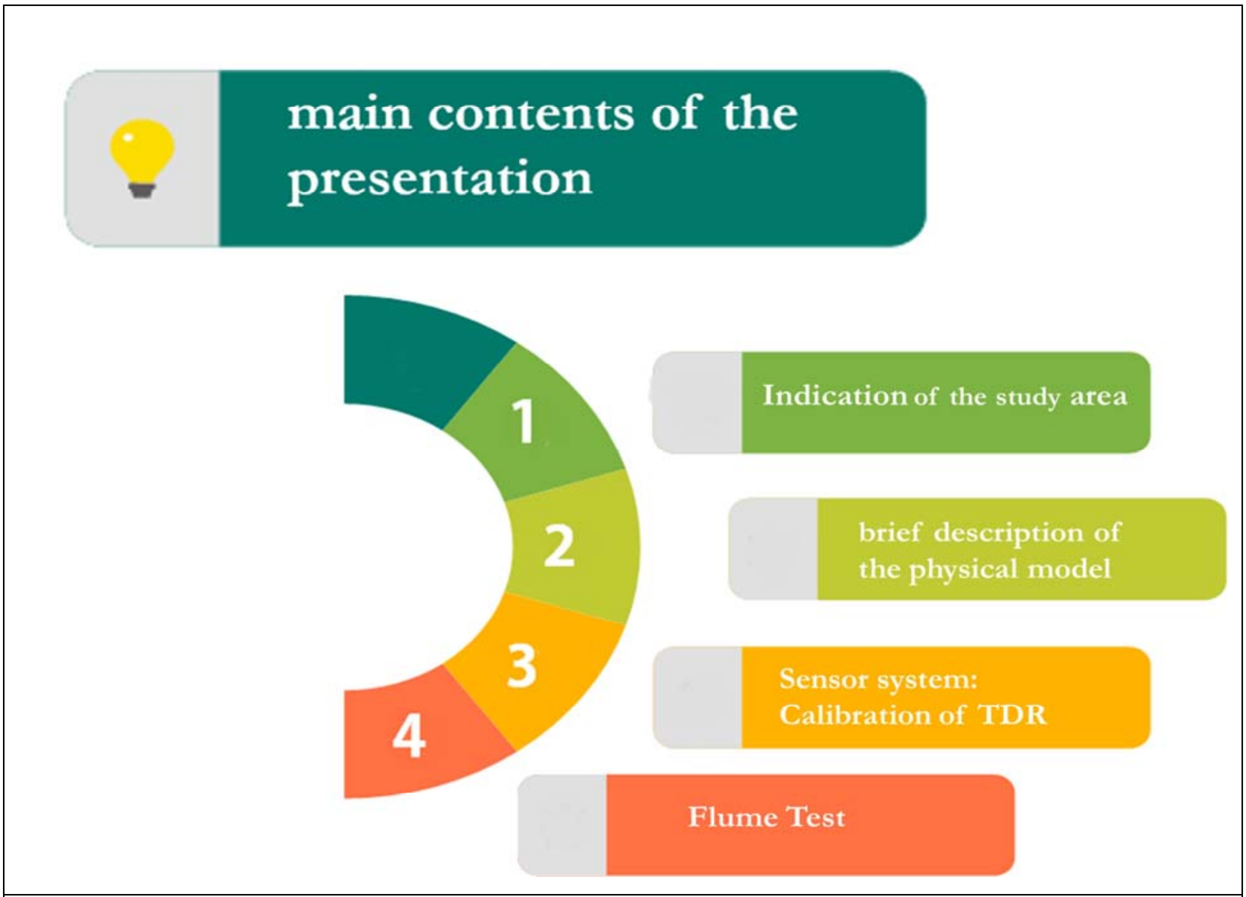
main contents of the presentation
1
2
3
4
Indication of the study area
brief description of the physical model
Sensor system: Calibration of TDR
Flume Test

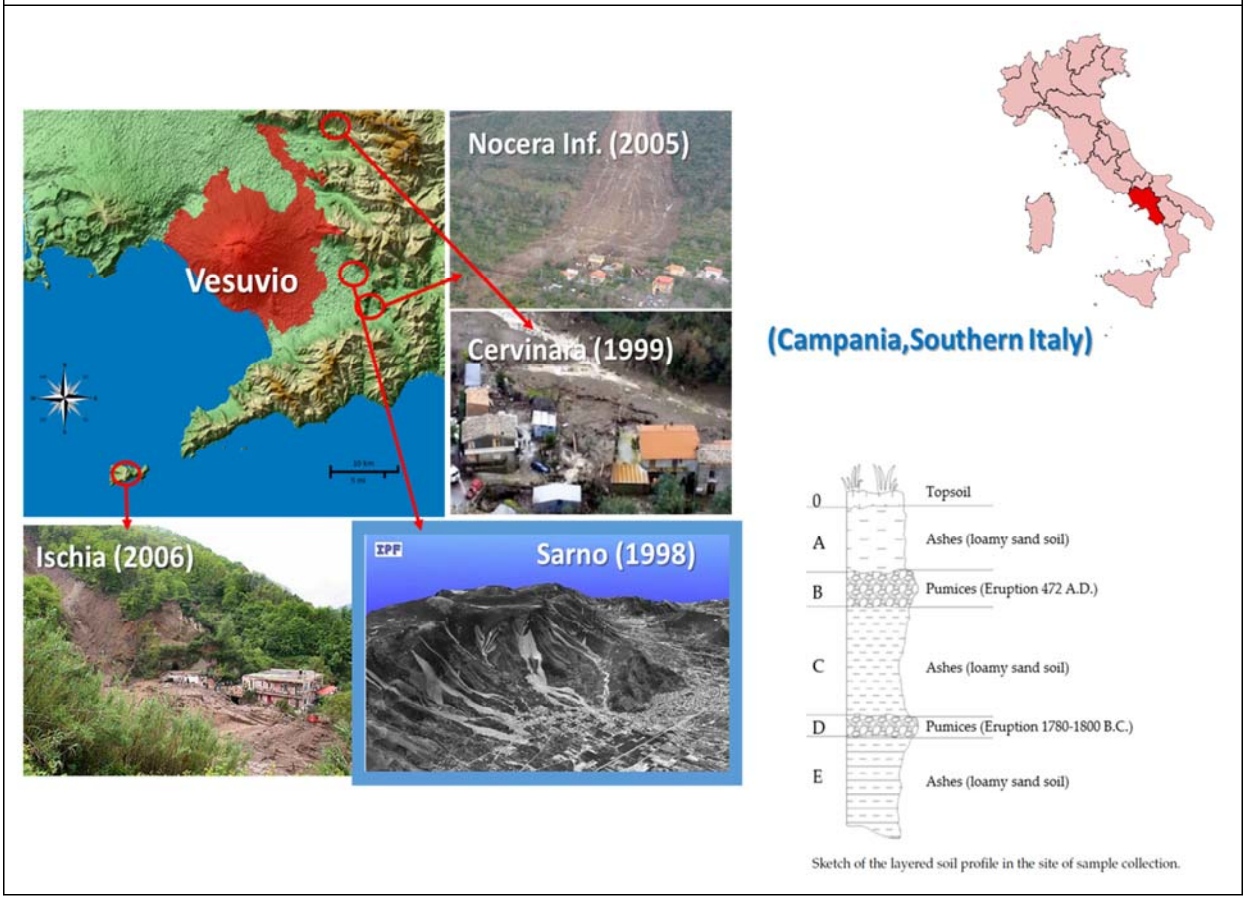
Nocera Inf. (2005)
Vesuvio
Cervinara (1999)
(Campania,Southern Italy)
Ischia (2006)
Sarno (1998)
0
A
B
C
D
E
Topsoil
Ashes (loamy sand soil)
Pumices (Eruption 472 A.D.)
Ashes (loamy sand soil)
Pumices (Eruption 1780-1800 B.C.)
Ashes (loamy sand soil)
Sketch of the layered soil profile in the site of sample collection.

Recurrent elements:

- the flowslides take place in shallow cohesionless air-fall deposits;
- the deposit is constituted by alternating ashy and pumiceous layers;
- the slope angle is higher than the friction angle of the cover;
- the deposit is initially unsaturated;
- the trigger of the process is rain water infiltration.

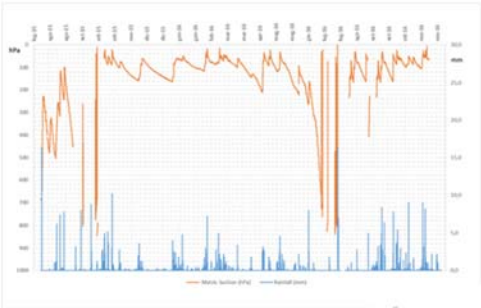

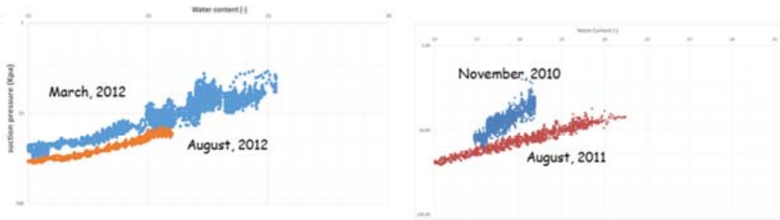

Channel	Lenght	Width	Height	Max Slope
Upper part	3 m	1 m	1 m	55°
Lower part	3 m	1 m	1 m	40°

Instrumented Flume

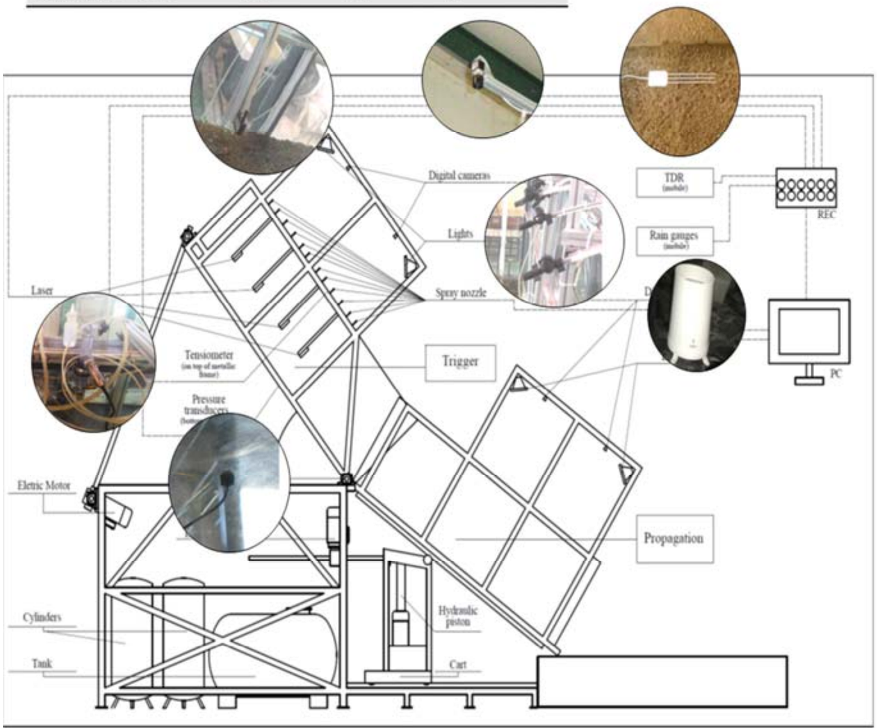

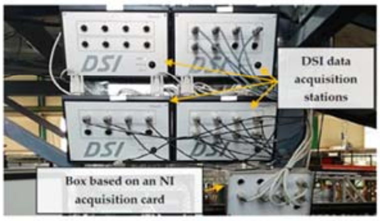

Figure 7: Acquisition stations.

Figure 2: Physical model: a) Side view b) Frontal view.

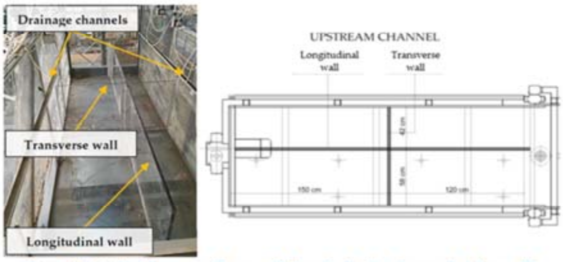

Figure 3: Detail of the upper flume, with longitudinal and cross dividing walls.

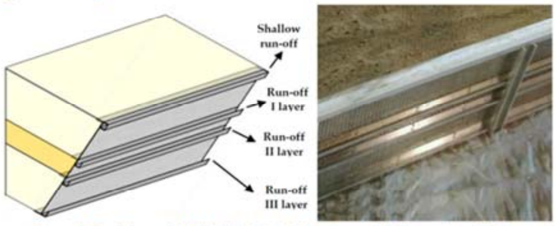

Figure 5: Draining grid laid at the foot of the slope with the water collection channels installed to measure run-off.

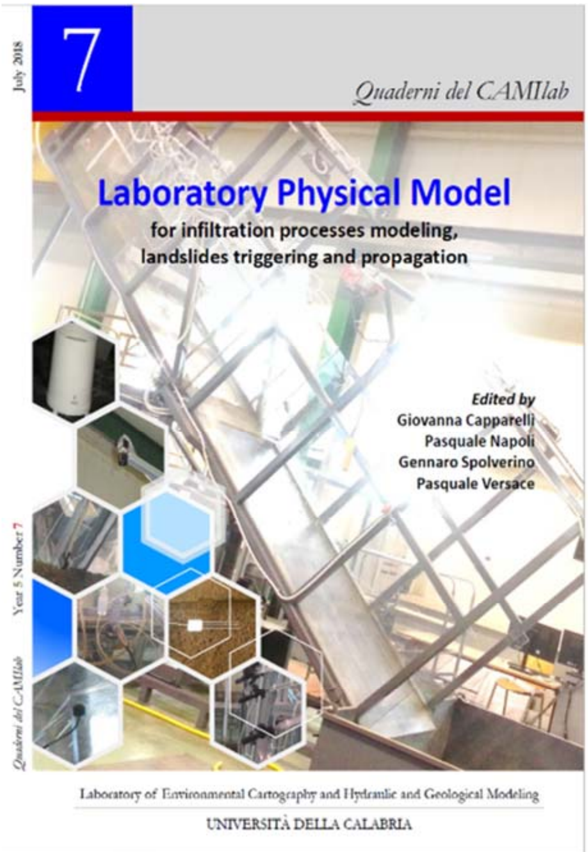

http://www.camilab.unical.it/web/camilab/laboratori

SENSOR SYSTEM

The instrumentation in the artificial channel is able to measure the main parameters that control the physical phenomenon, by the following equipment.

- **Tensiometers** (used to measure suction);
- **Pressure transducers** (used to measure pore water pressure);
- **TDR device** (used to measure soil water content);
- **Rainfall system** (used to simulate rainfall);
- **Laser sensors** (used to measure the soil profile and u_z displacements- in orthogonal direction);
- **High-resolution video cameras** (used to measure displacements along u_x and u_y –in plan)

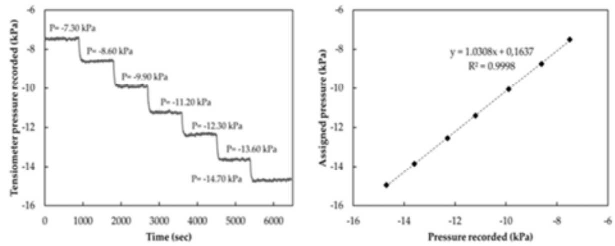

calibration of a ***tensiometer***.

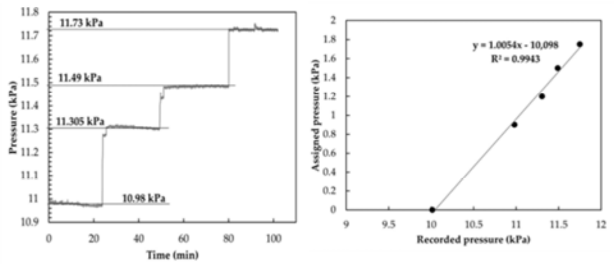

calibration of a ***pressure transducer***.

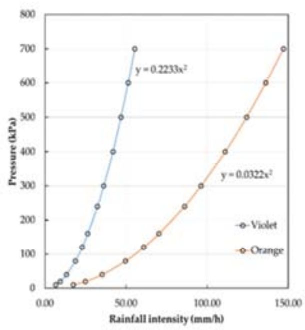

Rainfall system.

Image acquisition system and piv technique

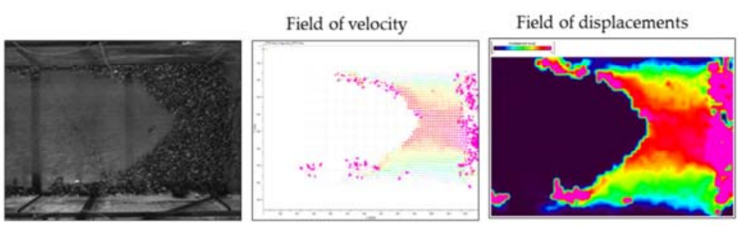

TDR Calibration

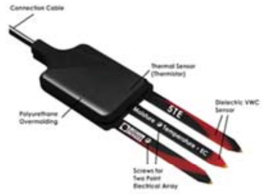

TDR systems are available for water content determination in porous media

Jones et al. Hydrol. Process. (2002)

bulk dielectric permittivity $\varepsilon_b = \left(\dfrac{ct}{2L}\right)^2$

c speed of light (velocity of electromagnetic waves)

t the travel time for the pulse to traverse the length of the embedded waveguide (down and back: 2L).

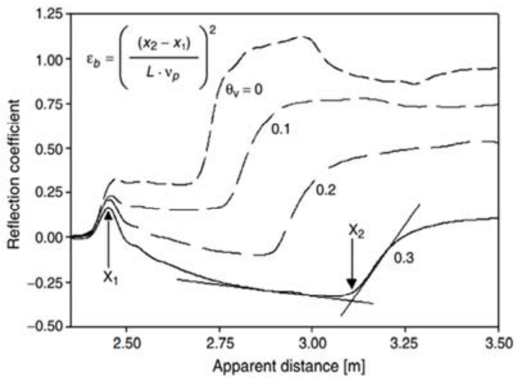

the apparent probe length (x_2- x_1) increases as the water content (and dielectric constant) increases, a consequence of reduced propagation velocity

TDR Calibration

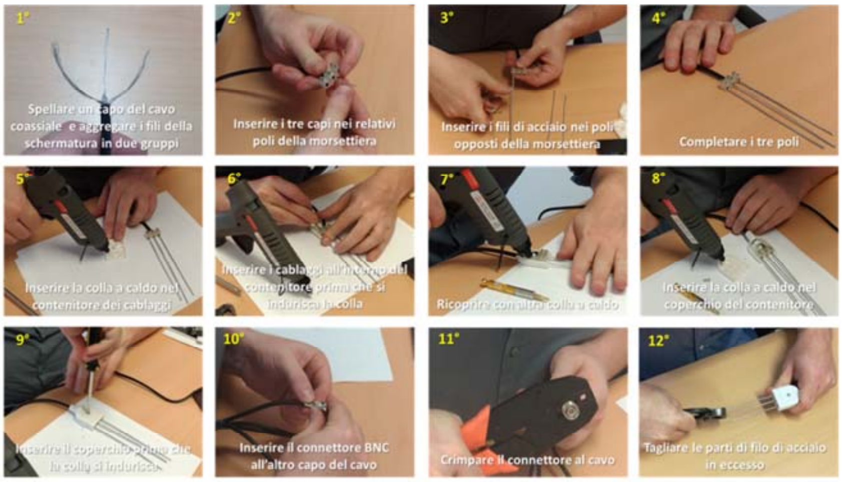

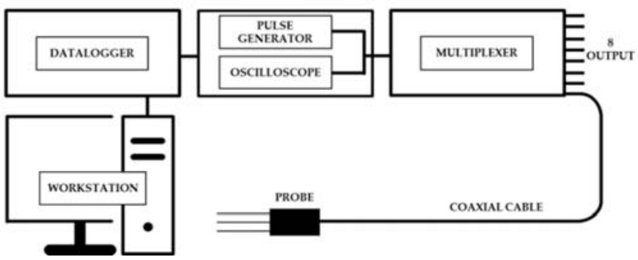

TDR Calibration

Relationships between ε_b and volumetric soil water content θ_v

Topp et al. 1980 . (in WRR)

a third-order polynomial to the observed relationships between ε_b and θ_v for multiple soils:

$$\theta_v = -5.3\times10^{-2} + 2.92\times10^{-2}\varepsilon_b - 5.5\times10^{-4}\varepsilon_b^2 + 4.3\times10^{-6}\varepsilon_b^3$$

New calibration

$$\theta_v = d + c\varepsilon_b + b\varepsilon_b^2 + a\varepsilon_b^3$$

Laboratory tests

TDR Calibration

Weight (water) [g]	Volumetric water content			
	θ = V_w /V_{tot}	θ (Topp)	Δ	εb
40	**0,066**	0,042	*0,024*	**3,50**
80	**0,106**	0,061	*0,045*	**4,26**
120	**0,146**	0,1035	*0,0425*	**6,06**
170	**0,196**	0,164	*0,032*	**8,88**
220	**0,246**	0,221	*0,025*	**11,87**
270	**0,296**	0,3305	*-0,0345*	**19,14**

$$\theta_v = d + c\varepsilon_b + b\varepsilon_b^2 + a\varepsilon_b^3$$

$$a = 4\times10^{-5}$$
$$b = 2.2\times10^{-3}$$
$$c = 4.6\times10^{-2}$$
$$d = -6.3\times10^{-2}$$

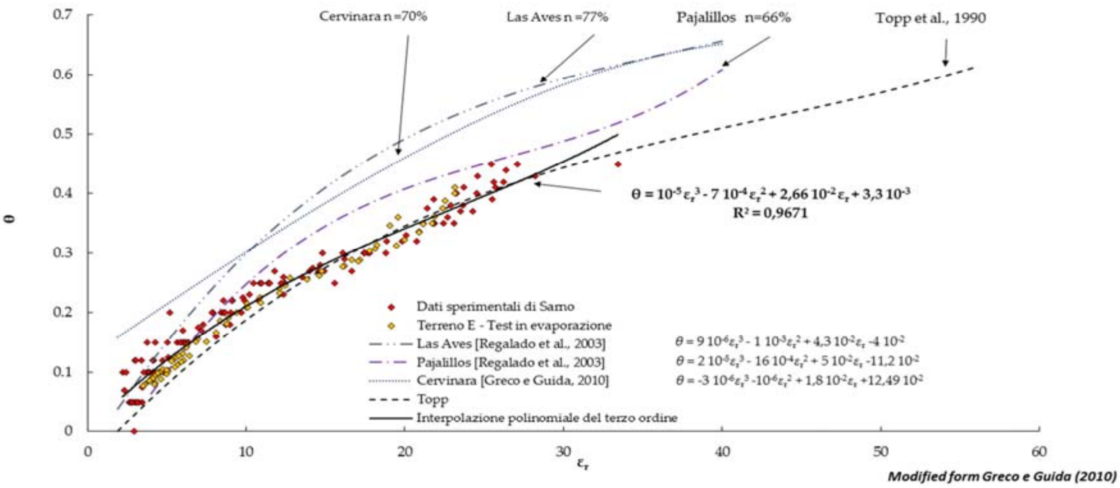

Modified form Greco e Guida (2010)

Measurement	Device	Manufacture/Type	Sensor	Sensor size		Transducer	Operating range	Linearity	Hysteresis	Output	Sampling Frequency
				Diameter	Height						
Matric suction	Tensiometer	Soil Moisture Corp/2100F	Porous ceramic cup	6 mm	25 mm	Current Transducer	0 - 100 Pa	0.0025	< 1%	4 - 20 mA	750 Hz

Measurement	Device	Manufacture/Type	Sensor	Sensor Probe size		Time Response of Combined Pulse Generator & Sampling Circuit	Maximum spatial resolution		Operating temperature range	Timing Resolution
				Diameter	Length					
Water content	TDR Apparatus	TDR100 Campbell Scientific	Small Probe	2 mm	75 mm	≤ 300 ps	1 cm a $\theta = 0.1\ m^3/m^3$	2 cm a $\theta = 0.2\ m^3/m^3$	− 40 /55 °C	12.2 ps
			Medium Probe	3 mm	150 mm	≤ 300 ps	2 cm a $\theta = 0.1\ m^3/m^3$	4 cm at $\theta = 0.2\ m^3/m^3$	− 40 /55 °C	12.2 ps
			Large Probe	5 mm	300 mm	≤ 300 ps	4 cm a $\theta = 0.1\ m^3/m^3$	8 cm at $\theta = 0.2\ m^3/m^3$	− 40 /55 °C	12.2 ps
			Home-made probe	2.2 mm	80 mm	≤ 300 ps	1 cm a $\theta = 0.1\ m^3/m^3$	2 cm at $\theta = 0.2\ m^3/m^3$	− 40 /55 °C	12.2 ps

Measurement	Device	Manufacture/Type	Sensor	Housig size (L - W - H)	Mesuring range	Resolution	Linearity	Output	Operating temperature	Sampling Frequency
Vertical displacement	Sensor displacement	LCL 45/100 - fae	Laser CMOS - array	62 mm -17 mm - 50 mm	100 mm	0.03 %	± 0.2%	4 - 20 Ma (analogic)	− 10 /60 °C	Lens C-Mount High Res

Measurement	Device	Manufacture/Type	Sensor	Housig size (L - W - H)	Frame rate	Resolution	Pixel size	Video Output	Image Area	Power consumption
Displacement ux - uy	Digital Camera	Basler/ICX445	1/3" progressive	42 mm - 29 mm - 29 mm	22 fps	1296 da 966	3.75 µm - 3.75 µm	YUV 4:2:2 Mono - Bayer	100 cm by 150 cm	2.5 W (PoE) 2.2 (AUX)

Accessory: Obiettivo C-Mount High Res - 1/2" - 4 mm - F/1.4 w/lock Basler Digital I/O cable with HRS 6-pin connector, 10 m Mega–Pixel Lens Fixed FL 8 mm - 2/3" - f/1.1 - f/16

Measurement	Device	Manufacture/Type	Sensor	Sensor size		Operating range	Resolution - Accuracy	Operating Temperature	Output	Compensated temperature
				Diameter	Height					
Pore water pressure	Pore pressure transducers	TE Connectivity Measurement Specialties	SENSOR 2PSIG 1/2NPT .5-	12.7 mm	25.4 mm	0 - 13.79 kPa	0.3 % - ± 1%	− 20 /70 °C	0 - 5 V	0 - 40°C

Measurement	Device	Manufacture/Type	Sensor	Sensor size		Operating range	Resolution	Maxiumum temporal Resolution
				Diameter	Height			
Rainfall intensity	Rain gauge	Oregon Scientific PCR800	Tiping bucket	87 mm	107 mm	0 - 999 mm/h	1 mm/h	1 min

Main characteristics and calibration parametrs of devices.

Soil Water Retention Curve

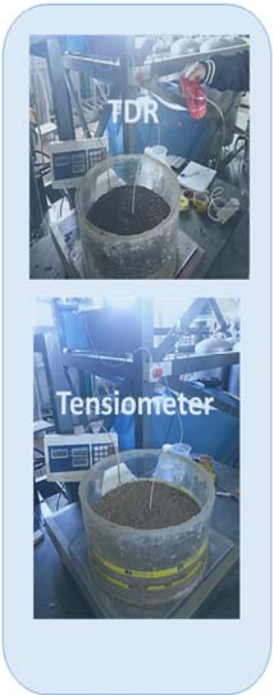

Infiltration test

Evaporation test

Suction and volumetric water content values were both measured during infiltration and evaporation phases

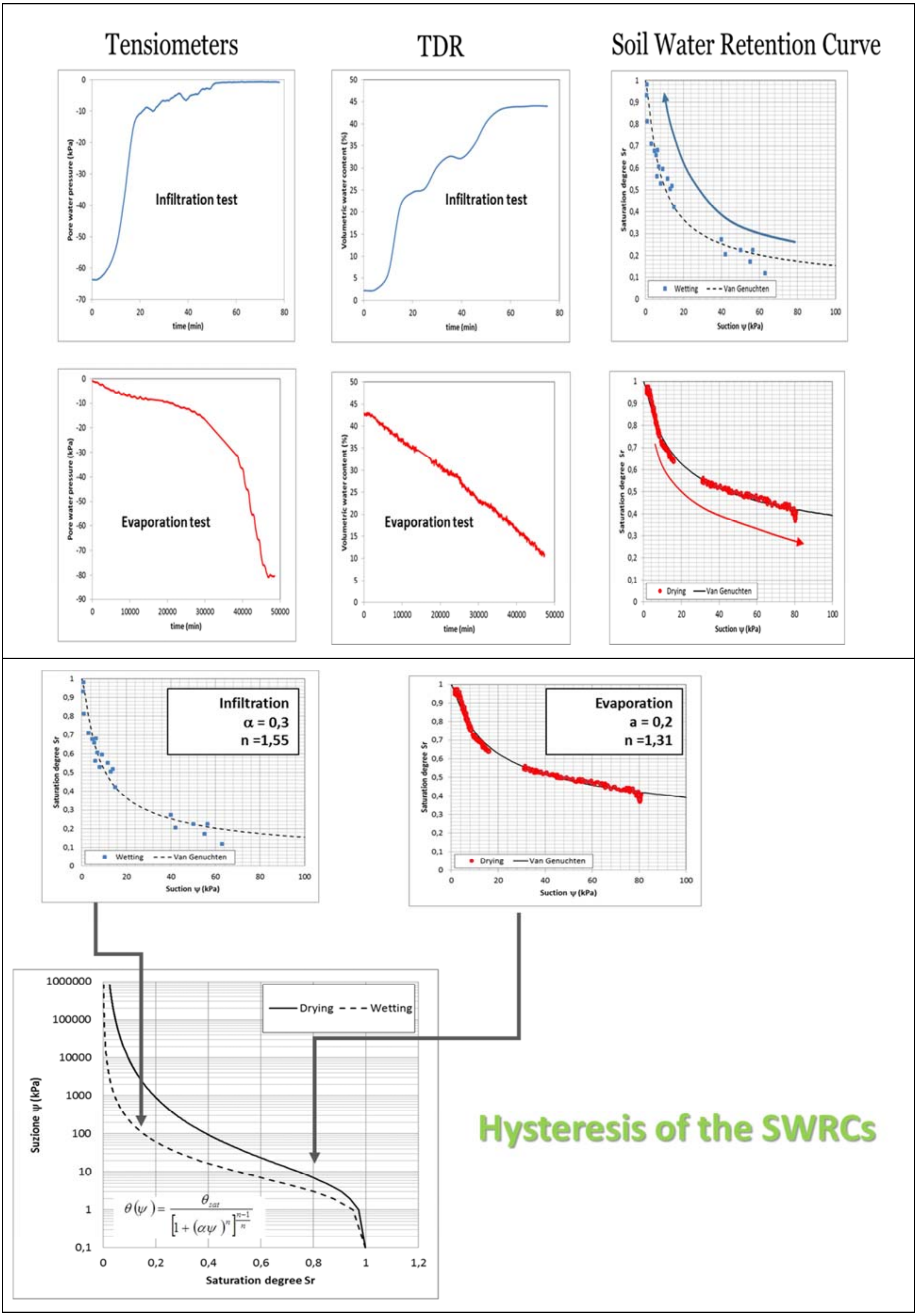
Tensiometers
TDR
Soil Water Retention Curve
Infiltration test
Infiltration test
Evaporation test
Evaporation test
Pore water pressure (kPa)
Volumetric water content (%)
time (min)
Saturation degree Sr
Suction ψ (kPa)
Wetting
Van Genuchten
Drying
Infiltration
α = 0,3
n =1,55
Evaporation
a = 0,2
n =1,31
Drying
Wetting
Suzione ψ (kPa)
Saturation degree Sr
$\theta(\psi) = \frac{\theta_{sat}}{\left[1 + (\alpha\psi)^n\right]^{\frac{n-1}{n}}}$
Hysteresis of the SWRCs

Flume Tests

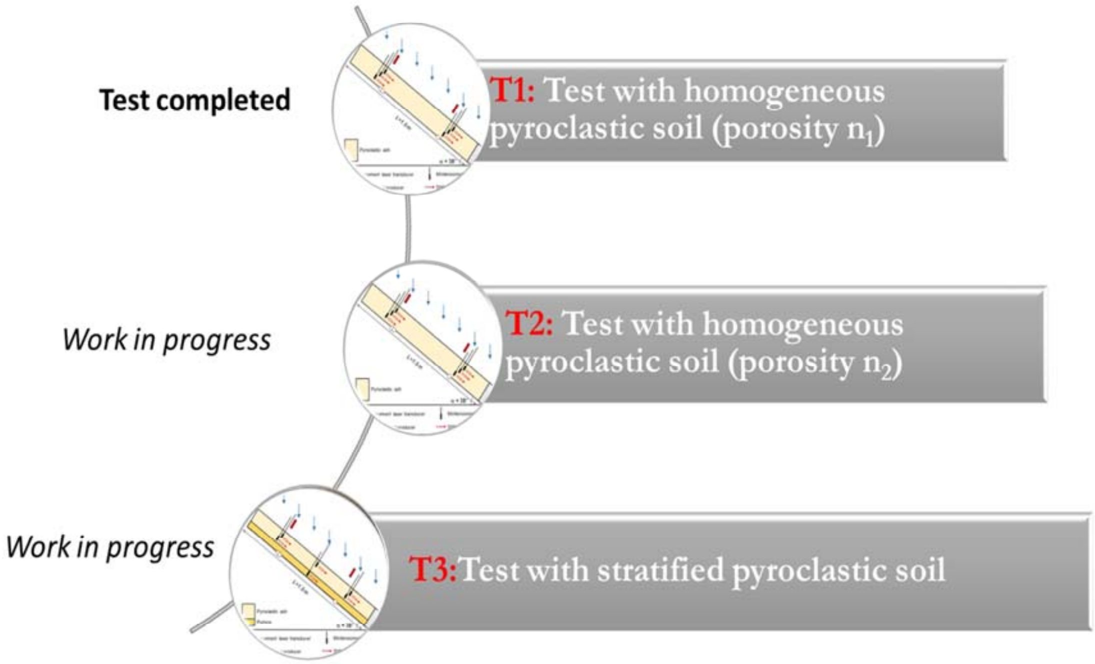

TEST T1

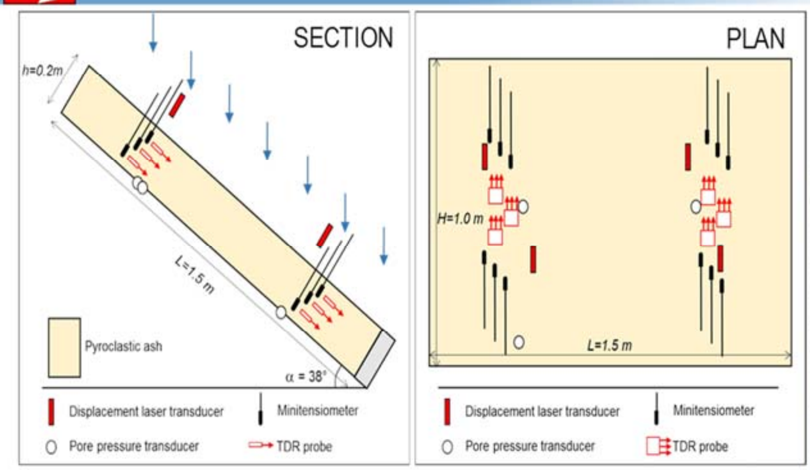

STEPs	Angle of inclination (degrees)	Rainfall intensity (mm/h)	Time
Infiltration horizontal slope	0	50	50 min
Evaporation	0	0	14 days
Redistribution	38	0	8 days
Failure	38	50	40 min

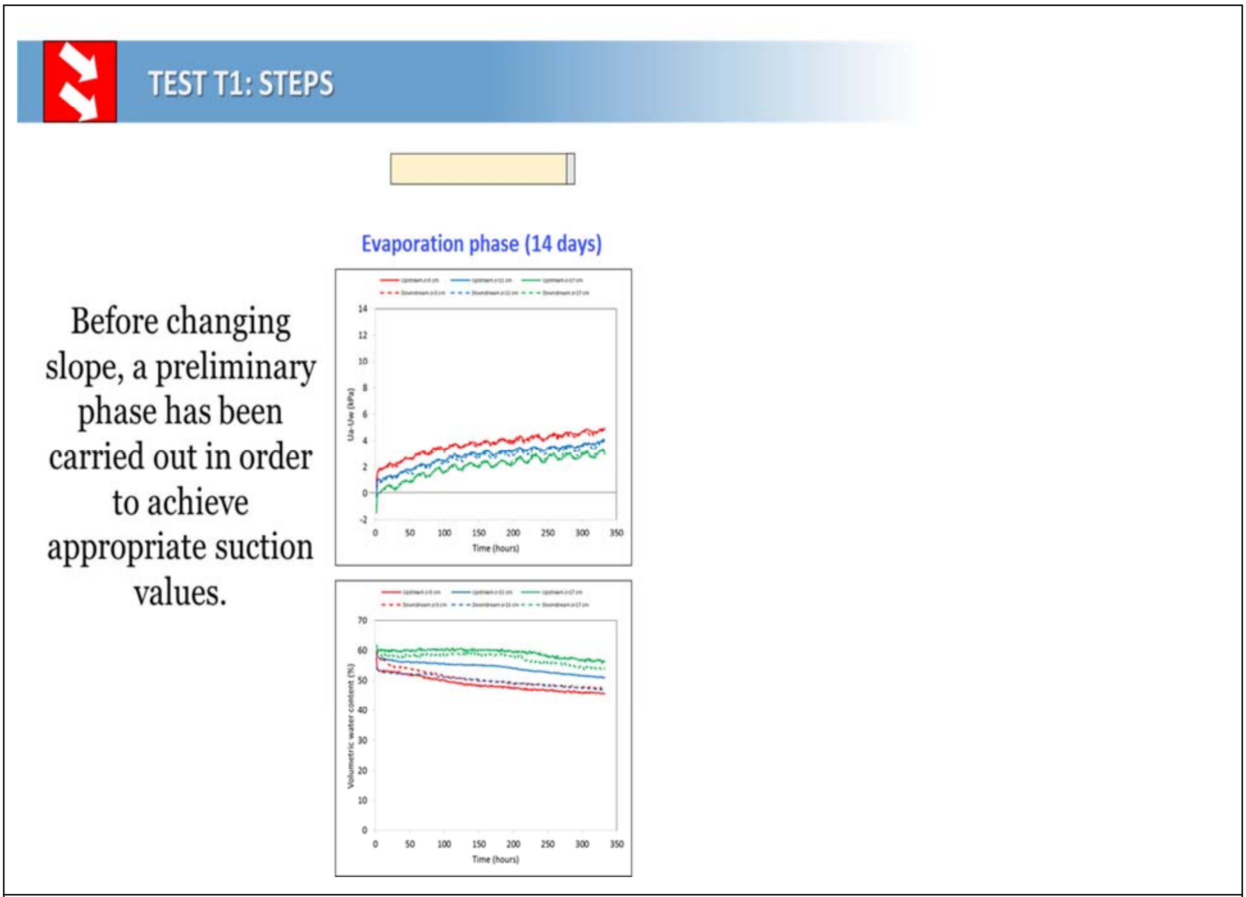
TEST T1: STEPS
Evaporation phase (14 days)
Before changing slope, a preliminary phase has been carried out in order to achieve appropriate suction values.
Ua-Uw (kPa)
Time (hours)
Volumetric water content (%)
Time (hours)

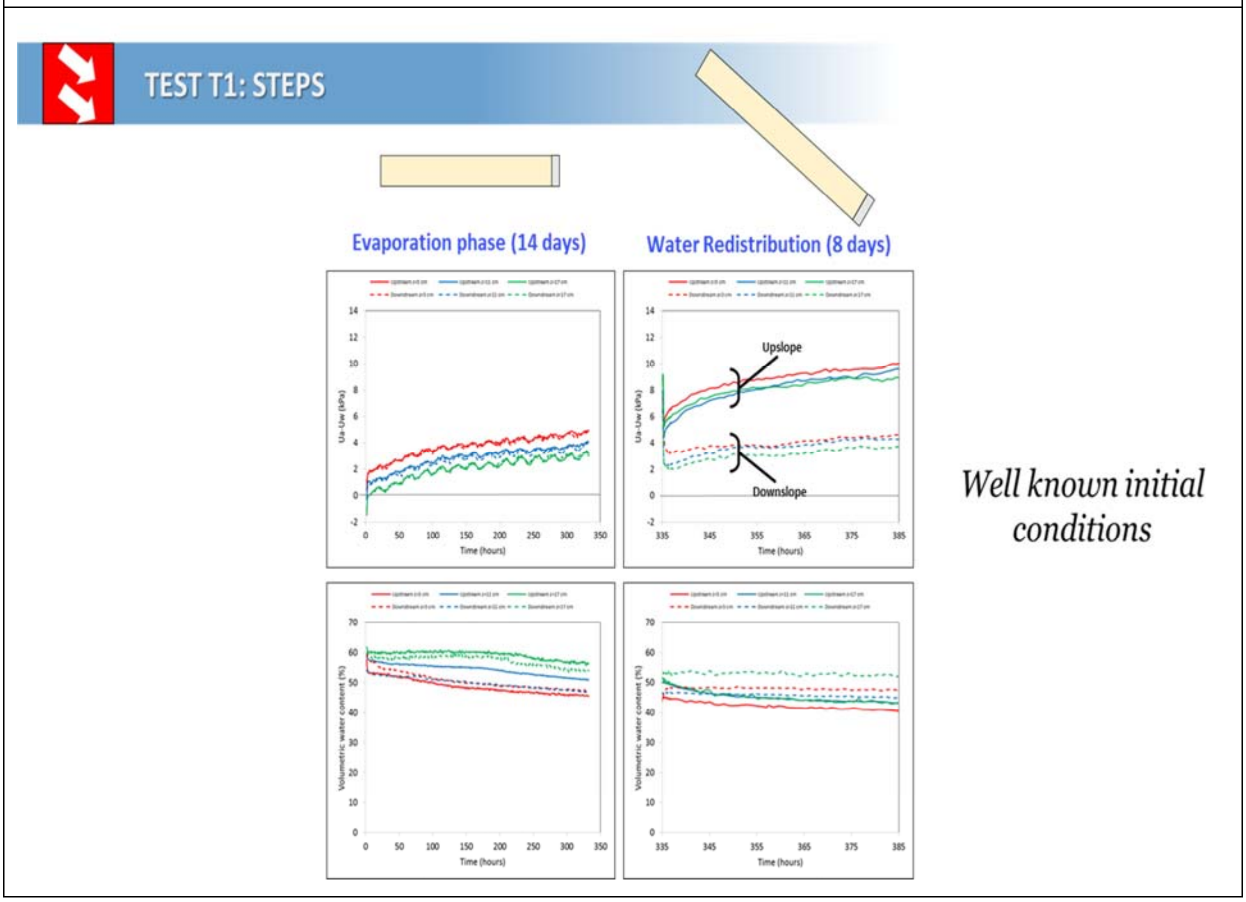
TEST T1: STEPS
Evaporation phase (14 days)
Water Redistribution (8 days)
Upslope
Downslope
Ua-Uw (kPa)
Volumetric water content (%)
Time (hours)
Well known initial conditions

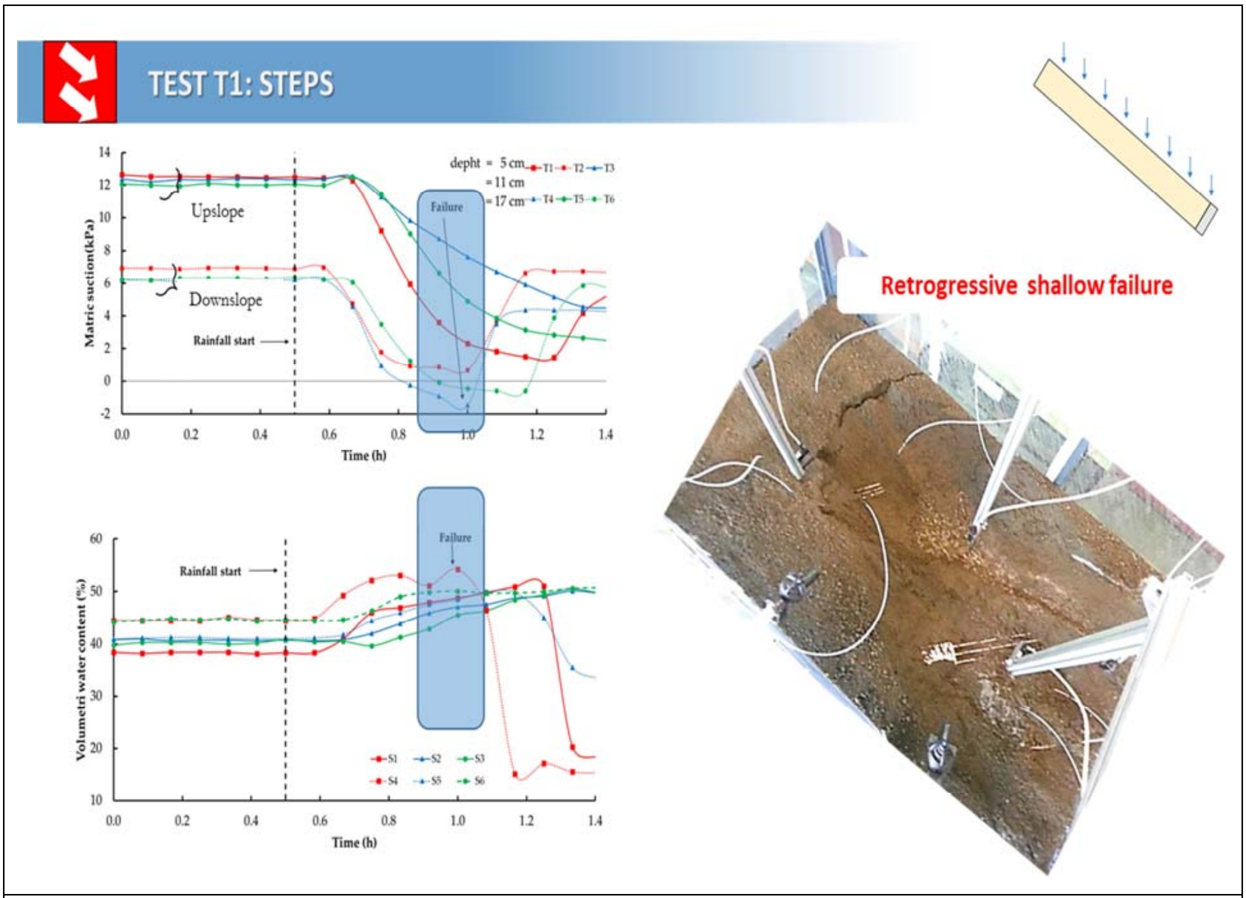
TEST T1: STEPS
depht = 5 cm
= 11 cm
= 17 cm
T1 T2 T3
T4 T5 T6
Upslope
Downslope
Failure
Rainfall start
Matric suction(kPa)
Time (h)
Volumetri water content (%)
S1 S2 S3
S4 S5 S6
Retrogressive shallow failure

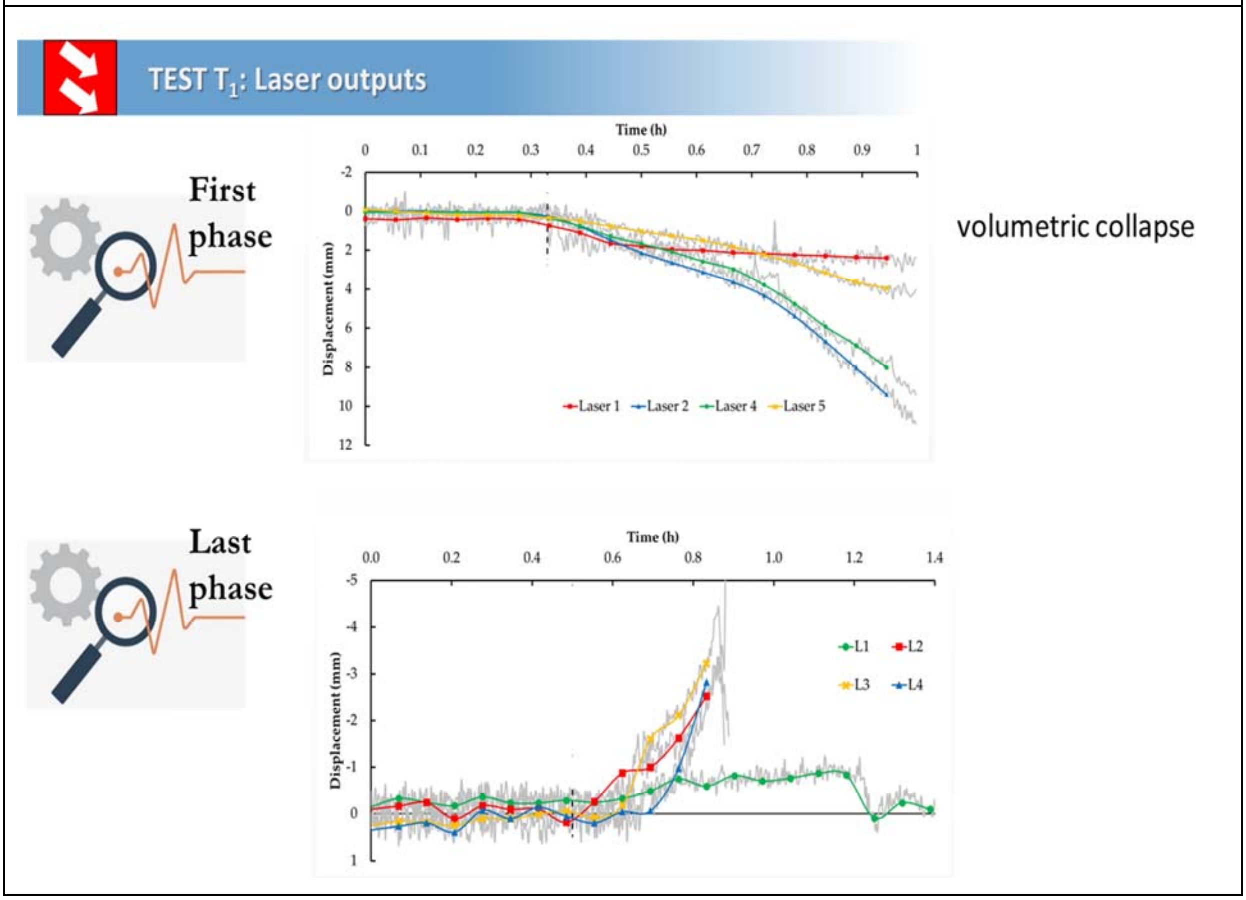
TEST T1: Laser outputs
First phase
Time (h)
Displacement (mm)
Laser 1 Laser 2 Laser 4 Laser 5
volumetric collapse
Last phase
L1 L2
L3 L4

- **(July 2019) Invited Talk on** *"Integrated Study of the Infiltration Processes in the Vesuvio Pyroclastic Soils Subject to Instability"* **WORLDCONGRESSONGEOLOGY&EARTHSCIENCE** London, UK https://geology-earthscience.com/

WORLD CONGRESS ON GEOLOGY & EARTH SCIENCE

- **Spolverino G., Capparelli G., and Versace P.** (2019). *An Instrumented Flume for infiltration process modeling, landslide triggering and propagation*. **Geosciences**, 9(3), 108; doi: 10.3390/geosciences9030108


geosciences

An Instrumented Flume for Infiltration Process Modeling, Landslide Triggering and Propagation

- **Capparelli G., Spolverino G. and Greco R.** (2018). Experimental determination of TDR calibration relationship for pyroclastic ashes of Campania (Italy). ***Sensors***, 18, 3727; doi:10.3390/s18113727

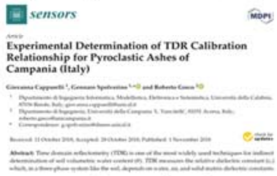
sensors

Experimental Determination of TDR Calibration Relationship for Pyroclastic Ashes of Campania (Italy)

- **Capparelli G., Spolverino G., Damiano E., Greco R., Olivares L.** (2018). *Physical model study of the infiltration processes in pyroclastic slopes subject to instability.* Vienna, Geophysical Research Abstracts Vol. 20, EGU2018-13625, 2018 **EGU General Assembly 2018**.

New tests with more layers of soil and different porosities

Comparison the evidences with the in situ measurements, with reference to the different scales effects .

Work in progress

Analysis of runoff and subsurfaces water flows

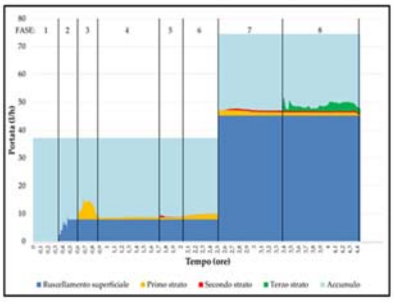

Accurate analysis of the permeability coefficients involved

giovanna.capparelli@unical.it

Integrated application of EO data and services for geohazard assessment: the EO4GEO project scenarios

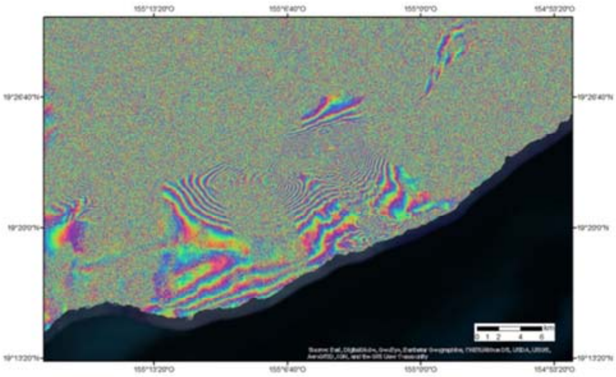

Daniele Spizzichino, Carlo Cipolloni, Valerio Comerci, Federica Ferrigno, Luca Guerrieri and Gabriele Leoni

IPL 2019 Symposium Paris
16-19 September

ISPRA - The Italian National Institute for Environmental Protection and Research
Via V. Brancati, 48 - 00144 ROMA; daniele.spizzichino@isprambiente.it

Abstract

EO4GEO project will define a long-term and sustainable strategy to fill the gap between supply of and demand for space/geospatial education and training taking into account the current and expected technological and non-technological developments in the space/geospatial and related sectors (e.g. ICT). The strategy will be implemented by the implementation of training modules directly usable in the context of Copernicus and other relevant programs; conducting a series of training actions for a selected set of scenarios in the three sub-sectors :1)integrated applications, 2) smart cities and 3) climate change to test and validate the approach. ISPRA will contribute significantly to the implementation of the real case studies through the landslide risk scenario concerning three different exposed categories: Linear infrastructure and transportation network; Cultural Heritage and Urban Area. The target of the IPL proposal is to define a standard methodology to use EO data and services (possibly open and free) to carry out landslide risk assessment, monitoring and mitigation. The landslide risk scenarios will be selected taking into account data availability and different typologies of phenomena (e.g. slow and very slow landslide, superficial and deep) as well as different vulnerability categories. Stakeholder, final user and landslide expert community (public and private) will be involved during the scenarios implementation. The proposal and the implementation of the project within the IPL framework could assure and guarantee one of the most important feedback among landslide worldwide expert.

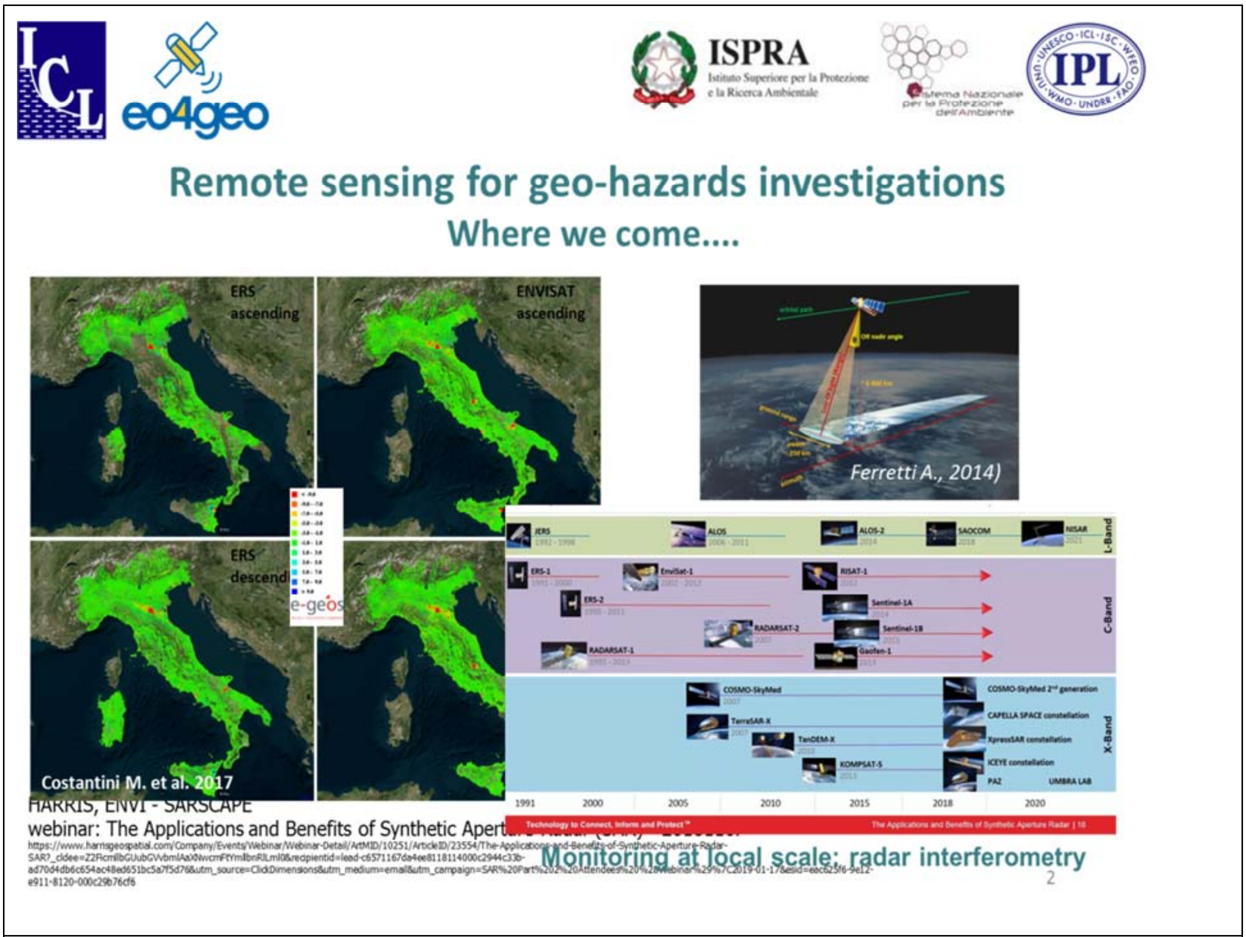
ISPRA
Istituto Superiore per la Protezione e la Ricerca Ambientale
Sistema Nazionale per la Protezione dell'Ambiente
IPL
Remote sensing for geo-hazards investigations
Where we come....
ERS ascending
ENVISAT ascending
ERS descend
e-geos
Costantini M. et al. 2017
Ferretti A., 2014)
JERS
ALOS
ALOS-2
SAOCOM
NISAR
L-Band
ERS-1
EnviSat-1
RISAT-1
ERS-2
Sentinel-1A
RADARSAT-2
Sentinel-1B
RADARSAT-1
Gaofen-1
C-Band
COSMO-SkyMed
COSMO-SkyMed 2nd generation
TerraSAR-X
CAPELLA SPACE constellation
TanDEM-X
XpressSAR constellation
KOMPSAT-5
ICEYE constellation
PAZ
UMBRA LAB
X-Band
1991
2000
2005
2010
2015
2018
2020
HARRIS, ENVI - SARSCAPE
webinar: The Applications and Benefits of Synthetic Apert
Monitoring at local scale: radar interferometry
2

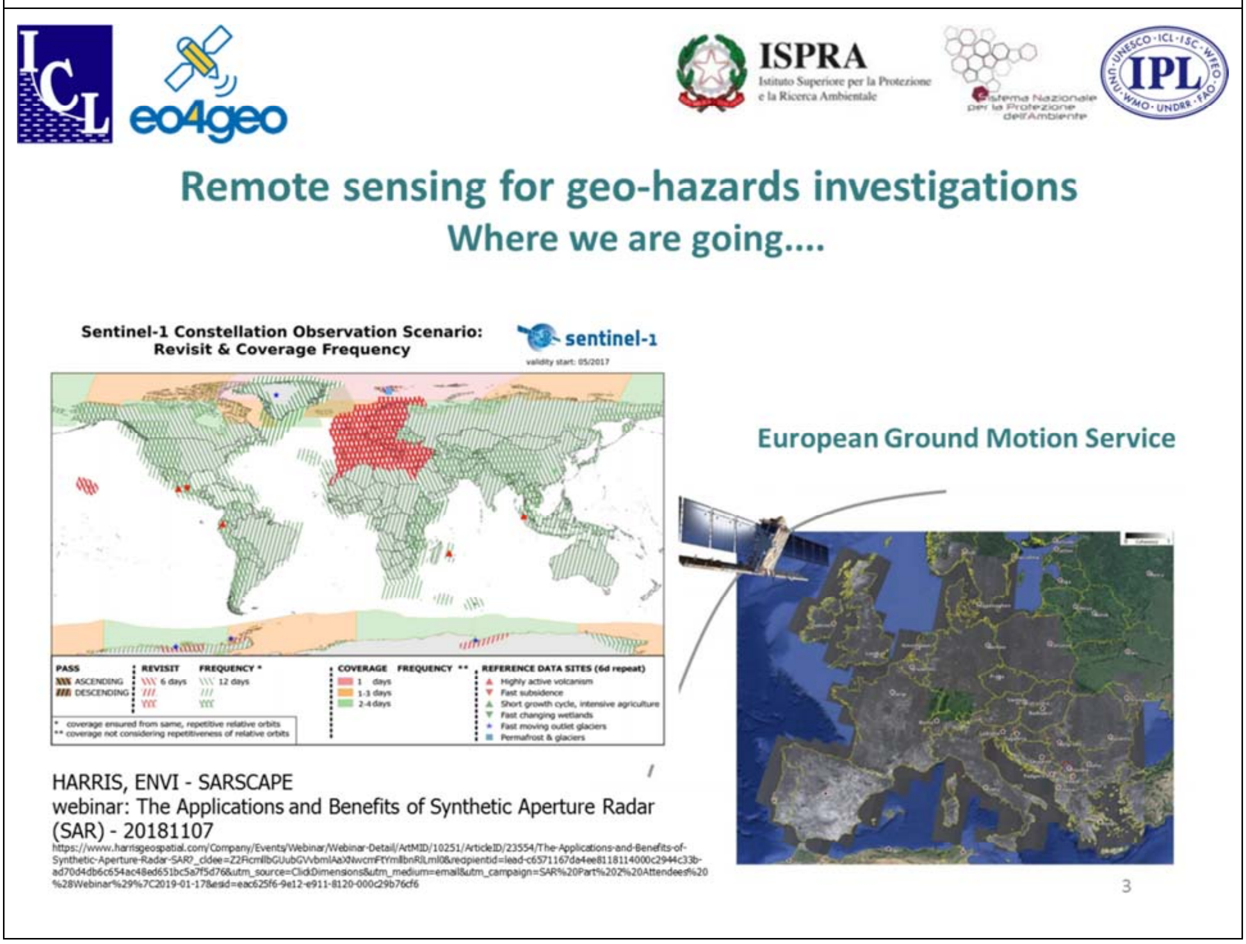
ISPRA
Istituto Superiore per la Protezione e la Ricerca Ambientale
Sistema Nazionale per la Protezione dell'Ambiente
IPL
Remote sensing for geo-hazards investigations
Where we are going....
Sentinel-1 Constellation Observation Scenario:
Revisit & Coverage Frequency
sentinel-1
validity start: 05/2017
European Ground Motion Service
HARRIS, ENVI - SARSCAPE
webinar: The Applications and Benefits of Synthetic Aperture Radar
(SAR) - 20181107
3

ISPRA
Istituto Superiore per la Protezione e la Ricerca Ambientale

Sistema Nazionale per la Protezione dell'Ambiente

EO4GEO Project

"Towards an innovative strategy for skills development and capacity building in the space geo-information sector supporting Copernicus User Uptake "

EO4GEO is an Erasmus+ Sector Skills Alliance gathering 26 partners from 12 countries from academia, private and public sector active in the education/training and space/geospatial sectors.

Duration: 4 years from January the 1st, 2018
Budget: 3,85 M€

Partnership: (from 16 EU Countries),
26 organisations + 22 (initially) Associated Partners
from Academia, Companies and networks, many of them Members of the Copernicus Academy Network

Addressed Copernicus Areas:
Integrated Applications, Smart Cities, Climate Change

4

ISPRA
Istituto Superiore per la Protezione e la Ricerca Ambientale

Sistema Nazionale per la Protezione dell'Ambiente

Data and services related to the space/geospatial sector **are still used in a sub-optimal way**

Bridge the skills gap between supply and demand of education and training in the **space/geospatial sector**

A lack of specialized technical and scientific skills impedes the uptake by private companies and other actors

Working in an multi- and interdisciplinary way and applying innovative solutions for its education and training actions including **case based and collaborative learning scenarios**

5

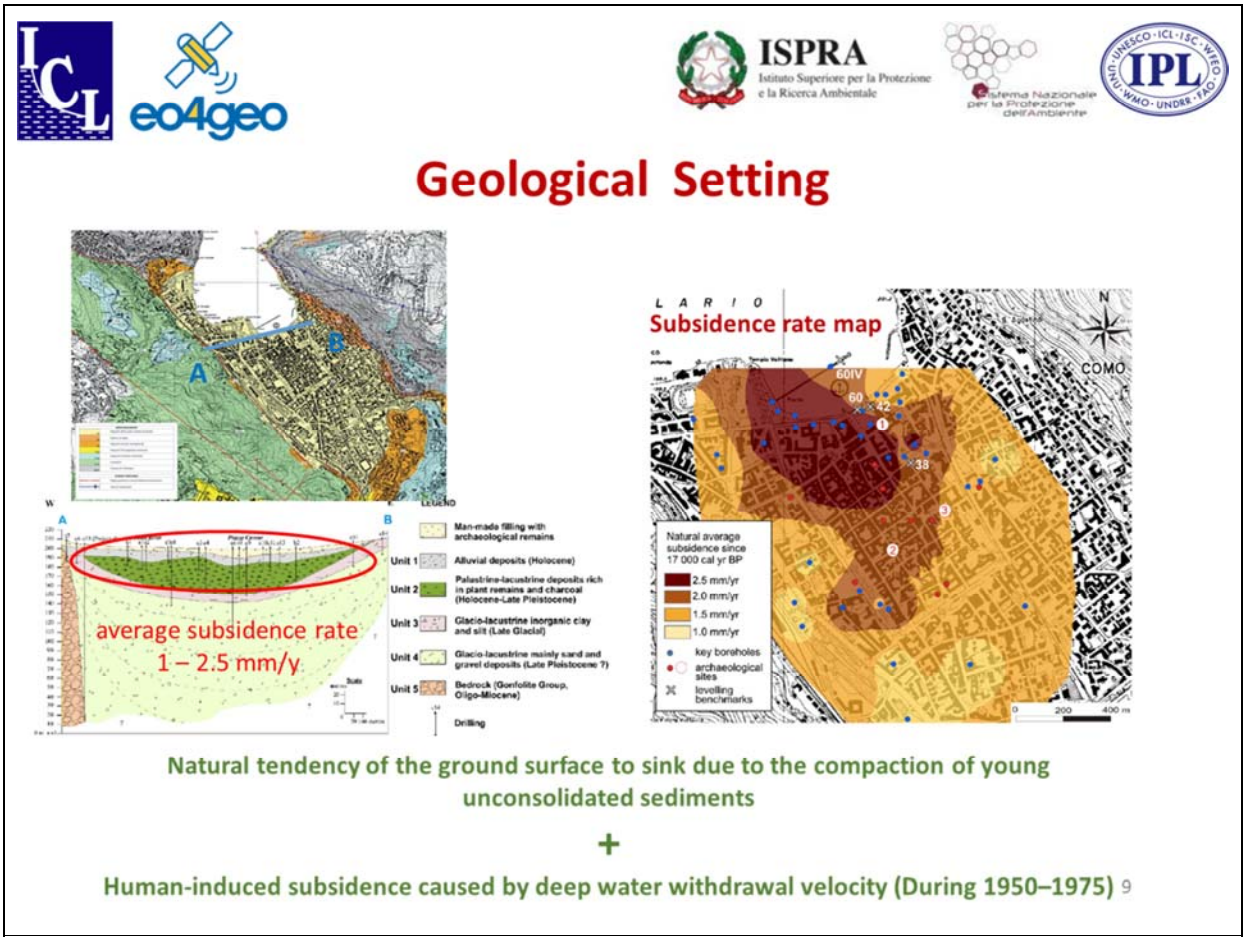
ICL
eo4geo
ISPRA
Istituto Superiore per la Protezione e la Ricerca Ambientale
Sistema Nazionale per la Protezione dell'Ambiente
UNESCO · ICL · ISC · WFEO · UNU · WMO · UNDRR · FAO
IPL
Geological Setting
A
B
LARIO
Subsidence rate map
COMO
N
60IV
60
42
38
Natural average subsidence since 17 000 cal yr BP
2.5 mm/yr
2.0 mm/yr
1.5 mm/yr
1.0 mm/yr
key boreholes
archaeological sites
levelling benchmarks
0 200 400 m
LEGEND
Man-made filling with archaeological remains
Unit 1 Alluvial deposits (Holocene)
Unit 2 Palustrine-lacustrine deposits rich in plant remains and charcoal (Holocene-Late Pleistocene)
Unit 3 Glacio-lacustrine inorganic clay and silt (Late Glacial)
Unit 4 Glacio-lacustrine mainly sand and gravel deposits (Late Pleistocene ?)
Unit 5 Bedrock (Gonfolite Group, Oligo-Miocene)
Drilling
average subsidence rate
1 – 2.5 mm/y
Natural tendency of the ground surface to sink due to the compaction of young unconsolidated sediments
+
Human-induced subsidence caused by deep water withdrawal velocity (During 1950–1975)
9

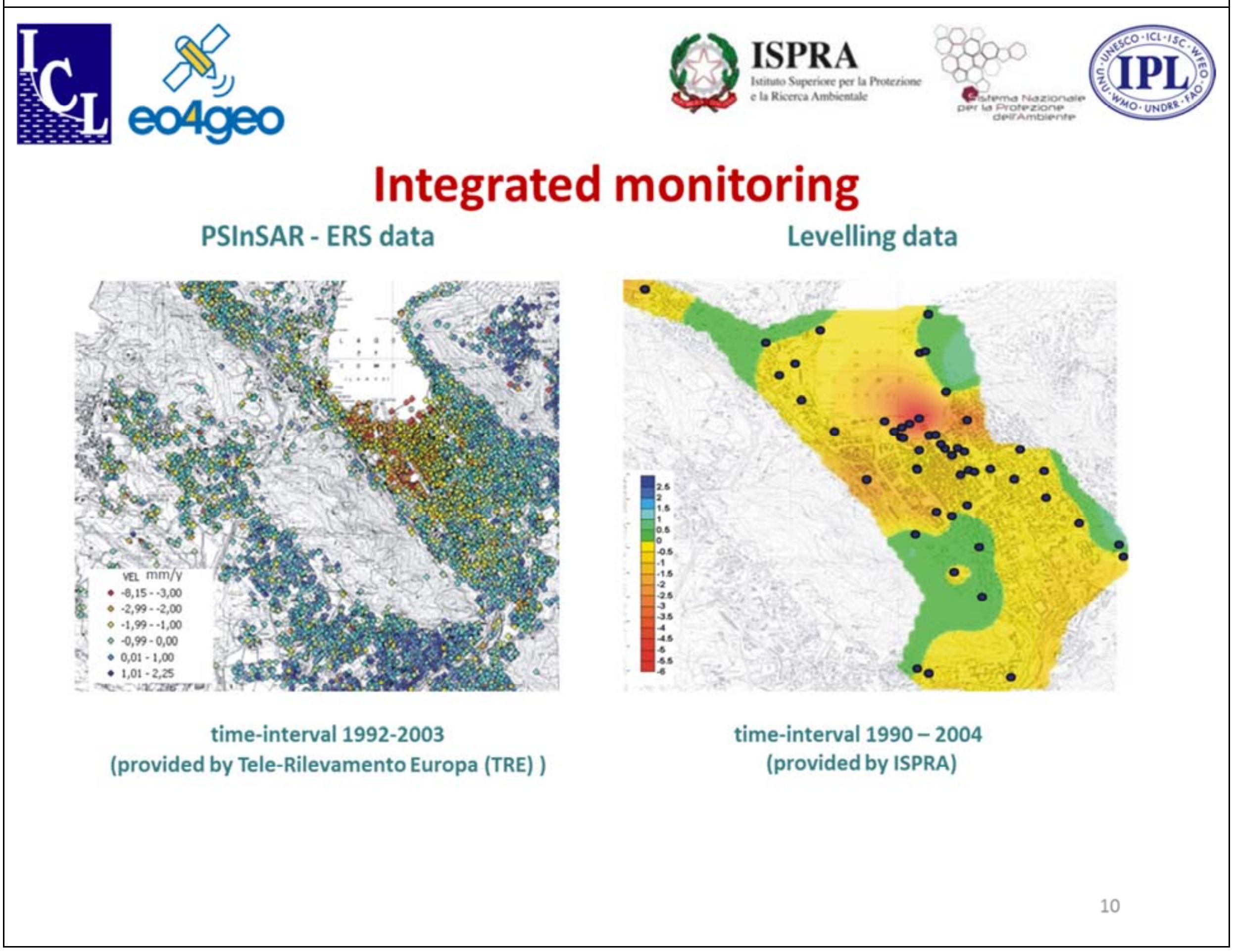
ICL
eo4geo
ISPRA
Istituto Superiore per la Protezione e la Ricerca Ambientale
Sistema Nazionale per la Protezione dell'Ambiente
UNESCO · ICL · ISC · WFEO · UNU · WMO · UNDRR · FAO
IPL
Integrated monitoring
PSInSAR - ERS data
Levelling data
VEL mm/y
-8,15 - -3,00
-2,99 - -2,00
-1,99 - -1,00
-0,99 - 0,00
0,01 - 1,00
1,01 - 2,25
2.5
2
1.5
1
0.5
0
-0.5
-1
-1.5
-2
-2.5
-3
-3.5
-4
-4.5
-5
-5.5
-6
time-interval 1992-2003
(provided by Tele-Rilevamento Europa (TRE))
time-interval 1990 – 2004
(provided by ISPRA)
10

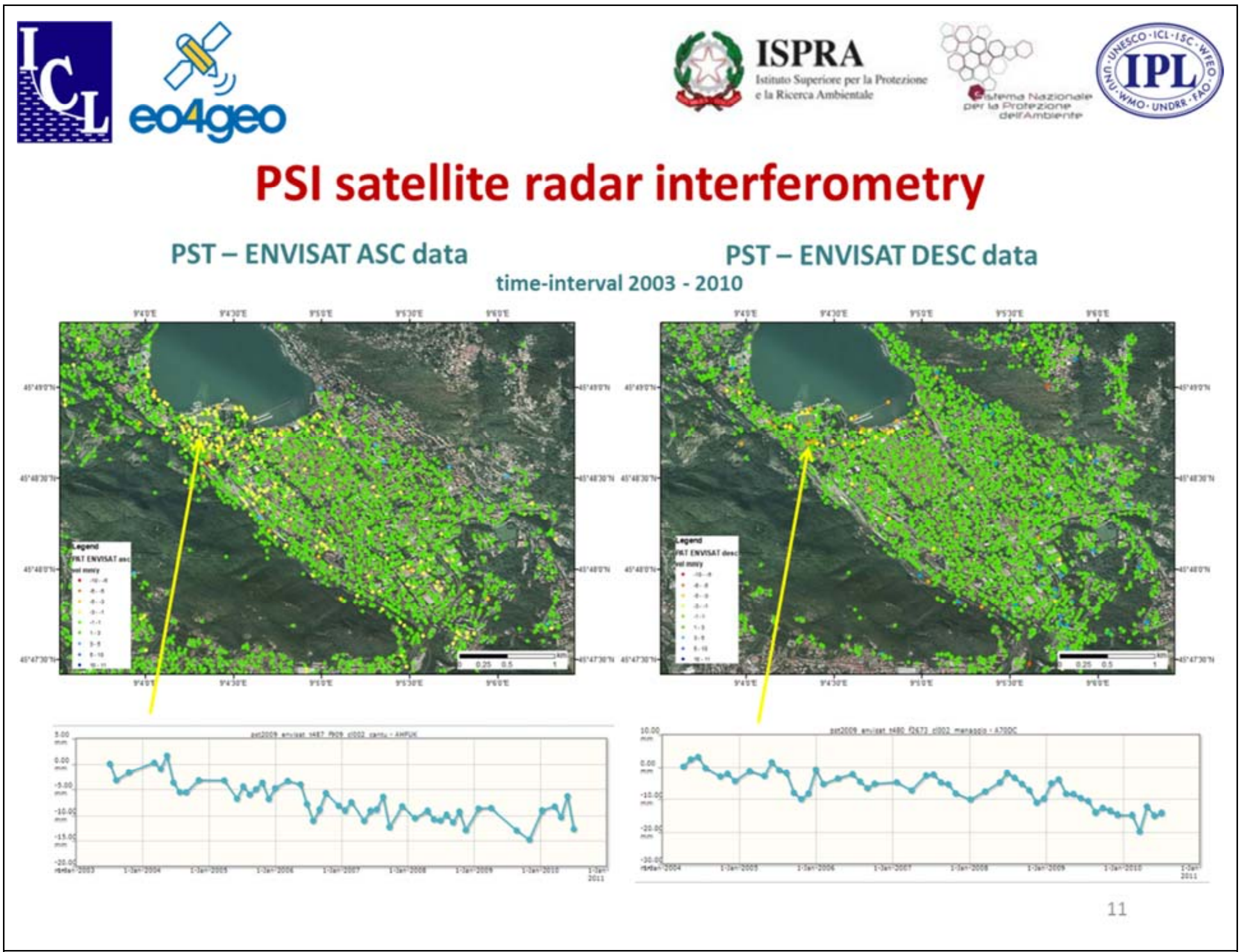
ISPRA
Istituto Superiore per la Protezione e la Ricerca Ambientale
Sistema Nazionale per la Protezione dell'Ambiente
eo4geo
IPL
PSI satellite radar interferometry
PST – ENVISAT ASC data
PST – ENVISAT DESC data
time-interval 2003 - 2010
11

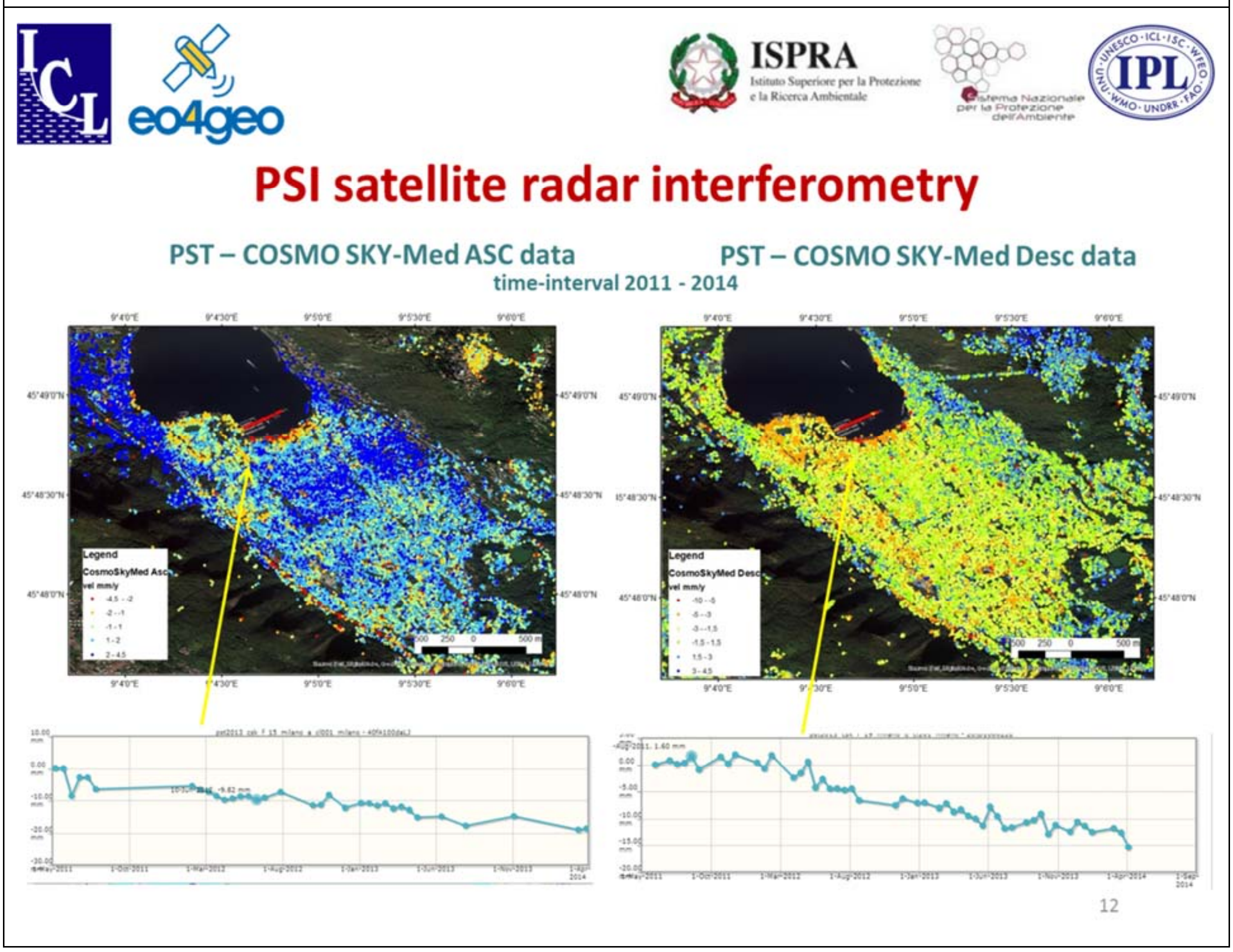
ISPRA
Istituto Superiore per la Protezione e la Ricerca Ambientale
Sistema Nazionale per la Protezione dell'Ambiente
eo4geo
IPL
PSI satellite radar interferometry
PST – COSMO SKY-Med ASC data
PST – COSMO SKY-Med Desc data
time-interval 2011 - 2014
Legend
CosmoSkyMed Asc
vel mm/y
Legend
CosmoSkyMed Desc
vel mm/y
12

ISPRA Istituto Superiore per la Protezione e la Ricerca Ambientale

Sistema Nazionale per la Protezione dell'Ambiente

Landslide affecting linear infrastructures

Case study : Petacciato, Italy

13

ISPRA Istituto Superiore per la Protezione e la Ricerca Ambientale

Sistema Nazionale per la Protezione dell'Ambiente

Geological and geomorphological setting

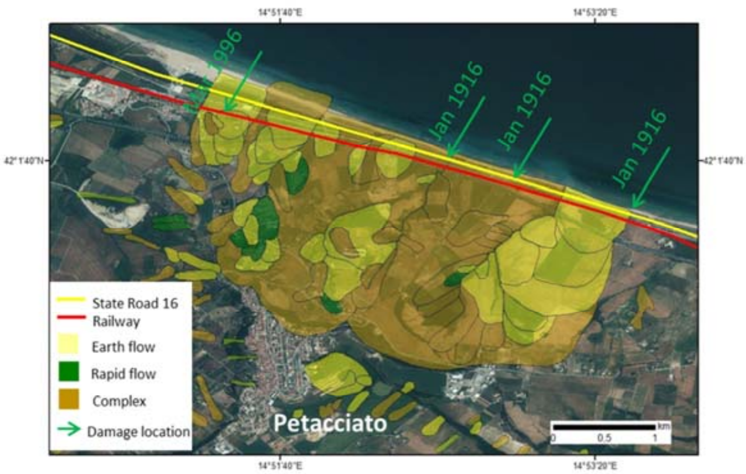

- Instability due to reactivation of landsliding ;
- very large piezometric levels at large depths in the slope;
- after the cut of a wood, intermittent landsliding started;
- fifteen main events have been recorded from1906 to 2015, in late winter–early spring;
- the largest movements occurred at the slope toe, damaging the railway and the motorway;
- retrogression of movements, reached the Petacciato village at the top within few days.

14

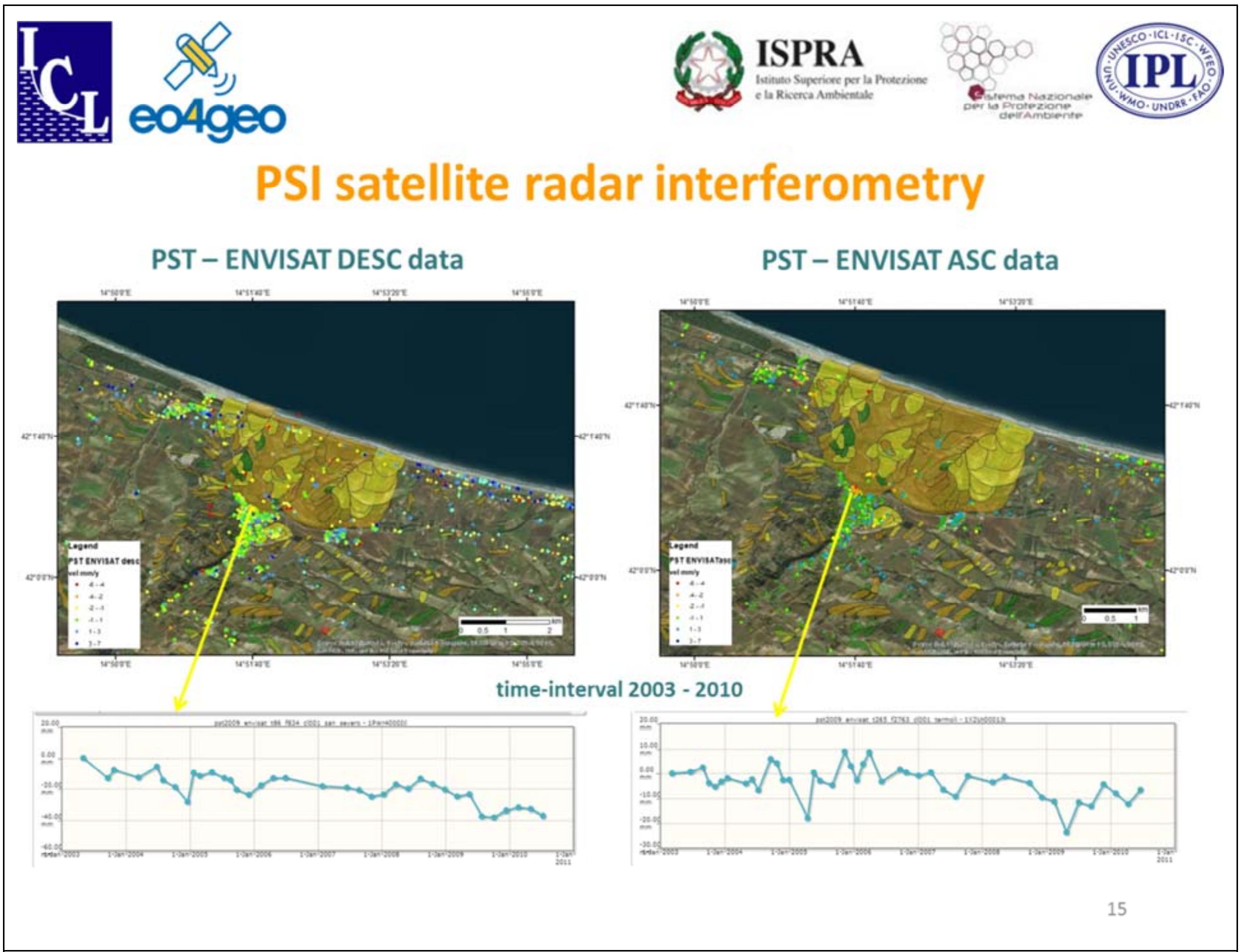

eo4geo
ISPRA
Istituto Superiore per la Protezione e la Ricerca Ambientale
Sistema Nazionale per la Protezione dell'Ambiente
IPL
UNESCO · ICL · ISC · WFEO · UNU · WMO · UNDRR · FAO
PSI satellite radar interferometry
PST – ENVISAT DESC data
PST – ENVISAT ASC data
time-interval 2003 - 2010
15

eo4geo
ISPRA
Istituto Superiore per la Protezione e la Ricerca Ambientale
Sistema Nazionale per la Protezione dell'Ambiente
IPL
UNESCO · ICL · ISC · WFEO · UNU · WMO · UNDRR · FAO
Landslide affecting cultural heritage sites
Case study: Baia Archaeological Park
Pozzuoli Gulf
Campi Flegrei
Baia
Baia Archaeological Park
Thermal bath
16

ICL
eo4geo
ISPRA
Istituto Superiore per la Protezione e la Ricerca Ambientale
Sistema Nazionale per la Protezione dell'Ambiente
IPL
Landslide affecting cultural heritage sites
business applications
esa
ARTEK - SATELLITE ENABLED SERVICES FOR PRESERVATION AND VALORISATION OF CULTURAL HERITAGE
ACTIVITY Demonstration Project
STATUS Ongoing
Source:http://artek.apps.nais-solutions.it/
GNSS
https://business.esa.int/projects/artek
17

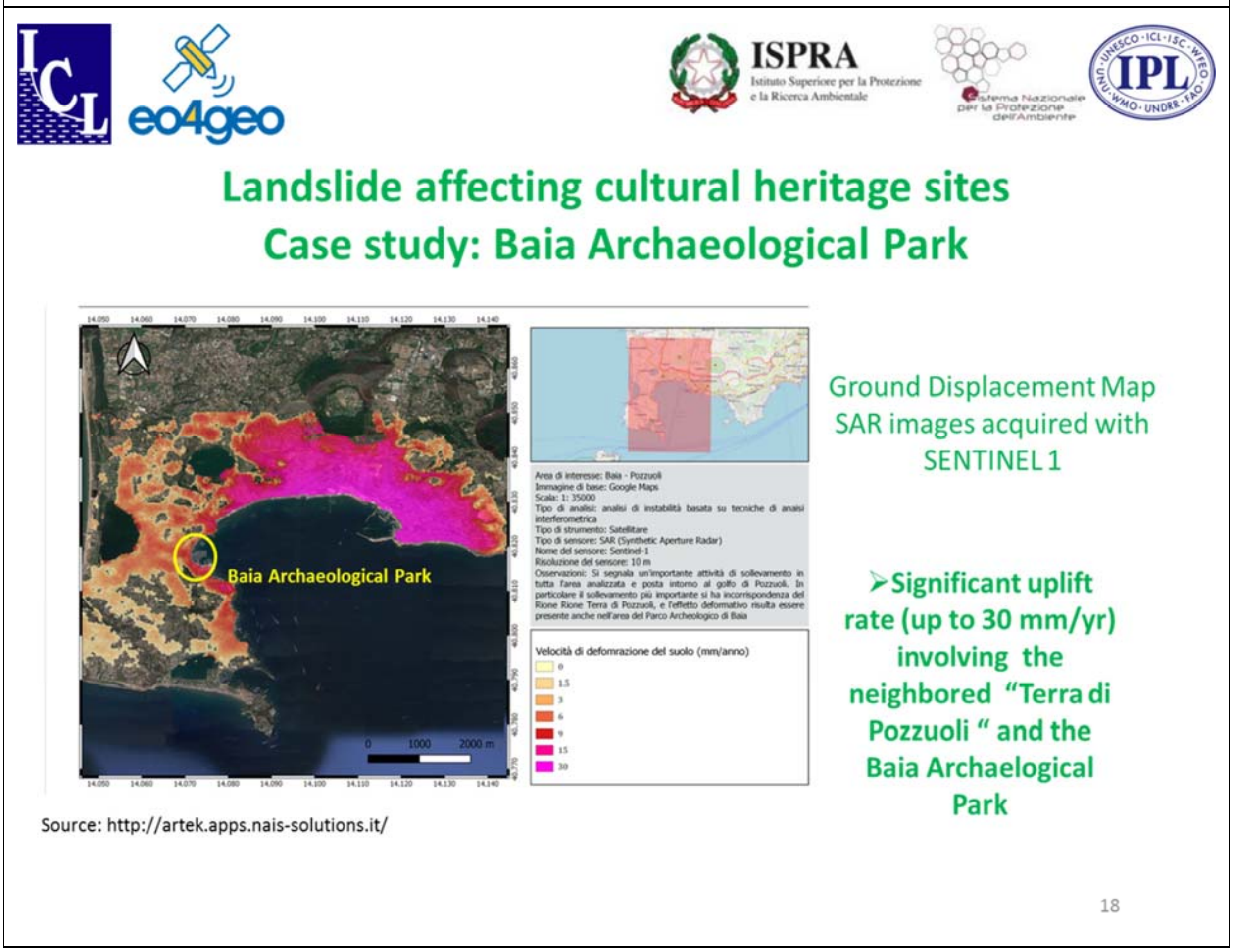

ICL
eo4geo
ISPRA
Istituto Superiore per la Protezione e la Ricerca Ambientale
Sistema Nazionale per la Protezione dell'Ambiente
IPL
Landslide affecting cultural heritage sites
Case study: Baia Archaeological Park
Baia Archaeological Park
0 1000 2000 m
Area di interesse: Baia - Pozzuoli
Immagine di base: Google Maps
Scala: 1: 35000
Tipo di analisi: analisi di instabilità basata su tecniche di anaisi interferometrica
Tipo di strumento: Satellitare
Tipo di sensore: SAR (Synthetic Aperture Radar)
Nome del sensore: Sentinel-1
Risoluzione del sensore: 10 m
Osservazioni: Si segnala un'importante attività di sollevamento in tutta l'area analizzata e posta intorno al golfo di Pozzuoli. In particolare il sollevamento più importante si ha incorrispondenza del Rione Rione Terra di Pozzuoli, e l'effetto deformativo risulta essere presente anche nell'area del Parco Archeologico di Baia
Velocità di defomrazione del suolo (mm/anno)
0
1.5
3
6
9
15
30
Ground Displacement Map SAR images acquired with SENTINEL 1
➢Significant uplift rate (up to 30 mm/yr) involving the neighbored "Terra di Pozzuoli " and the Baia Archaelogical Park
Source: http://artek.apps.nais-solutions.it/
18

Landslide affecting cultural heritage sites
Case study: Baia Archaeological Park

PST – ERS ASC data
time-interval 1993 - 2001

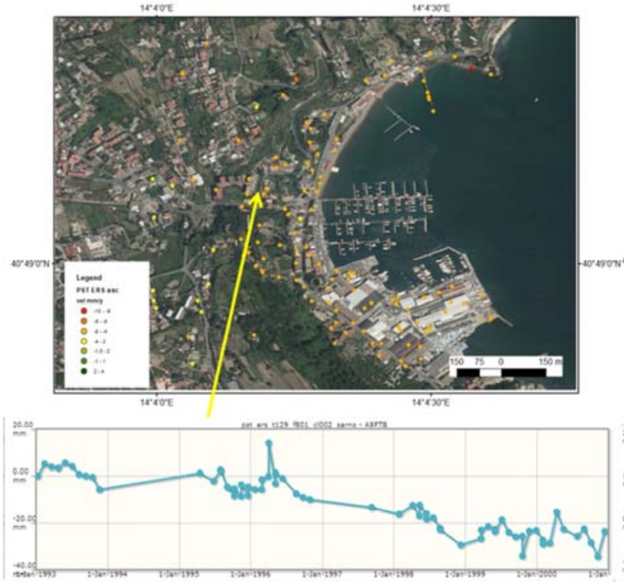

PST – CSK ASC data
time-interval 2011 - 2014

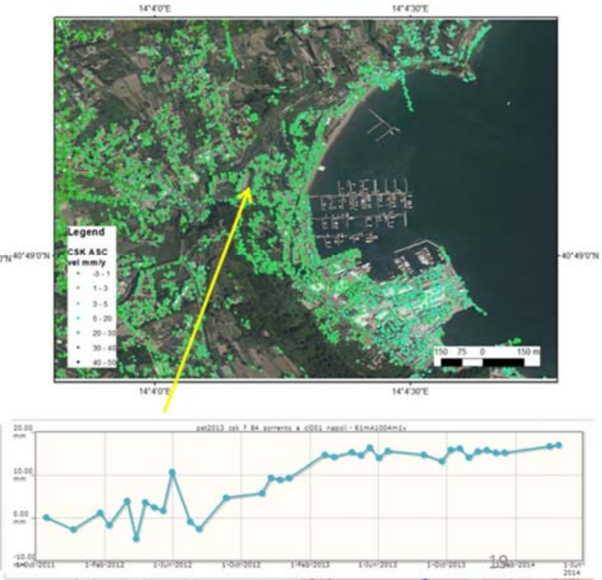

19

CONCLUSIONS

➢Development of a dynamic **collaborative platform** with associated **open tools**;

➢Conduct a series of **training actions** for the selected scenarios in different categories of exposed elements (e.g. linear infrastructure and transportation network, cultural heritage and urban areas);

➢define a standard methodology to use EO data and services favouring as much as possible open, accessible and free data, to carry out geo-hazard risk assessment, monitoring and mitigation

➢Dissemination and promotion EO4GEO project activities (e.g. International summer school, Copernicus academy, FPA)

20

Monitoring and modelling landslides at different scales

Settimio Ferlisi[(1)], Michele Calvello[(1)], Sabatino Cuomo[(1)], Dario Peduto[(1)], Maria Clorinda Mandaglio[(1)]

1) University of Salerno, Fisciano, Via Giovanni Paolo II 132
e-mail: scuomo@unisa.it

Abstract

GEG (Geotechnical Engineering Group) is part of the Department of Civil Engineering at the University of Salerno. It is a leading research group in Europe working on a number of boundary value problems involving natural geomaterials. Since a long time, special attention has been devoted to landslides triggered by extreme natural events, such as rainfall and earthquakes, which often produce serious human and economic consequences. Regarding this topic, GEG acquired a relevant expertise on: quantitative landslide risk assessment; landslide susceptibility and hazard zoning at different scales; numerical methods for modelling landslides; laboratory soil testing; local and regional early warning systems for the mitigation of the risk to life related to weather-induced landslides. Monitoring is another field of expertise, including the analysis, the interpretation and the assimilation within advanced geotechnical models of displacement measurements deriving from the processing of innovative spaceborne sensor images. Thus, GEG has been proposing novel scientific contributions in a number of topics such as: landslides, monitoring, modelling and early-warning.

The Geotechnical Engineering Group – UniSa (Salerno, Italy)

Currently the **Geotechnical Engineering Group** counts: 5 associate professors, 2 technicians, 3 post-doc fellows, 5 PhD students.

Ranked as **the first group in ITALY** (ANVUR VQR: 2004-2010, 2011-2014) for research quality in geotechnical engineering (National Agency for the Evaluation of University and Research Institutes.

Group picture

Laboratory activities

The Geotechnical Engineering Group: teaching activities

Bachelor degrees: Civil Engineering; Civil and Environmental Engineering

- ✓ Soil Mechanics (Prof. Michele Calvello, Prof. Maria Clorinda Mandaglio)

Master degrees: Civil Engineering; Environmental and Land Management Engineering

- ✓ Geotechnics (Prof. Sabatino Cuomo)
- ✓ Foundations (Prof. Settimio Ferlisi)
- ✓ Retaining walls (Prof. Dario Peduto)
- ✓ Slope stability (Prof. Maria Clorinda Mandaglio)
- ✓ Landslide risk (Prof. Michele Calvello)

Bachelor + Master degree in Building and Architectural Engineering

- ✓ Geotechnics (Prof. Settimio Ferlisi)

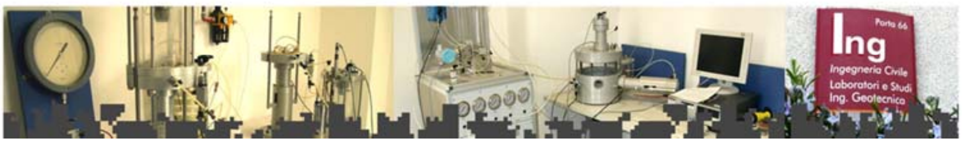

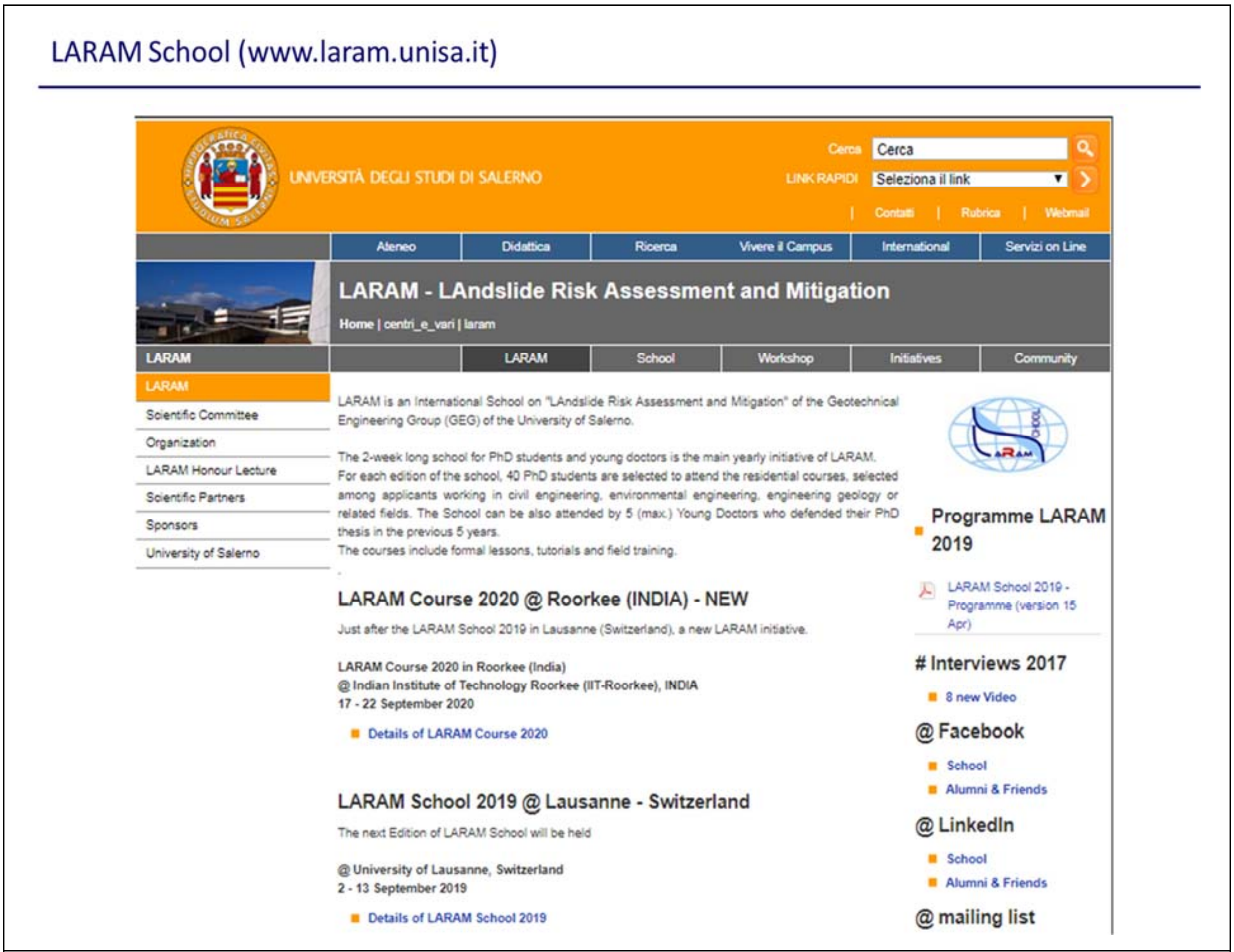
LARAM School (www.laram.unisa.it)
UNIVERSITÀ DEGLI STUDI DI SALERNO
Cerca
Cerca
LINK RAPIDI
Seleziona il link
Contatti | Rubrica | Webmail
Ateneo
Didattica
Ricerca
Vivere il Campus
International
Servizi on Line
LARAM - LAndslide Risk Assessment and Mitigation
Home | centri_e_vari | laram
LARAM
LARAM
School
Workshop
Initiatives
Community
LARAM
Scientific Committee
Organization
LARAM Honour Lecture
Scientific Partners
Sponsors
University of Salerno
LARAM is an International School on "LAndslide Risk Assessment and Mitigation" of the Geotechnical Engineering Group (GEG) of the University of Salerno.
The 2-week long school for PhD students and young doctors is the main yearly initiative of LARAM. For each edition of the school, 40 PhD students are selected to attend the residential courses, selected among applicants working in civil engineering, environmental engineering, engineering geology or related fields. The School can be also attended by 5 (max.) Young Doctors who defended their PhD thesis in the previous 5 years.
The courses include formal lessons, tutorials and field training.
LARAM Course 2020 @ Roorkee (INDIA) - NEW
Just after the LARAM School 2019 in Lausanne (Switzerland), a new LARAM initiative.
LARAM Course 2020 in Roorkee (India)
@ Indian Institute of Technology Roorkee (IIT-Roorkee), INDIA
17 - 22 September 2020
Details of LARAM Course 2020
LARAM School 2019 @ Lausanne - Switzerland
The next Edition of LARAM School will be held
@ University of Lausanne, Switzerland
2 - 13 September 2019
Details of LARAM School 2019
Programme LARAM 2019
LARAM School 2019 - Programme (version 15 Apr)
Interviews 2017
8 new Video
@ Facebook
School
Alumni & Friends
@ LinkedIn
School
Alumni & Friends
@ mailing list


LARAM School (www.laram.unisa.it)
Scientific Committee
David Alexander
University College London, UK
Eduardo Alonso
UPC, Barcelona, Spain
Zeliko Arbanas
University of Rijeka, Croatia
Michele Calvello
Università di Salerno, Italy
Nicola Casagli
Università degli Studi di Firenze, Italy
Leonardo Cascini (President)
Università di Salerno, Italy
Federica Cotecchia
Politecnico di Bari, Italy
Giovanni B. Crosta
Università Milano-Bicocca, Italy
Sabatino Cuomo
Università di Salerno, Italy
Claudio Di Prisco
Politecnico di Milano, Italy
Settimio Ferlisi
Università di Salerno, Italy
Alessio Ferrari
EPFL Lausanne, Switzerland
Thomas Glade
University of Vienna
Michel Jaboyedoff
Unisciences, Switzerland
Susanne Lacasse
NGI, Norway
Eric Leroi
URBATER, Roquevaire, France
Olga Mavrouli
University of Twente, Netherlands
Farrokh Nadim
International Centre for Geohazards, Oslo
Manuel Pastor
Universidad Politecnica de Madrid
Dario Peduto
Università di Salerno, Italy
Luciano Picarelli
Università "Luigi Vanvitelli", Italy
Robert Supper
Geologische Bundesanstalt für Österreich, Austria
Prof. Sivakumar Babu
Indian Institute of Science, India
Prof. Robin Fell
University of New South Wales, Australia
Prof. Dominic Lo
Hong Kong Geotechnical Engineering Office, China
Prof. Charles Ng
University of Science and Technology, China
Prof. Andy Take
Queen's University, Canada
Prof. Binod Tiwari
California State University, USA
Prof. Fawu Wang
Shimane University, Japan

LARAM School (www.laram.unisa.it) – since **2006**

News/Kyoto Commitment

Leonardo Cascini · Michele Calvello · Sabatino Cuomo · Michel Jaboyedoff · Dario Peduto

Landslides (2019) 16:1419–1421
DOI 10.1007/s10346-019-01193-9
Published online: 11 May 2019
© Springer-Verlag GmbH Germany part of Springer Nature 2019

LARAM School 2019: the yearly doctoral school on "LAndslide Risk Assessment and Mitigation"

LARAM

The International School on "LAndslide Risk Assessment and Mitigation" (LARAM) (http://www.laram.unisa.it) was founded at the University of Salerno in 2005 by Prof. Leonardo Cascini, who served as the Director of the School from 2005 to 2017, within the geotechnical engineering research group of the Department of Civil Engineering. The main objectives of LARAM are to develop high educational interdisciplinary programs for assessing, forecasting, and mitigating landslide risk at different scales and to promote the creation of training programs aimed at solving real landslide risk problems using the most advanced theories and methodologies in the fields of geotechnical engineering, geomechanics, geology, physical geography, mathematical modelling, monitoring, GIS techniques, risk management, and other relevant topics. These aims are achieved by means of yearly cycles of lectures, seminars, workshops, and conferences. The main yearly initiative of LARAM is the 2-week-long doctoral (http://www.laram.unisa.it/laram/sc_committee). The LARAM Scientific Committee, composed of esteemed experts in topics related to landslide risk, is renewed every 3 years. The Committee has always been very international with a majority of members having an expertise in the fields of geotechnical engineering or engineering geology. Before each edition of the doctoral school, the Scientific Committee sets the criteria for the students' selection and defines contents of the courses and lecturers, which are typically chosen among Committee members. Table 1 shows the current members of the Committee, in charge from 2018 to 2020.

LARAM School 2019

The 2019 edition of the LARAM School will be hosted by the University of Lausanne, Switzerland, from 2 to 13 September 2019 (Fig. 3). The LARAM class will be composed of 40 selected PhD students and up to five young doctors. The deadline for applications is May 31, 2019. Participants pay their own travel and accommodation

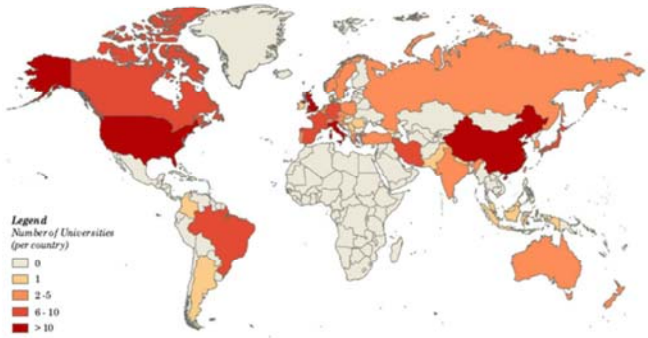

Fig. 1 Number of Universities per country providing the LARAM doctoral school with PhD students from 2006 to 2018

Landslides 16 • (2019) | 1419

Geotechnical Engineering Group - Salerno: Research Topics

- Unsaturated soil testing
- Landslide susceptibility, hazard and risk analysis and zoning (@different scales)
- DInSAR applied to slow-moving landslides and subsidence
- Early warning systems for rainfall-induced landslides
- Geosynthetics for soil reinforcement and protection structures
- Numerical modelling and inverse analysis of landslides
- Geotechnics for urban planning and land use management (@ different scales)

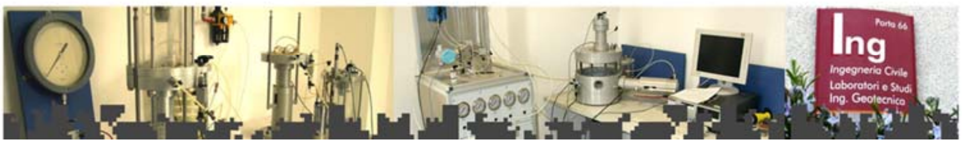

Unsaturated soil testing

Volumetric Pressure Plate Extractor

Suction-controlled Oedometer

Suction-controlled Direct shear

Richards Plate

Unsaturated Stress Path Triaxial Cell

Suction-controlled Simple shear

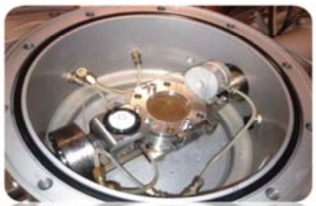

Soil mechanical behaviour

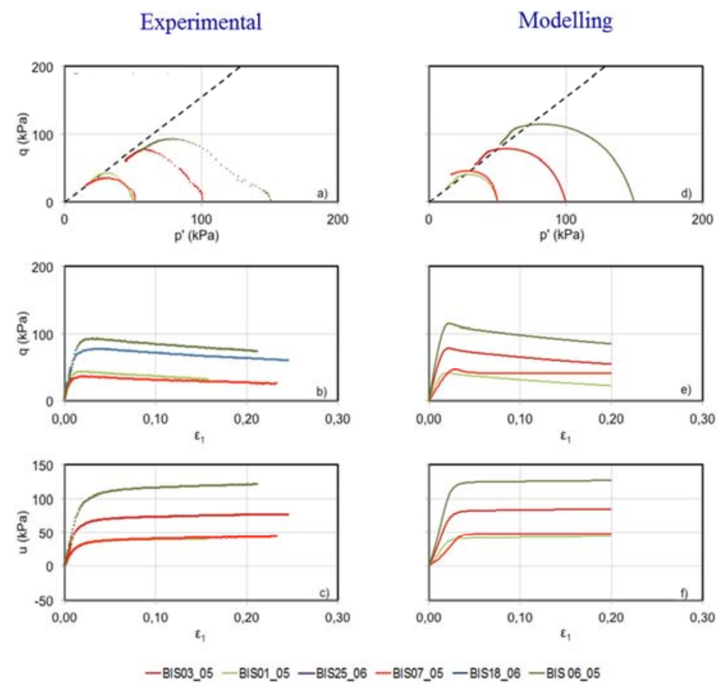

Cuomo, S., Moscariello, M., Manzanal, D., Pastor, M., & Foresta, V. (2018). Modelling the mechanical behaviour of a natural unsaturated pyroclastic soil within generalized plasticity framework. *Computers and Geotechnics*, *99*, 191-202.

Slope stability

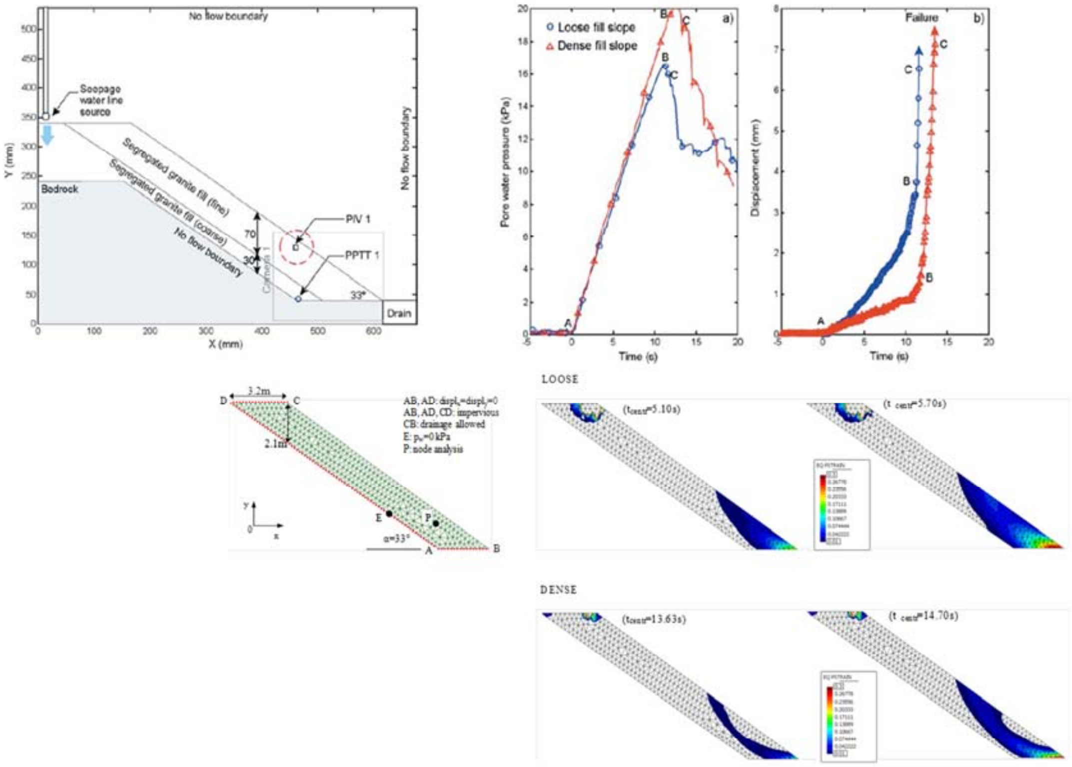

Cascini, L., Cuomo, S., Pastor, M., & Sacco, C. (2013). Modelling the post-failure stage of rainfall-induced landslides of the flow type. Canadian Geotechnical Journal, 50(9), 924-934.

Propagation

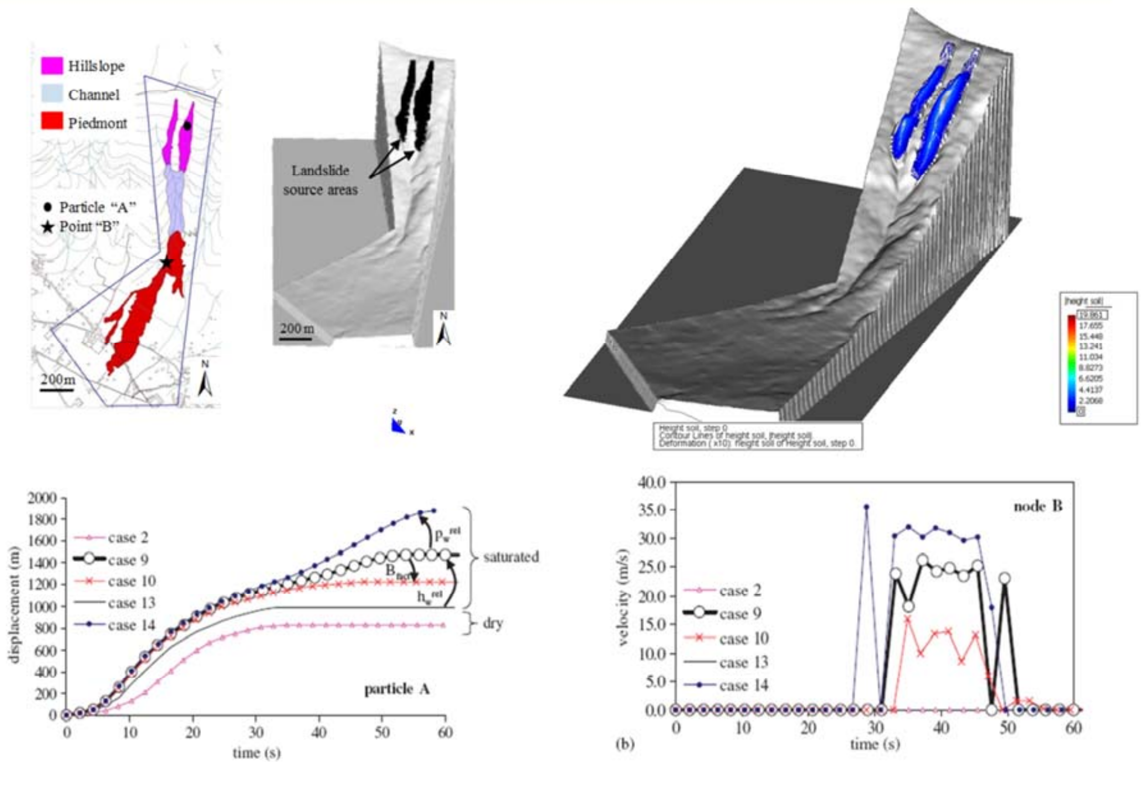

Cuomo S., Pastor M., Cascini L., Castorino G.C. (2014). Interplay of rheology and entrainment in debris avalanches: a numerical study. Canadian Geotechnical Journal

Inverse analysis of landslide propagation

Procedure: debris flow propagation modelling

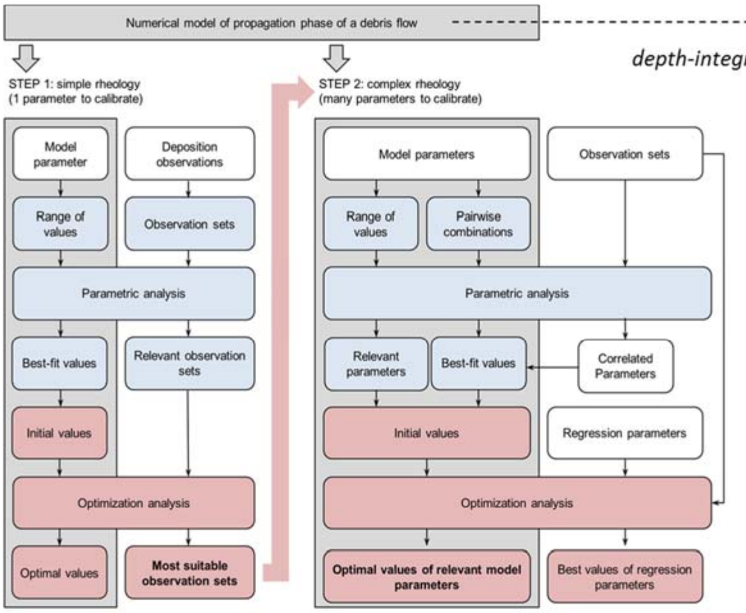

GeoFlow_SPH (Pastor et al. 2009)

depth-integrated hydro-mechanical coupled model

STEP 1

Simple rheology:
mixed-phase material

$$\tau_b = -\rho g h \cdot tan\phi_b \cdot \mathrm{sgn}(\overline{v})$$

STEP 2

Complex rheology:
two-phase model

$$\frac{dp_w^b}{dt} = \frac{\pi^2}{4h^2} c_v p_w^b$$

$$\tau_b = -(\rho g h - p_w^b) \cdot tan\phi_b \cdot \mathrm{sgn}(\overline{v})$$

Inverse analysis by non-linear regression with gradient-based algorithm (UCODE)

Calvello M, Cuomo S, Ghasemi P (2017). The role of observations in the inverse analysis of landslide propagation. Computers and Geotechnics. 92:11-21.

The role of observations

Step 1:

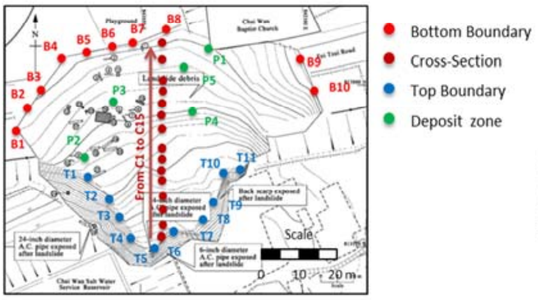

Parametric analysis

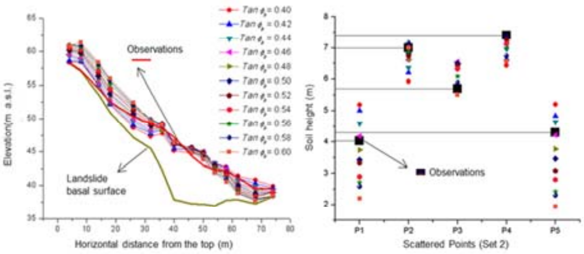

Table 1
Sets of observations used for model calibration.

No	Observations	Description of deposition height observations
1	C1 to C15	15 points along main cross section
2	P1 to P5	5 characteristic points in the deposition zone
3	B1 to B10	10 points along bottom boundary of deposition zone
4	T1 to T10	10 points along topmost boundary of the displaced mass
5	B1 to B10, T1 to T10	Set 3 + Set 4
6	B1 to B10, P3	Set 3 + one characteristic point (max height)
7	B1 to B10, P1	Set 3 + one characteristic point (building)
8	T1 to T10, P3	Set 4 + one characteristic point (max height)
9	T1 to T10, P1	Set 4 + one characteristic point (building)
10	B1 to B10, P1, P3	Set 3 + two characteristic points (max height, building)
11	B1 to B10, T1 to T10, P3	Set 3 + Set 4 + one characteristic point (max height)
12	B1-3-5-7-9, T1-3-5-7-9, P3	5 points from Sets 3 and 4 + one characteristic point (max height)
13	All	Set 1 + Set 2 + Set 3 + Set 4

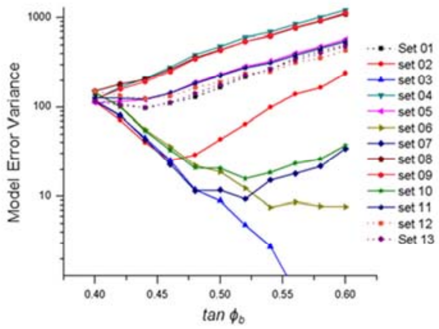

Calvello M, Cuomo S, Ghasemi P (2017). The role of observations in the inverse analysis of landslide propagation. Computers and Geotechnics. 92:11-21.

Calibration and vaildation

Step 2:

Study 2	Study 3	Study 4
Two-phase model	Two-phase model	Two-phase model
Frictional (Eqs. (2) and (3))	Frictional (Eqs. (2) and (3))	Frictional (Eqs. (2) and (3))
4	4	4
0.45, 0.50, 0.55, 0.60, 0.65, 0.70, 0.75	0.45, 0.50, 0.55, 0.60, 0.65, 0.70, 0.75	0.45, 0.50, 0.55, 0.60, 0.65, 0.70, 0.75
0.001, 0.005, 0.01, 0.05, 0.10	0.01	0.01
0.1	0.01, 0.05, 0.10, 0.15, 0.20	0.1
0.33	0.33	0.074, 0.14, 0.33, 0.44, 0.51
35	35	35

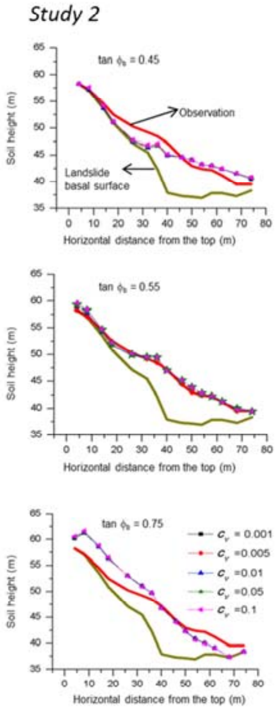

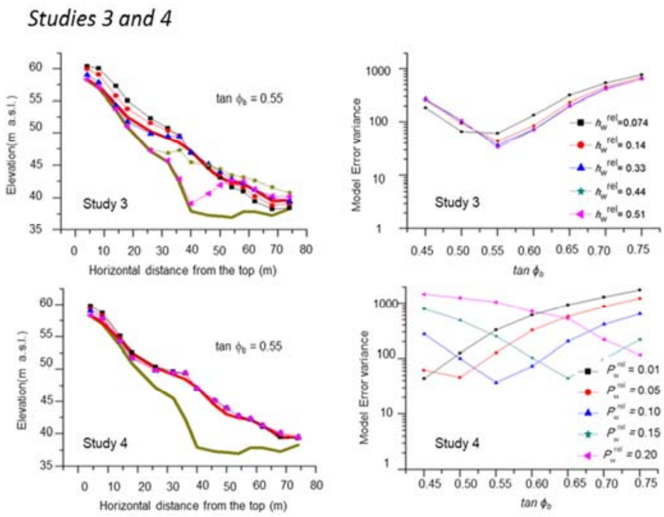

Calvello M, Cuomo S, Ghasemi P (2017). The role of observations in the inverse analysis of landslide propagation. Computers and Geotechnics. 92:11-21.

Slow moving landslides: diffusion, stages and displacement trends

Landslide in Italy IFFI project, 2007)

Slow moving landslides in Benevento Province (AdBN LGV, 2001)

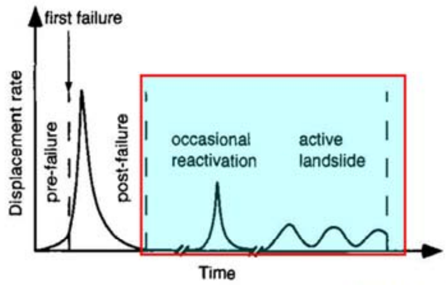

LEROUEIL ET AL. (1996)

Analysis of case studies at slope scale (Cascini et al., 2014)

COROMINAS ET AL. (2005); ANGELI ET AL. (1996); COMEGNA (2004); LOLLINO ET AL. (2006); SIMEONI ET AL. (2007); TOMMASI ET AL. (2006); TOMMASI ET AL. (2006); BERTINI ET AL. (1986); SHUZUI (2001)

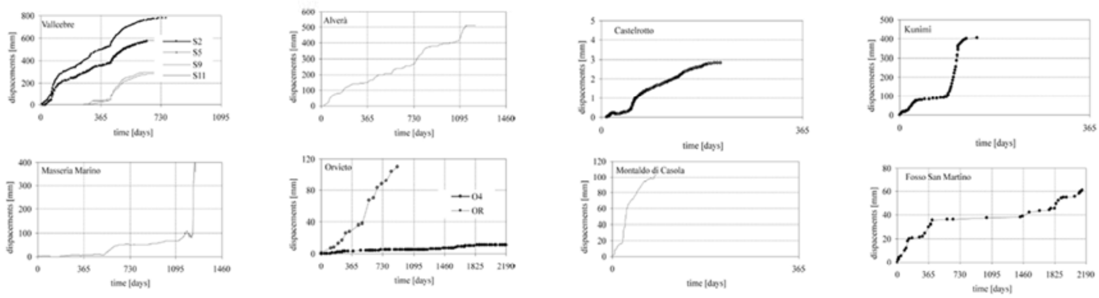

Cascini, L., Calvello, M., Grimaldi, G.M. (2014). Displacement trends of slow-moving landslides: classification and forecasting. Journal of Mountain Science, 11(3): 592-606.

Susceptibility zoning of shallow landslides in fine grained soils by statistical methods (1/2)

Procedure

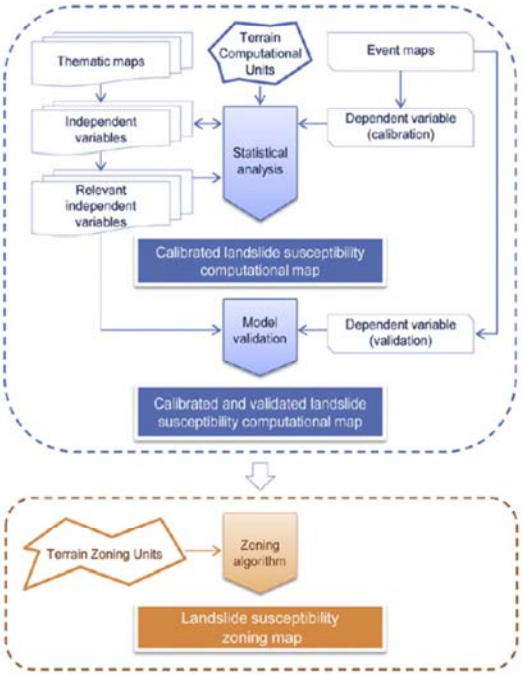

Fig. 1. Procedure to produce landslide susceptibility zoning maps at medium (1:25,000) and large (1:5000) scale.

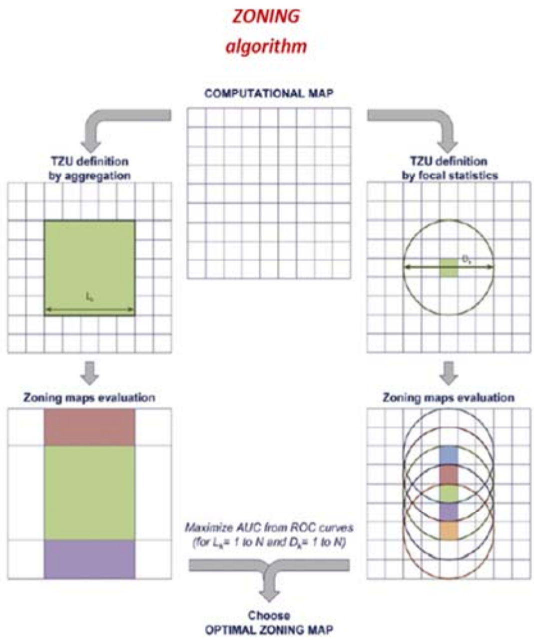

Fig. 2. Algorithm employed to optimise the size of the terrain units for landslide susceptibility zoning (TZUs).

Ciurleo M, Calvello M, Cascini L (2016). Susceptibility zoning of shallow landslides in fine grained soils by statistical methods. Catena, 139:250-264.

Susceptibility zoning of shallow landslides in fine grained soils by statistical methods (2/2)

Example: analysis at 1:5000 scale

Susceptibility computational map

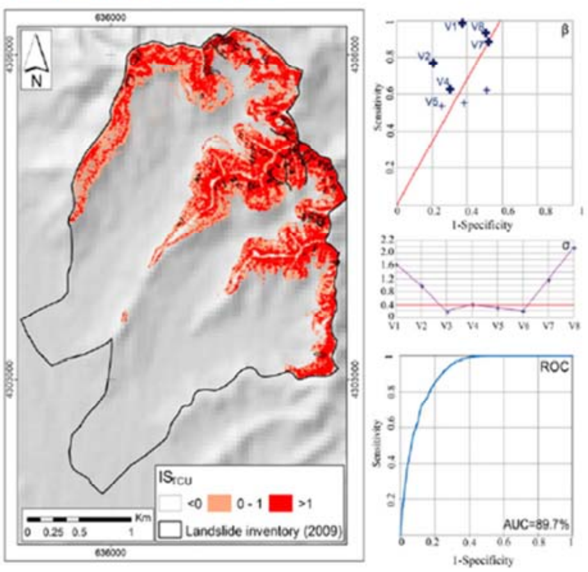

Fig. 12. Results of the statistical analysis at large scale: landslide susceptibility computational map; graphical representation of the bivariate success indexes, β_i, and bivariate standard deviation index of the normalized weights, σ_i; receiver operating characteristic curve.

Model validation

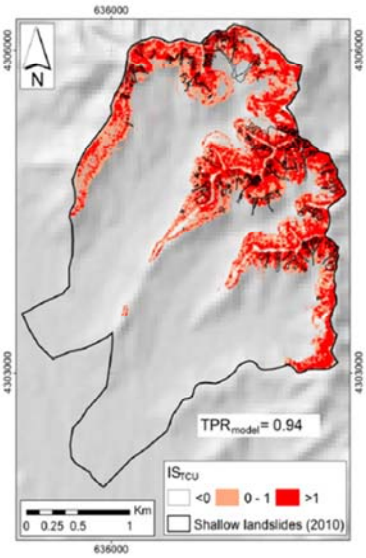

Ciurleo M, Calvello M, Cascini L (2016). Susceptibility zoning of shallow landslides in fine grained soils by statistical methods. Catena, 139:250-264.

Forecasting slow-moving landslides displacements over wide areas

Application of DInSAR techniques

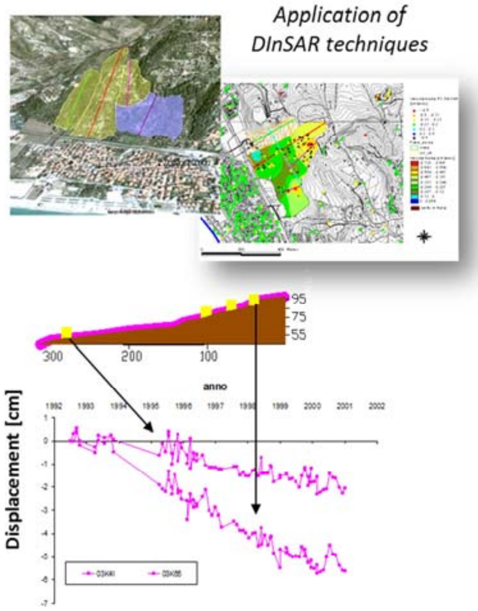

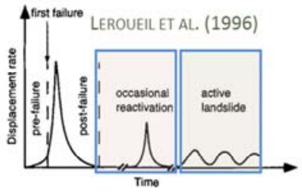

A framework for landslide displacements

$$D_i(t_j) = T_i(t_j)^x$$

x=1 Trend type I
x<1 for Trend type II
x>1 for Trend type III

CASCINI ET AL. (2014)

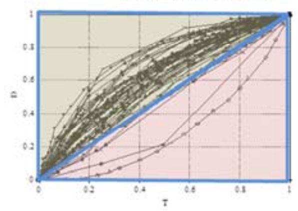

Trend type II forecasting

$$T_1 = \frac{t - t_{ref}}{\Delta t_{ref}}$$

$$d(t) = d_1 + \Delta t_{ref}\, M \left[\left(\frac{t - t_1}{\Delta t_{ref}} + 1 \right)^{\frac{v_{max}}{M}} - 1 \right]$$

$$v(t) = v_{max} \left(\frac{t - t_1}{\Delta t_{ref}} + 1 \right)^{\frac{v_{max}}{M} - 1}$$

t_{ref} reference time;
v_{max} measured velocity for T_1=1;
d_1=d(v_{max}) measured displacement for T_1=1;
t_1=t(v_{max}) measured time for T_1=1.

Cascini L, Calvello M, Grimaldi GM (2014). Displacement trends of slow-moving landslides: classification and forecasting. Journal of Mountain Science, 11(3): 592-606.

DInSAR techniques

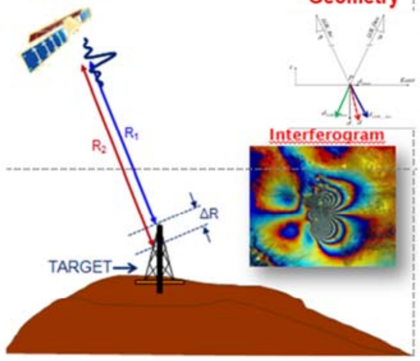

Main targets

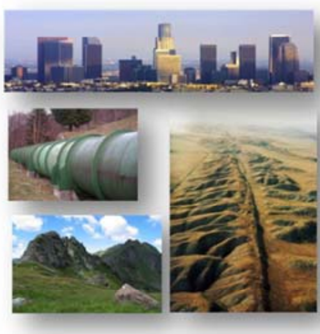

Alghoritms

- Permanent Scatterers (PS) (Ferretti et al., 2000;
- Small BAseline Subset (SBAS) (Berardino et al., 2002);
- Coherent Point Target Analysis (CPTA) (Mora et al., 2003);
- Interferometric Point Target Analysis (IPTA) (Wegmuller, 2003)
- Enhanced Spatial Differences (ESD) (Fornaro et al., 2007)
- Multi- Dimensional Imaging tecnique (Fornaro et al., 2009)

Sensors

Sensor	Band	Maximum measurable desplacement [cm/year ca.]	Incidence angle [°]	Revisiting time [days]	Archive	Resolution [m x m]
ERS	C	15	23	35	1992-2001	20x5
RADARSAT -1	C	21	10-59	24	1995-	10x5
RADARSAT -2	C	21	10-59	24	1997 up to now	10x5
J-ERS1	L	50	35	44	1992-1998	18x18
ALOS	L	47	18-43	46	2006-2011	16x16
ENVISAT	C	15	15-33	35	2002-2011	20x5
TerraSAR-X	X	35	—	8	2008- -	Up to 1x1
COSMOSky - Med	X	25	—	11	2008- -	Up to 1x1

Remote Sensing Extraordinary Plan (1992-2010)

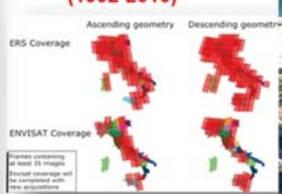

Podis-Tellus project Regione Campania

Perspective

3D displacement

DInSAR techniques to monitor subsidence phenomena: the Sarno case study

Comparison beetweern displacement map derived by topographic measures and DInSAR data

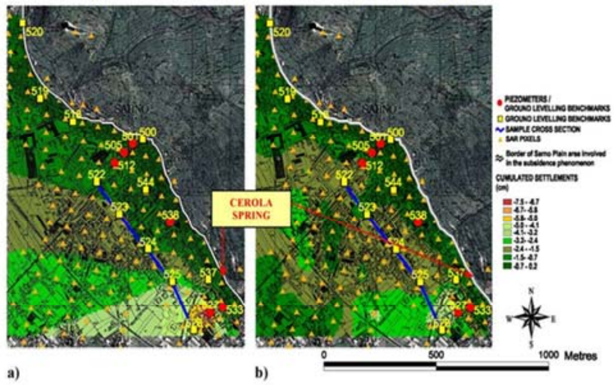

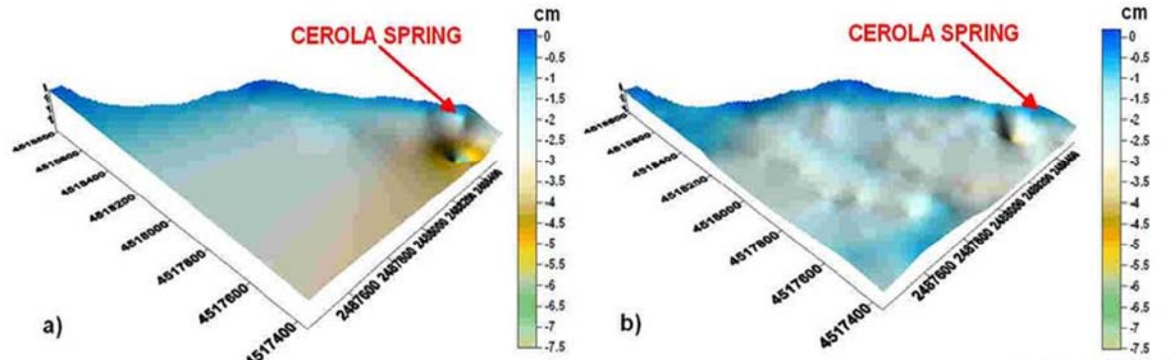

a) Topographic measures(July1992-October 1993)

b) dati SAR (June 1992- Novemb 1993).

Cascini et al. (2006)

Fast moving landslides: risk assessment

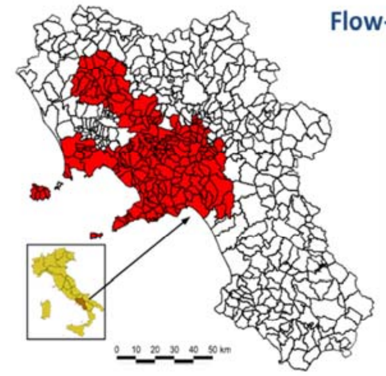

Flow-type landslides...

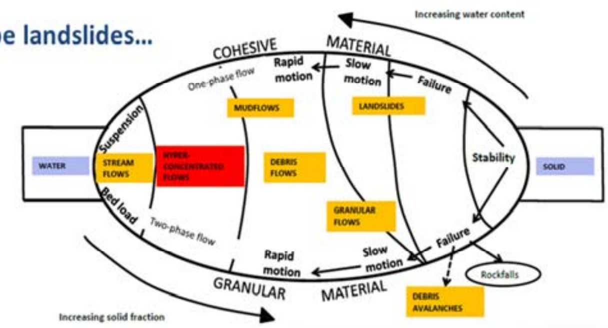

(Coussot & Meunier, 1996 mod.)

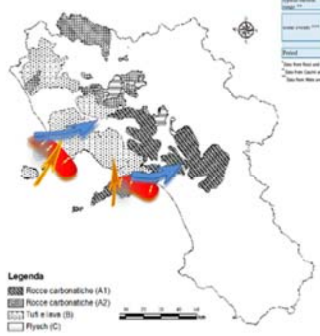

and societal risk

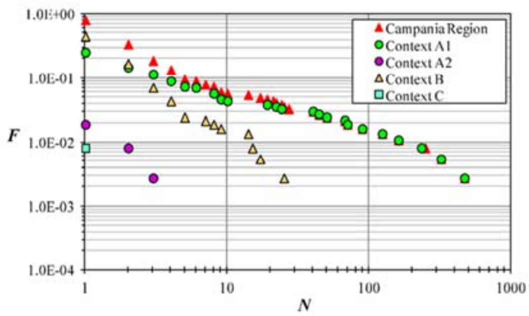

Quantitative landslide Risk Assessment (QRA): the Nocera Inferiore case study

Nocera Inferiore (southern Italy)
Region: Campania
Province: Salerno
Inhabitants (Census 2001): 46,540
Area: 20.8 km^2

Quantitative landslide Risk Assessment (QRA): the Nocera Inferiore case study

Individual risk related to the different phenomena

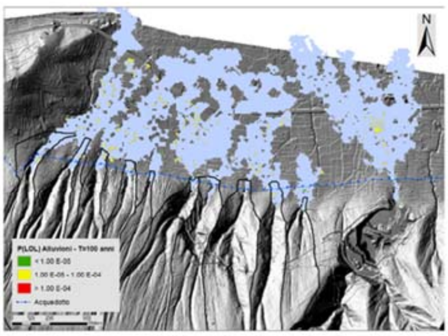

Flooding

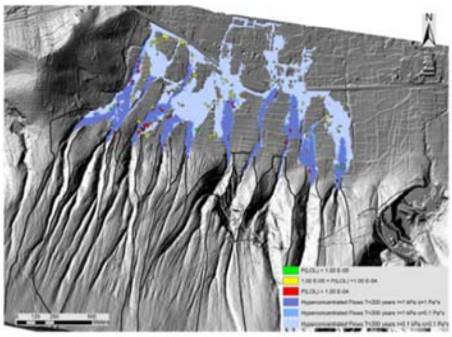

Hyperconcentrated flows

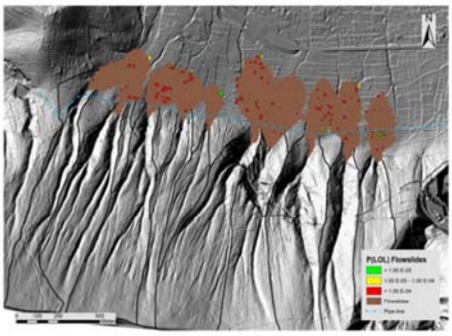

Flowslides

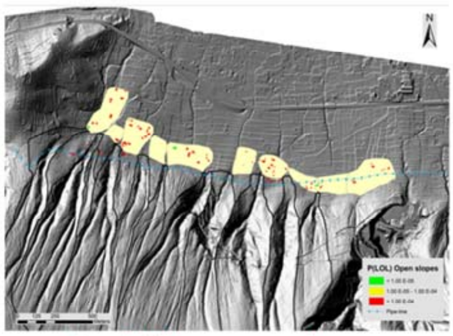

Landslides on open slopes

Quantitative landslide Risk Assessment (QRA): the Nocera Inferiore case study

Example(s) of risk mitigation option

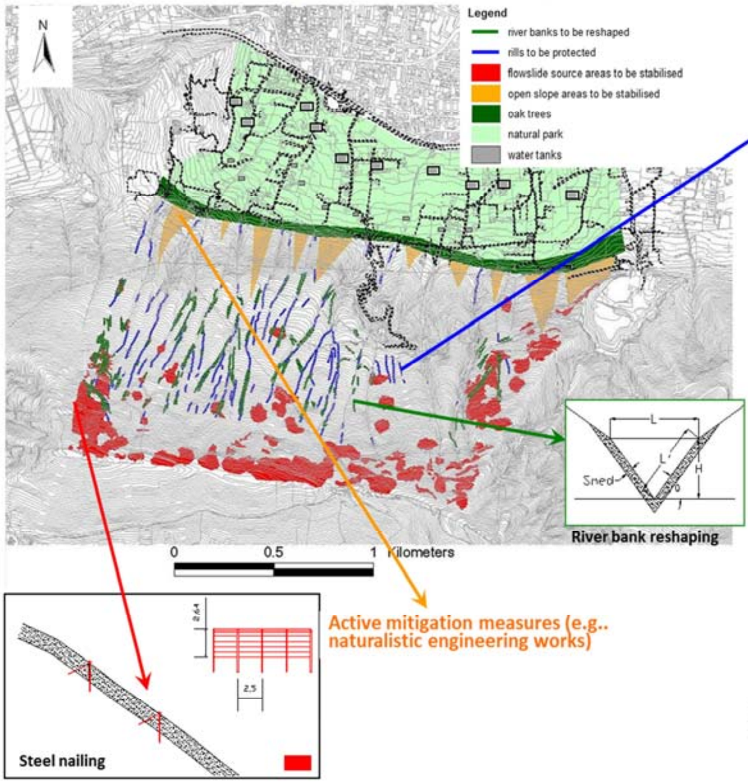

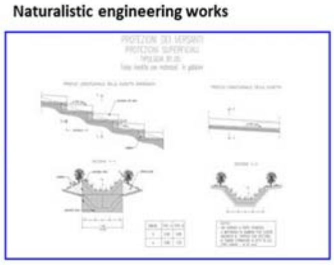

Active control works
- in the flowslide source areas
- along the river banks
- along the rills
- over the open slopes

Passive control works
- water tanks

Forestation

Natural park

The showed mitigation measures must be considered as typological examples.

Quantitative landslide Risk Assessment (QRA): the Nocera Inferiore case study

Participatory process

The partecipatory process was co-organised with the leader (IIASA) of the Area 5 (Risk management) of the **SafeLand Project**

The attendants of the meetings (15) were selected by the IIASA in order to have a balanced group in terms of gender, educational qualifications, age, profession, risk exposure, opinions about risk mitigation.

Quantitative landslide Risk Assessment (QRA): the Nocera Inferiore case study

Hypothesis of compromise solution

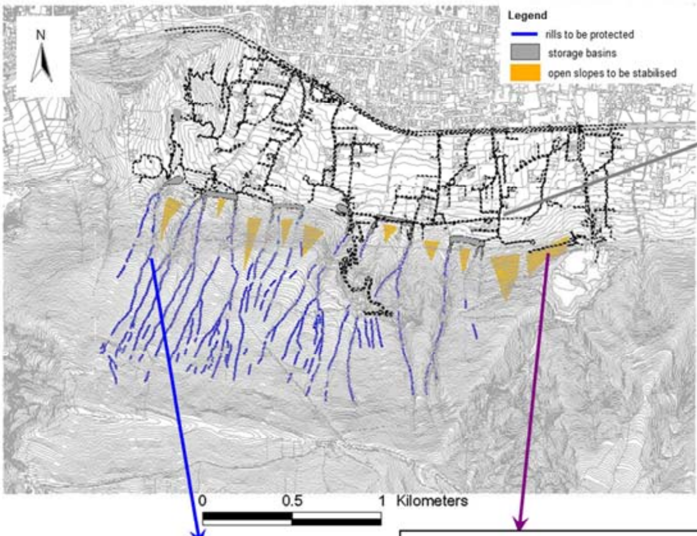

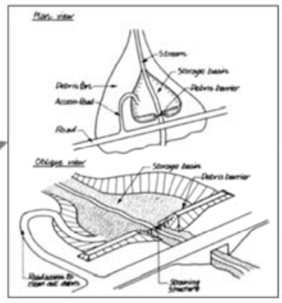

Storage basins

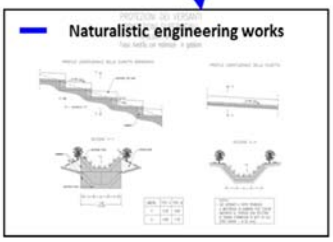

Possible types of mitigation measures

- **Soil cover removal**
- **Naturalistic engineering works**
- **Slope reshaping**

Active control works

- over the open slopes
- along the rills

Passive control works

- storage basins, located at the mouth of the basins, to be designed for alluvial phenomena due to rainfall having a return period T = 200 years

Monitoring

Territorial survey

Bed-entrainment control

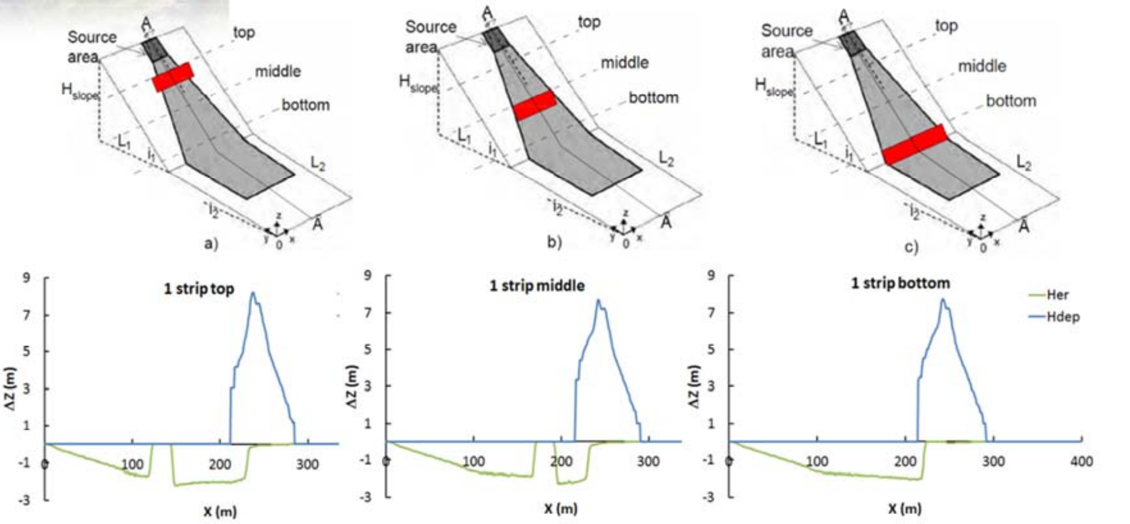

Cuomo, S., & Petrosino, S. (2019,). Two Control Works to Counteract the Inception of Debris Avalanches. In *National Conference of the Researchers of Geotechnical Engineering* (pp. 71-81). Springer, Cham.

Baffles

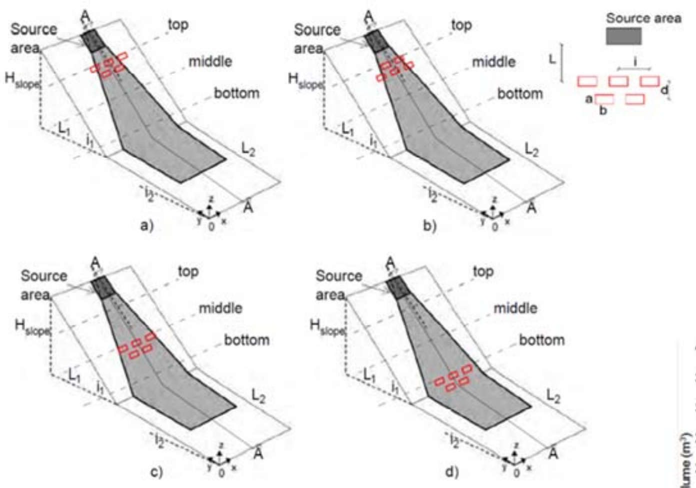

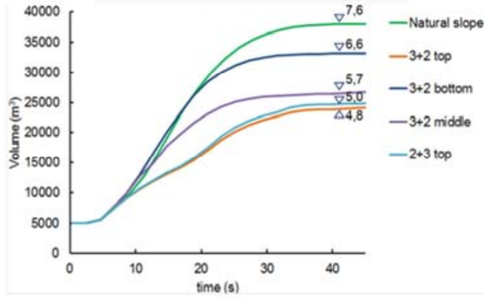

Cuomo, S., Cascini, L., Pastor, M., & Petrosino, S. (2017). Modelling the propagation of debris avalanches in presence of obstacles. In Workshop on World Landslide Forum (pp. 469-475). Springer, Cham.

Rigid barriers

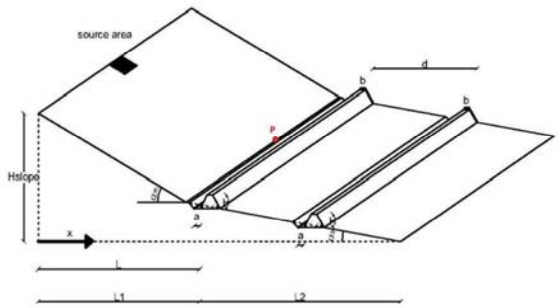

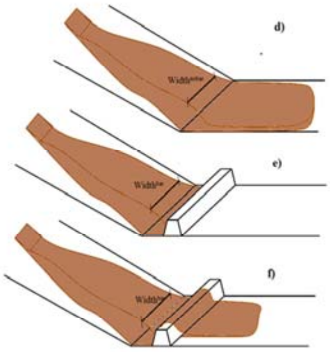

Index of Piedmont Runout Reduction (I_{PRR})

$$I_{PRR} = \frac{PR_{eng}}{PR_{nat}}$$

Index of Lateral Spreading (I_{LS})

$$I_{LS} = \frac{W_{eng}}{W_{nat}}$$

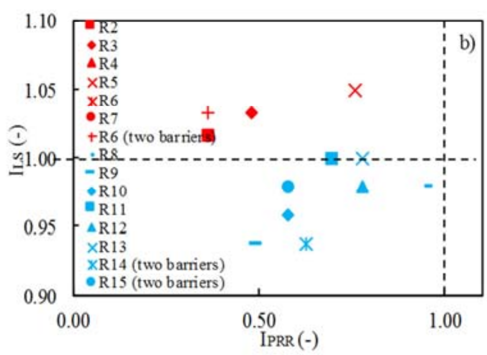

Cuomo, S., Moretti, S., & Aversa, S. (2019). Effects of artificial barriers on the propagation of debris avalanches. Landslides, 16(6), 1077-1087.

Deformable barriers reinforced by geosynthetics

Fig. 9 Deformed geometry at the end of impact I4 scenario and for materials in combo 1. The displacements are plotted in 1:1 scale for types A, B, C, while scaled down to 0.1 for type D

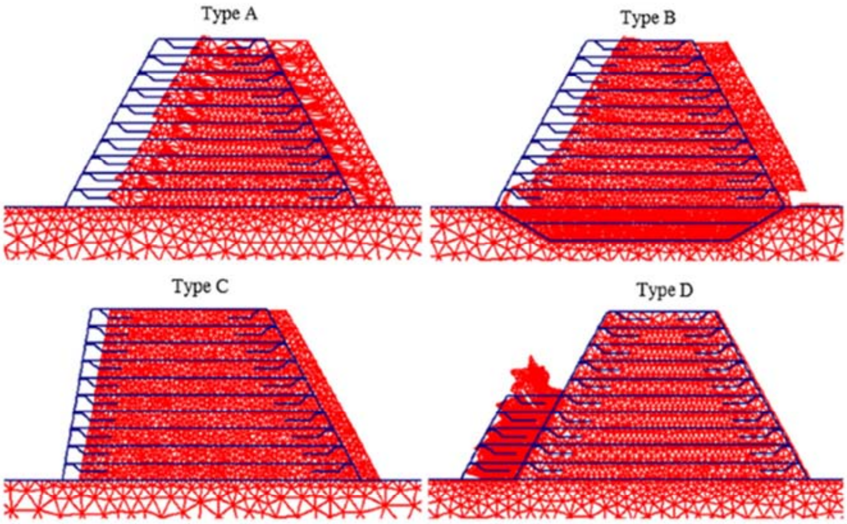

Cuomo, S., Moretti, S., Frigo, L., & Aversa, S. (2019). Deformation mechanisms of deformable geosynthetics-reinforced barriers (DGRB) impacted by debris avalanches. Bulletin of Engineering Geology and the Environment, 1-14.

Early Warning Systems for weather-induced landslides: components

Calvello et al. (2016)
Landslide risk perception: a case study in Southern Italy

Calvello, Piciullo (2016)
Assessing the performance of regional landslide early warning models: the EDuMaP method

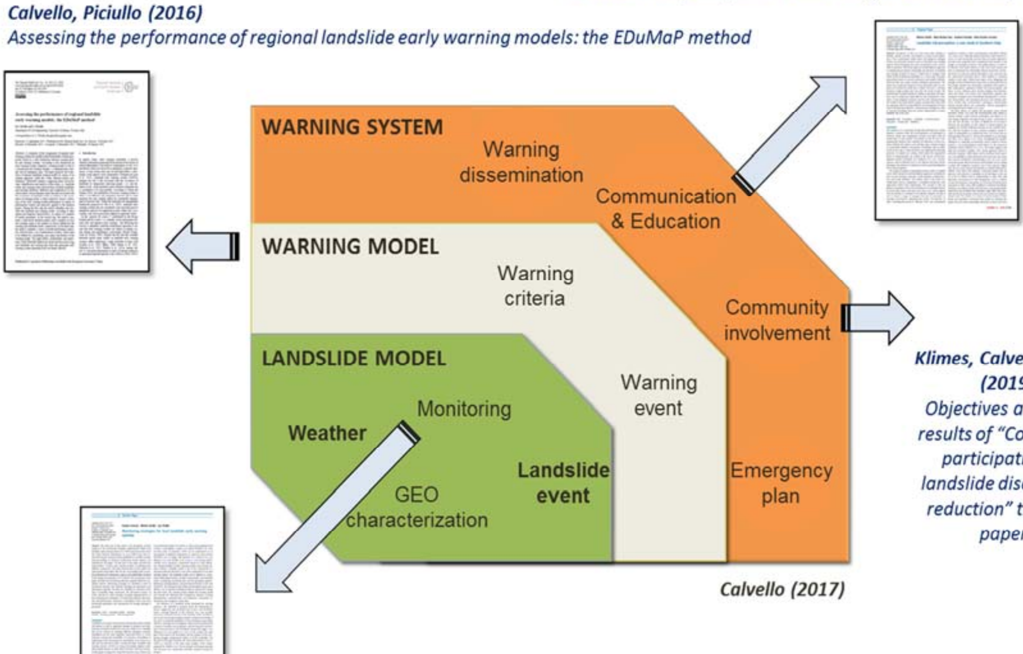

Klimes, Calvello, Auflic (2019)
Objectives and main results of "Community participation for landslide disaster risk reduction" thematic papers

Calvello (2017)

Pecoraro, Piciullo, Calvello (2019)
Monitoring strategies for local landslide early warning systems

Calvello M (2017). Early warning strategies to cope with landslide risk. Rivista Italiana di Geotecnica, 2/17:63-91

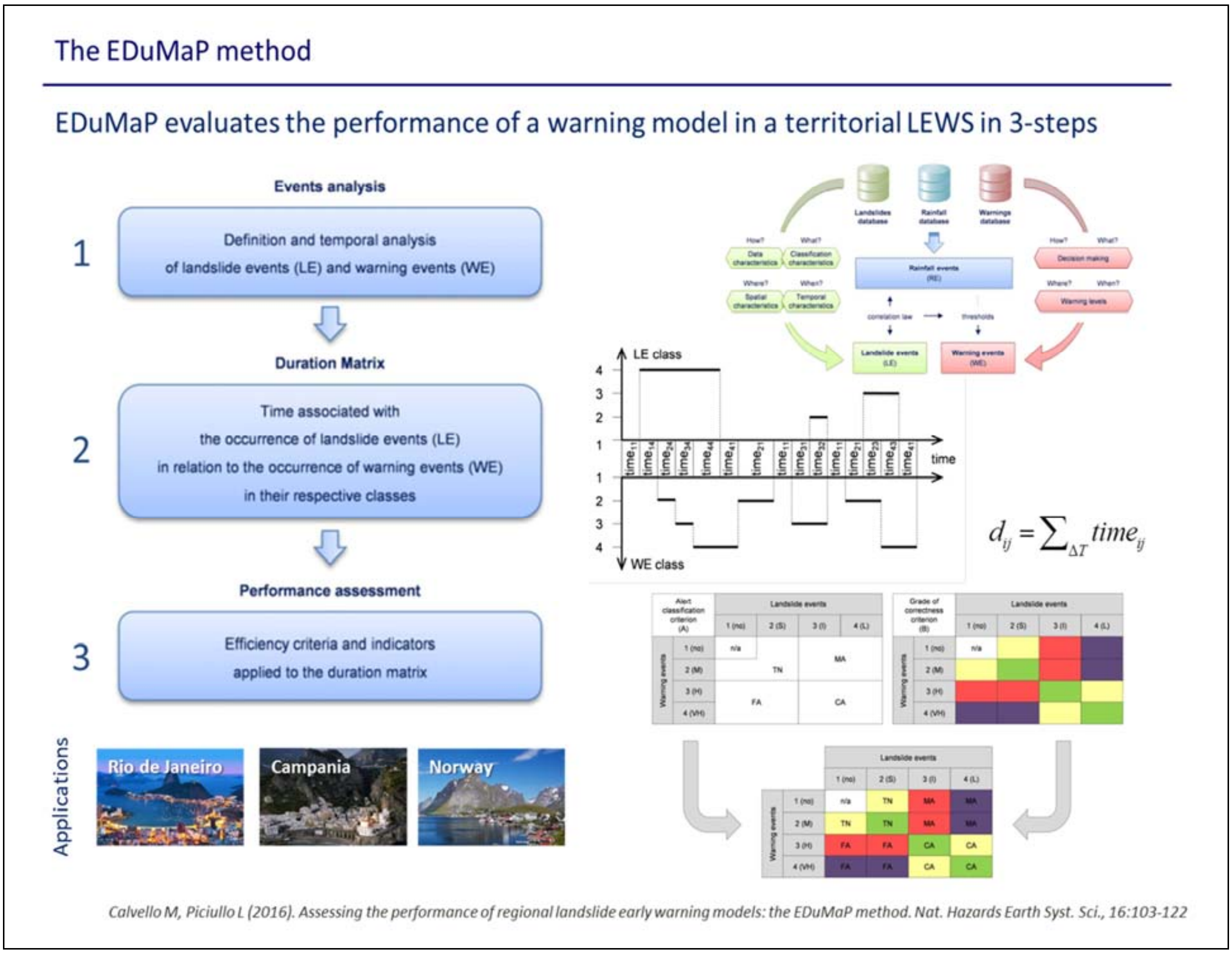
The EDuMaP method
EDuMaP evaluates the performance of a warning model in a territorial LEWS in 3-steps
Events analysis
1
Definition and temporal analysis
of landslide events (LE) and warning events (WE)
Duration Matrix
2
Time associated with
the occurrence of landslide events (LE)
in relation to the occurrence of warning events (WE)
in their respective classes
Performance assessment
3
Efficiency criteria and indicators
applied to the duration matrix
Applications
Rio de Janeiro
Campania
Norway
LE class
WE class
time
$d_{ij} = \sum_{\Delta T} time_{ij}$
Calvello M, Piciullo L (2016). Assessing the performance of regional landslide early warning models: the EDuMaP method. Nat. Hazards Earth Syst. Sci., 16:103-122

International Programme on Landslides

IPL Project Proposal 2019

Innovation in slow-moving landslide risk assessment of roads and urban sites by combining multi-sensor multi-source monitoring data

Main Project Fields:

A. Monitoring and Early Warning, **B.** Hazard Mapping, Vulnerability and Risk Assessment

Participants:

Dario Peduto[(1)], Biljana Abolmasov[(2)], Uroš Đurić[(3)], Settimio Ferlisi[(1)], Diego Reale[(4)]

Contributors:

Gianfranco Nicodemo[(1)], Milos Marionović[(2)], Antonio Marchese[(1)], Mariantonia Santoro[(1)], Giovanni Gullà[(5)], Gianfranco Fornaro[(4)]

1) University of Salerno – Geotechnical Engineering Group of Dept. of Civil Enginnering (Italy)
Via Giovanni Paolo II, 132 – 84084 – Fisciano (SA), e-mail: dpeduto@unisa.it

2) University of Belgrade – Department of Geotechnics, Faculty of Mining and Geology (Serbia)

3) University of Belgrade – Department of Geotechnical Engineering, Faculty of Civil Engineering (Serbia)

4) Institute for Electromagnetic Sensing of the Environment (IREA-CNR), Naples (Italy)

5) Research Institute for Geo-Hydrological Protection (CNR-IRPI), Cosenza (Italy)

16-19 September 2019, Salle IX, Fontenoy Building, UNESCO Headquarters in Paris, France

Abstract

Both Italy and Serbia suffer from widespread slow-moving landslides that, although not threatening human lives, recurrently cause damage to several densely populated urban areas as well as to numerous road sites with high traffic frequency and strategic importance. Accordingly, the need for easy-to-use tools that, at affordable costs, are capable of supporting decision makers in prioritizing risk mitigation measures turns out to be necessary. The project is aimed at developing and testing appropriate procedures for the use of innovative multi-temporal multi-sensor monitoring techniques jointly with multi-source field data for the landslide hazard, vulnerability and risk assessment in (slow-moving) landslide-affected areas. The proposed procedures will be double-tested in different geo-environmental contexts taking advantage of previous/ongoing studies carried out by the Project members in selected areas in both Italy and Serbia.

Introduction to the problem

Slow-moving landslides are widespread in different geological contexts all over the world and, although they usually have a low probability of generating "catastrophic" events (i.e. a significant loss of human life), often **cause significant damage to structures and infrastructures** with them interacting.

Types of slow-moving landslide according to Varnes (1978)

TYPE OF MOVEMENT		TYPE OF MATERIAL		
		BEDROCK	ENGINEERING SOILS	
			Predominantly coarse	Predominantly fine
FALLS		Rock fall	Debris fall	Earth fall
TOPPLES		Rock topple	Debris topple	Earth topple
SLIDES	ROTATIONAL	Rock slide	Debris slide	Earth slide
	TRANSLATIONAL			
LATERAL SPREADS		Rock spread	Debris spread	Earth spread
FLOWS		Rock flow (deep creep)	Debris flow	Earth flow (soil creep)
COMPLEX		Combination of two or more principal types of movement		

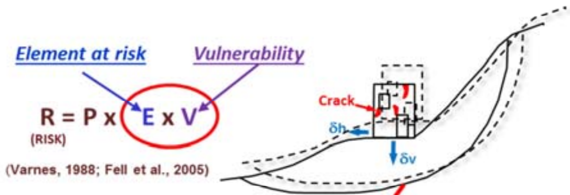

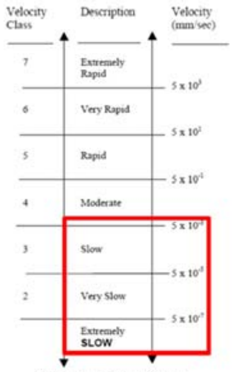

Velocity of landslides (Cruden e Varnes, 1996)

Consequences related to slow-moving landslides

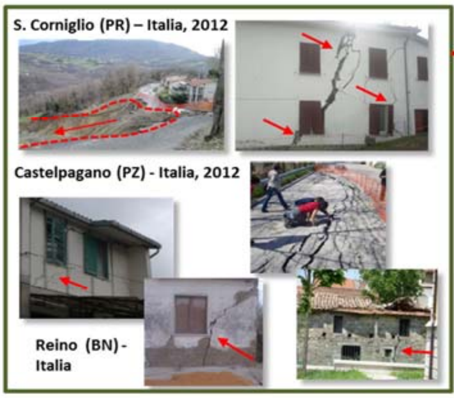

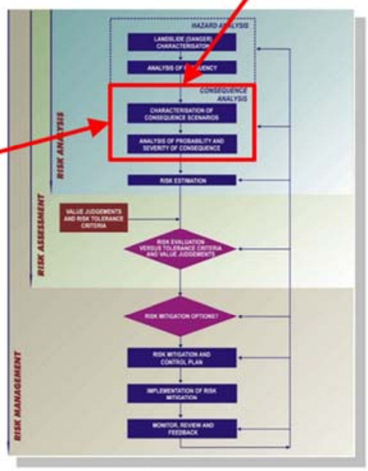

Framework for landslide risk management (Fell et al., 2008)

2/14

Background justification

Both **Italy and Serbia suffer from widespread slow-moving landslides** that recurrently cause **damage to several densely populated urban areas** as well as to numerous road sites with high traffic frequency and strategic importance. Accordingly, the need for easy-to-use **tools** that, at affordable costs, are capable of **supporting decision makers in prioritizing risk mitigation measures** turns out to be necessary. These tools, which should be differentiated according to the scale of analysis, require the availability of rich datasets collecting geological/geomorphological/geotechnical and monitoring data that can be extremely expensive over large areas.

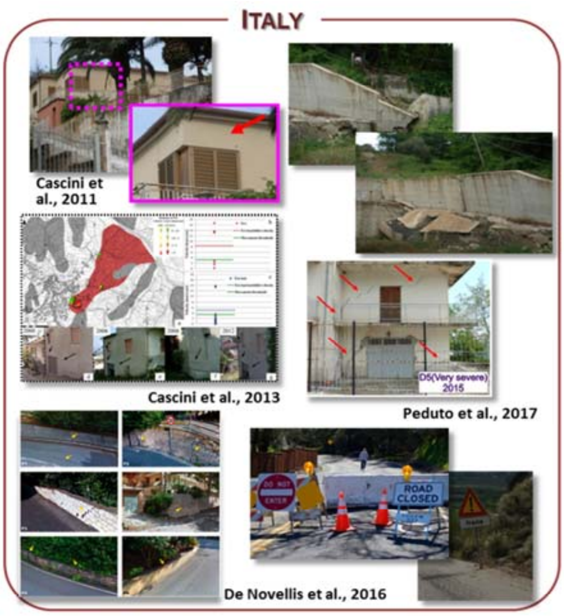

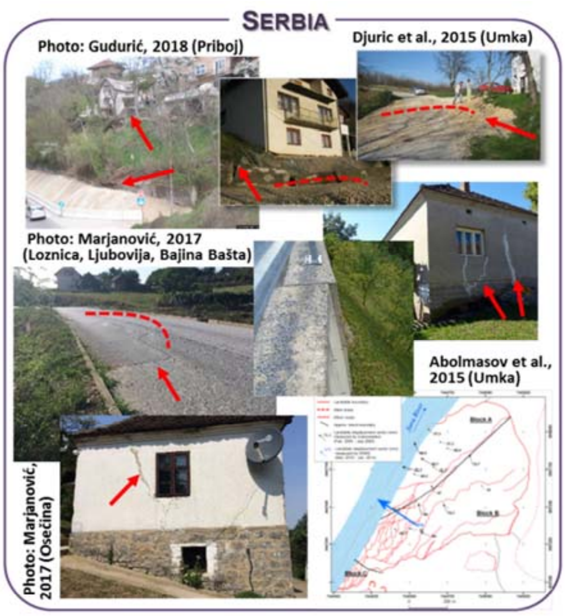

3/14

Objectives

The **project is aimed** at developing and testing **appropriate and integrated procedures** for the use of innovative multi-temporal multi-sensor monitoring techniques jointly with multi-source field data for the **landslide hazard, vulnerability and risk assessment** in (slow-moving) landslide-affected areas.

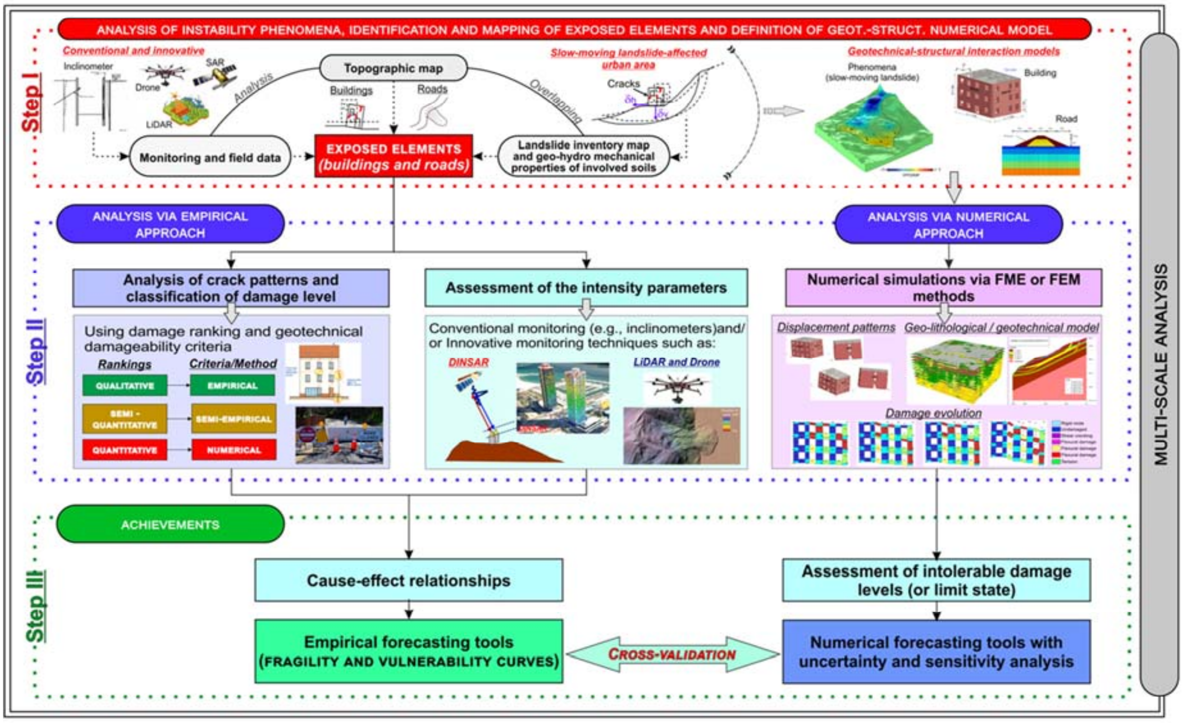

4/14

Project description

Building/Road Damage Analysis and Classification

- **Damage classification**

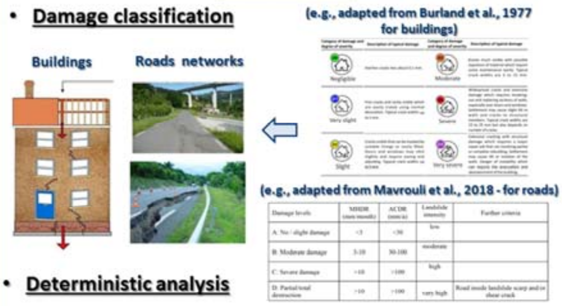

- **Deterministic analysis**

Adopting empirical, semi-empirical or numerical **geotechnical damageability criteria**:

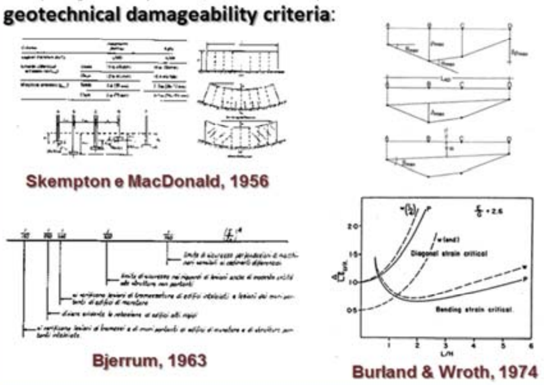

Fragility and Vulnerability Curves

The **forecast of building/road damages** can be addressed through the use of "**fragility and vulnerability curves**". These tools provide the conditional probability for every element at risk (e.g. building) to be in, or exceed, a certain damage state (or limit state) in function of the intensity of the phenomenon that generated it. They can be distinguished as **empirical, engineering judgmental, analytical and hybrid** (Zhang & Ng, 2005; Saeidi et al., 2009, 2012; Negulescu & Foester, 2010; Mavrouli et al., 2014; Peduto et al., 2017, 2018).

Three main types of input data:

1) **damage classification**
2) **building typology**
3) **intensity parameter**

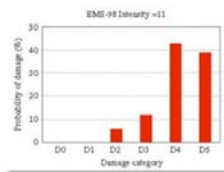

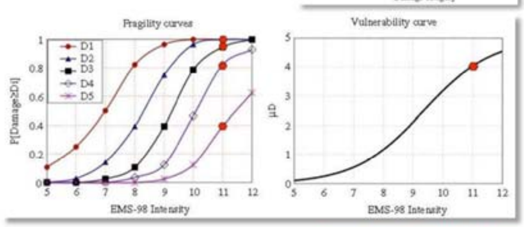

(Saeidi et al., 2009, 2012)

5/14

Project description

Multi-temporal DInSAR relying on processing of repeat-pass SAR images is a well-established remote sensing technique to derive wide-area and high-precision (mm/year) deformation monitoring

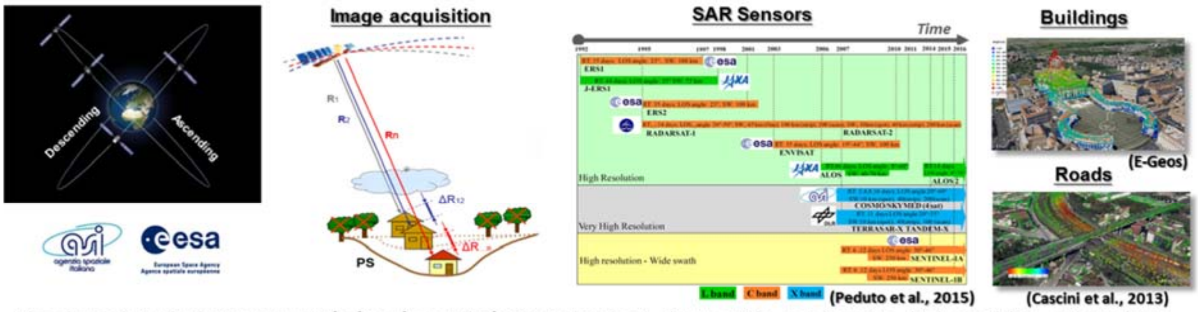

The **drone-based photogrammetric imaging** and **LiDAR technology** also provide non-invasive, high-precision end-products, while overcoming some limitations of the InSAR technology (limited coverage in vegetated areas and geometric constraints related to sensor acquisition).

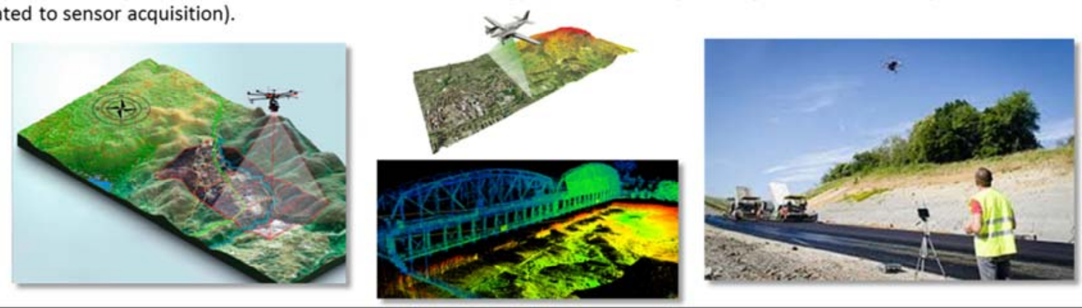

Combining these techniques can be beneficial from many aspects, all targeted at facilitating continuous, high-certainty data acquisition for early recognition and mitigation of the landslide risks along the roads and urban areas.

6/14

Project description

Main expected results

In the project, **empirical and numerical methods will be developed** – at different scales of analysis – to **analyze and forecast slow-moving landslide risk**.

The main expected achievements are:

i) **mapping** selected **road sections and urban sites in Serbia and Italy** that are **in slow-moving landslide-affected areas** using geological-geomorphological-geotechnical, Copernicus and Google Street view data as well as in-situ damage surveys and drone-based images used for 3D multi-temporal reconstruction;

ii) **classifying current damage** and collecting archive data for a multi-temporal analysis;

iii) **hazard assessment** via multi-source monitoring;

iv) **development of empirical and numerical methods for the vulnerability analysis and forecasting** of cause (displacement) – effect (damage) relationships at selected sites;

v) **quantitative risk analysis** corroborated also by numerical modelling in selected at high risk areas.

The project will also allow setting up a **group of experts interacting with local authorities and technicians** in both countries to disseminate the obtained results and bring them in the current best practice.

7/14

Study areas

The proposed procedures will be **double-tested in different geo-environmental contexts** taking advantage of previous/ongoing studies carried out by the Project members in selected areas in both Italy and Serbia. In particular, some study areas severely affected by slow-moving landslides will be selected in both countries: ***Calabria region*** and ***Cilento area***, southern Italy; and SW Belgrade suburb (***Umka landslide***) in Serbia.

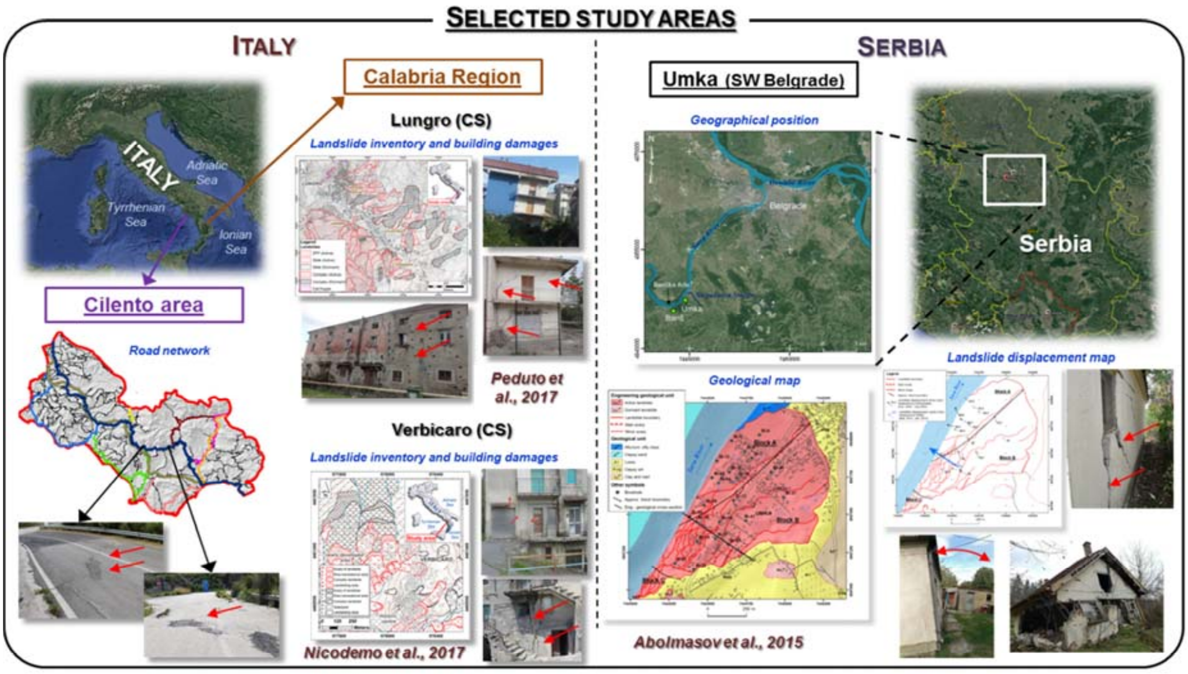

8/14

Duration, team work and necessary resources

➢ Project duration

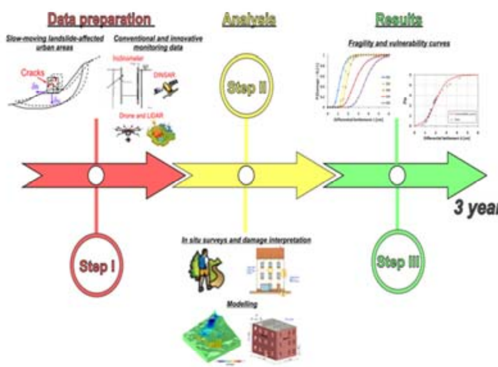

➢ Budget

- The total budget requirement is € 40,000

➢ Extra co-financings

- Extra co-financings for mobility of the project members will derive from Bilateral Erasmus funds for Staff/PhD student mobility exchange.

Erasmus+

➢ The Project will be jointly organized by

- Geotechnical Engineering Group (GEG), Department of Civil Engineering, University of Salerno (Italy)
- Faculty of Mining and Geology (FMG) and Faculty of Civil Engineering (FCE), University of Belgrade

➢ Envisaged cooperations

- Institute for Electromagnetic Sensing of the Environment (IREA-CNR), Naples (Italy)
- Research Institute for Geo-Hydrological Protection (CNR-IRPI), Cosenza (Italy)

dciv

University of Belgrade

istituto per il rilevamento elettromagnetico dell'ambiente

irpi Istituto di Ricerca per la Protezione Idrogeologica

9/14

Work Plan

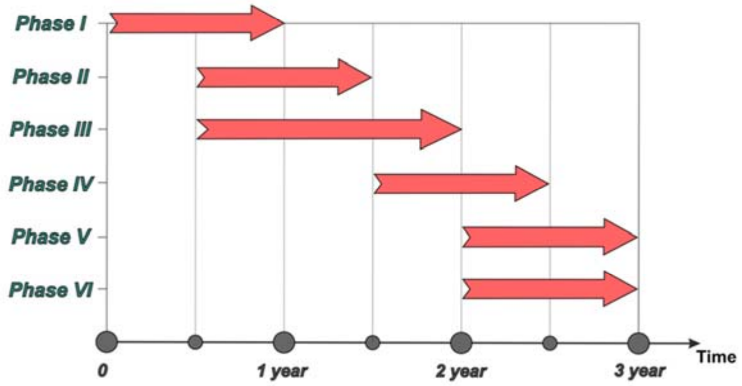

Phase I: **collection, review, harmonization** of data on landslides and exposed elements in the selected study areas also considering installation of corner reflectors (*GEG-UNISA, CNR-IRPI and FMG-UNIBG*).

Phase II: selection and **processing of SAR images** from constellations operating at different bandwidths and revisiting times. This will provide multi-temporal displacement time series (*GEG and IREA-CNR*).

Phase III: **landslide hazard assessment** based on (remote sensing and conventional) monitoring data (*GEG-UNISA, CNR-IRPI and FMG-UNIBG*).

Phase IV: empirical approaches to derive **fragility/vulnerability functions** relating displacements and damage on both roads and buildings at large scale (*GEG and UNIBG*).

Phase V: for most representative buildings and road sections **numerical analyses** will be performed to derive numerical vulnerability functions at selected sites (*GEG and UNIBG*).

Phase VI: by **combining the results on hazard and vulnerability**, **quantitative risk analysis** will be carried out. A comprehensive comparison of results from different study areas in both countries will be performed (*GEG and UNIBG*).

10/14

Deliverables

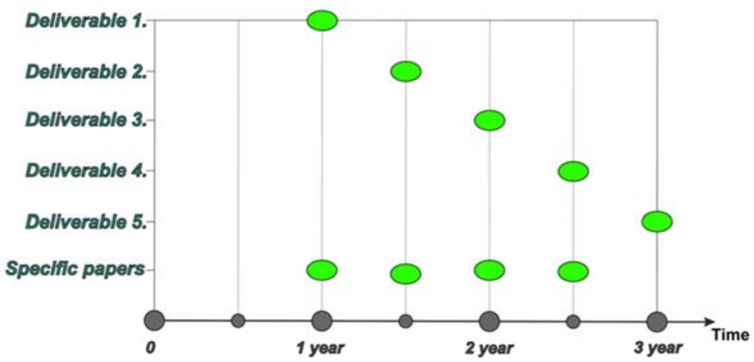

Deliverables:

Deliverable 1. Compilation of results of Phase I and Phase II (*end of 1st year*)

Deliverable 2. Compilation of results Phase III (*end of month 18th*)

Deliverable 3. Proposing empirical fragility/vulnerability curves (*Phase IV, end of month 24th*)

Deliverable 4. Numerical modeling on specific locations/landslide mechanism (Phase V) and quantitative risk assessment (*Phase VI, end of month 30th*)

Deliverable 5. Final report: discussion, comparison of obtained results (end of 3rd year)

Scientific papers:

Three original papers in *Landslides Journal*; *WLF5 - 3* papers related to: Session 2.5, 1 paper related to Session 3,2, 1 paper related to Session 5.1; *several papers on local symposia and conferences*.

11/14

Project beneficiaries and References

Project beneficiaries

- Direct beneficiaries will be local community/municipalities affected by landslides
- Local and regional authorities in both countries – housing sector, infrastructure authorities, Civil protection departments
- Results will be disseminated to PhD students and Young Doctors attending LARAM "LAndslide Risk Assessment and Mitigation" International School, yearly organized by GEG-UNISA with the contribution of several ICL members

Project beneficiaries and References

References

Abolmasov, B., Milenković, S., Marjanović, M., Đurić, U., Jelisavac, B. (2015). A geotechnical model of the Umka landslide with reference to landslides in weathered Neogene marls in Serbia. **Landslides** 12 (4): 689-702. DOI 10.1007/s10346-014-0499-4

Đurić D., et al. (2017) Using multiresolution and multitemporal satellite data for post disaster landslide inventory in the Republic of Serbia. **Landslides** 14 (4): 1467–1482. DOI: 10.1007/s10346-017-0847-2.

Marjanović M., Krautblatter M., Abolmasov B., Đurić U., Sandić C., Nikolić V. (2018) The rainfall-induced landsliding in Western Serbia: A temporal prediction approach using Decision Tree technique. **Engineering Geology** 232: 147–159. DOI:10.1016/j.enggeo.2017.11.021

Abolmasov B., Pejić M., Samardžić Petrović M., Đurić U., Milenković S. (2018) Automated GNSS monitoring of Umka landslide - Review of seven years experience and results. Proceeding of the 3rd Regional Symposium on Landslides in the Adriatic-Balkan Region, Ljubljana 2017, 11 - 13 October 2017 Ljubljana, Slovenia, pp65-70. Geological Survey of Slovenia. ISBN 978-961-6498-58-6

Đurić U., Marjanović M., Radić Z., Abolmasov B. (2019) Machine learning based landslide assessment of the Belgrade metropolitan area: Pixel resolution effects and a cross-scaling concept. **Engineering Geology** 256: 23-38. DOI:10.1016/j.enggeo.2019.05.007

Marjanović M., Abolmasov B., Milenković S., Đurić U., Krušić J., Samardžić-Petrović M. (2019). Multihazard Exposure Assessment on the Valjevo City Road Network. Spatial Modeling in GIS and R for Earth and Environmental Sciences, pp 671-688. (2019) Elsevier Inc. DOI: 10.1016/B978-0-12-815226-3.00031-4.

Peduto D. et al. (2017) Empirical fragility and vulnerability curves for buildings exposed to slow-moving landslides at medium and large scales, **Landslides**, 14(6):1993–2007, DOI : 10.1007/s10346-017-0826-7.

Ferlisi S., Gullà G., Nicodemo G., Peduto D. (2019) **Euro-Mediterranean Journal for Environmental Integration**, 4:20, https://doi.org/10.1007/s41207-019-0110-4.

Peduto D., Nicodemo G., M. Cuevas-Gonzáles, and M. Crosetto. Analysis of damage to buildings in urban centres on unstable slopes via TerraSAR-X PSI data: the case study of El Papiol town (Spain), **IEEE Geoscience and Remote Sensing Letters,** 10.1109/LGRS.2019.2907557.

Peduto D., Nicodemo G., Caraffa M., Gullà G. (2018). Quantitative analysis of consequences to masonry buildings interacting with slow-moving landslide mechanisms: a case study. **Landslides**, 15(10): 2017-2030, DOI 10.1007/s10346-018-1014-0.

Borrelli L., Nicodemo G., Ferlisi S., Peduto D., Di Nocera S., Gullà G. (2018*) Geology, slow-moving landslides, and damages to buildings in the Verbicaro area (north-western Calabria region, southern Italy)*, **Journal of Maps**, 14:2, 32-44, https://doi.org/10.1080/17445647.2018.1425164.

Calvello M., Peduto D., Arena L. (2017). *Combined use of statistical and DInSAR data analyses to define the state of activity of slow-moving landslides*. **Landslides**, 14 (2):473–489, DOI 10.1007/s10346-016-0722-6.

Gullà G., Peduto D., Borrelli L., Antronico L., Fornaro G. (2017). *Geometric and kinematic characterization of landslides affecting urban areas: the Lungro case study (Calabria, Southern Italy).* **Landslides**, 14 (1):171–188, DOI 10.1007/s10346-015-0676-0.

Cascini, L., Peduto, D., Pisciotta, G., Arena, L., Ferlisi, S., and Fornaro, G. (2013): *The combination of DInSAR and facility damage data for the updating of slow-moving landslide inventory maps at medium scale*, **Nat. Hazards Earth Syst. Sci.**, 13, 1527-1549, doi:10.5194/nhess-13-1527-2013.

Cascini L., Fornaro G., Peduto D. (2010). *Advanced low- and full-resolution DInSAR map generation for slow-moving landslide analysis at different scales.* **Engineering Geology**, 112 (1-4), 29-42, doi:10.1016/j.enggeo.2010.01.003.

13/14

Development of early warning technology of rain-induced rapid and long-travelling landslides in Sri Lanka

Kazuo Konagai [(1)], Asiri Karunawardena[(2)], A A Virajh Dias[(3)], Kyoji Sasssa[(1)], Khang Dang[(1)]

1) International Consortium on Landslide
2) National Building Research Organization (NBRO), Columbo, Sri Lanka
3) Central Engineering Consultancy Bureau (CECB), Columbo, Sri Lanka

Abstract

A coupled non-hydrostatic atmosphere-ocean-land general circulation model called Multi-Scale Simulator for the Geo-environment (MSSG) allows seamless transition from global to local areas in simulations of weather and climate. The developers of this cutting-edge computer-simulation platform, MSSG, at the Japan Agency for Marine-Earth Science and Technology (JAMSTEC) join the project to help develop a system for 24 hours-in-advance prediction of heavy rainfalls in mountains of Sri Lanka, taking into account of precise topographic effects on the cumulonimbus clouds development over upwind slopes for the better prediction of rainfalls in mountains. The landslide-prone areas in Sri Lanka are in general draped thick with weathered gneiss. Two pilot study sites are selected as representatives of two major types of rain-induced rapid and long-travelling landslides (RRLLs hereafter). One is Aranayaka landslide area in Kegalle District, 70 km east of Colombo, where a fluidized landslide mass flowed over a 2 km distance killing 125 people. The other is Athwelthota landslide area in Kalutara District, 62 km southeast of Colombo. Though the landslide of this type in not surprisingly large, they can occur all at once, and eventually cause extensive losses of human lives and properties as a whole. Careful field investigations at the two pilot sites, monitoring creeping movements of unstable debris masses still perched atop the exposed bare slopes, material testing and analyses including computer simulation are conducted to develop a model for the initiation and the motion of RRLL for predicting groundwater pressure build-up, and for identifying locations of RRLLs and their moving areas. The above-mentioned individual technologies are integrated as a practical RRLL early warning system. The performance of the developed RRLL early warning system will be examined at some additional testing site(s), and finally effective guidelines for the use of the system will be developed.

SATREPS: Science and Technology Research Partnership for Sustainable Development

Development of early warning technology of rain-induced rapid and long-travelling landslides in Sri Lanka

Kazuo KONAGAI, Leader
Principal Researcher, ICL, Prof. Emeritus, University of Tokyo

G1 Integrated research for early warning technology:
Kazuo KONAGAI, Asiri Karunawardena
G2 Time prediction of heavy rainfalls & site prediction of landslide initiation and motion:
Kazuo KONAGAI, Ryo ONISHI, Ryosuke UZUOKA, Shiho ASANO
G3 Risk communication and public education:
Katsuo SASAHARA, Munenari INOGUCHI , Go SATO

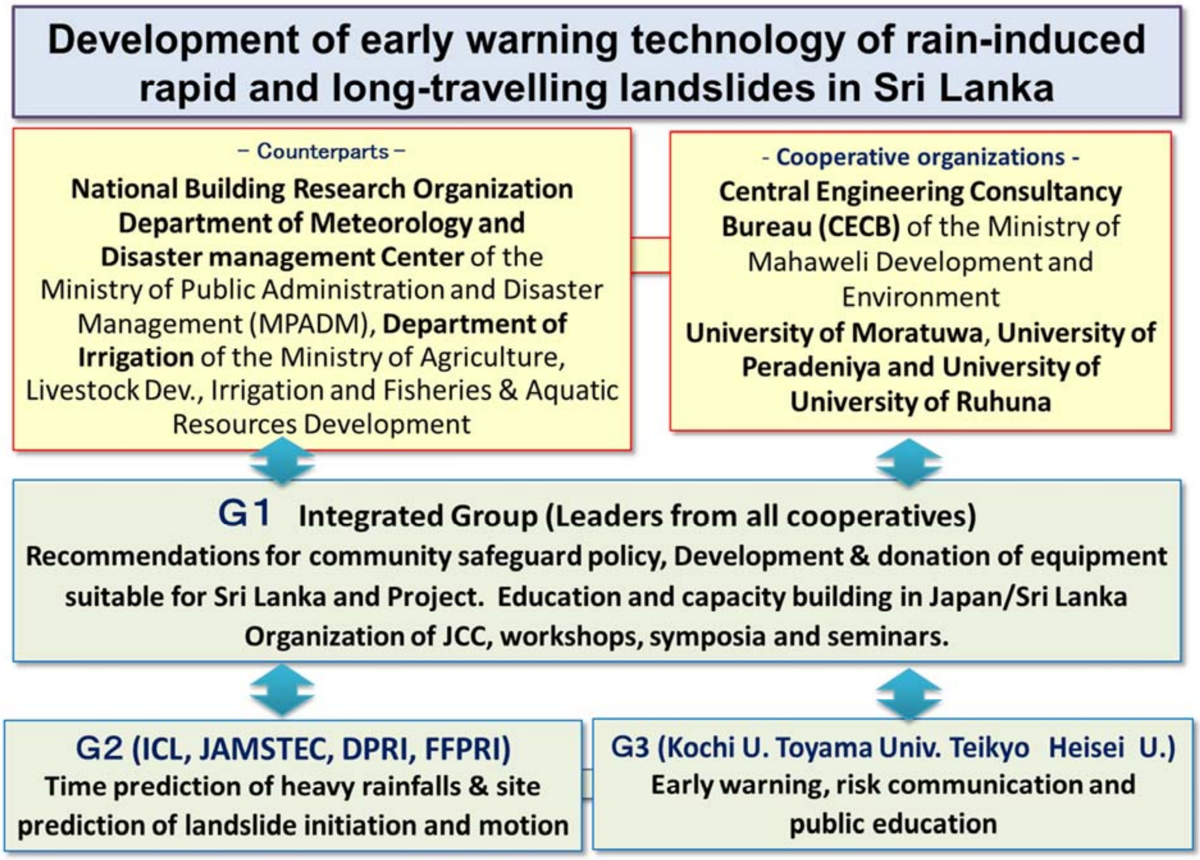

Landslides and casualties in recent years

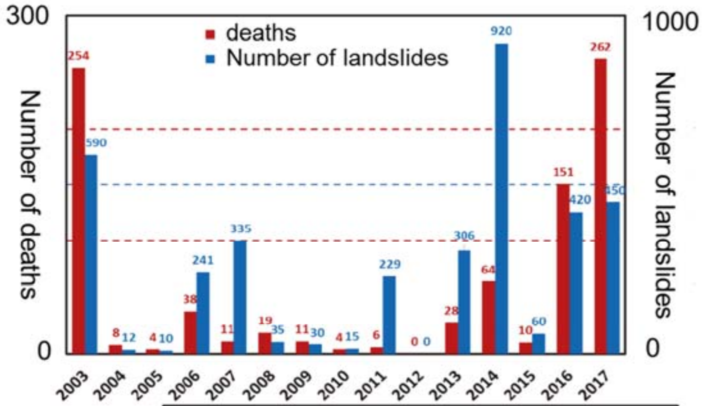

Fig. 1 Number of landslides and deaths

Landslide-prone areas overlap the tea growing regions in Sri Lanka. 6 out of total 8 world heritages in Sri Lanka are also located in these areas.

Fig. 3 Tea growing regions and world heritages

http://whc.unesco.org/en/statesparties/lk

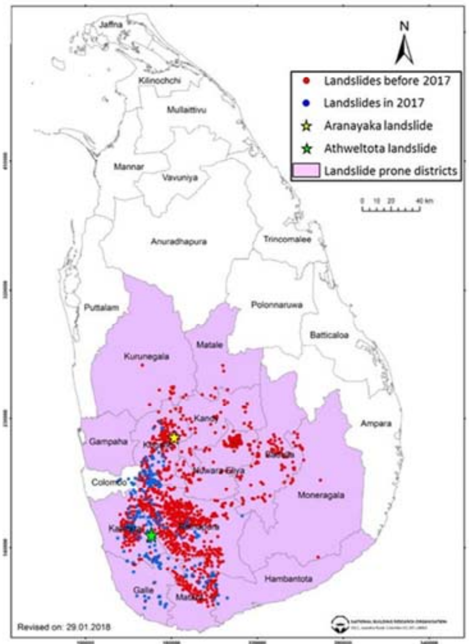

Fig. 2: Locations of landslides from 2000 to 2017 (From NBRO)
Purple: Landslide-prone provinces
Red: Landslides before 2017
Blue: Landslides after 2017

Why are RRLLs to be highlighted?

The technologies to stabilize reactivated and creeping landslide masses have much progressed because those locations can be easily identified. However, as for RRLLs, which have been causing serious destructions (photos below), neither their locations nor early signs of movement can easily be identified in advance. Therefore, development and implementation of an efficient early-warning system is a pressing need.

Aranayake landslide in 2016, Sri lanka: Debris mass from 600m altitude slid over a 2 km distance. 125 people were killed.

In June, 2018, a seasonal "Baiu" front extending over the western Japan became stationary causing thousands of RRLLs including this one in Yasuura, Hiroshima. The debris mass from 150m altitude slid over a 1 km distance killing one lady.

Why is ICL to be involved?

International Consortium on Landslides, a NPO founded in 2002, has been the important base of academic frontier of landslides, publishing an international monthly journal, “Landslides” with the Impact factor of 4.252 (2018).

ICL proposed the ISDR-ICL Sendai Partnerships 2015-2025 for global promotion of understanding and reducing landslide disaster risk at the Third World Conference on Disaster Risk Reduction (3rd WCDRR) in Sendai, Japan. It was accepted and singed by 16 organizations including the United Nations, international stakeholders, and National Organizations. NBRO and CECB also signed it.

Multi-Scale Simulator for the Geo-environment（MSSG）の適用

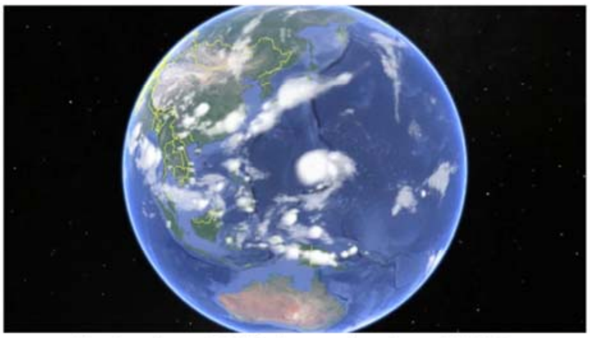

Estimation of 2018 Japan floods on MSSG

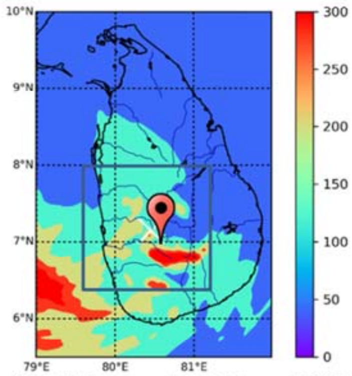

Estimation of 2016 Aranayake Rain on MSSG

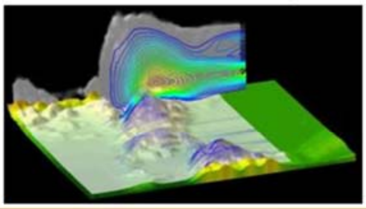

Our members (below) have clarified that cloud turbulence, with the presence of rugged terrain, accelerates development of water droplets. [Onishi, Matsuda & Takahashi, *J. Atmos. Sci.* (2015); Onishi & Seifert, *Atmos. Chem. Phys.* (2016)]

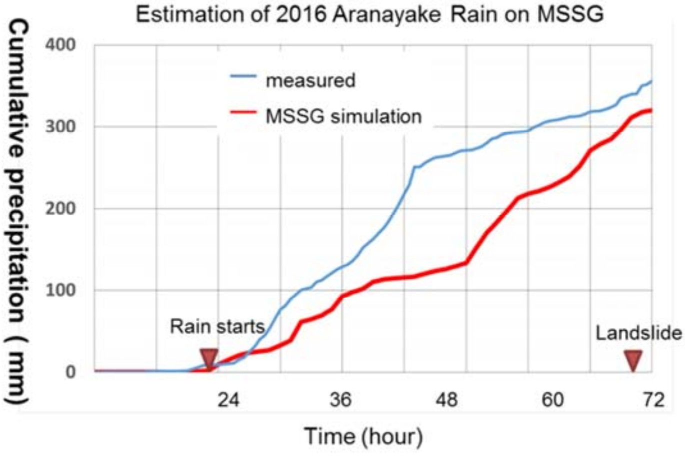

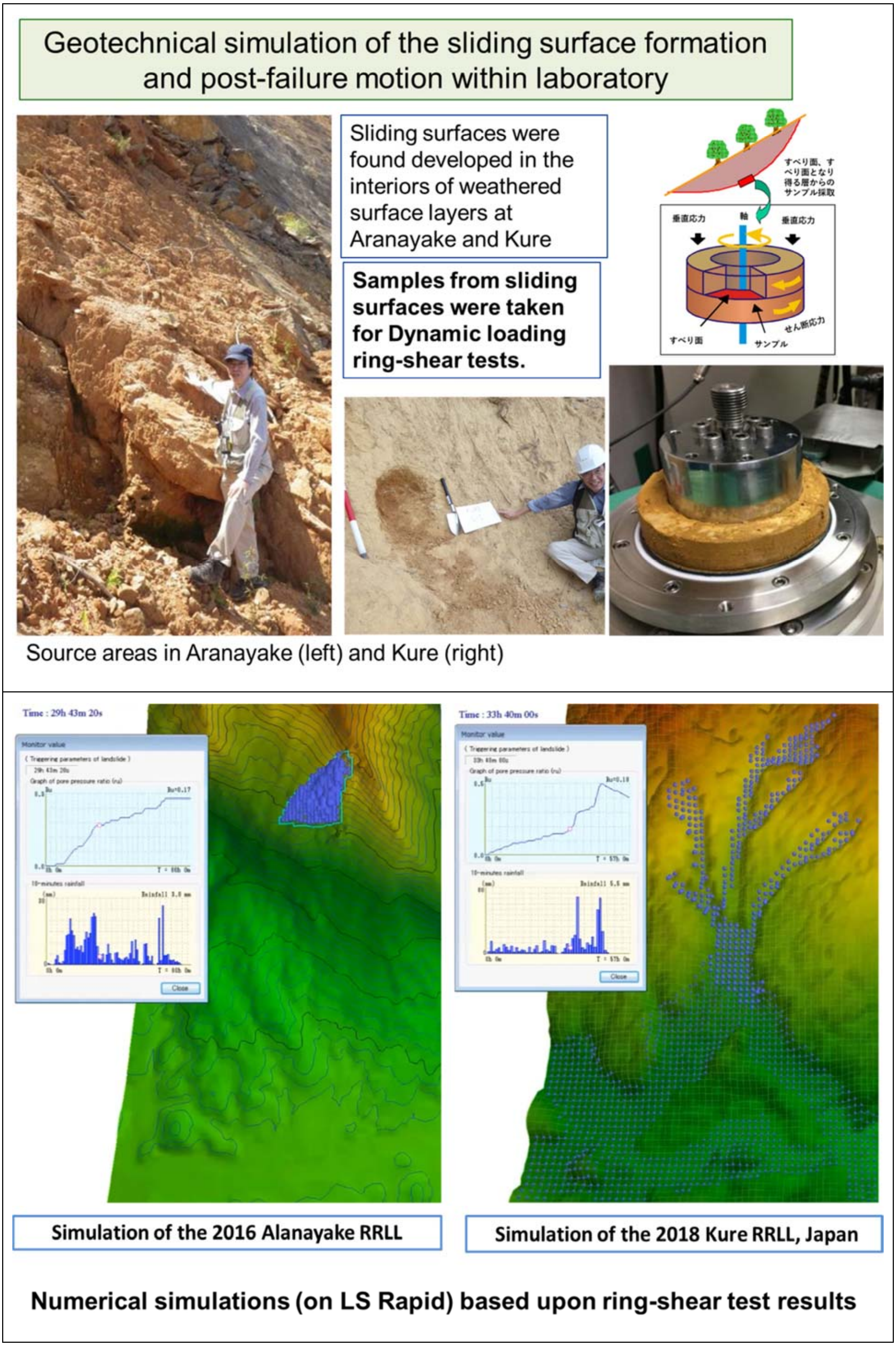
Geotechnical simulation of the sliding surface formation and post-failure motion within laboratory
Sliding surfaces were found developed in the interiors of weathered surface layers at Aranayake and Kure
Samples from sliding surfaces were taken for Dynamic loading ring-shear tests.
すべり面、すべり面となり得る層からのサンプル採取
垂直応力
軸
垂直応力
すべり面
サンプル
せん断応力
Source areas in Aranayake (left) and Kure (right)
Time : 29h 43m 20s
Time : 33h 40m 00s
Simulation of the 2016 Alanayake RRLL
Simulation of the 2018 Kure RRLL, Japan
Numerical simulations (on LS Rapid) based upon ring-shear test results

Technology for effective risk communication with community people in RRLL-prone areas

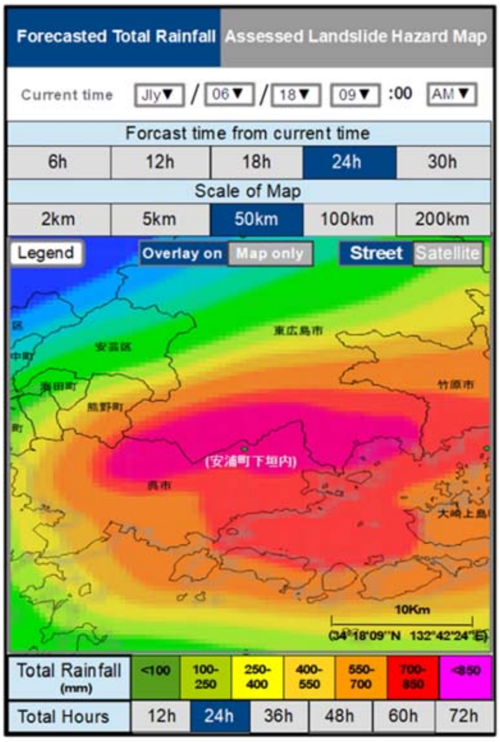

Time prediction of cumulative precipitation

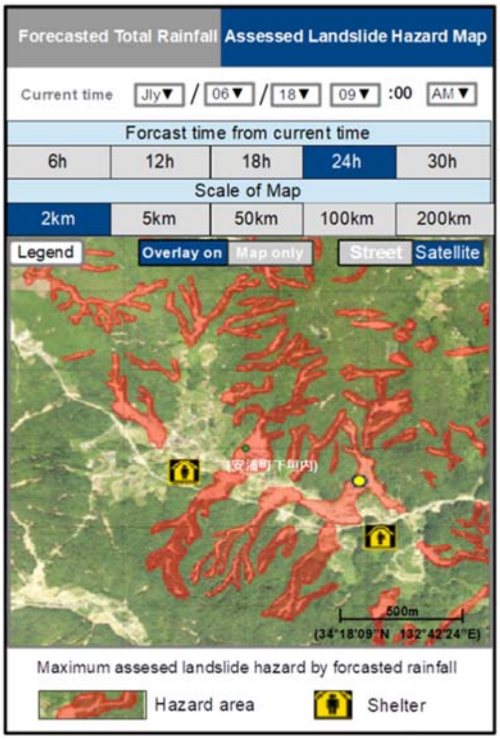

Site prediction of RRLLs

Workshop at the Ministry of Irrigation, Water Resources and Disaster Management

(2018/06/20)

Total about 20 officers and experts from NBRO, DOM, DMC, DMI of the ministry, CECB, Univ. of Moratuwa etc. joined the workshop, and expressed their firm willingness to help develop the proposed Early Warning System for RRLLs.

Assembly house of a local community, Debathgama Pallebage (47-A) : The door plate on the assembly house says that the number assigned to this local community is 47-A. The "A" in the trailing digit was assigned in the recent past. This implicitly says that the number of local community is increasing (2018/06/19).。

Plan of operation

Activities（JICA） / Sub-Activities	Year	1st Year (2020-2021)	2nd Year (2021-2022)	3rd Year (2022-2023)	4th Year (2023-2024)	5th Year (2024-2025)	Responsible Organization: Japan	Responsible Organization: Sri Lanka
		4-6, 7-9, 10-12, 1-3	4-6, 7-9, 10-12, 1-3	4-6, 7-9, 10-12, 1-3	4-6, 7-9, 10-12, 1-3	4-6, 7-9, 10-12, 1-3		
Output 1:								
1.1 Sri Lanka-Japan Joint research is conducted for developing a practical RRLL early warning system (RRLL EW system hereafter).	Plan / Actual							Practical work until mid-2nd year are by CECB & 3 univs & GETD (NBRO). Later works are by all.
1.2 The performance of the developed RRLL EW system is examined.	Plan / Actual							LRRMD. DOM, DMC, DOI
1.3 Guidline for RRLL EW system is developed.	Plan / Actual							NBRO, DMC, DOM, DOI
1.4 Human resource of engineers / researchers is developed.	Plan / Actual							Practical works until mid-2nd year are by CECB & 3 univs. Later works are by all.
Output 2:								
2.1 Rainfall prediction system in mountain slope is developed using "Multi-scale simulator for the Geo-environment (MSSG)".	Plan / Actual							Univs, DOM, GETD (NBRO)
Measuring system for landslides and slope deformations is developed.	Plan / Actual							CECB & Univs & GETD
2.2 MSSG model on a workstation at NBRO as a computing platform is developed.	Plan / Actual							NBRO (LRRMD)
Mechanical model is developed for predicting the initiation and motions of RRLLs.	Plan / Actual							Univs
2.3 RRLL EW system is developed and the system is examined at two pilot sites.	Plan / Actual							LRRMD (NBRO), DMC, DOM. DOI
Output 3:								
3.1 Augmented reality software is developed by integrating geospatial and location database.	Plan / Actual							Univs, DOM
3.2 Effective guidelines are developed through the two stages of study, at the pilot sites and then additional testing sites.	Plan / Actual							NBRO, DOM, DMC, DOI
3.3 Public education and capacity development are implemnted in communities and local administration offices.	Plan / Actual							Univs (initial years), HSPTD , DMC(3-5 years)

Summary: Urgency and importance of the project

- **Sendai Framework for Disaster Risk Reduction 2015-2030 highlights:** Priority 1: Understanding disaster risk
- **Agenda 2030: Sustainable development highlights:** Goal 11. Make cities and human settlements inclusive, safe, resilient and sustainable

For the goals mentioned above, International Consortium on Landslides (ICL) proposed the ISDR-ICL Sendai Partnerships. It was accepted and singed by 16 United Nations and international stakeholders, and national organizations including **NBRO** and **CECB**

NBRO joined the discussion for the the ISDR-ICL Sendai Partnerships, and signed it. NBRO seized this opportunity to propose this joint project for RRLL early warning system (March, 2015)

Given landslide disasters in 2016, the government of Sri Lanka has provided NBRO with the funding of 1.3 billion JPY over three fiscal years, and NBRO asked ICL to take an urgent action at the ICL meeting (March 2017)

ICL conducted field surveys in 2017 and 2018 in areas devastated by landslides (test sites). SATREPS project was prepared after thorough discussions with NBRO, CECEB, University of Moratuwa, University of Peradeniya, etc. and the proposal was submitted to the Japan Embassy (Aug. 2018)

This project is thus important to meet the urgent request from Sri Lanka and world community of natural disaster prevention

16-19 September 2019, UNESCO, Paris

Earthquake triggered landslides in Tephra deposit, Hokkaido, Japan

Fawu Wang, Shuai Zhang, Ran Li, Akinori Iio, Junichiro Furuyama

Shimane University, Japan

Abstract

In September 2018, a Mw6.6 earthquake occurred in Southern Hokkaido, Japan, just one day after a typhoon passed that area. More than 5000 landslides have been triggered, and caused severe damage on the houses, roads, farmland, rivers, and so on. Excepting one deep-seated landslide, most of the landslides are shallow landslides occurred in Tephra deposits. Field investigations were conducted on some typical landslides just one week after the earthquake, and a monitoring system was established in May 2019 to observe the rainfall water infiltration in the tephra deposit, in order to understand the moisture content and groundwater variation in whole season.

In this presentation, the field investigation results, in-situ soil mechanical test results, and up-to-date monitoring results will be presented to discuss the initiation mechanism and motion mechanism of the landslides. The effect of sliding zone thickness will be discussed, and a concept of "Soil weathering" and its controlling significance on landslide will be proposed.

Contents

2

1. Iburi earthquake and coseismic landslides

Magnitude: 6.7 (Mj)
Maximum seismic intensity: 7.0
Focal depth: 37 km
Casualties: 41 (landslide, 36)

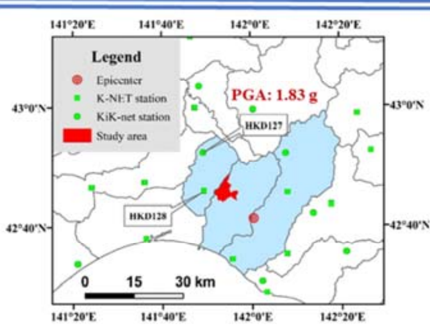

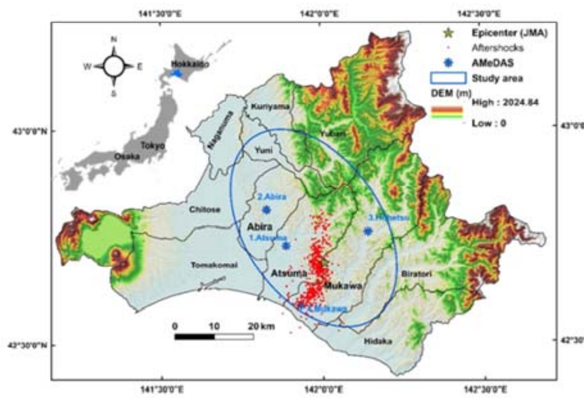

Mainshock and 631 aftershocks (M≥2.0) of the Iburi earthquake sequence

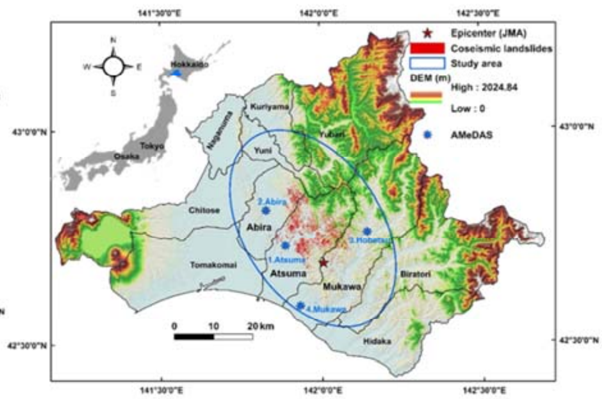

Coseismic landslide inventory (**5,625**)

3

1. Iburi earthquake and coseismic landslides

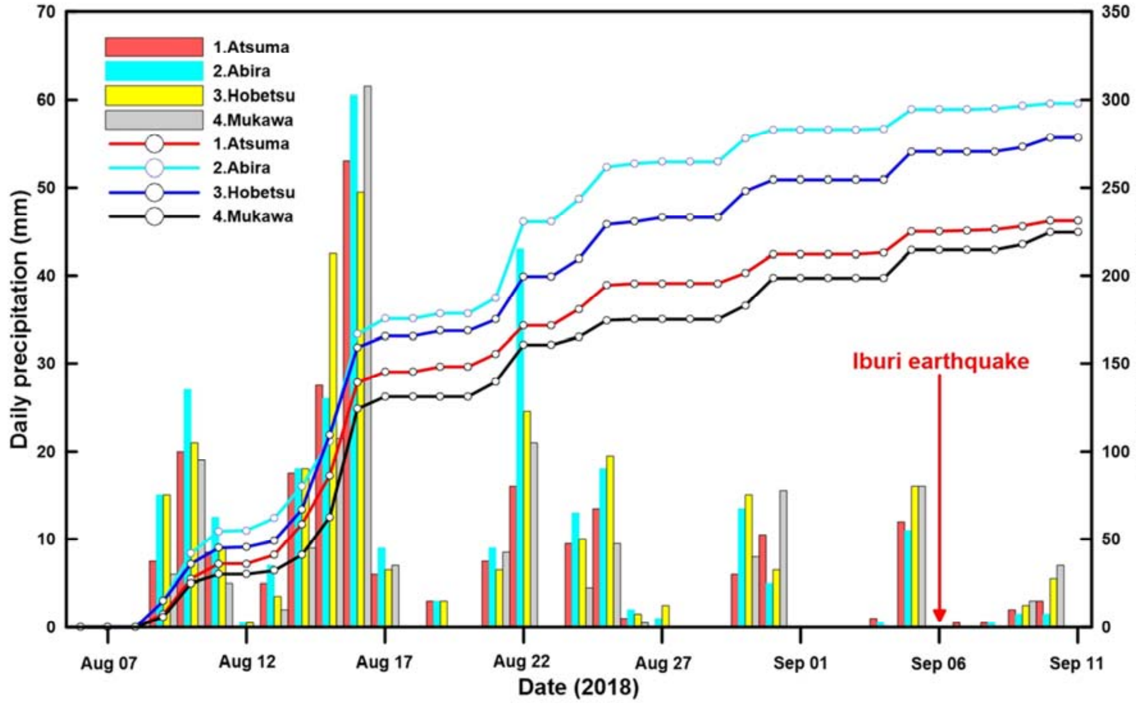

Daily and cumulative precipitation from 6 August 2018 to 11 September 2018

4

2. Spatial distribution of the Iburi landslides

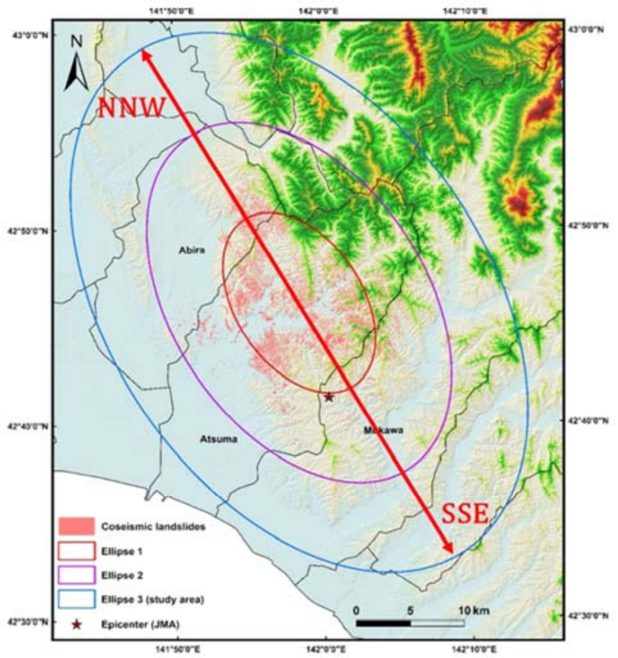

General spatial distribution: NNW/SSE

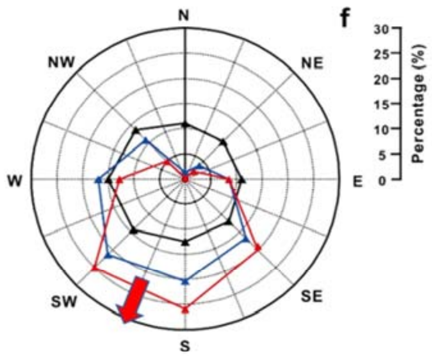

Preferred sliding direction : SSW

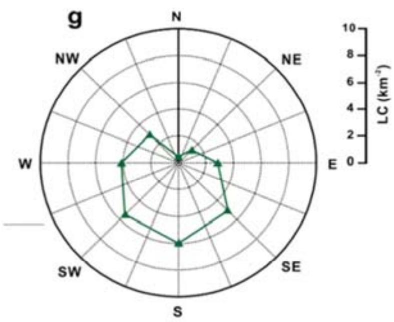

6

2. Spatial distribution of the Iburi landslides

Epicentral distance

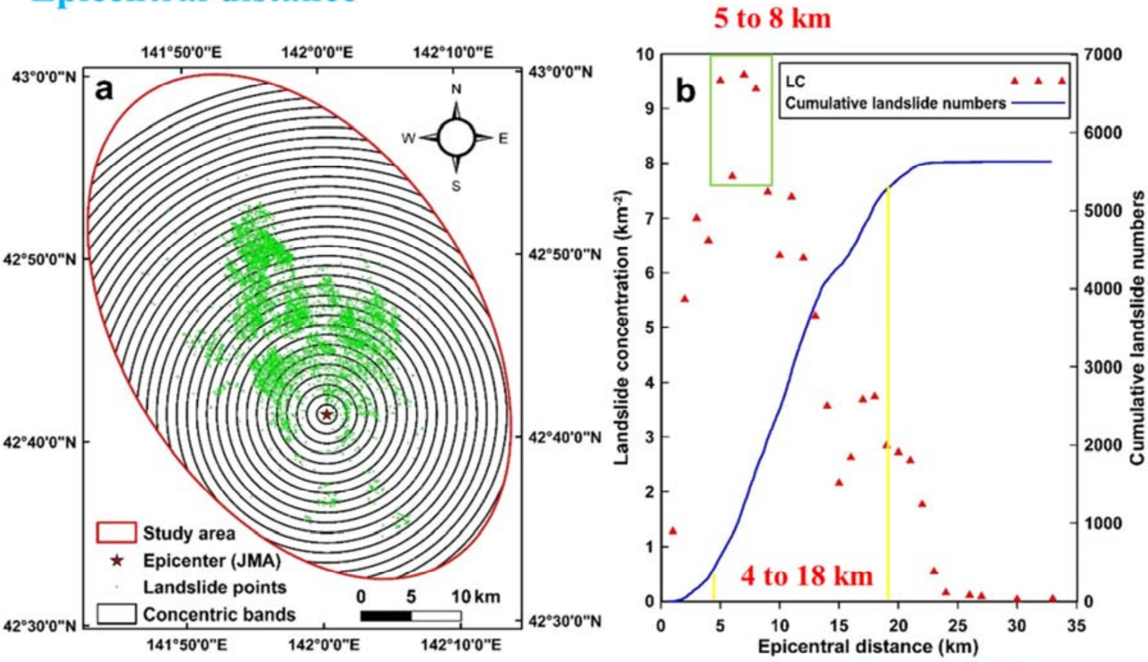

Relationship between **landslide occurrence** and **epicentral distance** 7

2. Spatial distribution of the Iburi landslides

Seismic intensity and PGA

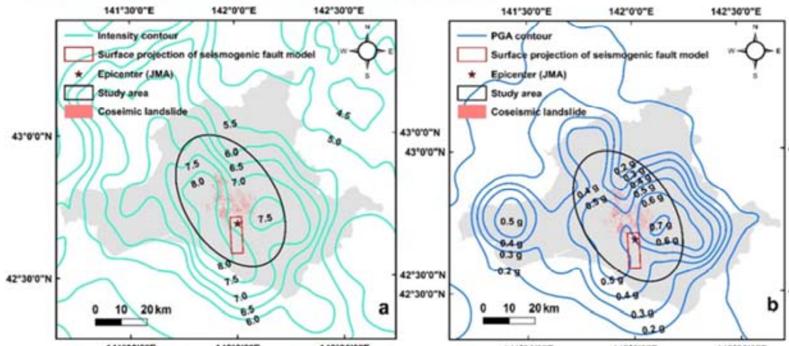

89.6% of the coseismic landslides are distributed in classes with seismic intensity 0f **7.0 - 8.0** and **86.2%** are concentrated in the area with PGA of **0.4 - 0.7 g**.

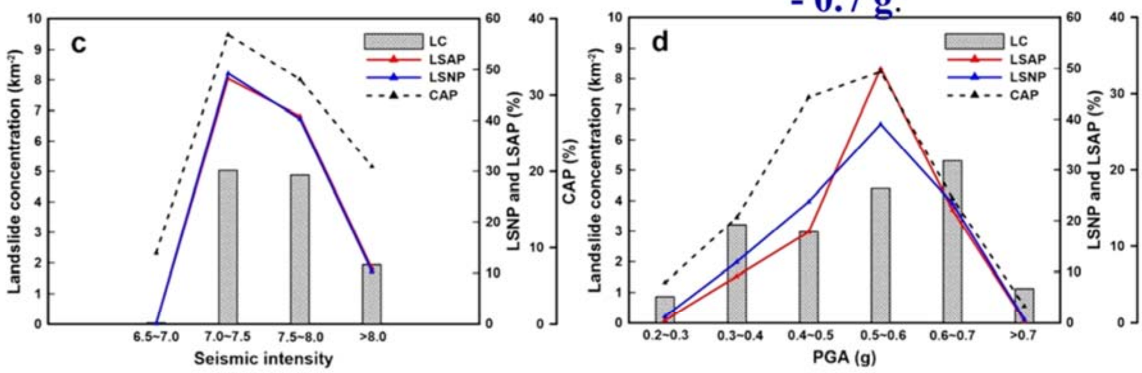

8

2. Spatial distribution of the Iburi landslides

Elevation and slope angle

1. **4,357** landslides occurred at elevations of **100 - 250 m**, corresponding to the LC of **7.1** per km^2.
2. **4,829** landslides occurred in slopes with mean slope angle at **15° - 35°**, corresponding to the LC of **8.4** per km^2.

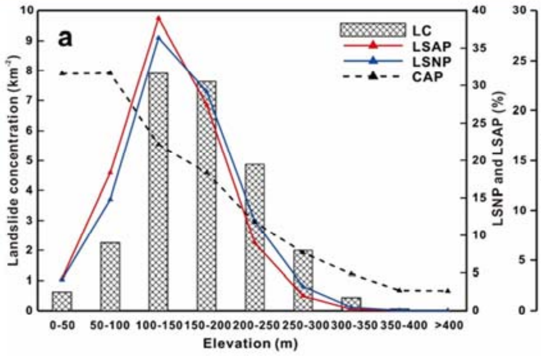

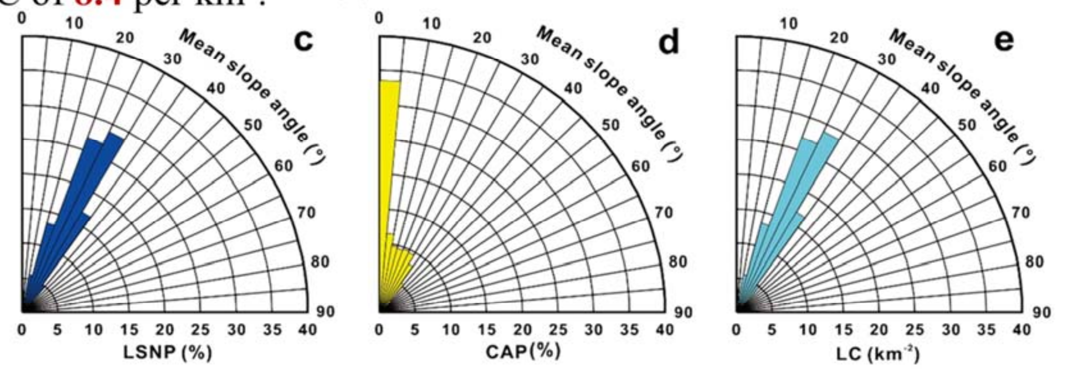

9

2. Spatial distribution of the Iburi landslides

Geological units & distance to faults

1. **N2sn** is the largest class area with the most concentrated landslides with a CAP of 43.0% and a LC of 8.1 per km^2. **N3sn** with the LC of 2.6 per km^2 is another remarkable class, accounting for 9.2% of the total occurrence and 6.6% of the total affected area.
2. The largest LC emerges in the class with a distance between **0.5 km and 0.6 km**, while the largest LSNP appears in the class with distance of **0.1 km to 0.2 km**.

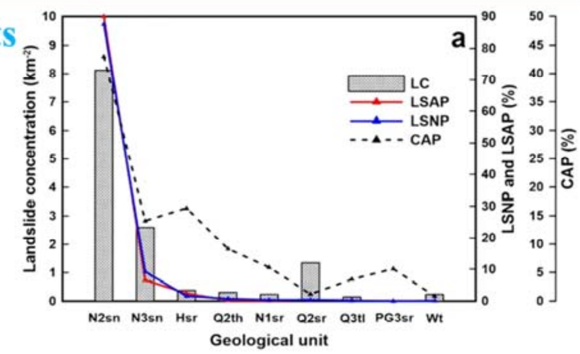

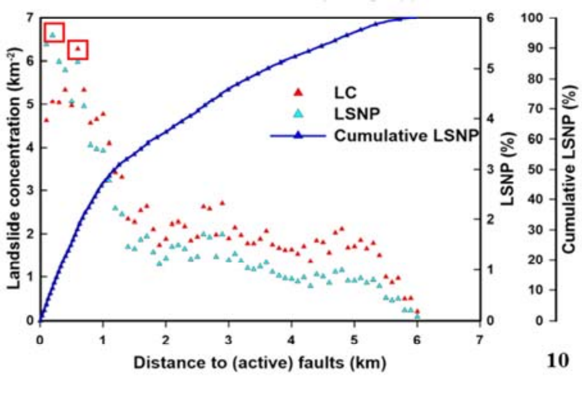

10

2. Spatial distribution of the Iburi landslides

Coseismic landslides in old landsliding area

Coseismic landslides: 5,625

Old landslides: 1,649

Intersected area:

110 old landslides;

109 coseismic landslides;

109 coseismic landslides occupying **2.6%** of the coseismic landslides area occurred in the old landslide area;

110 old landslides account for **6.7%** of the 1,649 old landslides.

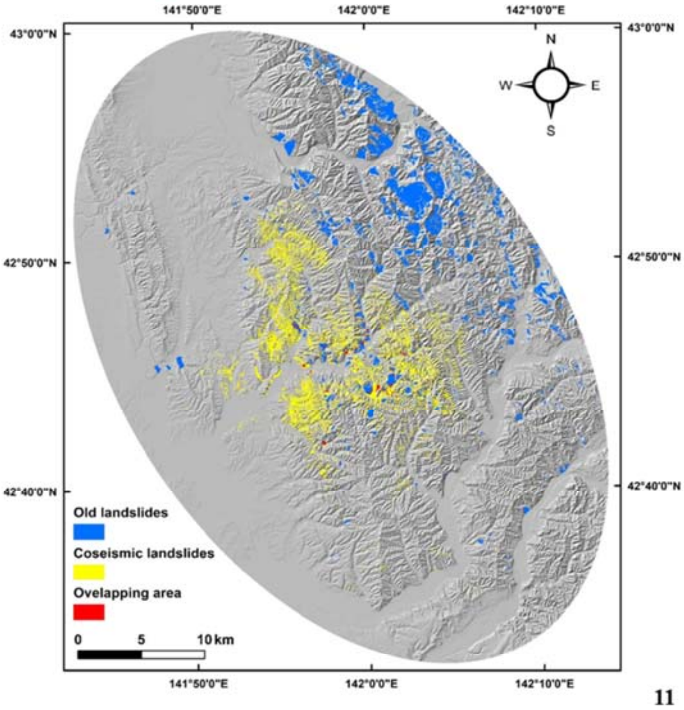

11

3. Types of the Iburi landslides

Two major types: **coherent shallow debris slide** and **disrupted mobilization of valley fill**.

One **deep-seated landslide** was confirmed.

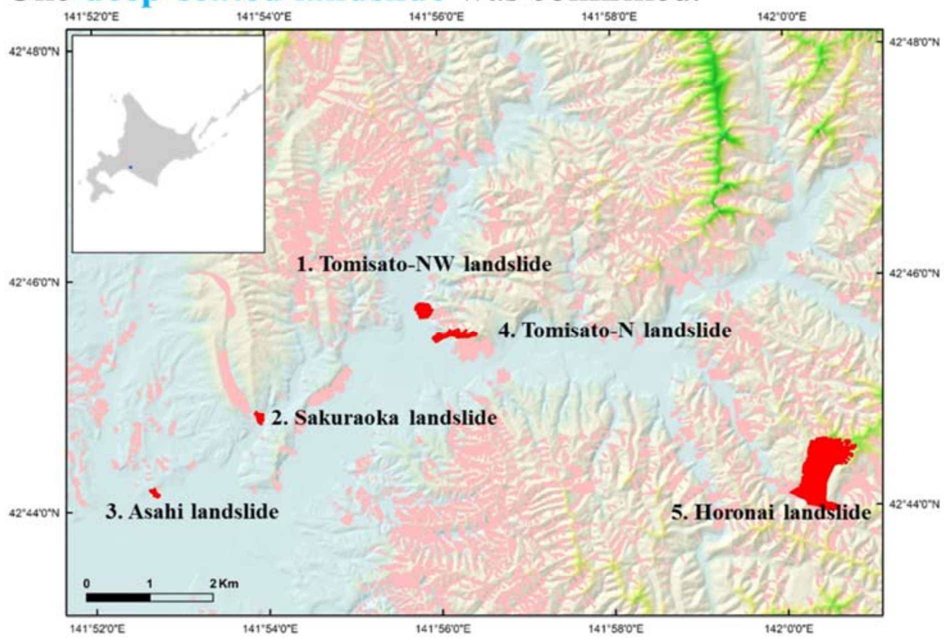

13

3. Types of the Iburi landslides

1. Tomisato-NW landslide

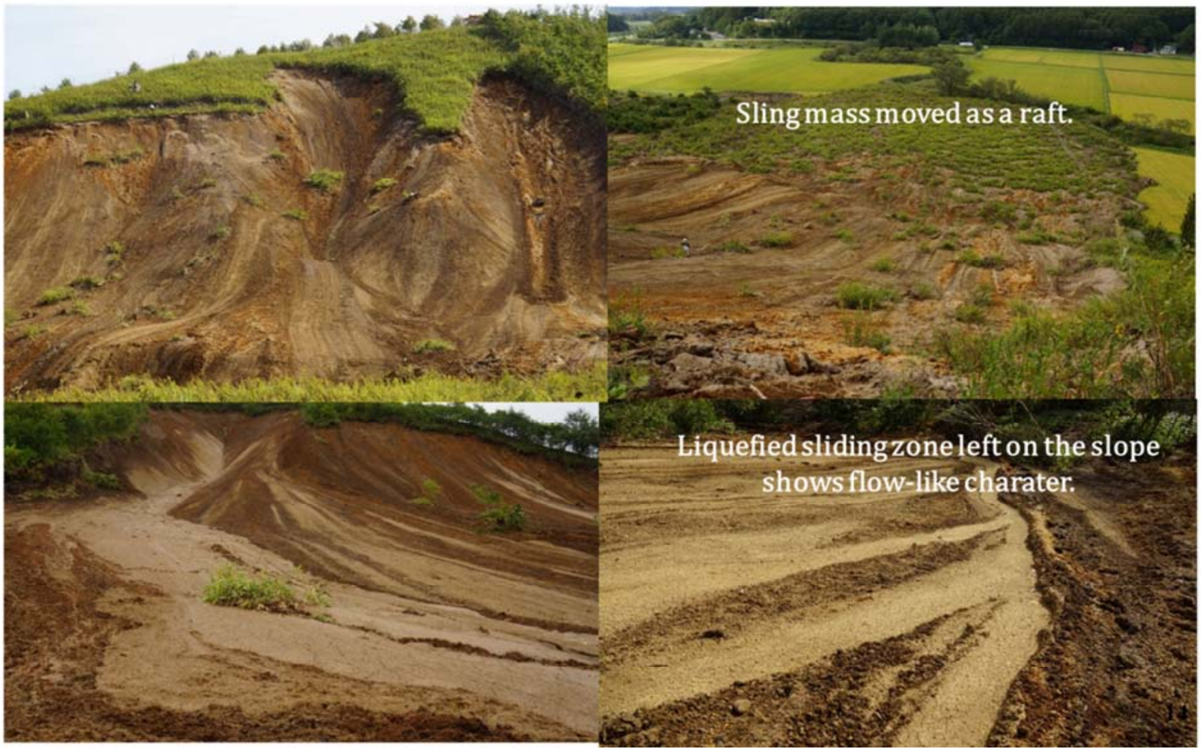

3. Types of the Iburi landslides

1. Tomisato-NW landslide

Flow-like sliding zone

15

3. Types of the Iburi landslides

1. Tomisato-NW landslide

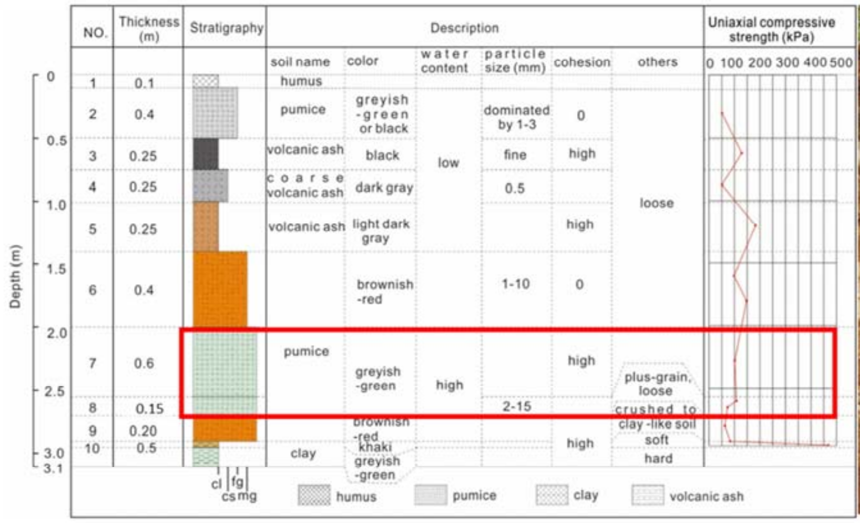

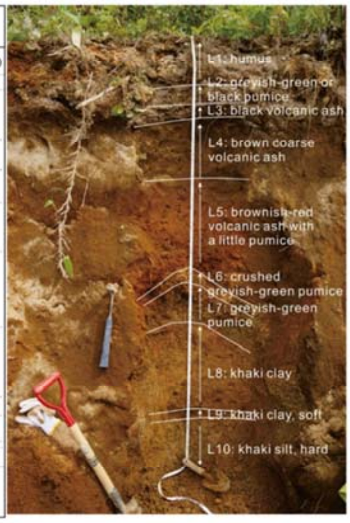

16

3. Types of the Iburi landslides

2. Sakuraoka landslide

17

3. Types of the Iburi landslides

2. Sakuraoka landslide

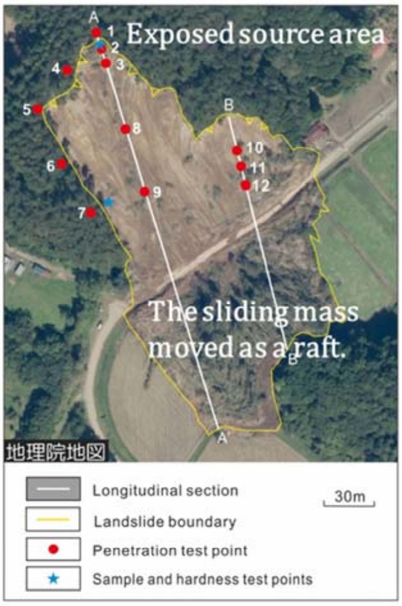

mobilized apparent friction angle: 10.6

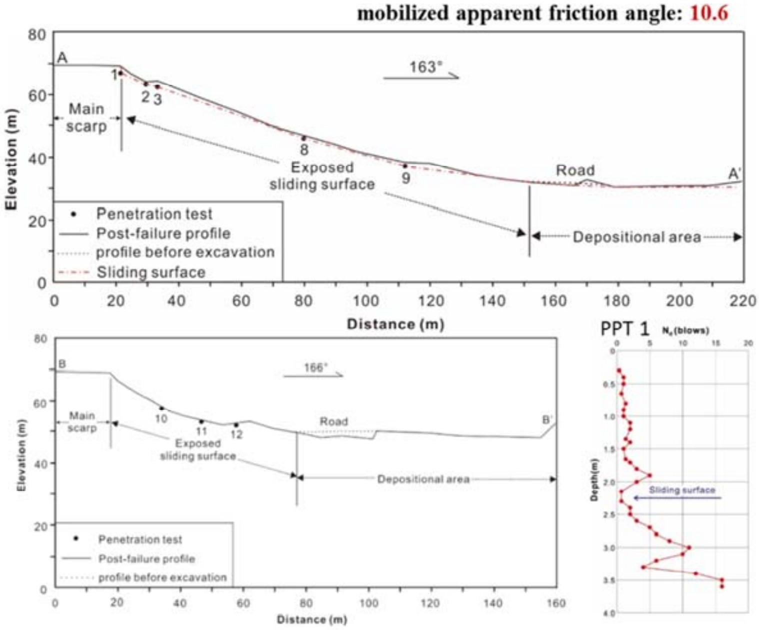

18

3. Types of the Iburi landslides

2. Sakuraoka landslide

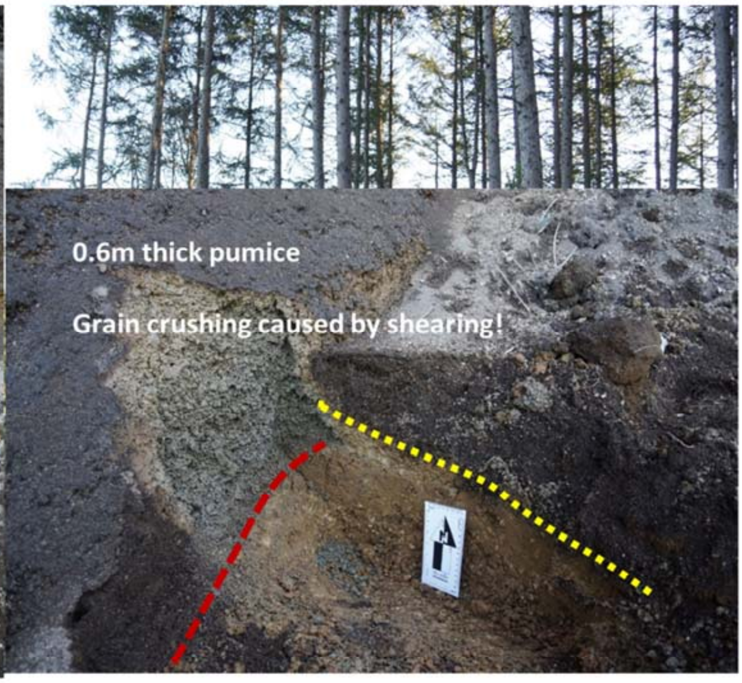

19

3. Types of the Iburi landslides

3. Asahi landslide

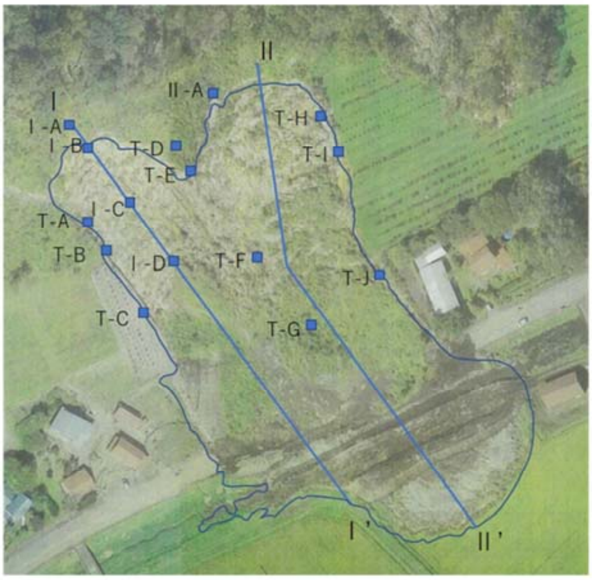

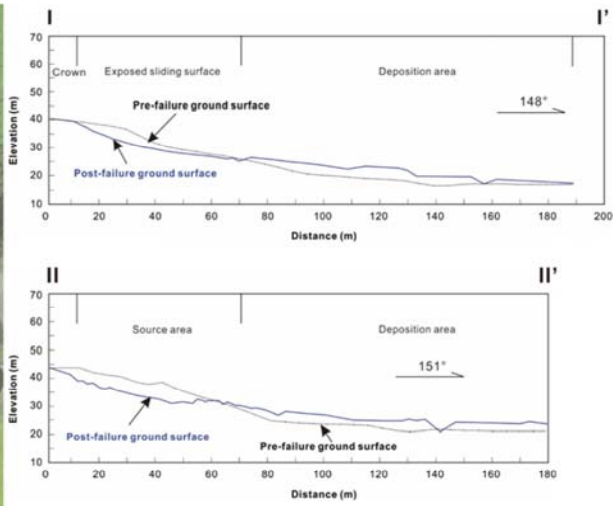

20

3. Types of the Iburi landslides

4. Tomisato-N landslide

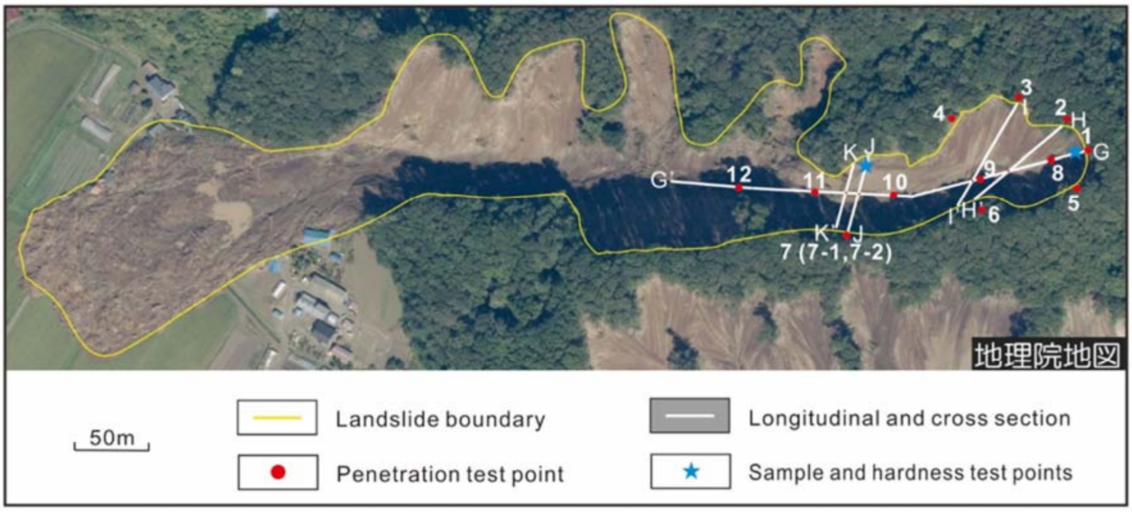

21

3. Types of the Iburi landslides

4. Tomisato-N landslide

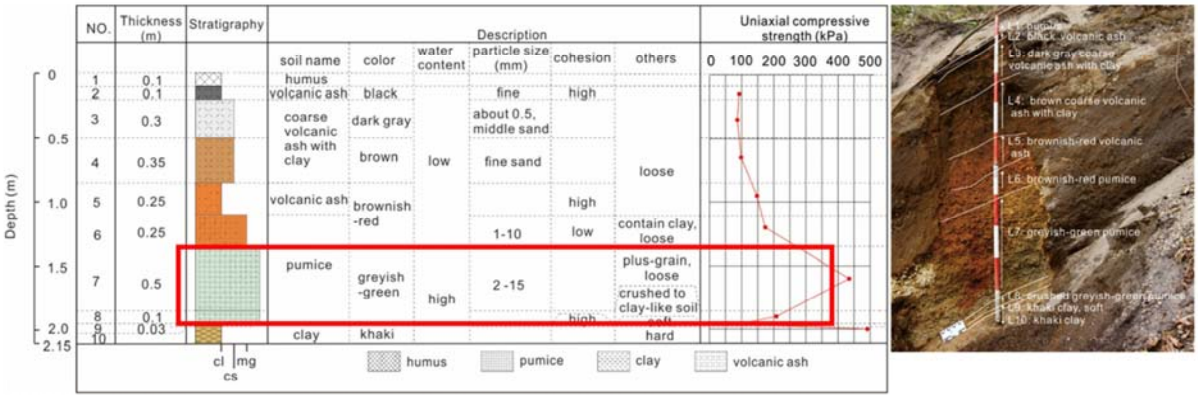

22

3. Types of the Iburi landslides

4. Tomisato-N landslide

Liquefaction may have occurred during the downslope skidding, and the sliding mass then flowed along the gully.

Another liquefaction occurred again.

23

3. Types of the Iburi landslides

5. Horonai landslide (deep-seated)

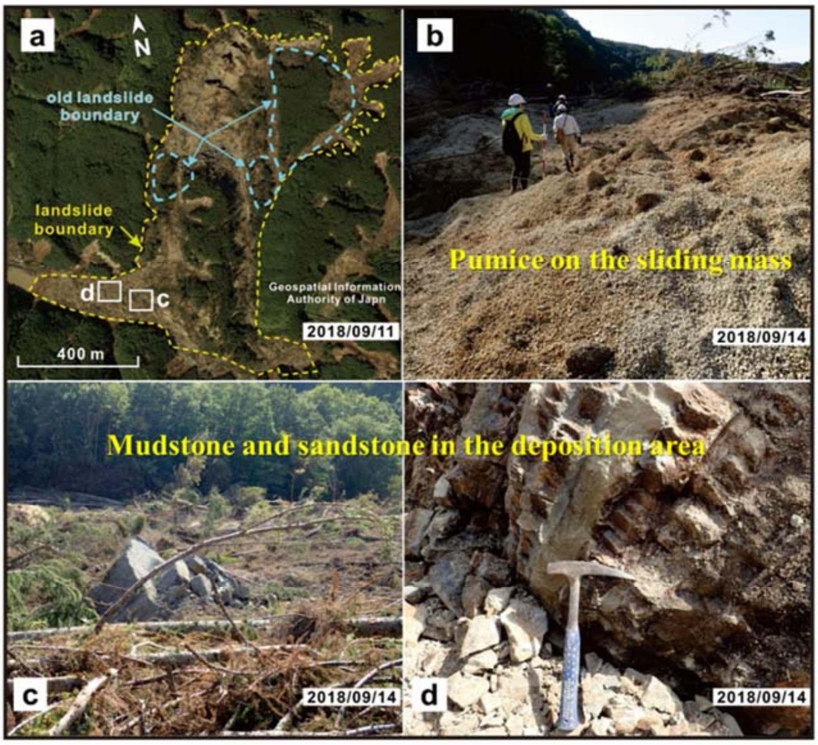

24

4. Failure and motion mechanism

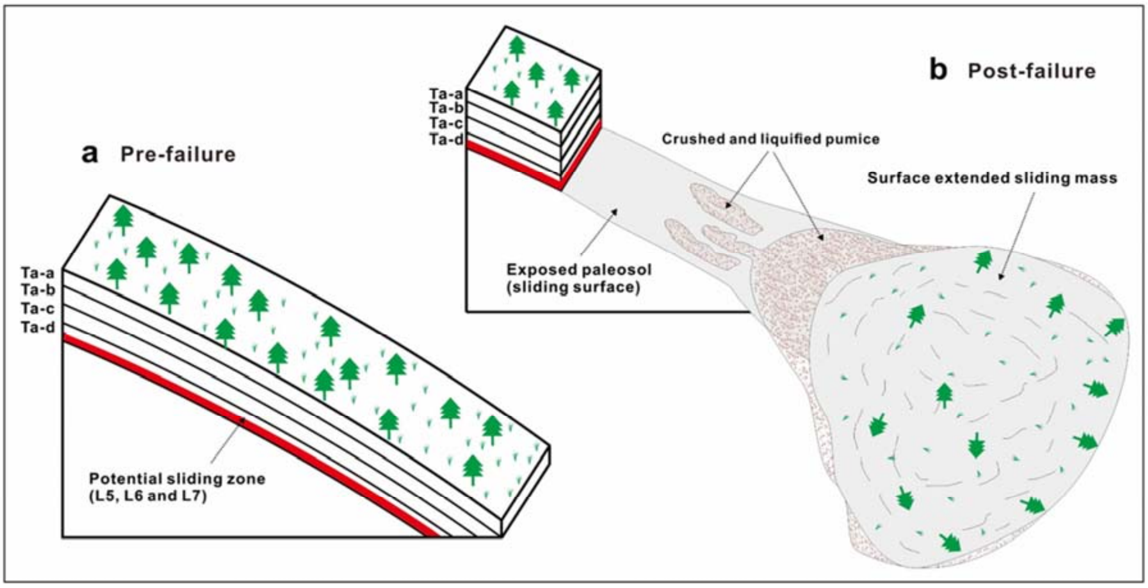

26

5. Initiation and motion simulation

Parameters used in the simulation

For sliding zone	
Initial apparent friction coefficient	0.10
Accumulation possibility of excess pore pressure	0.98
Lateral earth pressure coefficient (*K*)	0.9
Effective friction coefficient at sliding zone	0.84
Shear resistance of sliding zone at steady state	2 kPa
For sliding mass	
Unit weight of sliding mass	12.3 kN/m^3
Effective friction coefficient of the sliding mass	0.84

28

5. Initiation and motion simulation

Tomisato-NW landslide

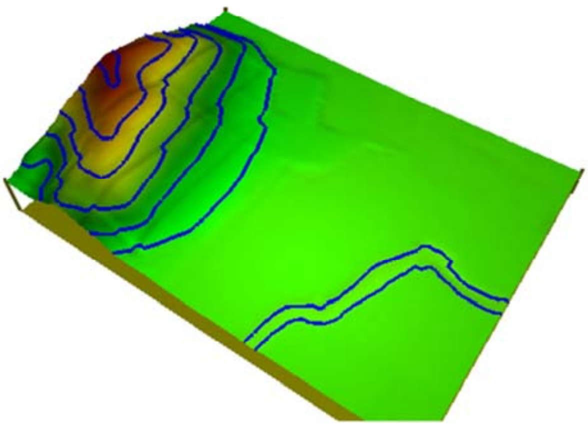

Asahi landslide

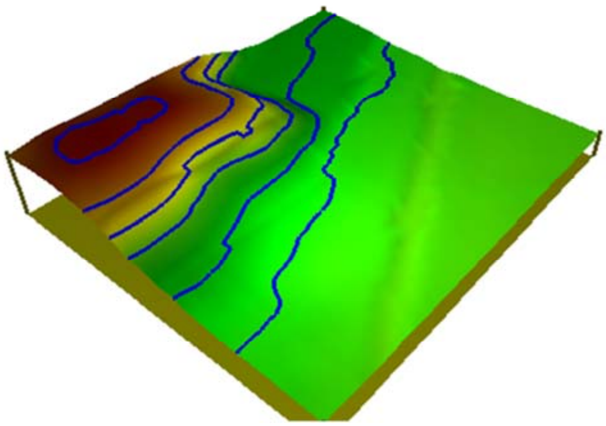

29

6. Conclusion remarks

1. Strong seismic ground motion is the main triggering factor for the coseismic landslide occurrence; high saturation of the soil that resulted from either the pond leakage or the preceding rainfall is responsible for the liquefaction and long run-out.
2. Sliding zone liquefaction occurred due to the collapse of loose structure in sandy soil; grain crushing liquefaction occurred due to the existence of the crushable soil.
3. During the sliding process, sliding zone may extend into the sliding mass because of shearing.

If the sliding mass is loose and fully saturated, spontaneous liquefaction may occur, and form a thick sliding zone; if the sliding zone is fully saturated and grain is easily crushable, the sliding zone may extend into the sliding mass.

31

6. Conclusion remarks

4. During the sliding process, sliding zone may be consumed because of wearing-out.

The sliding zone may be kept for long distance because all of the sliding mass may become to sliding zone; Sliding zone liquefaction will be limited in the crushable zone, and the sliding mass may move like a raft.

5. Possible sliding velocity and distance depends on the thickness and friction of the sliding zone.
6. Liquefaction is always accompanied by high speed and long run-out mass movement.

32

General characteristics of rock avalanches: comparison of Central Asian and Tibetan case studies

Alexander Strom(1, 2, 3)

1) Geodynamics Research Center – branch of JSC «Hydroproject Institute» Volokolamsk Highway 2, Moscow, Russia strom.alexandr@yandex.ru
2) Chang'an University, Xi'an, China
3) State Key Laboratory of Geohazard Prevention and Geoenvironment Protection, Chengdu, China

Abstract

Study of large-scale bedrock slope failures in Central Asia and in the south-eastern part of the Tibetan Plateau, in the Jinsha and Minjiang river basins, show that most of them have similar dual structure of the deposits with intensively fragmented interior and coarse blocky outer zone (carapace) and evidence of flow-like motion. In the Tibetan river basins with very deep and narrow valleys most of large-scare rock slope failures form natural dams just at the feet of the collapsed slopes. Many of Central Asian cases are characterized by longer runout. Nevertheless, we can easily find features from both regions that can be considered as analogues, either in the shape of the deposits (e.g. similar spreading of debris along and across river valleys), or in the internal structure (e.g. presence of blocks of the alluvium in rock avalanche debris), or in their role in river valleys evolution (e.g. short-term or long-term river blocking). Similar case studies from both regions will be demonstrated. It should be pointed out that vast majority of large-scale rock slope failures, despite mechanism of their initiation and runout distance, finally converted into rock avalanches and should be classified just as this type of flow-like landslides.

Study of large-scale bedrock slope failures in Central Asia and in the south-eastern part of the Tibetan Plateau, in the Jinsha and Minjiang river basins, show that most of them have similar dual structure of the deposits with intensively fragmented internal part and coarse blocky carapace.

Central Asia

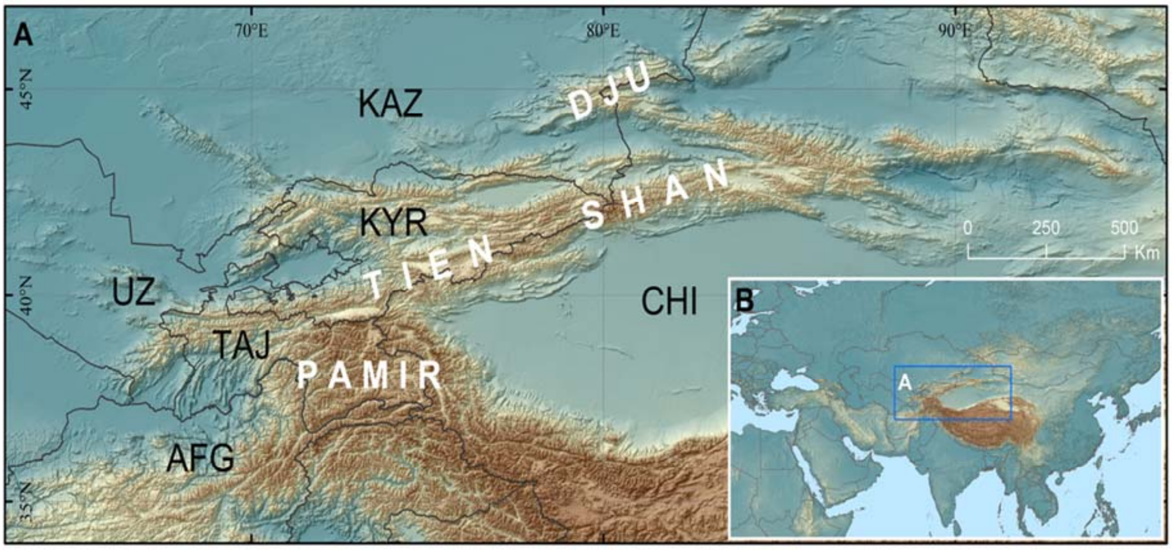

Eastern Tibet, Jinsha and Minjiang basins

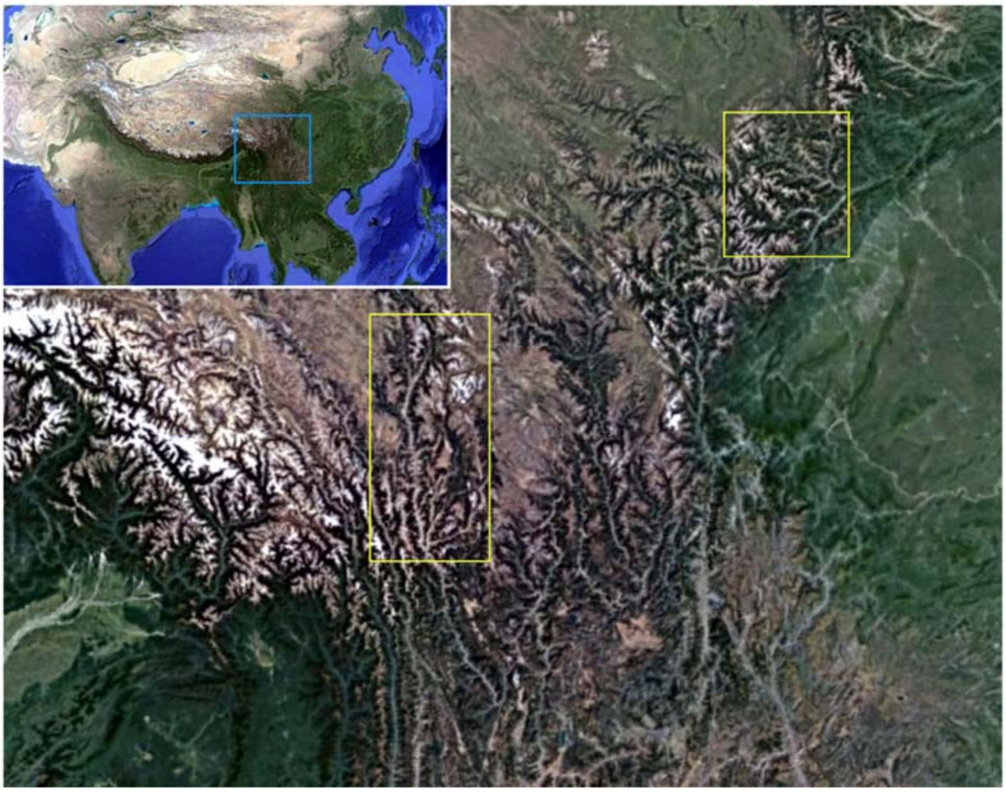

In both regions deposits even of those rock slope failures that occurred in deep and narrow valleys and formed natural dams just at the feet of the collapsed slopes have such internal structure typical of the flow-like rock avalanches.

Rockslide (rock avalanche) in the left tributary of the Jinsha River at28.377° N, 99.242° E

Intensively crushed debris with rare boulders imide and with preserved evidence of bedding in the internal part of the breached rockslide dam overlain by coarse boulder carapace

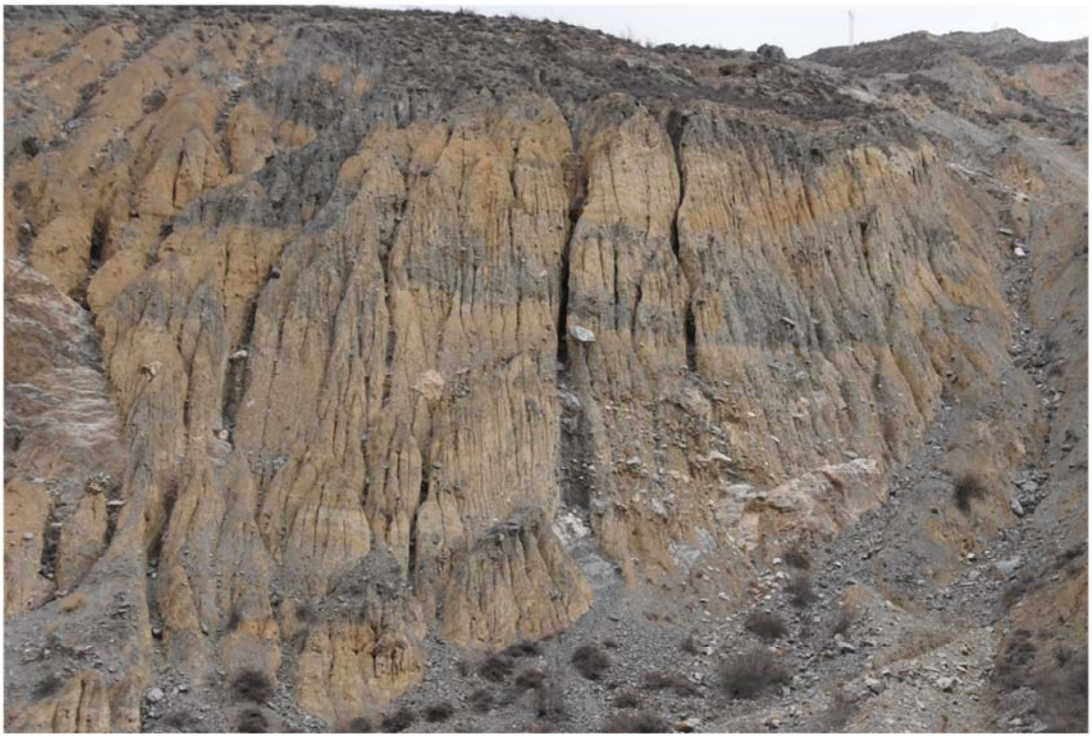

Dual structure of rockslide (rock avalanche) dam in the Jinsha River valley at 29.316° N, 99.074° E and sharp contact between fragmented and blocky zones.

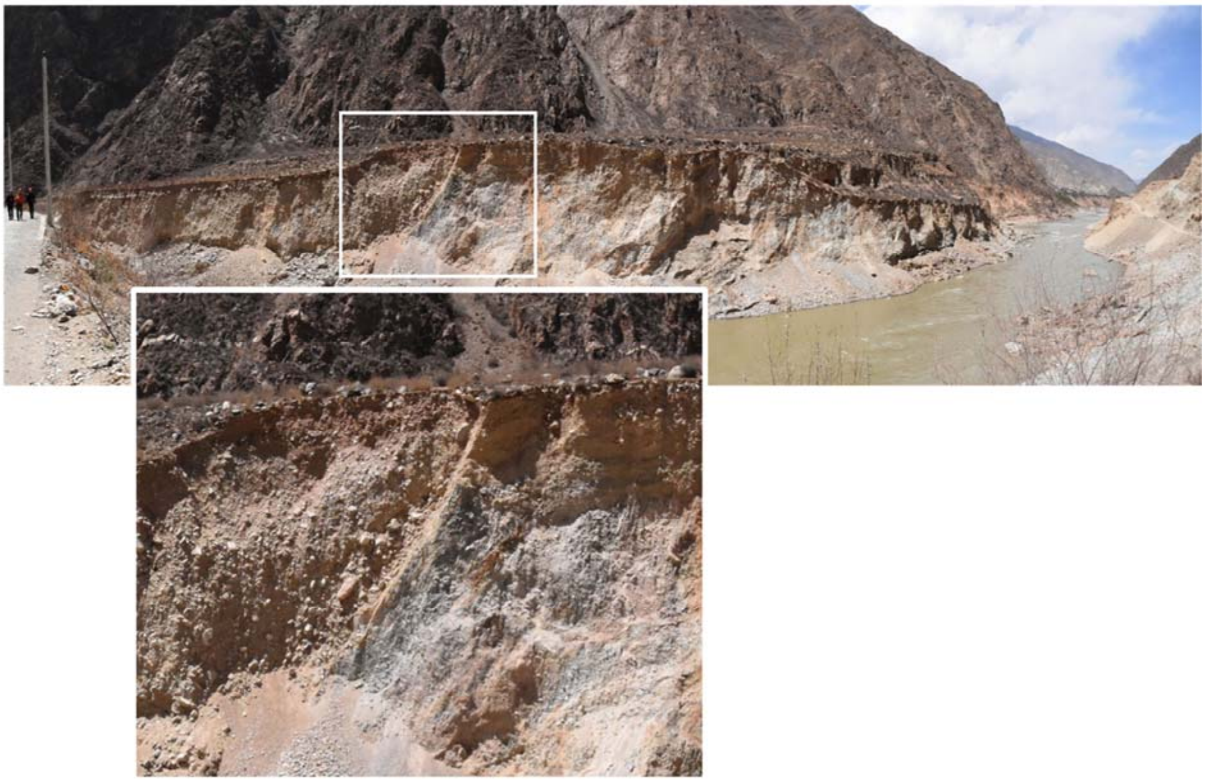

The Mini-Köfels rockslide (rock avalanche) in the Kokomeren River valley in Central Tien Shan (41.9° N, 74.286° E)

Red gneiss from the Mini-Köfels rockslide headscarp fragmented into homogenous fine-grained material (RS) that rest on the fluvial terrace (aQ).

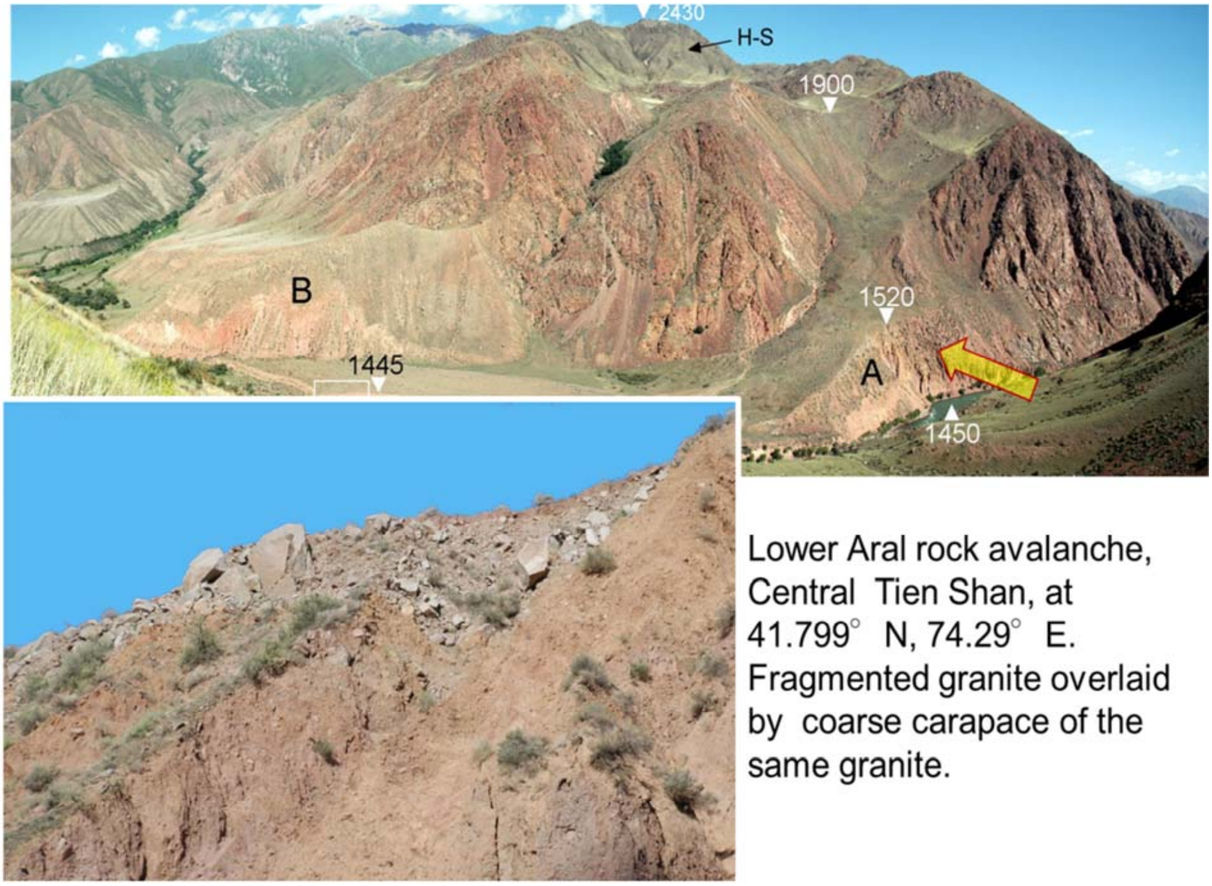

Lower Aral rock avalanche, Central Tien Shan, at 41.799° N, 74.29° E. Fragmented granite overlaid by coarse carapace of the same granite.

Sometimes big “blocks” of alluvium remain in rock avalanche debris, as it was found in the frontal part of the Karachauli rock avalanche in Central Tien Shan, at 41.733° N, 74.073° E.

Similar inclusion of the fluvial pebbles in rockslide deposits was observed at the upstream part of the Ancient Diexi rockslide in Minjiang River valley, Sichuan, China ”, at 32.041° N, 103.668° E.

Vast majority of large-scale catastrophic rock slope failures in both regions and, actually, worldwide, converted into rock avalanches regardless of the mechanism of their initiation and of the runout distance, and should be classified just as this type of highly mobile flow-like landslides.

Studying landslide movements from source areas to zone of deposition using a deterministic approach (IPL-226)

Jernej Jež(1), Tina Peternel(1), Mitja Janža(1), Mateja Jemec Auflič(1)

1) Geological Survey of Slovenia, Ljubljana, Dimičeva ulica 14, 1000, Ljubljana
e-mail: jernej.jez@geo-zs.si

Abstract

The main objective of this project is development of an interdisciplinary methodological approach for risk assessment of landslides and mass flows, which will include landslide origin (source areas) modelling, assessment of deposition volume, determination of rheological characteristics of the material, and modeling of the runout distance and the zone of deposition. The existing landslide susceptibility map will be upgraded for the wider catchment of Potoška planina and Stože landslides in a detailed scale which will be directly applicable in spatial planning, planning of prevention measures, and mitigation measures. Developed hydrogeological models for both study cases will enable spatially distributed and transient modelling of processes of the hydrological cycle. At the same time integration into slope stability model will significantly improve the accuracy of landslide prediction models. The results of modeling the rheological characteristics of the sampled soils will enable the prediction of the landslide source area, its spreading and possible mobilization into debris flow and 3D visualisation of potential landslide areas at different scales. These objectives will be achieved through extensive fieldwork in order to capture the data needed to improve the reliability of the modeling results.

Contents

- Objectives
- Problem identification
- Study area
- Results
- Project Beneficiaries
- Conclusions

2

Objectives

- Low speed landslides may cause failure of structures but are not usually dangerous for humans. While a highspeed, long-runout and wide-spreading landslides may cause a greater disaster.

- To reduce human loss from landslides and assess landslide hazard the following questions are pursued:
    - **where** can landslides occur (place of origin),
    - **when** (rheological properties of material, rainfall),
    - **how** extensive can they be (magnitude), and
    - **where** can landslides act (place of action)?

3

Objectives

- Developing a interdisciplinary methodology for risk assessment of landslides and debris flows, which will include
    - landslide origin (source areas) modelling,
    - assessment of deposition volume,
    - determination of rheological characteristics of the material, and
    - modeling of the runout distance and the zone of deposition.

4

Problem identification

- This IPL project is focused on **landslide investigations**, **deposition areas**, and the **geomechanical** and **rheological conditions** required for **mobilization** into a **debris flow**.

- The **landslide and debris flow origin** (source areas) was **determined** by previous studies using **spatiotemporal factors.**

- **Rainfall, velocity**, **volume** of deposit, **sliding**/flow **path**, and **deposition area** were not yet considered in studying the **dynamics of the landslide**.

5

Problem identification

- The following **key parameters** will be studied:
  - geological structure,
  - slope inclination (relief),
  - geomechanical characteristics of the soil,
  - catchment area of surface water and groundwater,
  - rainfall threshold.

6

Study area

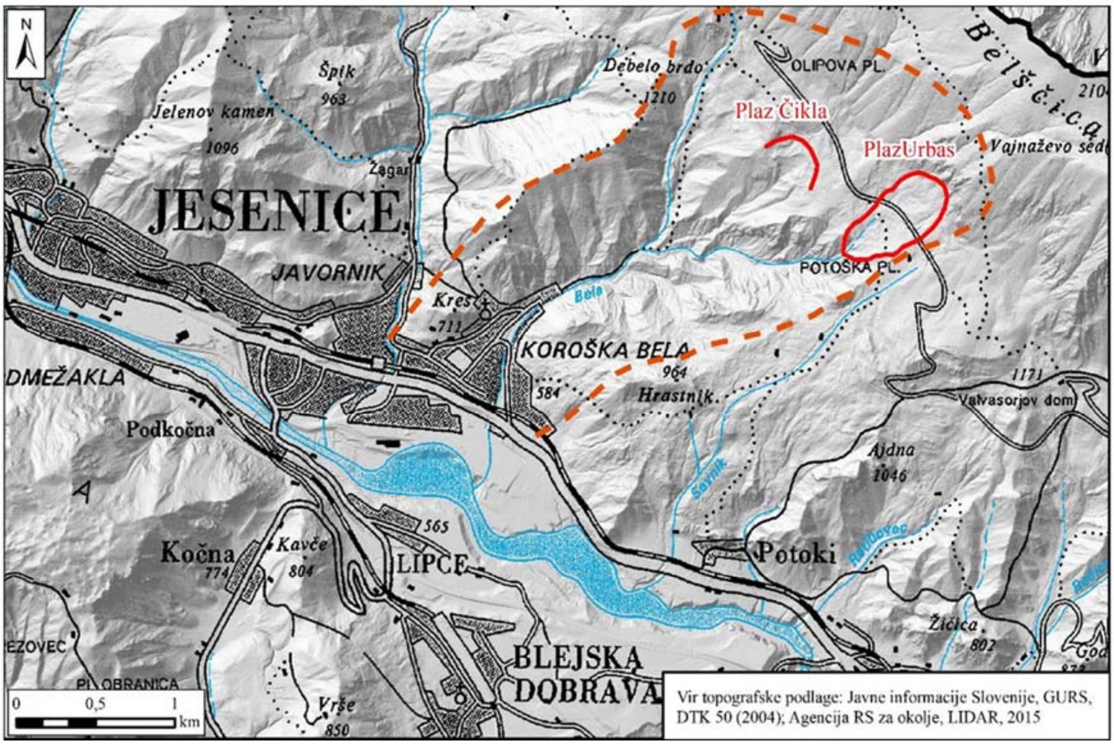

Study area

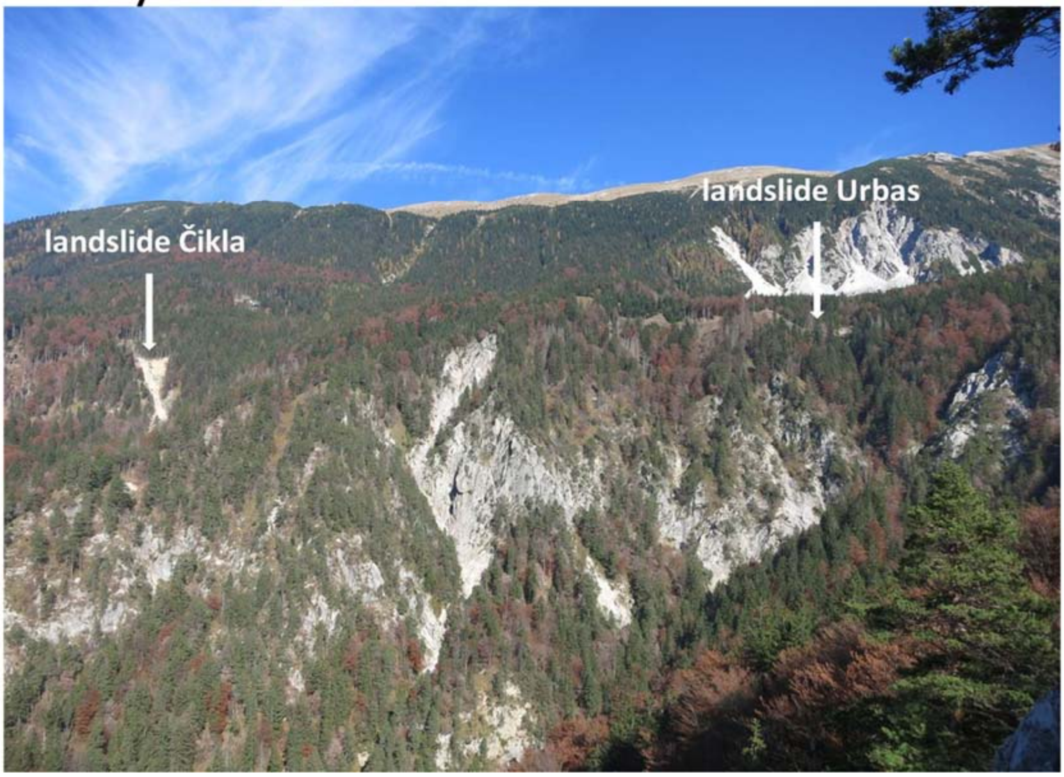

Study area – geological conditions

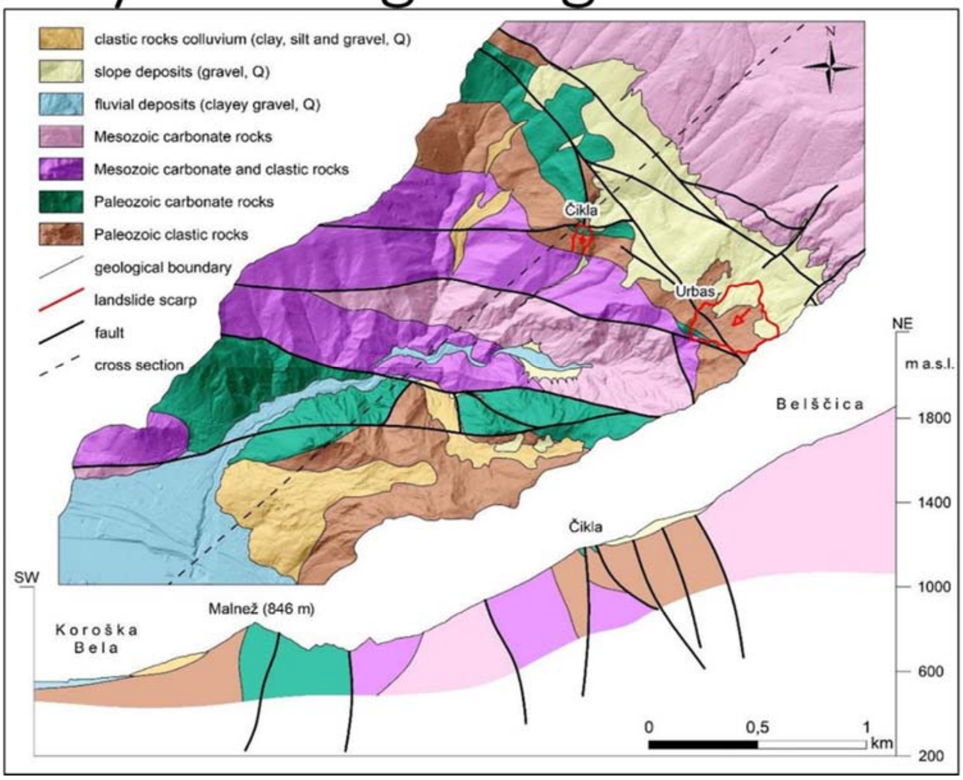


Study area
Landslide Čikla

The approach

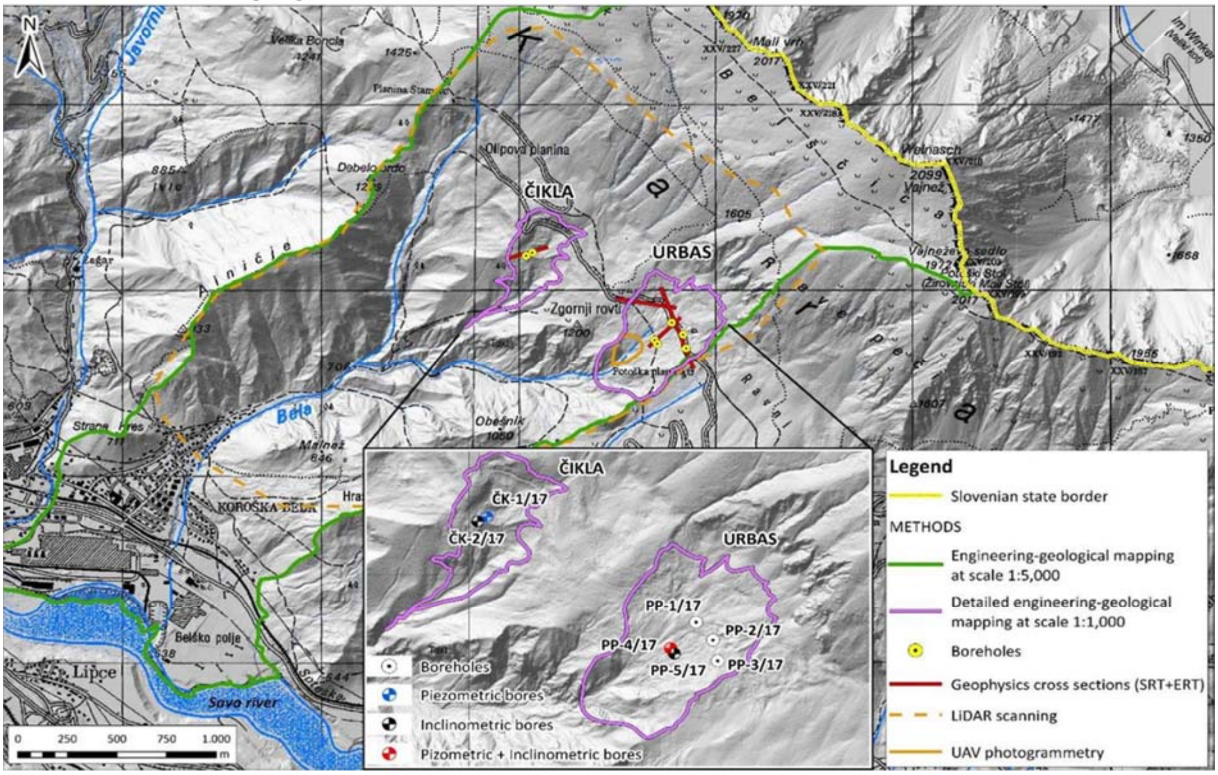

Research - Geological map and cross section of the hinterland of Koroška Bela (M 1:5.000)

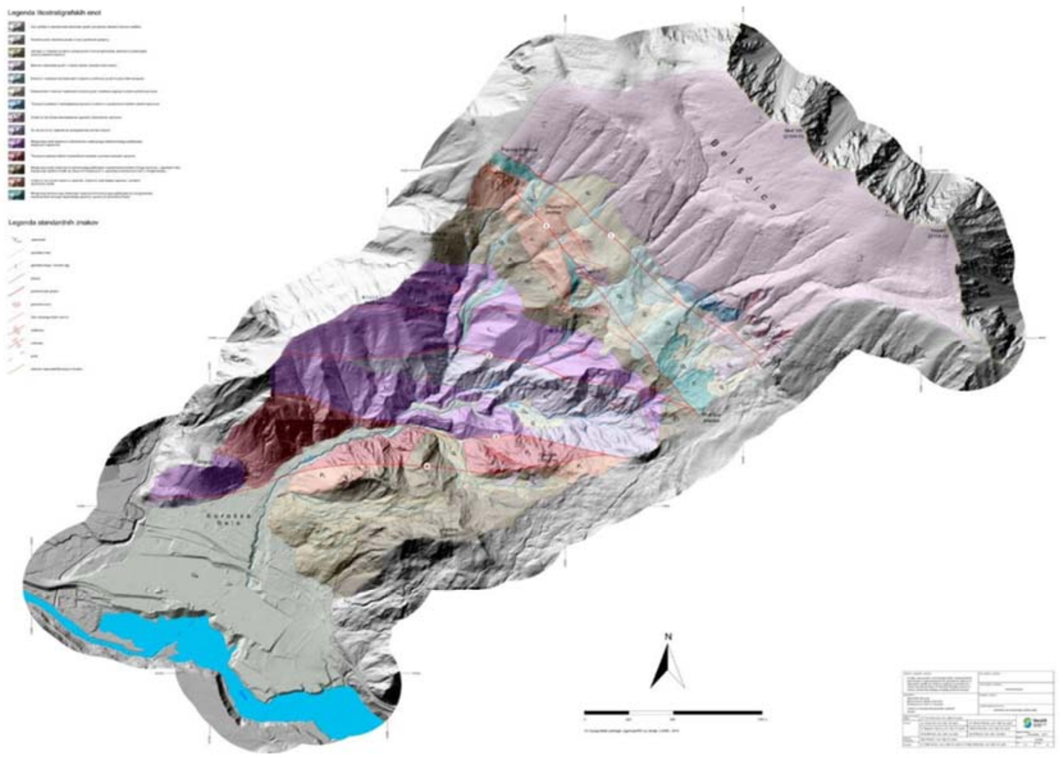

Research - Geological map and cross section of the hinterland of Koroška Bela (M 1:5.000)

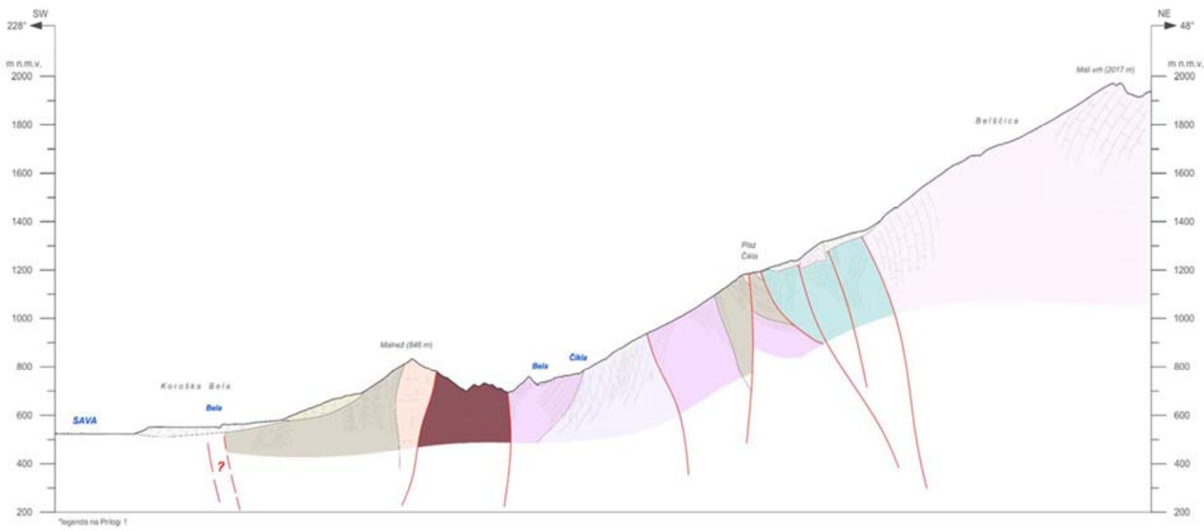

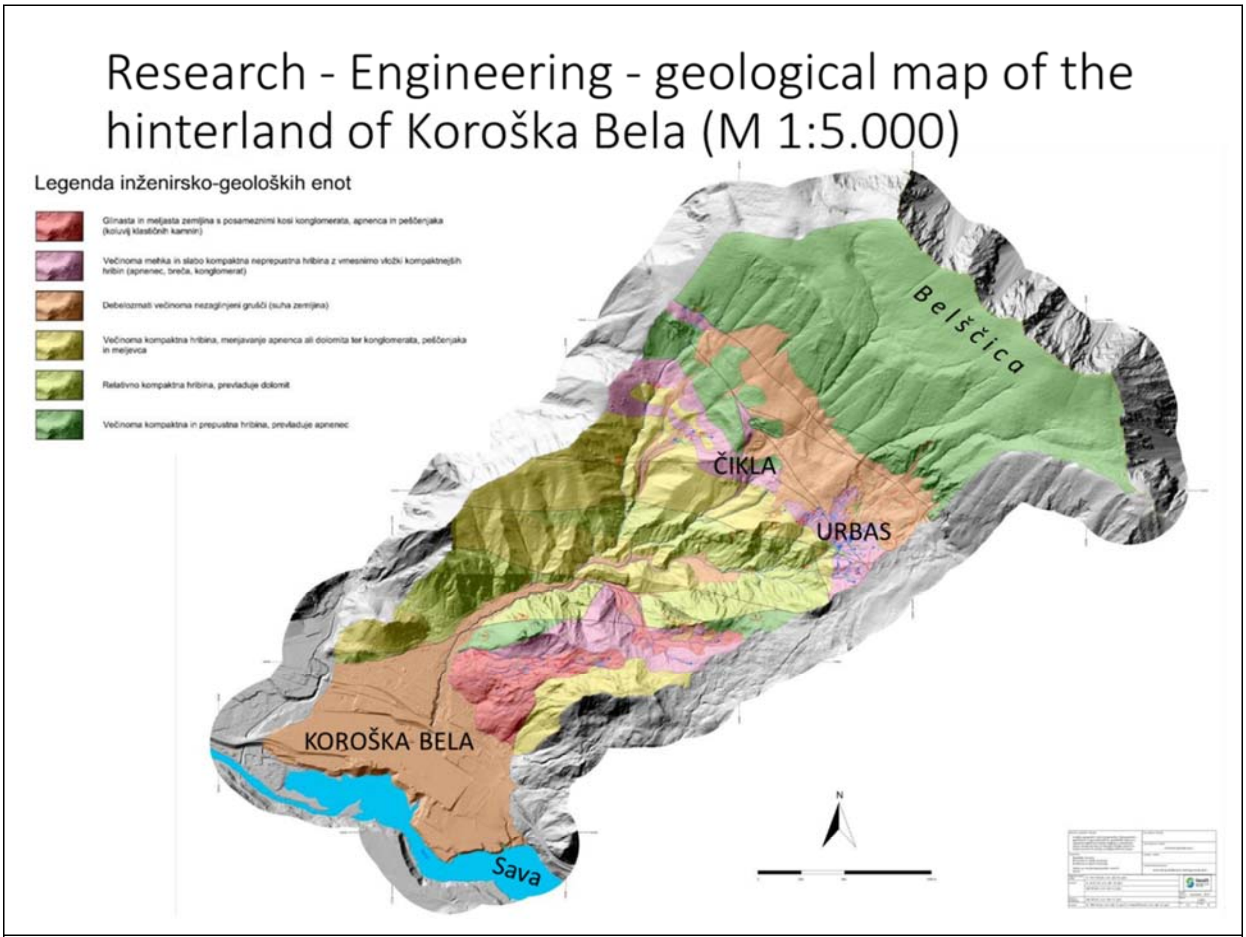
Research - Engineering - geological map of the hinterland of Koroška Bela (M 1:5.000)
Legenda inženirsko-geoloških enot
Glinasta in meljasta zemljina s posameznimi kosi konglomerata, apnenca in peščenjaka (koluvij klastičnih kamnin)
Večinoma mehka in slabo kompaktna neprepustna hribina z vmesnimo vložki kompaktnejših hribin (apnenec, breča, konglomerat)
Debelozrnati večinoma nezaglinjeni grušči (suha zemljina)
Večinoma kompaktna hribina, menjavanje apnenca ali dolomita ter konglomerata, peščenjaka in meljevca
Relativno kompaktna hribina, prevladuje dolomit
Večinoma kompaktna in prepustna hribina, prevladuje apnenec
Belščica
ČIKLA
URBAS
KOROŠKA BELA
Sava
N

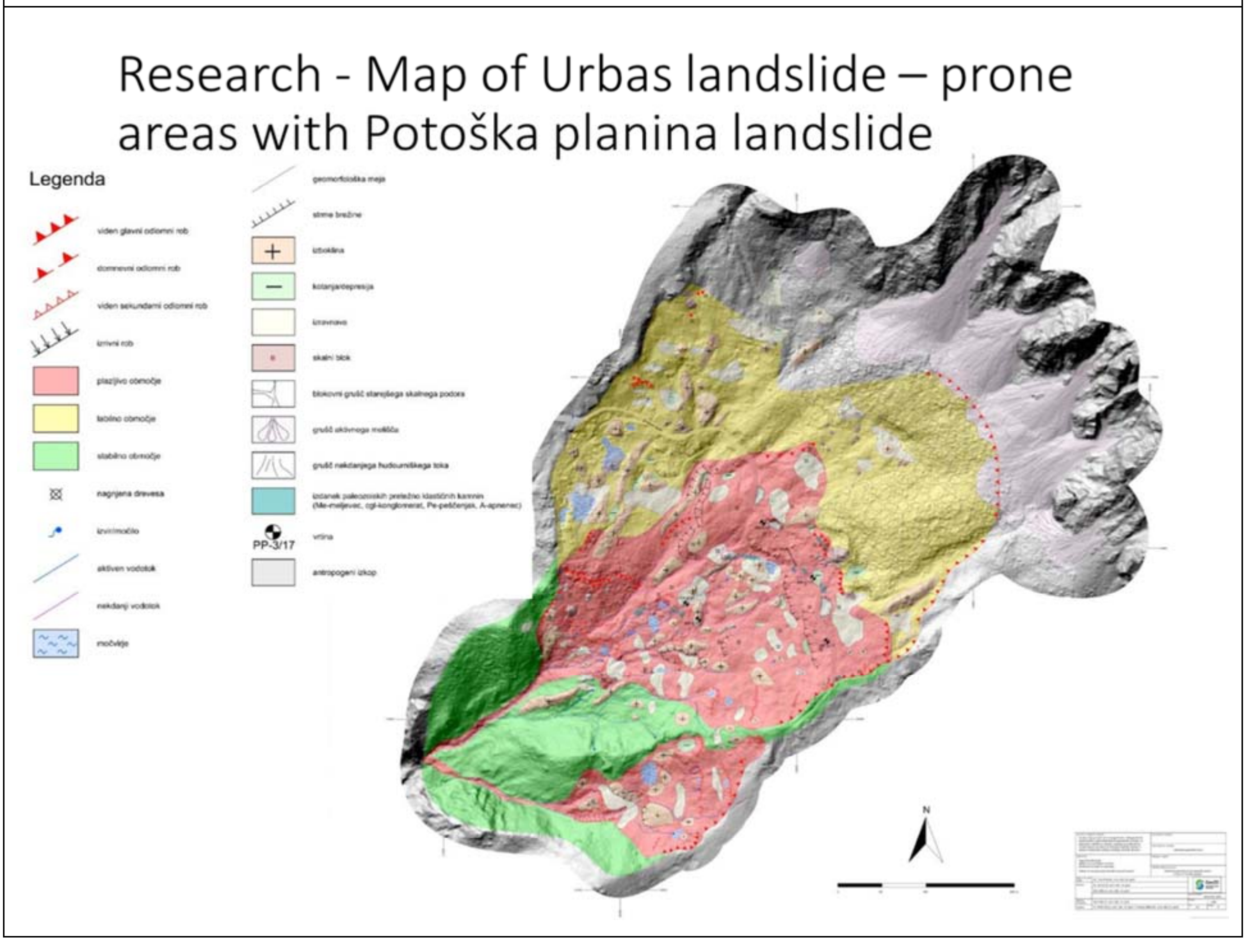
Research - Map of Urbas landslide – prone areas with Potoška planina landslide
Legenda
viden glavni odlomni rob
domnevni odlomni rob
viden sekundarni odlomni rob
plazljivo območje
labilno območje
stabilno območje
nagnjena drevesa
aktiven vodotok
nekdanji vodotok
močvirje
geomorfološka meja
strme brežine
izboklina
kotanja/depresija
skalni blok
blokovni grušč starejšega skalnega podora
grušč nekdanjega hudourniškega toka
vrtina
PP-3/17
antropogeni izkop
N

Research - Engineering - geological map of Čikla landslide

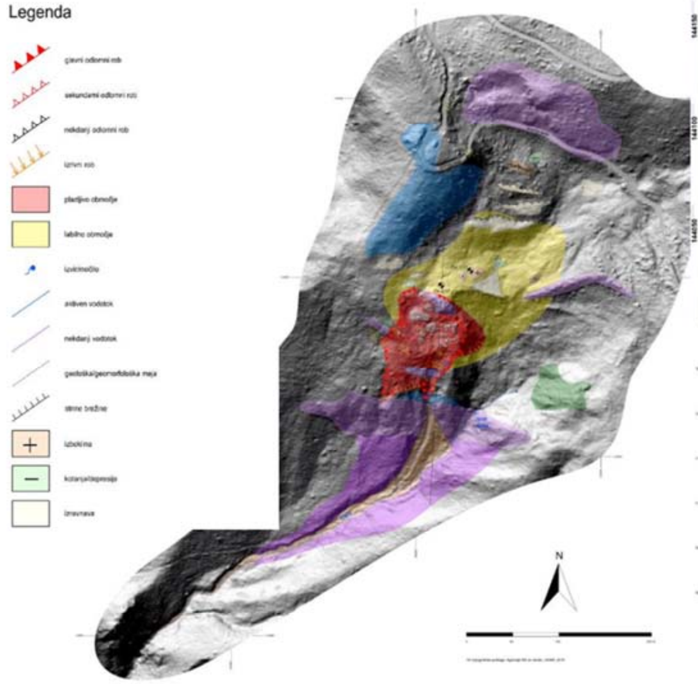

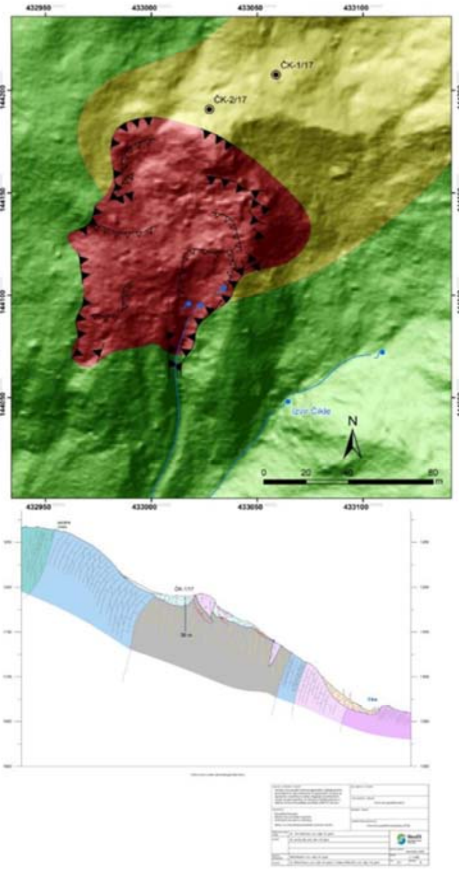

Research – Urbas landslide – core logging

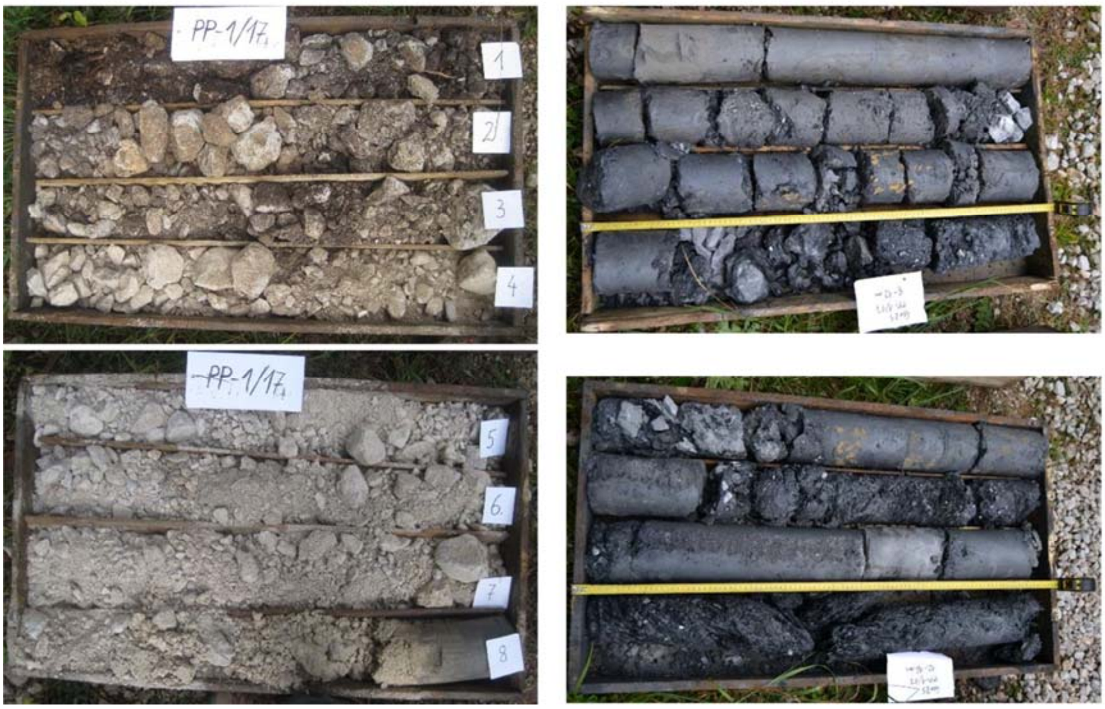

Research – Čikla landslide – core logging

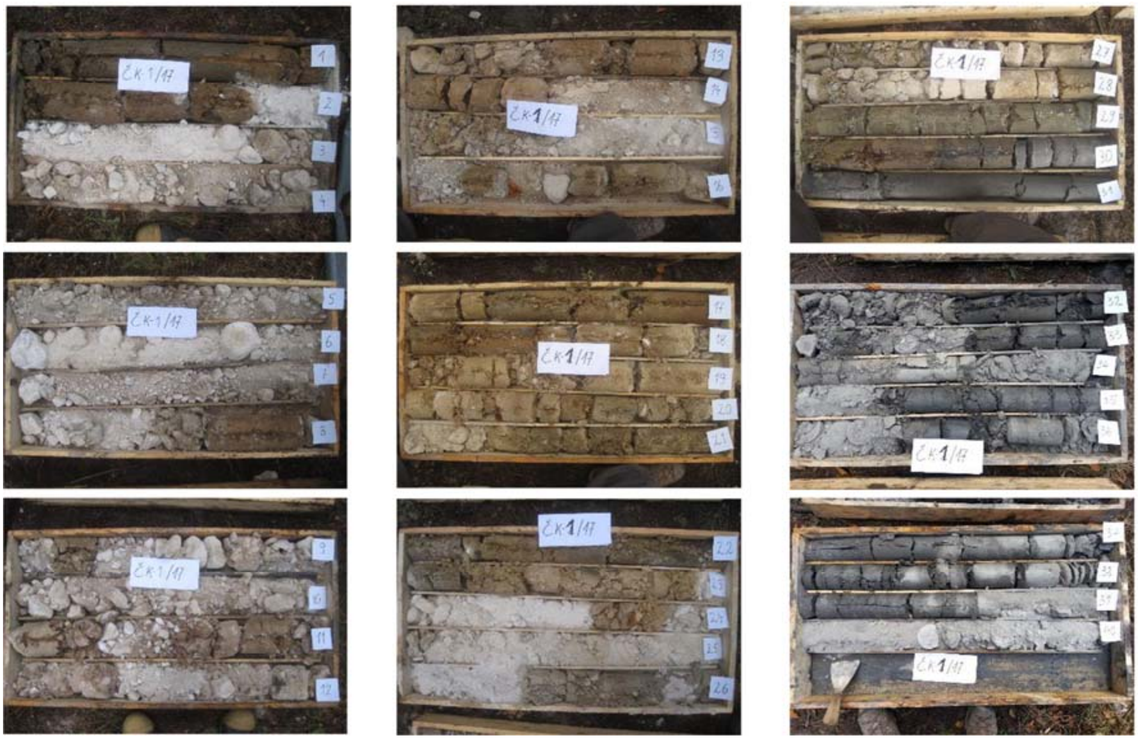

Research – monitoring system

- ✓ Monitoring of groundwater level
- ✓ Monitoring of inclinometers

(PP-5/17; ČK-2/17)

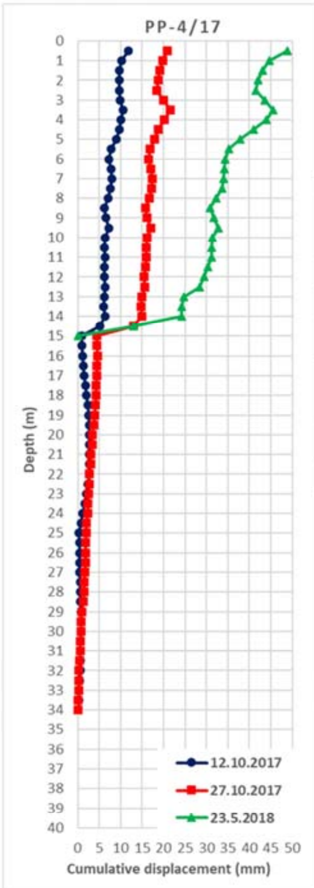

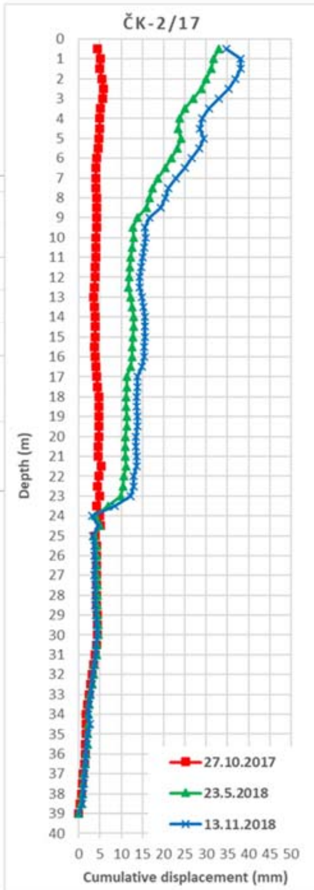

Research – geophysical investigations

- Seismic refraction method (SRT)
- Electrical resistivity tomografy (ERT)

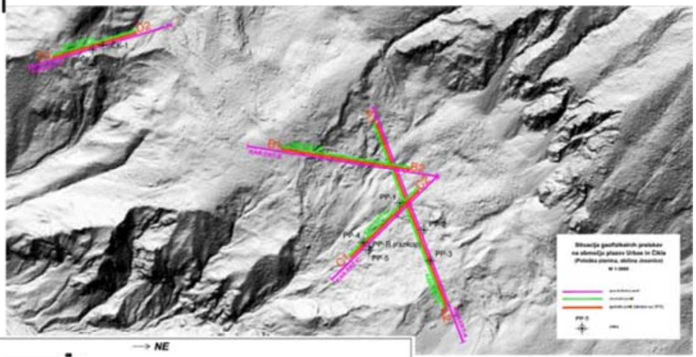

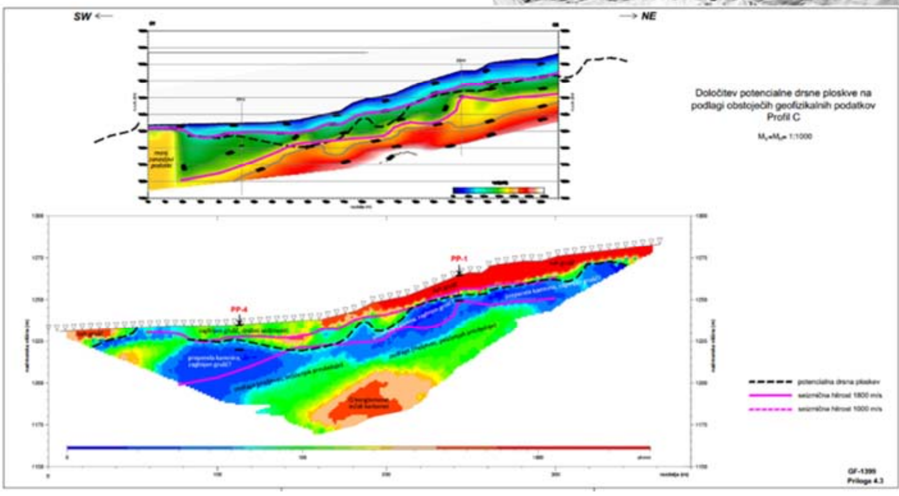

Volume calculation – Urbas landslide

3D reconstruction of landslide body and estimation of the thickness of sliding material was obtained from core logging, inclinometer measurements, hydrogeological measurements, geophysical research and data obtained from field mapping.

Volume calculation for Urbas landslide: 895,000 m^3

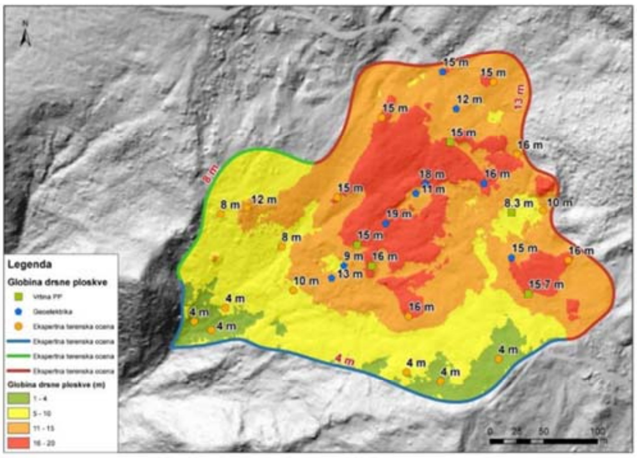

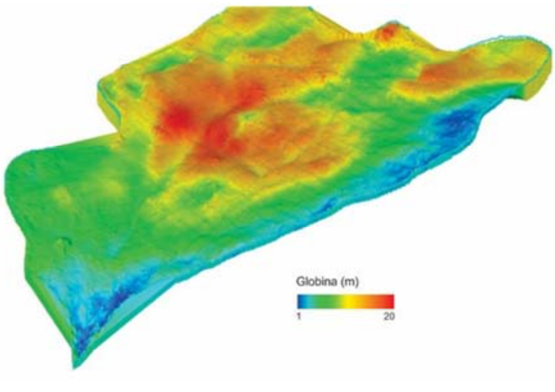

Volume calculation – Čikla landslide

3D reconstruction of landslide body and estimation of the thickness of sliding material was obtained from core logging, inclinometer measurements, hydrogeological measurements, geophysical research and data obtained from field mapping.

Volume calculation for Čikla landslide: 141,000 m3

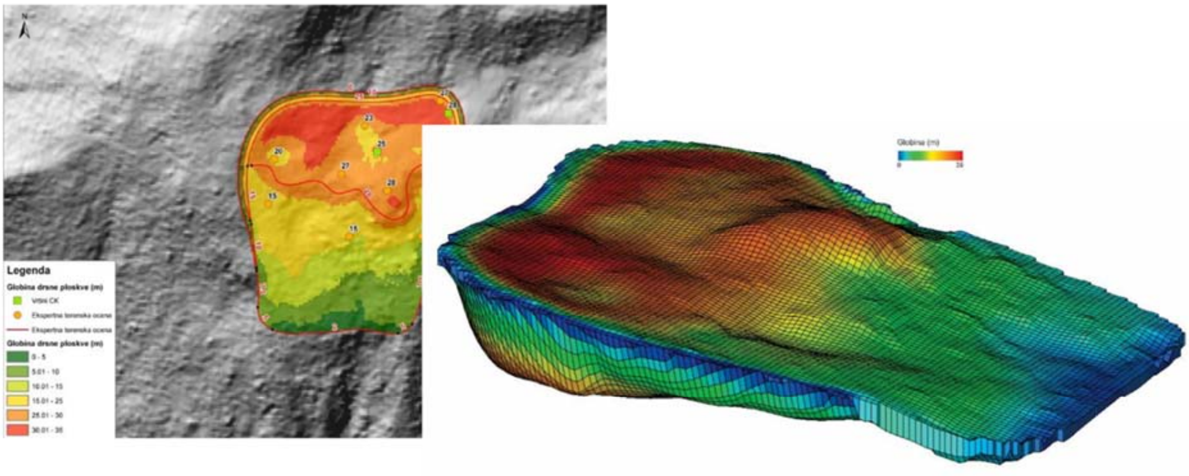

Conclusions

- Engineering-geological mapping showed that that more than 20 active landslide are located in the hinterland of Koroška Bela village. Urbas and Čikla landslide represent a direct risk to the settlement Koroška Bela.
- Presently, 2,200 people live in the area of the alluvial fan of past debris flow. With this risk in mind, landslide monitoring, debris flow modelling and assessing hazard is crucial for development of mitigation measures and effective disaster risk management.
- Modeling results show that potential debris flows with previously mentioned magnitudes would have catastrophic consequences on Koroška Bela torrential fan. Simulated depths of potential debris flow exceed 5m in some densely populated parts of the Koroška Bela fan. Therefore, application of mitigation measures is inevitable.

25

Future work

- In order to estimate the real effect of the tectonic, geological and meteorological conditions (e.g. amount of precipitation, snow melt, etc.) on the groundwater level and landslide dynamics further, upgraded application of established monitoring (e.g. rain gauges, geotechnical sensors, etc.) is in progress.
- Similarly, future additional research will focus on the relationship between precipitation, groundwater levels and landslide dynamics site in order to determine correlations between displacement rates and long-term rainy periods and/or snowmelt.
- Studies of magnitudes of previous debris-flow events and age-dating in order to assess the magnitudes of expected events in the future

26

IPL-216 Project Annual Report for 2018 and part of 2019

Diversity and hydrogeology of mass movements in the Vipava Valley, SW Slovenia

Timotej Verbovšek[(1)], Tomislav Popit[(1)], Jernej Jež[(2)], Jasna Smolar [(3)], Ana Petkovšek [(3)], Matej Maček[(3)]

1) University of Ljubljana, Faculty of Natural Science and Engineering, Aškerčeva cesta 12, 1000 Ljubljana, Slovenia, tomi.popit@ntf.uni-lj.si
2) Geological Survey of Slovenia, Dimičeva 14, 1000 Ljubljana
3) University of Ljubljana, Faculty of Civil and Geodetic Engineering, Jamova cesta 2, 1000 Ljubljana

ICL meeting, Paris, 16-19 September 2019

Abstract

The project is running mostly according to plan. The geological and geomorphological investigations (mapping and GIS analyses) are still taking place, with the aim of creation of a detailed engineering-geological map in GIS environment. We have gained additional several detailed information about the boreholes in the wider area of Ajdovščina town, including the hydrogeological data of the sediments. We have also performed measurements of physico-chemical parameters in the boreholes. These parameters show very different behavior in all measured boreholes, depending on their depth and location in the landslide. A detailed georeferenced 3D model of Stogovce landslide was also constructed in August 2018 by measuring the landslide with UAV (DJI Phantom 4).

Results have been published in two papers in Landslides Journal and several other peer-reviewed journals and conference proceedings. Besides the publications, some other activities were performed in 2018, among which we have promoted the Adriatic-Balkan network (ICL-ABN) network activities in the Vipava Valley with joint field work with students of University of Ljubljana + University of Zagreb, Faculty of Mining, Geology and Petroleum Engineering to Stogovce, Slano blato and Podboršt landslides, in June 2018. Several investigations are recently taking place, with aim to be published in peer-reviewed journals.

Study Area

- SW Slovenia, the upper Vipava Valley
- Mesozoic carbonates overthrusted on the Eocene flysch

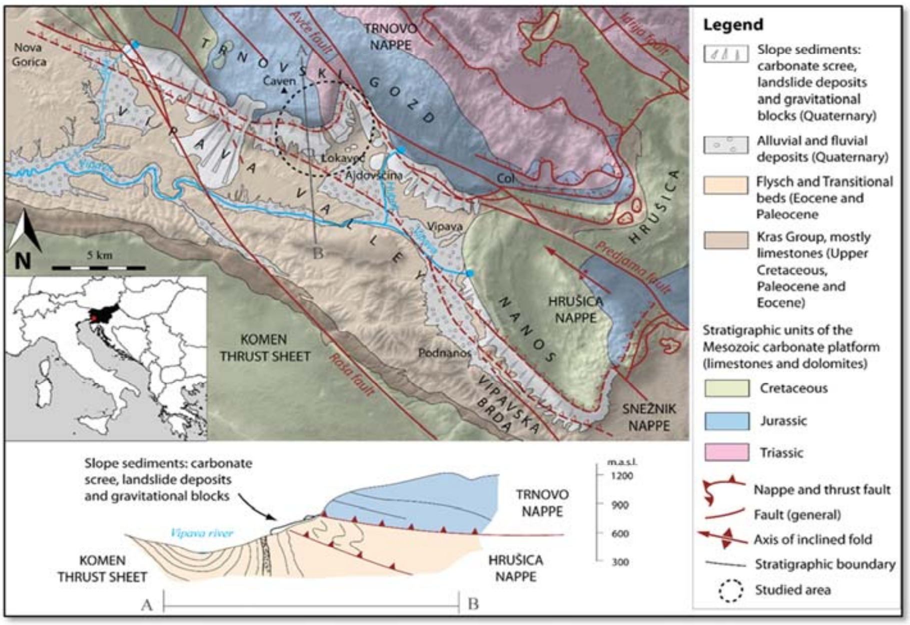

Project duration and objectives (from 2016 application)

- Project Duration: 3 years:
  - Year 1 (2017): Data collection and literature review of the mass movements in the Vipava Valley. Engineering-geological mapping of the area, creation of a GIS geodatabase.
  - Year 2 (2018): Continuation of previous year activities, plus hydrogeological measurements.
  - Year 3 (2019): Continuation of previous year activities, plus monitoring and geotechnical investigations.
- Objectives:
  - To create a landslide inventory (database) of the Vipava Valley in GIS environment.
  - Use of Cruden and Varnes classification, plus the use of updated Varnes classification (Hungr et al., 2014)
  - To perform a hydrogeological analysis of selected springs in this area, which are related to landslides.
  - To monitor the movement of some of the selected landslides, according to available budget.

2018 Activities – Papers

- Published papers in 2018 for Vipava Valley:
  - **Landslides** - Verbovšek, Timotej, Popit, Tomislav. GIS-assisted classification of litho-geomorphological units using Maximum Likelihood Classification, Vipava Valley, SW Slovenia. Landslides : Journal of the international consortium on landslides, ISSN 1612-510X. [Print ed.], 2018, vol. 15, iss. 7, str. 1415-1424, doi: 10.1007/s10346-018-1004-2
  - **Acta Geographica Slovenica** – Kocjančič M, Popit T, Verbovšek T, Gravitational sliding of the carbonate megablocks in the Vipava Valley, SW Slovenia, doi: 10.3986/AGS.4851
  - **Landslides** - Errera, Gerardo, Mateos, Rosa María, García-Davalillo, Juan Carlos, Grandjean, Gilles, Poyiadji, Eleftheria, Maftei, Raluca, Filipciuc, Tatiana-Constantina, Jemec Auflič, Mateja, Jež, Jernej, Podolszki, Laszlo, et al. Landslide databases in the Geological Surveys of Europe. Landslides : Journal of the international consortium on landslides, ISSN 1612-510X. [Print ed.], 2018, vol. 15, issue 2, str. 359-379, doi: 10.1007/s10346-017-0902-z.
  - **Geofluids** - PERANIĆ, Josip, ARBANAS, Željko, CUOMO, Sabatino, MAČEK, Matej. Soil-water characteristic curve of residual soil from a flysch rock mass. Geofluids, ISSN 1468-8123, 2018, letn. 2018, str. 1-15, ilustr. https://www.hindawi.com/journals/geofluids/2018/6297819/, doi: 10.1155/2018/6297819
  - **5th Slovenian Geological Congress** - Jemec Auflič, Mateja, Mikoš, Matjaž, Verbovšek, Timotej, Bavec, Miloš. Recent developments in landslide research in Slovenia. V: Jemec Auflič, Mateja (ur.), Mikoš, Matjaž (ur.), Verbovšek, Timotej (ur.). Advances in landslide research : proceedings of the 3rd Regional Symposium on Landslides in the Adriatic Balkan Region, 11-13 October 2017, Ljubljana, Slovenia. Ljubljana: Geological Survey of Slovenia. 2018, str. 119-124.
  - **5th Slovenian Geological Congress** - Verbovšek, Timotej, Mihevc, Nejc, Kočevar, Marko, Vrabec, Marko. Meritve premikov in podzemne vode na plazu Stogovce pri Ajdovščini = displacement and groundwater monitoring of the landslide Stogovce near Ajdovščina, SE Slovenia. V: Novak, Matevž (ur.), Rman, Nina (ur.). Zbornik povzetkov = Book of abstracts, 5. slovenski geološki kongres, Velenje, 3.-5. 10. 2018. Ljubljana: Geološki zavod Slovenije. 2018, str. 87-88.

2018 Activities – Mapping

- Production of GIS map of landslides in the project area, compilation of all known mass movements (in progress)

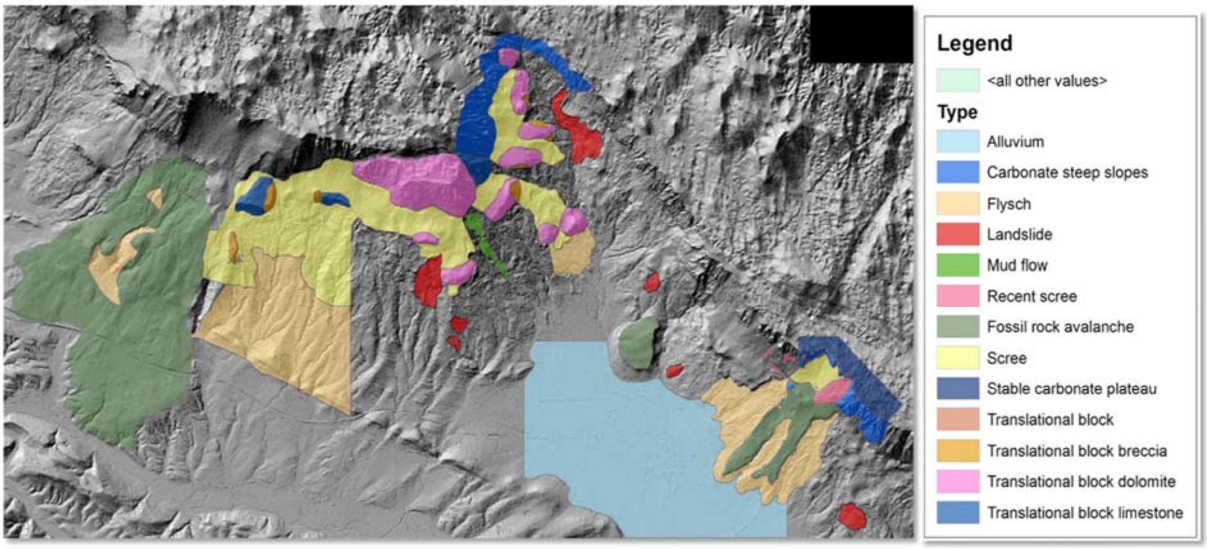

2018 Activities – Groundwater

- Monitoring of groundwater in Stogovce landslide
  - temperature, electroconduvity, water level (CTD diver)

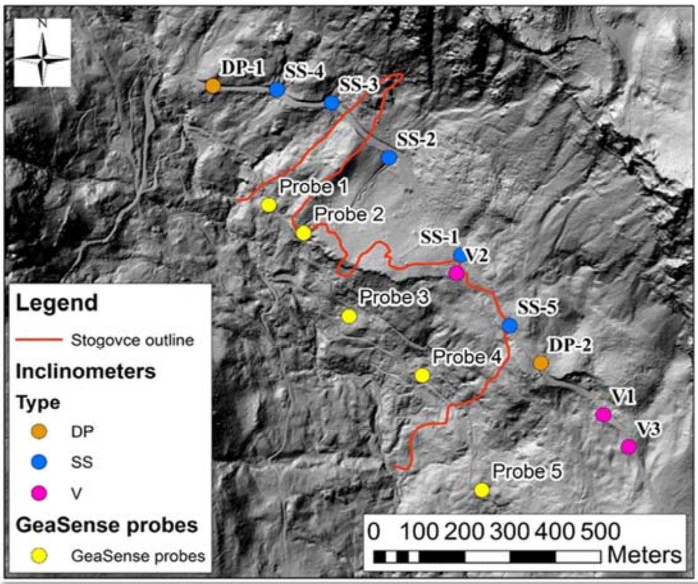

2018 Activities – Groundwater

- Monitoring of groundwater in Stogovce landslide

Level	SS-1	SS-2	SS-3	SS-4	SS-5	DP-2	V1	V2	V3
Depth (m)	*15.00*	*28.00*	*6.00*	*19.00*	*6.00*	*7.30*	*17.00*	*18.00*	*15.00*
Min (m)	12.50	25.11	3.13	*	1.43	7.24	12.71	12.02	10.44
Max (m)	14.18	26.40	4.91	*	3.02	7.40	12.82	16.61	12.53
Range (m)	1.68	1.29	1.78	*	1.59	0.16	0.11	4.59	2.09
H_water max (m)	2.50	2.89	2.87	*	4.57	0.06	4.29	5.98	4.56
H_water min (m)	0.82	1.60	1.09	*	2.98	-0.10	4.18	1.39	2.47

6 July 2018	SS-1	SS-2	SS-3	SS-4	SS-5	DP-2	V1	V2	V3
T (C)	11.5	11.9	11.9	*	11.3	*	8.4	10.9	10.9
EC (uS/cm)	547	451	152	*	795	*	845	539	421

2018 Activities – Groundwater

- V-2, V-3 and SS-2, **6.7.-27.9.2018**

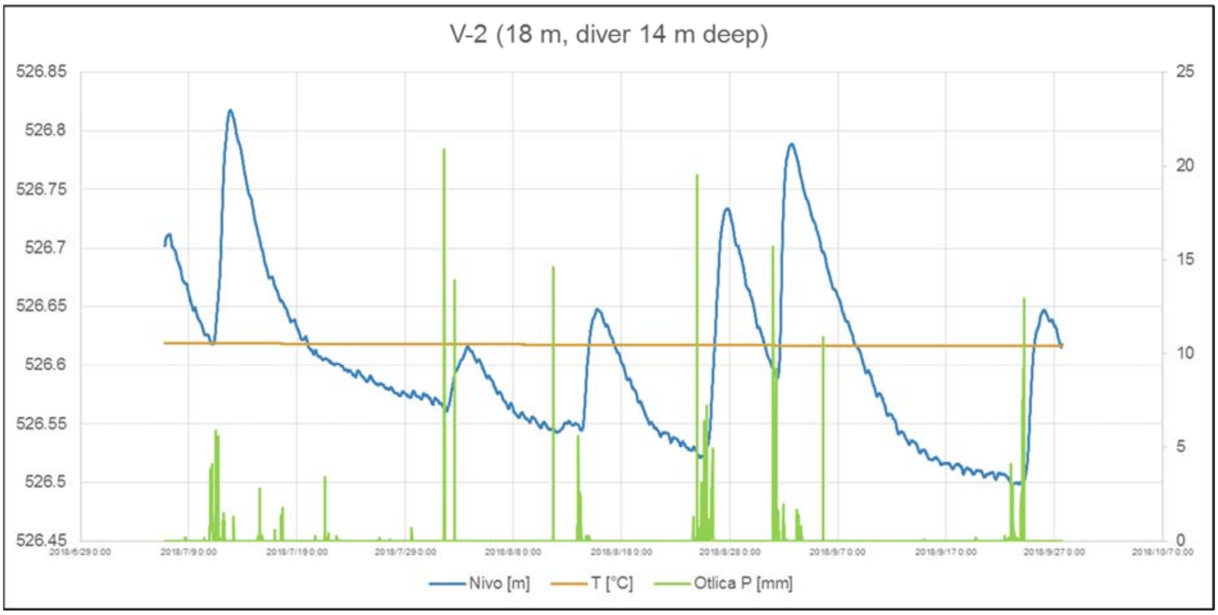

2018 Activities –Inclinometers

- **SS-1:**
- year 2011

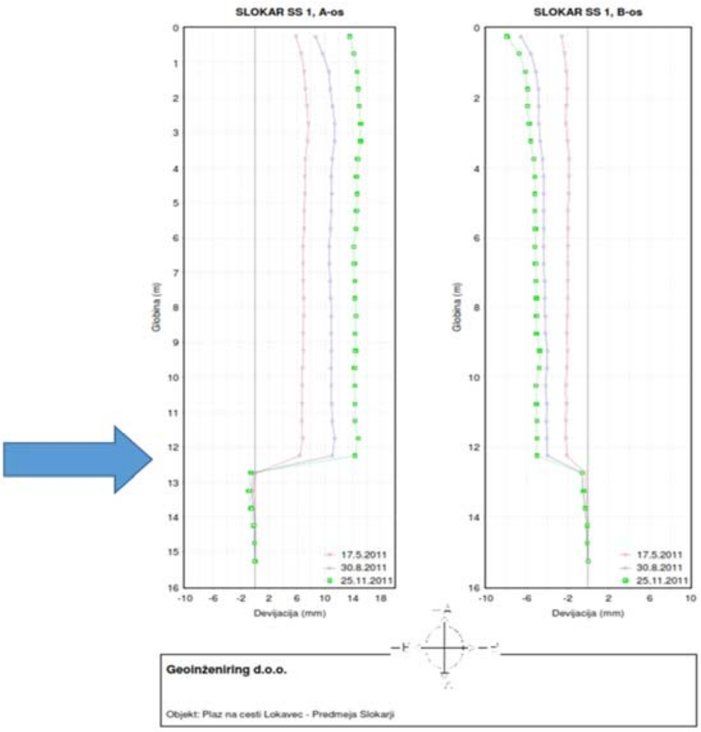

2018 Activities – Inclinometers

- **SS-2:**

- **0:** 22.11.2014
- **1:** 04.09.2015
- **2:** 09.08.2016
- **3:** 06.07.2018

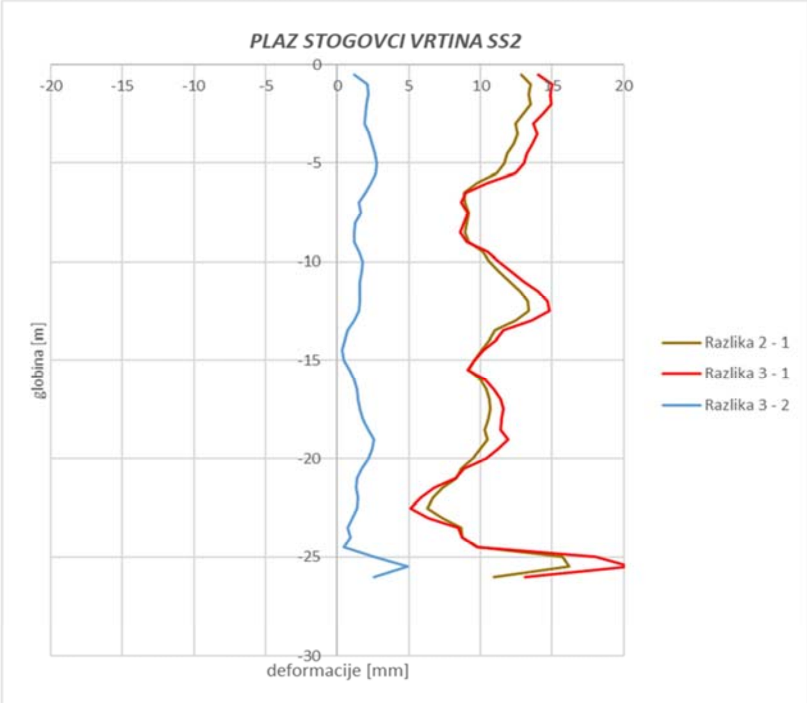

Precipitation

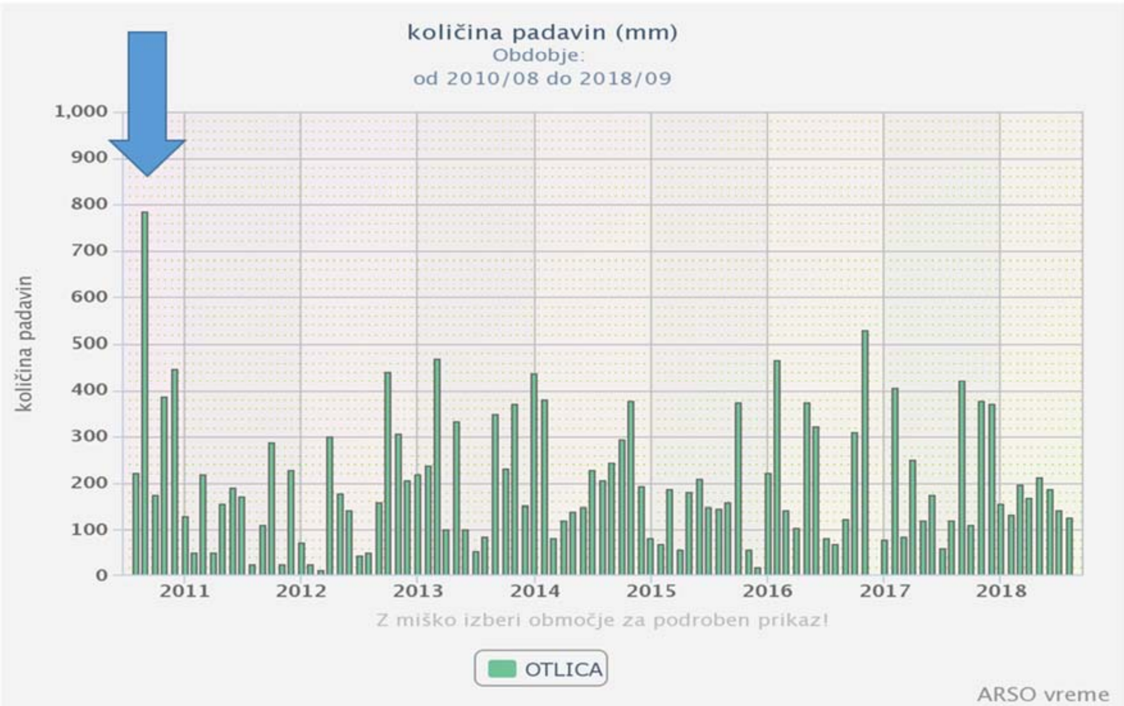

2018 Activities – Crack measurements

Simple crack opening measurements:

- Fixed point built-in
- Zero measurement (until now)

2018 Activities – Sampling

2018 Activities – Lab. investigations index tests results

Sample	Parameter / Method					
	natural water content, w (%)	fines content < 0.063 mm (%)	fines (< 0.063 mm)			
			w_L (%)	w_P (%)	w_A (%)	MB_F (g/kg)
	EN ISO 17892-1	EN ISO 17892-4	EN ISO 17892-4		DIN 18132	EN 933-9
STOGOVCI /this research	**1.62 - 4.29**	**11.8**	**29**	**20**	**44**	**10.7**
STOGOVCI /2010 - Nad sotočjem	8.4-10.6	18.5-19.9	26-31	15	41-48	12.9
STOGOVCI /2010 - Cesta	13.7-14.5	19.2-21.8	39	20	67-69	23
STOŽE / this research	**3.27**	**13.6**	**22**	**15**	**34**	**6.7**
STOŽE - Maček et al. 2017		15.6	25	15		
STOŽE - Majes et al. 2002		20-35	25	13		

Majes, B., Petkovšek, A., Logar, J. (2002) Primerjava materialnih lastnosti drobirskih tokov iz plazov Stože,Slano blato in Strug, GEOLOGIJA 45/2
Maček, M, Smolar, J., Petkovšek, A. (2017) Influences of Rheometer Size and the Grain Size on Rheological Parameters of Debris Flow, doi: https://doi.org/10.1007/978-3-319-53498-5_46
Smolar, J., Petkovšek, A., Majes. B. (2010) Poročilo o geomehanskih laboratorijskih preiskavah in ocena občutljivosti plazovine na utekočinjenje: na plazu Stogovce nad Ajdovščino. Strokovni elaborat UL FGG, KMTAL.

2018 Activities – Lab. investigations Grain size distribution curves

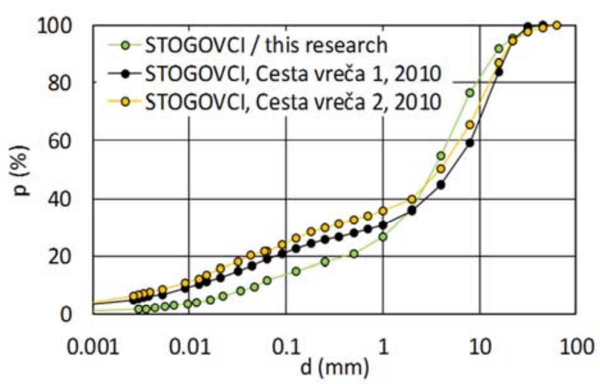

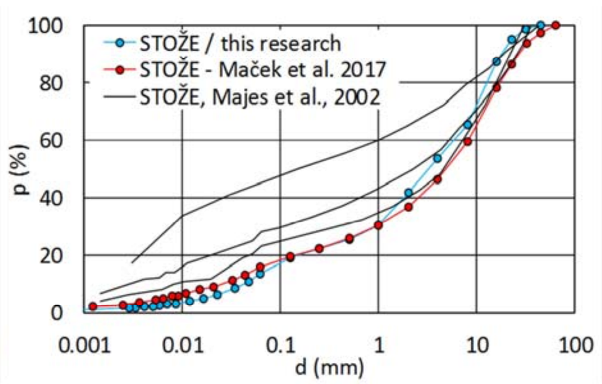

Majes, B., Petkovšek, A., Logar, J. (2002) Primerjava materialnih lastnosti drobirskih tokov iz plazov Stože,Slano blato in Strug, GEOLOGIJA 45/2
Maček, M, Smolar, J., Petkovšek, A. (2017) Influences of Rheometer Size and the Grain Size on Rheological Parameters of Debris Flow, doi: https://doi.org/10.1007/978-3-319-53498-5_46
Smolar, J., Petkovšek, A., Majes. B. (2010) Poročilo o geomehanskih laboratorijskih preiskavah in ocena občutljivosti plazovine na utekočinjenje: na plazu Stogovce nad Ajdovščino. Strokovni elaborat UL FGG, KMTAL.

2018 Activities – Lab. investigations Rheological properties

Laboratory vane (ELE)

Marsh cone (funnel) viscometer
4.76, 8, 9, 10, 11, 13 mm orifice

2018 Activities – Lab. investigations Rheological properties

DV3THB, Brookfield –
shear rate controlled coaxial cylinder rheometer

R_i<17mm
R_o=40mm

ConTec Viscometer 5,
Shear rate controlled coaxial cylinder rheometer,

R_i=100mm
R_o=145mm
D_{max}= 22 mm

2018 Activities – Lab. investigations Rheological properties

Specimens:

- fines (< 0.063 mm) - different water content (*w*)
- different fractions (from 0-0.063 mm to 0-22 mm) - different water contents

Determined parameters:

- water content, *w*
- density, ρ
- undrained shear strength, c_{ur}, yield stress, τ_y
- plastic (equivalent) viscosity, η_p

2018 Activities – Rheological properties calculation - rheometers

Bingham model

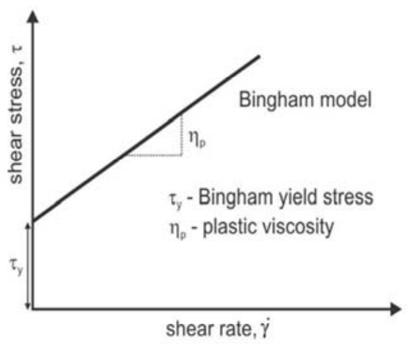

$$\tau = \tau_y + \eta_p \cdot \dot{\gamma}$$

Plug flow (Feys et al., 2013)

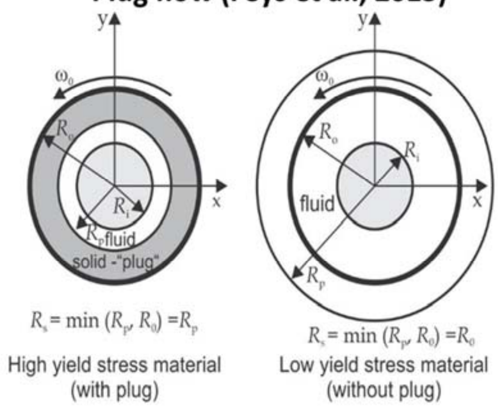

plug radius $R_p = \sqrt{\frac{T}{\tau_y \cdot 2 \cdot \pi \cdot h}}$

T – torque, h - height of the inner cylinder

change geometry for each point ($R_s = \min(R_p, R_o)$), iterative calculation

Feys, D., Wallevik, D.E., Yahia, A., Khayat, K.H., Wallevik, O.H. (2013) Extension of the Reiner–Riwlin equation to determine modified Bingham parameters measured in coaxial cylinders rheometers. Mater. Struct. 46(1–2), 289–311.

2018 Activities – Rheological properties calculation – Marsh funnel

- (equivalent) viscosity (Mohammed et al., 2014)

$d_{orifice}$=10 mm $$\eta_e = \rho \left(\frac{t - 5.5}{0.039} \right)^{\frac{5}{6}}$$

$d_{orifice}$=4.76 mm $$\eta_p = exp \left[ln \left(\frac{\frac{t - 24.5}{0.58}}{1.2} \right) + \ln(\rho) \right]$$

ρ - density
t – measured flow time

- viscosity and yield stress – complex semi analytical approach (Nguyen et al., 2006)

Mohammed M.H. et al. (2014) Rheological properties of cement-based grouts determined by different techniques. Engineering, 6, 217-229, doi: 10.4236/eng.2014.65026

Nguyen V.H. et al. (2006) Flow of Herschel–Bulkley fluids through the Marsh cone. Journal of Non-Newtonian Fluid Mechanics Volume 139, Issues 1–2.

2018 Activities – Rheological properties - Results

- results obtained using different test methods
- Sample: STOGOVCI, fines (< 0.063 mm)
- **comparable results**

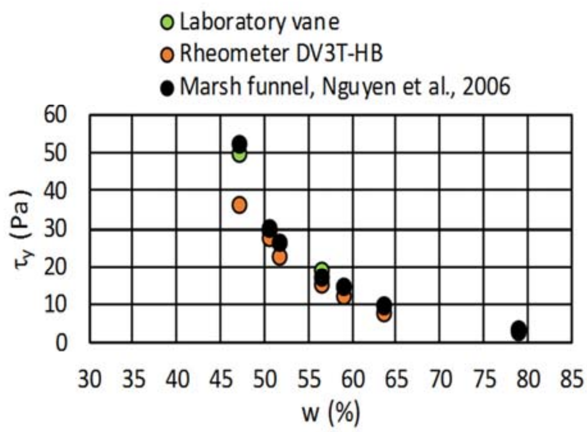

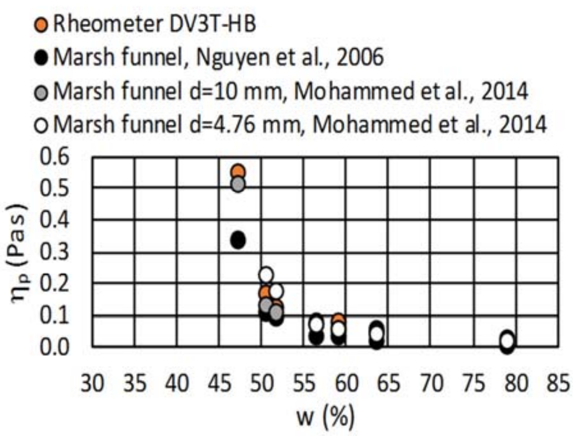

2018 Activities – Rheological properties - Results

- effect of maximum grain size
- Sample: STOŽE
- **rheological parameters are both water content and maximum grain size dependent**

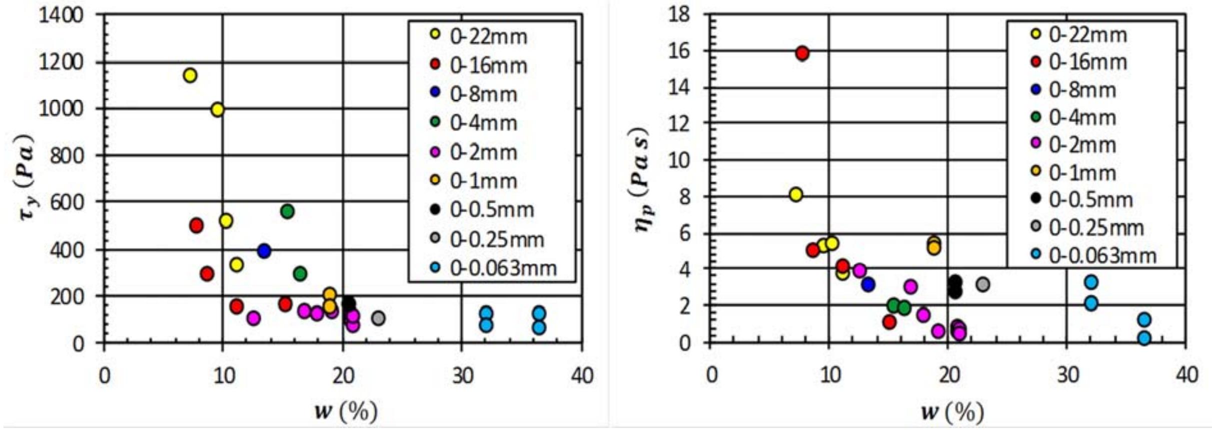

2018 Activities – Rheological properties - Results

- comparison of this results with results of first rheological investigations in 2002
- Sample: STOŽE

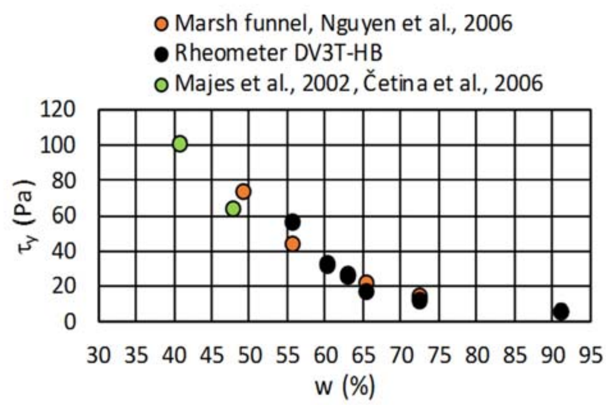

Majes, B., Petkovšek, A., Logar, J. (2002) Primerjava materialnih lastnosti drobirskih tokov iz plazov Stože,Slano blato in Strug, GEOLOGIJA 45/2
Četina, M., et al. (2006) Case Study: Numerical Simulations of Debris Flow below Stože, Slovenia. Journal of Hydraulic Engineering Vol. 132, Issue 2 (February 2006)

2018 Activities – Rheological properties - Results

- comparison with literature data

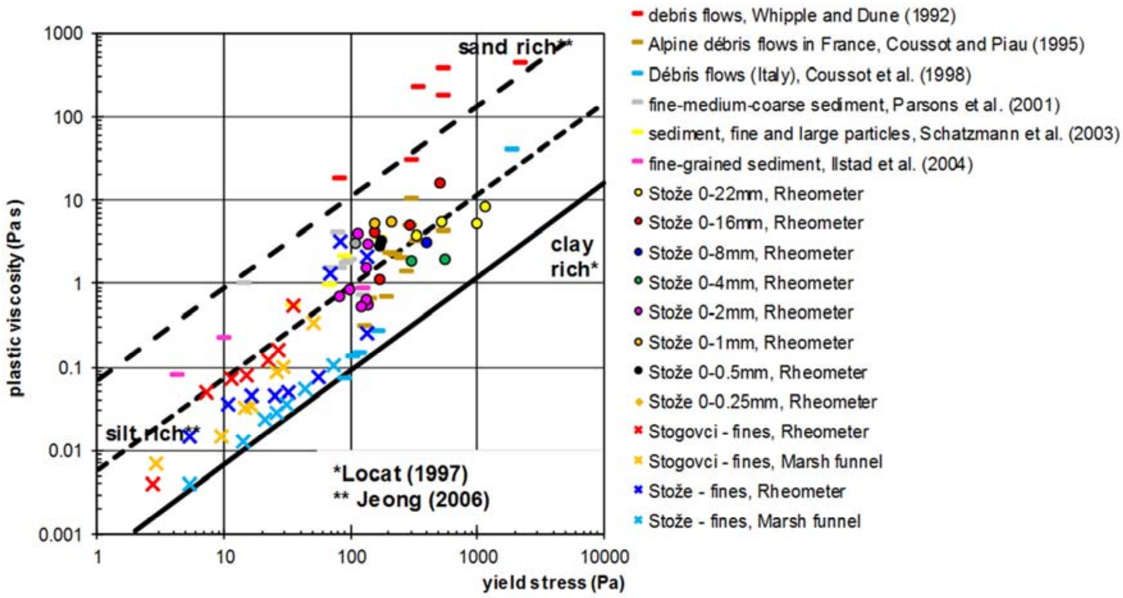

2018 Activities – Lab. investigations - Conclusions

- index properties are comparable with the results of previous investigations
- results obtained using different test methods are comparable
- rheological properties are water content and maximum grain size dependent.
  - The increase of water content decrease yield stress and plastic viscosity.
  - The increase of maximum grain size also tends to increase both parameters.

3D model and volume calculations

- UAV, August 2018
- 5 cm horizontal accuracy

3D model and volume calculations

- Google Earth

InSAR measurements

- preliminary results of monitoring of selected points and areas in Vipava valley by InSAR method (Sentinel-1A and ALOS-2 data)
- analyses started in May 2019 for period Sep 2016-Jan 2019

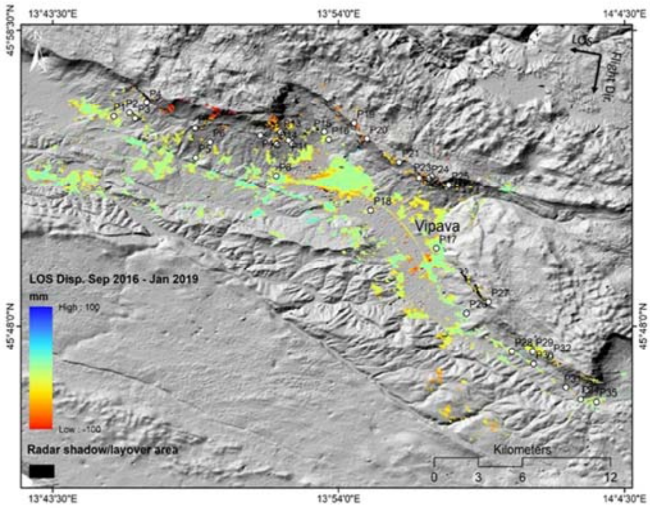

2018 Activities – Other

- **ICL-ABN activities**
  - **Field work with students of University of Ljubljana + University of Zagreb,** Faculty of Mining, Geology and Petroleum Engineering (Adriatic-Balkan network ICL ABN) to Stogovce, Slano blato and Podboršt landslides, June 2018.

Lithology, ecology, soils and socio-economic needs to be studied prior to conservation of the upper watershed of Mahaweli Ganga, Sri Lanka

A A Virajh Dias,

Project Director

Integrated Watershed and water resources management Project

Ministry of Mahaweli Development and Environment

Sri Lanka

Abstract

The upper Mahaweli watersheds are degrading, causing reduced crop yields, intensive erosion, landslides, downstream sedimentation and low river base flows. Soil erosion has observed in both natural and agricultural landscapes in different lithologies and soils under different types of land uses and vegetation covers. Appropriate land protective interventions were also experienced more than 200 years back and such interventions are promoting the facts of sustainability or loss of ground stability. Most of interventions usually meets societal acceptance or rejection in living terrain. The population in Mahaweli Basin amounts to more than 2.8 million, 15% of the total population of the country. The study shows that, among the many observations studied, native species, reservations, and social adoptability have statistically significant positive impact on soil conservation decisions. Similarly, erosion potential based on physical factors and type of soil in hill country shows a statistically insignificant impact on soil conservation decisions. This indicates that socio-economic factors act as determinants of soil conservation rather focuses only on physical factors. Thus, paper discusses the important societal adoptability indicators on soil conservations strategies which require more scientifically improved approach.

District	DSD_Name	No of GND	Area Ha	Total Population	MALE	FEMALE
Kandy	Akurana	34	3031.6	60,977	28,544	32,433
Kandy	Delthota	28	5116.7	29,185	13,444	15,741
Kandy	Doluwa	33	10016.9	49,480	23,426	26,054
Kandy	Ganga Ihala Korale	21	5247.6	40,279	18,964	21,315
Kandy	Harispattuwa	84	5007.5	87,955	41,763	46,192
Kandy	Gangawata	64	5869.4	157,572	75,898	81,674
Kandy	Kundasale	80	8082.0	127,282	60,049	67,233
Kandy	Medadumbara	94	19035.1	60,827	28,869	31,958
Kandy	Panwila	14	9194.9	26,185	12,106	14,079
Kandy	Pasbage Korale	29	12190.4	59,662	27,436	32,226
Kandy	Pathadumbara	54	4896.0	91,831	43,386	48,445
Kandy	Pathahewaheta	73	8350.2	57,219	27,832	29,859
Kandy	Poojapitiya	63	5114.4	55,561	26,228	29,333
Kandy	Thumpane	15	927.0	9,542	4,499	5,043
Kandy	Udadumbara	40	17703.3	14,711	7,158	7,553
Kandy	Udapalatha	51	9060.0	94,122	44,020	50,102
Kandy	Udunuwara	121	6088.0	107,661	51,899	55,762
Kandy	Yatinuwara	90	6520.7	101,407	48,213	53,194
Matale	Ukuwela	21	3448.1	14,231	6,764	7,467
Nuwara Eliya	Ambagamuwa	24	18441.7	88,586	42,117	46,469
Nuwara Eliya	Hanguranketha	131	22862.2	88,055	41,836	46,219
Nuwara Eliya	Walapane	125	32169.7	103,105	49,394	53,711
Nuwara Eliya	Kothmale	96	22372.3	100,437	48,256	52,181
Nuwara Eliya	Nuwara Eliya	72	48357.2	210,927	102,146	108,781
Badulla	Uva Paranagama	70	13728.2	82,186	39,681	42,505
Badulla	Welimada	64	19390.3	100,424	48,852	51,572
Badulla	Hali Ela	26	8587.0	35,154	16,798	18,356
Badulla	Bandarawela	26	4449.0	51,649	24,595	27,054
Badulla	Haputhale	23	5486.7	41,547	19,948	21,599
Badulla	Kandaketiya	14	8614.5	11,995	5,759	6,236
				2,159,754	1,029,880	1,130,346

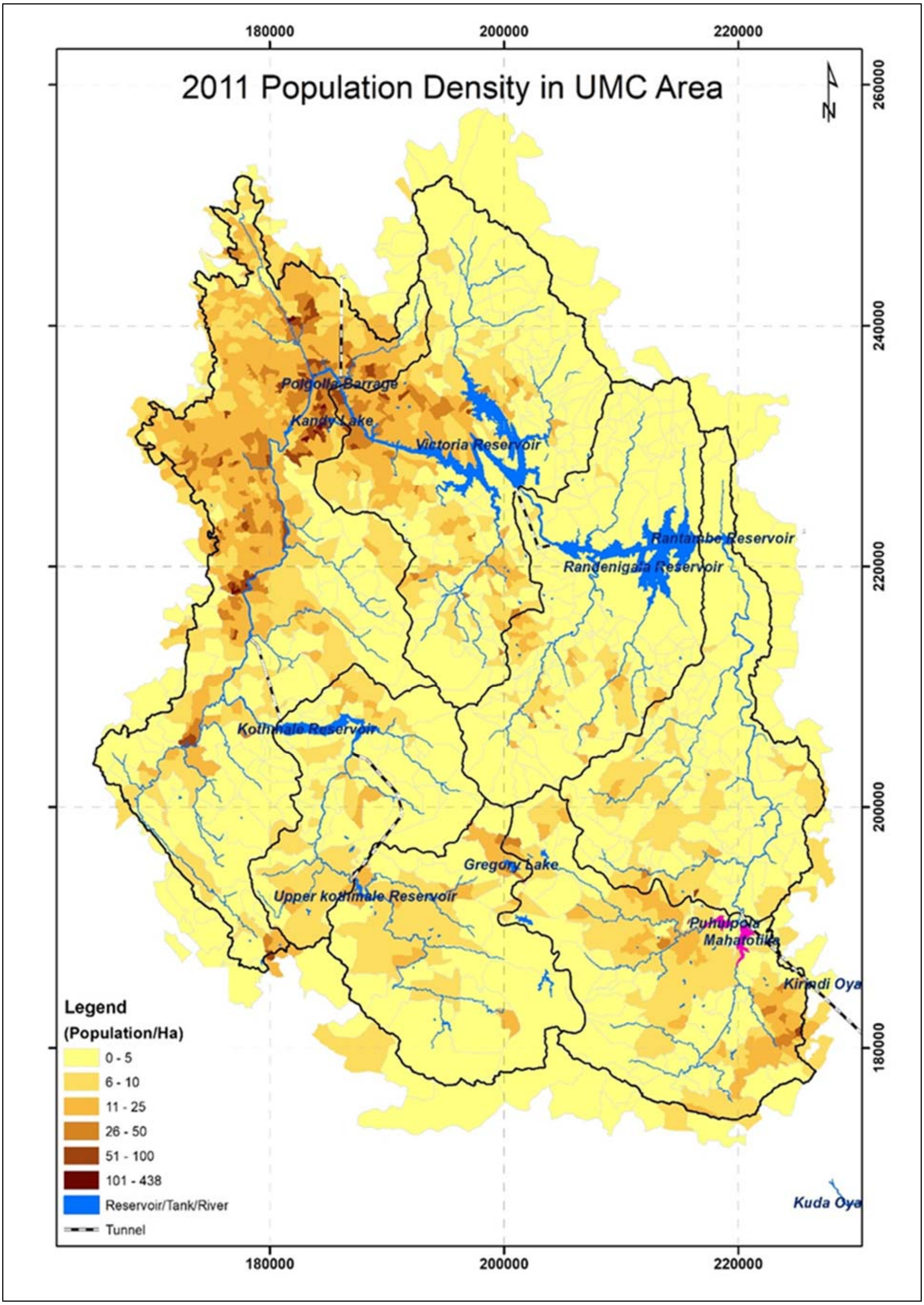
2011 Population Density in UMC Area
180000
200000
220000
260000
240000
N
Polgolla Barrage
Kandy Lake
Victoria Reservoir
Rantambe Reservoir
Randenigala Reservoir
Kotmale Reservoir
Gregory Lake
Upper kotmale Reservoir
Puhulpola
Mahatotila
Kirindi Oya
Kuda Oya
Legend
(Population/Ha)
0 - 5
6 - 10
11 - 25
26 - 50
51 - 100
101 - 438
Reservoir/Tank/River
Tunnel

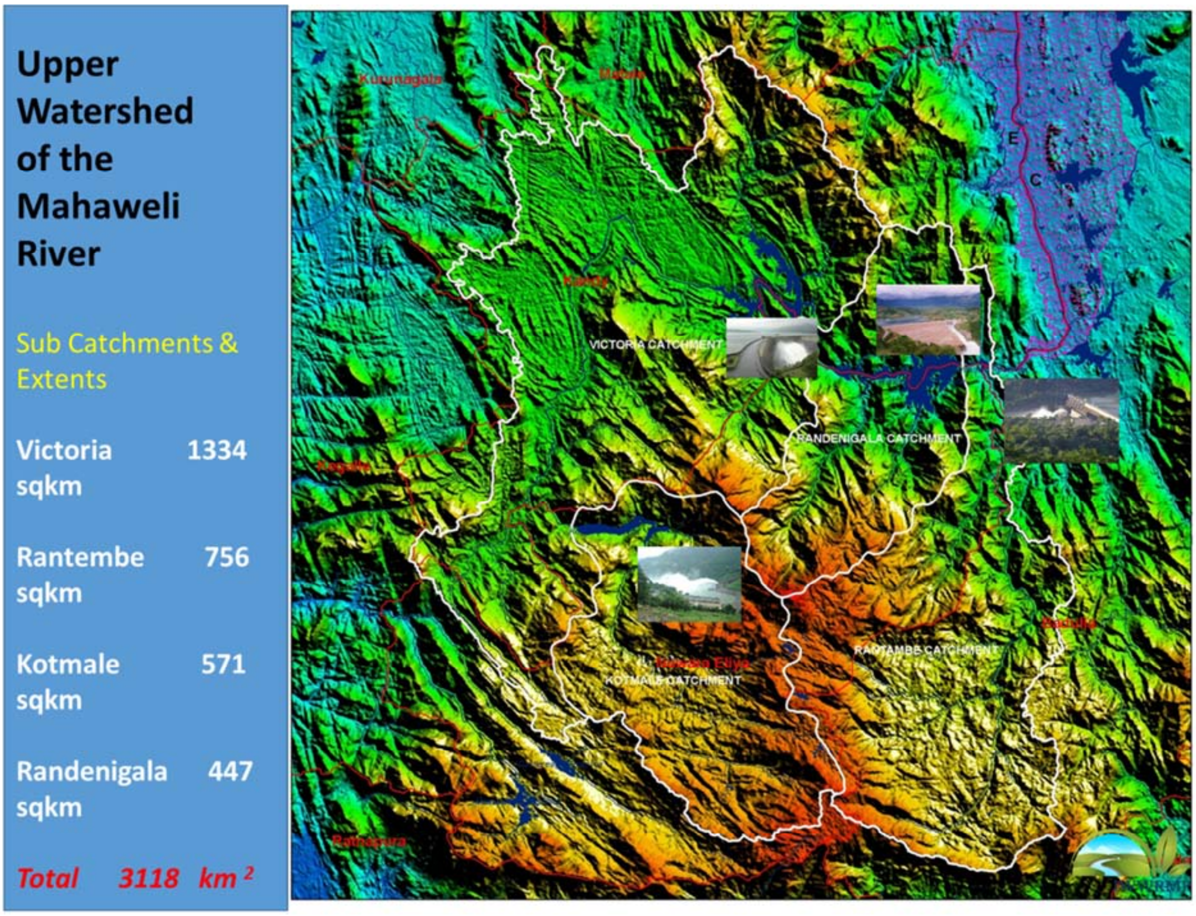
Upper Watershed of the Mahaweli River
Sub Catchments & Extents
Victoria 1334 sqkm
Rantembe 756 sqkm
Kotmale 571 sqkm
Randenigala 447 sqkm
Total 3118 km ^{2}
VICTORIA CATCHMENT
RANDENIGALA CATCHMENT
KOTMALE CATCHMENT

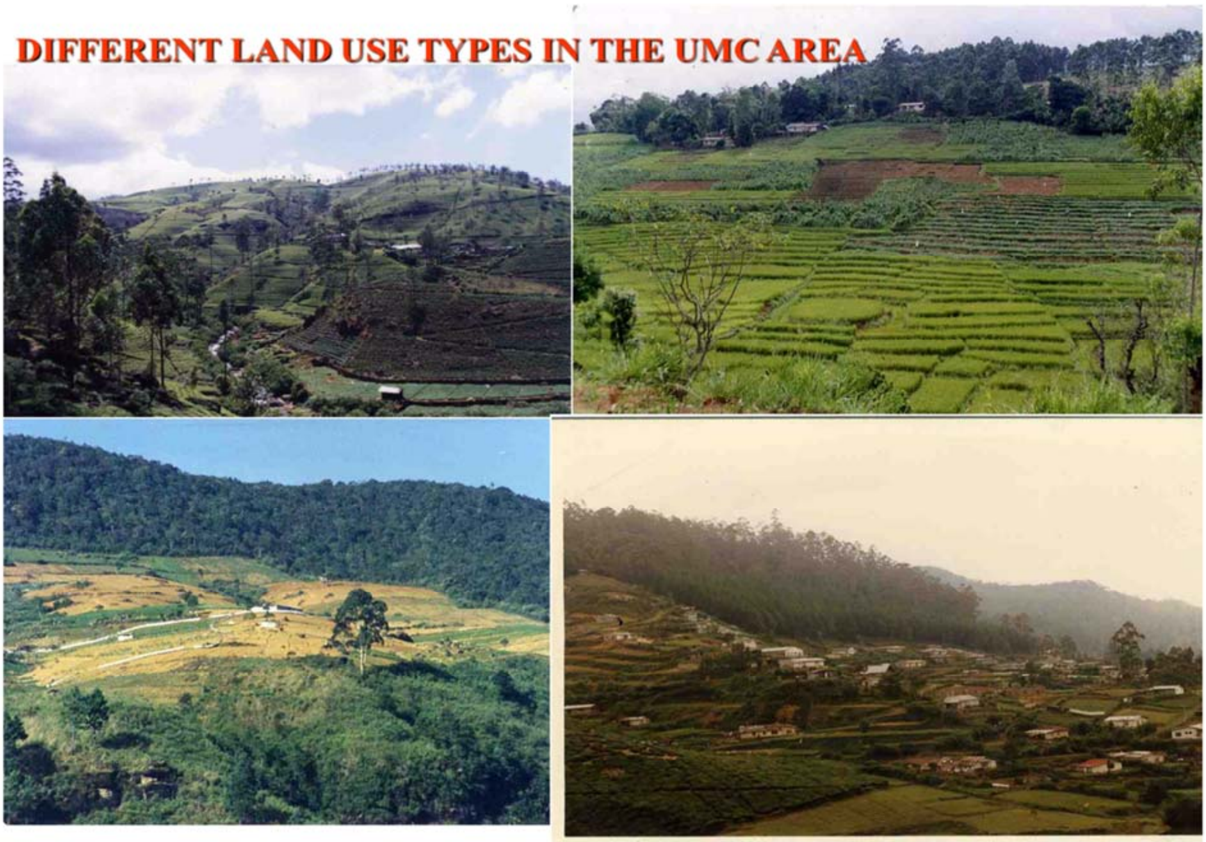
DIFFERENT LAND USE TYPES IN THE UMC AREA

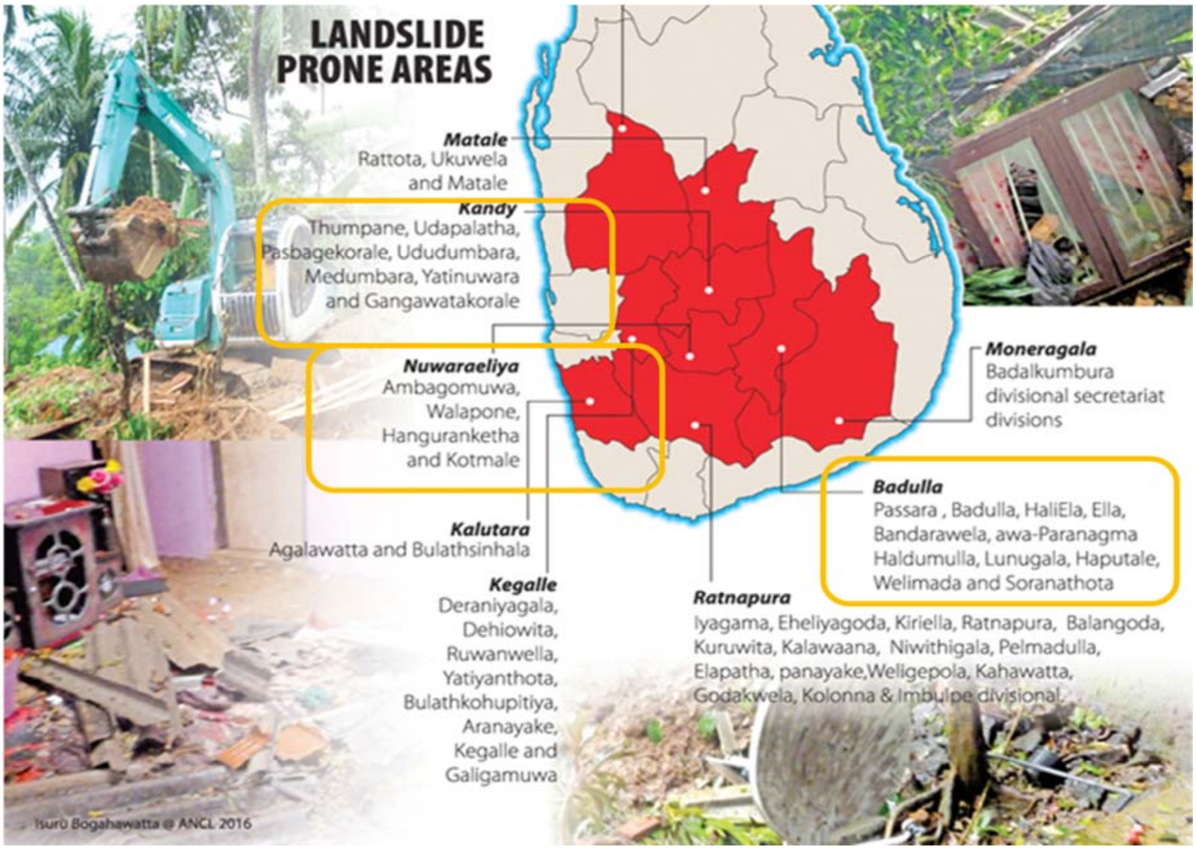
LANDSLIDE PRONE AREAS
Matale
Rattota, Ukuwela and Matale
Kandy
Thumpane, Udapalatha, Pasbagekorale, Ududumbara, Medumbara, Yatinuwara and Gangawatakorale
Nuwaraeliya
Ambagomuwa, Walapone, Hanguranketha and Kotmale
Kalutara
Agalawatta and Bulathsinhala
Kegalle
Deraniyagala, Dehiowita, Ruwanwella, Yatiyanthota, Bulathkohupitiya, Aranayake, Kegalle and Galigamuwa
Moneragala
Badalkumbura divisional secretariat divisions
Badulla
Passara , Badulla, HaliEla, Ella, Bandarawela, awa-Paranagma Haldumulla, Lunugala, Haputale, Welimada and Soranathota
Ratnapura
Iyagama, Eheliyagoda, Kiriella, Ratnapura, Balangoda, Kuruwita, Kalawaana, Niwithigala, Pelmadulla, Elapatha, panayake,Weligepola, Kahawatta, Godakwela, Kolonna & Imbulpe divisional
Isuru Bogahawatta @ ANCL 2016

Immediate Problems in the Upper Mahaweli Watershed

- **Deforestation, encroachment, forest fires and human-wild animal conflicts** in the forest areas in the catchment
- **On-farm and Off-farm Soil Erosion** leading to reduced land productivity
- **Increased Silt in river water and Siltation of Reservoirs** (which reduces their life span) while turbidity creates problems for drinking water supply & electricity generation(**Quality and Quantity**)
- **Landslides and unstable soil slopes creates additional siltation**
- **Reduced water flows** from the catchment to the Mahaweli river affecting drinking water supply, irrigation and electricity generation (**Quantity**)
- **Poor quality of Mahaweli water** (inorganic pollutants) create problems for drinking water supply (**Quality**)

IWWRMP

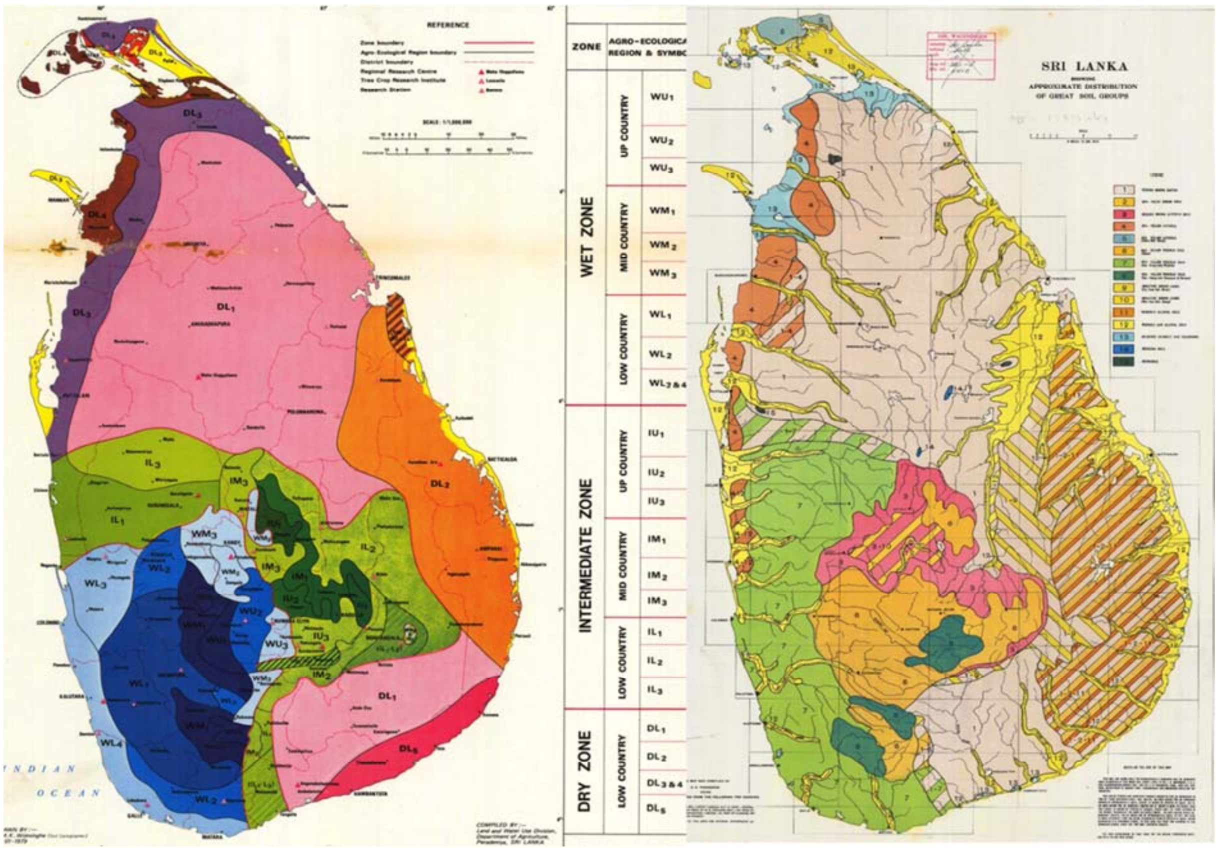

Increased Silt in River Water and Siltation of Reservoirs, Reduced water flows

13 Jul, 2019

The Ministry of Power and Renewable Energy states that the water bodies located around the hydro-power plants recorded the lowest water level in 29 years. Media spokesperson of the Ministry said that the overall water level recorded from the main water bodies belonging to the CEB has declined to 21.5%.

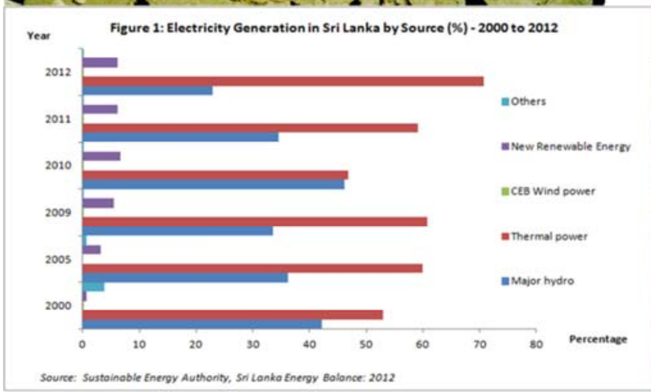

Increased Silt in River Water and Siltation of Reservoirs, Reduced water flows

	Original volume	Predicted Volume MCM	Actual (Measured) Volume (2015) MCM	Average rate for a year MCM	Capacity Loss MCM 2018
Rantembe	10.9 (1990)	3.9	5.95	0.2	5 (45.8%)
Randenigala	860.0 (1985)	830 (2017)	801.5 (2016)	1.89	62.37 (7.2%)
Victoria	717.53(1985)	688 (2017)	653	2.06	67.98 (9.4)
Pollgolla	4.66 (1971)		3.4 (2014)	0.02	1.26 (27.0)
					136.6 MCM

"deforestation and soil erosion has caused siltation in many of the major reservoirs, significantly reducing their water holding capacities"

- Kalawewa Reservoir - 123 MCM
- Parakrama Samudraya - 134 MCM

Source : Major Dams and Reservoir Division, Pollgola

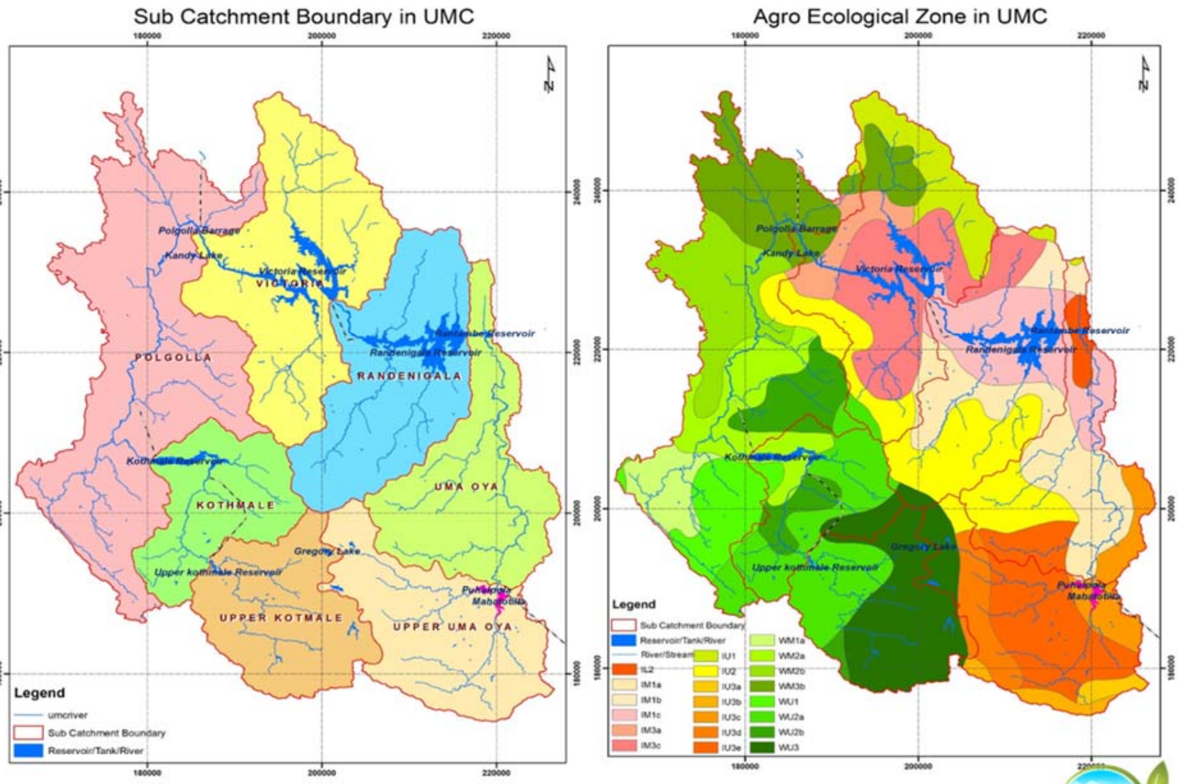

Catchment Sediment Monitoring Record

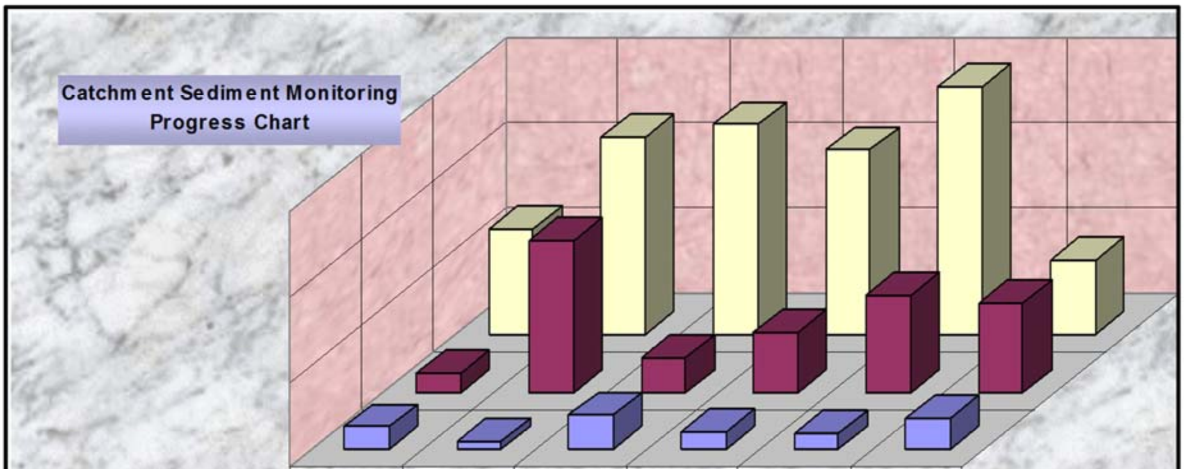

	Nilambe Oya	Uma Oya	Huluganga	Maha Oya	Belihul Oya	Atabage Oya
Run off in Mtrs.	1.37	0.54	2.05	1.03	0.95	1.86
Sediment Yield in t/ha/year	1.12	8.90	1.97	3.47	5.66	5.20
Catchment in Sq.km	6.13	11.49	12.26	10.78	14.47	4.35

IWWRMP

Project Objectives

- **Reduce soil erosion and resultant siltation of reservoirs**
- **Regulate water flow** to the Mahaweli River by improving water retention within the watershed
- **Reduce water pollution** (both point and non-point) to ensure good quality water for drinking purposes.
- **Improve biodiversity,** especially in forest land and wetlands, to provide enhanced ecosystem services
- **Enhance livelihoods** of watershed community as an incentive for SWC
- **Establish institutional and policy mechanisms** to sustain watershed management activities

IWWRMP

Plant Nurseries / Forestry plants


IWWRMP

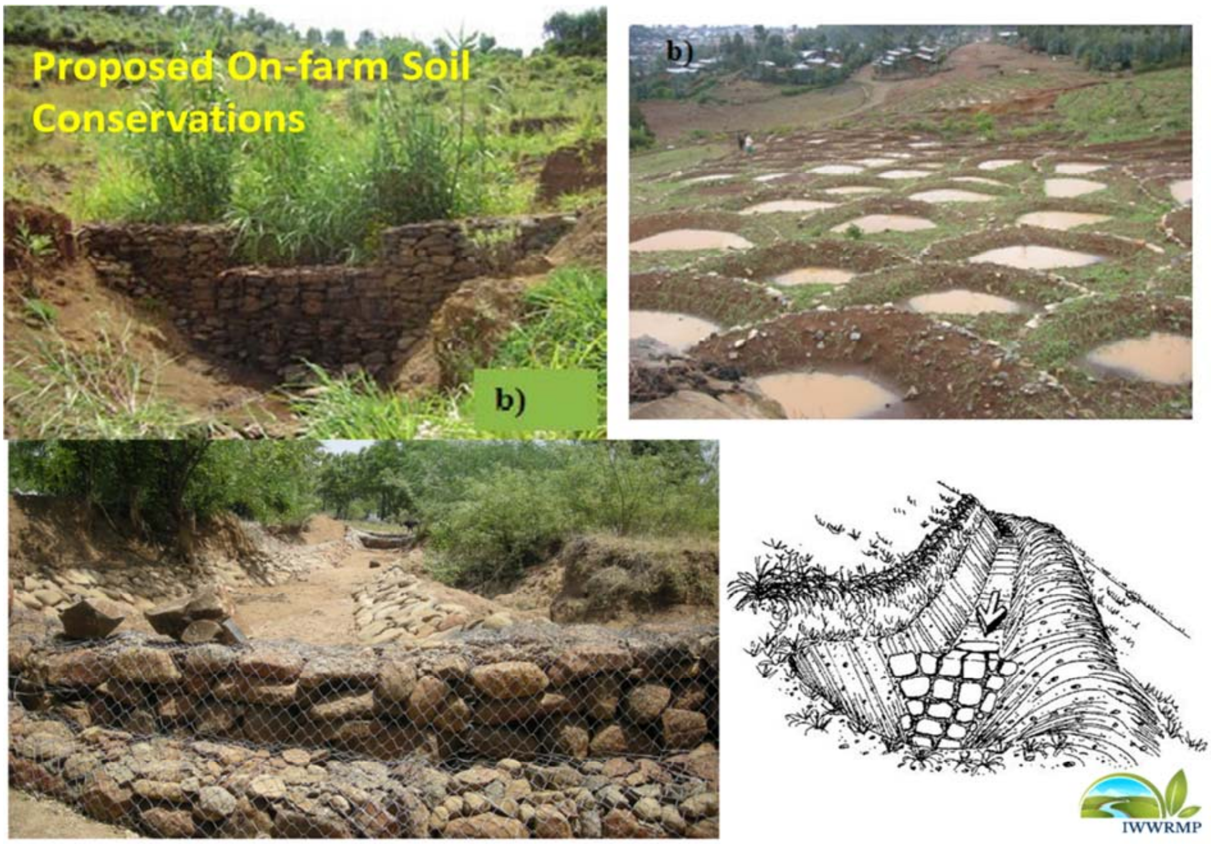
Proposed On-farm Soil Conservations
b)
b)
IWWRMP


Stone bunds: Simple yet effective water and soil conservation


Proposed On-farm Soil Conservations

Watershed management and community Income generation Improvement....

Increasing the Production of OFC and adaptation of new Agricultural Technologies to mitigate Climate Change Impacts

- Awareness increasing of farmers on Climate Change Impacts
- Adaptation of new technology to maximize production

  (SMART Farm initiatives through Public Private Producer Partnerships etc.)
- Increasing Productivity through integrated Farm Management

IWWRMP

"Mahaweli Turu Ithurum Tree Planting Program" for School children........

- School children of selected schools are encouraged to plant trees(Indigenous and threatened species) to make them Child Green Investors those who love the environment.
- Tree plants are purchased by MASL and the payments are deposited in their Bank accounts.

Awareness Creation on Catchment Conservation….

- Environmental Education Training Centers- Doragala and Pallekele
- Environmental Education Programs for School children and farmers (Exhibitions/Posters/leaflets/media programs)
- Establishment of Blue Green Mahaweli School (2018)

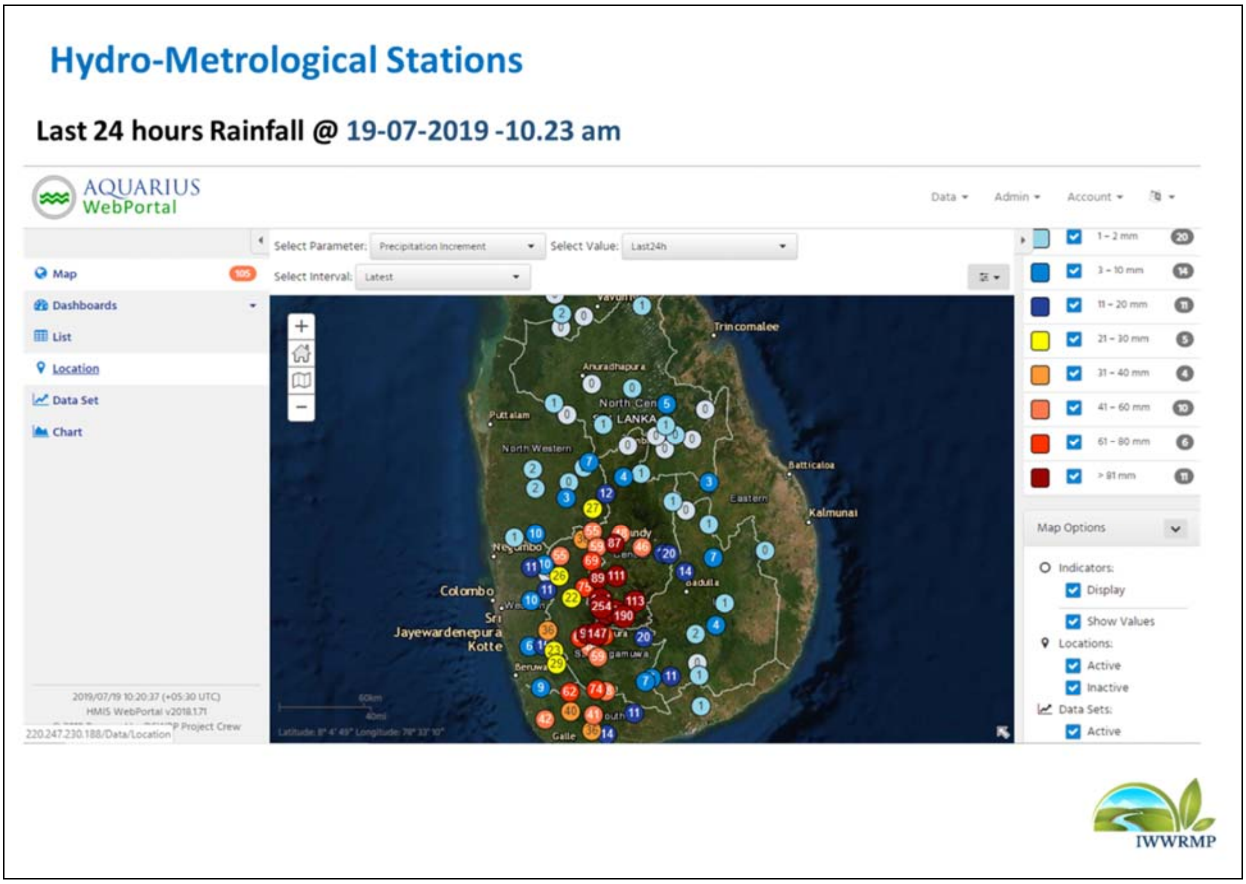
Hydro-Metrological Stations
Last 24 hours Rainfall @ 19-07-2019 -10.23 am
AQUARIUS
WebPortal
Data
Admin
Account
Map
Dashboards
List
Location
Data Set
Chart
Select Parameter:
Precipitation Increment
Select Value:
Last24h
Select Interval:
Latest
Trincomalee
Anuradhapura
Puttalam
North Western
Batticaloa
Eastern
Kalmunai
Colombo
Sri Jayewardenepura Kotte
Galle
1 - 2 mm
3 - 10 mm
11 - 20 mm
21 - 30 mm
31 - 40 mm
41 - 60 mm
61 - 80 mm
> 81 mm
Map Options
Indicators:
Display
Show Values
Locations:
Active
Inactive
Data Sets:
Active
IWWRMP

Comparison of soil module E50 of residual soil slope failures – Progress of the IPL 155

A A Virajh Dias, L K N S Kulathilaka & J.A.D.N.A Jayasuriya

Central Engineering Consultancy Bureau,
Colombo 7, Sri Lanka

Abstract

The comparison of soil module E50 of residual soil slope failures in two different rainfall precipitation zones is an experimental study to determine relationships between shear strength characteristics of soils which could be easily discussed on scenarios of the first-time occurrence failures and repetitive failures in residual soil formation. Therefore, more than 40 samples were selected along with the UDS samples for the determination of initial moisture content, initial void ration, dry density, shear strength parameters and secant modulus of E50. Comparing the results using a Poisson's ratio and shear strength of same soils yields a slight interrelationship and no significant observations on safety and the location of the critical slip surface.

Introduction

- The research IPL $_{155}$ is mainly a study on evaluation of inter-related shear strength characteristics of different precipitation regions would yield to understand the sensitivity that can be adopted in each region.
- Slope stability analysis enables the identification of landslides proven areas and risky areas, but the lack of knowledge in terms of variabiliy against friction angle, cohesion and elastic deformations of subsurface soil hinder the accurate interpretation of instability in natural slopes (Mallawarachihi, *et.al,2014*).
- The study has been continuously carried out over 40 UDS samples for the of initial moisture content, initial void ration, dry density, shear strength parameters and secant modulus of E_{50}.

IPL 155- Determination of Soil Parameters of Subsurface to be Used in Slope Stability Analysis in two Different Precipitations Zones of Sri Lanka- 2014

- Heavily precipitated zone in wet zone with annual average rainfall above 4000mm.
- Wet zone with annual average rainfall between 2500-3000 mm.

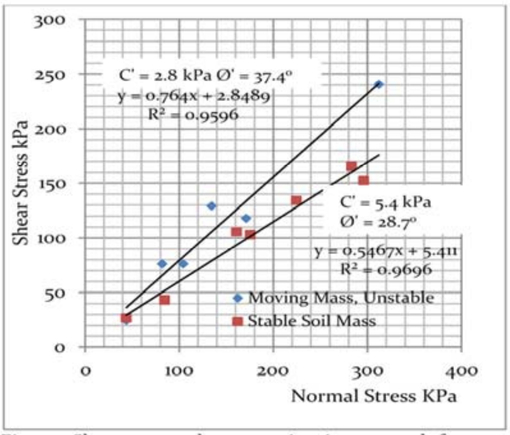

Fig. 5: Shear strength properties interpreted from a standard drained direct shear test in Zone 1

Rainfall Precipitation Zone	E_{50} (at EC- 100kPa - 120kPa) kN/m²	e_o	Number of landslides / slope failures
Zone 1: Balangoda to Bandarawela	39,286	0.838	09 nos of slope failures identified
Zone 1: Koslanda Landslide	41,957	0.810	one major landslide across the road
Zone 1: Gampola to Nuwara Eliya	35,182	0.937	07 number of slope identified
Zone 1: Watawala Landslide	10,714	1.15	one major landslide across the rail road
Zone 2: Colombo and sub regions	56,900	0.788	Newly formed earth cutting
	25,723	0.640	Newly formed earth cutting
	11,909	1.348	Newly formed earth cutting

Major residual Soil Slopes failures in Sri Lanka

May 2017 Athwelthota landslide in Kalutara District Sri Lanka, which killed 09 people. Landslide was initiated from residual soil origin.

May 2016 Aranayake landslide in Kegalle District, Sri Lanka, which killed 127 people. The image indicates landslide failure initiated in residual soil and boundary intact with weathered rock face.

Residual soils and elastic behavior of residual soils

- Rain induced failures in slopes made of residual soils are a major geotechnical hazards in Sri Lanka.
- Residual soils are formed by insitu weathering of metamorphic parent rock due to chemicals, water, and other environmental elements, without being transported.
- Another important issue is infiltration of rainwater into a residual soil slope may impair slope stability by changing the pore-water pressure in the soil which in turn controls the water content of the soil (Rahardjo, H, *et.al*, 2005).
- Usually unsaturated residual soils experience high matric suction (i.e., negative pore-water pressure) during dry periods, which contributes to the shear strength of the residual soil.
- The water content also impacts moduli. At low water contents the water binds the particles, increases the stress and suction between the particles and leads to a high soil moduli. Therefore, elastic moduli of residual soil indicate very high value during dry periods and subjects to losing its capacity during rain.

Idealized and real stress-strain behavior of soils

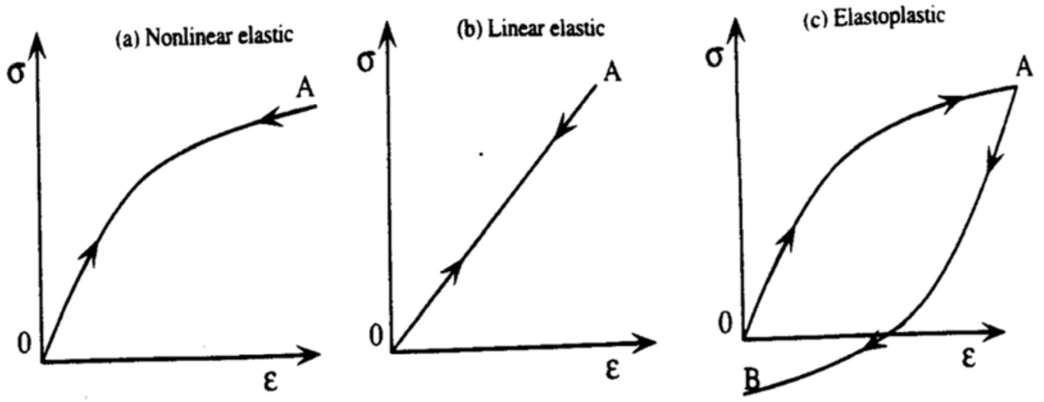

Idealized types of stress-strain behaviors: (a) nonlinear elastic Model, (b) linear elastic model, and (c) elastoplastic model

Idealized and real stress-strain behavior of soils

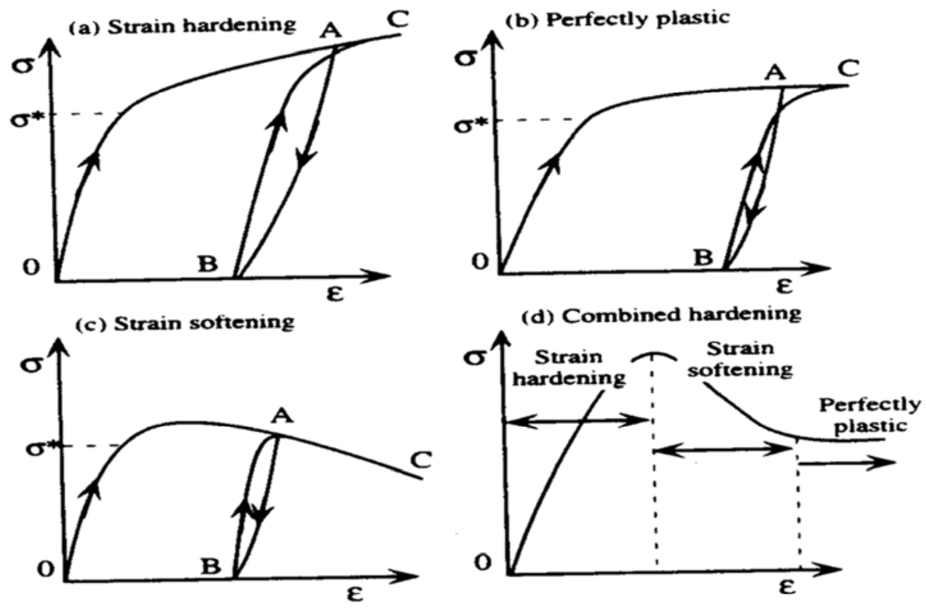

Various types of elastoplastic behaviors: (a) strain hardening, (b) perfectly plastic, (c) strain softening, and (d) combination of a to c.

Hooke's Law of Isotropic Elasticity

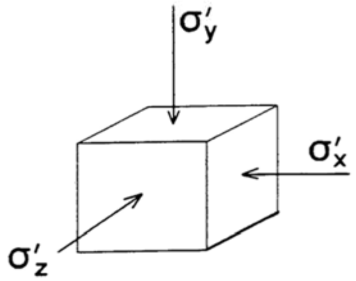

$$\varepsilon_x = \frac{1}{E}\left(\sigma'_x - \nu\sigma_y - \nu\sigma'_z\right)$$

$$\varepsilon_y = \frac{1}{E}\left(-\nu\sigma'_x + \sigma'_y - \nu\sigma'_z\right)$$

$$\varepsilon_z = \frac{1}{E}\left(-\nu\sigma'_x - \nu\sigma'_y + \sigma'_z\right)$$

E = Young's modulus
ν = Poisson's ratio

shear modulus	G	=	$E/(2 + 2\nu)$
bulk modulus	K	=	$E/(3 - 6\nu)$
oedometer modulus	E_{oed}	=	$G\,(2 - 2\nu)/(1 - 2\nu)$

Hooke's Law of Isotropic Elasticity

secant moduli

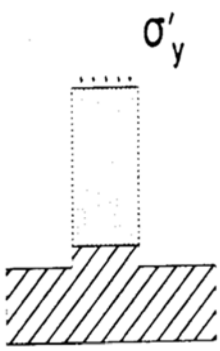

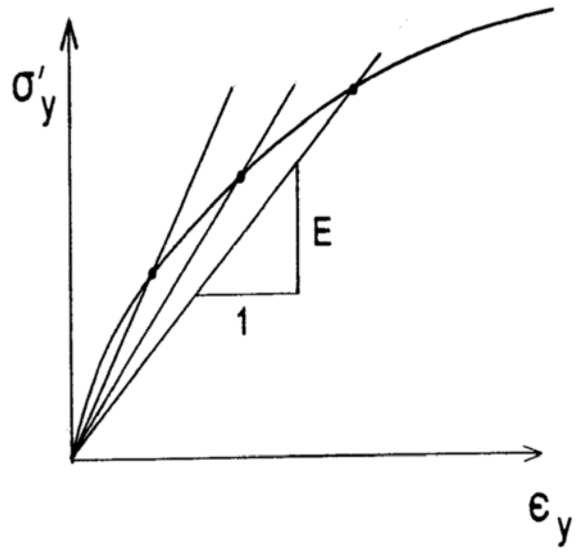

Computational Geotechnics

Determination of Soil Stiffness Parameters

Determination of E50 in a standard stress – strain plot of Consolidated Undrained Triaxial Test

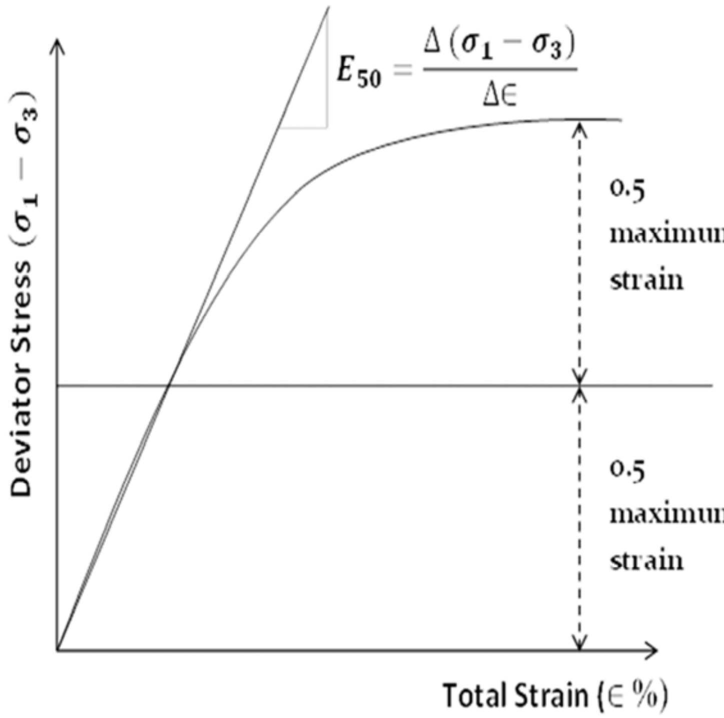

Determination of E50 in a standard stress – strain plot of Consolidated Undrained Triaxial Test

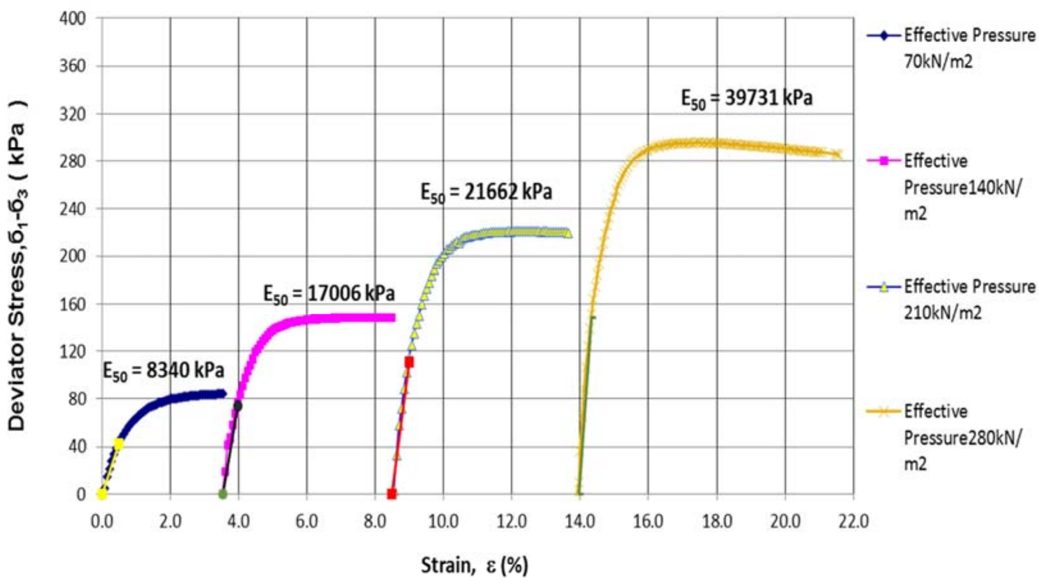

Summary of corresponding results

Sample Reference	Soil Description	MC (%)	Dry density (Mg/m^3)	Degree of Saturation	Void ratio, e_0	CU Triaxial Test		Effective confining pressure (kPa)	E_{50}
						C' kPa	Ø' deg		kPa
S180001	Gray, brown stiff clay with trace silt	31.97	1.31	0.90	1.02	6	25	70	8 340
								140	17 007
								210	21 662
								280	39 732
S180350	Yellowish brown clayey sand	28.93	1.64	0.98	0.81	6	29	50	13 045
								100	37 662
								150	54 542
S180351	Grayish brown sandy clay	38.01	1.26	0.91	1.09	14	28	50	29 856
								120	23 056
								190	31 828
S180354	Yellowish gray sandy clay	27.82	1.52	0.90	0.71	3	29	50	39 678
								100	22 286
								150	36 541
								200	41 681
S180780	Brownish gray clay with trace silt, trace fine sand, stiff, high plasticity, moist, CH	37.43	1.20	0.97	1.16	5	29	50	16 384
			1.26	0.91	1.06			100	14 216
			1.21	0.94	0.15			150	14 290
S172700	Dark brown slightly gravelly clayey silt	17.05	0.61	0.95	0.67	20	32	60	10 779
			1.61	0.92	0.67			120	30 699
			1.61	0.97	0.66			180	68 352
S172702	Light brown clayey sand	11.12	1.86	0.98	0.41	14	37	60	5 582
			1.86	0.91	0.41			120	8 570
			1.86	0.98	0.4			180	23 190
S180787	Grayish yellow soft to medium stiff clay	42.77	1.14	0.95	1.31	23	31	50	17 597
								100	35 736
								150	46 326
S172703	Yellowish brown slightly gravelly clayey sand	11.18	1.88	0.98	0.42	8	31	60	6 704
			1.89	0.94	0.41			120	14 854
			1.89	0.93	0.41			180	19 206

Summary of corresponding results.... Cont

Sample Reference	Soil Description	MC (%)	Dry density (Mg/m^3)	Degree of Saturation	Void ratio, e_0	CU Triaxial Test		Effective confining pressure (kPa)	E_{50}
						C' kPa	Ø' deg		kPa
S180798	Red, gray, brown medium stiff clay with sand	31.99	1.28	0.96	0.92	2	30	50	5 522
								100	7 452
S172705	Light brown clayey fine to coarse sand	9.86	1.93	0.94	0.38	26	35	60	13 000
			1.93	0.96	0.38			120	20 524
			1.92	0.92	0.38			180	32 659
S172708	Pinkish brown clayey gravel	14.07	1.83	0.96	0.47	8	38	60	6 556
			1.82	0.91	0.47			120	24 774
			1.83	0.99	0.47			180	25 387

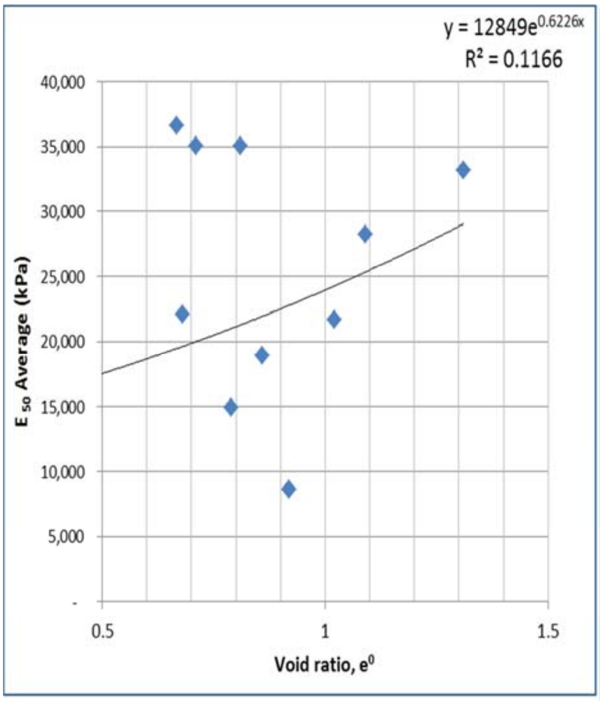

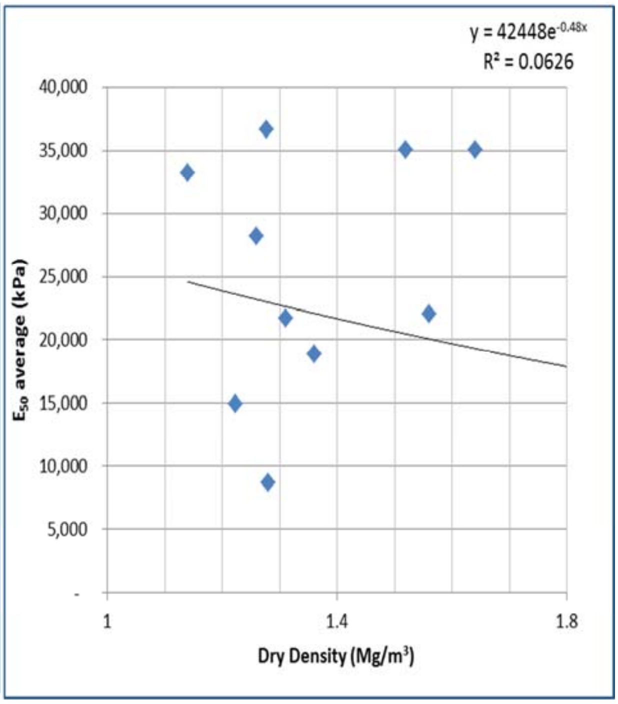

Discussion and Interpretation of results

- Void ratio, which is directly related to packing characteristics of geo-materials, has a strong impact on soil Young's moduli, E50. It is also suggested that the influence of void ratio can be taken into account by using an empirical void ratio function considering the values of E50. The study made an attempt to define a comparison between the void ratio and the elastic parameters.

- But coarse grain soils, if water content rises too much, the particles are pushed apart and the modulus is reduced. However, angle of internal friction will increase significantly. This is especially apparent when considering the stiffness of dried clay.

- Water content also impacts moduli. At low water contents the water binds the particles, increases the stress and suction between the particles and leads to a high soil moduli.

- If the soil has been subjected to stress in the past, it will impact the modulus. An over-consolidated soil will generally have a higher modulus than the same normally-consolidated soil (Briaud, J L, 2001).

- The experimental studying was difficult to rectify stress history and the deformity history. Stress history is created mainly due to rainfall precipitations, soil deposition, movement of soils, unloading effects and re-loading effect caused by erosion etc. The stresses in the past due to various deformities, loading and unloading, will impact the modulus

WCOE- International Training Course on Slope Land disaster Reduction

Louis Ge[1,2], Ko-Fei Liu[2], Kuo-Hsin Yang[2], Tai-Tien Wang[2]

1) National Taiwan University, No. 1, Sec. 4, Roosevelt Rd., Taipei 10617 e-mail: louisge@ntu.edu.tw
2) National Taiwan University, Department of Civil Engineering

Abstract

Landslide related disaster has become more and more important as the global warming effect increases. Given its unique geographical location and natural environment, Taiwan often experiences natural disasters, resulting in casualties and loss of property. Therefore, disasters, especially disaster prevention and mitigation, are a major concern of the Taiwanese society. Government authorities have closely paid attention to disaster prevention and control, allocating massive human and financial resources to disaster prevention and relief. Education has been recognized as the most effective way of reducing the loss due to disasters. This Training Course for Slope Land Disaster Reduction was established in 2013, and has been held for five times since then. Starting from 2019, the selected course participants will come from at least 7 countries around the world. With the aim to reduce the loss from slope land disasters, the course consists of in class lecturing, field exploration and observation, and cultural experiencing.

- Name of Organization
  National Taiwan University

- Name of Leader
  Prof. Louis Ge

- Core Members of the Activities

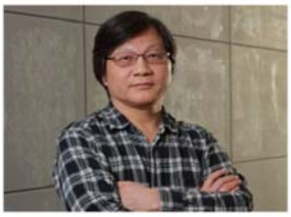

Prof. Ko-Fei Liu

Prof. Kuo-Hsin Yang

Prof. Tai-Tien Wang

Objectives

- Education has been recognized as the most effective way of reducing the loss due to disasters.
- This Training Course for Slope Land Disaster Reduction was established in 2013, and has been held for five times since then.
- Starting from 2019, the selected course participants will come from at least 7 countries around the world.
- With the aim to reduce the loss from slope land disasters, the course consists of in class lecturing, field exploration and observation, and cultural experiencing.

Justification

- Landslide related disaster has become more and more important as the global warming effect increases.
- Given its unique geographical location and natural environment, Taiwan often experiences natural disasters, resulting in casualties and loss of property.
- Government authorities have closely paid attention to disaster prevention and control, allocating massive human and financial resources to disaster prevention and relief.
- Studies on disaster prevention science and technologies have also been increasing in number in recent years.
- As part of the international society, we would like to contribute our know-how and share our experience in disaster prevention and mitigation so we human kind can live a better life.

Resources

- Organizing committee consists of a group of internationally active scholars.
- The Department of Civil Engineering is housing newly renovated classrooms.
- The budgets of running the training course is USD 60,000 each year, where at least 20 course participants will be full financially supported.
- There have been about 150 students from 26 countries all around the world participated this course since 2013.

Past Activities

1) Global Geo-disaster problem and scenario
2) Introduction to Emergency response procedure;
3) Landslide and debris flow hazard mapping
4) Landslide and Debris flow numerical simulation
5) Land use planning regulations and policy

6. Landslide field investigations
7. Debris flow warning system
8. Landslide and Debris flow monitoring system
9. Landslide mitigation methods and countermeasures
10. Hazard loss and Social Vulnerability for slope land problem.

Planned Activities

- There are 3 major activities in due course

1. Promotion of the training course
2. Training course on liquefaction prevention and mitigation, which is scheduled in Spring 2020
3. Publishing a disaster prevention manual, which covers the scientific and technological aspects of disaster prevention.

Beneficiaries of WCoE

- Each participant will apply what they learn from the training course to present their work on the last day. Those who pass the group project will be awarded a certificate. This document certified by ICL is crucially important to the success of the training course.

Ukraine's cultural heritage objects within landslide hazardous sites

IPL Project Proposal

Oleksandr Trofymchuk [(1)], Iurii Kalyukh [(2)], Oleksij Lebid [(1)]

1) Institute of Telecommunications and Global Information Space of National Academy of Sciences of Ukraine, Kyiv, Ukraine e-mail: kalyukh2002@gmail.com
2) Institute of Telecommunications and Global Information Space of National Academy of Sciences of Ukraine, Kyiv, Ukraine; State Research Institute of Building Constructions, Kyiv, Ukraine

Abstract

Ukraine has been a member of the "Landslides and Cultural & Natural Heritage" (LACUNHEN) thematic Network of the ICL since 2012. The purpose of the LACUNHEN - International Consortium on Landslides is to create a platform for scientists and practitioners who are ready to contribute to safeguarding relevant endangered Natural and Cultural Heritage sites. Within this view, landslides and more generally slope instabilities are an important factor endangering cultural heritage sites and its degradation, etc. More than 90% of the territory of Ukraine has complex ground conditions and about 120 000 sq. km of the Ukrainian territory are located in the zone with seismicity of natural origin with a magnitude varying from 6 to 9. Therefore, unpredictable changes of natural geological and man-made factors governing ground conditions may lead to dangerous deformation processes in the Ukraine heritage sites. That is why the new project "Ukraine cultural heritage objects within landslide hazardous sites" will devote certification of Ukraine cultural heritage objects within landslide hazardous sites: experimental and analytical research. We will be creating method of certification and assessment of technical state of the religious objects on hazardous landslide sites. The method includes: visual and vibrodynamic examination of the objects; recommendations for the repair and restoration.

- **PROJECT TITLE**:
UKRAINE CULTURAL HERITAGE OBJECTS WITHIN LANDSLIDE HAZARDOUS SITES

- **MAIN PROJECT FIELDS**
MITIGATION, PREPAREDNESS AND RECOVERY

- **TARGETED LANDSLIDES:**
MECHANISMS AND IMPACTS: LANDSLIDES THREATENING HERITAGE SITES

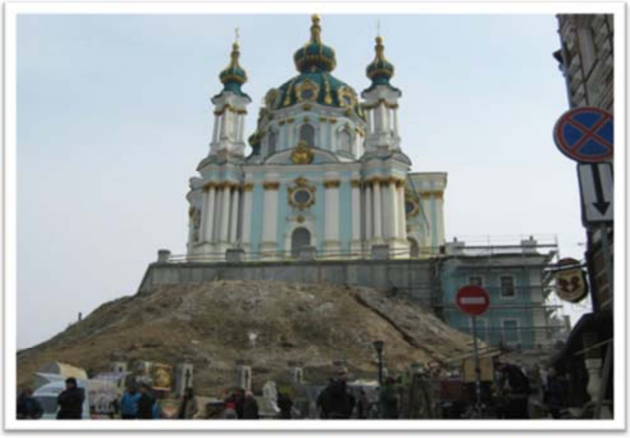

PROJECT LEADER:
- **Oleksandr Trofymchuk, Ph.D., Professor, Corresponding member of National Academy of Sciences of Ukraine, Director, Institute of Telecommunications and Global Information Space of National Academy of Sciences of Ukraine**

CORE MEMBERS OF THE PROJECT:
- **Yurii Kalyukh, Ph.D., Professor, Ukrainian State Research Institute of Building Constructions;**
- **Oleksij Lebid, Ph.D., Senior Researcher, Vice-Director, Institute of Telecommunications and Global Information Space of National Academy of Sciences of Ukraine;**
- **Berchun Victoriia, Scientific Researcher, Institute of Telecommunications and Global Information Space of National Academy of Sciences of Ukraine**

THE MAIN GOAL:
- **The main goal is certification of Ukrainian cultural heritage objects within landslide hazardous sites: experimental and analytical research etc. on the example of Kyiv-Pechersk Lavra.**

OBJECTIVES:
- **Development of methodology for certification religious buildings of Kyiv-Pechersk Lavra within landslide hazardous sites;**
- **Certification of religious buildings of Kyiv-Pechersk Lavra;**
- **Data collection and processing;**
- **Development of targeted database;**
- **Report preparation.**

STUDY AREA:
The certification of religious buildings of Kyiv-Pechersk Lavra within landslide hazardous sites. Kyiv region.

PROJECT DURATION:
January, 2020 – December 2022

PROJECT DESCRIPTION:

1ST PHASE: Method of certification and assessment of technical state of Kyiv-Pechersk Lavra objects in hazardous landslide sites will be developed. The method includes: visual and vibrodynamic examination of Kyiv-Pechersk Lavra objects within landslide hazardous sites; development of calculation model and calculations; comparative analysis of experimental and estimated data; recommendations for the repair and restoration and further operation of Kyiv-Pechersk Lavra objects within landslide hazardous sites.

2ST PHASE: Certification of some religious buildings of Kyiv-Pechersk Lavra will be performed.

3ST PHASE: data collection and processing, development of targeted database and report preparation.

Landslides as hazard for Moscow cultural heritage

Fomenko I.K. (1), Kropotkin M.P. (2), Gorobtsov D.N. (1), Nikulina M.E. (1)

1) Russian State Geological Prospecting University n. a. Sergo Ordzhonikidze (RSGPU), Moscow, Miklouho-Maklay's street, 23, e-mail: ifolga@gmail.com

2) National Research Moscow State University of Civil Engineering (NRU MGSU) 26, Yaroslavskoye Shosse, Moscow, Russia

Abstract Blocked landslides are widespread in Moscow. The displacement of such landslides connects with Upper Jurassic clays. As a rule, these landslides have huge web depth. This depends on the possibility of huge damage. The last one obstructs stabilizing measures. Landslides have regressive (inside slope) development and durable (tens and hundreds of years) periods of slow deformations (1-30 centimeter per year). Such deformations give place to short periods of activation with displacements of some meters and more.

In Moscow activation of such landslides threatens to cultural heritage, site which also a part of UNESCO. Landslide slope on Vorobievy Mountains where are Troicy Zhivonachalnoj temple, Andreevskij monastery, Muchenicy Tatiany temple under MSU is considered in depth.

Keywords
Landslides, slope stability, hazard, cultural heritage.

Introduction

Blocked landslides are widespread in Moscow. The displacement of such landslides connects with Upper Jurassic clays. Firstly, Pavlov A.V (1869-1947) near the Vorobievy Mountains explored them in 1908. It connected with the slope deformation close to east edge of Vorobievka village. The Viewing point situates there nowadays. Landslide occurred opposite pressure pond according to the M.V. Churinov data. This landslide carried the part of the slope along 250 m and destroyed the substructure of yacht club. Engineering investigations were carried in 1920 at the Vorobievy Mountains. It connected with International Red Stadium design and construction (1920-1925). The investigations in 1930 include deep drilling for design «hydro accumulating» power station, highway stream crossing, embankments and descents. Since 1960 and later on B.M. Danshin, M.V. Churinov, I.S. Rogozin, F.V. Kotlov, V.V. Kuntzel, K.A. Gulakjan, E.P. Emelianova, M.N. Paretzkaja, G.P. Postoev, S.D. Pigarina studied other landslides of Moscow: Fili, Kolomentskoe, Choroshevo and others. These specialists had different point of views about the landslides age, there activation factors, slump basis. This was due to lack of knowledge about landslide slopes and complete methods of stability assessment.

Deep blocked slopes detects in Moscow river valley on 12 sites (Shukino, Serebryanyj forest, Horoshevo-1, Fili-Kuntcevo, Nizhnie Mnevniki, Horoshevo-2, Poklonnaya Mountain, Vorobievy Mountains, Kolomenskoe, Moskvorechie, Chagino, Kapotnya) and in Shodnia river valley on 3 sites (Shodnia, Tushino, Kurkino) (fig.1).

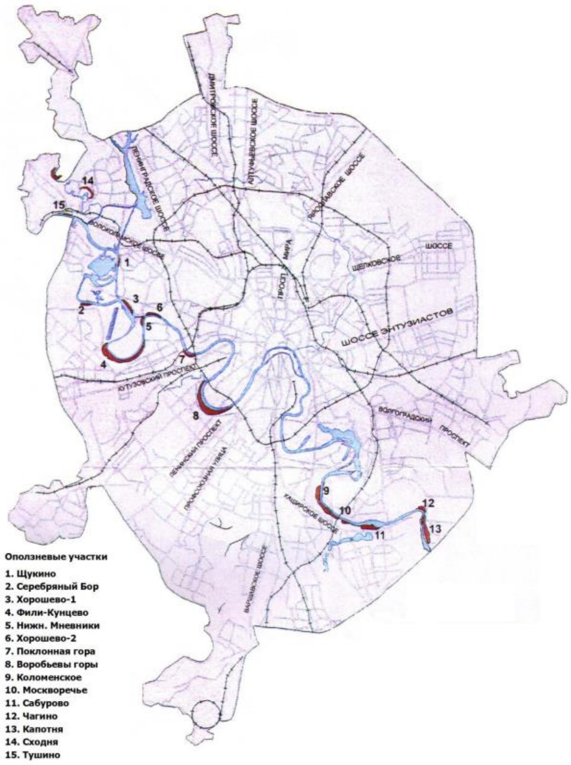

Figure 1. The areas of deep blocked landslides development in Moscow [9]

Slopes with deep landslides has specific relief: high abrupt slope (over landslide ledge) – in upper part; terrace with hilly and chine relief – in the middle and lower part. The spread of sliding area is various (from 0,5 to 3,0-3,5 km). The width (the length along landslide direction) is about 100-380 m. Planform is frontal, rarely it is circus. The volume of separate sliding blocks are about some hundred thousand m3. The volume of sliding body single circus is 5-7 mln. m3. Landslides characterizes by regressive (inside slope) growth and durable (tens and hundreds of years) periods of slow deformations which changes by periods of its activation with offset value about some meters and more [12].

The main reason of landslides origin was washout of the Moscow river high bank. Since 1770 6 floods with amplitude of water about 7,5 – 8,8 m were found on Moscow river. This means that water table treatment happened every 20-30 years. Since 1937 the river controlled by hydraulic structure. However, spring water level rise in 1955-1960 on Moscow river was 2-2,5 m. This caused the retreat of slope crest at a speed of 0,3-0,5 m/year.

More than half a century (in 1965), V.V. Kuntzel Has published a paper "About the age of deep landslides in Moscow and near Moscow areas connected with Jurassic clayey deposits [7]. Conclusions from this article are widely used in fields of the development history and structure of sliding slopes in Moscow. The article has two main points:

– vast majority of "ancient" landslides (huge sliding blocks) viewed on slopes have been taking shape along last 2000-3000 years;

– the duration of completely sliding cycle is 300-350 years (calculated on the Vorobievy Mountains example).

Figure 2. Hilly and depression relief at the base of slope in the Kolomenskoe near the Useknoveniya Glavy Ioanna Predtechi church. The relief is a result of the original sliding stages split

Moscow landslides activity assessment

Further, the illustration of slopes history development in Moscow with blocked landslides is given. Due to bank caving with the adequate height (more then 17-25 m above river level in low level) and upper Jurassic clayey deposits at the basement, the primary shear landslides forms with displacement surface close to circular cylindrical shape. Progressive erosion of sliding bodies front parts causes the slow "after main" displacement with the descent of their top parts. It induces changes in tense conditions of the virgin rock mass neighbouring part. If the top part of throwing back surface is in some position, so tense changes will be enough to break the balance of neighboring slope part. The last one also unplugs because of shear and detruncating along the surface close to circular cylindrical shape at descending part. This zone develops along shear surface of original block at the other part. Then the process is going to be cycle and develop in the way of "plateau". Sliding displacements also occur in detached blocks (in their front part, which is close to slump basis).

The main number of blocks and maximum length (along displacement direction) of sliding massive occurs on the highest slopes. Horizontal displacements of sliding massive are relatively low. The sub rotary displacements prevail with concomitant erosion as body end as upper part of "top" blocks. Changes in tense condition lead to stability disturbance of other blocks. They occur because of discharging horizontal tension. The last one happens thru low horizontal displacements and descent of top parts the previous blocks. It decreases vertical tensions on displacement surface.

The influence of low horizontal displacements on tense in massive may be illustrated by following example. Maximum value of riser the ditch bottom with the depth about 15-20 m in the generalized soil conditions is not higher than 20 cm. That means that it is 1-1,3% from width of excavated soils.

Usually soils is excavated fully from the trench. It may be raised (move upward) on 20 cm to complete the same result. This lead to full tension discharge (obviously, the transfer of lateral tension should be excluded). Therefore, the summary horizontal displacement about 1 - 3 m is enough to form 5 huge sliding blocks.

That way occur the conditions to renew creep flow in sliding massif. The slope becomes to be in limiting state while reaching the critical value. The catalyst of the main displacement with occurrence of new blocks were extremal floods on rivers. The last one lead to the growth of pore pressure in the displacement zone (especially on the top landslide submerged area).

Rapid flood recession leaveы behind the pore pressure dissipation in clayey soils. It also lead to sharp growth of hydraulic grades in sliding tongue massif. It increased the hydrodynamic pressure.

The tiny sub block forms when the influence of near slope crest discharge. This happens because minor displacement of sliding body tongue part could not reach deeply in the massif behind slope edge.

Maybe because of this the real displacement surface is going in massif near the slope edge, not in the depth.

In the result of bed deeping in Moscow river watercourse the additional nugatory technogenic influence on the stability occurs. In 1980 and 1981, washing the river watercourse was made. It may lead to the effect occurrence, which is similar to streambed erosion.

The massif displacement speed on sliding areas in Moscow are less than in 1960-1970 years. On some areas (Karamishevskaya embankment, Serebryanyj pine forest, Vorobievy Mountains and others) for the last 10-15 years, new surface manifestation occurs (in the form of tension joint). This could imply that the process is going to the other stage.

Data of regime observations for surface points and inclination supervisions also show notable differences in deformations:

– the displacement of sliding blocks is observed along the existing displacement zone on Kolomensky area of Chertanovsky manifold and on Choroshevo-1.

Instrumental observations for deep landslide growth on the stage of main displacement (Choroshevo-1 area) shows that the duration of first 2 stages (destruction of base rocks and displacement speed increasing) lasts for 8 months. Maximum displacement speeds are 35 mm/day.

Since 1985 until 2005 frame, which is near the landslide top, has went down on 476 mm and moved out of position to the river on 580 mm. The frame on the quay wall growth up to 226 mm and moved out of position to the river on 2032 mm [3]. It was observed near Chertanovsky manifold in Kolomensky area.
Distortion and changing the massif form prevails on Vorobievy Mountains.

Holy Trinity temple in Choroshevo

White Stone Holy Trinity temple stands on the high bank of the Moscow River for more than four centuries. It is one of the jewels of Russian architecture of XVI century (fig. 3).

It was constructed between 1596 and 1597 years and was finished when Boris Fedorovich Godunov has mounted the throne.
Piskarevski chronicler wrote about the temple erection: «In days of pious king and grand prince Fedor Ivanovich of all Russia… the stone temple in the village Choroshevo under the petition of boyar Boris Fedorovich Godunov» [10].

Figure 3. Holy Trinity temple in Choroshevo

The first mention about the sliding processes near the Holy Trinity temple in Choroshevo occurs since 18 century. In 1771 "landing slip near the Moscow river happened".

In 1877, a new threat of landing slip near the temple perturbed parishioners.

Choroshevo "undergo to inevitable and imminent danger of collapse and fall into the river" (according to "extra" internal memorandum of Moscow, district clerk from October 18, 1877). A special and imminent danger threatens the church and the house occupied by the parish board. Several cracks formed at the beginning of October in the coastal to the Moscow river area. The highest fracture situated on the mountain, which now has a length of more than 100 fathoms. This fracture begins in the middle of the church fence (near the fence, behind the house of the volost board), and then across the yard and garden of the merchant Egorova (two links of the fence already collapsed). Behind the garden of Egorova, the upper crack, descending downhill, will connect with another mountain crevice. The last one starts in the same place against the church, goes straight along the entire mountain in the space of half a mile and ends at the end of the rural buildings, where the bank of the river begins. The huge mass of earth, outlined by the upper crevice, connects with another crack. It quickly began to settle down and disappear without a trace, as if filling up an invisible underground void. More than 5 fathoms is from the Church to the edge of the collapse. The water keys began punching in Choroshevo closer to Konyushennaya Sloboda, between the right and left sides of the buildings. It was not happen before. If no measures takes, the destruction of buildings in the left side of the village Choroshevo will accelerate [1].

The church community returned to the issue of reinforcement the bank of the Moscow River that threatens to collapse. It happens in the year of the 300th anniversary of the Romanov dynasty, in a petition dated February 1913.

Holy Trinity temple (our historical holy) situates at the high bank (about 30 fathoms) of the Moscow River. This bank gradually creeping. It will cause inevitable falling to the church. In this case, the church situated more than 20-30 fathoms from the bank will be standing at the 3-5 fathoms from the abrupt coastal cliff.

Thirty years ago, there was a landslide near the coast and it cracked the church wall. Just one minor landslide and the church will inevitably fall. The parishioners and the rector of the church organize measures to eliminate the inevitable church falling. These measures include tree plantations, fences formation and do not bring good results because all of them were showered and destroyed during spring floods. Our parish, for their poverty, could not organize more capital measures. That's why with the fear and a broken heart, every spring, we are awaiting the destruction of the dear shrines" [2].

A.V. Pavlov, the professor of Russian University of Transport was the consulter. He told about the great threat to the temple. For this reason, it is necessary to force the bank or to luff the temple to the safe place [15].

Regular observations took place since 1975 and lasts until now. Until 2006 some minor mudslides occurred. They were 1-2 m along brow slope in length. High accuracy observations lasts since 1977 until 1984. They were taken place in 300 m down the river from Holy Trinity church. The highest average of frame displacement (86-91 mm) were near the river and decreased deep into the slope. They were 45-46 mm close to the top of the slope. Noticeable signs of deep deformations were not noticed [8, 9].

The main landslide displacement occuries in 2006. The length of wall disruption was 300 m, the height was 0,5-1,0 m, which then increased to 3 m. Wall disruption situated in 5 m from one of the cottages and 15 m from the church. It threatens to their safety (fig. 4-5).

Figure. 4. Wall disruption of sliding sub block and the widest part of slipping down the under rim part at the territory of Holy Trinity temple (12.10.06), sliding area Choroshevo-1

Figure 5 Sliding fracture of lower sliding blocks opposite the temple

In October 2006 observation network occurred. It include soils deformation frames and stamps (over than 50 signals). Lately there occurred bore halls (inclinometric, tensor, metric, and others) which were used for observations. There were also clinometers organized on load-carrying structure of cottages and church. Observations on soil frames conducted at a frequency of twice a week, and then every two weeks (since May 2007) [13].

Instrumental observations shows that planned displacement of sliding terrace was more than dissenting block. The frame situated at the base of the slope displaced on 84 mm. The displacement was on the central trunk. Other frames situated on dissenting block displaced on 57-68 mm. [6]. The fracture which separates block from delyapsiya unfold on 0,7-1,1 m in a year [14]. Activation of sliding process Matches with the construction of Zhivopisnyj Bridge, with driving of piles for temporary support in southwest area of Choroshevo alignment. At the end of 2007, the displacement speeds decreased to 2 mm in a month. However in January 7, 2008 after opening the traffic along the bridge the speeds increased by four, reached 2 mm in a week [14]. Therefore, the main reason of sliding process activation are tecnogenic loads.

Quantity slope stability assessment

There are many stability assessment methods at present. The preferred method of calculations depends from the type of sliding process and mechanism of sliding masses possible displacement. [4].

The class of limit equilibrium method (Spenser) and finite elements method (FEM) were used along the estimates. These methods applies for heterogeneous slopes.

Engineering and geological models were created for stability estimation. The results of the performed study of engineering and geological conditions of the investigated territory were the base for model construction. They allowed establishing boundaries between engineering and geological elements that differs in their physical and mechanical characteristics. The model of Coulomb-Mohr soil destruction was the main along calculations. [5].

The results of slope stability assessment with the definition of stability factor (Sf) are on the fig. 6 (Spenser method).

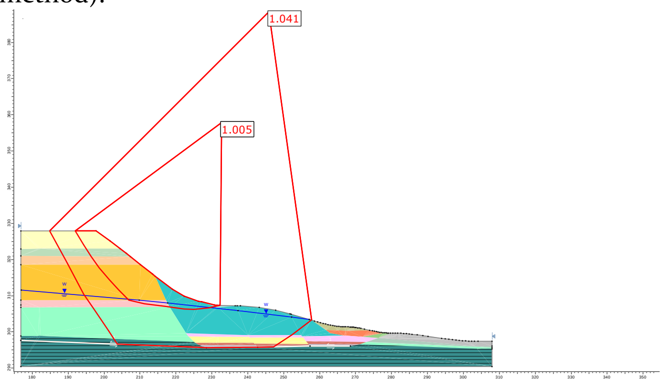

Figure 6 Geomechanical scheme with the results of slope stability estimation

In the result of sliding slope stability modeling by FEM the similar results received (fig. 7).

3D stability assessment realized for evaluation of the extent development the sliding process (by the limit equilibrium method (Spenser) (fig. 8).

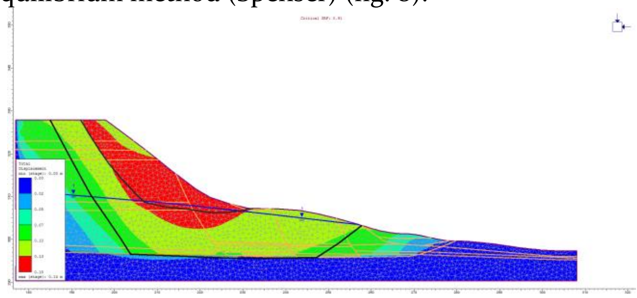

Figure 7. The estimation result by FEM method (Fs – 0.91). Black lines are the sliding surfaces estimated by Spenser method

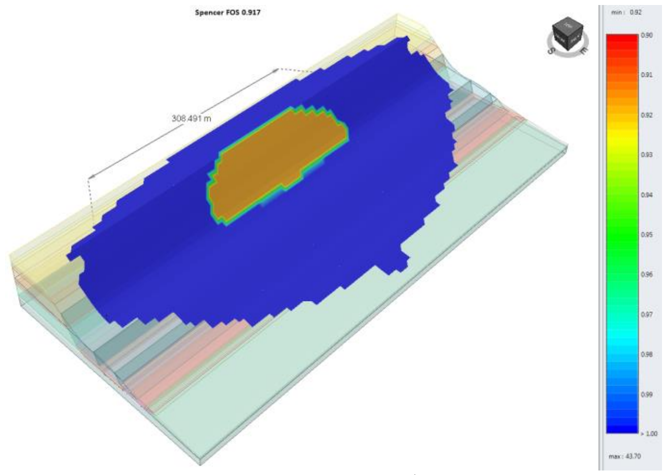

Figure 8. 3D slope stability assessment (by the limit equilibrium method (Spenser)

Estimated results about the landslide width (308 m) are well coordinate with the field data along engineering and geological investigations (300 m).

Conclusion

The analysis of data allows making a conclusion that there are two possible variants of sliding deformations.
According to the first variant the secondary landslide forms on the slope (Fs-1.005). Such scenario was proved along the geophysical investigations (fig. 9).

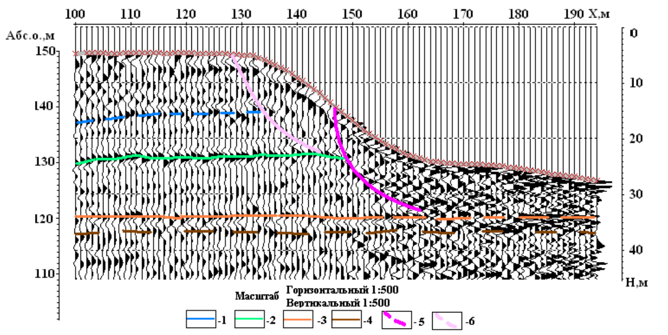

Figure 9. Deep seismogeological profile. 1 – the roof of the Cretaceous (?) deposits, 2 – the roof of the Volgian sediments; 3 – the roof of the Oxford clays; 4 – the roof of the Callovian clays; 5 - existing surface displacement; 6 – potential surface displacement

According to seismological profile, the block of secondary landslide forms on the sliding slope.

In concordance with the second variant, a new sliding block forms on the slope (Fs -1.04). Its sliding surface arranged to Upper Jurassic clays of Oxford stage. This variant was proved along inclinometric observations (fig.10).
Therefore, along the activation of sliding process there may be both variants when the process develops systematically. The secondary landslide formed on the first stage. Its activation on the second stage induced the new block formation with to Upper Jurassic clays of Oxford stage sliding surface. Maximum deformations were on the first stage. Second stage characterizes by long duration of sliding process.

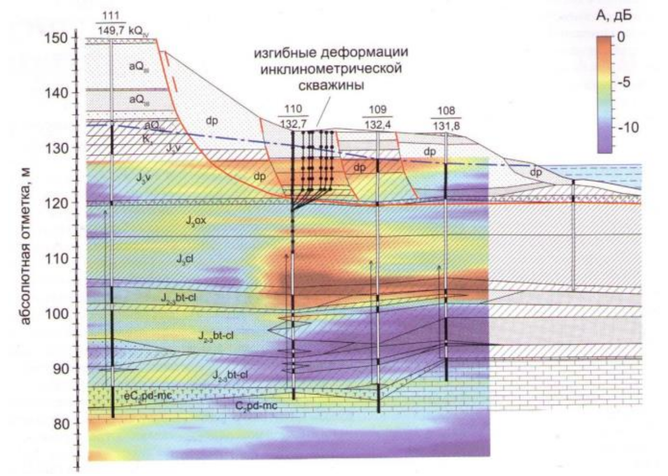

Figure 10. Geophysical profile and the results of inclinometric observations at the territory of Choroshevo-1. A – Amplitude of microseismic oscillation [16]

Correct ideas about the mechanism of landslide processes allow to predict them effectively and avoiding erroneous decisions on landslide protection.
This article prepared in the framework of the project IPL-238 «Landslides Threatening Russian Cultural Heritage Sites».

References

1. Copies of inventories archive CSA Moscow CIAM. F. 54. Op. 134. D. 330. The case of the Construction Department of the Moscow Provincial Board, on the proposal of the Chief City of the Province on business trip of the architect to inspect damage, was on the left Bank of Moscow in the village Horoshovo Moscow district. 1877-1878, L. 2. URL: http://kraevedmo.ru. [Last accessed: 27.07.2019].
2. Copies of inventories archive CSA Moscow. CIAM F. 454. Op. 3. D. 79. The case of the Construction Department of the Moscow Provincial Board, on the proposal of the Chief City of the Province on business trip of the architect to inspect damage, was on the left Bank of Moscow in the village Horoshovo Moscow district. L. 182-182 ob. URL: http://kraevedmo.ru. [Last accessed: 27.07.2019].
3. Engineering and geological conclusion of the department of monitoring of geological processes FSBI « Geocentr–Moscow » № 02/885 (94) from 12.09.2006 for the project "Construction of a dyuker Chertanovskaya channel deep-laid over the river Moscow».
4. Fomenko I. K. (2012) Current trends in slope stability calculations. Engineering Geology. № 6. pp. 44–53.
5. Fomenko I. K., Kurguzov K. V., Zerkal O. V. and Sirotkina O. N. (2019) Setting soil strength parameters for slope stability calculations. In Geotechnics Fundamentals and Applications in Construction: New Materials, Structures, Technologies and Calculations. vol. 2 of Proceedings in Earth and geosciences. CRC Press/Balkema Leiden. The Netherlands. pp. 59–64.
6. Gavrilov S.G., (2007) Results of observations of landslide slope deformations in the area between Karamyshevsky and Khoroshevsky straightening of the Moscow River as of November 08 2007. M.: SBI «Mosgorgeotrest». 15 p.

7. Kuntcel V.V. (1965) About age of the deep landslides of Moscow and Moscow region connected with Jurassic clay deposits. Bulletin of the Moscow society of nature testers. Department of Geology. T. XL (3). pp. 93-100.
8. Pareckaya M.N., Pigarina S.D., (1977) The report "Regional study of landslides at the Moscow territory ». M.: CIGGE. 356 p.
9. Pareckaya M.N., Raputov M.B., (1991) The report «Study of the regime of exogenous geological processes at the Moscow territory and the Moscow region (on the results of stationary study of landslide processes at the Moscow territory and the Moscow region from 1973 to 1989).) ». M.: MGGA. 371 p.
10. Piskarevskij letopisec (1978) Full collection of Russian Chronicles, T. 34, M. 200 p.
11. Recommendations for the assessment of geological risk in Moscow (2002). After the reduction of doctor of geological and mineralogical sciences A.L. Ragozina. Moskomarhitektura, GU GO CHS Moscow. M.: GUP NIAC. 49 p.
12. Tihonov A.V. (2007) Engineering and geological conclusion on the forecast of the landslide processes development in the area between Karamyshevsky and Khoroshevsky straightening of Moscow River. M.: FGUP «Geocentr-Mocow». 69 p.
13. Tihonov A.V. (2007) The monitoring project of landslide slope in the area between Karamyshevsky and Khoroshevskoe alignment of Moscow River. M.: FGUP « Geocentr-Mocow a». 38 p.
14. Tihonov A.V. (2009) Features of the mechanism of landslide process in Moscow on the example of the site Choroshevo-1. News higher educational institutions. Geology and exploration. №4. pp. 74-75.
15. Vajntraub L.R., Karpova M.G., Skopin V.V. (200) Temples of the Northwest district and Zelenograd. M. 90 p.
16. Volkov V.A., Tihonov A.V., Kalinina A.V., Ammosov S.M. (2012) Study of the structure of the active block landslide on the example of Karamyshevskaya embankment of the Moscow river. Georisk. №3. pp. 8–13.